Towards an *in vitro* model of Congenital Hyperinsulinism of Infancy

A thesis submitted to the University of Manchester for the degree of
Doctor of Philosophy
in the Faculty of Biology, Medicine and Health

2018

S M Mahbubur Rashid

School of Medical Sciences

Contents

Page no.

List of contents 2-8
List of figures 9-13
List of tables 14-15
Abbreviations 16-18
Abstract 19
Declaration 20
Copyright statement 21
Acknowledgement 22

Chapter 1 **23-46**
Introduction

1.1 Congenital hyperinsulinism of infancy 23

1.2 Biochemical features of CHI 23

1.3 Known genetic basis of CHI 24

1.4 Known mechanisms of CHI 28

1.5 Histological features of CHI 35

1.6 Management of CHI patients 37
1.6.1 Diagnosis of CHI 37
1.6.2 Treatment options for CHI 38

1.7 Studying model systems for understanding CHI 39
1.7.1 *In vivo* models for studying genes related to CHI 39
1.7.2 *In vitro* models for studying genes related to CHI 41

1.8 Network biology: an alternative approach to study CHI pathobiology 43

1.9 Aims of the study 45

Chapter 2 **47-92**
Materials and methods

2.1 Cell culture 47
2.1.1 Cell lines used in this study 47
2.1.2 Cell culture method 47
2.1.2.1 EndoCβH1 cell line 47
2.1.2.2 MIN6 cell line 48
2.1.2.3 CHI-iPS cell line 49
2.1.3 Cryopreservation and recovery of cells 49

2.2 Total RNA isolation, quantification, and conversion to cDNA 50
2.2.1 Collection of cells 50
2.2.2 RNA isolation 50
2.2.3 RNA quantification 51
2.2.4 Conversion of total RNA to cDNA by Reverse Transcription (RT) 51

2.3 Analysis of gene expression by Polymerase chain reaction (PCR) 52
2.3.1 Primers used for reverse-transcription PCR 52
2.3.2 Reverse-transcription PCR (RT-PCR) 52
2.3.3 Separation of PCR products and their visualisation 53
2.3.4 Primers validation 53
2.3.5 Relative quantitative PCR 54
2.3.5.1 SYBR Green-based qPCR 56
2.3.5.2 TaqMan probe-based quantitative PCR 57

2.4 Protein analysis 58
2.4.1 Immunofluorescence imaging study 58
2.4.2 Western blot analysis 59
2.4.2.1 Extraction of protein 59
2.4.2.2 Estimation of protein concentration 60
2.4.2.3 Protein separation, transfer to membrane and detection 60

2.5 Cell proliferation assay 62
2.5.1 Conventional cell counting method 62
2.5.2 CellTiter 96 AQ_{ueous} One Solution cell proliferation assay 62
2.5.3 Cell proliferation assay based on 5-Bromo-2-deoxyuridine incorporation 63

2.6 Glucose-stimulated insulin secretion (GSIS) assay 64
2.6.1 Isolation of Islet of Langerhans from mouse pancreas 64
2.6.2 Insulin secretion assay with cell lines 65
2.6.3 Insulin secretion assay with mouse pancreatic islets 67
2.6.4 Quantification of insulin content using enzyme-linked immunosorbent assay (ELISA) 68

2.7 CHI-iPS cell *in vitro* differentiation into insulin-producing beta cell 69

2.8 Gene knock-out using CRISPR-Cas9 gene editing method 73
2.8.1 Experimental design 73
2.8.2 Design and cloning of gRNAs targeted to edit critical exon 74
2.8.3 Transformation and cloning of plasmids, encoding gRNAs 76
2.8.3.1 Preparation of competent bacterial cells 76
2.8.3.2 Transformation of competent DH5α with plasmids, encoding gRNAs 77
2.8.3.3 Plasmid isolation from transformed cells for transfection experiments 77
2.8.4 Transfection of cells with CRISPR gRNAs 78
2.8.4.1 CHI-iPS cell transfection 78
2.8.4.2 EndoCβH1 cell transfection 79

2.8.5 Validation of transfection 81
2.8.5.1 DNA purification from cultured cells 81
2.8.5.2 Amplification of target region by PCR and purification of the amplicon 82
2.8.5.3 CHI-iPS cell transfection validation 83
2.8.5.4 EndoCβH1 cell transfection validation 83
2.8.6 Sorting potential edited cells 85
2.8.7 Clonal expansion of single CHI-iPS cell 85
2.8.8 Clonal expansion of single EndoCβH1cell 87

2.9 Gene knock-down experiments using short interfering RNAs 88

2.10 GSIS assay of siRNA-based knocked down EndocβH1 cells 89

2.11 Gene expression microarray analysis of CHI tissues 89

2.12 Computational analysis of CHI-related biological data 90
2.12.1 Analysis of differential gene expression and associated pathways 90
2.12.2 Finding protein-protein interaction partners, sorting and their validation 91
2.12.3 Integrated network visualization and analysis 91

2.13 Statistical analysis 92

Chapter 3 **93-145**
Derivation of CHI beta cells by modification of cell culture conditions

3.1 Introduction 93
3.1.1 Congenital hyperinsulinism in infancy and its predominant causes 93
3.1.2 CHI and its symptomatic functional attributes 94
3.1.3 Insulin secretagogues and their effect on cellular functions 95
3.1.4 Pancreatic beta cell lines and islets used in this study 96
3.1.5 Aim and objectives of this study 97

3.2 Results 99
3.2.1 Characterization of MIN6 and EndoCβH1 cells 99
3.2.1.1 Morphological features of beta cell lines 99
3.2.1.2 MIN6 and EndoCβH1 cells show characteristics of pancreatic beta cells 99
3.2.1.3 MIN6 and EndoCβH1 cells respond to glucose and secrete insulin 101
3.2.2 Effects of ISGs on MIN6 and EndoCβH1 cells proliferation 102
3.2.2.1 Effects on proliferation of MIN6 and EndoCβH1 cells acutely treated with ISGs 106
3.2.2.2 Effects on proliferation of MIN6 and EndoCβH1 cells chronically treated with ISGs 107
3.2.2.3 Effects on proliferation of MIN6 and EndoCβH1 cells acutely and chronically treated with tolbutamide in high concentration 109
3.2.2.3.1 Effects on proliferation of MIN6 and EndoCβH1 cells acutely treated with Tol^{high} 109

3.2.2.3.2 Effects on proliferation of MIN6 and EndoCβH1 cells chronically treated with Tol^{high} 110
3.2.2.4 Effects on proliferation of MIN6 and EndoCβH1 cells acutely and chronically treated with combinations of ISGs 112
3.2.2.4.1 Effects on proliferation of MIN6 and EndoCβH1 cells acutely and chronically treated with combinations of ISGs 112
3.2.2.4.2 Effects on proliferation of MIN6 and EndoCβH1 cells chronically treated with ISG_{mix} 113
3.2.3 Treatment with ISGs does not make any effect on insulin production of MIN6 and EndoCβH1 cells 115
3.2.4 Effects of ISGs on MIN6 and EndoCβH1 cells insulin secretion 118
3.2.4.1 Effects on insulin secretion of MIN6 and EndoCβH1 cells acutely treated with ISGs 121
3.2.4.2 Effects on insulin secretion of MIN6 and EndoCβH1 cells chronically treated with ISGs 125
3.2.4.3 Effects on insulin secretion of MIN6 and EndoCβH1 cells acutely and chronically treated with Tol^{high} 130
3.2.4.3.1 Effects on insulin secretion of MIN6 and EndoCβH1 cells acutely treated with Tol^{high} 130
3.2.4.3.2 Effects on insulin secretion of MIN6 and EndoCβH1 cells chronically treated with Tol^{high} 131
3.2.4.4 Effects on insulin secretion of MIN6 and EndoCβH1 cells acutely and chronically treated with ISG_{mix} 132
3.2.4.4.1 Effects on insulin secretion of MIN6 and EndoCβH1 cells acutely treated with ISG_{mix} 133
3.2.4.4.2 Effects on insulin secretion of MIN6 and EndoCβH1 cells chronically treated with ISG_{mix} 134
3.2.5 Chronic treatment of MIN6 and EndoCβH1 cells with ISGs had no affect on the expression of membrane-bound 137

3.3 Discussion 141

Chapter 4 **146-196**

Implementing CRISPR-Cas9 to knock out the *ABCC8* gene to generate *in vitro* CHI model cell line

4.1 Introduction 146
4.1.1 General 146
4.1.2 Experimental approaches used in this study 146
4.1.3 Stem cells and their potential for generation of CHI *in vitro* models 147
4.1.4 CRISPR/Cas9: an efficient gene editing tool to generate disease model 149
4.1.5 Aim and objectives of this study 152

4.2 Results 153
4.2.1 Characterization of CHI-iPS cells 153
4.2.2 CHI-iPS cells maintain expression of proteins characteristic for pluripotency 155
4.2.3 Differentiation of CHI-iPS cells into insulin-producing cells 156

4.2.3.1 Differentiation of CHI-iPS cells into insulin-producing cells following 5-stage protocol 157
4.2.3.2 Differentiation of CHI-iPS cells into insulin-producing cells following 7-stage protocol 161
4.2.4 Introduction of a homozygous mutation in CHI-iPS cells using CRISPR-Cas9 system 163
4.2.4.1 Design of guide RNAs and Single-stranded oligo donor targeted to introduce a homozygous mutation in CHI-iPS cells 163
4.2.4.2 Optimisation of cellular transfection method for transfection of CHI-iPS cells with plasmid DNA encoding gRNA 165
4.2.4.3 Transfection of CHI-iPS cells with gRNA encoding plasmid DNA and ssODN and validation of transfection 165
4.2.4.4 Single cell sorting and clonal propagation of CRISPR induced mutated CHI-iPS cells 166
4.2.4.5 Characterization of clonally propagated edited CHI-iPS cells 169
4.2.4.6 Applying alternative methods to transfect CHI-iPS cells and propagation of sorted single cells 174
4.2.5 Introduction of a deletion mutation in EndoCβH1 cells using CRISPR-Cas9 system to knock out *ABCC8* and *KCNJ11* genes 175
4.2.5.1 Design of guide RNAs targeted to knock out genes in EndoCβH1 cells 175
4.2.5.2 Optimising cell culture conditions to favour EndoCβH1 cell for expansion from single cells 179
4.2.5.3 Selection of transfection method for transfecting EndoCβH1 cells with plasmid DNA 180
4.2.5.4 Selection of best CRISPR guide RNAs to knock out *ABCC8* and *KCNJ11* genes in EndoCβH1 cells 183
4.2.5.5 Generation of *ABCC8* knock-out EndoCβH1 cell population and their characterization 185
4.2.6 Introduction of a deletion mutation in *ABCC8* gene in CHI-iPS cells 188
4.3 Discussion 189
4.3.1 General 189
4.3.2 CHI-iPS cell and its potential to generate insulin-producing cells 189
4.3.3 Introducing homozygous mutation in *ABCC8* gene in CHI-iPS cell line 192
4.3.4 Knocking out the *ABCC8* and *KCNJ11* genes in EndoCβH1 cell line 194

Chapter 5 **197-273**
Genome-wide gene expression microarray analysis of CHI-affected pancreatic tissues

5.1 Introduction 197
5.1.1 General 197
5.1.2 An overview of gene expression microarray 198

5.1.3 General approaches analysing data obtained from gene expression microarray 201
5.1.4 Explored web-based resources to analyse gene expression microarray data 202
5.1.5 Analysing gene expression microarray data using network biology 204
5.1.6 Aim and objectives of this study 205

5.2 Results 206
5.2.1 Tissues used for genome-wide analysis of gene expression 206
5.2.2 Validation of normalised expression data obtained from microarray analysis 207
5.2.3 Basic analysis of gene expression data obtained from microarray experiments 208
5.2.4 Analysing expression of genes potentially associated with CHI pathobiology 213
5.2.5 Exploring biological processes related to differentially expressed genes 220
5.2.6 Gene functional classification by Gene Ontology (GO) 223
5.2.6.1 Molecular functions altered in CHI conditions 223
5.2.6.2 Biological processes altered in CHI conditions 225
5.2.6.3 Cellular components altered in CHI conditions 227
5.2.7 High-throughput expression analysis of experimental microarray data 229
5.2.7.1 Analysing canonical pathways and processes associated with differentially expressed genes in CHI conditions 232
5.2.7.2 Analysing upstream regulators and their downstream effects of differentially expressed genes in CHI condition 239
5.2.7.3 IPA analysis of biological functions predicted to altered because of differentially expressed genes 245
5.2.8 Expression analysis of experimental microarray data using protein-protein interaction and network biology 249

5.3 Discussion 258
5.3.1 General 258
5.3.2 Experimental design and microarray experiments 259
5.3.3 Basic comparative analysis of genome-wide gene expression data generated from microarray experiments 261
5.3.4 Functional analysis of the differentially expressed genes in the experimental microarray datasets 265
5.3.5 Using network biology approach to identify key genes associated with CHI 269
5.3.6 Validation of the outcomes of the gene expression microarray experiments 271
5.3.7 Conclusion 273

Chapter 6 **274-291**

K_{ATP} channel knock-down and generation of transient *in vitro* CHI model

6.1 Introduction 274
6.1.1 General 274
6.1.2 Overview of siRNA-based gene silencing 275

6.1.3 siRNA: mechanism of action 276
6.1.4 Aim and objectives of this study 277

6.2 Results 279
6.2.1 siRNA-mediated knocking down of the expression of *KCNJ11* in EndoCβH1 cells 279
6.2.2 Glucose-stimulated insulin secretion assay of *KCNJ11* knocked down EndoCβH1 cells 281
6.2.2.1 KCNJ11KD cells have increased basal insulin secretion 282
6.2.2.2 GSIS assay of KCNJ11KD cells in the presence of insulin secretion inducer, tolbutamide 282
6.2.2.3 GSIS assay of KCNJ11KD cells in the presence of insulin secretion inhibitor, diazoxide 284
6.2.2.4 GSIS assay of KCNJ11KD cells in the presence of calcium channel inhibitor, nifedipine 285

6.3 Discussion 287

Chapter 7 **292-300**
Discussion

7.1 Summary 292
7.2 Contribution to the understanding of CHI 294
7.2.1 Establishment of CHI-like model cell line 294
7.2.1.1 IGS-based induction method 294
7.2.1.2 K_{ATP} channel gene-editing approach 295
7.2.1.3 siRNA-based KATP channel gene silencing approch 296
7.2.2 Differential gene expression study using microarray 297
7.3 Future perspecives 298
7.4 Concluding remarks 299

References 301-347

Appendix I 348-349

Appendix II 350-358

Appendix III 359-360

Word count: 77,840

List of Figures

Page no.

Chapter 1

Figure 1.1 Graphical representation of the components of the pancreatic beta cell K_{ATP} channel 29

Figure 1.2 Schematic representations of how mutations in K_{ATP} channels can cause uncontrolled insulin release in pancreatic beta cells 30-31

Figure 1.3 Summary of the common known causes of CHI in the pancreatic beta cell 34

Figure 1.4 A typical structural comparison between focal and diffuse CHI 36

Figure 1.5 Chromosomal aberration associated with a focal form of CHI 36

Chapter 2

Figure 2.1 A typical illustration of the phases of PCR 54

Figure 2.2 Typical steps of SYBR green and TaqMan assays 55

Figure 2.3 A typical diagram of different steps to differentiate CHI-iPS cells into insulin-producing cells 72

Figure 2.4 Schematic diagram of the critical steps of CRISPR-Cas9 mediated knockout experiments 73-74

Figure 2.5 Schematic map of the expression vector pX458 used in CRISPR-Cas9 mediated gene editing experiments 76

Figure 2.6 Schematic workflow for the validation of CRISPR-Cas9 induced gene editing 84

Chapter 3

Figure 3.1 Schematic representation of the insulin secretagogues and their mode of actions 96

Figure 3.2 Morphological shapes of pancreatic beta cell lines MIN6 and EndoCβH1 99

Figure 3.3 Immunofluorescence image of MIN6 cells showing expression of insulin 100

Figure 3.4 Expression of pancreatic beta cell markers in EndoCβH1 cells 101

Figure 3.5 Quantitative assays for glucose-stimulated insulin secretion in MIN6 and EndoCβH1 cells 102

Figure 3.6 Growth curve of MIN6 and EndoCβH1 cells showing the effect of insulin secretagogues on cell proliferation 103

Figure 3.7 CellTiter 96 A_{queous} Non-Radioactive Cell Proliferation assay-based growth curve of MIN6 and EndoCβH1 cells treated with insulin secretagogues 104

Figure 3.8 BrdU incorporation-based MIN6 cells proliferation assay 105

Figure 3.9 Effects of acute exposure to insulin secretagogues on MIN6 and EndoCβH1 cells proliferation 106

Figure 3.10	Effects of Chronic exposure of insulin secretagogues on MIN6 and EndoCβH1 cells proliferation	107
Figure 3.11	Cell proliferation of chronically insulin secretagogues treated MIN6 and EndoCβH1 cells in the presence of respective secretagogues	108
Figure 3.12	Effects of acute exposure of 500 µM tolbutamide on MIN6 and EndoCβH1 cells proliferation	110
Figure 3.13	Effects of chronic exposure of 500 µM tolbutamide on MIN6 and EndoCβH1 cells proliferation	111
Figure 3.14	Cell proliferation of chronically Tol^{high} treated MIN6 and EndoCβH1 cells in the presence of tolbutamide	112
Figure 3.15	Effects of acute exposure of mixture of insulin secretagogues on MIN6 and EndoCβH1 cells proliferation	113
Figure 3.16	Effects of chronic exposure of mixture of insulin secretagogues on MIN6 and EndoCβH1 cells proliferation	114
Figure 3.17	Cell proliferation of chronically treated MIN6 and EndoCβH1 cells in the presence of the respective mixture of insulin secretagogues	115
Figure 3.18	Expression of insulin in MIN6 cells chronically treated with insulin secretagogues	116
Figure 3.19	Expression of insulin in EndoCβH1 cells chronically treated with insulin secretagogues	117
Figure 3.20	Quantitative assays for glucose-stimulated insulin secretion in MIN6 cells treated with insulin secretagogues	119
Figure 3.21	Quantitative assays for glucose-stimulated insulin secretion in EndoCβH1 cells treated with insulin secretagogues	120
Figure 3.22	Quantitative assays for glucose-stimulated insulin secretion in MIN6 cells acutely treated with insulin secretagogues	121-122
Figure 3.23	Quantitative assays for glucose-stimulated insulin secretion in EndoCβH1 cells acutely treated with insulin secretagogues	122-123
Figure 3.24	Quantitative assays for glucose-stimulated insulin secretion in mouse islets acutely treated with insulin secretagogues	124
Figure 3.25	Quantitative assays for glucose-stimulated insulin secretion in MIN6 cells chronically treated with insulin secretagogues	126
Figure 3.26	Quantitative assays for glucose-stimulated insulin secretion in EndoCβH1 cells chronically treated with insulin secretagogues	127
Figure 3.27	Quantitative assays for glucose-stimulated insulin secretion in chronically treated MIN6 cells in the presence of insulin secretagogues	128-129
Figure 3.28	Quantitative assays for glucose-stimulated insulin secretion in chronically treated EndoCβH1 cells in the presence of insulin secretagogues	129-130
Figure 3.29	Quantitative assays for glucose-stimulated insulin secretion in MIN6 and EndoCβH1 cells acutely treated with 500 µM tolbutamide	131
Figure 3.30	Quantitative assays for glucose-stimulated insulin secretion in MIN6 and EndoCβH1 cells chronically treated with 500 µM tolbutamide	132
Figure 3.31	Quantitative assays for glucose-stimulated insulin secretion in MIN6 cells acutely treated with a mixture of insulin secretagogues	133
Figure 3.32	Quantitative assays for glucose-stimulated insulin secretion in EndoCβH1 cells acutely treated with a mixture of insulin secretagogues	134

Figure 3.33 Quantitative assays for glucose-stimulated insulin secretion in MIN6 cells chronically treated with a mixture of insulin secretagogues 135
Figure 3.34 Quantitative assays for glucose-stimulated insulin secretion in EndoCβH1 cells chronicallly treated with a mixture of insulin secretagogues 136
Figure 3.35 mRNA transcript profiles of membrane-bound channel proteins in chronically treated MIN6 cells 138
Figure 3.36 mRNA transcript profiles of membrane-bound channel proteins in chronically treated EndoCβH1 cells 139
Figure 3.37 Western blot analysis of chronically treated MIN6 and EndoCβH1 cells stained with anti-Kir6.2 and anti-β-Actin antibody 140

Chapter 4

Figure 4.1 Schematic illustration of types of stem cells and their source of origin 148
Figure 4.2 Schematic representation of CRISPR-Cas9 mediated gene editing 151
Figure 4.3 Morphological and genetic features of CHI-iPS cells 154
Figure 4.4 Expression of pluripotency markers in CHI-iPS cells 155-156
Figure 4.5 mRNA transcript profiles of beta cell-specific marker genes in CHI-iPS cells at different stages of 5-stage differentiation protocol 157
Figure 4.6 Gene expression changes of beta cell-specific marker genes in CHI-iPS cells at different stages of 5-stage differentiation protocol 159
Figure 4.7 Expression of beta cell-specific marker genes at the protein level in differentiated CHI-iPS cells after stage-4 and stage-5 (5-stage protocol) 160
Figure 4.8 Gene expression changes of beta cell-specific marker genes in CHI-iPS cells at different stages of 7-stage differentiation protocol 162
Figure 4.9 Schematic representation of guide RNAs, ssODN and primers designed for *ABCC8* gene modification in CHI-iPS cells 164
Figure 4.10 Relative green fluorescence emitted by CHI-iPS cells after transfection with plasmid encoding GFP using different transfection methods 165
Figure 4.11 Transfection of CHI-iPS cells with CRISPR guide RNA and ssODN, and validation of transfection 167
Figure 4.12 FACS data of GFP-expressing edited CHI-iPS cells 168
Figure 4.13 Single cell clonal propagation of edited CHI-iPS cells 168
Figure 4.14 Morphological features of clonal cells generated from CRISPR-edited CHI-iPS cells 169-170
Figure 4.15 Genetic screening and restriction enzyme profiles of clonal cells generated from edited CHI-iPS cells 170
Figure 4.16 Schematic representation of the genomic relation of clonal cells generated from edited CHI-iPS cells 172
Figure 4.17 Analysing insulin expression in clonal cells generated from edited CHI-iPS cells 173
Figure 4.18 Schematic representation of gene map of human *ABCC8* and *KCNJ11* genes 176

Figure 4.19	Schematic representation of the location of guide RNAs and primers designed for *ABCC8* and *KCNJ11* gene knock out experiments in EnodCβH1 cells	177-178
Figure 4.20	Relative transfection efficiencies of explored transfection kits used for EndoCβH1 cells	182
Figure 4.21	Transfection efficiencies of guide RNAs used to knock out *ABCC8* and *KCNJ11* genes in EndoCβH1 cells	184
Figure 4.22	Successfully transfected EndoCβH1 cells expressing GFP	186
Figure 4.23	Genetic screening of transfected EndoCβH1 cell population for *ABCC8* mutation	187
Figure 4.24	Genetic screening of *ABCC8* gene knocked out CHI-iPS cell population	188

Chapter 5

Figure 5.1	Schematic representation of two major types of arrays used in gene expression microarray	200
Figure 5.2	Quality control analysis of total RNA isolated from CHI tissues	207
Figure 5.3	M-A plot representing the normalisation state of microarray data	208
Figure 5.4	Intensity scatter plot showing the relative distribution of gene expression intensities of individual genes in control and disease conditions	209
Figure 5.5	Histogram plots showing the frequency of genes showing differential gene expression in microarray analysis	210
Figure 5.6	Pattern of gene expressions in three individual complete samples data in comparison with mean data	212-213
Figure 5.7	Differential expression in CHI tissues of known CHI genes and genes for hormones and receptors associated with blood glucose regulation	215-216
Figure 5.8	Differential expression in CHI tissues of genes associated with pancreas organogenesis and mature beta-cell generation	216
Figure 5.9	Differential expression in CHI tissues of genes previously predicted potentially associated with CHI and genes regulating insulin secretion	217
Figure 5.10	Differential gene expression pattern of identified potential CHI associated genes	218
Figure 5.11	Volcano plot to visualise statistically significant changes in gene expression	221
Figure 5.12	Classification of the differentially expressed genes based on the molecular functions	224
Figure 5.13	Classification of the differentially expressed genes based on the biological process	226-227
Figure 5.14	Breakdown of the major biological process category, cellular process, into sub-biological processes	227
Figure 5.15	Classification of the differentially expressed genes based on the cellular components associated with them	228-229
Figure 5.16	Significant canonical Pathways identified to be associated with differentially expressed genes in CHI conditions	233
Figure 5.17	Cardiac hypertrophy signalling pathway	236
Figure 5.18	CREB signalling in neurons	238

Figure 5.19 Schematic regulator effect network showing upstream regulators potentially associated with CHI to regulate the immune response of cells 243
Figure 5.20 Schematic regulator effect network showing upstream regulators potentially associated with CHI to regulate glucose sensitivity as well as neuron development 244
Figure 5.21 Visualisation of functional network related to nervous system development as well as molecular transport predicted by IPA analytical tool to be altered in CHI 247
Figure 5.22 Visualisation of functional network related to endocrine system development as well as cellular development predicted by IPA analytical tool to be altered in CHI 248
Figure 5.23 Integrated protein-protein interaction network generated based on interaction partners of top 50 differentially expressed genes being studied 252
Figure 5.24 Visualisation of filtered integrated protein-protein interaction network with at least 10 interaction partners 253

Chapter 6

Figure 6.1 Schematic illustration of the mode of action of siRNA-based gene silencing 277
Figure 6.2 Western blot experiment showing the time course of siRNA mediated knock-down of *KCNJ11* gene in EndoCβH1 cells 279
Figure 6.3 Western blot experiment showing the level of siRNA mediated knock down of *KCNJ11* gene in EndoCβH1 cells 280
Figure 6.4 Relative gene expression changes of *KCNJ11*, *ABCC8* and *INS* in knocked down EndoCβH1 cell population 281
Figure 6.5 Quantitative assays for glucose-stimulated insulin secretion in KCNJ11KD cells 282
Figure 6.6 Quantitative assay for glucose-stimulated insulin secretion in KCNJ11KD cells treated with tolbutamide 283
Figure 6.7 Quantitative assay for glucose-stimulated insulin secretion in KCNJ11KD cells treated with diazoxide 285
Figure 6.8 Quantitative assay for glucose-stimulated insulin secretion in KCNJ11KD cells treated with nifedipine 286

List of tables

Page no.

Chapter 1

Table 1.1	List of major CHI-associated genes and their general annotations	27

Chapter 2

Table 2.1	Typical RT-PCR reaction composition	52
Table 2.2	Typical SYBR Green-based qPCR reaction composition	56
Table 2.3	List of designed primers used in SYBR Green-based qPCR	56
Table 2.4	Typical TaqMan probe-based qPCR reaction composition	57
Table 2.5	Details of primary and secondary antibodies used in immuno-fluorescence assays	59
Table 2.6	Details of primary antibodies used in western blot assay	62
Table 2.7	Composition of KRH buffer	67
Table 2.8	Composition of cell lysis solution	68
Table 2.9	List of gRNAs and ssODNs used in this study	75
Table 2.10	List of transfection reaction conditions explored in this study (for 24-well plate)	81
Table 2.11	List of PCR primers used in transfection validation studies	82

Chapter 4

Table 4.1	Utilised alternative methods of single cell clonal propagation	175
Table 4.2	Attempted methods of EndoCβH1 single cell clonal propagation	180
Table 4.3	Reaction combinations for successful EndoCβH1 cell transfection (24-well plate)	181

Chapter 5

Table 5.1	Tissues used for genome-wide gene expression analysis	206
Table 5.2	List of potential CHI associated genes identified from basic analysis of experimental microarray data	218
Table 5.3	List of biological processes in which identified potential CHI associated genes participate	219
Table 5.4	List of statistically significant biological processes identified by DAVID knowledgebase altered in CHI conditions	222-223
Table 5.5	Summary of the IPA analysis of experimental microarray data	231
Table 5.6	Differentially expressed genes in the experimental microarray datasets found to be associated with the cardiac hypertrophy signalling pathway	237
Table 5.7	Differentially expressed genes in the experimental microarray datasets found to be associated with the CREB signalling pathway in neurons	239
Table 5.8	List of predicted of upstream regulators activated or inhibited	240-241

Table 5.9	List of target molecules and functions predicted to be regulated by the upstream regulators	241-242
Table 5.10	List of top functions networks predicted by IPA from experimental gene expression datasets	245-246
Table 5.11	List of top differentially expressed genes included for network biology analysis	249-250
Table 5.12	List of top differentially expressed genes not included for network biology analysis	250-251
Table 5.13	Analysed properties of the integrated PPI network generated from top 50 differentially expressed genes in dataset being used	254-255
Table 5.14	List of predicted genes by network biology potentially associated with CHI	256
Table 5.15	List of biological functions linked with genes predicted by network biology (generated by DAVID pathway database)	257

Abbreviations

$^{\circ}C$	Degree celsius
µg	Microgram
µl	Microlitre
µM	Micromolar
18-fluoro DOPA	Fluorine-18 L-3,4-dihydroxyphenylalanine
ADP	Adenosine diphosphate
ANOVA	One-way analysis of variance
AS	Adult stem
ATP	Adenosine triphosphate
BLAST	Basic Local Alignment Search Tool
bps	Base pairs
BrdU	5-Bromo-2-deoxyuridine
BSA	Bovine Serum Albumin
Ca^{2+}	Calcium ion
$CaCl_2$	Calcium chloride
cAMP	Cyclic adenosine monophosphate
Cas	CRISPR-associated
Cat. no.	Catalogue number
cDNA	complementary DNA
CHI	Congenital hyperinsulinism of infancy
CO_2	Carbon dioxide
CRISPR	Clustered Regularly Interspaced Short Palindromic Repeats
crRNA	CRISPR RNA
C_T	Threshold cycle
DAPI	4',6-Diamidino-2-Phenylindole
DAVID	Database for Annotation, Visualization and Integrated Discovery
Di-CHI	Diffuse form of CHI
DMEM	Dulbecco Modified Eagle Medium
DMSO	Dimethyl sulfoxide
DNA	Deoxyribonucleic acid
DNase	Deoxyribonuclease
dNTP	Deoxynucleotide triphosphate
DPBS	Dulbecco's phosphate buffered saline
DSB	DNA double-strand break
dsDNA	Double-stranded DNA
DTT	Dithiothreitol
ECM	Extracellular matrix
EDTA	Ethylene diamine tetra acetic acid
EGTA	ethylene glycol tetra acetic acid
ELISA	Enzyme-linked immunosorbent assay
ES	Embryonic stem

FACS	Fluorescence-activated cell sorting
FBS	Fetal Bovine Serum
FDR	False discovery rate
FGF	Fibroblast growth factor
Fo-CHI	Focal form of CHI
gDNA	Genomic DNA
GFP	Green fluorescent protein
GO	Gene Ontology
GOI	Gene of interest
gRNA	Guide RNA
GSIS	Glucose-stimulated insulin secretion
GTP	Guanosine triphosphate
H_20	Water
HCl	Hydrochloric acid
HDR	Homology-directed repair
HEPES	4-(2-hydroxyethyl)-1-piperazineethanesulfonic acid
hgDNA	Human genomic DNA
HRP	Horseradish peroxidase
Indel	Insertion-deletion
IPA	Ingenuity pathway analysis
iPS	Induced pluripotent stem
IQR	Inter-quartile range
ISG	Insulin secretagogue
ISG_{mix}	Mixture of ISGs
ITS-X	Insulin-transferrin-selenium-ethanolamine
K_{ATP}	ATP-sensitive potassium Channel
KCl	Potassium chloride
$KCNJ11^{KD}$	*KCNJ11* knocked down
KEGG	Kyoto Encyclopedia of Genes and Genomes
KH_2PO_4	Monopotassium phosphate
KRH	Krebs Ringer HEPES
LB	Luria-Bertani
lncRNA	Long non-coding RNA
Mg^{2+}	Magnesium ion
$MgCl_2$	Magnesium chloride
$MgSO_4$	Magnesium sulfate
miRNA	MicroRNA
ml	Millilitre
mM	Millimolar
mRNA	Messenger RNA
mV	Millivolt
NaCl	Sodium chloride
$NaHCO_3$	Sodium bicarbonate
ng	Nanogram
NGS	Normal goat serum

NHEJ	Non-homologous end joining
OD	Optical density
PAM	Protospacer Adjacent Motif
PCR	Polymerase chain reaction
PET	Positron emission tomography
PIP	Protein-protein interaction partner
PPI	Protein-protein interaction
PVDF	Polyvinylidene Fluoride
qPCR	Quantitative PCR
RIPA	Radio Immuno Precipitation Assay
RISC	RNA-induced silencing complex
RNA	Ribonucleic acid
RNAi	RNA interference
RNase	Ribonuclease
ROCKi	ROCK inhibitor
RPM	Rotation per minute
RPMI	Roswell park memorial institute
rRNA	Ribosomal RNA
RT	Reverse transcription
RTase	Reverse transcriptase
RT-PCR	Reverse-transcription PCR
SDS	Sodium dodecyl sulphate
SEM	Standard error of the mean
siRNA	Short interfering RNA
SMC4	Small molecule cocktail of 4 inhibitors
snoRNA	Small nucleolar RNA
SNP	Single nucleotide polymorphism
ssDNA	Single-stranded DNA
ssODN	Single-stranded oligonucleotide
SUR	Sulfonylurea receptor
T7EI	T7 endonuclease I
TBS	Tris Buffered Saline
TBS-T	TBS with Tween20
TF	Transcription factor
T_m	Melting (annealing) temperature
Tol^{high}	Higher concentration of tolbutamide
tracrRNA	Trans-activating crRNA
UniHi	United Human Interactome

Abstract

Towards an *in vitro* model of congenital hyperinsulinism of infancy

Congenital hyperinsulinism of infancy (CHI), one of the common forms of profound and persistent hypoglycemia in early childhood or infancy, is characterised by uncontrolled insulin secretion and beta cell hyperproliferation. Mutations in a number of genes have been identified to be associated with CHI; the most common being inactivating mutations in the *ABCC8* and *KCNJ11* genes encoding the SUR1 and Kir6.2 subunits of K_{ATP} channel in beta cells. However, for most of the cases, the aetiology of the disease is yet to be understood. Because of the limited availability of CHI tissue samples to be analysed, this study aimed to generate a model cell line that could mimic CHI-like behaviour in terms of insulin secretion and cell proliferation. Reports suggest that insulin could act as cell proliferation inducer, so we hypothesised that increased insulin secretion might promote pancreatic beta cells to acquire CHI-like characteristics. Insulin secretagogues (ISGs)- KCl (40 mM), tolbutamide (200 or 500 µM), leucine (10 mM), arginine (10 mM) and glibenclamide (10 µM) were tested for their abilities to promote cell proliferation or insulin secretion. No significant changes in insulin secretion or cell proliferation were observed in cells (MIN6 or EndoCβH1) acutely (48 hours) or chronically (up to 16 weeks) treated with ISGs. Also, there were no changes in expression of some of the key ion (Na^+, K^+ and Ca^{2+}) channels associated with the insulin secretion pathway. Thus, ISGs were not an appropriate option to transform beta cells into a CHI-like model system. As an alternative approach, K_{ATP} channel genes were edited (introducing single nucleotide polymorphism or deletion of a fragment) with CRISPR-Cas9. EndoCβH1, a human model pancreatic beta cell line, and CHI-iPS, an iPS cell line generated by our research group, were explored in this study. As part of this work, it was shown that insulin-producing beta cells could be generated from this CHI-iPS cell line through an already published controlled differentiation process. Our results showed successful cell transfection with gene editing tools followed by target gene editing in both CHI-iPS and EndoCβH1 cells. However, none of the clonal cell lines generated from edited single CHI-iPS cells could retain their stem cell properties after a couple of passages. For EndoCβH1 cell line, it was not possible to grow and expand a single cell. Thus, attempts were made to generate a population of cells with a greater proportion of gene-edited cells. However, only ~20% of cells were observed to have gene edited and this low proportion of edited cells made the cell population unfit for further analysis. As part of this study, genome-wide differential gene expression was studied on CHI pancreas tissue samples with a view to identify novel candidate genes related to this disease. Differential gene expression analysis identified 39 potential candidate genes related to insulin secretion pathways, pancreas developmental pathway and glucose homeostasis *etc*. A network biology approach was explored to identify candidate genes based on already published protein-protein interaction data. On this basis, 12 more potential CHI candidate genes were predicted which are associated with cell signalling, exocytosis, cell proliferation, immune response etc. To validate these new findings in future, approach was taken to generate transient CHI model cells by knocking down the expression of K_{ATP} channels using gene-specific short interfering RNA. Our results suggested ~55% of channel protein knockdown in the cell population. This knocked down cell population showed increased basal insulin secretion and other experiments with K_{ATP} channel opener and inhibitor also suggested this increased secretion was the result of loss-of-function of K_{ATP} channels. Due to time limitations, this cell population could not be used to validate the association of CHI candidate genes predicted by microarray analysis. However, our preliminary data suggest that this knocked down cell line can be considered as a potential CHI-like cell line for further studies.

Declaration

No portion of the work referred to in the thesis has been submitted in support of an application for another degree or qualification of this or any other university or other institute of learning.

Copyright statement

Acknowledgement

I would like to thank my PhD thesis supervisor Professor Mark J Dunne for his continuous guidance and encouragement. His invaluable support helps me to explore different things in the lab.

I would also like to thank my thesis co-supervisor Dr Jean-marc Schwartz for his critical suggestions and guidance.

I am grateful to Dr Karen Cosgrove for her critical suggestions on my work.

My special gratitude to the Commonwealth Scholarship Commission in the UK for funding my research project at the University of Manchester.

My heartiest thanks to Sophie Kellaway, Amna Gsour, Helga Palma, Aleksandra Toloczko, Saba Khan, Karolina Mosinska, Bing Han, Walaa Mal, Osama Basalem and Dr Alexander Ryan for making a happy and helpful working environment. Special thanks to Karolina Mosinska and Saba Khan for their continuous generous supports throughout my study period. I would like to express my gratitude to Dr Alexander Ryan for his critical review on my work.

I would like to thank Dr Antony Adamson (Transgenic unit), Dr Syed Murtuza Baker (Bioinformatics core facility) and Mr Roger Meadows (Bioimaging facility) for helping me in various ways to carry out my study. My special thanks to Ms Samantha Franks and Ms Joy Stewart (Postgraduate office) for their generous support.

In addition, I would like to thanks my friends at the UK for their encouragements and for their support during my frustration times.

Above all, my heartiest gratitude to my parents, brothers, sister and other family members for their sacrifices and endless support.

S M Mahbubur Rashid

Chapter 1

Introduction

1.1 Congenital hyperinsulinism of infancy

Congenital hyperinsulinism of infancy (CHI) is a lethal metabolic disorder of neonates and infants. It is usually characterised by severe, persistent hypoglycemia due to uncontrolled insulin secretion from pancreatic islet beta cells (Mcquarrie, 1954; Stanley and Baker, 1976; Thomas Jr *et al*, 1977; Dunne *et al*, 2004; Senniappan *et al*, 2012; Proverbio *et al*, 2013; Stevens *et al*, 2013; Arya *et al*, 2014; Stanley, 2016). This syndrome is one of the most common reasons for recurrent hypoglycemia of early aged individuals (Stanley, 1997; Meissner *et al*, 2003; Steinkrauss *et al*, 2005; Stevens *et al*, 2013). CHI has an estimated incidence of 1/30,000 to 1/50,000 children in random-mating populations of European descent, but the frequency can be as high as 1/2500 where high rates of consanguinity prevails (Glaser *et al*, 2000; Rahier *et al*, 2011; Arnoux *et al*, 2011; Senniappan *et al*, 2012; Rahman *et al*, 2015a; Stanley, 2016).

1.2 Biochemical features of CHI

Biochemical analysis of CHI patients reveals unregulated and uncontrolled secretion of insulin from pancreatic islet beta cells. The condition is further abetted by the inability of patients to generate sufficient levels of hormones (such as glucagon and cortisol) in serum that counter-act the action of insulin and maintain glucose homeostasis (Aynsley-Green *et al*, 2000; Hussain *et al*, 2003; Hussain *et al*, 2005a; Nessa *et al*, 2016). The uncontrolled secretion of insulin signals tissues (such as skeletal muscle, liver and adipose) to increase glucose uptake, leading to decreased plasma glucose and potentially for dangerous hypoglycaemia (Hussain *et al*, 2007; Arnoux *et al*, 2011; Nessa *et al*, 2016). This is further worsened by the simultaneous inhibition of glycogenolysis (glycogen breakdown for glucose production), gluconeogenesis (glucose manufacture from non-carbohydrate sources), lipolysis (catabolism of triacylglycerol into fatty acids, an energy substrate) and ketogenesis (production of ketone bodies, another energy substrates) mediated by the

increased levels of insulin (Hussain *et al*, 2007; Arnoux *et al*, 2011; Mohamed *et al*, 2012; Senniappan *et al*, 2012; Nessa *et al*, 2016). It is known that plasma glucose concentration needs to be above a threshold level to supply the sufficient amount of fuel to brain cells (Koh *et al*, 1988; Cryer 2007; Dunn-Meynell *et al*, 2009; Sprague and Arbelaez, 2011). Due to the insulin-induced hypoglycaemia, the brain becomes deprived of its essential primary and secondary energy sources from blood (Hussain *et al*, 2007). Therefore, failure of rapid recognition of this phenomenon may invite persistent neurological complications including brain damage, learning disability, seizures *etc*. (Aynsley-Green *et al*, 2000; Menni *et al*, 2001; Dunne *et al*, 2004; Steinkrauss *et al*, 2005; Avatapalle *et al*, 2013; Stevens *et al*, 2013; Arya *et al*, 2014). If unmanaged, CHI is lethal (Aynsley-Green *et al*, 2000; Dunne *et al*, 2004; Proverbio *et al*, 2013). However, clinically this condition shows heterogeneity as some patients may remain completely asymptomatic, some are mildly responsive to medical treatment while the others are unresponsive medically and might require pancreatectomy (Sempoux *et al*, 1998b; de Lonlay-Debeney *et al*, 1999; Hardy *et al*, 2007b; Arnoux *et al*, 2011; Banerjee *et al*, 2011; Senniappan *et al*, 2015).

1.3 Known genetic basis of CHI

A number of studies have been carried out to understand the aetiopathogenic process behind this disorder. Through genetic analysis, it was found that there are several genes that play key roles in the development of this syndrome. It was observed that the most common forms of CHI are because of the recessive inactivating mutations in the *ABCC8* and *KCNJ11* genes which encode the two sub-units (the accessory subunit, SUR1 and the pore-forming subunit, Kir6.2, respectively) of ATP-sensitive potassium (K_{ATP}) channels found on the membrane of pancreatic beta cells (Thomas *et al*, 1995; Thomas *et al*, 1996; Dunne *et al*, 1997; Huopio *et al*, 2000; Marthinet *et al*, 2005; Kapoor *et al*, 2013; Sang *et al*, 2014; Rahman *et al*, 2015a; Nessa *et al*, 2016). The sulfonylurea receptor (SUR1), a membrane protein, is encoded by the *ABCC8* (ATP-binding cassette transporter sub-family C member 8) gene. The *KCNJ11* (potassium channel inwardly rectifying subfamily J member 11) gene encodes the inward-rectifying potassium channel (Kir6.2). These two subunit genes of K_{ATP} channel are found to be clustered on human chromosome 11 at position 11p15.1 (Inagaki *et al*, 1995; Aguilar-Bryan and Bryan, 1999; Dunne *et al*, 2004; James *et al*, 2009; Adi *et al*, 2015). About 150 and 24 mutations have

been reported to be identified in *ABCC8* and *KCNJ11* genes, respectively, in CHI patients (Flanagan *et al*, 2009; Henquin *et al*, 2011; Rahman *et al*, 2015a). In the *ABCC8* gene, mutations are found in the promoter region, in exons 1-16, 21-30 and 32-39. No mutation was reported in *ABCC8* exons 17-20 and exon 31 in CHI patients. Some of these mutations were reported to cause the failure of proper assembly of channel components and hence, defective trafficking of the channels from the endoplasmic reticulum of the cell (Taschenberger et al, 2002; Flanagan *et al*, 2009; Nessa *et al*, 2016). These defective channel proteins then undergo protein degradation in lysosomes (Nessa *et al*, 2016). As a result, the level of the channel protein at the surface of the membrane is reduced, and thus, channel activity on the cell membrane is decreased (Yan *et al*, 2007; Flanagan *et al*, 2009; Nessa *et al*, 2016). This event hinders K^+ efflux from the cell through K_{ATP} channels that causes membrane depolarisation which ultimately leads to Ca^{+2} influx and insulin release from the cell (Dunne *et al*, 2004; James *et al*, 2009; Arya *et al*, 2014) (more details in section 1.4). Other mutations can impair the ability of the channel to be stimulated by metabolic state, and these mutations are normally located in the nucleotide binding domain of SUR1 (Huopio *et al*, 2002; Thornton *et al*, 2003; Flanagan *et al*, 2009). For *KCNJ11*, the mutations are distributed throughout the exon 1 of the gene and can reduce or abolish the channel activity (Nestorowicz *et al*, 1997; Marthinet *et al*, 2005; Flanagan *et al*, 2009). For both *ABCC8* and *KCNJ11*, types of mutation include deletion, missense, nonsense and frameshift mutations. So, the loss-of-function anomalies in these genes cause the channel to malfunction, and as mentioned above, K^+ efflux from the cell becomes impeded. This event leads to membrane depolarisation that promotes Ca^{+2}-mediated insulin release (Dunne *et al*, 2004; James *et al*, 2009; Arya *et al*, 2014) (more details in section 1.4).

Some other studies have also shown K_{ATP} channel-independent CHI. Recessive mutations in the *HADH* gene was reported to be associated with CHI (Clayton *et al*, 2001; Molven *et al*, 2004; Hussain *et al*, 2005b; Kapoor *et al*, 2009b; Senniappan *et al*, 2015). Dominant mutations in *GLUD1* (Stanley *et al*, 1998; Yorifuji *et al*, 1999; Kapoor *et al*, 2009a; Sang *et al*, 2014), *SLC16A1* (Otonkoski *et al*, 2007; Tosur and Jeha, 2017); *UCP2* (González-Barroso *et al*, 2008; Snider *et al*, 2013; Ferrara *et al*, 2017), *HNF4A* (Pearson *et al*, 2007; Kapoor *et al*, 2008; Flanagan *et al*, 2010; Stanescu *et al*, 2012), *GCK* (Glaser *et al*, 1998; Christesen *et al*, 2002; Cuesta-Muñoz *et al*, 2004; Dullaart *et al*, 2004), and *HNF1A* (Stanescu *et al*, 2012; Rozenkova *et al*, 2015) have also been described as being related to

the development of CHI. Details of these genes and their functions are described in the following section (section 1.4). In addition, using whole genomes single nucleotide polymorphism (SNP) genotyping and exome sequencing, it was possible to elucidate a number of genes (*CACNA1A*, *KCNH6*, *KCNJ10*, *NOTCH2*, *RYR3*, *SCN8A*, *TRPV3*, *TRPC5*, *ACACB*, *CAMK2D*, *CDKAL1*, *GNAS*, *NOS2*, *PDE4C*, *PIK3R3*, *PC*, *SLC24A6*, *CSMD1*, *SLC37A3*, *SULF1*, *TLL1*) which could also be associated with CHI (Proverbio *et al*, 2013). However, a significant proportion of CHI patients did not possess any recognisable genetic cause (Banerjee *et al*, 2011; Kapoor *et al*, 2013; Snider *et al*, 2013; Sang *et al*, 2014; Yorifuji, 2014; Senniappan *et al*, 2015).

Table 1.1: **List of major CHI-associated genes and their general annotations**

Gene	*locus*	*Protein*	*Biological functions related to pancreatic activity*
ABCC8	11p15.1	Sulfonylurea receptor 1 (SUR1)	Nucleotide-sensing subunit of K_{ATP} channels
KCNJ11	11p15.1	Inward rectifying potassium channel (Kir6.2)	Acts as an integral membrane protein and inward-rectifier type potassium channel
GLUD1	10q23.3	Glutamate dehydrogenase (GDH)	Catalyses the oxidative deamination of glutamate which plays an important role in regulating insulin secretion.
GCK	7p15.3-p15.1	Glucokinase	Phosphorylates glucose to produce glucose-6-phosphate, the first step in most glucose metabolism pathways which is essential for glucose-stimulated insulin secretion.
HADH	4q22–q26	L-3-hydroxyacyl-Coenzyme A dehydrogenase	Functions in the mitochondrial matrix to catalyse the oxidation of 3-hydroxyacyl-CoAs as part of the beta-oxidation pathway.
SLC16A1	1p12	Monocarboxylate transporter 1 (MCT1)	A proton-linked monocarboxylate transporter that catalyses the movement of many monocarboxylates, across the plasma membrane.
HNF4A	20q13.12	Hepatocyte nuclear factor 4 alpha	Controls the expression of several genes related to insulin secretion
UCP2	11q13	Uncoupling protein 2	Metabolic transporter of proton, phosphate, oxaloacetate, malate and aspartate in the mitochondrial membrane, regulates ATP synthesis
HNF1A	12q24.2	Hepatocyte nuclear factor 1-alpha	A transcription factor required for the expression of several genes.

~Biological functions are adapted from Gene database of National centre for biotechnology information (available at http://www.ncbi.nlm.nih.gov/gene/)

1.4 Known mechanisms of CHI

To control, mitigate or eradicate a disorder, it requires a great understanding of the mechanism by which it displays its effects. A number of studies have been carried out to understand the molecular mechanisms or pathways associated with CHI. However, very little information has been obtained, and it is not sufficient to explain all the cases of CHI (Stevens *et al*, 2014). It is evident that mutations in the pancreatic K_{ATP} channels are the most notable factor for the progression of this disease. The importance and involvement of these channels in beta cell activity were first described by Ashcroft *et al*. (1984). The K_{ATP} channel is a hetero-octameric complex that comprises of four Kir6.2 pore-forming subunits and four SUR1 accessory subunits (Figure 1.1) (Aguilar-Brayan *et al*, 1995; Inagaki *et al*, 1995; Clement IV *et al*, 1997; Mikhailov *et al*, 2005; Craig *et al*, 2008; James *et al*, 2009). Each SUR1 subunit has two cytosolic nucleotide-binding domains (NBDs). Occupancy of these NBDs with nucleotides stimulates the channel activity (Nichols *et al*, 1996; Gribble *et al*, 1997b; Shyng *et al*, 1997b; Zingman *et al*, 2001; Craig *et al*, 2008). In resting condition, when cytosolic ATP concentration is low, the channel becomes active and open as SUR1 NBDs are occupied with Mg^{2+}-ADP (Inagaki *et al*, 1995; Craig *et al*, 2008; James *et al*, 2009). Both Mg^{2+}-ADP and Mg^{2+}-ATP can bind to NBDs, but Mg^{2+}-ATP needs to be hydrolysed to become Mg^{2+}-ADP for activating the channel (Gribble *et al*, 1997b; Zingman *et al*, 2001; Craig *et al*, 2008). After glucose metabolism, when cytosolic ATP/ADP concentration ratio increases, the possibility of Mg^{2+}-ADP to bind with SUR1 decreases (Nichols *et al*, 1996; Craig *et al*, 2008). SUR1, not occupied with Mg^{2+}-ADP, then induces Kir6.2 to bind with ATP. Binding of ATP to this pore-forming Kir6.2 subunit results in the closure of the channel (Shyng *et al*, 1997a; Enkvetchakul *et al*, 2001; Craig *et al*, 2008).

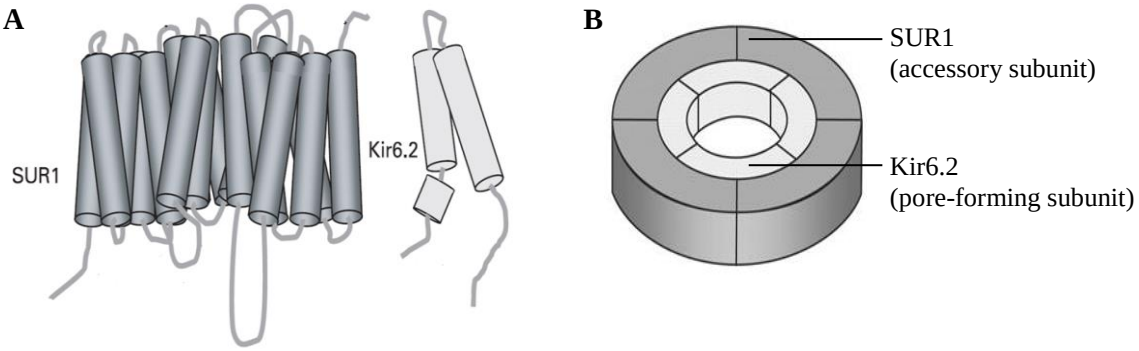

Figure 1.1: **Graphical representation of the components of the pancreatic beta cell K_{ATP} channel**. (A) The K_{ATP} channel is a two-subunit protein. One subunit, SUR1, consists of 17 transmembrane domains and the other subunit, Kir6.2, has two transmembrane segments. (B) Schematic representation of the multimeric arrangement of the K_{ATP} channel. The image is adapted from James *et al*. (2009).

This K_{ATP} channel controls the excretion of K^+ ions across cell membranes by sensing the membrane potential in the cell (Ashcroft, 1988). It is well known that in glycolysis, glucose, the first molecule in energy production cascade reactions, becomes phosphorylated by glucokinase and through further cascade of reactions generates ATP which results in an increase in the intracellular ATP/ADP ratio (Ashcroft *et al*, 1973, Nelson and Cox, 2008, p. 532). This increased ATP/ADP ratio inhibits K_{ATP} channel activity, as the binding of ATP leads to closure of the K_{ATP} channels. By preventing potassium efflux, membrane depolarisation occurs, with the membrane potential changing from approximately -65mV (basal level) to around 40mV (Cook and Hales, 1984; Dunne *et al*, 1994; Dunne *et al*, 2004; Craig *et al*, 2008). This membrane depolarisation subsequently opens L-type voltage-dependent calcium channels and it mediates an influx of Ca^{2+} that triggers the exocytosis of insulin from secretory granules of the beta cells (Dunne and Petersen, 1986; Hoenig and Sharp, 1986; Dunne *et al*, 1994; Kane *et al*, 1996; Nichols *et al*, 1996; Dunne *et al*, 2004).

Abnormalities in the subunit genes result in malfunction of K_{ATP} channels, and the beta cell plasma membranes become depolarised leading to the opening of L-type voltage-dependent calcium channels. Ultimately, Ca^{2+} enters into the cells and causes the uncontrolled insulin secretion (Inagaki *et al*, 1995; Nichols *et al*, 1996; Dunne *et al*, 1997;

Shyng *et al*, 1998; Eichmann *et al*, 1999) (Figure 1.2). The recessive inactivating mutations in *ABCC8* and *KCNJ11* results with defects in K_{ATP} channel biogenesis, defective channel trafficking from the endoplasmic reticulum and Golgi apparatus to the plasma membrane, and also alters the capability of the channels for cooperative binding with nucleotides (Dunne *et al*, 1997; Tanizawa *et al*, 2000; Cartier *et al*, 2001; Marthinet *et al*, 2005; Pinney *et al*, 2008). These mutations usually cause severe CHI which makes most of the patients unresponsive to medical treatment with diazoxide, a known K_{ATP} channel activator (Nichols *et al*, 1996; Flanagan *et al*, 2011; Ocal *et al*, 2011). Some of the mutations are found to act as dominant inactivating mutations and also lead to CHI (Huopio *et al*, 2000; Thornton *et al*, 2003; Pinney *et al*, 2008). The severity of patients with these dominant inactivating mutations appears to be much milder compared to that of those recessive inactivating mutations and patients with dominant mutations are usually responsive to diazoxide treatment (Pinney *et al*, 2008, Ocal *et al*, 2011). However, some patients with dominant mutations were also reported recently to be unresponsive to diazoxide treatment (Flanagan *et al*, 2011; MacMullen *et al*, 2011; Nessa *et al*, 2015)

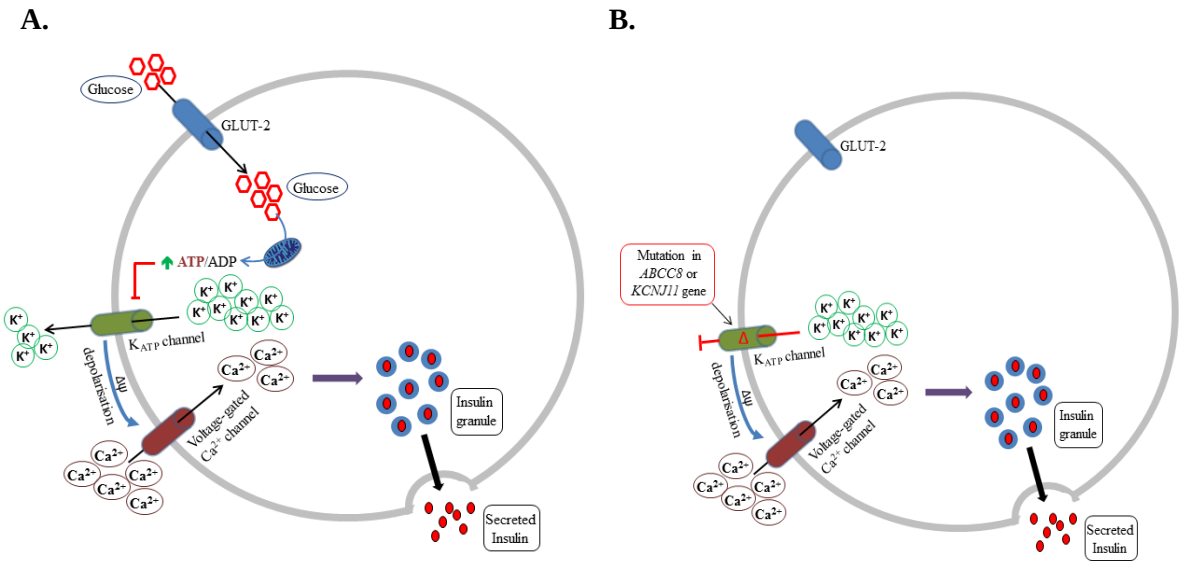

Figure 1.2: **Schematic representations of how mutations in K_{ATP} channels can cause uncontrolled insulin release in pancreatic beta cells.** Image A) shows the regulated insulin release from beta cells in normal condition. In resting condition, the K_{ATP} channel is kept open maintaining a membrane potential of approximately -65mV. Glucose after entering into the cells get metabolised through a cascade of reactions, and the concentration ratio of ATP to ADP increases. This event of increased ATP to ADP ratio then causes the

closure of the K_{ATP} channel. Then the cell membrane becomes depolarised which opens the L-type voltage-dependent calcium channels, and Ca^{2+} enters the cells. This event triggers the insulin exocytosis from beta cells. However, in CHI condition (B), mutations in either subunit of the K_{ATP} channel make the channel malfunctional and hence, efflux of K^+ is inhibited resulting in membrane deplorisation, Ca^{+2} influx and insulin release. This insulin release can happen in resting condition of the cell.

Dominant activating mutations in the *GLUD1* gene encoding Glutamate dehydrogenase are reportedly the second most common cause of CHI after *ABCC8* and *KCNJ11* (James *et al*, 2009; Palladino and Stanley, 2010; Lord and Leon, 2013). This enzyme catalyses the oxidative deamination of glutamate to α-ketoglutarate which in turn, enters in the tricarboxylic acid cycle and acts to generate cellular ATP (Stanley *et al*, 1998; Tanizawa *et al*, 2002; Kapoor *et al*, 2009a). This increases the intracellular ATP/ADP ratio which triggers the closure of the K_{ATP} channels and initiates insulin release through the actions of L-type voltage-dependent calcium channels. Some mutations also cause the reduction of sensitivity of this enzyme to the allosteric inhibitor, GTP and therefore keeps the rate of glutamate oxidation higher in the presence of leucine, the positive allosteric effector of *GLUD1* (Kelly *et al*, 2001; Stanley, 2004).

The gene *GCK* encodes glucokinase, one of the members of the hexokinase enzyme family that catalyses the transformation of glucose into glucose-6-phosphate, the rate-limiting step of glycolysis. Dominant activating mutations of *GCK* mediate the continuous passage of glucose into this reaction cycle by increasing the affinity of the enzyme for glucose (Matschinsky *et al*, 1993; Glaser *et al*, 1998; Christesen *et al*, 2002; Wabitsch *et al*, 2007). This ultimately leads to the overproduction of ATP which at the end increases the insulin secretion

Loss-of-function (recessive) mutations in the *HADH* gene has been reported to be associated with CHI (Clayton *et al*, 2001; Molven *et al*, 2004; Hussain *et al*, 2005b). *HADH* encodes the mitochondrial enzyme L-3-hydroxyacyl-coenzyme A dehydrogenase that catalyses the penultimate step in the β-oxidation of fatty acids (James *et al*, 2009; Kapoor *et al*, 2009b; Heslegrave and Hussain, 2013). However, the molecular mechanisms of how mutations in this gene cause unregulated insulin secretion are yet to

be completely understood. Studies suggest the high expression of *HADH* in beta cells and a low expression of other β-oxidation enzymes (Martens *et al*, 2007; James *et al*, 2009). Downregulation or knock out analysis of *HADH* shows an elevated insulin secretion that indicates the protective actions of the enzyme against inappropriately high secretion of insulin (Hardy *et al*, 2007a; Martens *et al*, 2007; James *et al*, 2009).

The gene *SLC16A1* encodes proton-linked plasma membrane monocarboxylate transporter 1 (MCT1). Dominant activating mutations in the promoter and intragenic regions of *SLC16A1* gene are noted to be associated with CHI (Otonkoski *et al*, 2007; Tosur and Jeha, 2017). Usually, pyruvate and lactate (products of glycolysis) do not have a direct effect on insulin secretion due to the low expression of MCT1 in beta cells (Ishihara *et al*, 1999; Lord and Leon, 2013; Koren and Palladino, 2016). However, mutations in the *SLC16A1* gene cause increased expression of MCT1 that allows the extracellular pyruvate/lactate to enter beta cells, which in turn is used as a substrate for mitochondrial oxidation to increase cytosolic ATP/ADP ratio (Ishihara *et al*, 1999, Otonkoski *et al*, 2007; Koren and Palladino, 2016). Affected patients suffer from hypoglycaemia within a short time after a period of intensive anaerobic exercise (Otonkoski *et al*, 2003, Otonkoski *et al*, 2007, James *et al*, 2009; Lord and Leon, 2013).

UCP2 gene encodes uncoupling protein 2 which is a metabolic transporter in the mitochondrial membrane. This protein transports protons and phosphate from cytosol in exchange of oxaloacetate and malate (the intermediate product of the tricarboxylic acid cycle), and aspartate from mitochondria (Vozza *et al*, 2014; Ferrara *et al*, 2017). By limiting the accessibility of oxaloacetate and malate, this protein reduces mitochondrial oxidative metabolism that eventually hinders ATP synthesis (González-Barroso *et al*, 2008, Ferrara *et al*, 2017). This role of *UCP2* is supported by the studies which show that over-expression of *UCP2* in isolated rat islets reduces ATP content and inhibits insulin secretion (Chan *et al*, 1999; Chan *et al*, 2001; Chan and Harper, 2006) and knockdown of *UCP2* in rat pancreatic beta cells stimulates insulin secretion (De Souza *et al*, 2007; Affourtit and Brand, 2008). Inactivation of UCP2 protein was reported in CHI patients (Ferrara *et al*, 2017) which could explain the plausible reasons behind the observed abnormal insulin secretion. Recently, it was reported that knocking out of *UCP2* in mice can lead to fetal hyperproliferation (Broche *et al*, 2018). So, mutations in *UCP2* can

explain the hyperproliferation observed in some CHI cases earlier (Kassem *et al*, 2000; Kassem *et al*, 2010; Lovisolo *et al*, 2010).

In addition to abnormalities in enzymes and structural proteins, CHI can be manifested due to anomalies in transcription factors (TFs). One of the representative examples is the *HNF4A* gene which encodes TF belongs to the nuclear hormone receptor superfamily (Duncan *et al*, 1998). Loss-of-function *HNF4A* mutations are associated with CHI (Pearson *et al*, 2007; Kapoor *et al*, 2008; Flanagan *et al*, 2010). Currently, it is not clear enough how mutations in *HNF4A* play a role to develop hypoglycaemia. However it was found that this is one of the widely acting TFs in beta cells that regulates several key genes involves in glucose metabolism and insulin secretion such as *SLC2A2* (encodes GLUT-2), *ALDOB* (encodes aldolase B), *PKL* (encodes L-pyruvate kinase), *UCP2* and *KCNJ11* (Wang *et al*, 2000a; Odom *et al*, 2004; Gupta *et al*, 2005; Kapoor *et al*, 2010; Nessa *et al*, 2016). It was reported that HNF4A protein could regulate the expression of approximately 40% of the genes expressed in hepatocytes and pancreatic islets (Odom *et al*, 2004; Kanazawa *et al*, 2010). So *HNF4A* deficiency might result in abnormal gene expression of one or more of these target genes that cause CHI as well as maturity-onset diabetes of the young (James *et al*, 2009; Kanazawa *et al*, 2010; Stanescu *et al*, 2012).

Another transcription factor that is related to CHI is HNF1A, also a member of the nuclear hormone receptor superfamily. Similar to *HNF4A*, loss-of-function *HNF1A* mutations are associated with CHI (Stanescu *et al*, 2012; Nessa *et al*, 2016). Since *HNF1A* and *HNF4A* are a part of a regulatory loop that regulates the expression of each other (Tian and Schibler, 1991; Hatzis and Talianidis, 2001; Kanazawa *et al*, 2010; Stanescu *et al*, 2012), so, *HNF1A* could act in a similar fashion like *HNF4A* to develop hypoglycemia.

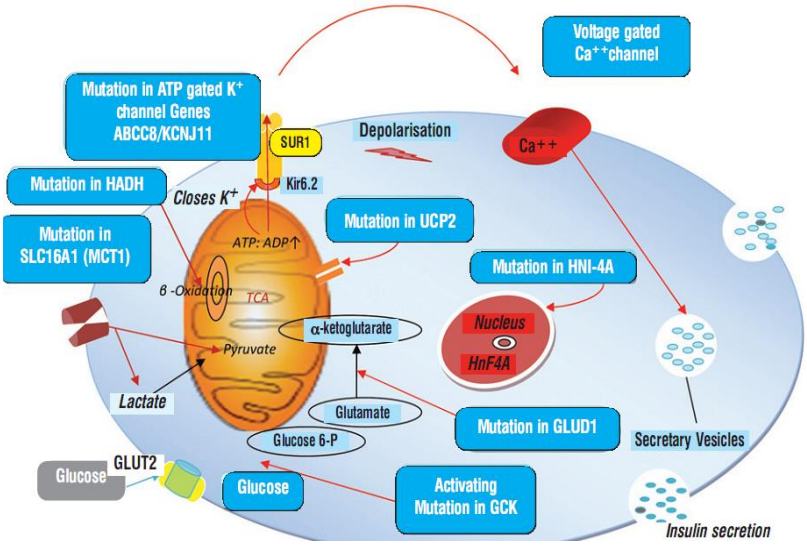

Figure 1.3: **Summary of the common known causes of CHI in the pancreatic beta cell**. ATP generation from glucose through metabolism cascades directs to the closure of K_{ATP} channels. This channel inhibition then leads to membrane depolarisation and Ca^{2+} influxes through L-type voltage-dependent calcium channels. The increased cytosolic calcium then triggers insulin secretion. Abnormalities related to this pathway leads to CHI. The image is adapted from Mohamed *et al*. (2012).

Though a lot of information related to CHI is reported in recent times, the mechanisms of the disease are not yet fully described. Also, prevention and long-term outcomes of the disorder are both incompletely resolved (Stevens *et al*, 2014). This is further complicated by the fact that along with genetic analysis, single nucleotide polymorphism (SNP) genotyping and exome sequencing provide new insights about the fact that CHI patients can carry multiple exonic mutations in different genes (mentioned in section 1.3) without having a mutation in known causative genes (Proverbio *et al*, 2013). However, due to the relatively small number of sample cases, it was not possible to associate all of these mutations with this disease. Consequently, a major proportion of the patients with CHI did not have any recognisable aetiology and mechanisms of the disease (Stevens *et al*, 2013).

1.5 Histological features of CHI

Histologically, two major forms of the disease have been observed -focal form of CHI (Fo-CHI) and diffuse form of CHI (Di-CHI) (Goossens *et al*, 1989; Fournet *et al*, 2001; Arnoux *et al*, 2011; Rahier *et al*, 2011; Mohamed *et al*, 2012; Arya *et al*, 2014). Fo-CHI is typically confined to specific areas of the pancreas where islets/beta cells are affected, while Di-CHI affects almost every beta cell of the pancreas (Hussain *et al*, 2008; Arnoux *et al*, 2011; Rahier *et al*, 2011; Mohamed *et al*, 2012) (Figure 1.4). In both of these conditions, the abnormal morphology is due to the result of the appearance of a group of oversized endocrine cells (compared to surrounding control acinar cells) with large cytoplasm and nuclei (Rahier *et al*, 1984; Sempoux *et al*, 1998b; Arnoux *et al*, 2011; Henquin *et al*, 2011; Mohamed *et al*, 2012). The presence of insulin granules is very limited in beta cells within the affected area probably due to the hypersecretion of insulin, while the beta cells outside the lesion are found with high storage of insulin (Rahier *et al*, 2011). Histological analyses also found that CHI affected beta cells showed an increased frequency of proliferation (Kassem *et al*, 2000; Lovisolo *et al*, 2010). Also, both of these forms showed a high frequency of cell apoptosis (Kassem *et al*, 2000; Kassem *et al*, 2010; Tornovsky-Babeay *et al*, 2014).

Some studies reported the focal form to be associated with mutations in *ABCC8* on the paternal allele and loss of a distal proportion of chromosome region 11p15 on the maternal allele (Figure 1.5) (de Lonlay *et al*, 1997; Verkarre *et al*,1998; Fournet *et al*, 2000; Fournet *et al*, 2001; Damaj *et al*, 2008, James *et al*, 2009). On the other hand, diffuse-CHI was mostly found to be associated with recessive inactivation of genes (most commonly *ABCC8* and *KCNJ11*) associated with this disease (Thomas *et al*, 1995; Thomas *et al*, 1996; Huopio *et al*, 2000; Hussain *et al*, 2008; James *et al*, 2009; Chandran *et al*, 2013; Nessa *et al*, 2015).

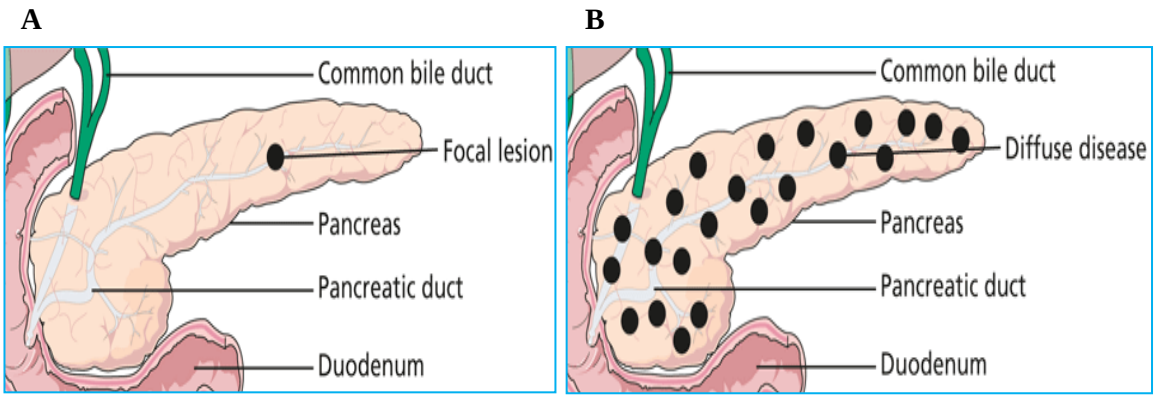

Figure 1.4: **A typical structural comparison between focal and diffuse CHI**. A particular tiny proportion of pancreas become transformed due to lesions (A). Unlike focal form, diffuse form suffers from lesions with almost all pancreatic cells (B). The image is adapted from the official web page of Great Ormond Street Hospital for Children, UK; available at http:// www.gosh.nhs.uk/medical-information/hyperinsulinism).

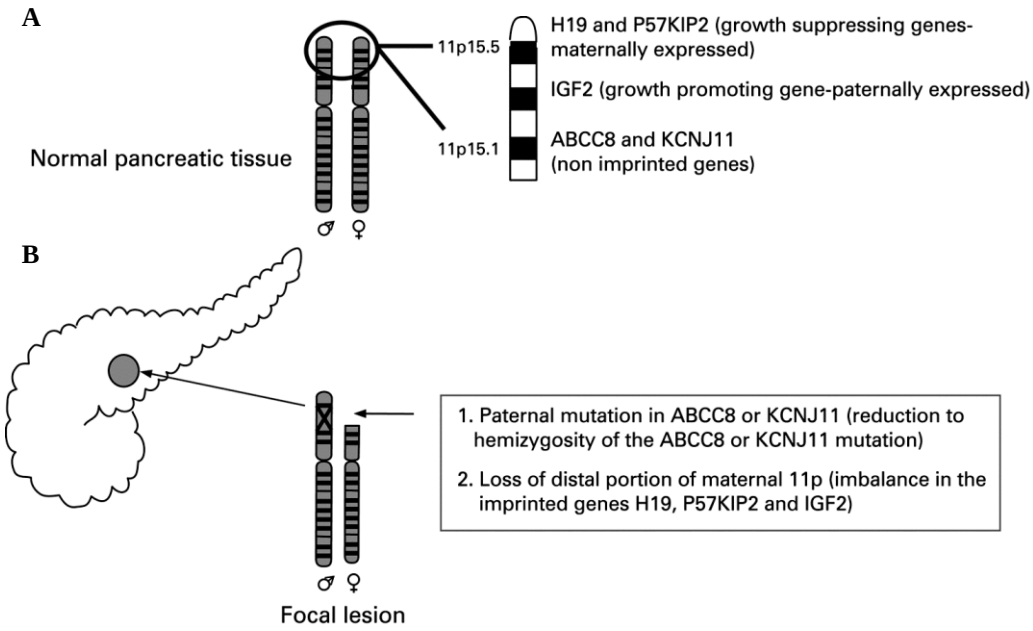

Figure 1.5: **Chromosomal aberration associated with a focal form of CHI**. Normal chromosomal loci 11p15 where growth regulatory imprinted genes like *H19* (encoding a tumour suppressor protein), *P57KIP2* (encoding a negative regulator of cell proliferation) and insulin-like growth factor 2 (IGF2) as well as CHI-associated genes *ABCC8* and *KCNJ11* are located (A). Loss of distal proportion in maternal allele (containing *H19*, *P57KIP2*, *IGF2*) of the loci causes the imbalance in these imprinted genes which induce hyperproliferation of cells and concurrent *ABCC8*/*KCNJ11* gene mutations in paternal allele following the loss of maternal alleles of the genes lead to focal CHI development (B).

Apart from these two forms, there are some cases in which the basic patterns of histological features are quite different. This atypical form of CHI is not very well defined and poorly understood. However, it was noted that it shows a diffuse type of pancreatic involvement but may be confined to some specific area of the pancreas (Delonlay *et al*, 2007). Some cases also show the pattern of chromosomal mosaicism (Hussain *et al*, 2008; Capito *et al*, 2011; Sempoux *et al*, 2011).

1.6 Management of CHI patients

1.6.1 Diagnosis of CHI

As mentioned above (section 1.2), frequent and persistent hypoglycaemia may cause abnormal neurodevelopment as well as brain damage. Therefore, rapid diagnosis of CHI and appropriate treatment is essential to avoid these neurologic abnormalities (Aynsley-Green *et al*, 2000; Giurgea *et al*, 2006; Hussain *et al*, 2007; Lord and Leon, 2013; Arya *et al*, 2014; Petraitiene *et al*, 2014). Detection of hypoglycaemia and measurement of plasma insulin and C-peptide levels are the initial criteria of diagnosis of CHI (Hussain, 2008; Mohnike *et al*, 2008; Arnoux *et al*, 2011; Arya *et al*, 2014). C-peptide or the connecting peptide is a short polypeptide that connects the A-chain with the B-chain of insulin in the proinsulin form (Bonser and Garcia-Webb, 1984). Insulin has a short half-life, but C-peptide has a longer half-life and indicates the endogenous insulin production as insulin and C-peptide are co-secreted in equimolar level (Hovorka and Jones, 1994; Arya *et al*, 2014). So, measurement of C-peptide is occasionally helpful for confirmation of the diagnosis (Arya *et al*, 2014). .It was reported that the level of plasma insulin is not always high in CHI patients (Stanley and Baker, 1976; Mohamed *et al*, 2012; Stanley, 2016). Therefore, the measurement of other markers is necessary along with insulin measurement. Since hypoglycaemia also suppresses lipolysis and ketogenesis (section 1.2), detection of low levels of ketone bodies and free fatty acids are other criteria of CHI diagnosis (Aynsley-Green *et al*, 2000; Hussain, 2008; Mohnike *et al*, 2008; Mohamed *et al*, 2012; Petraitiene *et al*, 2014). The requirement for high intravenous glucose (~10 mg/kg/min) is another feature of CHI diagnosis (Hussain, 2008; Mohnike *et al*, 2008; Mohamed *et al*, 2012; Lord and Leon, 2013; Petraitiene *et al*, 2014). In addition, glucagon injection-mediated increased glucose level is also an important feature of CHI

diagnosis (Aynsley-Green *et al*, 2000; Hussain, 2008; Mohnike *et al*, 2008; Lord and Leon, 2013; Petraitiene *et al*, 2014).

After preliminary diagnosis, further analyses should be carried out to identify the possible causes of the disease and to design appropriate management systems for patients. The recent introduction of non-invasive imaging technology that uses a positron emission tomography (PET) with Fluorine-18 L-3,4-dihydroxyphenylalanine (18-fluoro DOPA) offers an opportunity to distinguish Fo-CHI versus Di-CHI, as well as the location of focal lesions (Ribeiro *et al*, 2005; Hardy *et al*, 2007a; Hardy *et al*, 2007c; Mohnike *et al*, 2008; Arnoux *et al*, 2011). Genetic analysis of gene mutations is also important for confirming the diagnosis (Arnoux *et al*, 2011; Arya *et al*, 2014; Petraitiene *et al*, 2014).

1.6.2 Treatment options for CHI

Depending on the type of the disease, the treatments for CHI differ from simple medication to pancreatectomy (Hussain, 2008; Mohnike *et al*, 2008; Petraitiene *et al*, 2014). Diazoxide, a K_{ATP} channel opener and insulin secretion inhibitor, is the first drug of choice for the treatment of CHI (Dunne *et al*, 2004; Hussain, 2008; Arnoux *et al*, 2011; Mohamed *et al*, 2012; Petraitiene *et al*, 2014). Diazoxide binds to the K_{ATP} channel subunit, SUR1 and induces the channel to be open. Thus it prevents membrane depolarisation and consequently inhibits glucose-stimulated insulin secretion from the cells (Mariot *et al*, 1998; Schöfl *et al*, 2000; Dunne *et al*, 2004; Henquin *et al*, 2011). In the cases where patients do not respond to diazoxide, octreotide (a somatostatin analogue) is used which can activate somatostatin receptors and thus inhibit insulin release (Giurgea *et al*, 2006; Hussain, 2008; Arnoux *et al*, 2011). Although octreotide has been used for long-term management of some CHI patient, non-specificity of octreotide to bind to somatostatin receptors causes inhibition of cell growth by reducing growth hormone secretion (Harris, 1994; Hussain, 2008; Arya *et al*, 2014). Glucagon is used for emergency treatments; however, it was reported to be failed for long-term treatment of CHI (Aynsley-Green *et al*, 2000; Hussain, 2008; Arnoux *et al*, 2011; Mohamed *et al*, 2012; Senniappan *et al*, 2012). Nifedipine, a calcium channel blocker, has also been reported to be used for a few CHI cases (Bas *et al*, 1999; Eichmann *et al*, 1999; Shanbag *et al*, 2002). Nifedipine is an inhibitor of voltage-dependent L-type calcium channels, and thus it prevents the exocytosis of insulin-containing granules and consequently insulin

secretion (Giugliano *et al,* 1980; Dunne *et al,* 2004; Qureshi *et al,* 2015). However, most of the CHI patients did not respond to this drug and hence, it is not a drug of choice nowadays (Giurgea *et al*, 2006; Hussain, 2008; Petraitiene *et al*, 2014). A calcium independent pathway might be activated in these patients that could increase the rate of exocytosis and insulin secretion (Ämmälä *et al,* 1993; Komatsu *et al,* 1995; Sato *et al*, 1998; Heart *et al,* 2006). Recently, sirolimus, an inhibitor of mammalian target of rapamycin (mTOR), has been reported to be used for managing diazoxide un-responsive CHI patients (Senniappan *et al*, 2014). However, another study reported the limited efficacy of sirolimus on CHI treatment (Szymanowski *et al*, 2016).

In the cases where medication fails to improve the condition of CHI patients, surgery is recommended (Giurgea *et al*, 2006; Arnoux *et al*, 2011; Pierro and Nah, 2011; Petraitiene *et al*, 2014). For Di-CHI patients, sub-total to near-total pancreatectomy might be required, whereas Fo-CHI patients can be treated by focal lesionectomy (Fekete *et al*, 2004; Giurgea *et al*, 2006; Arnoux *et al*, 2011; Pierro and Nah, 2011; Mohamed *et al*, 2012; Arya *et al*, 2014).

1.7 Studying model systems for understanding CHI

To understand the aetiology and mechanism of CHI, numerous studies have been carried out in recent years. Many of these studies explored human tissues to understand the changes in cell morphology, expression of target proteins & metabolites, and the aftermath effect and response of drug administration. In addition, some studies were reported earlier where model organisms and cells were engineered *in vivo* and *in vitro* to reveal some answers to relevant queries related to CHI associated genes (details in the following sections 1.7.1 and 1.7.2).

1.7.1 *In vivo* models for studying genes related to CHI

There is no study reported earlier where *in vivo* model was used to study CHI directly. However, several studies were reported earlier where *in vivo* models were used to understand the role of certain genes in cells and some of these genes were identified to be associated with CHI lately. In one study, genetically modified mice, KirG132S (where a

glycine was substituted with serine at position 132 of Kir6.2 protein) were observed to secrete increased level of insulin and became hypoglycaemic because of the dominant-negative expression of the K_{ATP} channel (Oyama *et al*, 2006). Other studies were reported where K_{ATP} deficient transgenic homozygous mice were developed (Kir6.2$^{-/-}$ and SUR1 $^{-/-}$) (Miki *et al*, 1998; Seghers *et al*, 2000). Both of these mouse models showed impaired glucose-stimulated insulin secretion activity. Another study developed HADH$^{-/-}$ transgenic mice to observe the effect of *HADH* gene on glucose homeostasis (Li *et al*, 2010a). Hyperactivity of GLUD1 protein (glutamate dehydrogenase) was observed in this model system. Experiments using antibodies showed the protein-protein interaction between HADH and GLUD1. Observing the overall phenotype, it was postulated that HADH might have an inhibitory effect on GLUD1 and upon inactivation of HADH, GLUD1 become dysregulated and mediate insulin secretion in an uncontrolled fashion. Similar observations of loss-of-function mutations in the *HADH* gene and dominant activating mutations in the *GLUD1* gene were reported to be associated with insulin secretion observed in some CHI patients (Clayton *et al*, 2001; Molven *et al*, 2004; James *et al*, 2009; Lord and Leon, 2013) (more details of the function of these genes are described in section 1.4). Chan *et al*. (1999) reported that they used transgenic rats infected with an adenovirus (AdEGI-UCP-2) containing the full-length human *UCP2* coding sequence. Induction of the transgene resulted in overexpression of *UCP2* and decreased glucose-stimulated insulin secretion (GSIS) was observed. Two other studies employed the gene deletion method using the cre-loxP system to develop a transgenic mice model (*Hnf-4*$\alpha^{loxP/loxP}$, InsCre) to identify the role of a target protein (*HNF4A*) in glucose homeostasis (Gupta *et al*, 2005; Miura *et al*, 2006). The findings of those studies suggested that *HNF4A* regulates the expression of important insulin secretion regulatory genes including *KCNJ11*.

All of the studies on these *in vivo* model systems were aimed at identifying or validating the roles of genes in glucose metabolism and hence insulin release. None of the studies had any focus on CHI. However, these studies confirmed the glucose homeostasis-related roles of these CHI-associated genes. Since these models are not publicly open for further studies, they cannot be used for CHI-related studies by other research groups. Moreover, research findings from animal models do not correlate necessarily to the human systems (Seok et al, 2013; Burkhardt and Zlotnik, 2013; Justice and Dhillon, 2016; Sellers, 2017). Often differences in findings are observed between human and mouse responses and these

differences could be because of the evolutionary differences as well as differences in the cellular composition of tissues between these two species (Seok et al, 2013; Burkhardt and Zlotnik, 2013). All of these facts make the use of the current *in vivo* models for studying human disease limited (Sellers, 2017). Hence, stable and appropriate *in vitro* models that would behave as CHI-like disease model might be helpful for a better understanding of CHI pathobiology (details in section 1.7.2).

1.7.2 *In vitro* models for studying genes related to CHI

In vitro modelling or developing a cell-based research model that allows the study of the pathobiology of a disease will provide an alternative way of studying CHI (Guo *et al*, 2017). Although *in vivo* models are sometimes preferable to observe overall effects of an experiment in a living system in its natural environment, conducting experiments with these models is sometimes challenging to control. Moreover, as mentioned in the earlier section, research findings from animal models do not always correlate to the human systems (Seok et al, 2013; Burkhardt and Zlotnik, 2013; Justice and Dhillon, 2016; Sellers, 2017). On the other hand, as the experiments with *in vitro* models are carried out in isolated conditions (not in the natural environment), research findings may not be always accurate in predicting the effects inside a living system (Fearon *et al*, 2013; Jia *et al*, 2014; Justice and Dhillon, 2016). But, since the experiments are carried out in a highly controlled environment, and as the experiments are easier to set up with these models, *in vitro* modelling approach has already gained attention in the scientific community (Sherer *et al*, 2002; Fearon *et al*, 2013; Jia *et al*, 2014). Identification of multipotent progenitor pancreatic cells from CHI patients and the advancement of cell culture methodologies in the laboratory have enabled researchers to adopt this strategy. Advancement in downstream analytical procedures makes it easy to introduce perturbations in any *in vitro* model to follow the consequences.

A number of CHI-related studies had used advanced genomics and proteomics technology that involved knocking in/out the target gene of interest to analyse the expression pattern of proteins to correlate the effect of perturbation of these proteins to disease mechanism. For example, De Souza *et al*. (2007) and Affourtit and Brand, (2008) reported using gene-specific small interfering RNA (siRNA) to knock down *UCP2* in pancreatic beta cells that significantly increased glucose-stimulated insulin secretion

(GSIS). A similar phenomenon was observed in CHI patients with mutations in *UCP2* (Ferrara *et al*, 2017). In addition, Hardy *et al*. (2007c) and Martens *et al*. (2007) also utilised gene-specific siRNA in rodent (mouse and rat) cell models to understand the effect of *HADH* gene in CHI patients. The outcomes of these studies on *in vitro* rodent models indicated that the loss of function of this gene caused an uncontrolled increase of insulin secretion. Loss-of-function mutations in the *HADH* gene had been reported to be associated with CHI (Clayton *et al*, 2001; Molven *et al*, 2004; Hussain *et al*, 2005b). In addition to the use of antisense technology, some studies also used other *in vitro* analytical tools such as site-directed mutagenesis to introduce mutations in target genes (*ABCC8*, *KCNJ11* and *UCP2*) of pancreatic cells isolated from human and rodent model organisms (mouse, rat) to simulate the CHI condition (Cartier *et al*, 2001; Marthinet *et al*, 2005; González-Barroso *et al*, 2008). These studies found that mutations in *ABCC8* and *KCNJ11* can cause impaired channel trafficking and nonfunctional channels on the membrane. In addition, mutations in *UCP2* can make the gene product nonfunctional and can impair the regulation of insulin secretion. Recently, Guo *et al*. (2017) generated an *in vitro* CHI model from human embryonic stem cells by knocking out the *ABCC8* gene. Preliminary experiments with this *in vitro* model showed uncontrolled increased insulin secretion like CHI because of the mutations in the *ABCC8* gene.

The majority of the studies using *in vitro* models had focused on either identifying gene variance in clinical CHI samples, or validating causative mutations already suggested in the literature. One of the limitations of these *in vitro* studies was that the effects of the mutations in most of the studies were transient and hence the cell models could not be used again. In addition to these studies, some other studies had focused on identifying novel causative agents of CHI using high throughput analytical tools like gene expression microarrays (Kaestner *et al*, 2003; Lantz *et al*, 2004; Hardy *et al*, 2007c; Michelsen *et al*, 2011). However, the number of these kinds of genome-wide gene expression analyses is very limited since the number of CHI patients is very limited, and it is not always possible to collect live tissue samples from those patients to work with. In addition, unavailability of suitable progenitor cell lines, as well as control *in vitro* cell lines for comparative studies have also increased the difficulty. In past years, a number of functional model pancreatic beta cell lines (MIN6, INS-1, βHC *etc*.) have been generated from mouse and rat (Miyazaki *et al*. 1990; Asfari *et al*, 1992; Radvanyi *et al*, 1993). However, as mentioned earlier, the possibility of limited translational potentials of the

findings from the mouse models to human make the use of rodent cell line less desirable in CHI related study (Ravassard *et al*, 2011; Stevens et al, 2013). In 2011, Ravassard *et al*. developed a control model human pancreatic beta cell line (EndoCβH1) that expresses most of the beta cell-specific marker proteins and also releases insulin in response to glucose. So, modification of this human beta cell model to develop stable *in vitro* models that would behave like CHI tissue in respect of increased cell proliferation, insulin secretion and increased electrical activities might help us for better understanding about CHI pathobiology. Such a model CHI cell line would be helpful to overcome the limitations of the unavailability of CHI tissues for CHI related studies. Moreover, recent advancements in generating insulin-producing cells from the stem and induced pluripotent stem cells (Zhang *et al,* 2009; Rezania *et al,* 2012; Pagliuca *et al,* 2014; Rezania *et al,* 2014; Millman *et al,* 2016) would make the stem cells also a potential source for generation of CHI model cells. Guo *et al*. (2017) have reported (this work was published during the end of this current research study) to establish an *in vitro* CHI model from human embryonic stem cells.

1.8 Network biology: an alternative approach to study CHI pathobiology

In recent years, several studies have acquired useful information about the aetiology of CHI (Dunne *et al*, 2004; Senniappan *et al*, 2012; Stevens *et al*, 2013; Arya *et al*, 2014; Stanley, 2016). However, this information is not sufficient enough to fully explain the mechanisms of the disease as well as the long-term outcomes of the disorder. As a result, the best possible way of prevention of CHI is still to be resolved (Stevens *et al*, 2013).

As mentioned above, because of the rarity of the disease, as well as the limited access to the CHI-affected tissues, it can be difficult to draw an informative conclusion from the available information. Also, information gained from the study on animal models is not always reproducible in the human system due to the differences between human and animal systems (Hussain, 2005; Shanks *et al*, 2009). So, for a better understanding of the pathobiology of CHI, studies should adopt new strategies with a combination of the traditional approaches.

It is evident that the elements of biological systems rarely act independently in physiological conditions (Kitano, 2002; Leung and Cavalieri, 2003). Rather, every living system is a complete mesh (network) of activities, and every biomolecule in the system acts as part of complex networks of interacting macromolecules (Gu *et al*, 2002a; Smith, 2007; Jin *et al*, 2014; Kao *et al*, 2017). As a result, the combined effects of these coordinated activities establish the physiological properties of the living cell (Tyson *et al*, 2001). Systems biology and one of its analytical tool, network biology, are part of the new research strategies that focus on the interactions between the components of individual cells/tissues and their relationships to complex physiological and pathological processes (Barabási and Oltvai, 2004; Stevens *et al*, 2014). Network biology analyses the patterns of interactions between cellular components to understand their roles in complex biological functions linked with various metabolic and regulatory pathways (Barabási and Oltvai, 2004; Pujol *et al*, 2010; Stevens *et al*, 2014). It is an integrative approach to data analysis that includes analysing all aspects of datasets generated from genomics (the study of the whole genome), and post-genomic studies like transcriptomics, proteomics and metabolomics. Ultimately the analysed data then would help us to understand the pathobiology and to identify potential candidate gene(s) for further investigation (Loscalzo *et al*, 2007; Stevens *et al*, 2014).

The importance of systems biology using network biology is well acknowledged by the research community. In recent years, through the combination of traditional molecular techniques and computational biology approaches, a number of diseases are being redefined by identifying and analyzing the interconnected networks that are involved in the pathophysiology of the diseases (Calvano *et al*, 2005, Jesmin *et al*, 2010, Huan *et al*, 2013, Kumar *et al*, 2013, Lones *et al*, 2013, Sookoian and Pirola, 2013, Zhang *et al*, 2013). Pancreatic cancer is one of those diseases where systems biology approaches have been applied for identification of potential candidate genes for a better understanding of the disease (Omenn *et al*, 2010, Azmi *et al*, 2011).

This sort of analytical approach has not been used in CHI research extensively. However, the possibility of a systems biology approach to CHI study has already been highlighted by some recent initiatives and it is expected that this sort of analysis might facilitate the discovery of new insights for CHI management in the near future (Banerjee *et al*, 2013, Stevens *et al*, 2013, Stevens *et al*, 2014).

1.9 Aims of the study

Several previous studies have identified a number of mutations associated with CHI in the K_{ATP} channel subunits of pancreatic beta cells and also in genes involved in the insulin-secreting pathway. However, for many instances, the aetiology of the disease is yet to be identified. A number of studies have used *in vivo* and *in vitro* systems to increase the understanding of this disease, but the available information is still not sufficient to understand the pathobiology and necessary treatment of the diseased patient.

One of the problems in studying CHI is that the number of patients is very limited and it is not always possible to collect live tissue samples from those patients to work with. It seems that a suitable *in vitro* disease model might be helpful to decipher new insights to understand this disease properly.

Further, CHI is genotypically multifactorial, genes/proteins from multiple pathways are likely to be involved in the development of this disease. A transcriptomic dataset would be a highly valuable resource to help gain further understanding of how CHI is associated with altered expression of different genes and proteins. Within this context, it seems that a systems biology approach to analyse transcriptomic datasets with a view to identifying novel causative agents of CHI would be helpful for understanding their possible role in the progression of the disease.

Considering the abovementioned facts, **the aims of this PhD** were:

1. To generate model CHI β-cell lines through modification of cell culture conditions (Chapter 3), genetic manipulation (Chapter 4) and gene silencing (Chapter 6).
2. To generate an informatics resource of mRNA expression profiles derived from CHI β-cells for future studies of disease mechanisms (Chapter 5).

To support these aims the **broad objectives of the thesis** were:

a) To characterise a novel human β-cell line for use in CHI β-cell line derivation.
b) To characterise a widely-used mouse β-cell line for use in CHI β-cell line development.
c) To characterise a novel iPS-cell line obtained from CHI tissue for studies of the impact of genetic manipulation on CHI β-cell development.

d) To use molecular techniques to generate genetic constructs to support the manipulation of K_{ATP} channel gene expression by siRNA and using CRISPR-Cas9.
e) To explore genome-wide gene expression array to generate an mRNA expression profiles obtained from CHI pancreatic tissues.
f) To use informatics resources to analyse mRNA expression profiles to understand the mechanism of disease.

Chapter 2

Materials and methods

2.1 Cell culture

2.1.1 Cell lines used in this study

Two pancreatic beta cell lines – one from human (EndoCβH1) origin and one from mouse (MIN6) origin, were used in this study. EndoCβH1 cells were kindly provided by Dr Raphael Scharfmann at the French Institute of Health and Medical Research, Paris, France. MIN6 cells were kindly provided by Dr Jun-ichi Miyazaki at Osaka University, Japan. In addition, one human CHI tissue-derived induced pluripotent stem (CHI-iPS) cell line (generated in our laboratory) was also used (Kellaway, 2016).

2.1.2 Cell culture method

2.1.2.1 EndoCβH1 cell line

The EndoCβH1 cell line requires pre-coated surfaces. The coating medium was prepared using- 1x DMEM (4.5 g/L D-glucose, 4 mM L-glutamine) (Gibco, Thermo Fisher Scientific), antibiotics (100 units/ml penicillin and 100 µg/ml streptomycin (Gibco, Thermo Fisher Scientific), 2 µg/ml fibronectin from bovine plasma (Sigma-Aldrich) and 1% ECM (Sigma-Aldrich). Cell culture treated flasks/plates (Nunclon Delta Surface, Thermo Fisher Scientific) were incubated with coating medium in a 37°C incubator for at least 1 hour. Freshly prepared culture medium was required for optimum growth of the cells. The culture medium for this cell line was prepared using 1x DMEM (1 g/L D-glucose) (Gibco, Thermo Fisher Scientific), 2% albumin from bovine serum fraction V (Roche Diagnostics, USA), 50 µM β-mercaptoethanol (Sigma-Aldrich), 10 mM nicotinamide (VWR International, USA), 5.5 µg/ml transferrin (Sigma-Aldrich), 6.7 ng/ml sodium selenite (Sigma-Aldrich) and antibiotics (100 units/ml penicillin and 100 µg/ml streptomycin (Gibco, Thermo Fisher Scientific). Cells were allowed to grow

without changing medium and normally sub-cultured after seven days when the cells reached 70-80% confluency.

For passaging, EndoCβH1 cells were washed with Dulbecco's phosphate buffered saline (DPBS) (without $MgCl_2$ and $CaCl_2$) (Sigma-Aldrich) twice and incubated with 1x 0.05% (v/v) trypsin-EDTA (Gibco, Thermo Fisher Scientific) solution for 3 minutes. After trypsinisation, the inhibition of trypsin activity was carried out using 1x volume of neutralisation medium (80% DPBS (without $MgCl_2$ and $CaCl_2$), 20% FBS (fetal bovine serum; qualified heat-inactivated; Gibco, Thermo Fisher Scientific)) and 5x volume of culture medium. The cell suspension was transferred to a sterile 15 ml polypropylene tube (Corning Inc., USA) and centrifuged at 1200 rpm for 5 minutes (Hettich BOECO U-32, Germany). The cell pellet was re-suspended in culture medium and seeded in fresh medium on the ECM-coated culture flasks at a density of 75,000 cells/cm² and incubated them at 37°C in a humidified incubator with 5% CO_2. EndoCβH1 cells with passage number 65-80 were used in this study.

2.1.2.2 MIN6 cell line

MIN6 cells were grown in 1x DMEM (4.5 g/L D-Glucose, 4 mM L-Glutamine) (Gibco, Thermo Fisher Scientific), supplemented with 15% FBS (qualified heat-inactivated) (Gibco, Thermo Fisher Scientific), 75 µM β-mercaptoethanol (Gibco, Thermo Fisher Scientific) and antibiotics (100 units of penicillin and 100 µg of streptomycin per ml of media) (Gibco, Thermo Fisher Scientific) in cell culture treated flasks (Costar canted neck and vented flasks, Corning Inc., USA). The medium was changed in every three days before the cells were less than 50% confluent, and every two days once cells were more than 50% confluent. Cells were passaged once they reached 70-80% confluency.

For passaging, MIN6 cells were washed once with DPBS (without $MgCl_2$ and $CaCl_2$) (Sigma-Aldrich) briefly and then incubated with 1x 0.05% (v/v) trypsin-EDTA (Gibco, Thermo Fisher Scientific) for 3 to 5 minutes. Once the cells were fully detached from the surface, trypsin activity was inhibited by adding fresh culture medium (5x volume of trypsin solution used) and then transferred to sterile 15 ml polypropylene tube (Corning Inc., USA). The suspension was centrifuged at 550 rpm for 5 minutes (Hettich BOECO U-32, Germany). The cell pellet was re-suspended in culture medium and inoculated in

fresh culture medium inside sterile culture flasks at a density of 50,000 cells/cm². The cells were then incubated at 37°C in a humidified incubator with 5% CO_2. MIN6 cells with passage number 21-35 were used in this study.

2.1.2.3 CHI-iPS cell line

CHI-iPS cells require pre-coated surfaces for growth. The coating medium was prepared by diluting concentrated human recombinant vitronectin (VTN-N) (Gibco, Thermo Fisher Scientific) with DPBS (without $MgCl_2$ and $CaCl_2$) (Sigma-Aldrich) to make a final vitronectin concentration of 0.5 µg/cm^2 surface area. 100 µl of the diluted coating medium was used for 1 cm^2 surface area. Cell culture treated plates (Corning Inc., USA) were incubated with the coating medium at room temperature under the sterile condition for at least 1 hour. The culture medium for this cell line was prepared using 98% Essential 8 basal medium (DMEM/F12 (Ham) (1:1)) (Gibco, Thermo Fisher Scientific) and 2% Essential 8 supplement (50x) (Gibco, Thermo Fisher Scientific). The medium was changed every day and cells were normally sub-cultured after 3-4 days when the cells reached 70-80% confluency.

For passaging, CHI-iPS cells were washed once with DPBS (without $MgCl_2$ and $CaCl_2$) (Sigma-Aldrich) briefly and then incubated with 1x Versene solution (Gibco, Thermo Fisher Scientific) for 3 to 5 minutes at room temperature. Once the edges of the cell clusters were started to detach (observed under a microscope), Versene activity was inhibited by adding fresh culture medium. Using sterile plastic pipettes, the clusters were carefully detached (without making the single cell suspension) from the surface by slow pipetting. This cell suspension was then transferred to previously coated plates with appropriate dilutions. The cells were then incubated at 37°C in a humidified incubator with 5% CO_2. CHI-iPS cells with passage number 39-50 were used in this study.

2.1.3 Cryopreservation and recovery of cells

The cells were preserved in liquid nitrogen for long-term storage. For EndoCβH1 and MIN6, the cells were collected by trypsinisation and centrifugation as described above (respectively). MIN6 cells were resuspended in 1x cell freezing medium containing 90% culture medium and 10% DMSO (Sigma-Aldrich). EndoCβH1cells were resuspended in 1x cell freezing medium made of 90% FBS (Gibco, Thermo Fisher Scientific) and 10%

DMSO (Sigma-Aldrich). The CHI-iPS cells were harvested as described above and were collected by centrifugation (Hettich BOECO U-32, Germany) at 200xg for 4 minutes. The cells were then resuspended in 1x cell freezing medium (90% culture medium, 10% DMSO (Sigma-Aldrich)). For all three cell lines, cells were then frozen at -80°C for a short period followed by transfer to liquid nitrogen (-196°C) for longer storage.

When required, the cells were collected from liquid nitrogen and were warmed to 37°C using a water bath. 1 ml of cell suspension was then resuspended in 9 ml of medium and then centrifuged (as described above, respective of cell lines) at room temperature. The supernatant was discarded, and the cell pellet was then resuspended in fresh medium. The cells were transferred to ready to use culture flasks/plates and incubated in a 37°C incubator.

2.2 Total RNA isolation, quantification, and conversion to cDNA

2.2.1 Collection of cells

After reaching 70-80% confluency, cells were detached from the culture flask/plates and collected as cell pellets following the protocols described above (section 2.1.2). The pellets were washed with DPBS (without $MgCl_2$ and $CaCl_2$) (Sigma-Aldrich). The washed pellets were used for extracting total RNA.

2.2.2 RNA isolation

Total RNA of the cells was isolated using the RNeasy Mini Kit and QIAshredder columns (both from Qiagen Ltd., UK) according to the manufacturer's protocol. Briefly, the pelleted cells were lysed with 350 µl or 600 µl of buffer RLT (depending on the number of cells) which was supplemented with 1% β-mercaptoethanol. The cell lysate was then transferred to a QIAshredder spin column and centrifuged for 2 minutes at maximum speed using a benchtop centrifuge machine (Minispin Plus, Eppendorf, UK). One volume of 70% ethanol (Sigma-Aldrich) was added to the lysate, mixed properly by pipetting and then the lysate was transferred to an RNeasy silica-gel mini-column for allowing the RNA to bind to membrane inside the column. The sample was then centrifuged at 10,000xg for 15 seconds followed by washing with wash buffer RW1 once. RNase-free

DNase I solution (10 µl of DNase I in 70 µl of Buffer RDD, both reagents from Qiagen Ltd, UK) was applied to the membrane and incubated at room temperature for 15 minutes to prevent any genomic DNA carryover. The column was washed again with Buffer RWI once, then with RPE buffer twice. Finally, total RNA was eluted using RNase-free water in RNase-free microcentrifuge tube. The extracted RNA was then stored at -80°C.

2.2.3 RNA quantification

The quantity and quality of extracted RNA samples were determined using the NanoDrop ND-2000 UV-Vis spectrophotometer (Thermo Fisher Scientific). An A_{260}/A_{280} ratio in the range of 1.8-2.2 was considered pure. Also, A_{260}/A_{230} ratio and the absorbance graph were used for measurement of purity.

2.2.4 Conversion of total RNA to cDNA by Reverse Transcription (RT)

The extracted pure total RNAs were then converted to complementary DNA (cDNA) using the Precision nanoScript Reverse Transcription kit (Primerdesign Ltd, UK), using the manufacturer's protocol. Briefly, a maximum of 2 µg of total RNA sample was added to 1 µl of oligo-(dT) primers and 1 µl of random primers (9 nucleotides in length), and adjusted to a volume of 10 µl with nuclease-free water. The sample was then incubated at 65°C for 5 minutes and then quickly cooled on ice. A master mix of 2 µl of 10x reaction buffer, 2 µl DTT (100 mM), 1 µl of dNTPs (10 mM each), 4 µl of nuclease-free water, and 1 µl of Reverse transcriptase (RTase) was added to the pre-chilled sample. The mixture was incubated at 25°C for 5 minutes, followed by incubation at 55°C for 20 minutes to activate the RTase enzyme. The reaction was heat inactivated by incubation at 75°C for 15 minutes. All the incubation steps were carried out in a Veriti 96-well Thermal Cycler (Applied Biosystems, Thermo Fisher Scientific). To detect any genomic contamination in subsequent steps, a negative (RT-ve) control for each sample was generated following the same procedure except in place of RTase, 1 µl of nuclease-free water was added. Finally, cDNA samples were stored at -20°C for short-term storage or at -80°C for longer storage.

2.3 Analysis of gene expression by Polymerase chain reaction (PCR)

2.3.1 Primers used for reverse-transcription PCR

All of the gene-specific primers used in this study were designed using the Primer3 (v.0.4.0) (http://bioinfo.ut.ee/primer3-0.4.0/primer3/) primer designing web tool and NCBI Primer-BLAST (http://www.ncbi.nlm.nih.gov/tools/primer-blast/). The cut-off parameters used for the designed primers were at-least 50% GC content and a size of 18-25 bases. Primers were purchased from Eurofins Genomics, Germany. The supplied lyophilized primers were suspended in nuclease-free water (Ambion, Thermo Fisher Scientific) to make 100 µM stock solutions and then diluted and divided into aliquots of 10 µM working concentration with nuclease-free water. The primers were stored at -20°C. Primer sequences and optimised annealing temperatures (T_m) for all individual primer pairs are provided as additional information (Appendix I).

2.3.2 Reverse-transcription PCR (RT-PCR)

RT-PCR was performed in a Veriti Thermal Cycler (Applied Biosystems, Thermo Fisher Scientific) using reagents from Invitrogen (Thermo Fisher Scientific). The reagent composition of a typical RT-PCR reaction is mentioned in Table 2.1. As a control, 100 ng of genomic DNA (gDNA) (Human/Mouse, Promega, UK) was used. For a negative control, nuclease-free water was used in place of the template to cross-check the possible contamination in the reagents used. The PCR reaction conditions were as follows: an initial denaturation at 94°C for 5 minutes, then 30-35 cycles each with denaturation at 94°C for 30 seconds, annealing (annealing temperature for each primer set is provided in Appendix I) for 30 seconds, and elongation at 72°C for 45 seconds followed by a final extension at 72°C for 5 minutes.

Table 2.1: **Typical RT-PCR reaction composition**

Reagent	***Final concentration***	***Volume (µl)***
10x reaction buffer (without $MgCl_2$)	1x	2.5
10 mM dNTP mixture	0.2 mM	0.5
50 mM $MgCl_2$	1.5 mM	0.75
Forward/Revese primer (10 µm)	0.5 µM	1.25
Template cDNA	~50 ng	1 - 2
Taq DNA Polymerase (5 U/µl)	0.06 U/µL	0.3
Nuclease-free water	--	Up to 25

2.3.3 Separation of PCR products and their visualisation

PCR products were electrophoretically separated on a 1.5-3% agarose gel (depending on amplicon size) containing GelRed nucleic acid gel staining solution (1:10,000) (Biotium Inc., USA) in 1x TAE running buffer at 100 volts. Blue/Orange 6x loading dye (Promega, UK) was added to the PCR products prior to load into the wells of the gel. Either the Quick-load 100 bp or Fast DNA ladder (both from New England Biolabs, UK) was used as a size marker. After electrophoresis, DNA bands in the gel were observed and photographed by using a UV gel documentation system (Biorad Chemidoc MP imaging system, Bio-Rad Laboratories, USA).

2.3.4 Primers validation

To authenticate the PCR products as the genes of interest, the gene-specific PCR products were sequenced. The PCR products were purified using a PCR purification kit (QIAquick, Qiagen, UK) according to the manufacturer's protocol. In brief, 1 volume of DNA (PCR product) was thoroughly mixed with 5 volumes of Buffer PB. The mixture was then transferred to a silica-based membrane containing columns so that the DNA can bind to the membrane. The sample was centrifuged at 13,000 rpm for 60 seconds using a benchtop centrifuge machine (Minispin Plus, Eppendorf, UK). After discarding the flow-through, which contains the other PCR reagents, the sample was washed with 0.75 ml of Buffer PE and then, centrifuged at 13,000 rpm for 60 seconds. In the end, 30-50 µl nuclease-free water was added to the membrane and the purified DNA was eluted by centrifuging at 13,000 rpm for 60 seconds.

The purified PCR products along with their corresponding primers (forward and reverse, separately) were sent for DNA sequencing, which was conducted by The University of Manchester DNA Sequencing Facility (University of Manchester, UK). The sequences were then analysed using bioinformatics web tools – NCBI Nucleotide Blast (https://blast.ncbi.nlm.nih.gov/Blast.cgi) and ClustalW (http://www.genome.jp/tools/clustalw/) to confirm product identity.

2.3.5 Relative quantitative PCR

Relative quantitative PCR (qPCR), also known as real-time PCR, is a state-of-the-art technique that merges amplification and detection steps into a single step and provides the information in real-time. As a result, this method does not require time-consuming gel electrophoresis for detection. More importantly, the resulting information is truly quantitative. So, the qPCR approach is quite the opposite compared to conventional PCR methods, which detect the product at the end stage and is not truly quantitative.

Experimentally, PCR reactions can be sub-divided into three distinct phases- exponential, linear and plateau (VanGuilder *et al*, 2008) (Figure 2.1). Traditional PCR methods analyse the end-product, at the plateau phase. On the other hand, the qPCR method collects reaction information at the exponential phase and thus providing a more sensitive detection method.

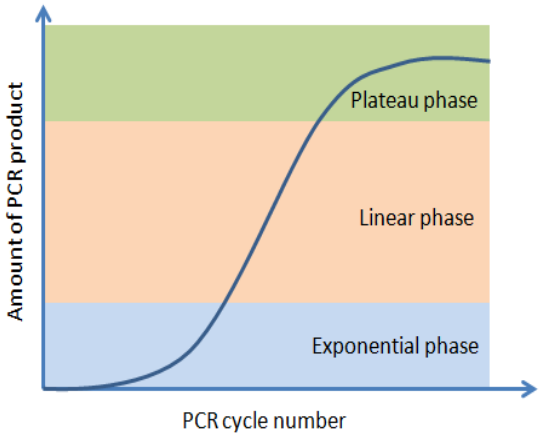

Figure 2.1: **A typical illustration of the phases of PCR.** PCR reactions start with the exponential phase, where the reactions produce the double amount of the product after each cycle. The reagents then become used up and therefore less available. So, ultimately, the reaction rate decreases, the amount of products no longer doubles after each cycle. In the long run, the reactions enter the plateau phase, where reactions slow down and eventually, stop to amplify any more products. The image was adapted from VanGuilder *et al*. (2008).

In this study, two popular methods of qPCR were used. One was SYBR Green dye-based assay which uses a non-specific dye that binds to minor grooves of double-stranded DNA (dsDNA) only (Schneeberger *et al*, 1995; Cao and Shockey, 2012; Kumar *et al*, 2012). The other one was TaqMan probe-based assay that uses sequence-specific single-stranded DNA (ssDNA) probe labelled with a fluorescent reporter and a quencher dye (Holland *et al*, 1991; Cao and Shockey, 2012; Kumar *et al*, 2012). Both of the methods are outlined briefly in Figure 2.2.

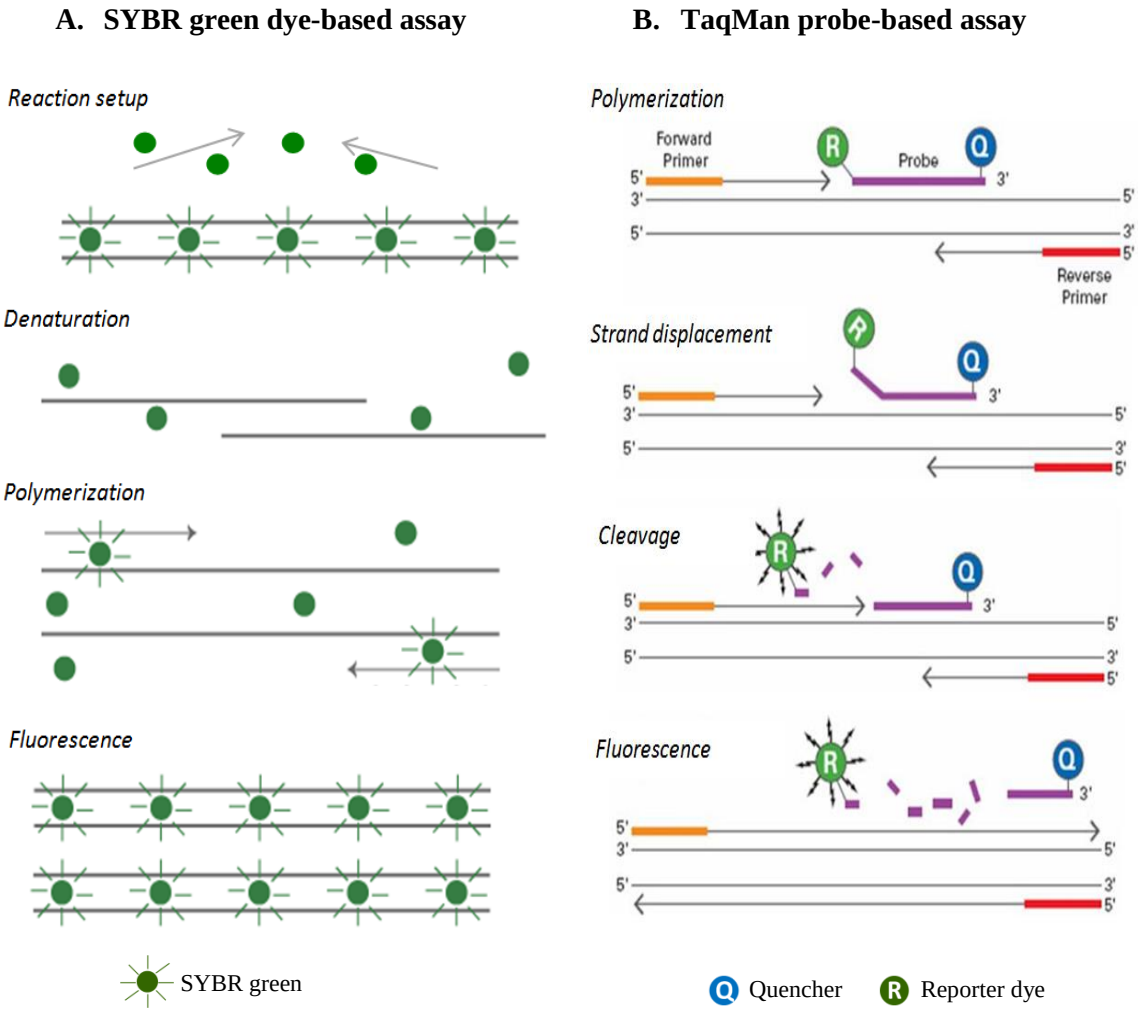

Figure 2.2: **Typical steps of SYBR green and TaqMan assays.** Panel A) SYBR green dye fluoresces only when bound to double-stranded DNA. After denaturation, the dye is released, and fluorescence is inhibited. After completion of the polymerisation, the dye again binds to double-stranded DNA, resulting in increased fluorescence. Panel B) TaqMan probe, attached with a fluorescent reporter dye and a quencher dye, bind to the target gene. During the DNA extension step, probe DNAs are displaced and are cleaved by the polymerase. So, the reporter dye becomes separated from the quencher and emits fluorescence. For both of the methods, the relative amount of fluorescence is proportional to the amount of product generated. Images were adapted from Thermo Fisher Scientific website (https://www. thermofisher.com/uk/).

2.3.5.1 SYBR Green-based qPCR

The RNA was extracted and converted to cDNA following the protocol described section 2.2. Precision 2x real time master mix (Primerdesign Ltd, UK), which contains SYBR green as the primary dye and ROX as a reference dye, was used in this study. 50 ng of cDNA was used for the PCR reaction. The reaction volume was set to 20 µl, and the composition that was used is mentioned in Table 2.2. The qPCR primers for target genes were designed following the protocol mentioned in section 2.3.1. *18S rRNA* and *GAPDH* primers purchased from Primerdesign Ltd, UK were used as the endogenous controls. The list of primers used in this assay is mentioned in Table 2.3.

Table 2.2: **Typical SYBR Green-based qPCR reaction composition**

Reaction components	***Amount (µl)***
2x Master Mix	10
Primer (10 µM)	1
Nuclease-free water	4
cDNA (10 ng/µl)	5

Table 2.3: **List of designed primers used in SYBR Green-based qPCR**

Gene name/ NCBI ref. no	***Primer***	***Primer sequence 5′ → 3′***	***Product size (bp)***
INS (human) NM_001185097.1	Forward	CCAGGACAGGCTGCATCAG	117
	Reverse	CCATGGCAGAAGGACAGTGA	
NEUROD1 (human) NM_002500.4	Forward	TCCGGAGGCCCCAGGGTT	104
	Reverse	CGCCCATCAGCCCACTCT	
NKX6.1 (human) NM_006168.2	Forward	CGTTGGGGATGACAGAGAGT	110
	Reverse	CGAGTCCTGCTTCTTCTTGG	
NGN3 (human) NM_020999.3	Forward	CTTCGTCTTCCGAGGCTCT	110
	Reverse	CTATTCTTTTGCGCCGGTAG	
PDX1 (human) NM_000209.3	Forward	CGTCCGCTT GTTCTCCTC	96
	Reverse	CCTTTCCCATGGATGAAGTC	
SST (human) NM_001048.3	Forward	CCCAGACTCCGTCAGTTTCT	205
	Reverse	CCATAGCCGGGTTTGAGTTA	

The reaction volume was transferred into a single well of a V-bottomed 96-well optical plate (Life Technologies, Thermo Fisher Scientific). Each sample was prepared in triplicate, and a negative control (nuclease-free water instead of cDNA) was also prepared

for each primer. The plate was then sealed with an optical film (Life Technologies, Thermo Fisher Scientific) and spun at 1500 rpm for 1 minute in a tabletop centrifuge machine (Hettich BOECO U-32, Germany) at room temperature. The plate was then placed for PCR reaction in a real-time thermal cycler (StepOnePlus Real-Time PCR System, Thermo Fisher Scientific). The reaction program was - initial denaturation at 95°C for 10 minutes, then 40 cycles at 95°C for 30 seconds, followed by 61°C for 1 minute. Results of the PCR were analysed using StepOnePlus system software (Thermo Fisher Scientific) and MS Excel (Microsoft corp., USA).

2.3.5.2 TaqMan probe-based quantitative PCR

For TaqMan probe-based qPCRs, TaqMan Fast Advanced Master Mix (Thermo Fisher Scientific) with ROX as a reference dye was used. The quantitative expressions of *KCNJ11*, *ABCC8* and *INS* were assayed by this method. The expression of *GAPDH* was used as endogenous control. All the target gene-specific probes and endogenous control specific probe were purchased from Thermo Fisher Scientific. 50 ng of cDNA was used for the PCR reaction. The reaction volume was set to 20 µl, and the typical reaction composition is mentioned in Table 2.4.

Table 2.4: **Typical TaqMan probe-based qPCR reaction composition**

Reaction components	***Amount (µl)***
2x Master Mix	10
20x TaqMan gene probe	1
Nuclease-free water	5
cDNA (12.5 ng/µl)	4

Similar to the protocol for SYBR Green-based qPCR (mentioned above), the reaction volume was transferred into a single well of a V-bottomed 96-well optical plate (Life Technologies, Thermo Fisher Scientific). Each sample was prepared in triplicate, and a negative control (nuclease-free water instead of cDNA) was also prepared for each primer. The plate was then sealed with an optical film (Life Technologies, Thermo Fisher Scientific) and spun at 1500 rpm for 1 minute in a tabletop centrifuge machine (Hettich BOECO U-32, Germany) at room temperature. The plate was then placed for PCR reaction in a real-time thermal cycler (StepOnePlus Real-Time PCR System, Thermo Fisher Scientific). The reaction program was - initial incubation at 48°C for 15 minutes,

polymerase activation at 95°C for 10 minutes, and 40 cycles of denaturation at 95°C for 15 seconds and 60°C for 1 minute. The data were collected at the end of each cycle. Results of the PCR were analysed using StepOnePlus system software (Thermo Fisher Scientific) and MS Excel (Microsoft corp., USA).

2.4 Protein analysis

2.4.1 Immunofluorescence imaging study

Cells were detached from the culture flasks/plates and collected as cell pellets following the protocol described in section 2.1.2. The cells were then re-suspended and seeded into culture medium on sterilised 15 mm diameter glass coverslips (Scientific Laboratory Supplies, UK) in 24-well plates (Corning Inc., USA). The cells were then allowed to grow in a 37°C incubator until the cells reached 70-80% confluency. The used culture medium was then removed, and cells were fixed with 4% paraformaldehyde (Sigma-Aldrich) in DPBS buffer for 20 minutes at room temperature. The cells were washed with DPBS three times. Coverslips with cells were then permeabilised with 0.1% Triton X-100 (Sigma-Aldrich) in DPBS for 20 minutes at room temperature. To minimise the background staining from non-specific binding, cells were incubated with 10% normal goat serum (NGS) (Gibco, Thermo Fisher Scientific) in DPBS for 1 hour at room temperature. The cells were incubated with primary antibody (details listed in Table 2.5) in DPBS containing 3% NGS overnight at 4°C. After that cells were washed with DPBS three times for 5 minutes each. Cells were then incubated with secondary antibody conjugated with a fluorescent protein (details listed in Table 2.5) in DPBS containing 3% NGS for 1 hour at room temperature. The cells were then washed three times with 0.1% Tween-20 (Sigma-Aldrich) in PBS for 5 minutes each. Cells were then mounted on glass slides (Thermo Fisher Scientific) with mounting media containing DAPI (ProLong Gold antifade reagent, Thermo Fisher Scientific) and allowed to cure for 24 hours in the dark at room temperature. The stained cells were viewed under an Olympus BX51 Snapshot widefield microscope and images were captured with Coolsnap ES camera (Photometrics, USA) using MetaVue imaging software (Molecular Devices, USA). Specific band-pass filters (in accordance with the fluorescent protein conjugated with secondary antibody)

were used for viewing and capturing the images. Images were then analysed using ImageJ (National Institute of Health, USA).

Table 2.5: **Details of primary and secondary antibodies used in immunofluorescence assays**

Antibody	***Host***	***Specificity***	***Dilution***	***Source***
Primary				
Anti-Insulin	Rabbit	Polyclonal	1:200	Cat. no.- ab63820 Abcam PLC, UK
Anti-Nanog	Rabbit	Polyclonal	1:50	Cat. no.- ab21624 Abcam PLC, UK
Anti-NeuroD1	Rabbit	Polyclonal	1:200	Cat. no.- 12080-1-AP Proteintech, USA
Anti-Oct4	Rabbit	Polyclonal	1:200	Cat. no.- ab19857 Abcam PLC, UK
Anti-Somatostatin	Rat	Monoclonal	1:150	Cat. no.- MAB354 Millipore UK Ltd
Anti-Sox2	Rabbit	Polyclonal	1:500	Cat. no.- ab97959 Abcam PLC, UK
Anti-SSEA4	Mouse	Monoclonal	1:70	Cat. no.- ab16287 Abcam PLC, UK
Secondary				
Alexa Fluor 488-conjugated Anti-Rabbit	Goat	Polyclonal	1:200	Cat. no.- A11008 Thermo Fisher Scientific
Alexa Fluor 488-conjugated Anti-Mouse	Goat	Polyclonal	1:200	Cat. no.- A11008 Thermo Fisher Scientific
Cy3-conjugated Anti-Rat	Goat	Polyclonal	1:200	Cat. no.- ab6953 Abcam PLC, UK
Cy5-conjugated Anti-Rabbit	Goat	Polyclonal	1:200	Cat. no.- ab6564 Abcam PLC, UK

2.4.2 Western blot analysis

2.4.2.1 Extraction of protein

To have a sufficient amount of whole cell protein, cells were grown in T80 culture flasks until 70-80% confluency was achieved. Radio Immuno Precipitation Assay (RIPA) buffer (150 mM NaCl, 0.1% Triton X-100, 0.5% sodium deoxycholate, 0.1% Sodium dodecyl sulphate (SDS), 50 mM Tris, pH 8.0, 1x protease inhibitor) was used for extraction of

whole cell protein. In brief, the cells were detached and collected as cell pellets according to the protocol mentioned above (section 2.1.2) and washed with ice-cold DPBS twice. 500 µl of RIPA buffer was then added to the cell pellet. The cells were then resuspended gently and incubated at 4°C for 30 minutes with occasional vortexing to ensure the complete lysis of the cells. The sample was then centrifuged (PrismR, Labnet International, USA) at 13,000 rpm for 20 minutes at 4°C. The supernatant was transferred to a clean pre-chilled microcentrifuge tube on the ice. The sample was stored at -20°C for short-term storage and at -80°C for long-term storage.

2.4.2.2 Estimation of protein concentration

To measure the concentration of total protein of different samples, Bradford reagent (Sigma-Aldrich) was used. The formation of a coloured complex (which shows maximum absorption at 595 nm) between the dye, Brilliant Blue G, and proteins in solution is the basis of this procedure. The amount of absorption is proportional to the amount of protein present in the solution. Quick Start Bovine Serum Albumin (BSA) Standard kit (0, 0.125, 0.25, 0.5, 0.75, 1.0, 1.5 and 2.0 µg/µl) (Bio-Rad Laboratories, USA) was used as protein standard. Briefly, 10 µl of each protein standard was added to a well of 96-well plate (Corning Inc., USA) in three technical replicates. Then 10 µl of a sample protein solution (in 1:10 and 1:100 dilution separately) to be tested was added in triplicate to the wells of the plate. 100 µl of Bradford assay reagent was added to the wells and incubated at room temperature for 5 minutes at dark. The optical density (OD) was measured using a plate reader (Synergy HT, BioTek Instruments, Inc.) and the readings of OD were extracted using Gen5 software (BioTek Instruments, Inc.). Protein concentrations were measured from the OD data using MS Excel (Microsoft Corp., USA) and GraphPad Prism 6 (GraphPad Software, Inc., USA) software programmes.

2.4.2.3 Protein separation, transfer to membrane and detection

Separation

40 ng of total protein from each sample was used for gel separation. At first, protein samples were denatured by incubating with Laemmli loading buffer (2% SDS, 5% β-mercaptoethanol, 10% glycerol, 0.01% Bromophenol blue, 62.5 mM Tris-HCl, pH 6.8) at 95°C for 5 minutes. Proteins from each samples were then loaded in 12% Mini-protean

stain-free pre-cast polyacrylamide gels (Bio-Rad Laboratories, USA) and then separated by electrophoresis using 1x Tris-Glycine running buffer (25 mM Tris base, 190 mM glycine, 0.1% SDS pH 8.3) at 15 mA in Mini-PROTEAN3 Cell electrophoresis system (Bio-Rad Laboratories, USA). ColorPlus Prestained Protein Ladder (New England Biolabs, UK) was used as a protein marker and run along with the protein samples.

Transfer of proteins to the membrane

After electrophoresis, the protein gel was placed in the middle of the sandwich assembly (on top of a PVDF (Polyvinylidene Fluoride) membrane) of the Trans-Blot Turbo mini transfer pack (Bio-Rad Laboratories, USA). The sandwich assembly was then placed in a tray of the Trans-Blot Turbo transfer system (Bio-Rad Laboratories, USA). Recommended set program (in accordance with the molecular weight of target proteins) was run to transfer the proteins from gel to PVDF membrane.

Target protein detection

Following the transfer of the proteins from gel to a membrane, the membrane was taken out of the sandwich carefully. The membrane was then incubated with milk blocking reagent (5% skimmed milk (Sigma-Aldrich) in Tris Buffered Saline (TBS) (20 mM Tris-Cl pH 7.6, 150 mM NaCl) with 0.1% Tween-20 (TBS-T)) for 1 hour at room temperature on an orbital shaker (Gyro rocker, Stuart Scientific, UK) to block the free spaces of the membrane. The membrane was then incubated with the primary antibody (details in Table 2.6) diluted in milk blocking reagent overnight at 4°C. Following the incubation, the membrane was washed three times with TBS-T for 5 minutes each. Afterwards, the membrane was incubated with the horseradish peroxidase (HRP)-conjugated secondary antibody (anti-rabbit IgG, HRP-linked antibody; Cat. no.- 7074, Cell Signaling Technology, UK) diluted (1:10000) in milk blocking reagent for 1 hour at room temperature on the orbital shaker. Next, the membrane was rinsed three times with TBS-T for 10 minutes each. Following the washing, the membrane was incubated with Immobilon Western Chemiluminescent HRP Substrate (EMD Millipore., UK) for 2 minutes. The membrane was then exposed to photographic film (Kodak Biomax MR Film, Sigma-Aldrich) and developed using an automatic X-ray film processor (JP-33, JPI Healthcare, USA).

Table 2.6: **Details of primary antibodies used in western blot assay**

Antibody	***Host***	***Specificity***	***Dilution***	***Source***
Anti-Kir6.2	Rabbit	Polyclonal	1:2000	Cat. no.- APC-020, Alomone labs, Israel
Anti-Beta Actin	Rabbit	Polyclonal	1:5000	Cat. no.- ab95437, Abcam, UK

2.5 Cell proliferation assay

2.5.1 Conventional cell counting method

Cells were cultured with normal growth media until they reached ~70-80% confluency according to the protocols mentioned in section 2.1.2. To observe the effect of different insulin secretagogues (ISGs) (potassium chloride, tolbutamide, arginine, leucine and glibenclamide) (described in detail in chapter 3) on the cell growth, different composition of culture media (with or without ISGs) were prepared and used in this assay. All the ISGs used in this study were purchased from Sigma-Aldrich. In brief, cells were seeded in culture media (with or without individual ISG) on 24-well plates (Corning Inc., USA) and allowed to grow at 37°C. After every 24 hours (up to 192 hours), cells were detached from three different wells for every individual condition and collected as cell pellet using tabletop centrifuge machine (Minispin Plus, Eppendorf, UK). The centrifugation was carried out at room temperature, and the speed was optimised as - 2000 rpm for 10 minutes (MIN6) and 3000 rpm for 5 minutes (EndoCβH1). The cell pellets were then resuspended in 1 ml of individual media and kept in ice. Then, the number of cells was counted separately using a glass hemocytometer (Hawksley, UK). Trypan blue (Sigma-Aldrich) was used to determine the live cells. The growth rate was analysed for eight days. A growth curve was plotted using MS Excel (Microsoft Corp., USA) software to observe the pattern of the growth rate of cells in different conditions.

2.5.2 CellTiter 96 AQ_{ueous} One Solution cell proliferation assay

CellTiter 96 AQ_{ueous} One Solution (Promega, UK) proliferation assay is based on a colourimetric method for determining the number of viable cells in the cell sample. The principal ingredients for this assay is a solution of a novel tetrazolium compound [3-(4,5-

dimethylthiazol-2-yl)-5-(3-carboxymethoxyphenyl)-2-(4-sulfophenyl)-2H-tetrazolium, inner salt; MTS] and an electron coupling reagent (phenazine ethosulfate; PES). MTS is metabolically converted by cells into a coloured, culture medium soluble formazan product, which can be measured by taking absorbance at 490 nm directly from 96-well assay plates without any downstream processing (Technical bulletin, CellTiter 96 AQ_{ueous} One Solution cell proliferation assay, Promega, UK)

In brief, define number of cells (16,000 for MIN6 and 24000 for EndoCβH1) in 100 µl culture media were grown in 96-well plates at 37°C. The cells were seeded in three wells for each of the experimental condition, and for each day of the assay. Every 48 hours, the assay was carried out by treating the cells for 2 hours at 37°C with 20 µl of assay reagent directly added to the respective wells. Absorbance at 490 nm was then measured using a plate reader (Synergy HT, BioTek Instruments, Inc.) and the readings of absorbance were extracted using Gen5 software (BioTek Instruments, Inc.). The absorbance measured in this assay is directly proportional to the number of viable cells. In addition, absorbance at 490 nm of cells from each condition was measured after 24 hours. Along with the experimental conditions, negative controls for each condition (respective culture media only, without any cell) were also used and were undergone the same procedure to measure the background absorbance. The overall absorbance was normalised by subtracting background absorbance and absorbance after 24-hour experiments from experimental readings.

2.5.3 Cell proliferation assay based on 5-Bromo-2-deoxyuridine incorporation

Cells were seeded in culture medium on 15 mm diameter cover-slips in 24-well plates (Corning Inc., USA) and allowed to grow in a 37°C incubator for 48 hours. After 48 hours, the used culture media were removed, and the cells were treated with BrdU (5-Bromo-2-deoxyuridine) labelling reagent (Molecular Probes, Thermo Fisher Scientific) diluted (1:100) in culture media for 2 hours at 37°C. After 2 hours, the media was replaced with fresh culture media and incubated for another 24 hours at 37°C. The cells were fixed with 4% paraformaldehyde (Sigma-Aldrich) in DPBS buffer (Sigma-Aldrich) for 20 minutes at room temperature. The cells were washed with DPBS three times. Cover-slips with cells were then taken out and placed in a glass beaker containing 50 ml of sodium citrate buffer (10 mM, pH 6.0) and heated at high power (800 watts) in a

microwave oven (Panasonic NN-E250) for 2 minutes and then at medium power for another 5 minutes. The cells were then allowed to cool to room temperature. Cover-slips with cells were then transferred to a fresh 24-well plate and then permeabilised with 0.1% Triton X-100 (Sigma-Aldrich) in DPBS for 20 minutes at room temperature. To minimise the background staining from non-specific binding, cells were incubated with 10% NGS (Gibco, Thermo Fisher Scientific) in DPBS for 1 hour at room temperature. Cells were then incubated with primary antibody (rat anti-BrdU antibody, Bio-Rad Laboratories, USA) containing 3% NGS in DPBS overnight at 4°C. After that, cells were washed with DPBS three times for 5 minutes each. Cells were then incubated with secondary antibody (goat anti-rat antibody, Abcam, UK) in 3% NGS in DPBS for 1 hour at 37°C followed by three washes with 0.1% Tween-20 (Sigma-Aldrich) in DPBS for 5 minutes each. Cells were then mounted on glass slides (Thermo Fisher Scientific) with mounting media containing DAPI (ProLong Gold antifade reagent, Thermo Fisher Scientific) and allowed to cure for 24 hours in the dark at room temperature. The stained cells were viewed under an Olympus BX51 Snapshot widefield microscope and images were captured with Coolsnap ES camera (Photometrics, USA) using MetaVue imaging software (Molecular Devices, USA). Specific band pass filters were used for viewing and capturing the images. Images were then analysed using ImageJ software (National Institute of Health, USA).

2.6 Glucose-stimulated insulin secretion (GSIS) assay

2.6.1 Isolation of Islet of Langerhans from mouse pancreas

8-10 weeks old six mice (C57BL/6) were collected from the Biological Services Facility, University of Manchester. The mice were sacrificed by cervical dislocation. After dissecting the mice, the pancreases were rapidly removed and placed in cold Krebs Ringer HEPES (KRH) buffer (the composition of KRH buffer is given in Table 2.7). In brief, the pancreas was inflated with cold collagenase V (1 mg/ml) (Sigma-Aldrich, catalogue no. C-9263) dissolved in KRH buffer through the bile duct using a syringe and needle. Spleen and fat tissues were trimmed, and the inflated pancreas was transferred into a 50 ml polypropylene tube (RNase/DNase free, Corning Inc., USA) containing collagenase solution. To enzymatically digest the pancreas and to have the islets in the solution, the tube containing pancreas was placed into a 37°C water bath for strictly 10

minutes with occasional swirling by hand. Ice-cold RPMI 1640 (Gibco, Thermo Fisher Scientific) supplemented with 10% FBS and antibiotics (100 units of penicillin and 100 µg of streptomycin per ml of media) was then added to the pancreas sample to inhibit the action of the collagenase. The sample was then centrifuged (Hettich BOECO U-32, Germany) at 1400 rpm for 1.5 minutes at 10°C and the supernatant was discarded. The sample was washed with supplemented ice-cold RPMI and centrifuged at 1400 rpm for 1.5 minutes at 10°C. This step was carried out three times. Following the washing steps, the islet sample was resuspended in supplemented RPMI, and filtered through a metallic sieve (a typical tea strainer) to separate the islets from undigested tissues. The filtrate was then centrifuged (Hettich BOECO U-32, Germany) at 1500 rpm for 1.5 minutes at 10°C and the supernatant was discarded. The supernatant was removed completely by inverting the tube onto a tissue paper. The sample was then resuspended with 15 ml Histopaque (Sigma-Aldrich). Supplemented ice-cold RPMI was then added very gently to the islet suspension to create a smooth interface between re-suspended islets (in Histopaque) and RPMI. The solution was then centrifuged (Hettich BOECO U-32, Germany) at 3510 rpm for 24 minutes at 10°C (with the slowest acceleration and slowest breaking speed to ensure the integrity of density gradient). The islets, suspended at the density interface after centrifugation, were then collected carefully into a new tube using micropipette. The isolated islets were then washed three times with supplemented RPMI and centrifuged at 1500 rpm for 1.5 minutes at 10°C. After the final wash, the islets were resuspended in RPMI 1640 supplemented with 5.5 mM glucose, 10% FBS and antibiotics (100 units of penicillin and 100 µg of streptomycin per ml of media), and then transferred to a petri dish, and incubated overnight in an incubator at 37°C with air having 5% CO_2. On the following day, healthy and clean islets were hand-picked using a micropipette under a microscope (Leica MS 5, Leica Microsystems, UK) for insulin secretion assay.

2.6.2 Insulin secretion assay with cell lines

The general protocol of GSIS assay for MIN6 and EndoCβH1 cell lines followed in this study is slightly different.

For MIN6 cell line, 100,000 cells/cm^2 were seeded in culture media in 96-well plates (Corning Inc., USA) and allowed to grow in a 37°C incubator for 48 hours. Then the culture media were replaced with KRH buffer supplemented with 1 mM glucose (Sigma-Aldrich) and incubated for 45 minutes at 37°C growth incubator. After 45 minutes, the

buffer was removed, and cells were incubated separately with KRH buffers with different target glucose concentrations (2 mM, 5.5 mM, 10 mM, 20 mM and 25 mM) at 37°C for 60 minutes. After the incubation, the buffers were collected from the culture wells, centrifuged at 4000 rpm (Hettich BOECO U-32, Germany) for 5 minutes at 4°C. The supernatants were collected and kept on ice. To measure the total insulin content of cells of respective culture wells after each treatment, the cells were lysed with KRH buffer supplemented with 2% Triton X-100 (Sigma-Aldrich) at room temperature for 15 minutes with occasional vortexing. Samples were then centrifuged at 4000 rpm for 5 minutes at 4°C and supernatants were collected and kept on ice. Collected supernatant samples were either stored at -20°C for at most four weeks, or were used for assaying the quantification of insulin using ALPCO insulin (Mouse) ELISA kit (ALPCO, USA) following the manufacturer's recommended protocol.

For the assay for EndoCβH1 cell line, 226,000 cells/cm^2 were seeded in culture media in 96-well plates (Corning Inc., USA) and allowed to grow in a 37°C incubator for 48 hours. Then the culture media were replaced with glucose starving media (1x DMEM (without glucose) (Gibco, Thermo Fisher Scientific), 2% albumin from bovine serum fraction V, 50 μM β-mercaptoethanol, 10 mM, 5.5 μg/ml transferrin, 6.7 ng/ml sodium selenite and antibiotics (100 units/ml penicillin and 100 μg/ml streptomycin), supplemented with 2.8 mM glucose) and incubated overnight (not more than 18 hours) at 37°C (Ravassard *et al*, 2011; Krishnan *et al*, 2015). On the day of experiments, the culture media were replaced with KRH buffer supplemented with 0.5 mM glucose (Sigma-Aldrich) and incubated for 60 minutes at 37°C. After the incubation, the buffers were removed, and cells were incubated separately with KRH buffers with different target glucose concentrations (0.5 mM, 2.8 mM, 11 mM, 15 mM and 20 mM) at 37°C for 60 minutes. Next, the buffers were collected from the culture wells, centrifuged at 4000 rpm (Hettich BOECO U-32, Germany) for 5 minutes at 4°C and supernatants were collected and kept on ice. To measure the total insulin content of cells of respective culture wells after each treatment, the cells were lysed with cell lysis solution (composition mentioned in table 2.8) at room temperature for 15 minutes with occasional vortexing. Samples were then centrifuged at 4000 rpm for 5 minutes at 4°C and supernatants were collected and kept on ice. Collected supernatant samples were either stored at -20°C for at most four weeks, or were used for assaying the quantification of insulin using ALPCO insulin (human) ELISA kit (ALPCO, USA) following the manufacturer's recommended protocol.

2.6.3 Insulin secretion assay with mouse pancreatic islets

Isolated mouse pancreatic islets (section 2.6.1) were incubated overnight in RPMI1640 medium (Gibco, Thermo Fisher Scientific) in 6-well plate (Corning Inc., USA) at 37°C incubator. After that, groups of three similar sized healthy islets were hand-picked for each experimental condition, transferred to 1.5 ml microcentrifuge tubes and were incubated for 15 minutes at 37°C with KRH buffers containing 1 mM glucose. After the incubation, the buffers were replaced with KRH buffers with either 2 mM or 20 mM glucose concentrations at 37°C for 30 minutes. After the incubation, the buffers were collected from the culture wells, centrifuged at 4000 rpm (Hettich BOECO U-32, Germany) for 5 minutes at 4°C. The supernatants were collected and kept on ice. To measure the total insulin content of the group of islets of respective treatment, the islets were lysed with KRH buffer supplemented with 1 mM glucose and 2% Triton X-100 (Sigma-Aldrich) at room temperature for 15 minutes with occasional vortexing. Samples were then centrifuged at 4000 rpm for 5 minutes at 4°C and supernatants were collected and kept on ice. Collected supernatant samples were either stored at -20°C for at most four weeks, or were used for assaying the quantification of insulin using ALPCO insulin (Mouse) ELISA kit (ALPCO, USA) following the manufacturer's recommended protocol.

Table 2.7: **Composition of KRH buffer**

Reagents/Chemicals	***Concentration***
NaCl	129.0 mM
KCl	4.8 mM
$MgSO_4.6H_2O$	1.2 mM
KH_2PO_4	1.2 mM
$NaHCO_3$	5.0 mM
HEPES	10 mM
$CaCl_2$	2.5 mM
BSA	0.1% w/v
pH ~ 7.4	

Table 2.8: **Composition of cell lysis solution**

Reagents/Chemicals	***Final volume***
Tris pH 8.0, 1 M	1 ml
Triton X-100	500 µl
Glycerol	5 ml
5 M NaCl	1.37 ml
0.2 M EGTA	500 µl
H_20	Upto 50 ml
One anti-protease tablet (Roche Diagnostics, USA) per 10 ml of solution	

2.6.4 Quantification of insulin content using enzyme-linked immunosorbent assay (ELISA)

ALPCO insulin (Mouse) ELISA kit (ALPCO, USA) was used for quantification of insulin content in different experimental mouse islet and MIN6 samples. Supplied concentration standards (0.188, 0.50, 1.25, 3.75, 6.90 ng insulin/ml) were used for this assay. The protocol, in brief, 10 µl of concentration standards and the experimental samples were added to the antibody-coated wells in triplicate. 75 µl of antibody conjugate was added to the individual well and incubated for 2 hours at room temperature with continuous shaking (AM89B, Dynex Technologies, USA) at 700-900 rpm. After the incubation, the contents of the wells were decanted and washed six times with wash buffer manually using a wash bottle equipped with a wash nozzle. After the final wash, any residual wash buffer and bubbles from the wells were removed by inverting and firmly tapping the plate on absorbent paper towels. Following the washing steps, 100 µl of TMB Substrate was added to each well and incubated for 15 minutes at room temperature with continuous shaking at 700-900 rpm. Finally, 100 µl of stop solution was added to each well and mixed gently. Absorbance at 450 nm was then measured using a plate reader (Synergy HT, BioTek Instruments, Inc.) and the readings of absorbance were extracted using Gen5 software (BioTek Instruments, Inc.). The absorbance measured in this assay is directly proportional to the amount of insulin present in the experimental samples. Further analysis was performed using MS Excel (Microsoft Corp., USA) and GraphPad Prism 6 (GraphPad Software, Inc., USA) software programmes.

To quantify the insulin content from EndoCβH1 experimental samples, ALPCO insulin (human) ELISA kit (ALPCO, USA) was utilised. Supplied concentration standards (3, 10, 30, 100, 200 µIU insulin/ml) were used for this assay. The protocol is quite similar to the protocol for mouse insulin. In brief, 25 µl of concentration standards and the experimental samples were added to the antibody-coated wells in triplicate. 100 µl of detection antibody was added to the individual wells and incubated for 1 hour at room temperature with continuous shaking (AM89B, Dynex Technologies, USA) at 700-900 rpm. After the incubation, the contents of the wells were decanted and washed six times with wash buffer manually using a wash bottle equipped with a wash nozzle. After the final wash, any residual wash buffer and bubbles from the wells were removed by inverting and firmly tapping the plate on absorbent paper towels. Following the washing steps, 100 µl of TMB Substrate was added to each well and incubated for 15 minutes at room temperature with continuous shaking at 700-900 rpm. Finally, 100 µl of stop solution was added to each well and mixed gently. Absorbance at 450 nm was then measured using a Synergy HT plate reader, and the readings of absorbance were extracted using the Gen5 software. Further analysis was performed using MS Excel (Microsoft Corp., USA) and GraphPad Prism 6 (GraphPad Software, Inc., USA) software programmes.

2.7 CHI-iPS cell *in vitro* differentiation into insulin-producing beta cell

CHI-iPS Cells were cultured following the protocol mentioned in section 2.1.2.3. After reaching ~70–80% confluency, cells were rinsed twice with 1× DPBS (without Mg^{2+} and Ca^{2+}) (Thermo Fisher Scientific). The cells were detached from the surface by incubating the cells with 1x Versene at room temperature for 3-5 minutes. Released cells were rinsed with E8 medium and centrifuged at 110xg (Hettich BOECO U-32, Germany) for 3 min at room temperature. The resulting cell pellet was re-suspended into single cell suspension in E8 medium supplemented with 10 µM ROCK Inhibitor (ROCKi) (Y-27632 dihydrochloride, Sigma-Aldrich). 1.5 x 10^6 cells were seeded per well of 6-well plate (Corning Inc., USA) pre-coated with Matrigel Basement Membrane Matrix (Scientific Laboratory Supplies, Corning Inc., USA) and incubated for 48 hours at 37°C. The cells were differentiated into insulin-producing cells by following recently published 5-stage and 7-stage differentiation protocols (Rezania *et al,* 2012; Rezania *et al,* 2014). The culture conditions of different stages of differentiation are mentioned below.

7-stage differentiation protocols

Stage-1 (*definitive endoderm*): Three days of treatment were required for the cells to be differentiated into this stage. Undifferentiated CHI-iPS cells, plated on Matrigel-coated surfaces, were rinsed with 1× DPBS (without Mg^{2+} and Ca^{2+}). Then the cells were incubated with MCDB 131 medium (Gibco, Thermo Fisher Scientific) supplemented with 10 mM glucose (Sigma-Aldrich), 1.5 g/l sodium bicarbonate (Sigma-Aldrich), 2 mM L-glutamine (Sigma-Aldrich), 0.5% (w/v) BSA (fatty acid free, Roche Diagnostics, USA), 100 ng/ml Activin A (Sigma-Aldrich), and 3 µM Chir99021 (Sigma-Aldrich) for day 1 only. For day 2, cells were cultured with MCDB 131 (like day 1) modified with 0.3 µM Chir99021. On day 3, the used medium was replaced with fresh supplemented MCDB 131 (like day 1) without Chir99021, and the cells were incubated for another 24 hours.

Stage-2 (*primitive gut tube*): Two days were required to achieve this stage. On day 4, the used medium was discarded, and stage-1 cells were rinsed once with 1X DPBS (without Mg^{2+} and Ca^{2+}). Then the cells were incubated for 2 days with MCDB 131 supplemented with 10 mM glucose, 1.5 g/l sodium bicarbonate, 2 mM L-glutamine, 0.5% (w/v) BSA, 0.25 mM ascorbic acid (Sigma-Aldrich) and 50 ng/ml of fibroblast growth factor-7 (FGF7, PeproTech EC Ltd., UK).

Stage-3 (*posterior foregut*): Two days were required for this differentiation stage. On day 6, the used medium was discarded and stage-2 cells were cultured for two days in MCDB 131 supplemented with 10 mM glucose, 2.5 g/l sodium bicarbonate, 2 mM L-glutamine, 2% (w/v) BSA, 0.25 mM ascorbic acid, 50 ng/ml FGF7, 0.25 µM SANT-1 (Sigma-Aldrich), 1 µM retinoic acid (Sigma-Aldrich), 100 nM LDN193189 (Stemgent Inc., USA), 0.5% (v/v) insulin-transferrin-selenium-ethanolamine (ITS-X, Thermo Fisher Scientific), and 200 nM TPB (Calbiochem, Merck Millipore, UK).

Stage-4 (*pancreatic endoderm, $PDX1^+/NKX6.1^+$ cells*): Three days were required for this stage. On day 8, stage-3 cells were incubated for 3 days with MCDB 131 supplemented with 10 mM glucose, 2.5 g/l sodium bicarbonate, 2 mM L-glutamine, 2% (w/v) BSA, 0.25 mM ascorbic acid, 2 ng/ml FGF7, 0.25 µM SANT-1, 0.1 µM retinoic acid, 200 nM LDN193189, 0.5% (v/v) ITS-X, and 100 nM TPB.

Stage-5: (*pancreatic endocrine precursors, PDX1$^+$/NKX6.1$^+$/NEUROD1$^+$ cells*): Three days were required for this stage. On day 11, stage-4 cells were treated for 4 hours with the culture medium used in stage-4 supplemented with 10 µM ROCKi. Cells were then washed with 1× DPBS (without Mg^{2+} and Ca^{2+}) and incubated with 1x Versene at room temperature for 3-5 minutes. The cells were dissociated from the surface using cell scraper (2-position blade, Sarstedt, Germany) and re-dissolved in ROCKi supplemented stage 4 culture medium. The cell suspension was centrifuged at 110xg for 3 min at room temperature, and the resulting cell pellet was re-suspended as single cells at a density of 50,000 cells/µl. 10 µl of cell suspension was added as a spot on a polyester membrane filter (0.4 µm) insert pre-loaded in 6-well culture plate (Corning Inc., USA). Under the filter insert, the well of the 6-well plate was filled with MCDB 131 supplemented with 20 mM glucose, 1.5 g/l sodium bicarbonate, 2 mM L-glutamine, 2% (w/v) BSA,0.25 µM SANT-1, 0.05 µM retinoic acid, 100 nM LDN193189, 0.5% (v/v) ITS-X, 1 µM T3 (3,3′,5-Triiodo-L-thyronine sodium salt; Sigma-Aldrich), 10 µM Repsox (Sigma-Aldrich), 10 µM zinc sulphate (Sigma-Aldrich), and 10 µg/ml of heparin (Sigma-Aldrich). Thus, the cells were allowed to grow at an air-liquid interface for three days. Culture medium was changed every day.

Stage-6 (*NKX6.1$^+$/insulin$^+$ cells*): Fifteen days were required for this stage. On day 14, stage-5 cells were incubated for the first 7 days with MCDB 131 supplemented with 20 mM glucose, 1.5 g/l sodium bicarbonate, 2 mM L-glutamine, 2% (w/v) BSA, 100 nM LDN193189, 0.5% (v/v) ITS-X, 1 µM T3, 10 µM Repsox, 10 µM zinc sulphate, 100 nM gamma secretase inhibitor XX (Merck Millipore, UK); and further supplemented with 10 µg/ml heparin from day 8 to day 15. Culture medium was changed every day.

Stage-7 (*NKX6.1$^+$/insulin$^+$/MAFA$^+$cells*): Another fifteen days were required for this final stage. On day 29, stage-6 cells were cultured in MCDB 131 supplemented with 20 mM glucose, 1.5 g/l sodium bicarbonate, 2 mM L-glutamine, 2% (w/v) BSA, 0.5% (v/v) ITS-X, 1 µM T3, 10 µM Repsox, 10 µM zinc sulfate, 1 mM N-acetyl-L-cysteine (Sigma-Aldrich), 10 µM Trolox (Merck Millipore, UK), and 2 µM R428 (Selleckchem, USA) for first 7 days and further supplemented with 10 µg/ml of heparin from day 8 to day 15. Culture medium was changed every day.

5-stage differentiation protocols

The first four stages of this protocol are similar to the first four stages of the 7-stage protocol mentioned above. In this method, stage-4 cells were differentiated directly to insulin-producing cell clusters. In brief, on day 11, stage-4 cells were detached using 1x Versene and cell scraper following the procedures mentioned above in stage-5. The dissociated cells were pipetted gently into cell clumps. The cell clumps were then transferred to an ultra-low attachment 6-well plate (Corning Inc., USA) containing DMEM high glucose (Thermo Fisher Scientific) supplemented with 10 µM Repsox, 100 nM LDN193189, 1 µM T3, 100 nM gamma-secretase inhibitor XX, 10 µg/ml heparin, and 1% (v/v) B27 (Thermo Fisher Scientific) and incubated for 7 days.

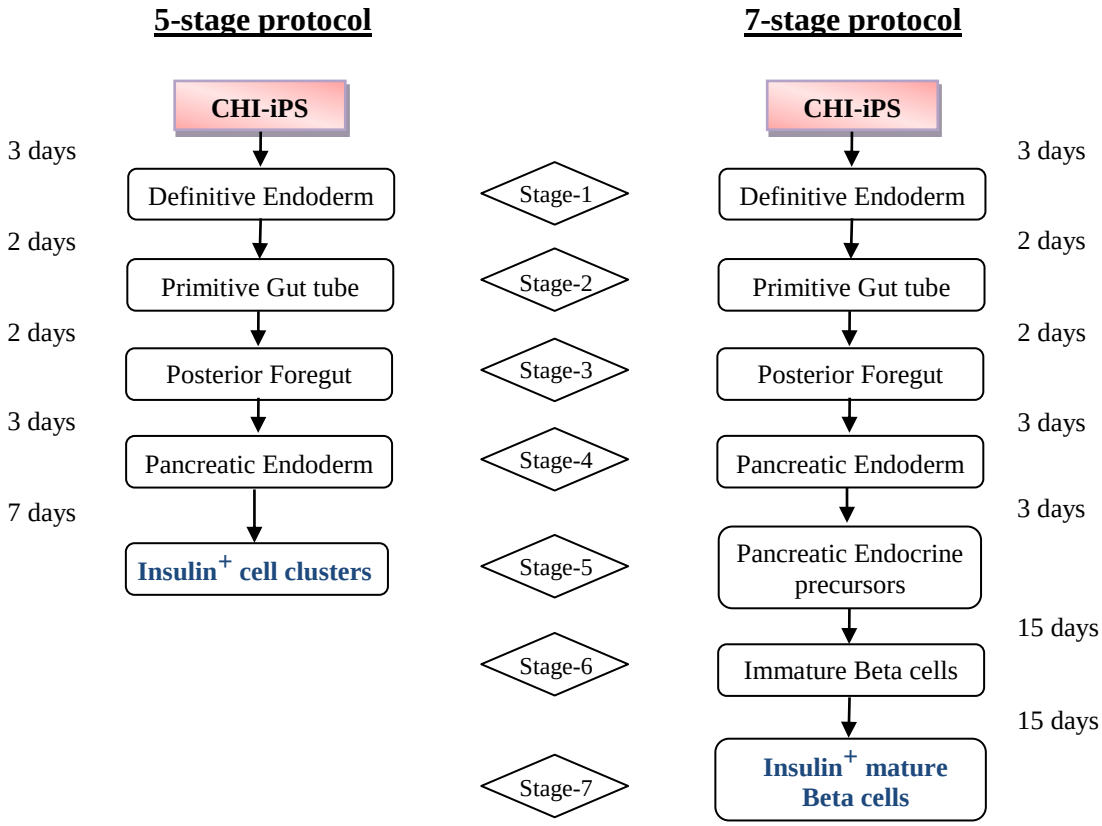

Figure 2.3: **A typical diagram of different steps to differentiate CHI-iPS cells into insulin-producing cells.** Both 5-stage and 7-stage protocols are illustrated here. In both protocols, treatments of CHI-iPS cells in the first four stages are similar. The 5-stage protocol ends with insulin^{+} islet-like cell clusters, and the protocol requires 17 days. On the other hand, the 7-stage protocol ends with insulin^{+} mature beta cells. This protocol requires 43 days.

2.8 Gene knock-out using CRISPR-Cas9 gene editing method

2.8.1 Experimental design

Experiments were designed for introducing a site-specific mutation in the *ABCC8* gene (G21350A) in CHI-iPS cells, and for introducing a random deletion mutation in both the *ABCC8* (exon 2) and the *KCNJ11* (exon 1) genes in EndoCβH1 cells. To carry out editing experiments, it is necessary to design effective guide RNA (gRNA) and single-stranded oligonucleotide (ssODN) (as appropriate). The experiments for this knockdown approach were designed with the support of the Transgenic Unit, the University of Manchester, UK. The overall steps of the gene editing experiments are depicted as a schematic diagram (Figure 2.4).

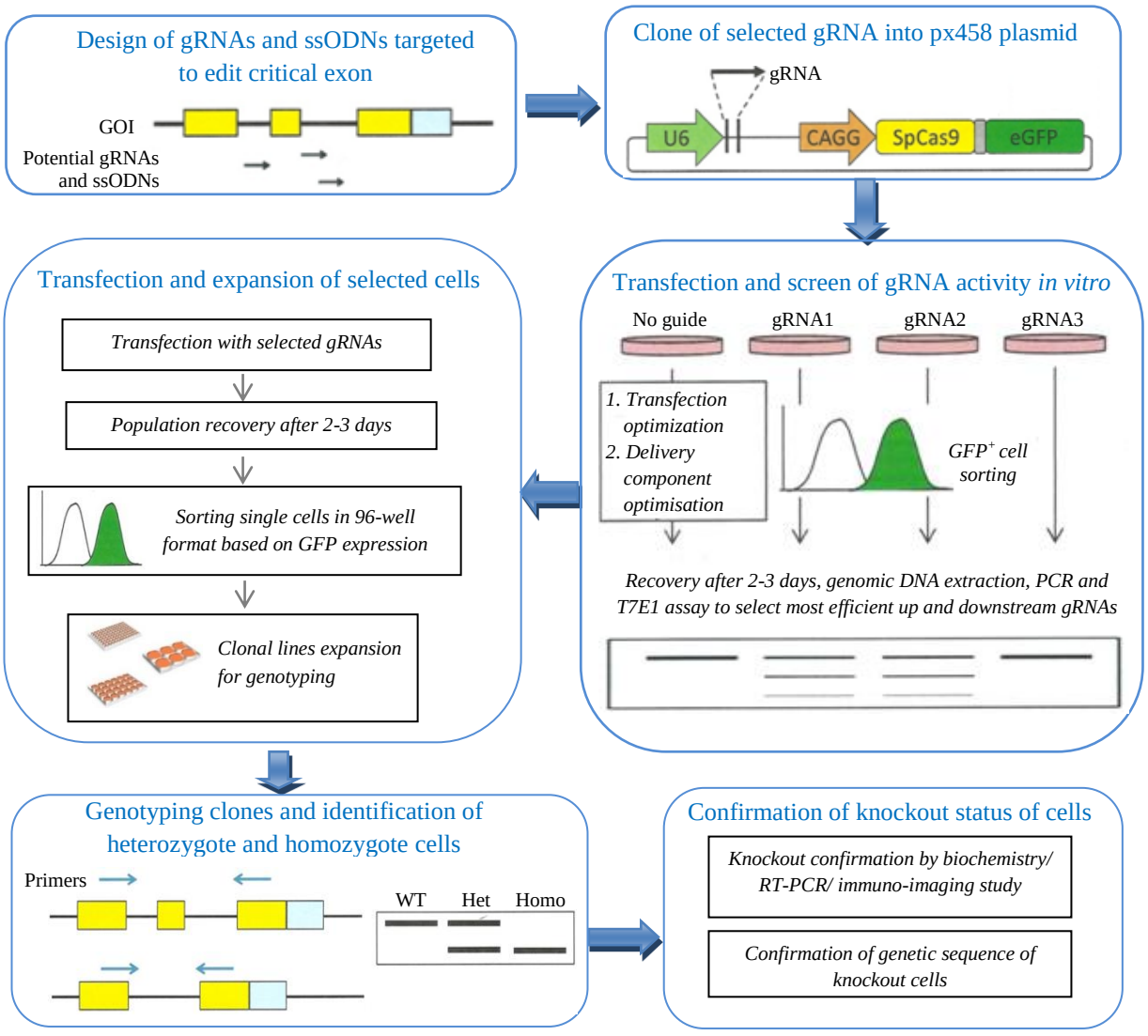

Figure 2.4: **Schematic diagram of the critical steps of CRISPR-Cas9 mediated knockout experiments**. The CRISPR-Cas9 method offers an efficient and reliable means to introduce targeted changes to the genome of living cells. The major components of this gene-editing system include a non-specific endonuclease (Cas9) and target sequence-specific guide RNAs (gRNA). gRNAs can bind to target DNA sequences because of sequence complementarity. Cas9 can recognise the gRNA-DNA complex and can introduce a DNA double-strand break (DSB) at the target. This DNA damage is then repaired by the host repair pathways. The repair mechanism can either introduce precise target mutations or can introduce unpredictable random mutations like insertion, deletion, or frameshifting depending on the repair pathways. Designing potential guide RNAs (gRNAs) and single-stranded oligonucleotides (ssODNs) (required for introducing precise target mutations) is the most important step of this gene-editing experiment. The potential gRNAs are cloned into transfer vectors and analysed for their editing efficiency in target cell lines. Based on the analysis, suitable gRNAs were selected and transfected (with ssODNs, for site-specific mutation introduction) into the cells. Transfection-positive cells are then sorted as single cells and allowed to propagate clonally. Clonal cell lines with target gene modification are selected through genotyping and allowed to propagate for downstream experiments.

2.8.2 Design and cloning of gRNAs targeted to edit critical exon

gRNAs against target genomic loci were designed with the help of the Genome Editing Services at the Transgenic Unit, the University of Manchester, UK. Briefly, gRNAs were designed to flank a critical exon of the gene of interest. Transfection of a combination of guides would result in the removal of this exon and knockout of the gene by deletion and/or frameshift mutation. To introduce a precise mutation in the target gene, ssODNs were designed and transfected along with gRNAs which upon excision would repair the DNA directed by the ssODN.

gRNAs and ssODNs were designed using the web tool developed by the Sanger Institute and available at http://www.sanger.ac.uk/htgt/wge/. gRNAs were designed in a way to minimize the potential off-site genomic mismatches (Ran *et al*, 2013; Kim *et al*, 2014).

The CHI-iPS cell line is heterozygous with an *ABCC8* exon-6 mutation. CRISPR oligonucleotides were designed to introduce a second mutation (homozygous) at the mutated locus of the *ABCC8* gene. Effective gRNAs were designed to delete critical

exons of *ABCC8* and *KCNJ11* genes in EndoCβH1 cell line. *ABCC8* is a multi-exonic gene. It contains 39 exons, and it is 83961 bp in length. Among all the exons, exon 2 shows well-conserved sequences and thus, was predicted to be a critical exon of the gene. Hence, the gRNAs for *ABCC8* were designed to splice out the exon 2 in EndoCβH1 cells. On the other hand, *KCNJ11* is a small gene with 4086 bp length, and it has only one coding exon. Therefore, gRNAs for *KCNJ11* were designed against this exon to introduce a deletion mutation. Designed gRNA sequences and ssODNs are provided in Table 2.9.

Table 2.9: **List of gRNAs and ssODNs used in this study**

Cell line	***Oligonucleotides***	***Sequences (5′ → 3′)***
CHI-iPS	*ABCC8*_gRNA1	GCCGACCTGCTGGGCTTCGC
	*ABCC8*_gRNA2	CCGACCTGCTGGGCTTCGCC
	*ABCC8*_ssODN	GCCATCTGGCAGGCACTCAGCCAT GCCTTCGGGAGGCGCCTGGTCCTC AGCAGCACTTTCCGCATCTTGGCCG ACCTGCTGGGCTTCGCCAGGCCACT GTGCATCTTTGGGATCGTGGACCA CCTTGGGAA
EndoCβH1	*ABCC8*_gRNA1	TAGTTTGTGTGTACCAGCCT
	*ABCC8*_gRNA2	TGTAGGTGTCACCCTCACCA
	*ABCC8*_gRNA3	GGGCCTTTCAGGAAGTACCC
	*ABCC8*_gRNA4	GGATGTAGTAACAAAAGACA
	*KCNJ11*_gRNA1	GAGGCTGGTATTAAGAAGTG
	*KCNJ11*_gRNA2	GAGGCCCTAGGCCACGTCCG
	*KCNJ11*_gRNA3	AACACCCTGGATGAGCAGCA
	*KCNJ11*_gRNA4	AGTGTGGCTGGTCAATCGTG

Selected guides were cloned into expression vector pSpCas9(BB)-2A-GFP (PX458) (plasmid # 48138, Addgene, USA) (Figure 2.5). According to the protocol described by Ran *et al*. (2013), the cloned vector was then transformed, sequence verified, and supplied as mini-prepped DNA by the Transgenic unit, University of Manchester, UK.

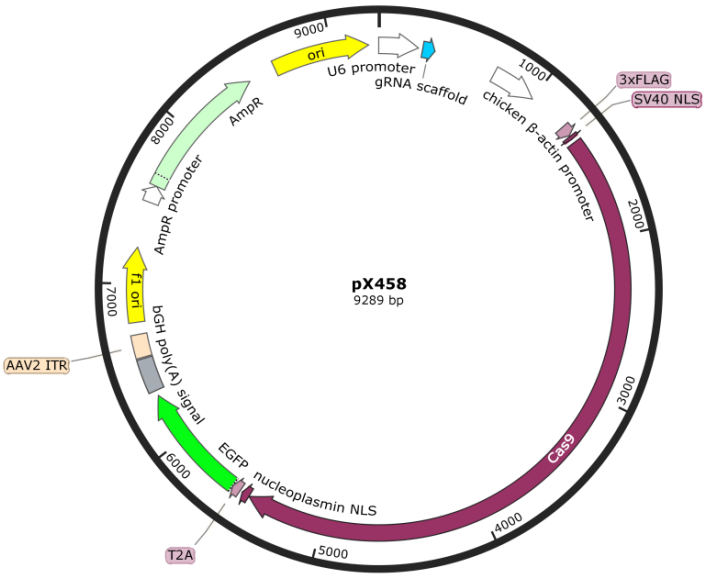

Fig: 2.5 **Schematic map of the expression vector pX458 used in CRISPR-Cas9 mediated gene editing experiments**. The image was drawn using SnapGene 3.3.3 software (SnapGene, USA).

2.8.3 Transformation and cloning of plasmids, encoding gRNAs

The supplied mini-prepped plasmid was not in sufficient amount to carry out the optimisation and downstream experiments. Hence, the amount of plasmid was amplified using bacterial transformation system.

2.8.3.1 Preparation of competent bacterial cells

E. Coli DH5α Cells are a renowned, versatile strain that is very amenable to competence and can be used in numerous cloning applications. The procedure, in brief, DH5α cells were grown in 5 ml Luria-Bertani (LB) medium (purchased from Media preparation and decontamination facility, University of Manchester, UK) overnight at 37°C with 150 rpm continuous shaking (ES-20 Shaker-incubator, Grant Instruments Ltd., UK). 1 ml of the overnight culture was then transferred into 100 ml LB medium and incubated at 37°C with 250 rpm continuous shaking for 3 hours. After that, the culture was placed in an ice bath for 10 minutes. The chilled culture was then transferred to a pre-chilled 50 ml

polypropylene tube (Corning Inc., USA) and the cells were pelleted by centrifugation (Hettich BOECO U-32, Germany) at 4000 rpm, 4°C for 10 minutes. The supernatant was discarded, and the pellet was then resuspended very gently in ice-cooled 100 mM $CaCl_2$ and incubated on ice for 10 minutes. The cells were pelleted again by centrifugation at 4000 rpm, 4°C for 10 min. The resuspension in ice-cooled 100 mM $CaCl_2$, followed by centrifugation steps were carried out once again with the cell pellet. Finally, the cells were resuspended in 1ml (for each 100 ml culture) ice-cooled 100 mM $CaCl_2$ solution containing 25% glycerol. 50 µl of cell suspension was aliquoted in pre-chilled 1.5 ml microcentrifuge tube and stored in -80°C freezer for long-term preservation.

2.8.3.2 Transformation of competent DH5α with plasmids, encoding gRNAs

The previously frozen competent DH5α cells in a microcentrifuge tube were thawed on ice for 5-10 minutes. 2 µl of a plasmid, encoding a gRNA, was added to the bacterial solution and incubated on ice for 5 minutes. The cells were then challenged with heat shock in a 42°C water bath for exactly 1 minute, and immediately the cells were transferred on ice and incubated for 5 minutes. 500 µl of LB media was added to the tube, and the cell suspension was incubated at 37°C for 1 hour with 220 rpm continuous shaking. The cells were then pelleted by centrifugation (Minispin Plus, Eppendorf, UK) at 8000xg for 2 min at room temperature. 400 µl of the supernatant was discarded, and the cell pellet was resuspended again in the remaining media. The cells were then spread on culture plate made of LB media with agar (LA) supplemented with ampicillin antibiotic (100 µg/ml) and incubated overnight in a 37°C incubator (Mini incubator, Labnet International, USA). On next day, a single colony of transformed cells were picked and further cultured overnight in a 37°C incubator for downstream applications.

2.8.3.3 Plasmid isolation from transformed cells for transfection experiments

Plasmids were isolated only from fresh overnight cultures and by using Plasmid mini kit (Qiagen Ltd., UK) following the recommended protocol of the manufacturer. In brief, a single colony of transformed DH5α bacteria from a freshly overnight culture was picked, inoculated into a 50 ml LB medium with ampicillin (100 µg/ml) and incubated at 37°C overnight with 250 rpm continuous shaking (ES-20 Shaker-incubator, Grant Instruments Ltd., UK). After incubation, the cells were harvested by centrifugation (Hettich BOECO U-32, Germany) at 6000xg for 15 min at 4°C. After discarding the supernatant, the cell

pellet was resuspended completely in 0.3 ml of Buffer P1 that contain RNase A (100 µg/ml). 0.3 ml Buffer P2 was added to the solution, mixed vigorously by inverting the tube several times, and then incubated at room temperature for 5 minutes. After that, 0.3 ml of pre-chilled Buffer P3 was added, mixed thoroughly by inverting the tubes several times, and then incubated on ice for 5 minutes. The solution was then centrifuged (PrismR, Labnet International, USA) at 13,000 rpm for 10 minutes at 4°C. In the meantime, a Qiagen-tip 20 column filter was equilibrated by adding 1 ml Buffer QBT into the column and allowing the column to be empty by gravitational force. From the centrifuged solution, the supernatant was carefully transferred to the equilibrated column and allowed the solution to pass through the resin filter by gravity flow. The column was then washed twice with supplied Buffer QC, followed by elution of plasmid DNA with Buffer QF. The eluted plasmid solution was then mixed thoroughly with 0.7 volumes of isopropanol (room temperature) and then precipitated by immediate centrifugation at 15000xg for 30 minutes. The supernatant then decanted carefully, and the pellet was washed with 70% ethanol and centrifuged at 15000x g for 10 minutes. The washed plasmid pellet was dried completely by leaving it open for 10-15 minutes in air and then finally redissolved in a suitable volume of TE buffer. The dissolved plasmid DNA was then kept at -20°C for long-term storage.

2.8.4 Transfection of cells with CRISPR gRNAs

2.8.4.1 CHI-iPS cell transfection

To transfect CHI-iPS cells with plasmids, electroporation-based Amaxa Primary Cell 4D-Nucleofector X Unit (Lonza, Switzerland) transfection system was found to be the most efficient. The optimised protocol, in brief, the iPS cells were grown in 6-well plates (Corning Inc., USA) following the protocol mentioned above (section 2.1.2.3) until the cells reached 70-80% confluency. On the day of nucleofection, the used medium was replaced with fresh growth medium supplemented with ROCKi (Sigma-Aldrich) and incubated for about 1 hour at 37°C. In the meantime, culture plates were coated, and nucleofection reagents were prepared. Wells of the 6-well plates were coated with Matrigel Basement Membrane Matrix (Scientific Laboratory Supplies, Corning Inc., USA) in 1:30 dilution. Fresh nucleofection reagent was prepared by adding P3

supplement to the P3 nucleofector solution (Lonza, Switzerland) in 1:4.5 ratio. For a transfection reaction, 2.5 µg of gRNA- encoding plasmid and 200 pmole of ssODN were mixed in a total of 20 µl of complete nucleofection reagent. After the 1 hour incubation, the spent culture medium was removed, and the cells were washed with PBS once. Then the cells were incubated with Accutase (STEMCELL Technologies, UK) at 37°C for 5-6 minutes to detach the edge of the cell clusters. After removal of Accutase solution, the cells were detached from the surface by adding. The cells were resuspended properly to make a single cell suspension. 500,000 cells (per well of 6-well plate) were collected for each reaction by centrifugation at 110xg (Hettich BOECO U-32, Germany) for 3 min at room temperature and re-suspended in 80 µl of complete nucleofection reagent. 20 µl of plasmid solution was combined promptly to this 80 µl of cell suspension, and the whole mixture was transferred into a nucleocuvette. The nucleocuvette was placed into the nucleofection chamber and pre-set program CB-150 was run. The nucleofected cells in the nucleocuvette were incubated 10 min at room temperature. The cells were then mixed with pre-warmed growth medium supplemented with ROCKi, transferred to a pre-coated well of the culture plate, and incubated at 37°C for 24 hours. After the incubation, The spent medium was replaced with fresh culture medium (without ROCKi supplementation) and incubated at 37°C for another 24 hours. One set of transfected cells were used for validation of transfection using BstNI (New England Biolabs, UK) restriction enzyme profiling (protocol is described in section 2.8.5.3) and the other set of transfected cells were sorted as single cell (protocol is described in section 2.8.6) in 96-well plate (Corning Inc., USA) and incubated at 37°C for clonal propagation.

In addition, in an attempt to introduce deletion mutation in *ABCC8* gene, CHI-iPS cells were also transfected with the plasmids encoding the gRNAs against the gene (designed for EndoCβH1 cell line) using Amaxa transfection system following the protocols mentioned above.

2.8.4.2 EndoCβH1 cell transfection

A number of commercially available transfection reagents were explored to find out the most efficient method to transfect EndoCβH1 cells with the plasmid DNA. Lipid-based ViaFect (Promega, UK) transfection reagent was found most effective compared to other reagents. The optimised protocol, in brief, the cells were grown in 6-well plates (Corning

Inc., USA) with 3x seeding density for 24 hours. On the day of transfection, fresh transfection complex was prepared by adding plasmids and Viafect transfection reagent into serum-free Opti-MEM (Thermo Fisher Scientific) medium in a fresh tube and incubating at room temperature for 10 minutes. For a single well of a 6-well plate, 5 µg of plasmid DNA was found to be better effective. For transfection with two plasmids encoding two gRNAs, 2.5 µg of each plasmid was added. For 1 µg of plasmid DNA, 3 µl of ViaFect transfection reagent was most effective to form the complex and overall transfection.

The used medium from the cell culture was replaced with 1 ml serum-free Opti-MEM medium, followed by, 250 µl of transfection complex was added to the culture. The plate was swirled gently for a few times and then incubated at 37°C for not more than 12 hours. After the incubation period, the used medium was replaced with fresh growth medium and incubated at 37°C for 48 hours. One set of transfected cells were used for validation of transfection using T7 nuclease digestion (protocol is described in section 2.8.5.4) and another set of transfected cells were sorted as single cell (protocol is described in section 2.8.6) in 96-well plate (Corning Inc., USA) and incubated at 37°C for an attempt of clonal propagation.

In some experiments, a plasmid, encoding a puromycin resistance gene, was used to select transfected clones. On those occasions, 1.5 µg of each of the two plasmids containing gRNAs and 2 µg of puromycin-encoding plasmid was added to form the complex with ViaFect reagent.

As mentioned, a number of transfection reagents from different vendors were explored in different combinations. The purpose was to find out the most suitable condition which would offer the highest yield of transformed cells. The different combinations investigated in this study are listed in Table 2.10.

Table 2.10: **List of transfection reaction conditions explored in this study (for 24-well plate)**

Lipofectamine 3000 (Thermo Fisher Scientific)		
Cell seeding density	*Plasmid DNA (µg)*	*P3000 reagent (µl)*
1x / 2x / 3x	1	1 / 1.5 / 2 / 3 / 5
1x / 2x / 3x	2	1 / 2 / 4 / 6 / 10
1x / 2x / 3x	3	3 / 6 / 9
Lipofectamine LTX (Thermo Fisher Scientific)		
Cell seeding density	*Plasmid DNA (µg)*	*LTX reagent (µl)*
1x / 2x / 3x	1	2 / 3 / 4 / 5
1x / 2x / 3x	2	2 / 3 / 4 / 5
1x / 2x / 3x	3	3 / 5 / 6
ViaFect (Promega, UK)		
Cell seeding density	*Plasmid DNA (µg)*	*transfection reagent (µl)*
1x / 2x / 3x	1	1 / 2 / 3 / 5
1x / 2x / 3x	2	1 / 2 / 4 / 6 / 10
1x / 2x / 3x	3	3 / 6 / 9
FuGENE HD (Promega, UK)		
Cell seeding density	*Plasmid DNA (µg)*	*transfection reagent (µl)*
1x / 2x / 3x	1	1 / 2 / 3 / 5
1x / 2x / 3x	2	1 / 2 / 4 / 6 / 10
1x / 2x / 3x	3	3 / 6 / 9
Amaxa Nucleofector P3 (Lonza, Switzerland)		
Cell seeding density	*Plasmid DNA (µg)*	
1x / 2x / 3x	1 / 2 / 3	
Amaxa Nucleofector R (Lonza, Switzerland)		
Cell seeding density	*Plasmid DNA (µg)*	
1x / 2x / 3x	1 / 2 / 3	

2.8.5 Validation of transfection

2.8.5.1 DNA purification from cultured cells

Genomic DNA of the cells was isolated using the QIAamp DNA Mini Kit (Qiagen Ltd., UK) according to the manufacturer's protocol. In brief, cells were detached from the culture flask/plates and collected as cell pellet following the protocols described above (section 2.1.2.1 for EndoCBH1, section 2.8.4.1 for CHI-iPS). The pellet was washed once with DPBS (without $MgCl_2$ and $CaCl_2$) (Sigma-Aldrich). The cell pellet was resuspended in DPBS to a final volume of 200 µl, and 20 µl of proteinase K was added to the suspension. Followed by, 200 µl of Buffer AL was added to the sample, mixed by pulse-

vortexing for 15 seconds and incubated at 56°C for 10 minutes. After incubation, 200 µl ethanol (98%) (Sigma-Aldrich) was added to the sample and mixed again by pulse-vortexing for 15 s. Then, the mixture was carefully transferred to the QIAamp Spin Column (in a 2 ml collection tube) and centrifuged (Minispin Plus, Eppendorf, UK) at 8000 rpm for 1 minute. The filtrate was discarded, 500 µl of Buffer AW1 was added into the column and centrifuged again with the same condition. The filtrate was discarded again. 500 µl of Buffer AW2 was added into the column and centrifuged at 14,000 rpm for 3 minutes. Finally, the column was placed in a clean microcentrifuge tube, 150 µl Buffer AE was added and incubated at room temperature for 1 minute. Then the tube was centrifuged at 8000 rpm for 1 minute to elute the genomic DNA into the tube. The extracted DNA was then stored at -20°C.

2.8.5.2 Amplification of target region by PCR and purification of the amplicon

The target areas of the gene of interests were amplified through PCR by using specific primers designed against the flanking regions of mutation sites. All of the primers were designed, purchased and processed using the protocol mentioned above (section 2.3.1). The primer sequences for the validation study are mentioned in Table 2.11.

Table 2.11: **List of PCR primers used in transfection validation studies**

Gene	***Primer orientation***	***Primer sequences (5′ → 3′)***	***Annealing temperature (°C)***
ABCC8 (exon 6)	Forward	AGGCCCAGCCGTGAATTAG	58
	Reverse	AGAGTAGGATACCCTTGGGGC	
ABCC8 (exon 2)	Forward	CATTTTGGTGGGCTGTGACA	60
	Reverse	TTGAATGGTGGGCTGAGGAT	
KCNJ11	Forward	GACCTAGTGATCTGCCCTCC	62
	Reverse	GATTGTTCTTCCCCAGCCAC	

PCR was performed in a Veriti Thermal Cycler (Applied Biosystems, Thermo Fisher Scientific) using reagents from Invitrogen (Thermo Fisher Scientific). The reaction composition is mentioned above (Table 2.1). The reaction conditions were as follows: an initial denaturation at 94°C for 5 minutes, then 35 cycles each with denaturation at 94°C for 30 seconds, annealing for 30 seconds, and elongation at 72°C for 45 seconds followed by a final extension at 72°C for 5 minutes.

Successful PCR was confirmed by electrophoretically separating the products on a 1.5% agarose gel following the protocol mentioned in section 2.3.3. After electrophoresis, DNA bands in the gel were observed and photographed using a UV gel documentation system (Biorad Chemidoc MP imaging system, Bio-Rad Laboratories, USA).

The PCR products were purified using a PCR purification kit (QIAquick, Qiagen, UK) according to the manufacturer's protocol described in section 2.3.4. The concentration of PCR products was measured using the NanoDrop ND-2000 UV-Vis spectrophotometer (Thermo Fisher Scientific) following the manufacturer's protocol.

2.8.5.3 CHI-iPS cell transfection validation

Following the CRISPR homology-directed repair, substitution mutation was introduced in the cells which changed the restriction enzyme cutting site recognised by BstNI (New England Biolabs, UK) (Figure 2.6). The protocol, in brief, 300 ng of purified PCR amplicon was added to in total of 25 µl solution that contained 1x NEBuffer 3.1 and 10 units of BstNI enzyme. The solution was incubated at 60°C in a water-bath for 60 minutes to digest the DNA. The digested product was then checked electrophoretically on a 3% agarose gel following the protocol mentioned in section 2.3.3. After electrophoresis, DNA bands in the gel were observed and photographed using a UV gel documentation system (Biorad Chemidoc MP imaging system, Bio-Rad Laboratories, USA).

2.8.5.4 EndoCβH1 cell transfection validation

Following the CRISPR editing strategy, indel mutations were introduced in the cells, and this Cas9 induced deletion can be assessed by T7 endonuclease I (T7EI) assay. T7EI (New England Biolabs, UK) recognises and cleaves mismatched heteroduplex DNA which arises from hybridisation of wild-type and mutant DNA strands (Figure 2.6). The protocol in brief, 200 ng of purified PCR amplicon was added to in total of 10 µl annealing buffer (10 mM Tris HCl pH 7.5, 50 mM NaCl, 1 mM EDTA) and performed hybridization reaction in a Veriti Thermal Cycler (Applied Biosystems, Thermo Fisher Scientific) subjected to the following reaction conditions: 95°C for 10 minutes, 95–85°C at −2°C/second, 85°C for 1 minute, 85–75°C at −2°C/second, 75°C for 1 minute, 75–65°C at −2°C/second, 65°C for 1 minute, 65–55°C at −2°C/second, 55°C for 1 minute, 55–45°C at −2°C/second, 45°C for 1 minute, 45–35°C at −2°C/second, 35°C for 1 minute, 35–25°C

at −2°C/second, 25°C for 1 minute, and hold at 4°C. After the hybridisation reactions, 1x NEBuffer 2 and 5 units of T7EI were added to the hybridised sample in a reaction volume of 20 µl. The mixture was then incubated at 37°C in a water-bath for 30 minutes to digest the re-annealed DNA. The digested product was then checked electrophoretically on a 3% agarose gel following the protocol mentioned in section 2.3.3. After electrophoresis, DNA bands in the gel were observed and photographed by using a UV gel documentation system (Biorad Chemidoc MP imaging system, Bio-Rad Laboratories, USA).

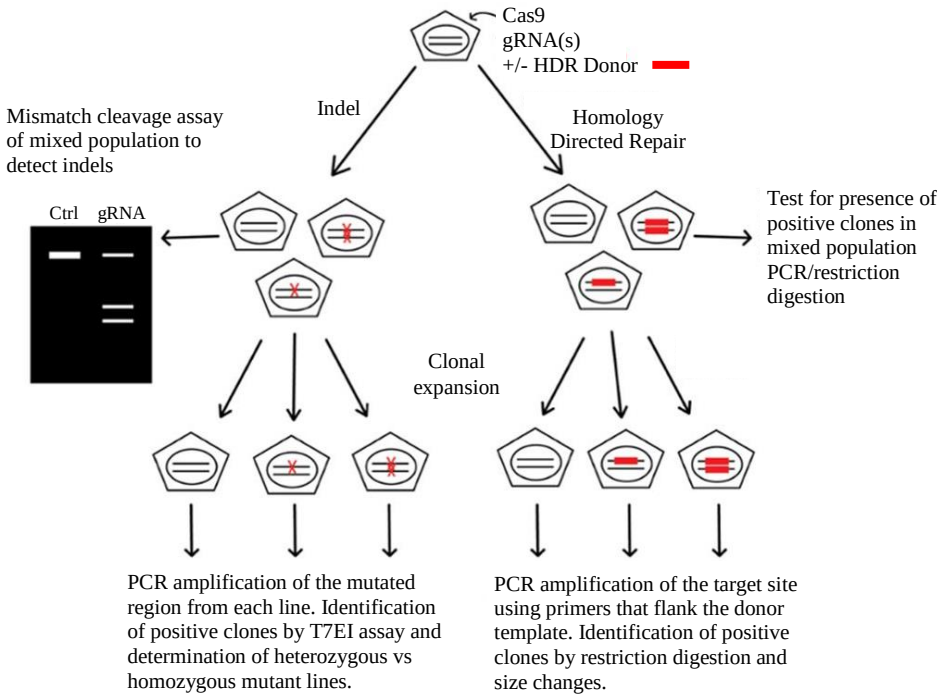

Figure 2.6: **Schematic workflow for the validation of CRISPR-Cas9 induced gene editing**. The CRISPR-Cas9-mediated gene editing method can introduce mutations in a proportion of cells in a cell population. For downstream experiments, the cells with target mutations need prior identification and validation. A single-stranded oligonucleotide (ssODN) is used as homology-directed repair donor where the precise mutation is required in the target locus of a cell. After confirming the presence of cells with target mutations in a cell population (through PCR or restriction digestion assay), the cells are clonally propagated. Clonal cells with target mutations are then identified by PCR or restriction digestion assay and can be used for further analyses. In the experiments where random mutations are introduced to knock-out the expression of a target gene, the presence of cells with mutations in a cell population are confirmed by T7 endonuclease I (T7EI) assay. The cells are then clonally propagated and clonal cells with target mutations are then identified by T7EI assay for further analyses.

2.8.6 Sorting potential edited cells

The cultured cells were detached and collected as cell pellet from the growing surface according to the protocol mentioned above (section 2.1.2.1 for EndoCβH1, section 2.8.4.1 for CHI-iPS). The cell pellet was resuspended thoroughly in a modified culture medium to make a single cell suspension. The growth medium composition was modified by not adding any serum and by having HEPES at a final concentration of 25 mM. The cell suspension was further diluted in a way to have the cell concentration in the range 5 x 10^6 per ml. The diluted cell suspension was then filtered through a 50-micron cup-type filter (Filcon, BD Biosciences, USA) and transferred to a 5 ml Falcon Round-Bottom Polypropylene Tube (Corning Inc., USA). The filtered cell suspension was then handed over to the Flow Cytometry Core Facility of the University of Manchester, UK. The cells were sorted based on the expression of the green fluorescent protein (GFP) using BD FACSARIA FUSION (BD Biosciences, USA). Finally, the sorted cells were collected either as single cell in wells of 96-well plate (Corning Inc., USA) and incubated at 37°C to allow the cells to grow, or collected altogether in a 15 ml polypropylene tube (Corning Inc., USA) to culture them normally as a mixed population for further analysis.

2.8.7 Clonal expansion of single CHI-iPS cell

From sorted GFP-expressing CHI-iPS cells, some clonal cell lines were established. The method in brief, 96-well plates were coated with Matrigel Basement Membrane Matrix (Scientific Laboratory Supplies, Corning Inc., USA) at 1:30 dilution. The sorted single cells were collected in wells of pre-coated 96-well plates containing growth medium supplemented with ROCKi. The cells were cultured in a 37°C incubator for 48 hours. After this incubation spent media were replaced with fresh growth medium (with ROCKi supplementation) very gently and incubated at 37°C for another 6 days. Eight days after sorting, used media were replaced with fresh usual growth media (without ROCKi supplementation) very gently and continued to grow at 37°C until sufficient confluency was achieved to sub-culture the cells. In this stage, the culture media were replaced in every other day.

Although the method mentioned above generated survived single cells, the cells lost their viability as a stem cell. So, some other methods were explored to generate viable iPS cells from the transfected single cells. The methods are as follows-

Option-1: Sorted single cells were cultured in normal culture media (with ROCKi supplementation) in Matrigel pre-coated 96-well plate at 37°C for 24/48 hours (in separate experiments), followed by replacement of used media by fresh medium (without ROCKi supplementation). The incubation was continued for 2-3 weeks.

Option-2: Sorted single cells were cultured in normal culture media (with ROCKi supplementation) in Matrigel pre-coated 96-well plate at 37°C for one/two weeks (in separate experiments) without changing growth medium, followed by replacement of used medium by fresh medium (without ROCKi supplementation). The incubation was continued in a total of three weeks.

Option-3: Sorted single cells were cultured in vitronectin (Gibco, Thermo Fisher Scientific) pre-coated (0.5 µg/cm^2) 96-well plates following the protocols mentioned option-1 and 2.

Option-4: Sorted single cells were cultured in normal culture media supplemented with small molecule cocktail of 4 inhibitors (SMC4) (1 µM Chir99021, 0.4 µM PD0325901, 2 µM SB431542, and 5 µM Thiazovivin) (all reagents from Sigma-Aldrich). The cells were cultured either Matrigel or Vitronectin pre-coated 96-well plates following the protocol similar to option-1 and 2.

Option-5: Sorted single cells were cultured with Cellartis DEF-CS Xeno-Free Culture medium (Takara Bio Inc, Japan). 96-well plates were pre-coated with Matrigel or Vitronectin or iMatrix-511 (0.5 µg/cm^2) (Clontech, Takara Bio inc., Japan) (in separate experiments). Sorted single cells were seeded in pre-coated plates and cultured at 37°C for 3 weeks. The culture media were replaced in every 48 hours.

Option-6: The cells were co-transfected with puromycin encoding plasmid (PX459, V2.0) (Addgene plasmid # 62988) and were cultured in growth medium supplemented with puromycin (2 µg/ml) for 48 hours to select puromycin-resistant cells only. In one approach, the survived cells were seeded as single cells in 96-well plates by limiting dilution (0.8 cell per well) and cultured following option-1 to 5 in separate experiments. In another approach, single cells were isolated using Scienceware cloning cylinders (Sigma-Aldrich) or Scienceware cloning discs (Sigma-Aldrich) following manufacturer's

protocol. In brief, the location of the target cell to isolate was marked with a marker pen on the bottom of the culture plate with the help of a microscope (Olympus CKX1 inverted microscope, Olympus Corporation, Japan). The growth medium was removed and cells were washed with DPBS twice. To use a cloning cylinder, the cylinder was placed over a single cell and pressed gently to attach the cylinder to the surface firmly. Then the cell was detached using Accutase inside the cylinder, transferred to a well of 96-well plate (Corning Inc., USA) and allowed to grow at 37°C following the protocols mentioned in option-1 to 5. To use a cloning disc, the disc was first soaked in the Accutase solution and then placed on the marked cell. The cell was then incubated at 37°C for 5 minutes. After incubation, the disc was picked out from the plate and placed in a well of 24-well plate (Corning Inc., USA). Since the cell adhered to the discs after detachment, so it was transferred to the individual well. The cell was then incubated at 37°C and allowed to grow following the protocols mentioned in option-1 to 5.

2.8.8 Clonal expansion of single EndoCβH1cell

A number of methods were explored to expand clonal cells to establish as cell lines. However, none of them was successful. Some of the methods that were used to culture single EndoCβH1 cells are as follows-

Method-1: Single cells were sorted either by FACS or limiting dilution (0.8 cell per well) and cultured in normal growth media in 24-/ 96-well plate at 37°C for up to 12 weeks with the replacement of used medium by the fresh medium in every 5 days.

Method-2: Single cells were sorted either by FACS or serial dilution and cultured in normal growth media in 24-/ 96-well plate at 37°C for up to 2 weeks without media replacement. Then, spent media was replaced by the fresh medium in every 5 days for up to 12 weeks.

Method-3: Single cells were sorted either by FACS or serial dilution and cultured with previously used normal culture media in a 24-/ 96-well plate at 37°C for either 5 days or 2 weeks without media replacement (in separate experiments) (like method -1 and 2). Then, spent media was replaced by the fresh medium in every 5 days for up to 12 weeks.

Method-4: Single cells were sorted either by FACS or serial dilution and cultured with growth medium supplemented with either ROCKi or SMC4 following the protocol for method-1 and 2.

Method-5 The cells were transfected with puromycin encoding plasmid (PX459, V2.0) (Addgene plasmid # 62988) and were cultured in growth medium supplemented with puromycin (4 µg/ml) for 48 hours to select puromycin-resistant cells only. After 48 hours, the spent medium was replaced with fresh growth medium (without puromycin supplementation) and were cultured for 5 more days. From the survived cells, single cells were sorted following the methods described in option-6 for CHI-iPS cells and cultured following the protocols for method-1 to 4 for EndoCβH1

2.9 Gene knock-down experiments using short interfering RNAs

Pre-designed Silencer Select Short interfering RNA (siRNAs) (Ambion, Thermo Fisher Scientific) was used to transiently knockdown the expression of *KCNJ11* gene in EndoCβH1 cells. The protocol, in brief, the cells were seeded 2x concentration in a pre-coated well of a 6-well plate (Corning Inc., USA) and allowed to grow at 37°C for 24 hours. Before transfection, siRNA solutions were freshly prepared. 5 µl of siRNA solution (of 10 µM stock) was diluted into 250 µl of serum-free Opti-MEM medium (Gibco, Thermo Fisher Scientific). 15 µl of lipid-based Lipofectamine RNAiMAX reagent (Invitrogen, Thermo Fisher Scientific) was diluted into 250 µl of Opti-MEM medium. 250 µl of diluted siRNA solution was mixed with 250 µl of diluted RNAiMAX reagent and incubated at room temperature for 10 minutes to make siRNA-lipid complex. After the incubation, the used growth medium was replaced with 1 ml of fresh growth medium, and 250 µl of the siRNA-lipid complex solution was added to it. The cells were then incubated at 37°C for 72 hours. After that, the used growth medium with siRNA-lipid complex was replaced with fresh growth medium containing freshly prepared siRNA-lipid complex solution following the above-mentioned method and incubated at 37°C for another 72 hours. This two 3-day phases of treatment were found to be the most efficient to knock-down the gene in this cell line. Further treatment of the cells with the siRNA reagent was observed to be fatal for the cells.

2.10 GSIS assay of siRNA-based knocked down EndocβH1 cells

The cells were seeded 2x concentration in a pre-coated well of a 96-well plate (Corning Inc., USA) and allowed to grow at 37°C for 24 hours. Before transfection, siRNA solutions were freshly prepared. 0.5 µl of siRNA solution (of 10 µM stock concentration) was diluted into 25 µl of serum-free Opti-MEM medium (Gibco, Thermo Fisher Scientific). Also, 1.5 µl of lipid-based Lipofectamine RNAiMAX reagent (Invitrogen, Thermo Fisher Scientific) was diluted into 25 µl of Opti-MEM. 25 µl of diluted siRNA solution was mixed with 25 µl of diluted RNAiMAX reagent and incubated at room temperature for 10 minutes to make siRNA-lipid complex. After the incubation, the used growth medium was replaced with 80 µl of fresh growth medium, and 20 µl of the siRNA-lipid complex solution was added to it. The cells were then incubated at 37°C for 72 hours. After that, the used growth medium with siRNA-lipid complex was replaced with fresh growth medium containing freshly prepared siRNA-lipid complex solution following the above-mentioned method and incubated at 37°C for another 72 hours. Finally, the transfected cells were used for GSIS assay following the protocol mentioned in section 2.6.

2.11 Gene expression microarray analysis of CHI tissues

Pancreatic tissues from CHI patients were freshly collected after surgery from Royal Manchester Children's Hospital, Manchester, UK. Total RNAs of the tissues were isolated using TissueLyser II (Qiagen Ltd., UK) and ISOLATE II RNA Mini Kit (Bioline, UK). The protocol in brief- 30 mg of individual tissues were weighed out and added to 600 µl of buffer RLY (containing 6.5 µl β-mercaptoethanol). The tissues were then placed in the TissueLyser adapter set, and the TissueLyser was operated twice for 2 min at 20–30 Hz. The tissue lysates were then transferred to ISOLATE II filters and centrifuged for 1 minute at 11000xg using a benchtop centrifuge machine (Minispin Plus, Eppendorf, UK). One volume of 70% ethanol (Sigma-Aldrich) was added to the homogenized lysates, mixed properly by pipetting and then the lysates were transferred to ISOLATE II RNA mini columns allowing the RNAs to bind to membrane inside the columns. The samples were then centrifuged at 11,000xg for 30 seconds followed by washing with desalting buffer MEM once and centrifuged at 11,000xg for 1 minute. 95 µl of RNase-free DNase I reaction mixture (10 µl of DNase I in 90 µl of Buffer RDN) was

applied to each of the column membranes and incubated at room temperature for 15 minutes to prevent any genomic DNA carryover. The columns were washed with Buffer RWI once, then with RW2 buffer twice. Finally, total RNA from tissues were eluted using RNase-free water in RNase-free microcentrifuge tube.

The extracted RNA of different tissue samples were then handed over to Genomic Technologies Core Facility (GTCF) of the University of Manchester, Manchester, UK. In the facility, the extracted RNAs were assessed for the quality, quantity and size using RNA ScreenTape assays (Agilent Technologies, USA). Microarray analysis was then performed by the GTCF using GeneChip Human Transcriptome Array 2.0 according to GeneChip protocols (Affymetrix, Thermo Fisher Scientific). Raw microarray data were then analysed by Bioinformatics Core Facilities, University of Manchester, Manchester, the UK for technical quality control of the arrays, normalisation, and statistical analysis. The state of data normalisation was checked by generating an M-A plot. An M-A plot is a graphical method for visualising the intensity-dependent ratio of raw microarray data. Here, "M" corresponds to the binary log of intensity ratio (lesion/control) and "A" stands for the average log intensity of the gene expression (Dudoit *et al*, 2002; Quackenbush, 2002; Yang *et al*, 2002; Smyth and Speed, 2003). The calculation formulas of M and A are as follows-

$$\mathrm{M} = \log_2\left(\frac{\mathrm{R}}{\mathrm{G}}\right) = \log_2(\mathrm{R}) - \log_2(\mathrm{G})$$

$$\mathrm{A} = \frac{1}{2}\log_2(\mathrm{RG}) = \frac{1}{2}(\log_2(\mathrm{R}) + \log_2(\mathrm{G}))$$

Here R indicates gene expression intensities in lesion tissues and G indicates intensities in control tissues (Tseng *et al*, 2001; Dudoit *et al*, 2002; Yang *et al*, 2002). The normalised data file was then used for further gene expression analysis using multiple computer software.

2.12 Computational analysis of CHI-related biological data

2.12.1 Analysis of differential gene expression and associated pathways

The normalised microarray data were analysed using free command-based statistical software environment R, version 3.4.0 (www.r-project.org), MS Excel (Microsoft corp.,

USA), Ingenuity pathway analysis (IPA) (Qiagen Bioinformatics, Qiagen, UK), and the statistical software GraphPad Prism 6 (GraphPad Software Inc., USA). Pathway analyses were conducted using the Database for Annotation, Visualization and Integrated Discovery (DAVID) version 6.7 (https://david-d.ncifcrf.gov), IPA, and Panther classification systems (http://www.pantherdb.org/pathway).

2.12.2 Finding protein-protein interaction partners, sorting and their validation

Through preliminary analysis, a number of potential candidate genes associated with CHI were identified. A large number of databases are available for biologists that offer information related to protein-protein interactions (PPIs) of candidate genes. Databases such as DIP (http://dip.doe-mbi.ucla.edu/dip/Main.cgi), BioGRID (http://thebiogrid.org/), HPRD-BIN (http://hprd.org/index_html), and I2D (http://ophid.utoronto.ca/ophidv2.204/) were used primarily to gather the PPI data. Later, pathway databases like KEGG (http://www.genome.jp/kegg/), REACTOME (http://www.reactome.org/) were used. To facilitate the findings, UniHi (United Human Interactome) (http://www.unihi.org/), a web-based PPI-finding tool was used. All of these search tools provide authentic data already published in the literature.

2.12.3 Integrated network visualisation and analysis

With the listed potential genes and their protein-protein interaction partners (PIPs), networks were generated and analysed with a free bioinformatics tool, Cytoscape (http://www.cytoscape.org/). Data was filtered to generate a viable metabolic network model with the genes/proteins that got at least 10 interaction partners. The network was analysed based on the network properties including average shortest path length (ASP), betweenness centrality (BC), closeness centrality (CC), clustering coefficient (CCo), and degree which are the measurement of the confidence of network prediction. ASP is a measurement that indicates an average number of steps that is required by a node in a network to communicate with another node. It is a measure of efficiency to transfer information between nodes in a network (Ye *et al*, 2010; Mao and Zhang, 2013). BC of a node in a network is a measurement that indicates the level of control or influence of the node over the transferring information to the other nodes in the network (Newman, 2005; Yoon *et al*, 2006). CC is a measure describing how fast information can transfer from a given node to other nodes in a network, *i.e*. how close a node in a network to all of the

other nodes (Newman, 2005). CCo is a measure that describes how well a node in a cluster is connected with neighbour clusters (Barabási and Oltvai, 2004). The degree is the most basic measurement of a node that indicates the number of other nodes it is connected within a network (Barabási and Oltvai, 2004).

2.13 Statistical analysis

All the relevant data are presented as a mean ± standard error of the mean (SEM). All data were statistically analysed using the GraphPad Prism 6 (GraphPad Software Inc., USA). Comparisons were made using Student's t-test or one-way analysis of variance (ANOVA) followed by Bonferroni's post-test, as appropriate. P-values of less than 0.05 were considered significant.

Chapter 3

Derivation of CHI beta cells by modification of cell culture conditions

3.1 Introduction

3.1.1 Congenital hyperinsulinism in infancy and its predominant causes

Congenital hyperinsulinism in infancy (CHI) is one of the most common causes of persistent hypoglycemia in early childhood or infancy (Stanley, 1997; Meissner *et al*, 2003; Steinkrauss *et al*, 2005; Stevens *et al*, 2013). This potentially lethal disease is characterised by the inappropriate release of insulin from the pancreatic beta cells (Stanley and Baker, 1976; Thomas Jr *et al*, 1977; Dunne *et al*, 2004; Senniappan *et al*, 2012; Proverbio *et al*, 2013; Arya *et al*, 2014). Mutations in several genes have been identified to be associated with this condition (James *et al*, 2009; Mohamed *et al*, 2012; Lord and Leon, 2013; Yorifuji, 2014; Nessa *et al*, 2015; Rahman *et al*, 2015a). The most common being inactivating mutations in the *ABCC8* and *KCNJ11*, genes encoding the subunits (SUR1 and Kir6.2, respectively) of K_{ATP} channel in beta cell (Thomas *et al*, 1996; Dunne *et al*,1997; Huopio *et al*, 2000; Dunne *et al*, 2004; Kapoor *et al*, 2013; Nessa *et al*, 2016). However, a significant proportion of CHI patients have no recognisable genetic causes (Banerjee *et al*, 2011; Kapoor *et al*, 2013; Sang *et al*, 2014; Yorifuji, 2014; Senniappan *et al*, 2015).

In order to regulate insulin secretion, pancreatic beta cells utilise a signal transduction system that connects intracellular metabolic changes in the beta cell for inactivation of K_{ATP} channels. In CHI, loss-of-function of this channel can cause membrane potential changes inappropriately, *i.e.* without increased glucose levels. This membrane depolarisation then leads to calcium influx and hence, irregular uncontrolled increased insulin release (James *et al*, 2009).

3.1.2 CHI and its symptomatic functional attributes

CHI tissues were reported to be associated with altered sensitivity to glucose, irregular exocytosis and hence, uncontrolled irregular insulin secretion (Thomas Jr *et al,*1977; Aynsley-Green *et al,* 1981; Dunne *et al,* 1997; Grimberg *et al,* 2001; Senniappan *et al,* 2012; Nessa *et al,* 2016). In normal pancreatic beta cells, glucose, the first molecule in energy production cascade reactions, become phosphorylated and through the further chain of reactions, ATP is generated. Generation of ATP through glycolysis results in an increase of the intracellular ATP/ADP ratio (Ashcroft *et al,* 1973). ATP binds to K_{ATP} channels and leads to their closure. This closure of the channels prevents K^+ efflux via the channel and thus membrane depolarisation results (Cook and Hales, 1984; Dunne *et al,* 1994; Dunne *et al,* 2004; Craig *et al,* 2008). This membrane depolarisation subsequently opens voltage-gated calcium channels that mediate Ca^{2+} influx and insulin is released from secretory granules through exocytosis (Dunne *et al,* 1994; Kane *et al,* 1996; Nichols *et al,* 1996; Dunne *et al,* 2004). However, in the majority of CHI cases, where the K_{ATP} channel is malfunctional, the beta cell plasma membrane becomes depolarised constantly. This leads to an uncontrolled constitutive Ca^{2+} influx and insulin secretion (Inagaki *et al,* 1995; Dunne *et al,* 1997; Shyng *et al,* 1998; Eichmann *et al,* 1999).

It has also been reported that the affected beta cells in both Fo-CHI and Di-CHI tissues are associated with increased cell proliferation (Kassem *et al,* 2000; Kassem *et al,* 2010; Lovisolo *et al,* 2010). Increased cell proliferation in Fo-CHI patients may be associated with the losses of *H19*, a maternally expressed tumour suppressor gene and *CDKN1C*, encoding a negative regulator of cell proliferation, $p57^{KIP2}$, and activation of paternally expressed insulin-like growth factor 2 (IGF2) (Fournet *et al,* 2000; Fournet *et al,* 2001; Kassem *et al,* 2001; James *et al,* 2009; Avrahami *et al,* 2014). On the other hand, increased nuclear expression of *CDK6* and *CDKN1B* (encoding $p57^{KIP1}$) might be associated with the increased cell proliferation observed in Di-CHI (Salisbury *et al,* 2015). Alternatively, increased level of secreted insulin could be the reason of CHI-related hyperproliferation since insulin is reported to act as a potential growth factor (Hill and Milner, 1985; Ish-Shalom *et al,* 1997; Heni *et al,* 2011; Gong *et al,* 2016; Li *et al,* 2017). Insulin has a low affinity for insulin-like growth factor (IGF) receptors and can bind to IGF receptors in high concentration. Thus upon binding to the IGF receptors, insulin can mediate growth promoting effects (Hill and Milner, 1985; Boucher *et al,* 2010).

3.1.3 Insulin secretagogues and their effect on cellular functions

A number of previous studies reported that some synthetic chemicals and amino acids act as insulin secretagogues (ISG). ISGs are widely used in type 2 diabetes where they prompt beta cells to secrete more insulin (Proks *et al,* 2002; Schmitz *et al,* 2002; Lund *et al,* 2009; Swinnen *et al,* 2010; Schramm *et al,*2011; Scheen, 2016).

A number of studies have reported that potassium chloride (KCl) (Gembal *et al,* 1992; Amin *et al,* 2002; Johnson *et al,* 2007a; Hatlapatka *et al,* 2009; Hatlapatka *et al,* 2011; Cheng *et al,* 2012), sulfonylureas (*e.g*. tolbutamide and glibenclamide) (Mariot *et al,* 1998; Giersbergen *et al,* 2002; Proks *et al,* 2002; Ishiyama *et al,* 2006; Hatlapatka *et al,* 2009) and specific amino acids (*e.g*. arginine and leucine) (Charles *et al,* 1982; Smith *et al,*1997; Ishiyama *et al,* 2006; Yang *et al,* 2010; Cheng *et al,* 2012) perform as ISGs in pancreatic beta cells. These ISGs modulate insulin secretion by acting directly or indirectly on membrane-bound K_{ATP} channel proteins in beta cells.

KCl at a high concentration can trigger beta cell membrane depolarisation independent of the K_{ATP} channel and as a result, can open voltage-gated calcium channel to influx Ca^{2+} that causes insulin release (Gembal *et al,* 1992; Hatlapatka *et al,* 2009; Hatlapatka *et al,* 2011). Sulfonylureas are effective K_{ATP} channel blockers. Sulfonylureas work by binding to the *ABCC8*-encoding SUR1 subunit of K_{ATP} channels and hence promote closure of the channels. Consequently, the inhibition or closure of this channel causes membrane depolarisation, calcium influx and finally insulin release (Ashcroft and Rorsman, 1989; Mariot *et al,* 1998; Aguilar-Bryan and Bryan, 1999; Proks *et al,* 2002; Ishiyama *et al,* 2006). Arginine is a positively charged amino acid under physiological conditions, and its uptake by the cell is electrogenic. So, it was hypothesized that arginine induces membrane depolarisation directly through its positive charge and evokes Ca^{2+} influx and stimulates insulin secretion (Henquin and Meissner, 1981; Charles *et al,* 1982; Smith *et al,*1997; Ishiyama *et al,* 2006). Leucine was reported to be transaminated to α-ketoisocaproate (KIC), and KIC closes K_{ATP} channel and induces the depolarisation of plasma membrane (Bränström *et al,* 1998; Yang *et al,* 2010). Also, Leucine was reported to activate glutamate dehydrogenase (GDH) allosterically to convert glutamate to α-ketoglutarate (αkG) (Stanley, 2004; Stanley, 2009; Yang *et al,* 2010). αkG, in turn, acts to increase the intracellular ATP/ADP ratio that leads to K_{ATP} channel closure and insulin

secretion (Stanley *et al*, 1998; Tanizawa *et al*, 2002; Kapoor *et al*, 2009a). The modes of action of the secretagogues are illustrated in Figure 3.1 in a simplified way.

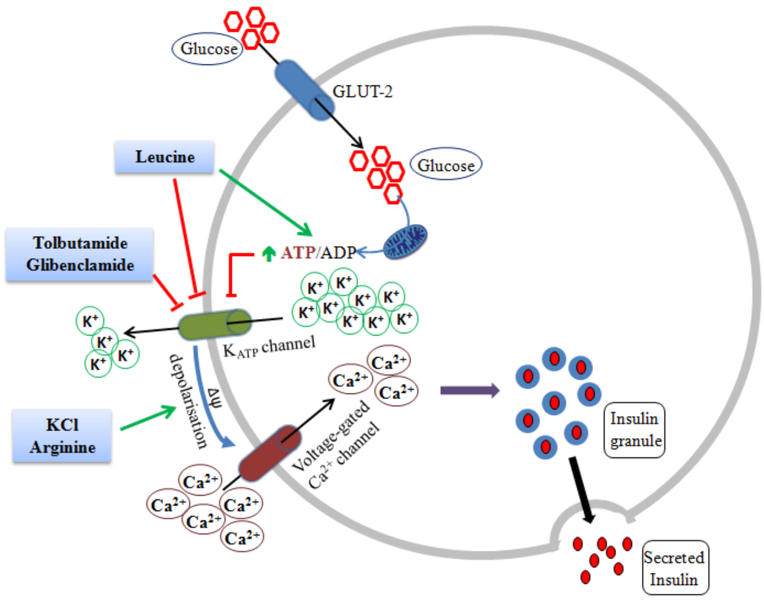

Figure 3.1: **Schematic representation of the insulin secretagogues and their mode of actions**. Tolbutamide, glibenclamide and leucine inactivate K_{ATP} channels whereas KCl and arginine depolarise membrane and thus induce Ca^{2+} influx via L-type voltage-gated calcium channels and stimulate insulin secretion. The pointed arrow in green colour shows positive action whereas the red coloured solid line with blunt end indicates negative action.

3.1.4 Pancreatic beta cell lines and islets used in this study

Two functional model pancreatic beta cell lines, one from human origin (EndoCβH1) and the other from mouse origin (MIN6), were considered for this study.

The EndoCβH1 cell line was derived from human fetal pancreatic bud which was modified with simian virus 40 large T antigen (SV40LT) and human telomerase reverse transcriptase to express beta cell-specific markers (Ravassard*et al*, 2011). Ravassard and colleagues showed that this cell line displayed characteristics of pancreatic beta cells as it expressed many of the beta cell-specific markers (*INS*, *PDX1*, *NKX6.1*, *NEUROD1*) without significant expression of other pancreatic cell type markers. This finding was supported by Gurgul-Convey *et al.* (2015). This cell line was reported to secrete insulin in

response to glucose and ISGs (such as KCl, leucine, glibenclamide) (Ravassard *et al,* 2011; Andersson *et al,* 2015; Gurgul-Convey *et al,* 2015; Krishnan *et al,* 2015). A number of recent studies have reported using this cell line as a functional model beta cell line (Fred *et al,* 2015; Scoviille *et al,* 2015; Axelsson *et al,* 2017; Grieco *et al,* 2017).

The MIN6 cell line was derived from a mouse insulinoma and established by targeted expression of SV40LT antigen gene in transgenic mice (Miyazaki *et al,* 1990). The cell line was reported to secrete insulin in response to glucose and ISGs as native pancreatic cells (Miyazaki *et al,* 1990; Ishihara *et al,* 1993; Johnson *et al,* 2007a; Cheng *et al,* 2012). MIN6 is one of the widely used functional model rodent beta cell lines (Vanderford *et al,* 2008; Weir and Bonner-Weir, 2011; Antonucci *et al,* 2015; Hilderink *et al,* 2015).

In addition, mouse pancreatic islets were used in this study. The purified islets were extracted from C57BL/6 mice, one of the widely used inbred strains of mouse (Fergusson *et al,* 2014; da Silva *et al,* 2016). This mouse strain was reported earlier to be used in a number of insulin secretion related studies (Henquin *et al,* 2006; Imai *et al,* 2007; Fergusson *et al,* 2014; Roat *et al,* 2014).

3.1.5 Aim and objectives of this study

Since CHI is a poorly understood disease, the **aim of this series of studies** was to generate an *in vitro* CHI β-cell line to support additional studies of the mechanisms of the disease.

In order to support this aim, the objectives of this chapter, in general, were to use insulin-secreting cell lines and to manipulate cell culture conditions. The objectives were as follows-

a) To characterise the basic properties of a novel human pancreatic β-cell line, EndoCβH1 and the mouse pancreatic β-cell line, MIN6.
b) To examine the actions of insulin-secretagogues on cell proliferation in the EndoCβH1 and MIN6 cell lines.

c) To investigate the actions of insulin-secretagogues on insulin production in the EndoCβH1 and MIN6 cell lines.
d) To examine the actions of insulin-secretagogues on insulin secretion in the EndoCβH1 and MIN6 cell lines.
e) To study the actions of insulin-secretagogues on the expression of core ion channel proteins in the EndoCβH1 and MIN6 cell lines.

3.2 Results

3.2.1 Characterization of MIN6 and EndoCβH1 cells

3.2.1.1 Morphological features of the beta cell lines

Both the MIN6 and EndoCβH1 cell lines (Figure 3.2) were observed to maintain their growth in formulated culture media. The growth of MIN6 cells was faster compared to EndoCβH1 cells. Through manual cell counting, it was observed that after 7 days of culture in media, the number of MIN6 cells was increased 6.36 ± 0.82 (average ± SEM, n=3, r = 2) times. For EndoCβH1, the number was 1.91± 0.74 (n = 3, r = 2) times. Since the growth rate of these two cell lines was different, so the downstream similar types of experiments with these two cell types were designed differently in terms of cell seeding density and cell incubation time for growth in some cases (described in the materials and methods chapter).

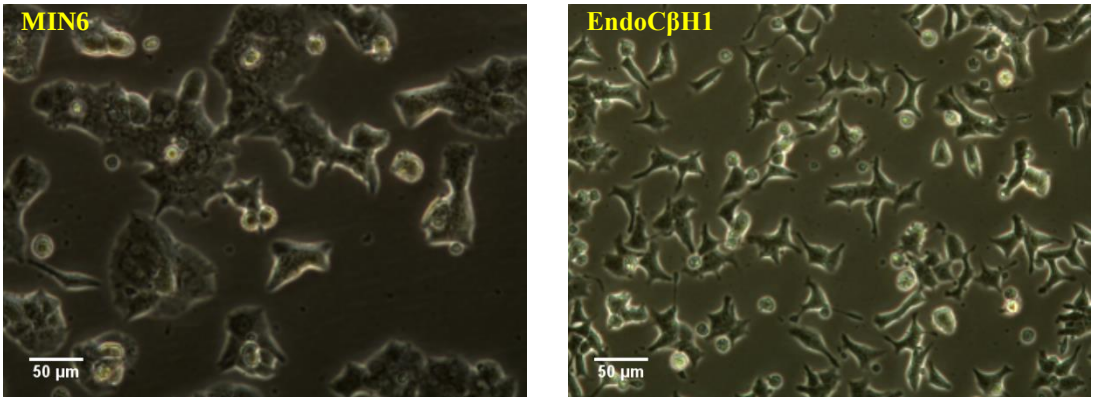

Figure 3.2: **Morphological shapes of pancreatic beta cell lines MIN6 and EndoCβH1**. The cells were on day 7 of culture. These bright field images were taken using an Olympus CKX41 inverted microscope at 20x magnification.

3.2.1.2 MIN6 and EndoCβH1 cells show characteristics of pancreatic beta cells

MIN6 is well characterised and has been used as a model beta cell line previously (Miyazaki *et al,* 1990; Ishihara *et al,* 1993; Johnson *et al,* 2007a; Vanderford *et al,* 2008; Cheng *et al,* 2012; Antonucci *et al,* 2015). So, this cell line was not characterised again in details in this study. The MIN6 cells undergoing studies were checked for their

insulin expression ability. The cells were observed to be capable of insulin expression, and it was confirmed by immunofluorescence study (Figure 3.3).

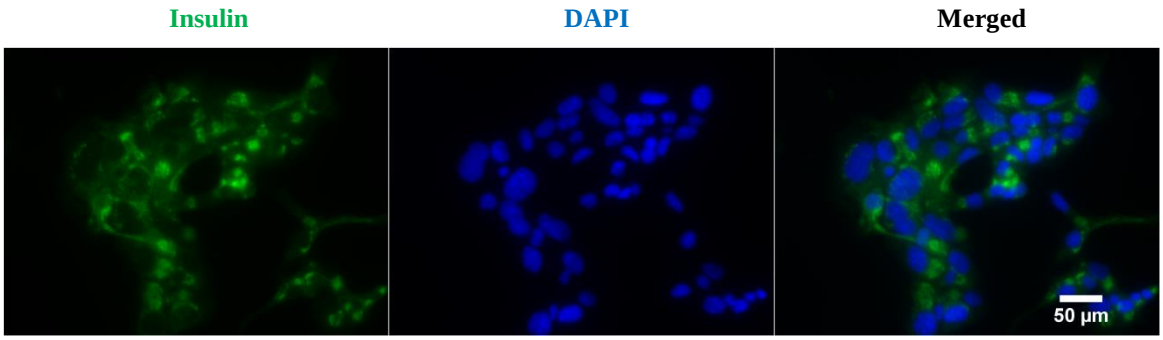

Figure 3.3: **Immunofluorescence images of MIN6 cells showing expression of insulin**. Nuclei (DNA) were stained with DAPI (blue). Insulin was stained as green. The images were captured using an Olympus BX51 upright microscope using appropriate band-pass filters and merged using ImageJ software.

The EndoCβH1 cell line was newly developed at the beginning of this research project and was not reported to be used by any other research group apart from Ravassard *et al.* (2011). Primarily, the cells were investigated for their ability to express some of the important beta cell-specific markers genes at the mRNA level. Transcription of a gene (at mRNA level) does not indicate the expression and function of its protein product. However, it can suggest the possibility of the expression of that gene at the protein level (Vogel and Marcotte, 2012). There are some marker genes which are normally transcribed and expressed as proteins in the pancreatic beta cells (Pan and Wright, 2011). Ravassard and colleagues reported earlier that EndoCβH1 cells transcribe as well as translate some of the key beta cell-specific marker genes - *INS*, *PDX1*, *NKX6.1* and *NEUROD1* (Ravassard *et al*, 2011). RT-PCR data showed that the cells undergoing studies were positive for expressing all of these markers at the mRNA level (Figure 3.4 A). Furthermore, immunofluorescence was used to confirm the expression of insulin at the protein level in the cells (Figure 3.4 B).

Since both of the cell types were expressing pancreatic beta cell-specific markers including insulin, it was concluded that both the cell lines were maintaining their beta

cell-like characteristics. Therefore, the cells were considered for downstream experiments.

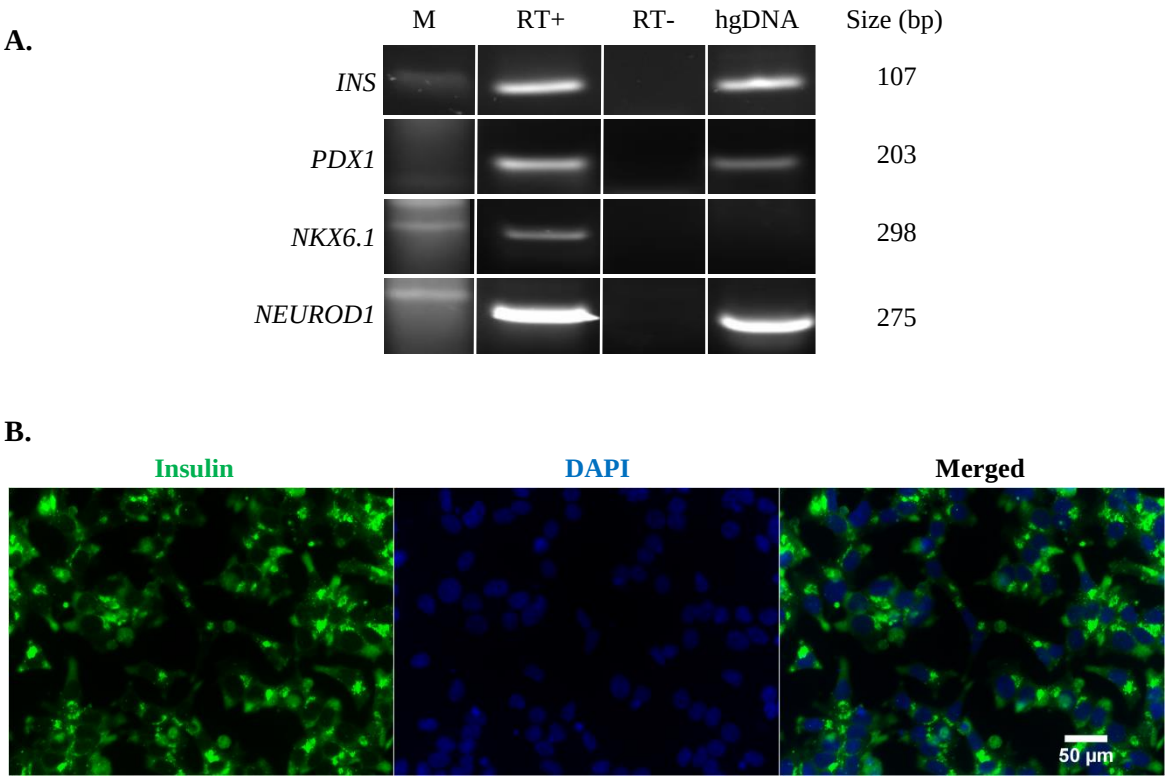

Figure 3.4: **Expression of pancreatic beta cell markers in EndoCβH1 cells**. A. RT-PCR products showing the mRNA expression of the markers. M: DNA ladder, RT+: presence of reverse transcriptase for cDNA synthesis, RT-: absence of reverse transcriptase, hgDNA: Human genomic DNA. B. Immunofluorescence imaging study showing the expression of insulin (green) at the protein level in EndoCβH1cells. Nuclei were stained with DAPI (blue). The Image was captured using an Olympus BX51 upright microscope.

3.2.1.3 MIN6 and EndoCβH1 cells respond to glucose and secrete insulin

To confirm that the beta cell models were responsive to glucose stimulation, insulin secretion was measured following the protocols mentioned in section 2.6.2. As previously reported in the literature, increased insulin secretion was observed in response to higher concentrations of glucose (Figure 3.5) (Ishihara *et al*, 1993; Johnson *et al*, 2007a; Ravassard *et al*, 2011; Krishnan *et al*, 2015). In MIN6 cells glucose was able to stimulate insulin secretion. Compared to low glucose (2 mM & 5.5 mM), 10 mM, 20 mM and 25

mM were able to induce insulin secretion significantly. In EndoCβH1 cells, 11 mM, 15 mM and 20 mM glucose were able to induce insulin secretion, compared to low (0.5 mM & 2.8 mM) glucose. The glucose concentrations for MIN6 were selected observing the glucose-stimulated insulin secretion (GSIS) patterns in the literature (Ishihara *et al*, 1993; Johnson *et al*, 2007a). The glucose concentrations for EndoCβH1 were used extensively by Ravassard *et al.* (2011). Despite the differences in concentrations, both cell types were observed to respond to glucose as like native beta cells.

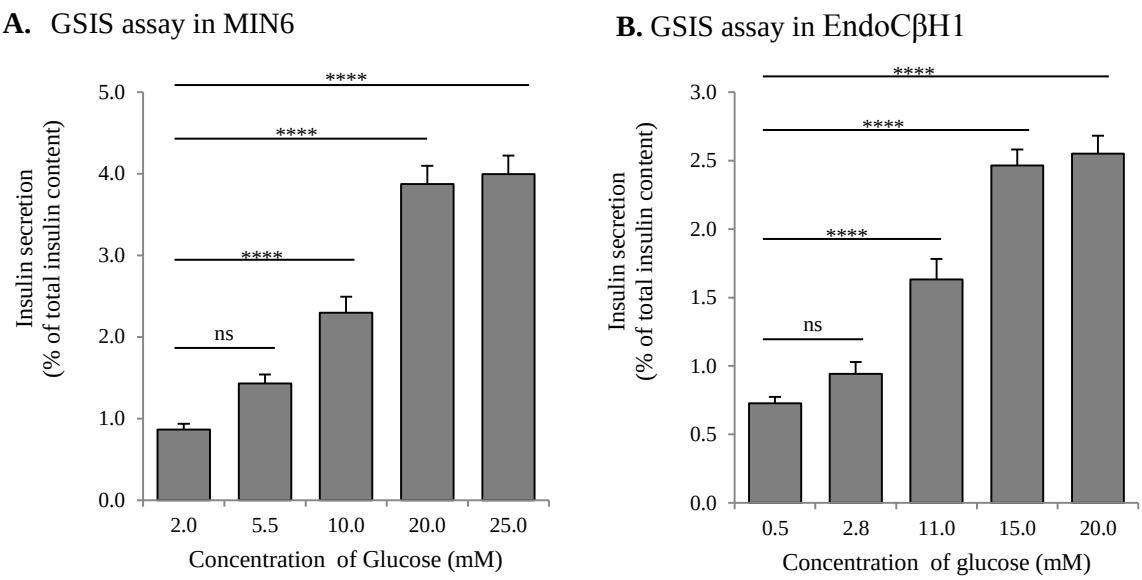

Figure 3.5: **Quantitative assays for glucose-stimulated insulin secretion in MIN6 and EndoCβH1 cells**. ~70% confluent cells were used for the studies. Values were normalised and expressed as the percentage of the amount of insulin secreted by the cells from the total insulin content of the cells in individual conditions. n = 3; 3 independent experiment; **** - p <0.0001; ns = not significant; One-Way ANOVA. Data are presented as mean ± SEM.

3.2.2 Effects of ISGs on MIN6 and EndoCβH1 cells proliferation

Insulin secretagogues (ISGs) that promote beta cells to secrete insulin, were investigated to determine whether they could induce beta cell proliferation. The reason for doing these studies was to mimic the actions of CHI through chronically depolarizing the cells, raising intracellular Ca^{2+} and looking to see whether these manipulations had an action on cell proliferation, which is a key feature of the CHI pancreas (Kassem *et al*, 2000; Kassem *et al*, 2010; Lovisolo *et al*, 2010).

Five different ISGs (KCl, 40 mM; tolbutamide, 200 µM; arginine, 10 mM; leucine, 10 mM; and glibenclamide, 10 µM) were used to treat the MIN6 and EndoCβH1 cells. These ISGs were reported to be efficient in inducing beta cells to secrete more insulin (Proks *et al*, 2002; Schmitz *et al*, 2002; Lund *et al*, 2009; Swinnen *et al*, 2010; Schramm *et al*,2011). The concentrations of these ISGs were reported earlier to be capable of inducing insulin secretion (Johnson *et al*, 2007a; Hatlapatka *et al*, 2009; Yang *et al*, 2010; Cheng *et al*, 2012). Cells were grown for eight days (192 hours) in culture media containing individual ISG. The number of cells was counted manually using a hemocytometer every 24 hours. Growth curves were plotted to observe the effect of these stimuli on cell growth (Figure 3.6). It was observed that neither of the ISGs was able to induce any effect on cell proliferation in both MIN6 and EndoCβH1 cells. The cell proliferation was not statistically significant at each time point compared to untreated control MIN6 and EndoCβH1 cells.

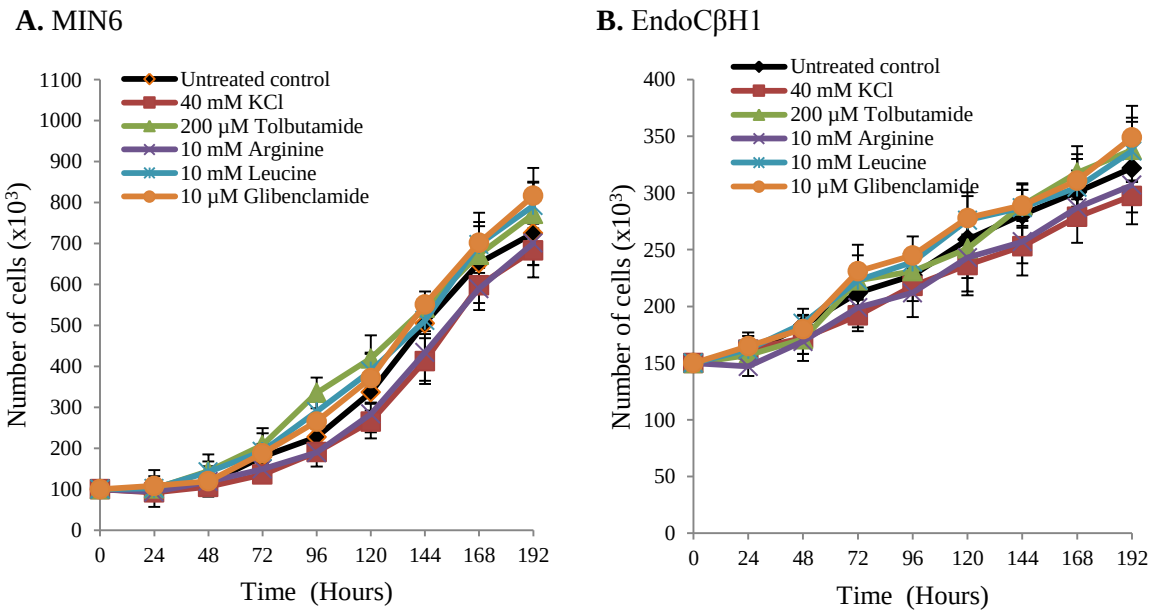

Figure 3.6: **Growth curve of MIN6 and EndoCβH1 cells showing the effect of insulin secretagogues on cell proliferation**. Cells were grown for 192 hours in culture media containing individual insulin secretagogues. Cells were counted in every 24 hours. n = 3; 3 independent experiments; one-way ANOVA across treatments at each time point. Data are presented as mean ± SEM.

To further verify this method of manual counting to examine cell proliferation, the effects of ISGs on cell proliferation were measured using two chemical-incorporating methods. The first method was using CellTiter 96 A_{queous} Non-Radioactive Cell Proliferation Assay kit (Figure3.7) (detail protocol in section 2.5.2). The data from these assays were found similar to the data from manual counting. No significant changes in cell proliferation were observed in cells exposed to ISGs compared to untreated control cells at individual time points.

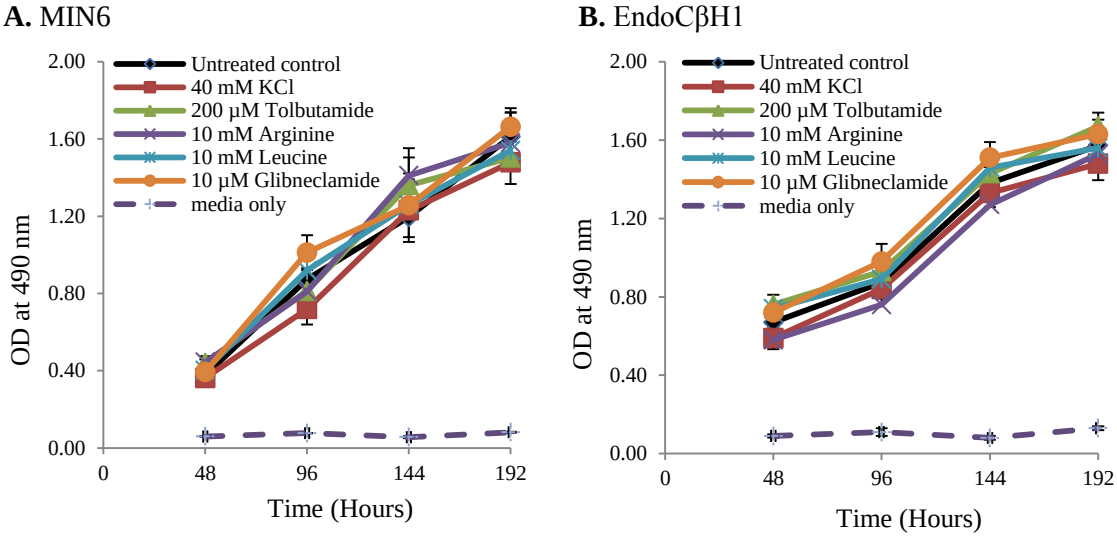

Figure 3.7: **CellTiter 96 A_{queous} Non-Radioactive Cell Proliferation assay-based growth curve of MIN6 and EndoCβH1 cells treated with insulin secretagogues**. Cells were grown for 192 hours in culture media containing individual insulin secretagogues. The absorbance of cell suspensions was measured in every 48 hours. The absorbance of culture media was measured to normalise the background noise. n = 3; 3 independent experiments; one-way ANOVA across treatments at each time point. Data are presented as mean ± SEM.

The second chemical-incorporating method was based on utilising BrdU (5-Bromo-2-deoxyuridine) as a labelling reagent. EndoCβH1 cells did not show any incorporation of BrdU inside the cells (data not shown). MIN6 cells were grown for 48 hours with or without ISGs. The cells were then incubated with BrdU for 2 hours following another 24-hours growth with or without respective ISGs (details in section 2.5.3). The incorporation of BrdU in genomic DNA was evaluated by immunofluorescence imaging (Figure 3.8 A). The number of actively dividing cells (that incorporated BrdU) were counted using

ImageJ software. The data from this assay were similar to those observed in the previous two methods, and no significant changes in the numbers of actively dividing cells (which indicates cell proliferation) were observed in the different treatment conditions compared to untreated control cells (Figure 3.8 B).

So, the results from these three methods indicate that the ISGs used in this study did not have any effect on beta cell proliferation normally. So, further experiments were designed to examine if the cells could acquire permanent changes in proliferation property because of prolonged exposure (acute or chronic) to ISGs.

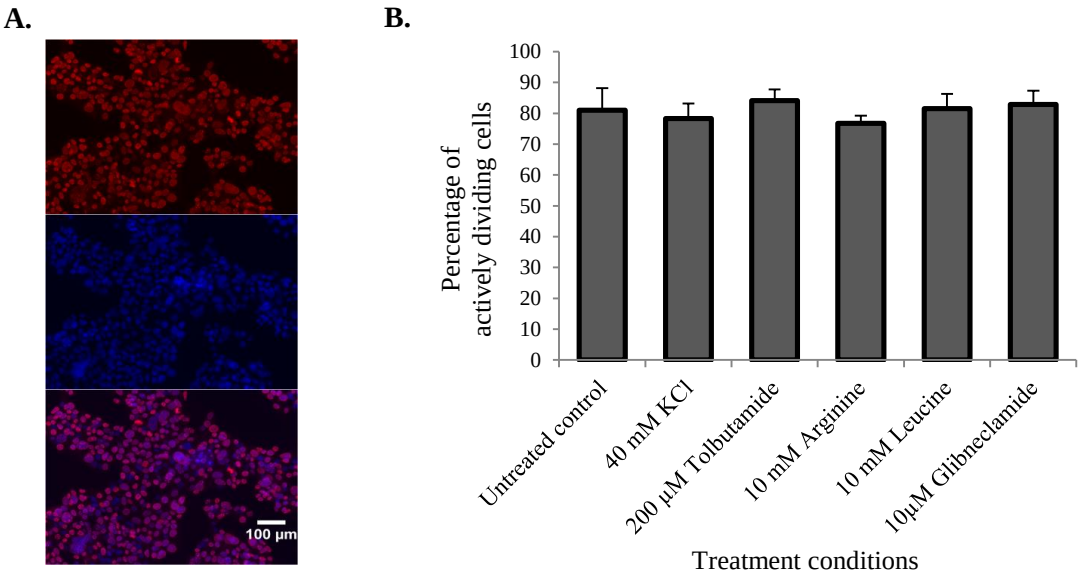

Figure 3.8: **BrdU incorporation-based MIN6 cells proliferation assay**. A. Representative immunofluorescence images of BrdU incorporation (red) in genomic DNA of MIN6 cells 24 hours after the BrdU treatment. Nuclei were stained with DAPI (blue). Images were taken using an Olympus BX51 upright microscope. B. Percentage of the number of actively dividing cells in different treatment conditions. n = 3; 3 independent experiments; one-way ANOVA. Data are presented as mean ± SEM.

3.2.2.1 Effects on the proliferation of MIN6 and EndoCβH1 cells acutely treated with ISGs

Proliferation assays were carried out to investigate the effect of acute (48 hours) exposure of ISGs on beta cell proliferation. Both the MIN6 and EndoCβH1 cells were grown in growth media with ISGs for 48 hours. Then these treated cells were cultured in normal culture media (without any ISG) and allowed to grow for a further 144 hours (6 more days). Cells were counted manually using a hemocytometer every 24 hours. Growth curves were plotted to observe the effect of these stimuli on cell growth (Figure 3.9). With time, the cell numbers were increased. However, compared to untreated control cells, neither the MIN6 (Figure 3.9 A) nor the EndoCβH1 (Figure 3.9 B) cells showed any significant changes in proliferation at different time points after acute exposure to the different treatment conditions.

A. MIN6

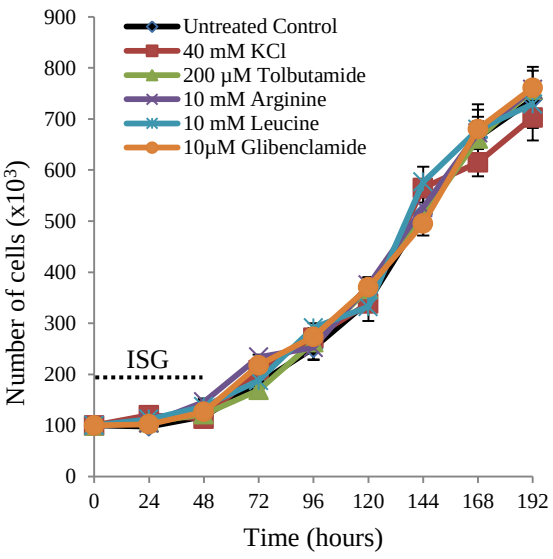

B. EndoCβH1

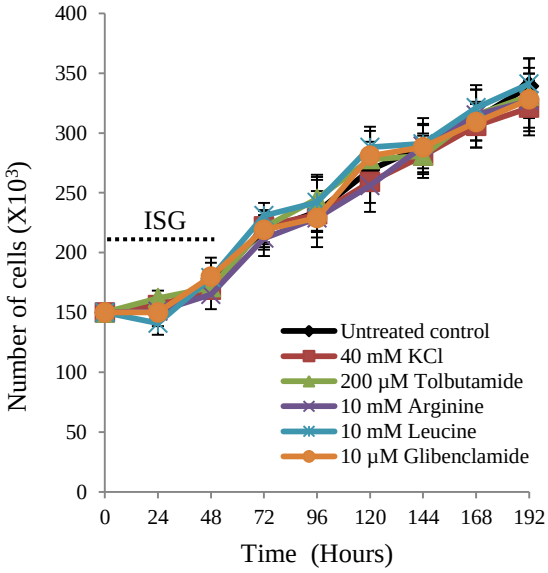

Figure 3.9: **Effects of acute exposure to insulin secretagogues on MIN6 and EndoCβH1 cells proliferation**. Panel A and B represent the growth curve of acutely (48 hours) treated MIN6 and EndoCβH1 cells, respectively, with secretagogues. Dotted lines indicate the time duration when the cells were exposed to secretagogues. n = 3; 3 independent experiments; one-way ANOVA across treatments at each time point. Data are presented as mean ± SEM.

3.2.2.2 Effects on the proliferation of MIN6 and EndoCβH1 cells chronically treated with ISGs

Since acute exposure of ISGs did not show any effect on cell proliferation, so, MIN6 and EndoCβH1 cells were grown in growth media with ISGs continuously for up to 16 weeks. After every week of the treatment, the treated cells were collected and cultured in normal growth media (without ISG) for up to 192 hours. Cells were counted manually using a hemocytometer every 24 hours. Growth curves were plotted to observe the effect of these stimuli on cell growth (Figure 3.10). With time, the cell numbers were increased. However, compared to untreated control cells, neither the MIN6 (Figure 3.10 A) nor the EndoCβH1 (Figure 3.10 B) cells showed any significant changes in proliferation at different time points after the chronic exposure to the different treatment conditions.

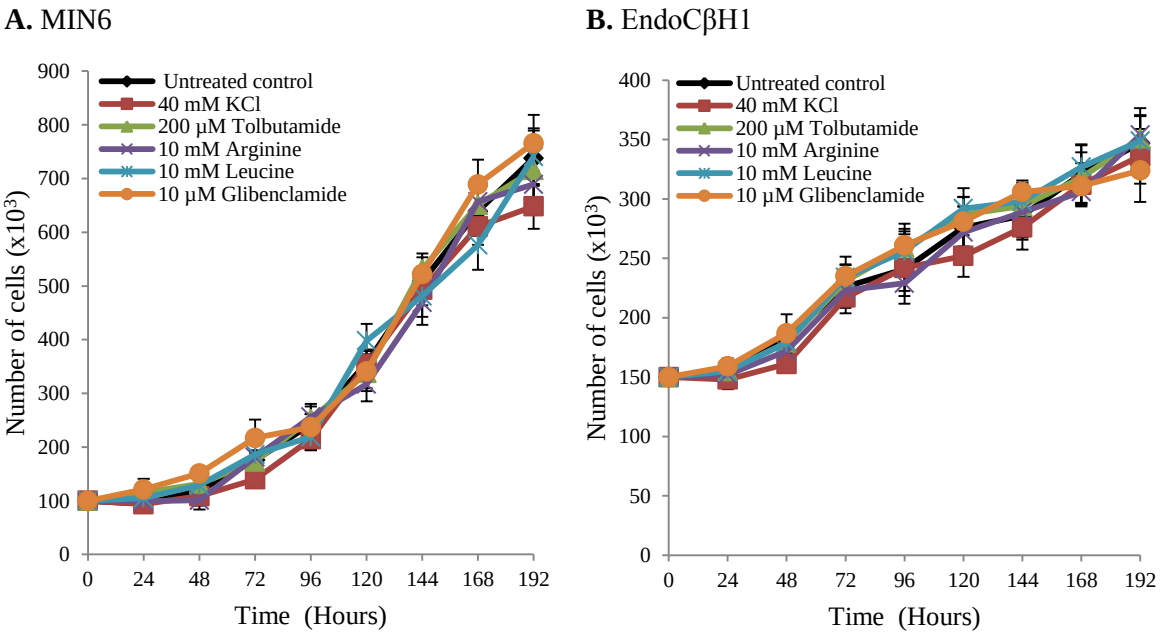

Figure 3.10: **Effects of Chronic exposure of insulin secretagogues on MIN6 and EndoCβH1 cells proliferation**. Panel A and B show representative growth curve of chronically treated MIN6 and EndoCβH1 cells, respectively (after week 5, 6 and 7). The chronically treated cells were grown in normal culture media (without secretagogues) to analyse the effect on proliferation. n = 3; 3 independent experiments; one-way ANOVA across treatments at each time point. Data are presented as mean ± SEM.

After every week, the chronically treated cells were also analysed for their proliferation in the presence of ISGs to examine whether the treated cells retained their sensitivity to respective ISGs. To do these proliferation assays, the treated cells were collected and cultured in growth media (with respective ISG) and allowed to grow for 192 hours. Cells were counted manually using a hemocytometer every 24 hours and growth curves were plotted and analysed (Figure 3.11). With time, the cell numbers were increased. However, compared to untreated control cells, neither the MIN6 (Figure 3.11 A) nor the EndoCβH1 (Figure 3.11 B) cells showed any significant changes in proliferation in different time points after the chronic exposure to the different treatment conditions.

From these observations, it was concluded that neither acute nor chronic exposure of cells to ISGs, at the concentrations used here, had any effect on the proliferation of either MIN6 or EndoCβH1 cells.

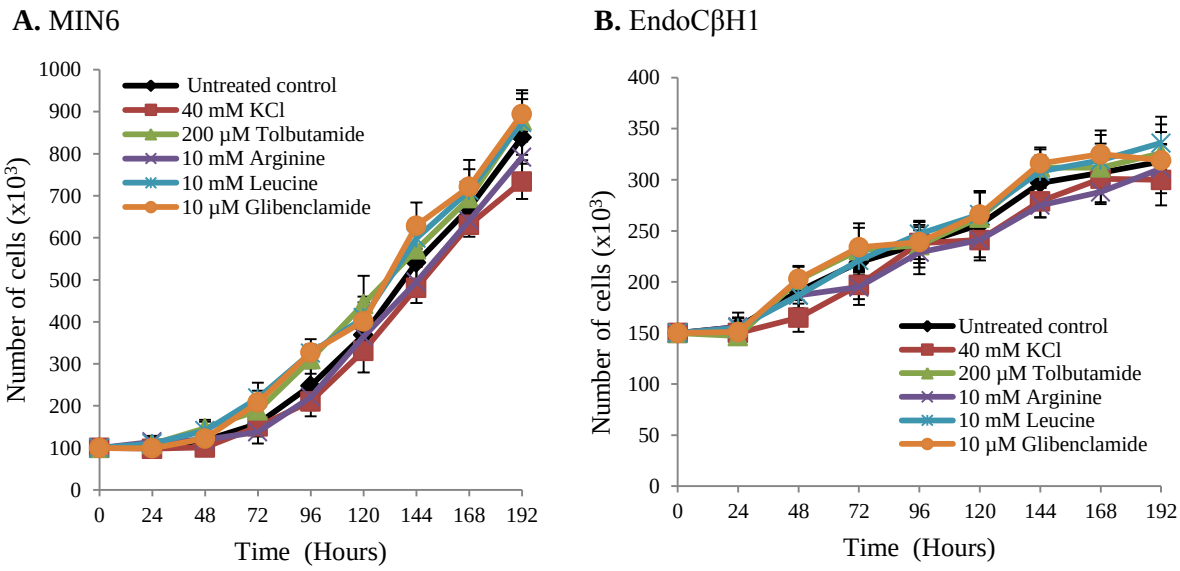

Figure 3.11: **Cell proliferation of chronically insulin secretagogues treated MIN6 and EndoCβH1 cells in the presence of respective secretagogues**. Panel A and B show representative growth curve of chronically treated MIN6 and EndoCβH1 cells, respectively (after week 5, 6 and 7). The chronically treated cells were grown in culture media with respective secretagogues to analyse the effect on proliferation. n = 3; 3 independent experiments; one-way ANOVA across treatments at each time point. Data are presented as mean ± SEM.

3.2.2.3 Effects on the proliferation of MIN6 and EndoCβH1 cells acutely and chronically treated with tolbutamide in high concentration

Some previous studies reported the use of higher concentration of tolbutamide (500µM) in treating different cell types (Huang *et al,* 1995; Ammala *et al*, 1996a; Ammala *et al*, 1996b; Gribble *et al,* 1997a). These studies used this higher concentration of tolbutamide to induce insulin secretion from beta cells or to inhibit K_{ATP} channel activity for analysing electrochemical properties of beta cells. Although the reasons for using this high concentration of tolbutamide were different from the present study, it was thought useful to investigate whether this higher concentration (500µM) of tolbutamide (Tol^{high}) could induce increased cell proliferation. Since the concentration (200µM) of tolbutamide used in the experiments described in previous sections did not have any effect on proliferation of MIN6 and EndoCβH1 cells, it was hypothesised that these cells could be sensitive to this higher concentration of tolbutamide (Tol^{high}) to acquire increased cell proliferation property. Since this high tolbutamide concentration was not reported earlier to be toxic for cells, both MIN6 and EndoCβH1 cells were treated with Tol^{high} acutely and chronically (as in sections 3.2.2.1 and 3.2.2.2).

3.2.2.3.1 Effects on the proliferation of MIN6 and EndoCβH1 cells acutely treated with Tol^{high}

Both the MIN6 and EndoCβH1 cells were grown in the presence of Tol^{high} for 48 hours. These treated cells were then cultured in normal media (without Tol^{high}) and allowed to grow for a further 144 hours. Cells were counted manually using a hemocytometer every 24 hours. Compared to untreated control cells, neither the MIN6 (Figure 3.12 A) nor the EndoCβH1 (Figure 3.12 B) cells showed any significant changes in proliferation in different time points after acute exposure to the Tol^{high}.

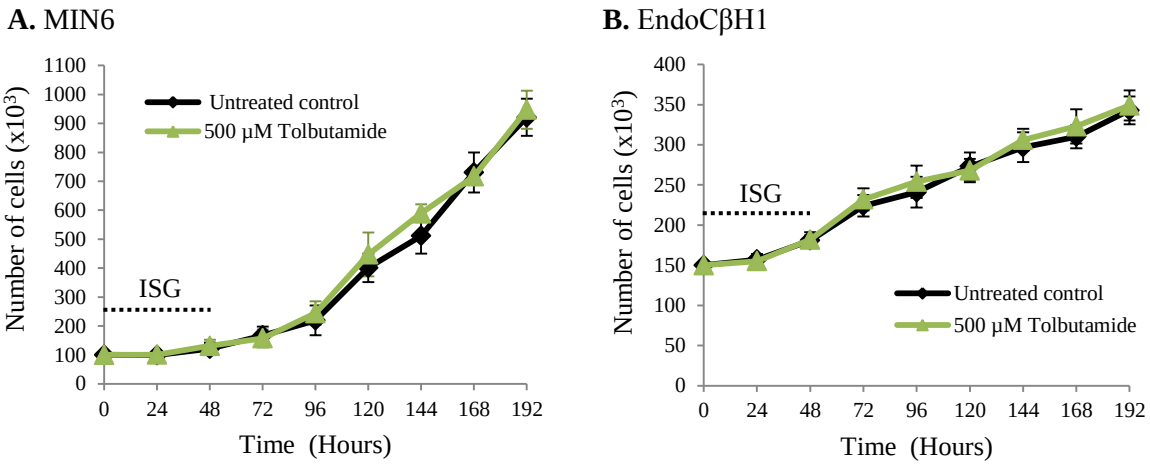

Figure 3.12: **Effects of acute exposure of 500µM tolbutamide on MIN6 and EndoCβH1 cells proliferation**. Panel A and B represent the growth curve of acutely (48 hours) treated MIN6 and EndoCβH1 cells, respectively. Dotted lines indicate the time duration when the cells were exposed to tolbutamide. n = 3; 3 independent experiments; t-test at each time point. Data are presented as mean ± SEM.

3.2.2.3.2 Effects on the proliferation of MIN6 and EndoCβH1 cells chronically treated with Tol^{high}

MIN6 and EndoCβH1 cells were grown in growth media with Tol^{high} continuously for up to 12 weeks. After every week, the treated cells were analysed for the growth curve experiments. The treated cells were collected and cultured in normal growth media (without Tol^{high}) and allowed to grow for 192 hours. Cells were counted manually using a hemocytometer every 24 hours. Compared to untreated control cells, neither the MIN6 (Figure 3.13 A) nor the EndoCβH1 (Figure 3.13 B) cells showed any significant changes in proliferation in different time points after the chronic exposure to Tol^{high}.

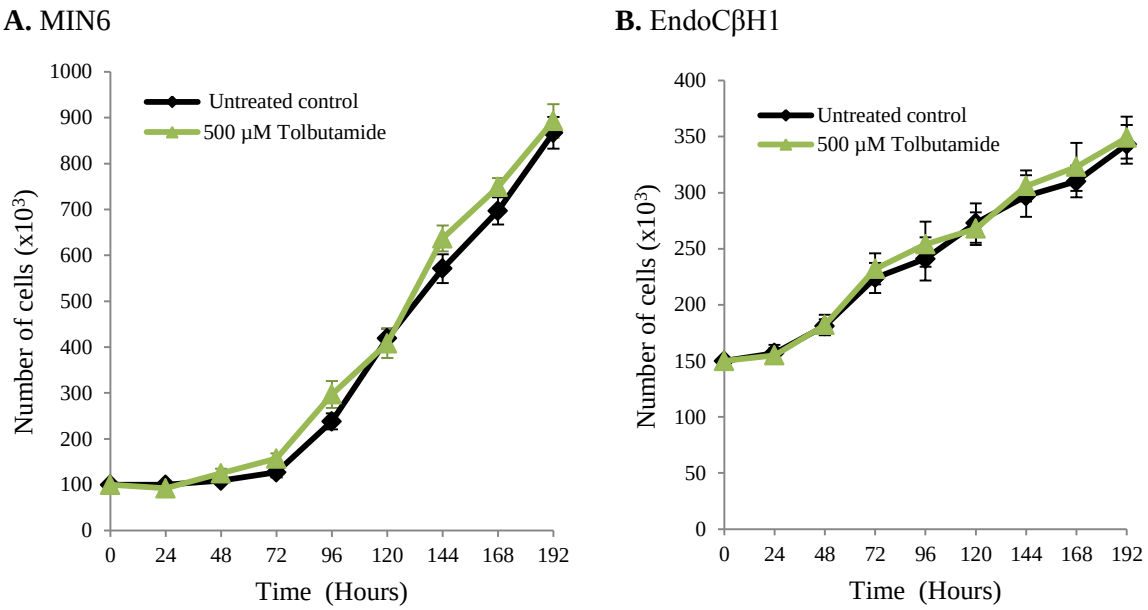

Figure 3.13: **Effects of chronic exposure of 500µM tolbutamide on MIN6 and EndoCβH1 cells proliferation.** Panel A and B represent the growth curve of chronically treated MIN6 and EndoCβH1 cells, respectively (after week 5, 6 and 7). The chronically treated cells were grown in normal culture media (without tolbutamide) to analyse the effect on proliferation. n = 3; 3 independent experiments; t-test at each time point. Data are presented as mean ± SEM.

After every week, the chronically treated cells were also analysed for their proliferation in the presence of Tol^{high}. The treated cells were collected and cultured in growth media (with tolbutamide) and allowed to grow for 192 hours. Cells were counted manually using a hemocytometer every 24 hours and growth curves were analysed (Figure 3.14). Compared to untreated control cells, neither the MIN6 (Figure 3.14 A) nor the EndoCβH1 (Figure 3.14 B) cells showed any significant changes in proliferation in different time points.

From these observations, it was concluded that neither acute nor chronic exposure to tolbutamide, even at this higher concentration (500µM), had any effect on the proliferation of either MIN6 or EndoCβH1 cells.

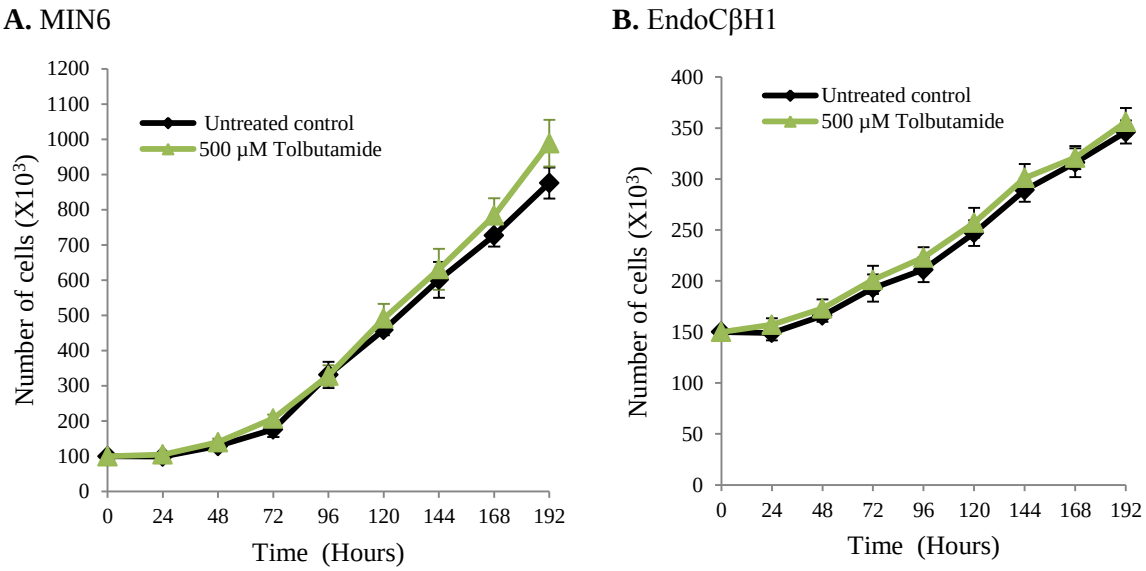

Figure 3.14: **Cell proliferation of chronically Tol^{high} treated MIN6 and EndoCβH1 cells in the presence of tolbutamide**. Panel A and B show representative growth curve of chronically treated MIN6 and EndoCβH1 cells, respectively (after week 5, 6 and 7). The treated cells were grown in culture media with tolbutamide to analyse the effect on proliferation. n = 3; 3 independent experiments; t-test at each time point. Data are presented as mean ± SEM.

3.2.2.4 Effects on the proliferation of MIN6 and EndoCβH1 cells acutely and chronically treated with combinations of ISGs

As a final attempt, cells were treated acutely and chronically with a mixture of two ISGs (ISG_{mix}). It was hypothesised that the combination of two ISGs might create a strong selection pressure to the cells to acquire the desirable changes in cell proliferation. KCl was used in every combination as it can induce membrane depolarisation independent of K_{ATP} channel (Gembal *et al*, 1992; Hatlapatka *et al*, 2009; Hatlapatka *et al*, 2011).

3.2.2.4.1 Effects on the proliferation of MIN6 and EndoCβH1 cells acutely treated with ISG_{mix}

As previous, both the MIN6 and EndoCβH1 cells were grown in the presence of ISG_{mix} for 48 hours. These treated cells were then cultured in normal media (without ISGs) and

allowed to grow for a further 144 hours. Cells were counted manually using a hemocytometer every 24 hours. Compared to untreated control cells, neither the MIN6 (Figure 3.15 A) nor the EndoCβH1 (Figure 3.15 B) cells showed any significant changes in proliferation in different time points after acute exposure to the ISG_{mix}.

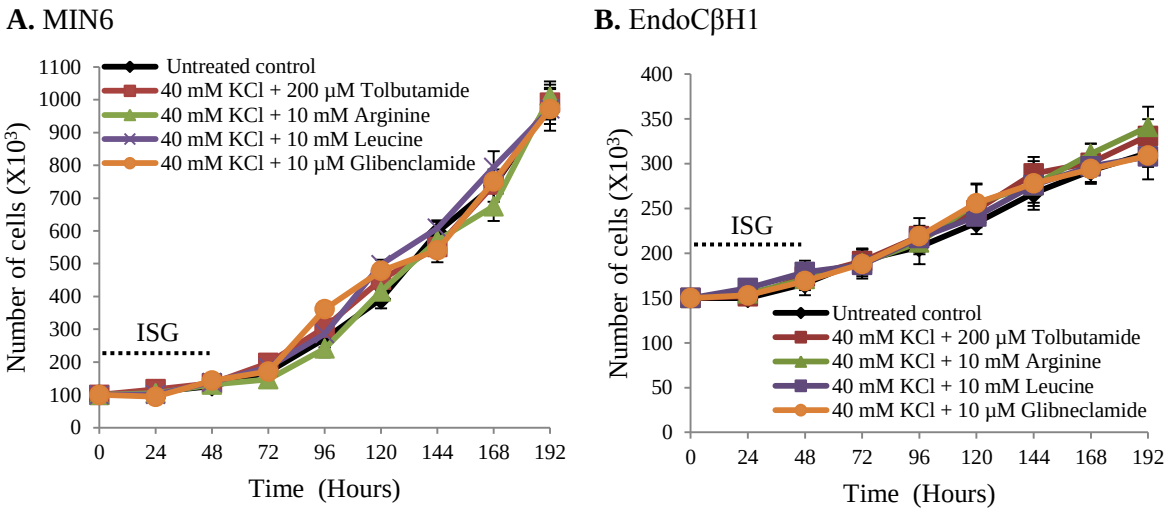

Figure 3.15: **Effects of acute exposure of the mixture of insulin secretagogues on MIN6 and EndoCβH1 cells proliferation**. Panel A and B represent the growth curve of acutely (48 hours) treated MIN6 and EndoCβH1cells, respectively. Dotted lines indicate the time duration when the cells were exposed to secretagogues. n = 3; 3 independent experiments; one-way ANOVA across treatments at each time point. Data are presented as mean ± SEM.

3.2.2.4.2 Effects on the proliferation of MIN6 and EndoCβH1 cells chronically treated with ISG_{mix}

MIN6 and EndoCβH1 cells were grown in growth media with ISG_{mix} continuously for up to 12 weeks. After every week, the treated cells were analysed for the growth curve experiments. The treated cells were collected and cultured in normal growth media (without ISGs) and allowed to grow for 192 hours. Cells were counted manually using a hemocytometer every 24 hours. Again, compared to untreated control cells, neither the MIN6 (Figure 3.16 A) nor the EndoCβH1 (Figure 3.16 B) cells showed any significant changes in proliferation in different time points after the chronic exposure to ISG_{mix}.

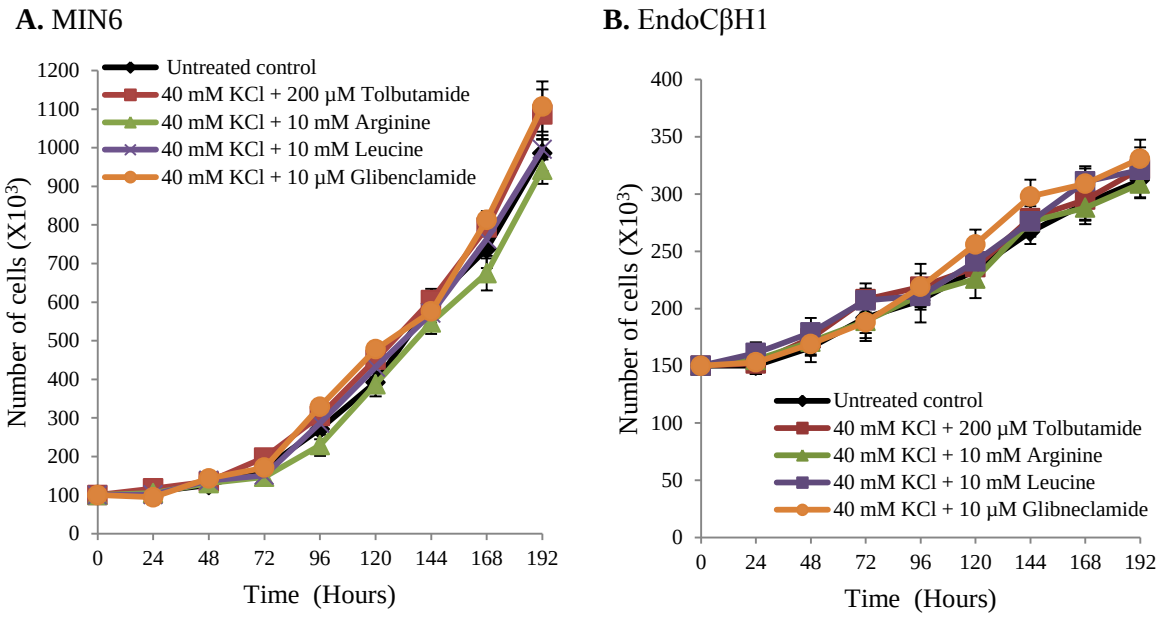

Figure 3.16: **Effects of chronic exposure of the mixture of insulin secretagogues on MIN6 and EndoCβH1 cells proliferation**. Panel A and B represent the growth curve of chronically treated MIN6 and EndoCβH1 cells, respectively (after week 5, 6 and 7). The chronically treated cells were grown in normal culture media (without any secretagogues) to analyse the effect on proliferation. n = 3; 3 independent experiments; one-way ANOVA across treatments at each time point. Data are presented as mean ± SEM.

After every week, the chronically treated cells were analysed for their proliferation in the presence of ISGs. The treated cells were collected and cultured in growth media (with respective ISGs) and allowed to grow for 192 hours. Cells were counted manually using a hemocytometer every 24 hours and growth curves were plotted and analysed (Figure 3.17). Compared to untreated control cells, neither the MIN6 (Figure 3.17 A) nor the EndoCβH1 (Figure 3.17 B) cells showed any significant changes in proliferation in different time points.

So, from the observations mentioned above, it was concluded that modifying cell culture conditions by adding insulin secretagogues was not an appropriate technique to induce cell hyperproliferation in pancreatic beta cell lines, MIN6 and EndoCβH1.

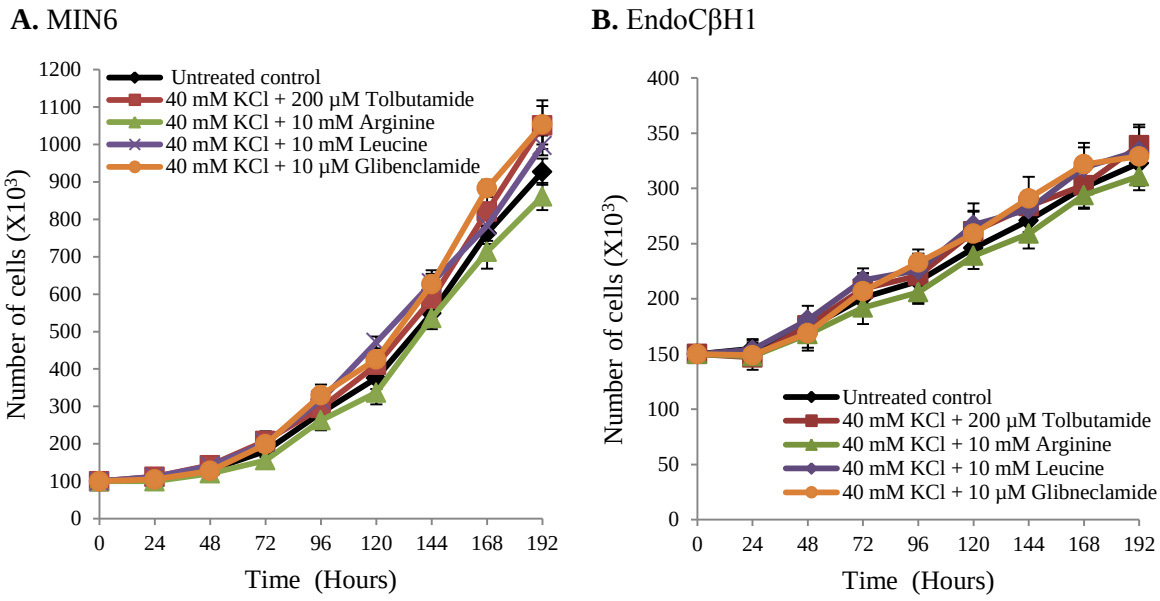

Figure 3.17: **Cell proliferation of chronically treated MIN6 and EndoCβH1 cells in the presence of the respective mixture of insulin secretagogues**. Panel A and B show representative growth curve of chronically treated MIN6 and EndoCβH1 cells, respectively (after week 5, 6 and 7). The treated cells were grown in culture media with respective secretagogues to analyse the effect on proliferation. n = 3; 3 independent experiments; one-way ANOVA across treatments at each time point. Data are presented as mean ± SEM.

3.2.3 Treatment with ISGs had no effect on insulin production of MIN6 and EndoCβH1 cells

Both MIN6 and EndoCβH1 cells were examined to assess if continuous exposure to ISGs had any effect on insulin production (at protein level) in cells. From immuno-fluorescence studies, it was observed that all the chronically treated cells maintained their ability to produce insulin at the cellular level without any visible changes (Figure 3.18 and Figure 3.19 for MIN6 and EndoCβH1, respectively). This finding was confirmed by the amount of total insulin content in both the cell types treated with ISGs. No significant changes were observed in total insulin content in each of the ISG-treated cells compared to untreated cells.

So, it was concluded that chronic exposure to insulin secretagogues had no effect on overall insulin production in beta cells.

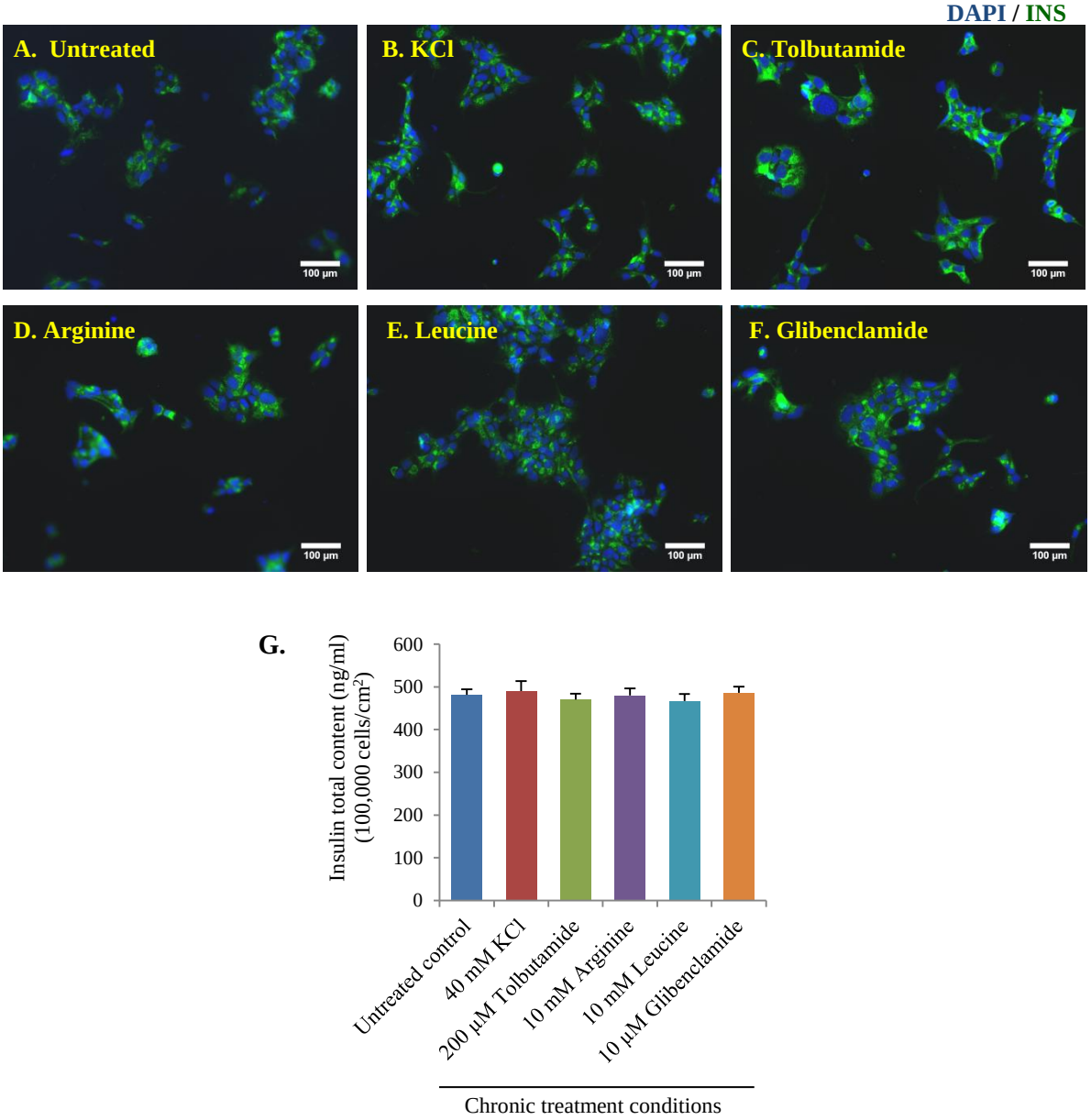

Figure 3.18: **Expression of insulin in MIN6 cells chronically treated with insulin secretagogues**. A – F: Representative immunofluorescence images of MIN6 cells stained with anti-insulin antibody. Individual images correspond to MIN6 cells untreated (A) and treated with different secretagogues (B-E). Cells were chronically treated with ISGs for 10 weeks. Green fluorescence represents insulin. Nuclei were stained with DAPI (blue). Images were taken using an Olympus BX51 upright microscope. G: Total insulin content of MIN6 cells chronically treated in different conditions (after week 8, 9 and 10). n = 3; 3 independent experiments; one-way ANOVA. Data are presented as mean ± SEM.

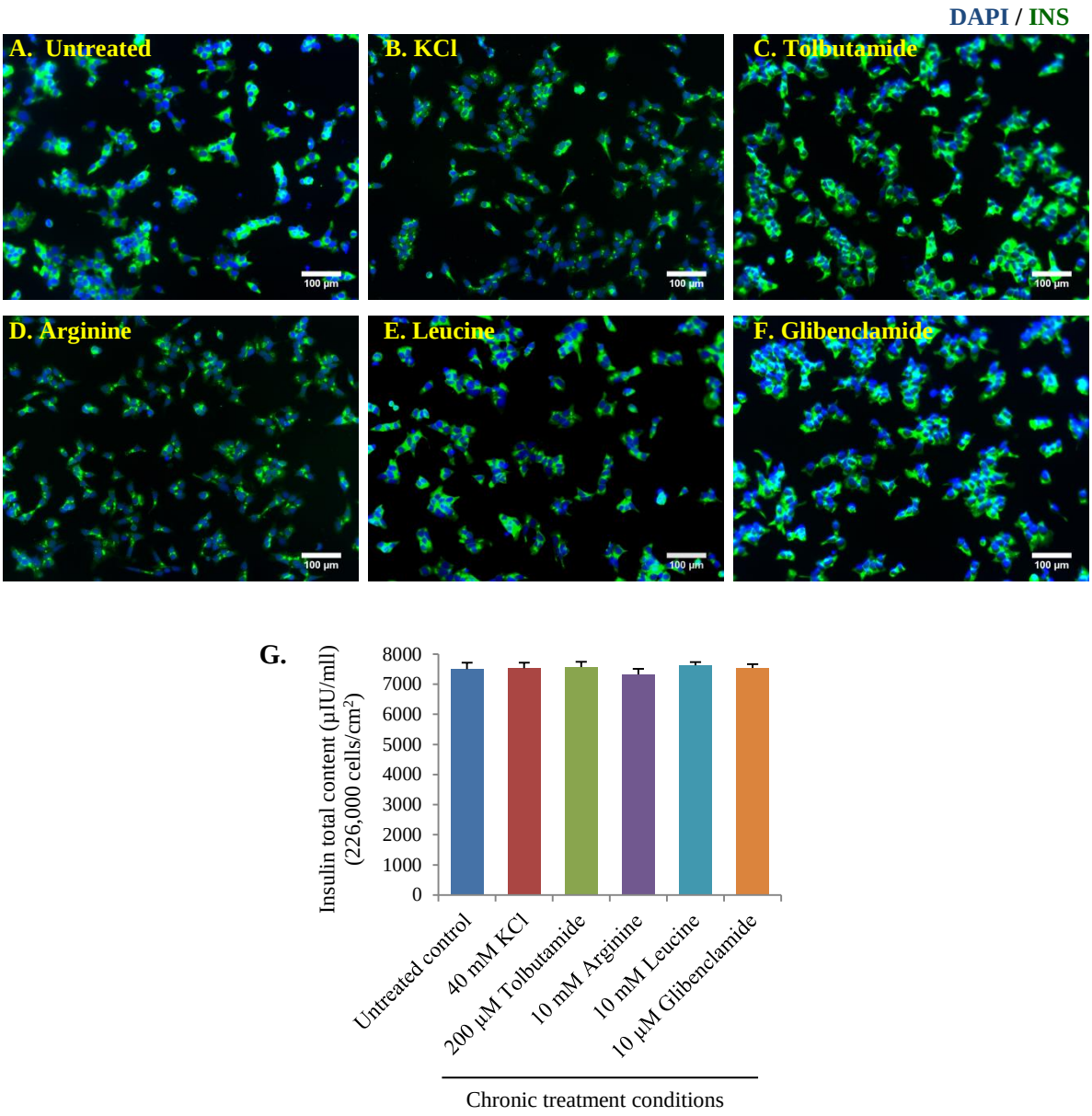

Figure 3.19: **Expression of insulin in EndoCβH1 cells chronically treated with insulin secretagogues**. A – F: Representative immunofluorescence images of cells stained with anti-insulin antibody. Individual images correspond to cells untreated (A) and treated with different secretagogues (B-E). Cells were chronically treated with ISGs for 10 weeks. Green fluorescence represents insulin. Nuclei were stained with DAPI (blue). Images were taken using an Olympus BX51 upright microscope. G: Total insulin content of EndoCβH1 cells chronically treated in different conditions (after week 8, 9 and 10). n = 3; 3 independent experiments; one-way ANOVA. Data are presented as mean ± SEM.

3.2.4 Effects of ISGs on MIN6 and EndoCβH1 cells insulin secretion

To investigate the capacity of cells to secrete insulin in response to ISGs, insulin secretion assays were carried out. The ISGs were added to KRH buffers separately, and the cells were incubated in the buffers (in the presence of low and high glucose content) for specific periods of time (see materials and methods chapter for more details).

Significantly higher amounts of insulin were released in the presence of high glucose (20 mM and 15 mM for MIN6 and EndoCβH1, respectively) compared to the secretion in low glucose (2 mM and 0.5 mM for MIN6 and EndoCβH1, respectively) (Figure 3.20 and Figure 3.21) as it was observed in Figure 3.5. The amount of secretion was observed to be much higher in both low and high glucose conditions when the cells were treated with ISGs. So, this observation indicates that both MIN6 and EndoCβH1 cells are sensitive to ISGs and can release more insulin upon stimulation by ISGs. Further experiments were designed to examine if the cells could acquire permanent changes in glucose sensitivity and hence insulin secretion property because of prolonged exposure (acute or chronic) to ISGs.

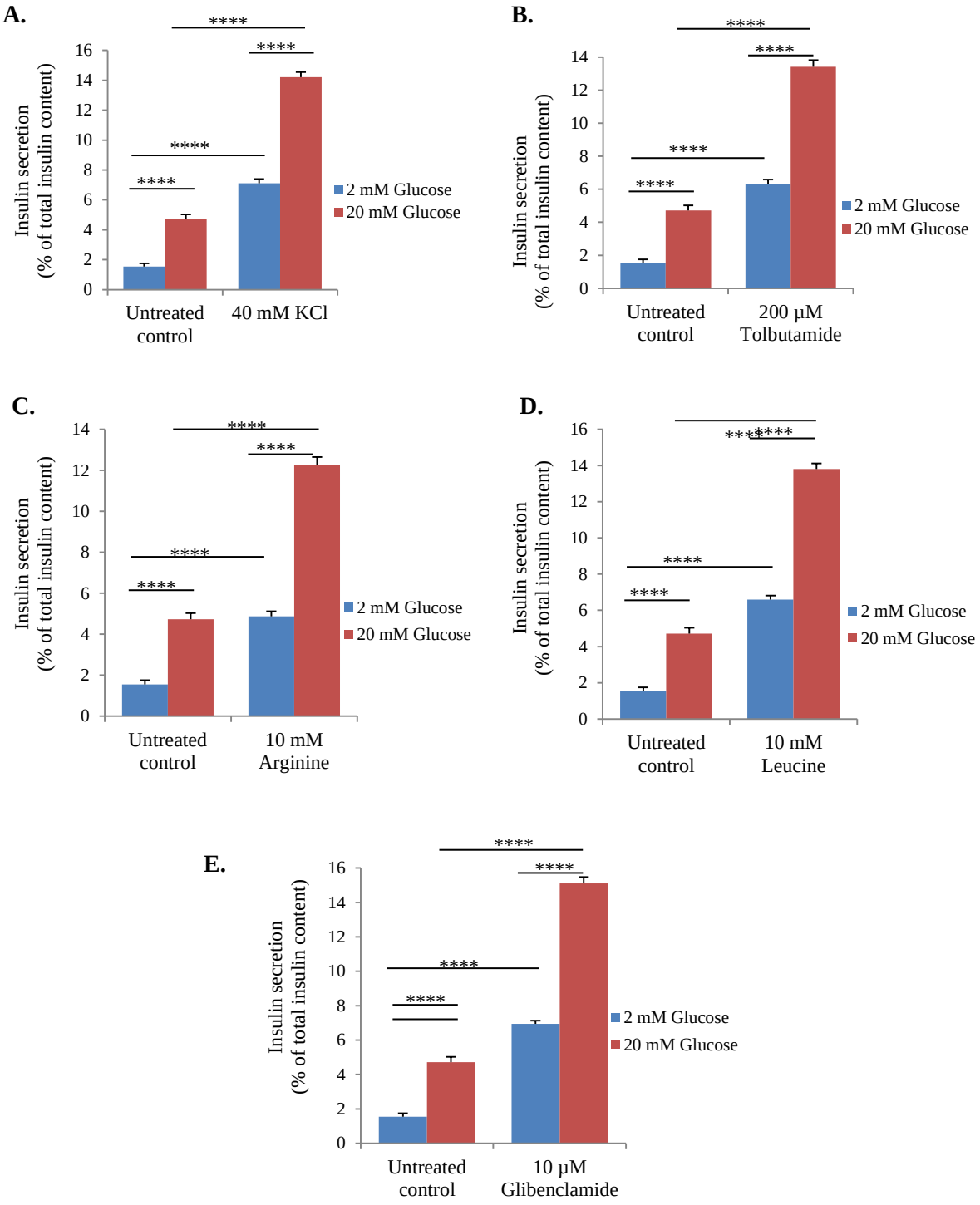

Figure 3.20: **Quantitative assays for glucose-stimulated insulin secretion in MIN6 cells treated with insulin secretagogues**. Secretion data of MIN6 untreated and treated with KCl (A), tolbutamide (B), arginine (C), leucine (D) and glibenclamide (E) are represented here. The assay was carried out in KRH buffer with individual secretagogues. Values were normalised and expressed as the percentage of the amount of insulin secreted by the cells from the total insulin content of the cells in individual conditions. n = 3; 3 independent experiments; **** - $p < 0.0001$; t-test. Data are presented as mean ± SEM.

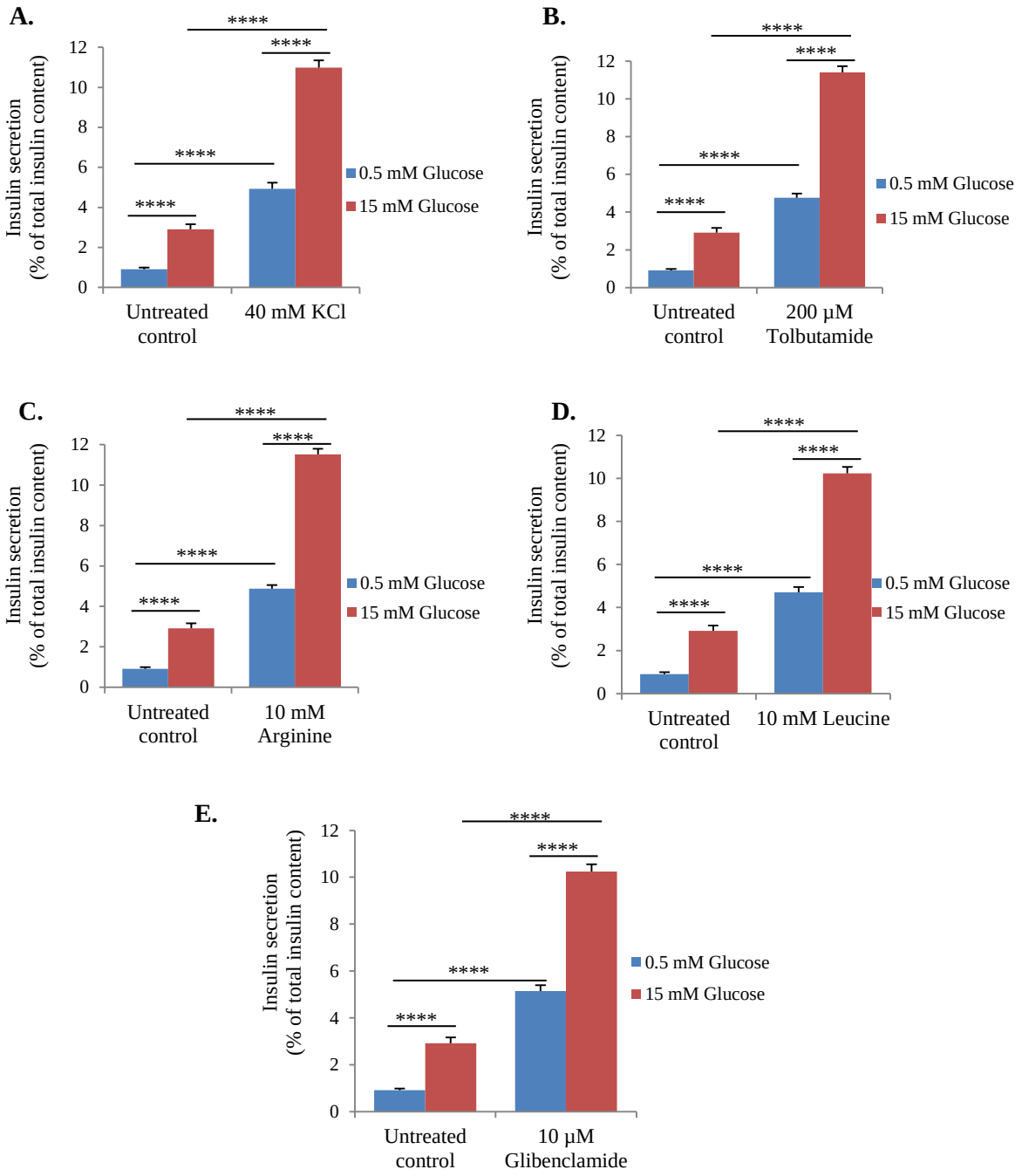

Figure 3.21: **Quantitative assays for glucose-stimulated insulin secretion in EndoCβH1 cells treated with insulin secretagogues**. Secretion data of EndoCβH1 cells untreated and treated with KCl (A), tolbutamide (B), arginine (C), leucine (D) and glibenclamide (E) are represented here. The assay was carried out in KRH buffer with individual secretagogues. Values were normalised and expressed as the percentage of the amount of insulin secreted by the cells from the total insulin content of the cells in individual conditions. n = 3; 3 independent experiments; **** - $p < 0.0001$; t-test. Data are presented as mean ± SEM.

3.2.4.1 Effects on insulin secretion of MIN6 and EndoCβH1 cells acutely treated with ISGs

To examine whether acute exposure of cells to ISGs have a role in changing glucose sensitivity, and therefore in insulin secretion, both cell types were cultured in growth media containing individual ISG for 48 hours. These treated cells were then incubated in the KRH buffers (without any ISG) having low or high glucose content.

Both untreated and treated MIN6 and EndoCβH1 cells were observed to be sensitive to glucose concentration and significantly higher amounts of insulin were released in the presence of high glucose (Figure 3.22 and Figure 3.23 for MIN6 and EndoCβH1, respectively). However, no significant changes in insulin secretion were observed in acutely ISG-treated cells compared to untreated control cells in either low or high glucose conditions.

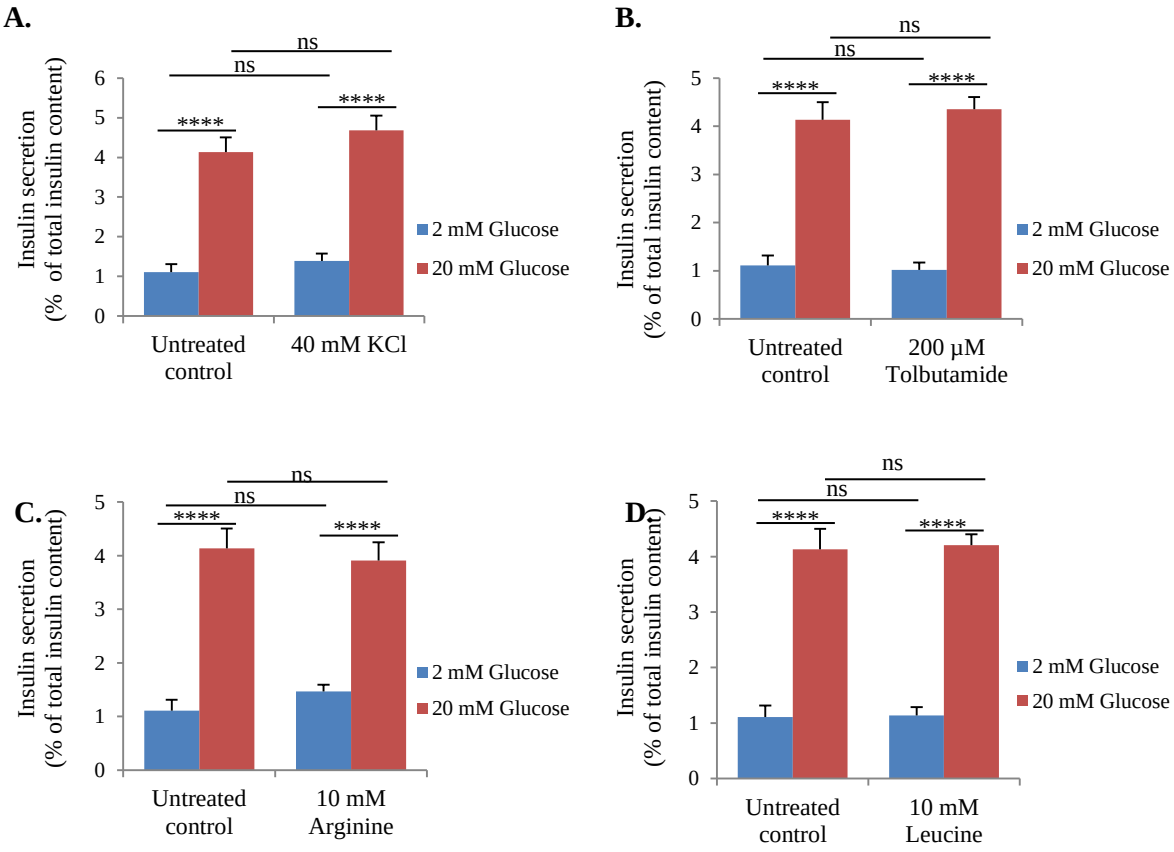

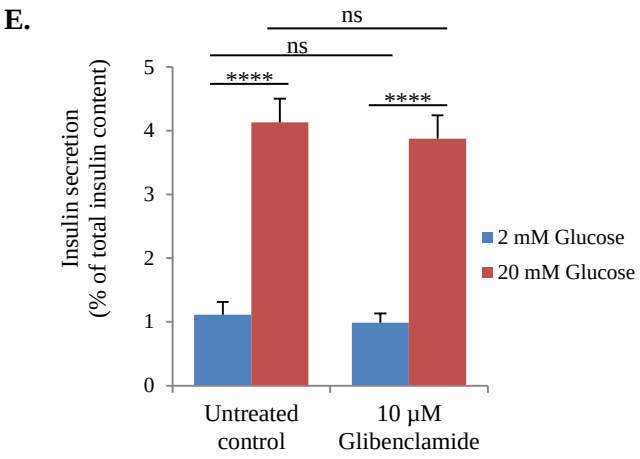

Figure 3.22: **Quantitative assays for glucose-stimulated insulin secretion in MIN6 cells acutely treated with insulin secretagogues**. Secretion data of MIN6 untreated and treated with KCl (A), tolbutamide (B), arginine (C), leucine (D) and glibenclamide (E) are represented here. The assay was carried out in KRH buffer without any secretagogues. Values were normalised and expressed as the percentage of the amount of insulin secreted by the cells from the total insulin content of the cells in individual conditions. n = 3; 3 independent experiments; **** - $p < 0.0001$; ns = not significant, t-test. Data are presented as mean ± SEM.

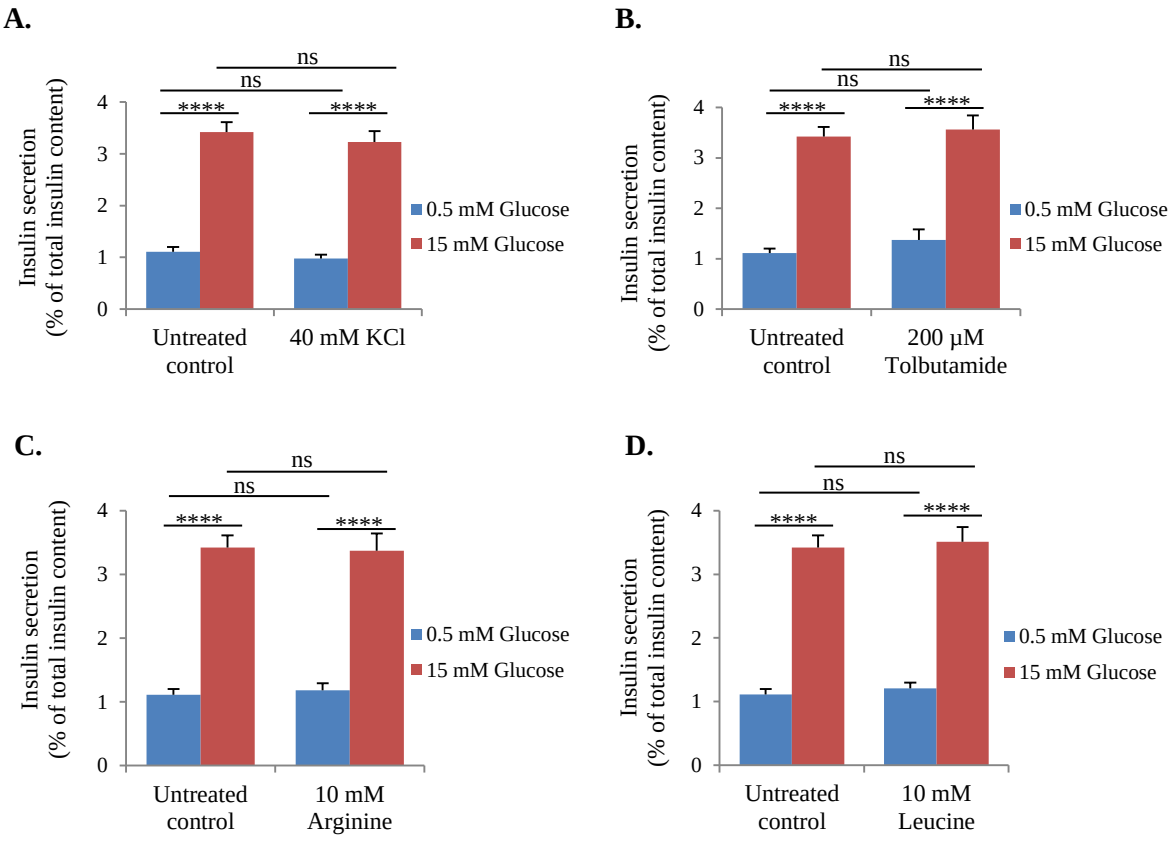

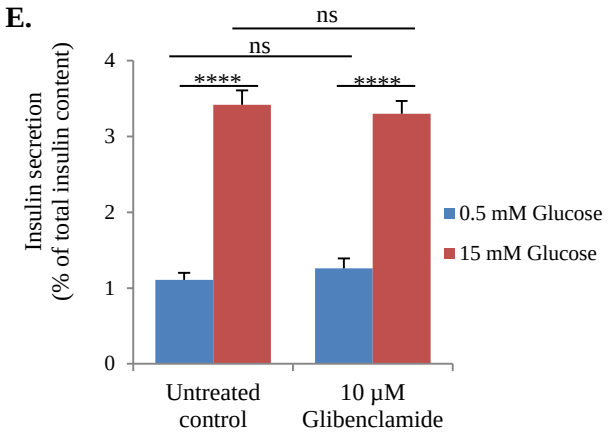

Figure 3.23: **Quantitative assays for glucose-stimulated insulin secretion in EndoCβH1 cells acutely treated with insulin secretagogues**. Secretion data of EndoCβH1 untreated and treated with KCl (A), tolbutamide (B), arginine (C), leucine (D) and glibenclamide (E) are represented here. The assay was carried out in KRH buffer without any secretagogue. Values were normalised and expressed as the percentage of the amount of insulin secreted by the cells from the total insulin content of the cells in individual conditions. n = 3; 3 independent experiments; **** - $p < 0.0001$; ns = not significant, t-test. Data are presented as mean ± SEM.

Some previous studies also used purified islets to observe the effect of ISGs on insulin secretion capacity of islets (Gullo *et al*, 1991; Annelo *et al*, 1999; Mullooly *et al*, 2014). As an alternative approach, in addition to cell lines, highly purified mouse pancreatic islets were used in this study to investigate whether the islets could show the higher secretion capacity after acute treatment with ISGs and act as CHI. Purified islets were incubated in nutrient media containing individual ISG for 48 hours. These treated islets were then incubated in the KRH buffers (without any ISG) having low or high glucose content. As with both MIN6 and EndoCβH1 cells, significantly higher amounts of insulin were released from islets in the presence of high glucose (Figure 3.24). Also, no significant changes in insulin secretion were observed in acutely ISG-treated islets compared to untreated control islets in both low and high glucose conditions.

So, it can be inferred from the observations as mentioned above that acute treatment with ISGs was not an appropriate technique to induce increased insulin secretion capacity in pancreatic beta cells and mouse islets.

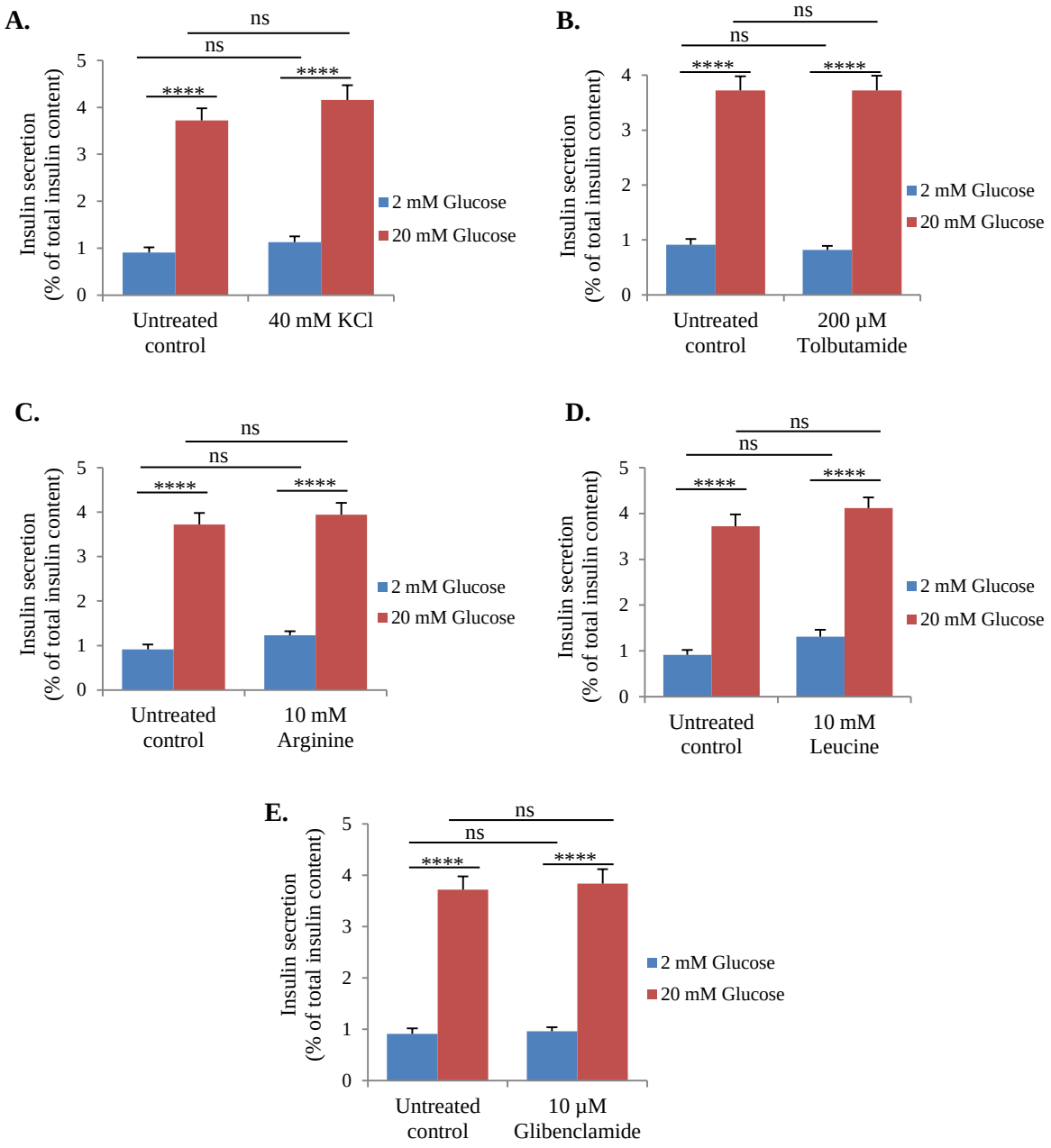

Figure 3.24: **Quantitative assays for glucose-stimulated insulin secretion in mouse islets acutely treated with insulin secretagogues**. Secretion data of islets untreated and treated with KCl (A), tolbutamide (B), arginine (C), leucine (D) and glibenclamide (E) are represented here. The assay was carried out in KRH buffer without any secretagogue. Values were normalised and expressed as the percentage of the amount of insulin secreted by the cells from the total insulin content of the cells in individual conditions. n = 3; 3 independent experiments; **** - $p < 0.0001$; ns = not significant; t-test. Data are presented as mean ± SEM.

3.2.4.2 Effects on insulin secretion of MIN6 and EndoCβH1 cells chronically treated with ISGs

To examine whether chronic exposure to ISGs could change the glucose sensitivity of the cells, and therefore change in insulin secretion capacity, both cell types were cultured in growth media containing individual ISG for up to 16 weeks. After every week, the treated cells were collected and analysed for their insulin secretion property. The treated cells were incubated in the KRH buffers (without any ISG) having low or high glucose content and analysed for insulin secretion.

Similar to the acute exposures, both untreated and chronically treated MIN6 and EndoCβH1 cells were observed to be sensitive to glucose concentration. Significantly higher amounts of insulin (near about 4 fold for MIN6 and more than 3 fold for EndoCβH1) were released in the presence of high glucose (Figure 3.25 and Figure 3.26 for MIN6 and EndoCβH1, respectively). However, there were no changes in insulin secretion in acutely ISG treated cells compared to untreated control cells in either low or high glucose conditions.

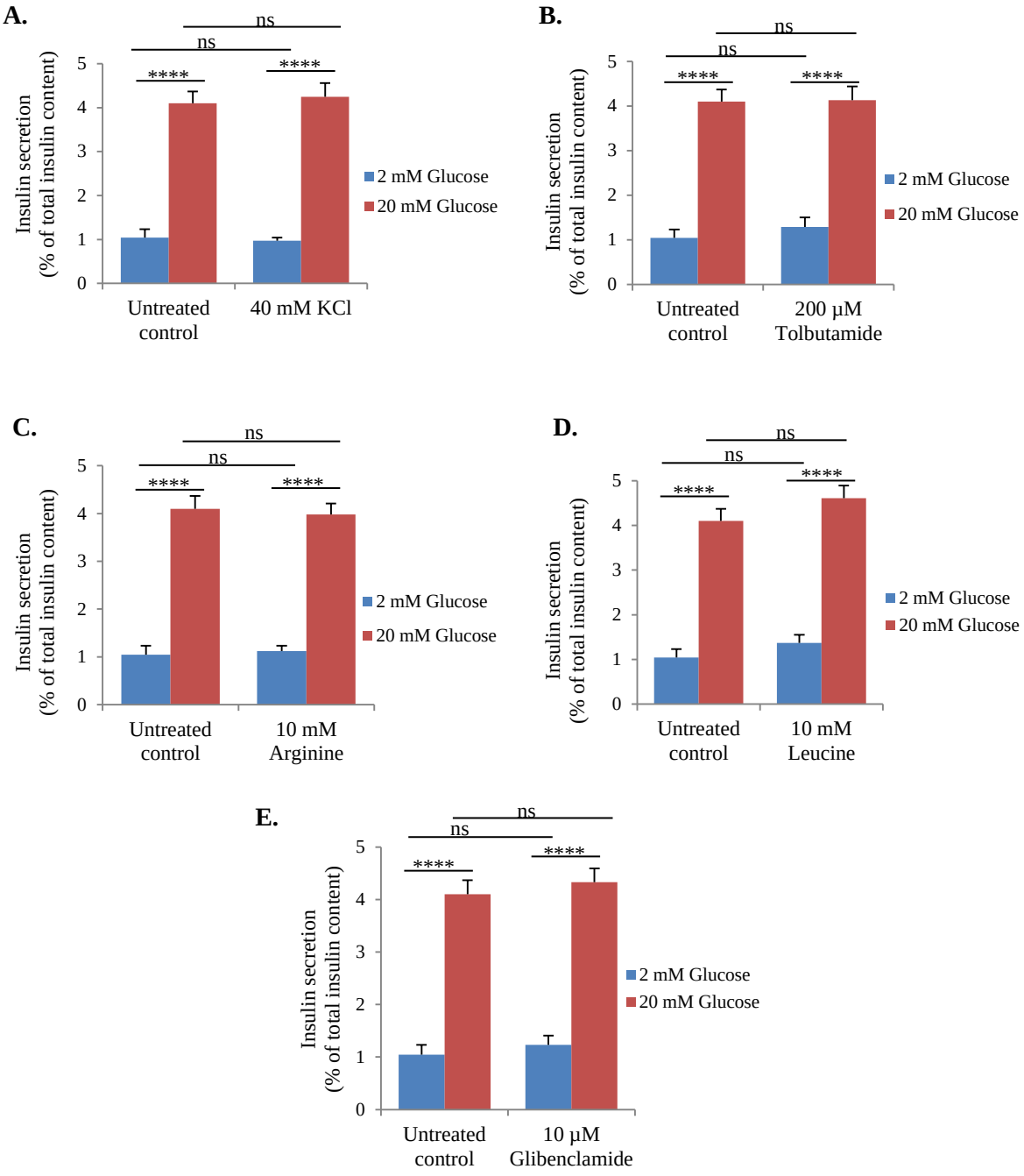

Figure 3.25: **Quantitative assays for glucose-stimulated insulin secretion in MIN6 cells chronically treated with insulin secretagogues**. Secretion data of cells untreated and chronically treated with KCl (A), tolbutamide (B), arginine (C), leucine (D) and glibenclamide (E) (after week 5, 6, and 7) are represented here. The assay was carried out in KRH buffer without any secretagogues. Values were normalised and expressed as the percentage of the amount of insulin secreted by the cells from the total insulin content of the cells in individual conditions. n = 3; 3 independent experiments; **** - $p < 0.0001$; ns = not significant; t-test. Data are presented as mean ± SEM.

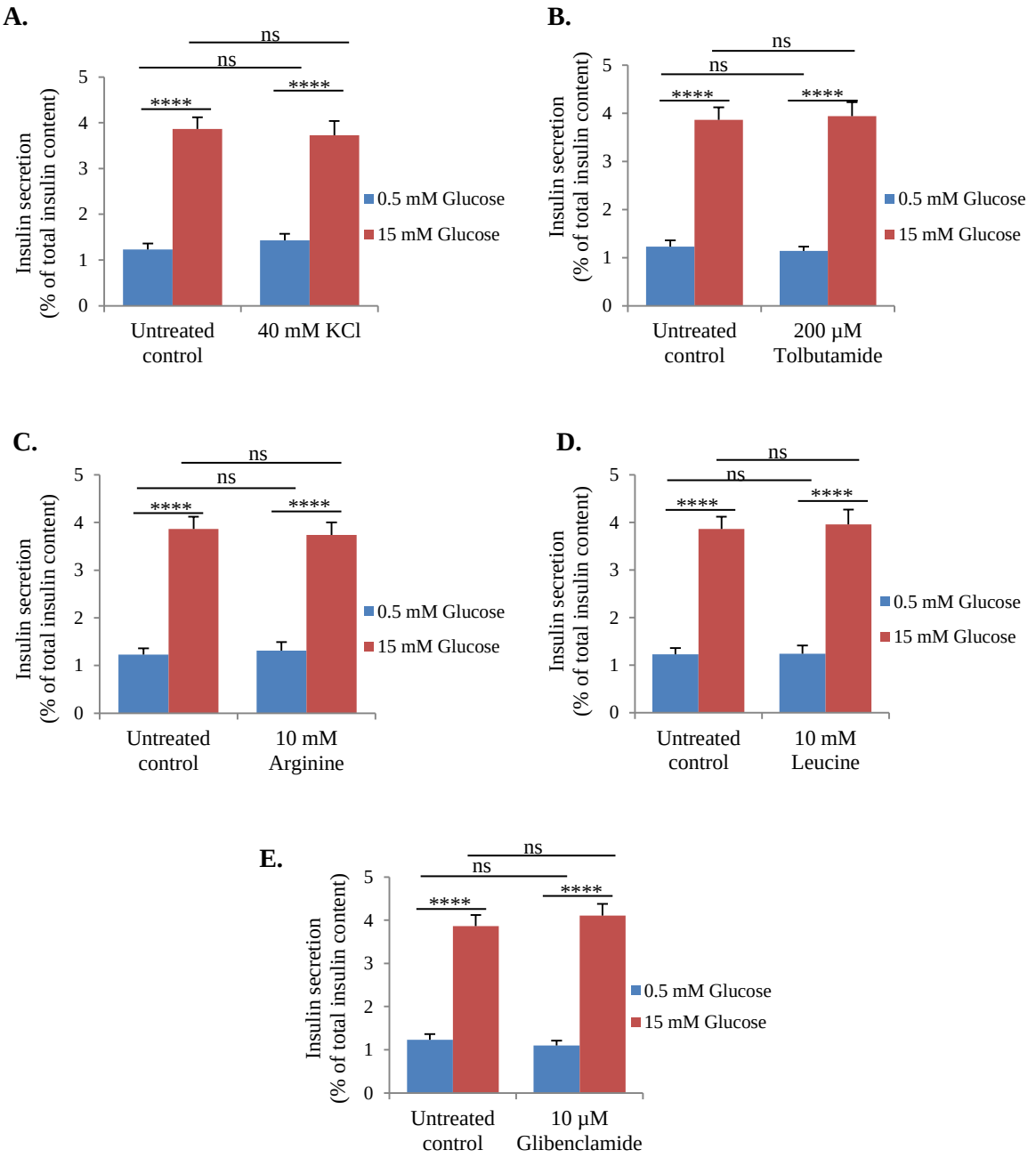

Figure 3.26: **Quantitative assays for glucose-stimulated insulin secretion in EndoCβH1 cells chronically treated with insulin secretagogues**. Secretion data of cells untreated and treated with KCl (A), tolbutamide (B), arginine (C), leucine (D) and glibenclamide (E) (after week 5, 6, and 7) are represented here. The assay was carried out in KRH buffer without any secretagogue. Values were normalised and expressed as the percentage of the amount of insulin secreted by the cells from the total insulin content of the cells in individual conditions. n = 3; 3 independent experiments; **** - $p < 0.0001$; ns = not significant; t-test. Data are presented as mean ± SEM.

The chronically treated cells were then assessed to examine whether the chronic treatment caused any alteration in cells for their sensitivity to the respective ISG for insulin release. The treated cells were collected and incubated in the KRH buffers (with respective ISG) having low or high glucose content and analysed for insulin secretion.

Both the cell types were observed to retain their sensitivity to the ISG with which the cells were treated chronically. Similar to the secretion observed in untreated cells (Figure 3.20 and Figure 3.21), significantly higher amounts of insulin were released from both the cell types in the presence of high glucose compared to the secretion in low glucose (Figure 3.27 and Figure 3.28 for MIN6 and EndoCβH1, respectively). The amount of secretion was observed to be significantly higher in both low and high glucose conditions when the cells were treated with ISGs. So, based on these observations mentioned above it was concluded that similar to acute treatment, chronic treatment with ISGs was also not a suitable way to alter insulin secretion ability of pancreatic beta cells.

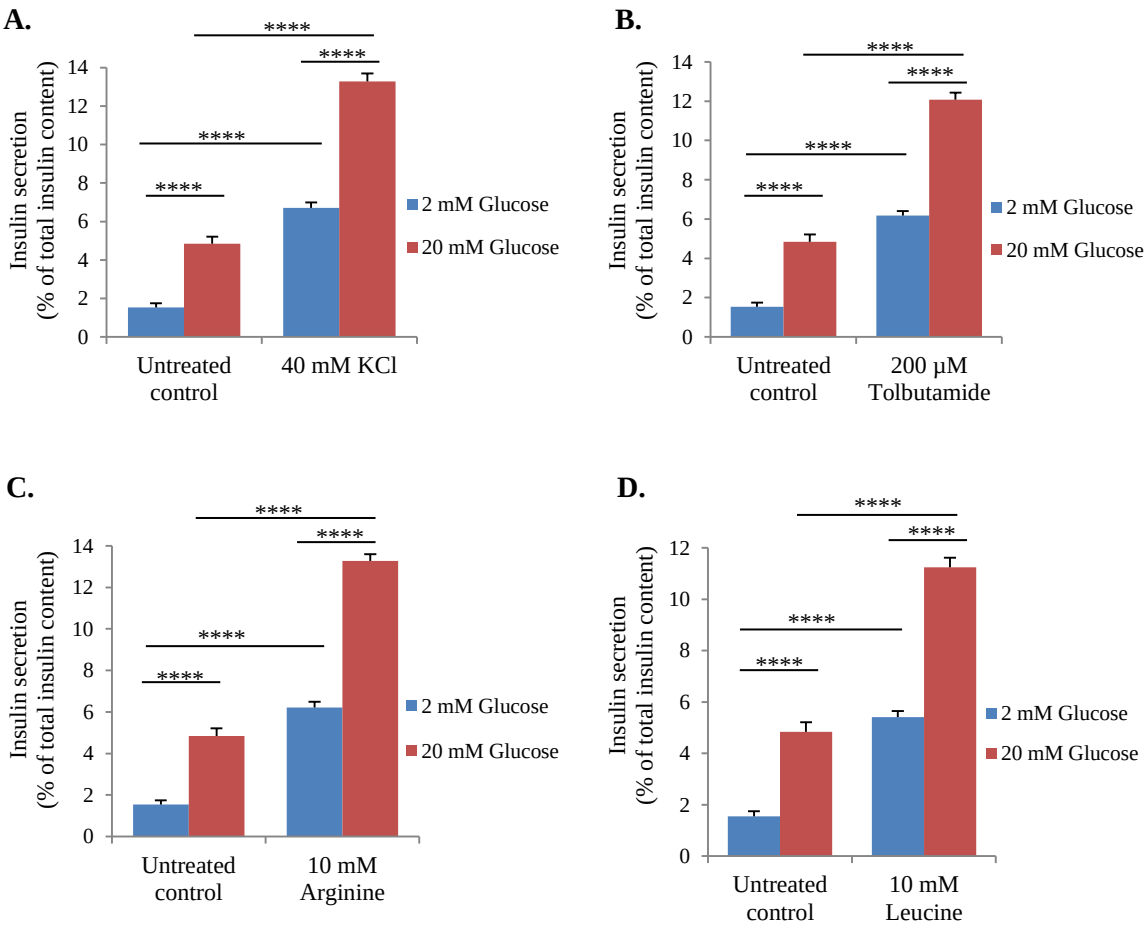

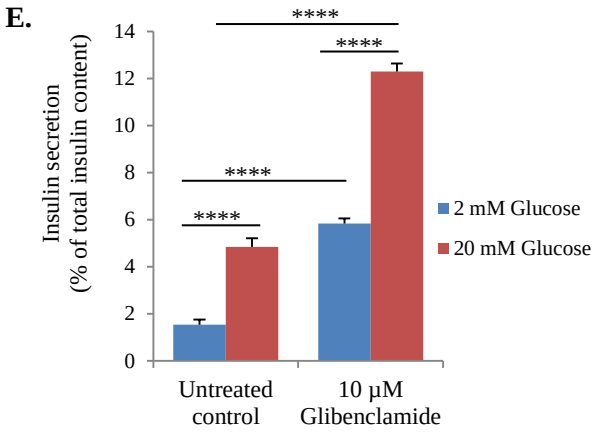

Figure 3.27: **Quantitative assays for glucose-stimulated insulin secretion in chronically treated MIN6 cells in the presence of insulin secretagogues**. Secretion data of cells untreated and treated with KCl (A), tolbutamide (B), arginine (C), leucine (D) and glibenclamide (E) (after week 5, 6, and 7) are represented here. The assay was carried out in KRH buffer with respective secretagogues. Values were normalised and expressed as the percentage of the amount of insulin secreted by the cells from the total insulin content of the cells in individual conditions. n = 3; 3 independent experiments; **** - $p < 0.0001$; t-test. Data are presented as mean ± SEM.

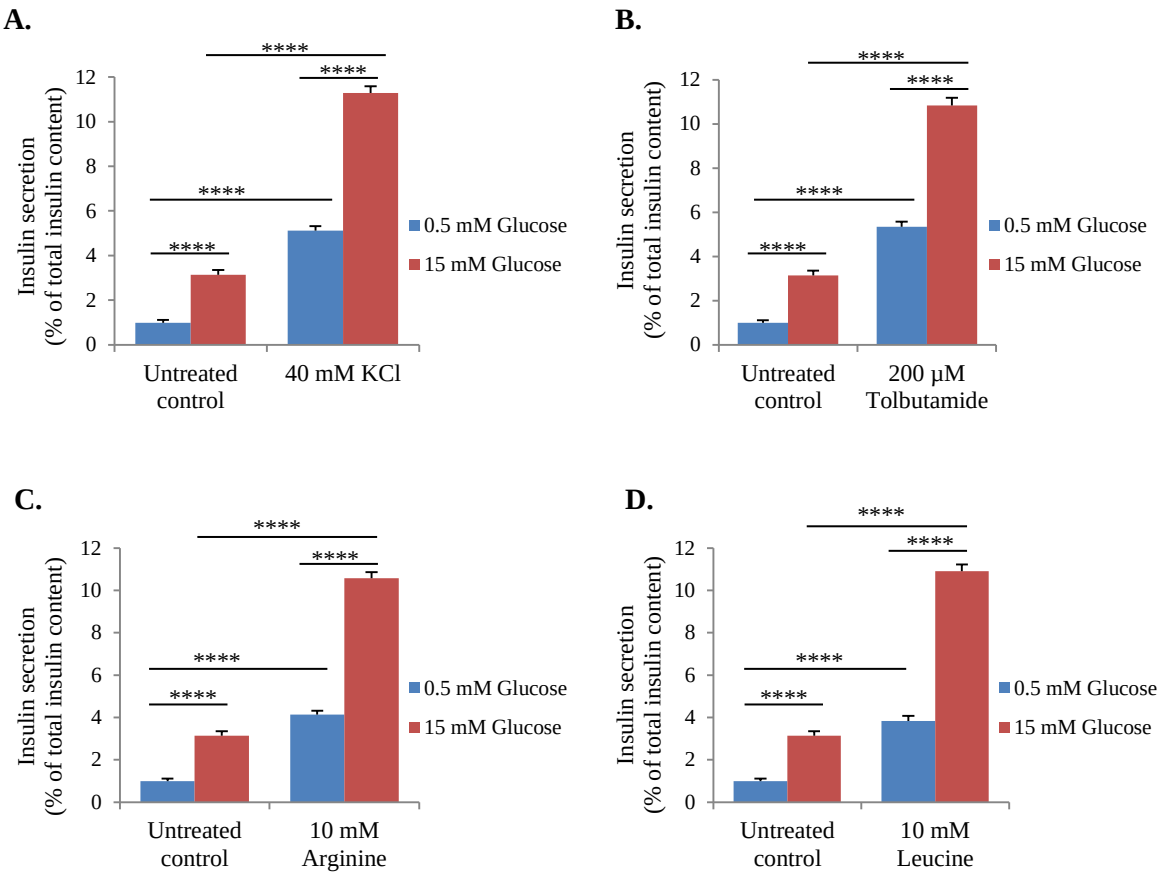

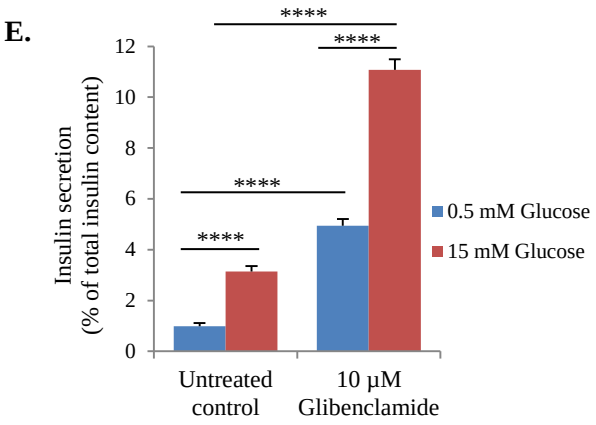

Figure 3.28: **Quantitative assays for glucose-stimulated insulin secretion in chronically treated EndoCβH1 cells in the presence of insulin secretagogues**. Secretion data of cells untreated and treated with KCl (A), tolbutamide (B), arginine (C), leucine (D) and glibenclamide (E) (after week 5, 6, and 7) are represented here. The assay was carried out in KRH buffer with respective secretagogues. Values were normalised and expressed as the percentage of the amount of insulin secreted by the cells from the total insulin content of the cells in individual conditions. n = 3; 3 independent experiments; **** - $p < 0.0001$; t-test. Data are presented as mean ± SEM.

3.2.4.3 Effects on insulin secretion of MIN6 and EndoCβH1 cells acutely and chronically treated with Tol^{high}

As mentioned in section 3.2.2.3, as an alternative approach, both the cell types were treated with Tol^{high} (500 µM tolbutamide) acutely and chronically. The treated cells were analysed for their sensitivity to glucose and therefore change in insulin secretion.

3.2.4.3.1 Effects on insulin secretion of MIN6 and EndoCβH1 cells acutely treated with Tol^{high}

Both the cell types were cultured in growth media containing Tol^{high} for 48 hours. The treated cells were then incubated in the KRH buffers (without Tol^{high}) having low or high glucose content.

Both untreated and treated beta cell types were observed to secrete significantly higher amounts of insulin in the presence of high glucose (Figure 3.29). However, no significant

changes in insulin secretion were observed in acutely tolbutamide-treated cells compared to untreated control cells in both low and high glucose conditions.

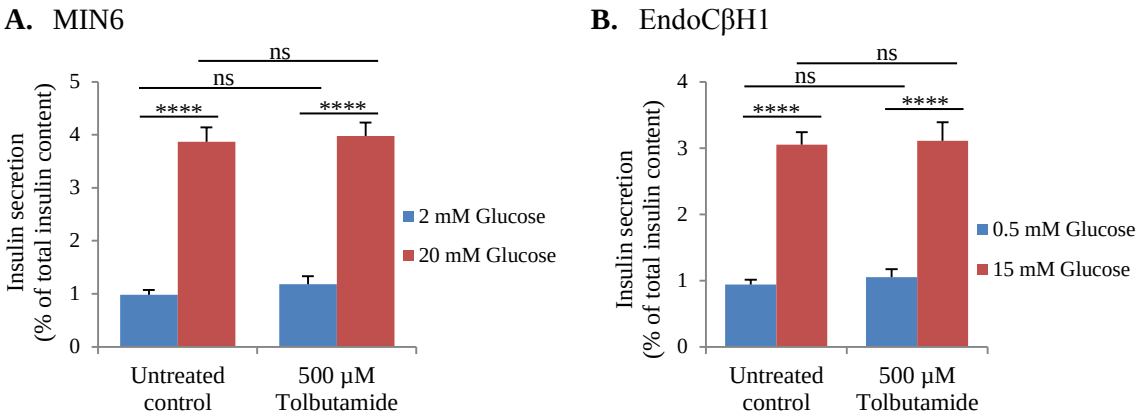

Figure 3.29: **Quantitative assays for glucose-stimulated insulin secretion in MIN6 and EndoCβH1 cells acutely treated with 500µM tolbutamide**. The image illustrates the secretion data of MIN6 (A) and EndoCβH1 (B) untreated and treated with tolbutamide. The assay was carried out in KRH buffer without tolbutamide. Values were normalised and expressed as the percentage of the amount of insulin secreted by the cells from the total insulin content of the cells in individual conditions. n = 3; 3 independent experiments; **** - $p < 0.0001$; ns = not significant; t-test. Data are presented as mean ± SEM.

3.2.4.3.2 Effects on insulin secretion of MIN6 and EndoCβH1 cells chronically treated with Tol^{high}

Both the cell types were cultured in growth media containing Tol^{high} for up to 12 weeks. After every week, the treated cells were collected and incubated in the KRH buffers (without Tol^{high}) having low or high glucose content and analysed for insulin secretion.

Similar to the acute exposures, both untreated and chronically treated MIN6 and EndoCβH1 cells were observed to secrete significantly higher amounts of insulin in the presence of high glucose (Figure 3.30). Again, there were no changes in insulin secretion in chronically tolbutamide-treated cells compared to untreated control cells in both low and high glucose conditions.

So, it can be inferred from the observations mentioned in this section 3.2.4.3 that treatment (acute or chronic) with tolbutamide (even in high concentration) was not an appropriate technique to induce insulin secretion ability in pancreatic beta cells.

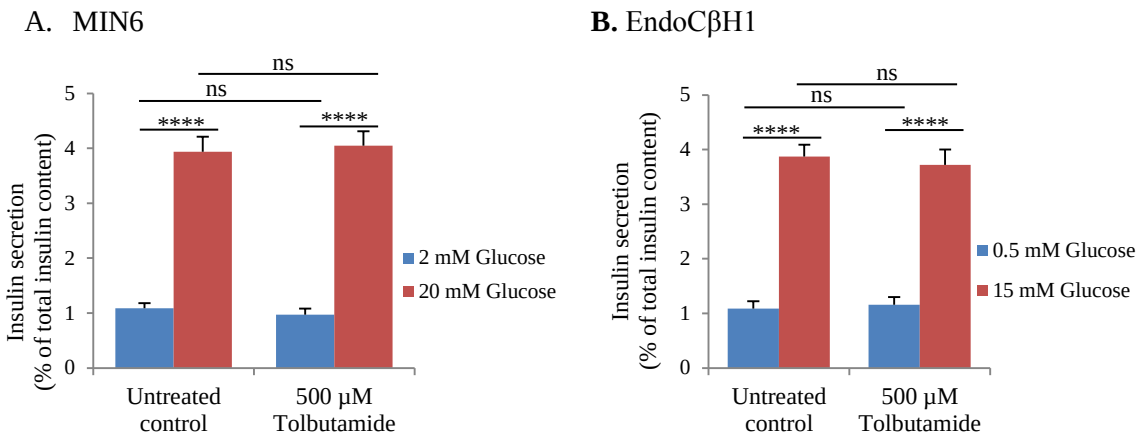

Figure 3.30: **Quantitative assays for glucose-stimulated insulin secretion in MIN6 and EndoCβH1 cells chronically treated with 500µM tolbutamide**. The image illustrates the secretion data of MIN6 (A) and EndoCβH1 (B) untreated and treated with tolbutamide. The assay was carried out in KRH buffer without tolbutamide. Values were normalised and expressed as the percentage of the amount of insulin secreted by the cells from the total insulin content of the cells in individual conditions. n = 3; 3 independent experiments; **** - $p < 0.0001$; ns = not significant; t-test. Data are presented as mean ± SEM.

3.2.4.4 Effects on insulin secretion of MIN6 and EndoCβH1 cells acutely and chronically treated with ISG_{mix}

In section 3.2.2.4, it was mentioned that as the final approach, both the cell types were treated acutely and chronically with ISG_{mix} (a mixture of two ISGs). As before, the treated cells were analysed for their sensitivity to glucose and therefore change in insulin secretion.

3.2.4.4.1 Effects on insulin secretion of MIN6 and EndoCβH1 cells acutely treated with ISG_{mix}

Both the cell types were cultured in growth media containing ISG_{mix} for 48 hours. The treated cells were then incubated in the KRH buffers (without ISG_{mix}) having low or high glucose content. Similar to previous approaches, both untreated and treated MIN6 and EndoCβH1 cells were observed to secrete significantly higher amounts of insulin in the presence of high glucose (Figure 3.31 and Figure 3.32 for MIN6 and EndoCβH1, respectively). And, again, there were no changes in insulin secretion in acutely ISG_{mix} treated cells compared to untreated control cells in either low or high glucose conditions.

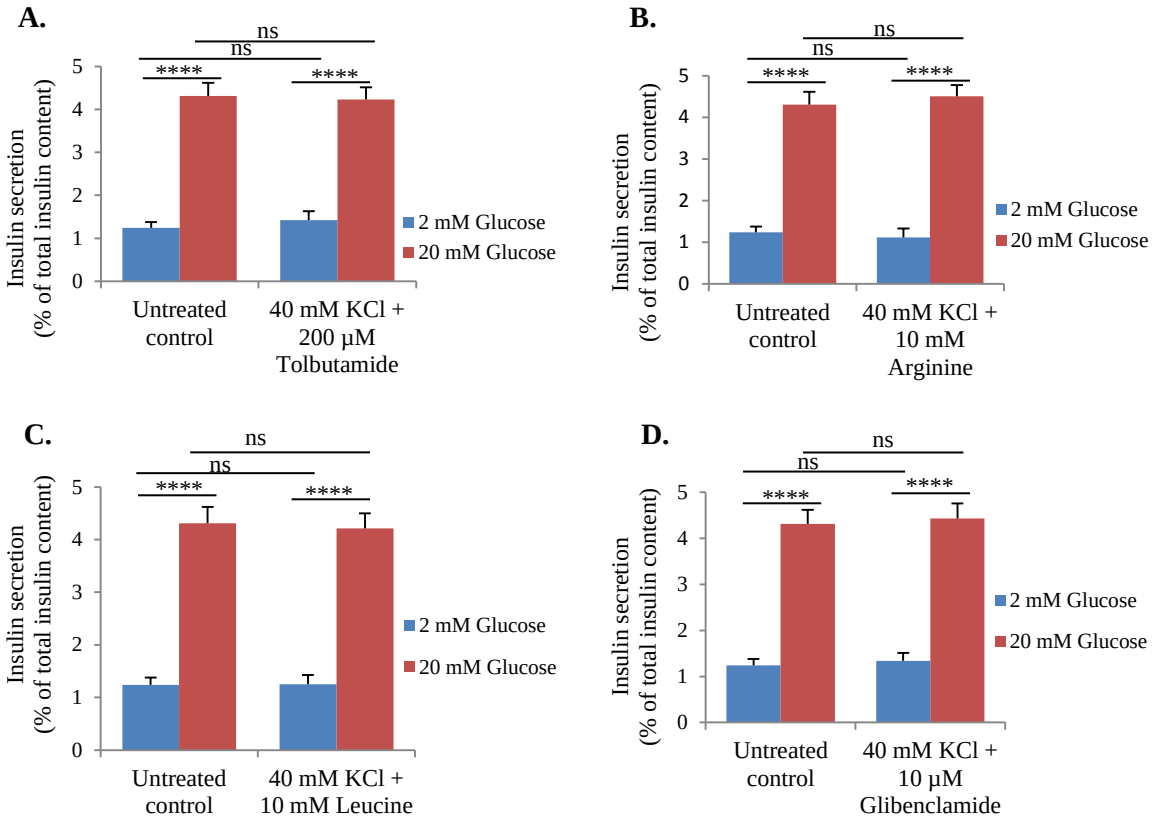

Figure 3.31: **Quantitative assays for glucose-stimulated insulin secretion in MIN6 cells acutely treated with a mixture of insulin secretagogues**. Secretion data of MIN6 untreated and treated with KCl + tolbutamide (A), KCl + arginine (B), KCl + leucine (C) and KCl + glibenclamide (D) are represented here. The assay was carried out in KRH buffer without any secretagogues. Values were normalised and expressed as the percentage of the amount of insulin secreted by the cells from the total insulin content of the cells in individual conditions. n = 3; 3 independent experiments; **** - $p < 0.0001$; ns = not significant; t-test. Data are presented as mean ± SEM.

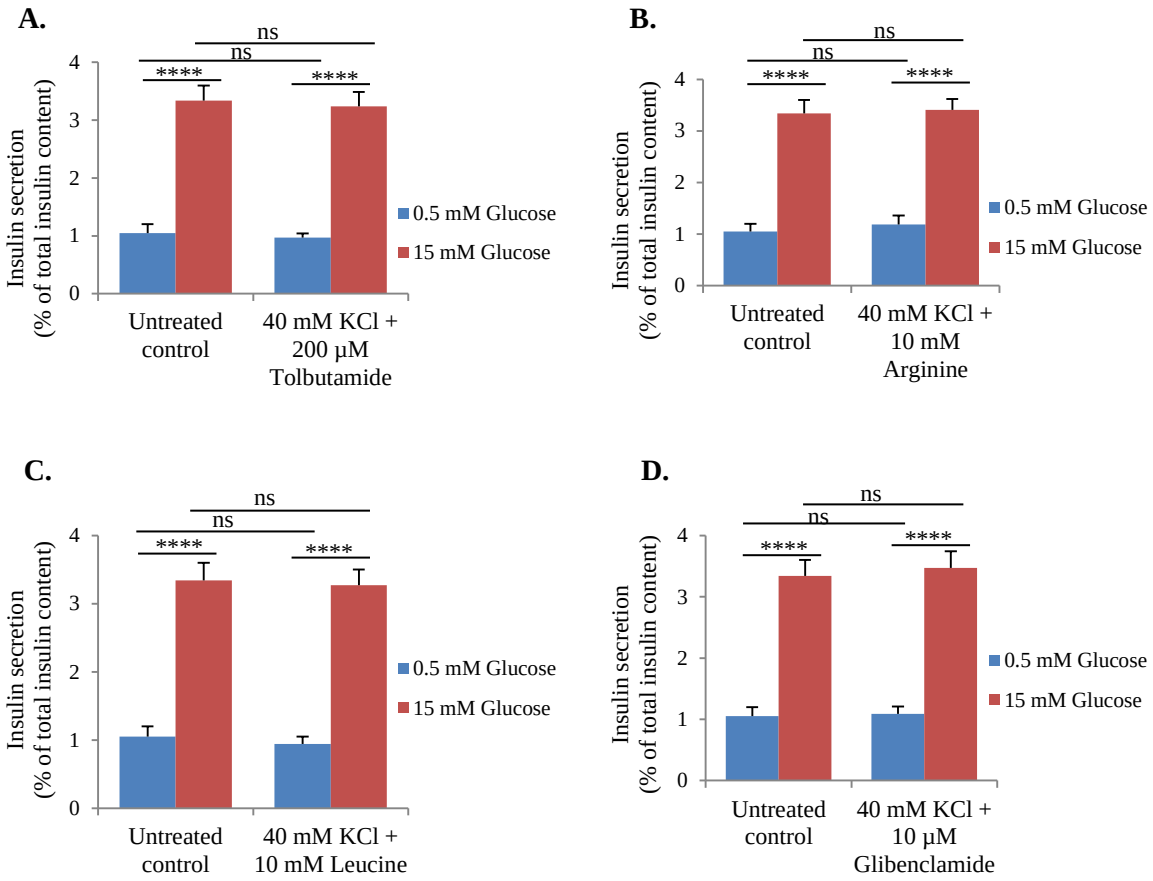

Figure 3.32: **Quantitative assays for glucose-stimulated insulin secretion in EndoCβH1 cells acutely treated with a mixture of insulin secretagogues**. Secretion data of cells untreated and treated with KCl + tolbutamide (A), KCl + arginine (B), KCl + leucine (C) and KCl + glibenclamide (D) are represented here. The assay was carried out in KRH buffer without any secretagogues. Values were normalised and expressed as the percentage of the amount of insulin secreted by the cells from the total insulin content of the cells in individual conditions. n = 3; 3 independent experiments; **** - $p < 0.0001$; ns = not significant; t-test. Data are presented as mean ± SEM.

3.2.4.4.2 Effects on insulin secretion of MIN6 and EndoCβH1 cells chronically treated with ISG_{mix}

Both MIN6 and EndoCβH1 cell types were cultured in growth media containing ISG_{mix} for up to 12 weeks. After every week, the treated cells were collected and analysed for their insulin secretion property. The treated cells were incubated in the KRH buffers (without any ISG) having low or high glucose content and analysed for insulin secretion.

Similar to acute treatments, both untreated and treated MIN6 and EndoCβH1 cells were observed to secrete significantly higher amounts of insulin in the presence of high glucose (Figure 3.33 and Figure 3.34 for MIN6 and EndoCβH1, respectively). And, again, no changes were observed in insulin secretion in chronically ISG_{mix} treated cells compared to untreated control cells in either low or high glucose conditions.

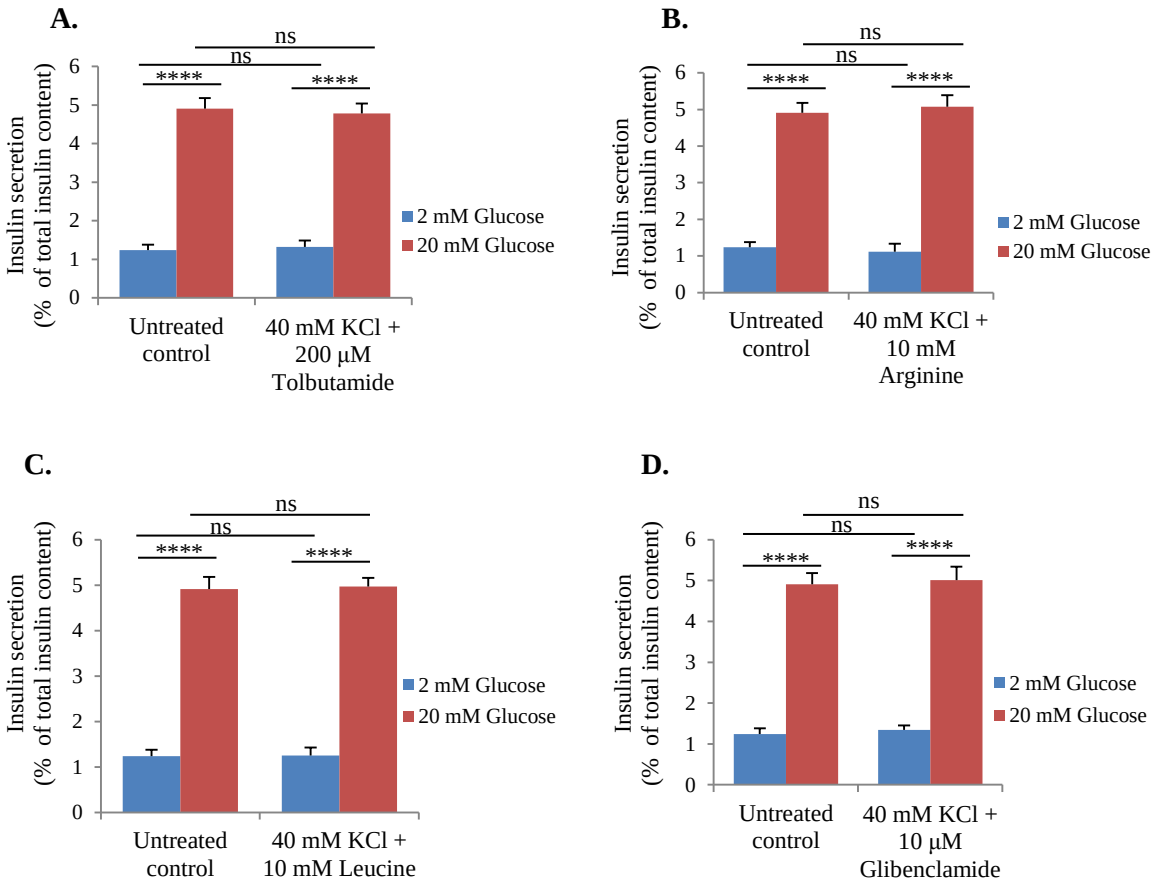

Figure 3.33: **Quantitative assays for glucose-stimulated insulin secretion in MIN6 cells chronically treated with a mixture of insulin secretagogues**. Secretion data of MIN6 untreated and treated with KCl + tolbutamide (A), KCl + arginine (B), KCl + leucine (C) and KCl + glibenclamide (D) are represented here. The assay was carried out in KRH buffer without any secretagogues. Values were normalised and expressed as the percentage of the amount of insulin secreted by the cells from the total insulin content of the cells in individual conditions. n = 3; 3 independent experiments; **** - $p < 0.0001$; ns = not significant; t-test. Data are presented as mean ± SEM.

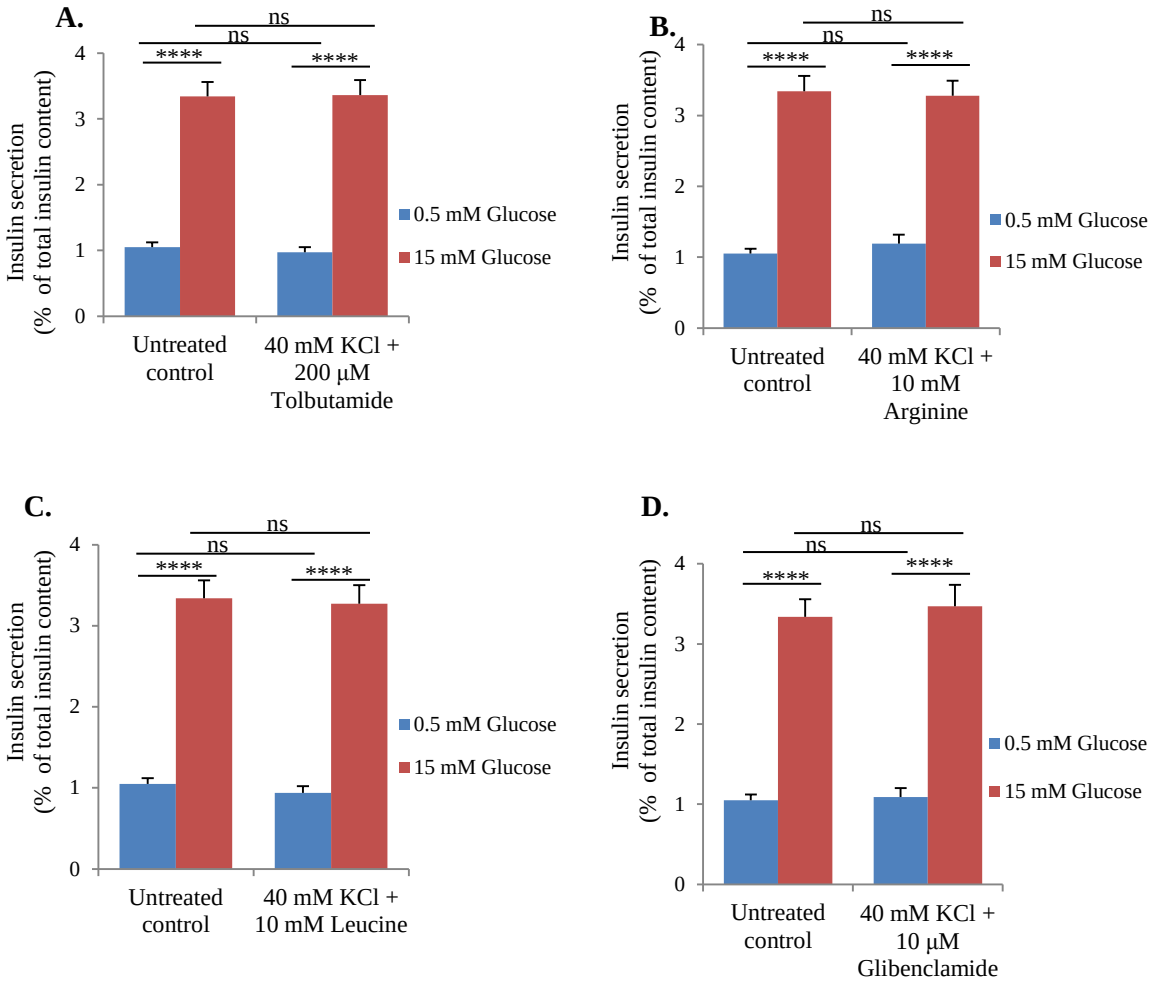

Figure 3.34: **Quantitative assays for glucose-stimulated insulin secretion in EndoCβH1 cells chronically treated with a mixture of insulin secretagogues**. Secretion data of EndoCβH1 untreated and treated with KCl + tolbutamide (A), KCl + arginine (B), KCl + leucine (C) and KCl + glibenclamide (D) are represented here. The assay was carried out in KRH buffer without any secretagogues. Values were normalised and expressed as the percentage of the amount of insulin secreted by the cells from the total insulin content of the cells in individual conditions. n = 3; 3 independent experiments; **** - $p < 0.0001$; ns = not significant; t-test. Data are presented as mean ± SEM.

So, based on the findings mentioned in this section, it can be concluded that similar to the treatments with individual ISGs, treatment with a combination of two ISGs was also ineffective as a means to alter insulin secretion capacity of pancreatic beta cells.

3.2.5 Chronic treatment of MIN6 and EndoCβH1 cells with ISGs had no effect on the expression of membrane-bound ion channels

Since treatment (acute or chronic) with ISGs had no effects on beta cell properties (cell proliferation, insulin production, and insulin secretion), it was hypothesised that the potential changes in these beta cell properties mentioned above might be counteracted by other alterations, particularly in other membrane-bound ion channel proteins important for cell metabolism and electrolyte balance. Cellular metabolism, especially, glucose homeostasis, as well as cell proliferation, are reported to be regulated by electro-physical properties of the cell (Efanova *et al*, 1998; Dunne *et al*, 2004; James *et al*, 2009; Kassem *et al*, 2010). Alteration in any of the ion (*e.g.* Na^{+}, K^{+}, Ca^{+2}) channels present in beta cells due to the treatment with ISGs could restore any changes in electro-physical properties of cells that could affect cell properties mentioned above. So, RT-PCR experiments were designed to screen any alteration of ion channels at RNA level since the change in transcription of a gene can sometimes indicate a possibility of change in protein expression and functions.

Mouse and human pancreatic beta cell membrane contain different ion channels. Gene targets were chosen according to the cell type (MacDonald and Wheeler, 2003; Yan *et al*, 2004; Vignali *et al*, 2006; Braun *et al*, 2008; Rorsman *et al*, 2012). For MIN6 cells, expression of genes encoding calcium channels including *CACNA1A*, *CACNA1B*, *CACNA1C*; potassium channels including *ABCC8*, *KCNJ11*, *KCNB1*, *KCNB2*, *KCNMA1*; and sodium channel *SCN9A* were evaluated (Figure 3.35). For EndoCβH1 cells, expression of genes encoding calcium channels including *CACNA1H*, *CACNA1D*; potassium channels including *ABCC8*, *KCNJ11*, *KCNB1*, *KCNB2*, *KCNC2*; and sodium channel including *SCN8A, SCN9A* were evaluated (Figure 3.36). These particular channel subunit genes were reported to be conserved and prominently expressed in mouse and human beta cells (MacDonald and Wheeler, 2003; Vignali *et al*, 2006; Braun *et al*, 2008). Insulin expression was also analysed for both the cell types. *GAPDH* was used as a quantitative control for both cell types. With comparison to untreated cells, no significant changes in the expression of membrane ion channels were observed in MIN6 and EndoCβH1 cells chronically treated with ISGs.

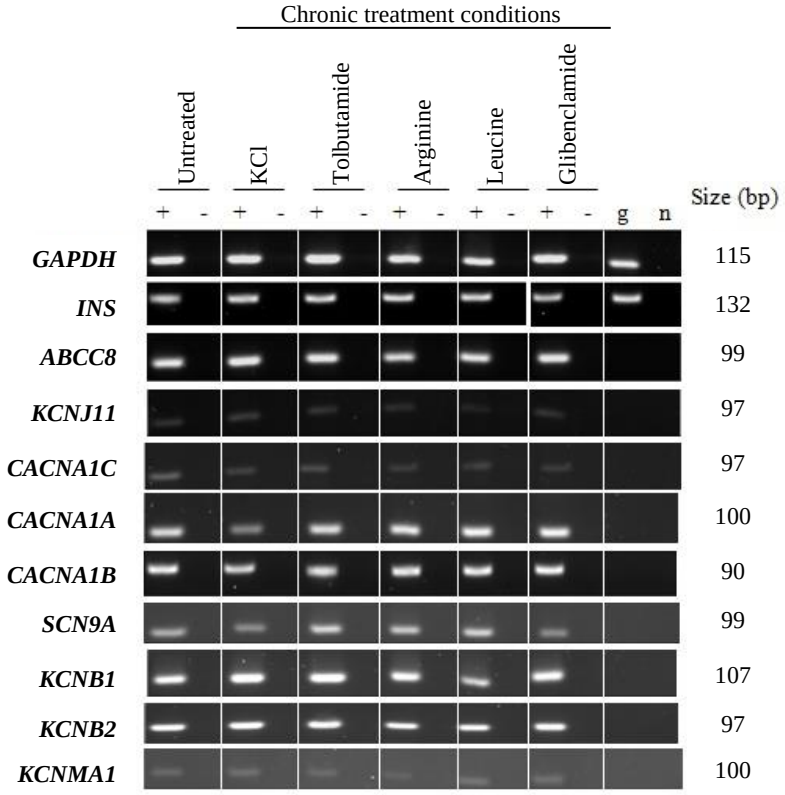

Figure 3.35: **mRNA transcript profiles of membrane-bound ion channel proteins in chronically treated MIN6 cells**. The representative mRNA expressions were analysed from cells chronically treated for 10 weeks. The lanes correspond to mRNA isolated from cells in different treatment conditions. 'g' represents mouse genomic DNA and 'n' represent PCR negative control.'+' and '-' represent cDNA positive and negative control respectively.

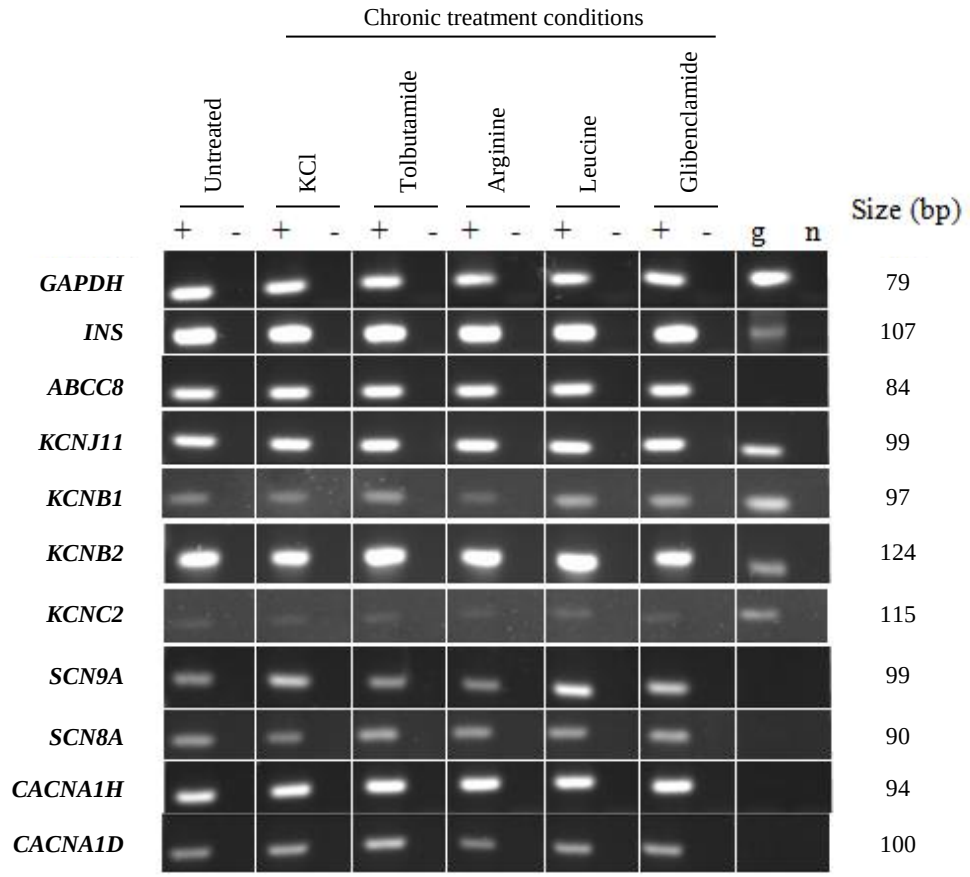

Figure 3.36**: mRNA transcript profiles of membrane-bound ion channel proteins in chronically treated EndoCβH1 cells**. The representative mRNA expressions were analysed from cells chronically treated for 10 weeks. The lanes correspond to mRNA isolated from cells in different treatment conditions. 'g' represents mouse genomic DNA and 'n' represent PCR negative control.'+' and '-' represent cDNA positive and negative control respectively.

Here, in these assays, no significant changes occurred in gene transcription of any of the ion channels analysed. However, it was not possible to rule out the possibility that protein production could be affected since mRNA levels do not necessarily equate to protein levels. To examine this, western blot experiments were carried out using protein extracted from untreated and chronically treated MIN6 and EndoCβH1 cells. K_{ATP} channel proteins were considered preliminarily to correlate the findings at mRNA level with protein level. Only Kir6.2 protein expression was examined, as unfortunately, antibodies against SUR1 were unsuitable for western blot analysis. From the analysis, it was observed that chronic

exposure of cells to ISGs did not have a significant effect on Kir6.2 protein production in the cell (Figure 3.37).

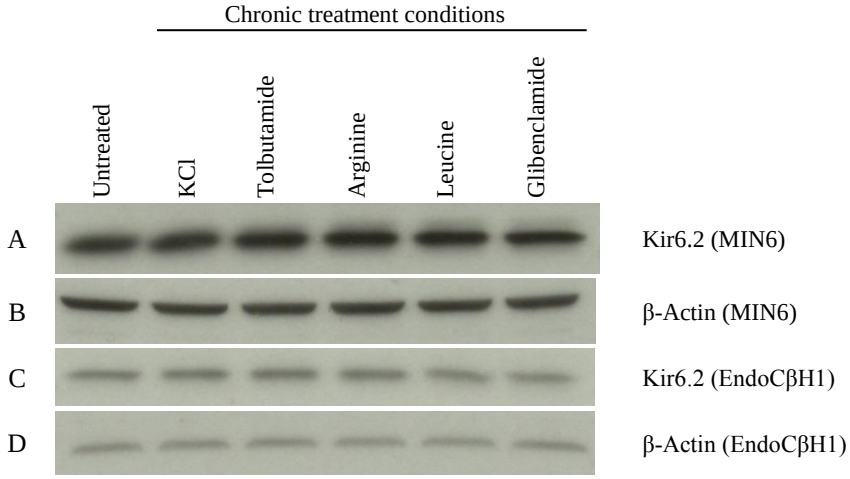

Figure 3.37: **Western blot analysis of chronically treated MIN6 and EndoCβH1 cells stained with anti-Kir6.2 and anti-β-Actin antibody**. Proteins were extracted from cells treated for 10 weeks. A and B show the expression in MIN6 cells whereas C and D show the expression in EndoCβH1 cells. The lanes correspond to proteins detected from cells treated in different conditions. β-Actin was used as a loading control. Samples were separated in 12% polyacrylamide gels. Membranes were incubated separately with the antibodies.

It is well known that the expression of a gene at mRNA and protein levels do not always correlate with each other as well as with its level of functional activity. However, it can suggest some preliminary links to follow for downstream analysis. Both the RT-PCR and western blot data indicated the similar findings that ISGs had no effect on K_{ATP} channels expression. However, based on mRNA profile only, it was not possible to rule out the potential changes of other ion channels at the protein level, either protein expression or functional expression of channels at the cell surface which would influence ion flux and thus, cellular metabolism. Analysing functional activities of these ion channels would require a lot of time. The main focus of the study described in this chapter was to develop an *in vitro* condition to modulate model beta cells to behave as CHI-like cells. Since the approaches described in this chapter did not alter any cell properties (cell proliferation and insulin secretion) and the cells did not behave as CHI-like cells, so it was decided not to continue with these approaches anymore. Thus, functional activity studies on these ion channels were not carried out.

3.3 Discussion

The aim of the study was to generate an *in vitro* condition in which a model pancreatic beta cell line could be made to behave in a similar manner to CHI tissues. A very widely used mouse pancreatic beta cell line, MIN6 and a recently developed human model cell line, EndoCβH1 were used for this purpose.

The foremost features of CHI are increased insulin secretion from beta cells as well as beta cell hyperproliferation. Since insulin can act as a potential growth factor, so it was postulated that modifying cell culture conditions by the addition of insulin secretagogues (ISGs), alone or in combination, could induce the cells to transform into cell models that could behave similar to CHI cells (in terms of insulin secretion and cell proliferation). However, all the analyses and their data confirmed that implemented chemical induction method by using insulin secretagogues was not sufficient to transform the pancreatic beta cells into a CHI-like model cell line.

As it is mentioned in section 3.1.1, CHI is a metabolic disorder affecting neonates and early infants. This disorder is characterised by severe, persistent hypoglycemia due to inappropriate increased insulin secretion from pancreatic islet β-cells (Stanley and Baker, 1976; Dunne *et al,* 2004; Senniappan *et al,* 2012; Proverbio *et al,* 2013; Arya *et al,* 2014). In addition to the uncontrolled insulin secretion, the other major feature of CHI is hyperproliferation of affected beta cells compared to normal, unaffected cells. This increased proliferation was observed both in Fo-CHI and Di-CHI tissues (Kassem *et al,* 2000; Kassem *et al,* 2010; Lovisolo *et al,* 2010; Salisbury *et al,* 2015). Although, one study was reported not to find any significant association of CHI with beta cell hyperproliferation (Sempoux *et al*, 1998a).

Increased uncontrolled insulin secretion is the major feature of CHI, and also insulin was reported to act as a potential growth factor (Hill and Milner, 1985; Ish-Shalom *et al,*1997; Desbois-Mouthon *et al*, 2000; Beith *et al,* 2008; Heni *et al,* 2011; Li *et al,* 2017). Insulin has a low affinity to insulin-like growth factor (IGF) receptors and can bind to IGF receptors in high concentration. Thus upon binding to the IGF receptors, insulin can mediate growth promoting effects (Hill and Milner, 1985; Boucher *et al*, 2010). So, hyperproliferation observed in CHI tissues could be linked with this increased insulin

secretion. Further, increased proliferation of beta cells has been reported in rodent models to be associated with glucose sensing and insulin secretion pathways (Porat *et al,* 2011; Dadon *et al,* 2012). So, considering these facts in mind, it was hypothesised in this study that chemical induction of beta cells using secretagogues for increased insulin secretion might promote cells to acquire behaviour similar to CHI in terms of insulin secretion and cell hyperproliferation.

Five ISGs - KCl, two sulfonylureas (tolbutamide, glibenclamide) and two amino acids (arginine, leucine) were used in this study to induce the cells for hyperproliferation and insulin hypersecretion.

Previously, Popiela and Moore, (1991) reported increased cell proliferation in rat islet cells in the presence of tolbutamide. In contrast, tolbutamide was also reported to reduce cell proliferation in pancreatic islets and some other mammalian cell types (Efanova *et al,* 1998; Sanchez-Alvarez *et al,* 2006). The continuous presence of leucine in the growth medium was suggested to stimulate cell proliferation in a mammalian cell line (porcine ectoderm cell) (Kim *et al,* 2013). Increased cell proliferation was evidenced when mammalian cell types (human endometrial cell, human dermal fibroblast cell, rat islet cell, porcine ectoderm cell) were incubated continuously with arginine (Green *et al,* 2013; Kim *et al,* 2013; Fujiwara *et al,* 2014; Mullooly *et al,* 2014). Cells were treated with the secretagogues for 1 - 4 days in all of these studies mentioned above. There is no previous report of this proliferation study with KCl and glibenclamide. None of the earlier studies was carried out on MIN6 and EndoCβH1 cell line. Since secretagogues were found to increase cell proliferation in some cell types, so it was assumed that ISGs might affect these beta cell lines and increase cell proliferation. The experiment was designed to monitor the cell proliferation up to eight days as the untreated cells usually reached 70-80% confluency after eight days. However, neither of the cell types (MIN6 and EndoCβH1) showed any changes in cell proliferation while growing continuously in the presence of the ISGs for eight days. So, it can be inferred that the continuous presence of ISGs in growth medium might not be able to produce any direct effect on the proliferation of MIN6 and EndoCβH1 cells normally.

Hence, as alternative approaches, the experiments were designed to treat the beta cells with ISGs for either short (acute, 48 hours) or long (chronic, up to 16 weeks) period of

time and then evaluate the possible changes in proliferation of the cells without the presence of ISGs. It was hypothesised that short to prolonged exposure of cells to ISGs could bring permanent changes in cells which would affect the proliferation property of the cells. No previous studies were reported earlier where the cells were treated with ISGs for a certain period of time and then evaluate the changes in cell proliferation in the absence of that particular ISG. Experimental data in this study suggested that ISGs were unable to induce any changes in the cells that might influence cell proliferation whether cells were treated acutely or chronically with the ISG individually. Some studies also reported the use of higher concentration of tolbutamide (500 µM) in treating different cell types (Huang *et al,* 1995; Ammala *et al,* 1996a; Ammala *et al,* 1996b; Gribble *et al,* 1997a). Again higher concentration of tolbutamide could not bring any change in both MIN6 and EndoCβH1 cell proliferation. As an alternative approach, experiments were designed to treat cells with a mixture of two ISGs where KCl was used in all combination as a K_{ATP} channel-independent cell depolariser (Gembal *et al,* 1992; Hatlapatka *et al,* 2009; Hatlapatka *et al,* 2011). It was assumed that the combination of ISGs could have more stimulation effect to induce cell hyperproliferation. Again, no success was there with this approach. So, based on the experimental data, it can be inferred that increased secreted insulin through the actions of ISGs might not have any effect on cell proliferation in either MIN6 or EndoCβH1 beta cells.

A number of studies were reported earlier showing the response of MIN6, EndoCβH1 and other beta cell lines to ISGs in different glucose concentrations. The cells were reported to secrete higher amount of insulin in the presence of ISGs both in low and high glucose conditions (Landgraf *et al,* 1974; Gembal *et al,* 1992; Johnson *et al,* 2007a; Cheng *et al,* 2012; Andersson *et al,* 2015). In one study, arginine was shown capable to increase insulin release only in high glucose condition, not in low glucose condition (Ishiyama *et al,* 2005. Both the MIN6 and EndoCβH1 cell undergoing studies showed similarly increased insulin secretion in the presence of ISGs.

However, it was reported in some studies that acute (18-48 hours) exposure of cells and islets with ISG might impair cellular properties including glucose-stimulated insulin release. Tolbutamide and glibenclamide were reported to reduce sensitivity to glucose and lowered insulin release in acutely treated cells (Brennan *et al,* 2006). Insulin secretion from islets was reported to be lowered after acute treatment with arginine (Mullooly *et al,*

2014). After acute treatment with leucine, lowered insulin secretion was reported by Anello *et al.* (2001) and Liu *et al.* (2012) whereas increased secretion was reported by Yang *et al.* (2006). In contrast, no significant changes in insulin secretion in cells were observed by Yang *et al.* (2004) and Mullooly *et al.* (2014) after acute treatment with leucine. Nonetheless, pancreatic islets were reported to acquire increased insulin secretion capacity after one week of chronic treatment with leucine (Yang *et al*, 2004) whereas reduced secretion ability was reported for cells treated with glibenclamide for two weeks (Ball *et al*, 2000). No other study was reported on cells treated with other ISGs or with ISGs continuously for 12-16 weeks.

So variability was observed in different cell types in terms of insulin secretion after acute or a couple of weeks of treatment with ISGs in earlier reports. However, it was hypothesised that MIN6 or EndoCβH1 cells could be amenable to short or prolong exposure (several weeks) to ISGs and this treatment could bring permanent changes in either of these cell types which could alter mechanisms of the cells to secrete higher amount of insulin continuously without proper stimulations. So, the experiments were designed to treat the beta cells with individual ISGs or a mixture of two ISGs for either short (acute, 48 hours) or long (chronic, up to 16 weeks) period of time and then evaluate the possible changes in the cells for insulin secretion without the presence of ISGs.

From the experimental data, it was observed that ISGs used in this study individually or as a mixture were unable to induce any significant changes in insulin secretion while the beta cells or mouse islets (as a control cell model) were treated acutely (for 48 hours) or chronically. So, based on the experimental data, it can be inferred that ISGs are unable to induce any change in insulin secretion mechanism in either MIN6 or EndoCβH1 beta cells after acute or chronic treatments.

It was reported previously that mouse and human pancreatic beta cells contain different membrane-bound ion channels in addition to K_{ATP} channels (MacDonald and Wheeler, 2003; Yan *et al*, 2004; Vignali *et al*, 2006; Braun *et al*, 2008; Rorsman *et al*, 2012). These channels act in an integrated fashion to control the electrolyte balance and hence, cell metabolism. As acute or chronic treatment of cells with ISGs showed no effect on insulin secretion as well as cell proliferation, it was hypothesised that the potential effects of ISGs could be counteracted by any other alterations in any of these membrane-bound ion

channel proteins. No reports were published earlier regarding the expression profiles of ion channels in beta cells acutely or chronically treated with ISGs. So experiments were designed for chronically treated both the MIN6 or EndoCβH1 cells to investigate the expression of some ion (Na^+, K^+ and Ca^{2+}) channel genes at mRNA level according to the cell source (mouse or human). Although the change of mRNA level does not necessarily correlate with the change of the protein expression level and downstream functions, sometimes some changes in mRNA level can lead to new findings to explain the reasons behind that. Chronic treatments with ISGs were unable to induce any changes in ion channels expression at mRNA level both in MIN6 and EndoCβH1 cells. Since confirming the functional activities of these ion channels would take time and as these analyses were beyond this present research focus, functional activity studies on these ion channels were not carried out. Hence, it was not possible to conclude whether these ion channels were altered to minimise the effect of ISGs in terms of insulin secretion or cell proliferation.

Briefly, the major features of CHI are cell hyperproliferation and increased uncontrolled insulin secretion from beta cells. This study attempted to induce pancreatic model beta cell lines, MIN6 and EndoCβH1 to acquire characteristics similar to CHI cells in terms of cell proliferation and insulin secretion. This induction was carried out by modifying growth medium composition through the addition of ISGs. Since ISGs are reported earlier for their capability to induce insulin hypersecretion in cells and since insulin can act as a growth factor, so it was believed that treatment (either acute or chronic period of time) of beta cells with ISGs could stimulate the cells to be CHI-like. However, neither acute nor chronic treatments with any of the ISGs could bring any change in MIN6 or EndoCβH1 cells in terms of cell proliferation and insulin secretion. So, it can be concluded that chemical induction using ISGs was not an appropriate method of choice to transform beta cells into a CHI-like model cell line.

Chapter 4

Implementing CRISPR-Cas9 to knock out the *ABCC8* gene to generate *in vitro* CHI model cell line

4.1 Introduction

4.1.1 General

It is described in the previous chapter (Chapter 3) that chemical induction by using insulin secretagogues was not an appropriate method of choice to transform the pancreatic beta cells into a CHI-like model cell line. It is mentioned earlier that malfunctional ATP-sensitive potassium (K_{ATP}) channels found on the membrane of pancreatic beta cells are associated with CHI in most of the CHI cases (Dunne *et al*, 1997; Marthinet *et al*, 2005; Kapoor *et al*, 2013; Sang *et al*, 2014; Nessa *et al*, 2016). It was therefore hypothesised that introducing mutations in K_{ATP} channel genes (*ABCC8* and *KCNJ11*) to make the channels malfucntional would promote CHI characteristics in cells. Hence, experiments were conducted to introduce mutations to knock-out the activity of K_{ATP} channels with a view to generating a CHI-like model cell line

4.1.2 Experimental approaches used in this study

Two cell lines were utilized in this gene editing-based approach of generating CHI-like model cell lines. One cell line was EndoCβH1 and the other one was an iPS (induced pluripotent stem) cell line. EndoCβH1 is described in section 3.1.4. The iPS cell line was derived in our laboratory from *ex vivo* expanded pancreas tissue of a Fo-CHI patient. This CHI tissue-derived iPS (CHI-IPS) cell line was established by targeted expression of key genetic factors (Oct3/4, Sox2, Klf4 and c-Myc) necessary for reprogramming somatic cells into iPSCs. This reprogramming was performed through retrovirus-mediated gene transduction (using Sendai reprogramming kit, Life Technologies, Thermo Fisher Scientific) and conducted by Dr Sophie Kellaway (Kellaway, 2016). Successful reprogramming to iPS cells and their pluripotency was confirmed by immunofluorescence, flow cytometry and differentiation studies (Kellaway, 2016).

The CHI-iPS cell line was originally established from a Fo-CHI pancreatic tissue with a heterozygous recessive mutation in the *ABCC8* gene (details in section 4.2.1). The cells that were used to make the CHI-iPS cell line were from the healthy tissue at the edge of the focal lesion. The cells were healthy, carried the recessive allele, and did not show insulin over-secretion as like CHI (Kellaway, 2016). So, the heterozygous recessive mutation might not have any deleterious effect on *ABCC8* expression *in vitro* which, otherwise, induced CHI in some cells *in vivo*. It was assumed that homozygous mutation might be helpful to induce CHI in *in vitro* condition. Malfunctional K_{ATP} channels because of homozygous mutations in the *ABCC8* gene were reported earlier in CHI patients (Yan *et al*, 2007; Flanagan *et al*, 2009; Rahman *et al*, 2015a; Nessa *et al*, 2016). Therefore, it was hypothesised that introduction of a second mutation at the mutated locus of CHI-iPS cells, so that both copies of the *ABCC8* gene would be mutated, would have the potential to make the gene inactive or malfunctional. Malfunctional K_{ATP} channels because of deletion mutations in the *ABCC8* or *KCNJ11* gene were also reported earlier in CHI patients (James et al, 2009; Flanagan et al, 2012; Fan et al, 2015). Hence, it was also hypothesised that the introduction of a deletion mutation in either of the *ABCC8* or the *KCNJ11* gene would make the channels malfunctional. So, different experimental approaches were considered to edit the *ABCC8* or the *KCNJ11* gene by introducing either homozygous or deletion mutations.

It was reported that iPS cells preserve an epigenetic memory of the original somatic tissue from which they have been established, and this epigenetic memory helps iPS cells for the differentiation towards the cells of origin (Kim *et al*, 2010; Bar-Nur *et al*, 2011; Vaskova *et al*, 2013; Liang and Zhang, 2013). Since CHI-iPS cell line was originally established from a Fo-CHI pancreatic tissue, so it was hypothesised that the use of this iPS cell line would be helpful for the differentiation into pancreatic beta-like cells.

4.1.3 Stem cells and their potential for generation of CHI *in vitro* models

Stem cells, a class of undifferentiated cells, are able to differentiate into many different cell types in the body during early life and growth. These cells play a crucial role in the development and/or body repair processes. These cells have the capability to grow without limit in *in vitro* culture condition (Wu *et al*, 2016; Paterson *et al*, 2017). When a stem cell divides, each new cell has the capability to differentiate into another type of cell

or to remain as a stem cell (Pittenger *et al,* 1999; Bach *et al,* 2000; Liu *et al,* 2000; Odorico *et al,* 2001).

Two types of stem cells have been primarily studied- embryonic stem (ES) cells and adult stem (AS) cells (Kao *et al,* 2011). ES cells are isolated from blastocyst stage embryos and are considered to be pluripotent, *i.e.* they are able to differentiate into almost any cell type (Hwang *et al,* 2004; Johnson *et al,* 2008; Narsinh *et al,* 2011). These cells are easy to grow *in vitro*. AS cells are found inside of different types of tissue and considered to be multipotent, *i.e.* these cells have limited ability to differentiate into other cell types (Oshima *et al,* 2001; Toma *et al,* 2001; Beltrami *et al,* 2003). AS cells are very limited in number in mature tissues and their origin in most tissues are still not conclusive (Boisset and Robin, 2012; Sidhu *et al,* 2012). A third type of stem cells, induced pluripotent stem (iPS) cells, are basically engineered somatic cells which are genetically reprogrammed to be ES-like cells and these cells are not very different in terms of pluripotency compared to ES cells (Takahashi and Yamanaka, 2006; Leeper *et al,* 2010; Okita and Yamanaka, 2011; Koh and Piedrahita, 2014). All of the stem cell lines are important models for understanding cell development and biology.

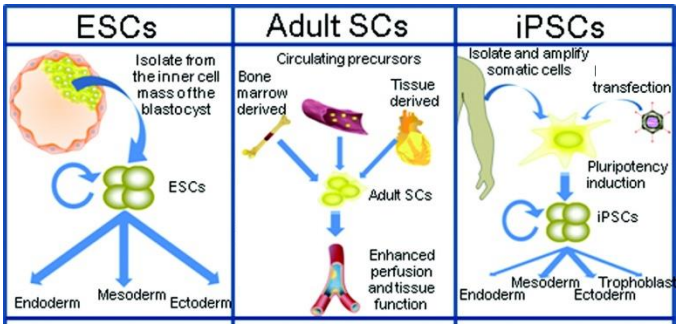

Figure 4.1: **Schematic illustration of types of stem cells and their source of origin**. Embryonic stem cells are isolated from blastocyst of embryos and these cells are pluripotent, *i.e.* these cells can produce any cells of endodermal, mesodermal or ectodermal lineage. Adult stem cells are isolated from bone marrow, circulation or resident tissues. These cells are multipotent and cannot be differentiated into cells of ectodermal or endodermal lineage. These cells are partially lineage committed and hence, can give rise to the cells of their origin to enhance tissue functions. On the other hand, induced pluripotent stem cells are reprogrammed somatic cells that can behave similarly to embryonic stem cells. The image is adapted from Leeper *et al*. (2010).

A number of previous studies have established a range of differentiation protocols to transform ES and iPS cells into mature and functional insulin-producing pancreatic beta cells (Zhang *et al,* 2009; Rezania *et al,* 2012; Pagliuca *et al,* 2014; Rezania *et al,* 2014; Millman *et al,* 2016). None of these studies was reported to use pancreatic progenitor cells to produce insulin-producing cells. However, successful generation of insulin-producing cells from ES and iPS cell lines indicated the possibility of generating a CHI disease model cell line from either stem cell type (Musunuru, 2013; Sterneckert *et al,* 2014). More recently, two studies were reported to generate *ABCC8* deficient human ES cell lines with knocked out K_{ATP} channels (Guo *et al,* 2016; Guo *et al,* 2016a). These findings illustrate the possibility of stem cell-based CHI models.

4.1.4 CRISPR/Cas9: an efficient gene editing tool to generate disease model

The emerging technology of genome editing provides the ability to introduce a variety of genetic alterations with high efficiency and target specificity. The alteration could be as small as a single-nucleotide modification or could be a whole gene addition or deletion (Musunuru, 2013).

Among the various high-throughput genome editing tools, the CRISPR-Cas9 method offers efficient and reliable means to introduce precise and targeted changes to the genome of living cells (Cong *et al,* 2013; Ran *et al,* 2013). CRISPR (Clustered Regularly Interspaced Short Palindromic Repeats) and CRISPR-associated (Cas) genes are essential in microbial adaptive immunity. This is a defence mechanism of microbial organisms to get rid of invading foreign genetic materials using RNA-guided nuclease systems (Musunuru, 2013; Ran *et al,* 2013; Kim *et al,* 2014; Maruyama *et al,* 2015).

Among the three types (I-III) of CRISPR systems identified so far in a wide variety of bacteria and archaea, the Type II CRISPR system is the most widely used system that has been modified for genome engineering (Ran *et al,* 2013; Kim *et al,* 2014; Maruyama *et al,* 2015). This Type II system consists of a non-specific endonuclease (Cas9), a CRISPR RNA (crRNA) array that encodes the guide RNAs (gRNA) and a trans-activating crRNA (tracrRNA) that mediates the processing of the crRNA array (Ran *et al,* 2013). The gRNA is composed of a user-defined 20 nucleotide "guide" or "spacer" sequence which delineates the target DNA sequence to be modified and a "scaffold" sequence which is

required for Cas9 proteins to bind to the target area (Musunuru, 2013; Ran *et al,* 2013). In this editing method, the target DNA must be present immediately upstream of a 5'-NGG Protospacer Adjacent Motif (PAM) sequence. Upon binding, Cas9 introduces a DNA double-strand break (DSB) at the target locus mediated by the gRNAs. This DNA damage is repaired by either the error-prone non-homologous end joining (NHEJ) pathway or the high-fidelity homology-directed repair (HDR) pathway (Figure 4.2) (Cong *et al,* 2013; Ran *et al,* 2013; Maruyama *et al,* 2015; Chu *et al,* 2015). As mentioned, NHEJ is an error-prone repair process, and so unpredictable random mutations like insertion, deletion, or frameshifting could result in the genome (Ran *et al,* 2013; Wang *et al,* 2013; Wu *et al,* 2013; Maruyama *et al,* 2015). For introducing controlled mutation, single-stranded oligonucleotide (ssODN), homologous to the target site, should be added along with guide RNAs. The HDR pathway is promoted by the addition of ssODN (Yang *et al,* 2013; Wang *et al,* 2013; Maruyama *et al,* 2015). Experimental strategies inducing multiple DSBs can furthermore facilitate to mediate larger deletions in the genome (Chen *et al,* 2011; Cong *et al,* 2013). Both of the editing methods have the capability to accomplish the desired editing outcome (Ran *et al,* 2013).

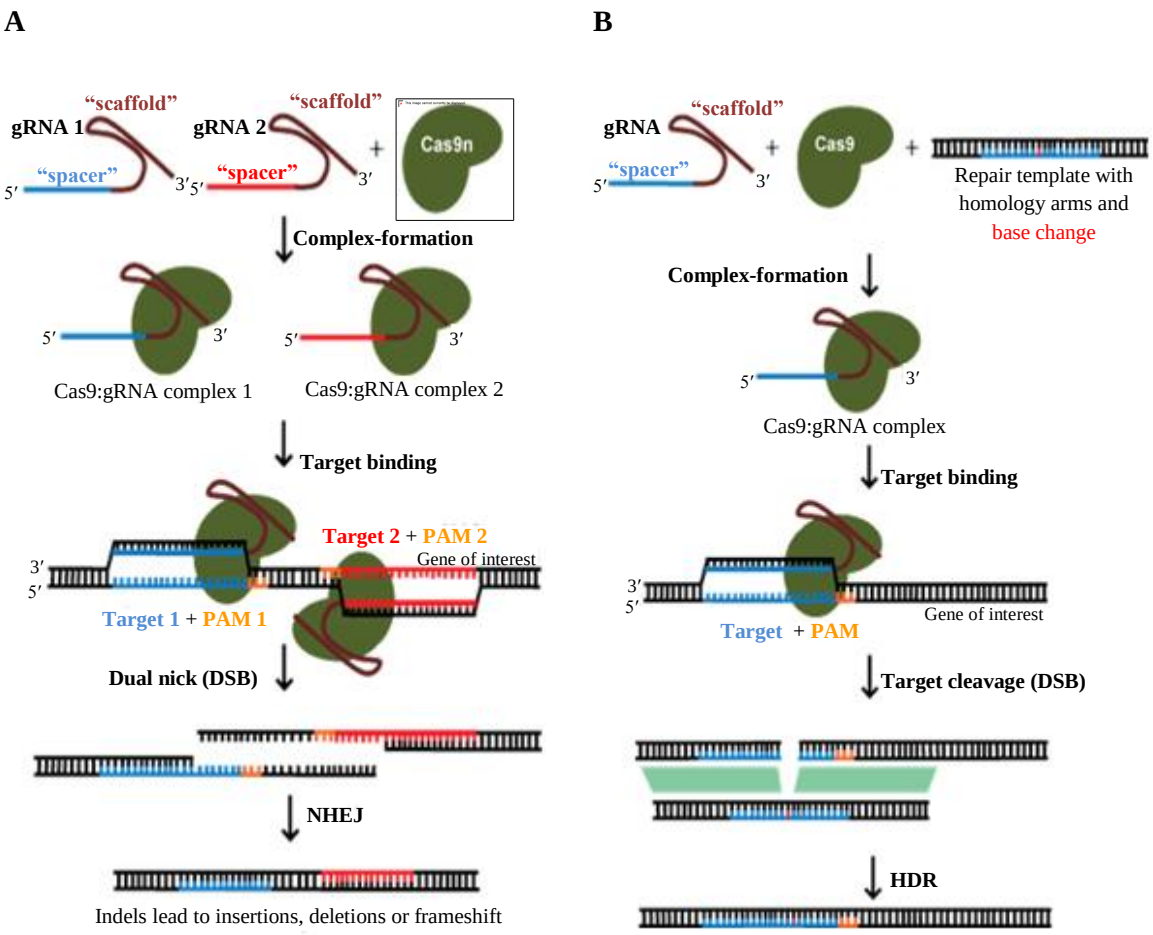

Figure 4.2: **Schematic representation of CRISPR-Cas9 mediated gene editing**. gRNAs form complex binding with a Cas9 endonuclease. Spacer sequences direct the complexes to the target genomic locus, followed by the introduction of DSB facilitated by Cas9. DSB can be repaired in one of two ways. A) In the error-prone NHEJ pathway, the nicks are rejoined by endogenous DNA repair machinery results in random indel mutations. These mutations within the coding region of a gene can result in frameshifts, which can change the downstream protein sequences and/or can create a premature stop codon, resulting in gene knockout. B) On the other hand, supplied repair templates activated the high fidelity and precise HDR pathway can edit and repair the error precisely. Images are adapted from https://www.addgene.org/crispr/guide.

Multiple studies were reported earlier to show the effectiveness of the CRISPR-Cas9 method by editing target genes precisely. This method was used widely for genome editing applications in experimental *in vitro* and *in vivo* model systems (Hsu *et al*, 2014; Sander and Joung, 2014). The application of the CRISPR/Cas9 system to edit target genes in human pluripotent stem cells has facilitated approaches for generating *in*

vitro human disease models (Musunuru, 2013; González, 2016; Yu and Cowan, 2016). The CRISPR-Cas9 method was also reported to be used to generate *ABCC8* deficient human ES cell lines which showed malfunctional K_{ATP} channels (Guo *et al,* 2016; Guo *et al,* 2016a). From these *ABCC8* deficient ES cell lines, insulin-producing CHI-like model cell line was reported to be established in a very recent report (Guo *et al,* 2017). A higher insulin secretion was observed in this *ABCC8* deficient cell type similar to the CHI tissues. This increased insulin secretion was reported to be rescued by drugs (nifedipine, octreotide) commonly used in CHI treatment. Hence, this study illustrates the feasibility of differentiating stem cell as a CHI-like model cell line.

4.1.5 Aim and objectives of this study

The **aim of this series of studies** was to generate genetically manipulated models of CHI β-cells to support additional studies of the mechanisms of disease. Two independent approaches were used. First, CRISPR-induced manipulation of CHI-iPS, a human induced pluripotent stem cell line and second, CRISPR-induced modulation of EndoCβH1 human β-cells.

In order to support this aim, the objectives of this Chapter were:-

a) To characterise the basic properties of a novel human induced pluripotent stem cells lines, CHI-iPS.
b) To demonstrate that CHI-iPS cells can be differentiated towards insulin-producing beta-like cells.
c) To generate a genetic model of CHI β-cells from CHI-iPS cells using CRISPR-Cas9 System.
d) To generate a genetic model of CHI β-cells from EndoCβH1 cells using CRISPR-Cas9 System.

4.2 Results

4.2.1 Characterization of CHI-iPS cells

Before conducting gene editing experiments on CHI-iPS cells, some analyses were conducted to characterise the cells to check if they maintained their stem cell properties. Since this study aimed to generate a beta cell line from the CHI-iPS cells which would be capable to produce insulin, the differentiation method to transform the CHI-iPS cells into insulin-producing beta cells was optimized before conducting gene editing experiments. The following sections (4.2.1 – 4.2.3) describe these analyses.

CHI-iPS cells showed robust growth in supplemented 8 culture media (Figure 4.3 A). Within 4 days, the number of cells increased four-fold. The cells carry a heterozygous recessive mutation in the *ABCC8* gene. Location of the mutation was identified as base number 21350 by DNA sequence analysis. A purine transition (from G to A) is introduced because of the point mutation and as a result, amino acid, glycine is replaced by arginine in the final protein product (Figure 4.3 B and C).

A

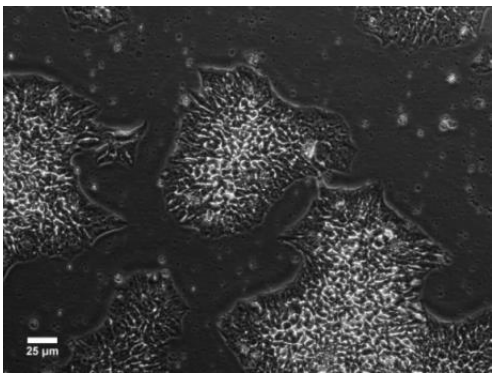

B

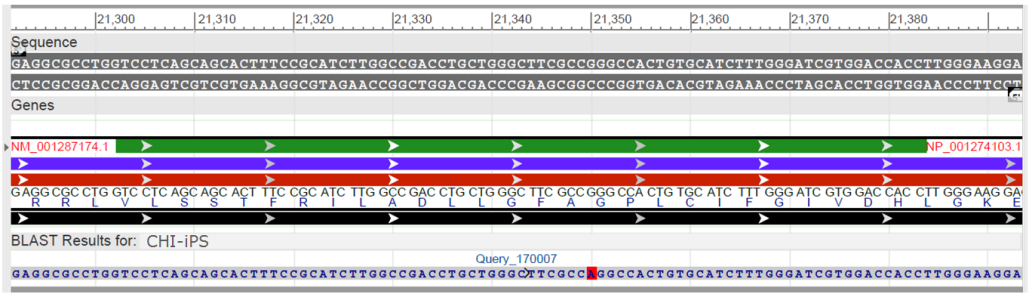

C

DNA sequence	…… TGCTGGGCTTCGCC**G/A**GGCCACTGTGCATC……
Mutation location	21350 G>A
Change of codon	GGG (**glycine**) > AGG (**arginine**)

Figure 4.3: **Morphological and genetic features of CHI-iPS cells**. A) CHI-iPS cells, grown in culture media on day 2. The cells grow in aggregated form and have a compact cluster like cell shape. The bright field images were taken using an Olympus CKX41 inverted microscope at 20x magnification. B) Nucleotide-BLAST (accessed at https://blast.ncbi.nlm.nih.gov/Blast.cgi?PAGE_TYPE=BlastSearch) analysis confirmed the location and genre of the mutation. C) Summary of the genetic features of the heterozygous mutation in cells.

4.2.2 CHI-iPS cells maintain expression of proteins characteristic for pluripotency

The CHI-iPS cell line was earlier characterized in our laboratory for its stem cell characteristics and pluripotency (Kellaway, 2016). Before conducting downstream experiments, the cells were checked if they maintained their stem cell properties. Here, immunofluorescence studies were carried out to look for the expression of the stem cell markers- Nanog, Oct4, Sox2 and SSEA4. Nanog, Oct4 and Sox2 are already reported in many studies as important transcription factors (TFs) that act in a concerted core regulatory network and determine stem cell pluripotency (Chambers *et al*, 2003; Okumura-Nakanishi *et al*, 2005; Zhou *et al*, 2011; Amini *et al*, 2014). SSEA4, an early embryonic glycolipid antigen, has also been reported using as a marker for undifferentiated pluripotent human stem cells (Henderson *et al*, 2002; Gang *et al*, 2007). Immunofluorescence studies were conducted to confirm the expression of a set of pluripotency marker proteins in CHI-iPS cells (Figure 4.4). The cells were found to express all four markers- Nanog, Oct4, Sox2, and SSEA4. As a negative control, an anti-insulin antibody was used, determining that CHI-iPS did not express any insulin. So these result indicated that CHI-iPS cells maintained stem cell features and so were suitable for further experiments.

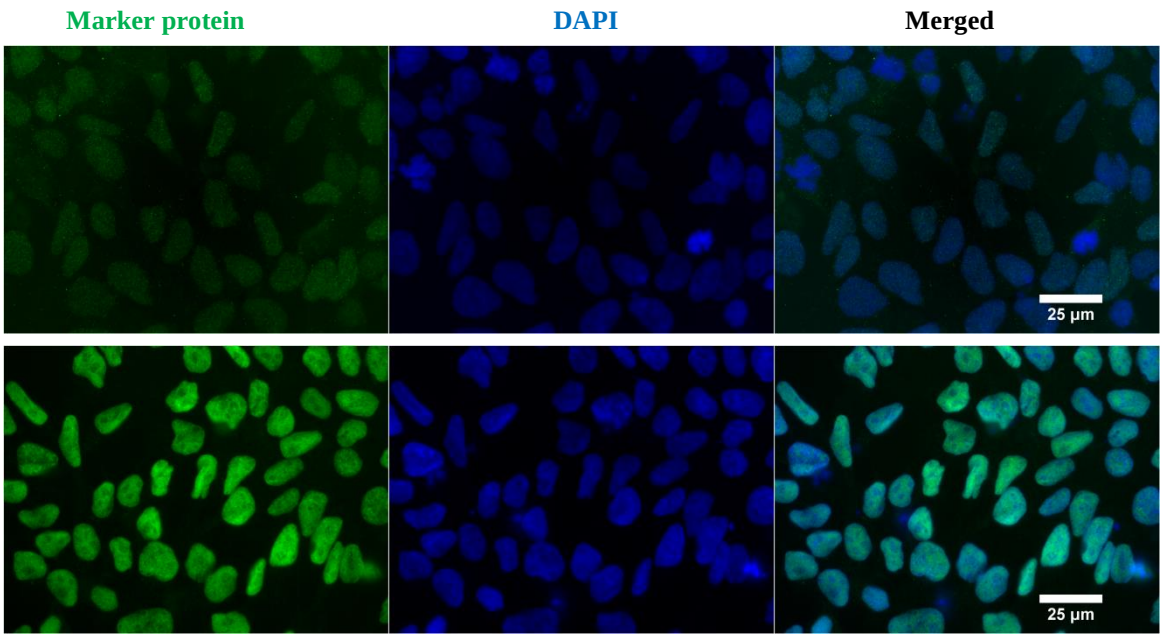

(Continued on next page..)

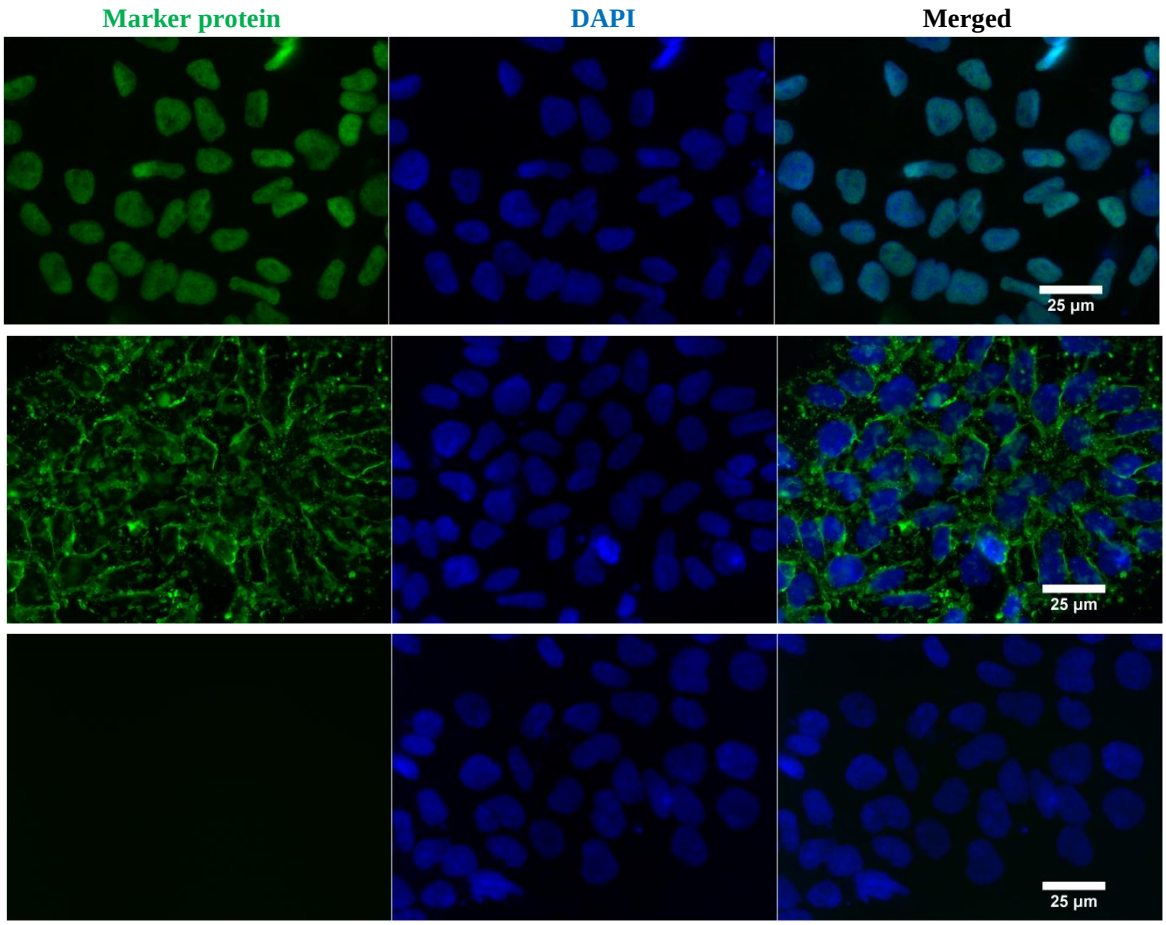

Figure 4.4: **Expression of pluripotency markers in CHI-iPS cells**. Individual images correspond to immunofluorescence images stained with anti-Nanog (A), anti-Oct4 (B), anti-Sox2 (C), anti-SSEA4 (D) and anti-Insulin (E) antibody. Green represents the expression of marker proteins. Nuclei were stained with DAPI (blue). Images were taken using an Olympus BX51 upright microscope.

4.2.3 Differentiation of CHI-iPS cells into insulin-producing cells

Before conducting gene-editing experiments, CHI-iPS cells were investigated to observe the ability of the cells to differentiate into insulin-producing cells. A number of earlier studies reported to differentiate human and mouse ES and iPS cells established from different sources of stem cells into insulin-producing cells through chemical modification of culture systems (Zhang *et al*, 2009; Rezania *et al*, 2012; Pagliuca *et al*, 2014; Rezania *et al*, 2014; Millman *et al*, 2016).

Two different approaches were utilized here (section 2.7 for more details). The first approach was a 5-stage protocol (Rezania *et al*, 2012; Rezania *et al*, 2014) that ended

with insulin-producing cell-clusters. The second one was a 7-stage protocol (Rezania *et al,* 2014) that generated insulin-producing mature beta-like cells. Since it was not certain which cell types (cell clusters or beta-like cells) would be feasible for CHI model cells, so both the protocols were optimised for CHI-iPS cell line.

4.2.3.1 Differentiation of CHI-iPS cells into insulin-producing cells following 5-stage protocol

At first, the 5-stage differentiation protocol was explored for CHI-iPS cells. After completion of every stage, the expression of some key beta cell-specific markers (*INS*, *PDX1*, and *NEUROD1*) was examined through RT-PCR (Figure 4.5). PDX1 was observed to be expressed from differentiation stage-3, whereas *NEUROD1* was being expressed from stage-4. Both of the markers were being expressed until stage-5. Expression of insulin was observed only in the final cluster-like stage (stage-5) that indicated the differentiation of CHI-iPS cells into pancreatic islet-like cluster structure. Expression of markers at stage-5 was similar to that of observed in EnodCβH1, a model mature beta cell line.

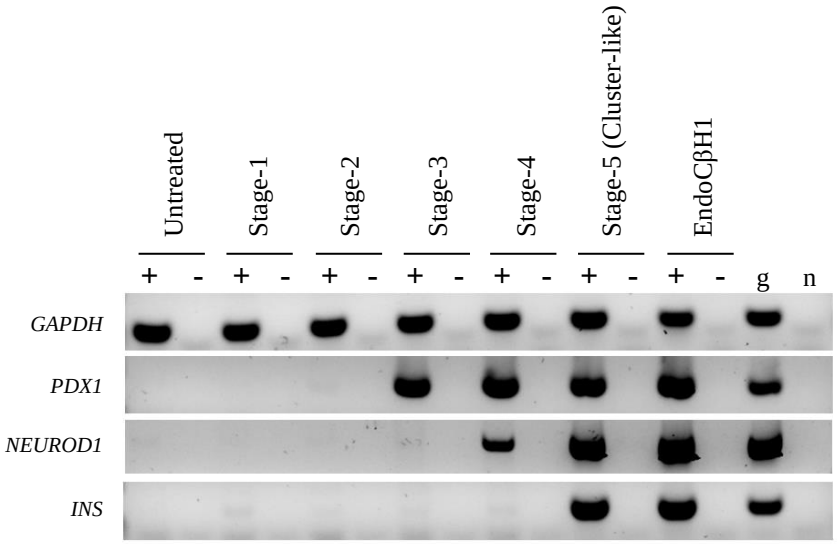

Figure 4.5: **mRNA transcript profiles of beta cell-specific marker genes in CHI-iPS cells at different stages of the 5-stage differentiation protocol**. The lanes correspond to mRNA isolated from CHI-iPS (untreated) cells, cells after stage-1, cells after stage-2, cells after stage-3, cells after stage-4, cells after stage-5 and EnodCβH1 cells (as a positive control) (7). 'g' represents human genomic DNA and 'n' represent PCR negative control. '+' and '-' represent cDNA positive and negative control respectively. Expression of *GAPDH* was analysed as a quantitative control.

This pattern of expression of beta cell-specific markers was analysed quantitatively using q-PCR. After completion of every stage of the protocol, q-PCR was conducted to analyse the expression of *PDX1*, *NEUROD1*, *NKX6.1*, Neurogenin-3 (*NGN3*), and *INS*. Figure 4.6 shows the q-PCR data for 5-stage differentiation protocol. *PDX1* was found to be expressed from stage-3 treatment (68-fold higher compared to untreated CHI-iPS) and the expression was continued in higher amount until stage-5. Compared to the expression level after stage-3 (which marks the formation of posterior foregut) (Rezania *et al*, 2012; Rezania *et al*, 2014), the expression of *PDX1* was significantly higher (p-value <0.0001) after stage-4 (pancreatic endoderm and endocrine precursors) and stage-5 (islet-like cell clusters) (Rezania *et al*, 2012; Rezania *et al*, 2014). No significant change was observed in *PDX1* expression after stage-5 compared to the level of stage-4. Expression of *NEUROD1* and *NKX6.1* was first observed after stage-4 and expressions were continued after stage-5 at a significantly higher amount. Expression of *NGN3* (an endocrine progenitor marker) (Gu *et al*, 2002b; Afrikanova *et al*, 2012; Ma *et al*, 2012) was observed only after stage-5 and the level of expression was low (~5.5-fold compared to untreated cells) related to the expression of other markers analysed. Expression of insulin (*INS)* and somatostatin (*SST*) (expressed by delta cells, a marker for pancreatic islets) (Wang *et al*, 2014; Brereton *et al*, 2015; Lau *et al*, 2016) only in stage-5 indicated the differentiation of CHI-iPS cells into pancreatic islet-like cluster structure. In this experiment, where expression of markers in any stage was very low or undetectable, threshold cycle (C_T value) of q-PCR for those markers was observed to be >38. It was reported that C_T >35 is not reliable and can be considered as very low or no expression at all (Goni *et al*, 2009; Mar *et al*, 2009; McCall *et al*, 2014; van Vuren *et al*, 2016). Gene expression changes in q-PCR are measured as fold change ($2^{-\Delta\Delta CT}$), so a change of expression close to zero value always resulted with a fold change close to 1 (as observed in Figure 4.6 for expression of *NKX6.1* and *NGN3*).

Immunofluorescence studies were also conducted to confirm the expression of some of the marker genes at the protein level since suitable antibodies only for these marker proteins were available during the study. Figure 4.7 A illustrates the expression of NEUROD1 in differentiated cells after stage-4. No insulin was expressed in those cells at this stage (Figure 4.7 B) or earlier stages (data not shown). The stage-5 cells were found to express insulin and somatostatin proteins, which again indicated the differentiation of CHI-iPS cells into pancreatic islet-like cell clusters (Figure 4.7 C-D).

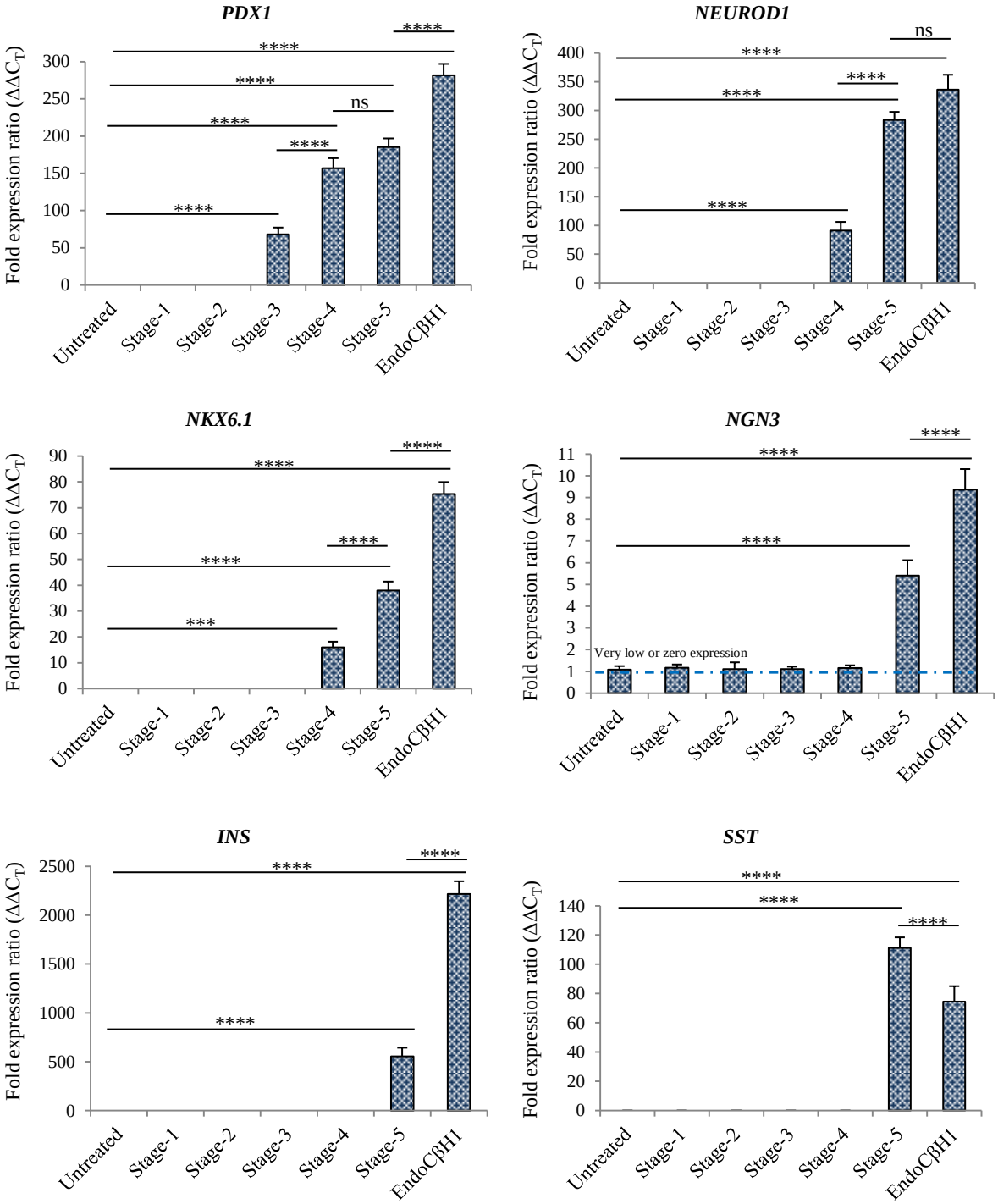

Figure 4.6: **Gene expression changes of beta cell-specific marker genes in CHI-iPS cells at different stages of the 5-stage differentiation protocol**. Expression patterns of *PDX1*, *NEUROD1*, *NKX6.1*, *NGN3*, *INS* and *SST* are illustrated here. Values were normalised with the expression of *GAPDH* in each condition. EnodCβH1 cells were used as positive control. Blue dotted line in the graph for *NGN3* expression indicates the level for very low or zero expression. n = 3; 3 independent experiments; **** - $p < 0.0001$; *** - $p < 0.001$; ns = not significant; one-way ANOVA. Data are presented as mean ± SEM.

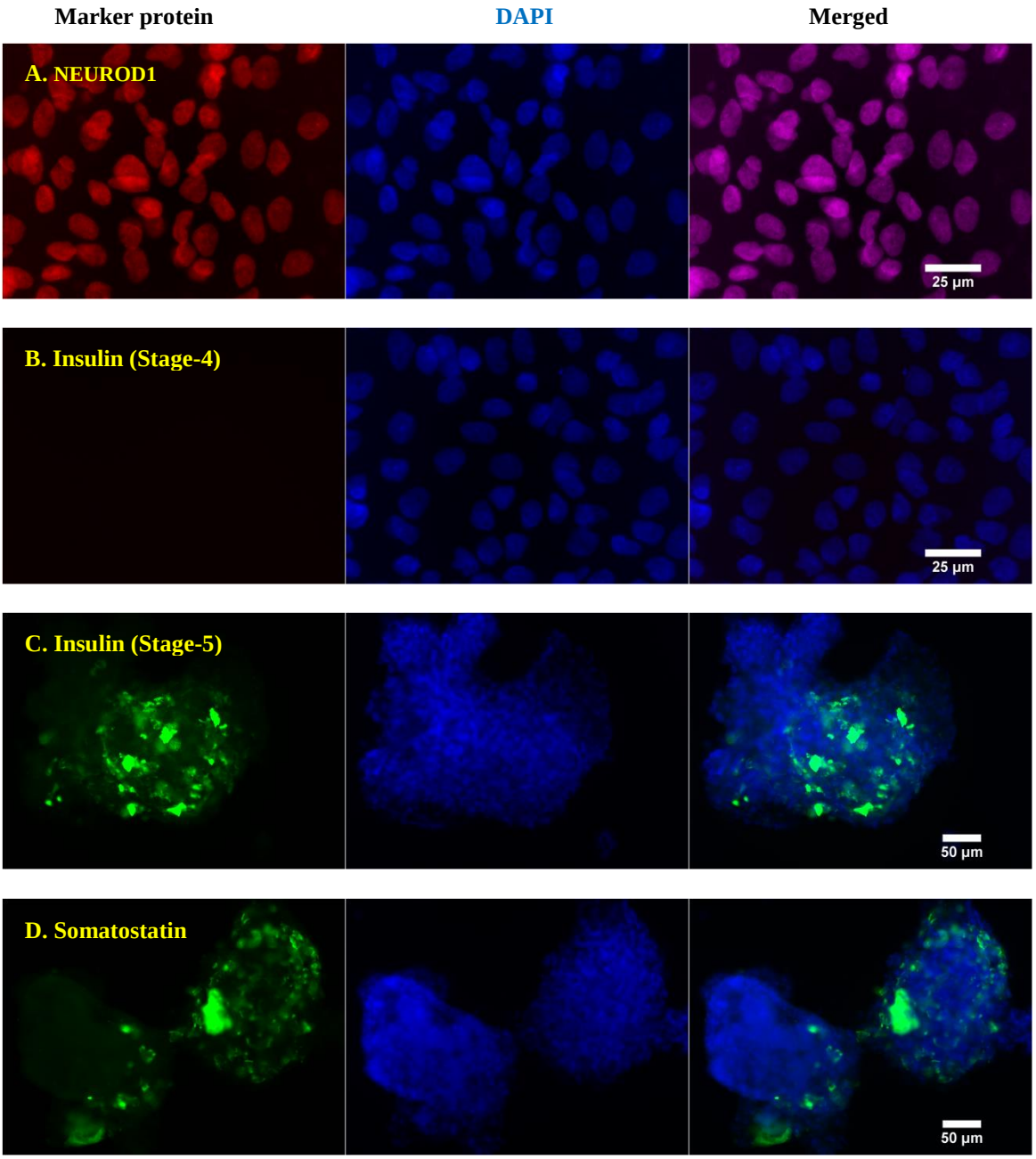

Figure 4.7: **Expression of beta cell-specific marker genes at the protein level in differentiated CHI-iPS cells after stage-4 and stage-5 (5-stage protocol).** Individual immunofluorescence images correspond to protein expression of NEUROD1 (after stage-4) (A), insulin (after stage-4) (B), insulin (after stage-5) (C), and somatostatin (after stage-5) (D). Green and red fluorescents represent the expression of marker proteins. Nuclei were stained with DAPI (blue). Images were taken using an Olympus BX51 upright microscope.

4.2.3.2 Differentiation of CHI-iPS cells into insulin-producing cells following 7-stage protocol

7-stage differentiation protocol was also explored for CHI-iPS cells to transform them into insulin-producing cells. After completion of every stage, expression of beta cell-specific markers (*PDX1*, *NEUROD1*, *NKX6.1*, *NGN3* and *INS*) was examined quantitatively through RT-PCR as like the 5-stage protocol performed earlier. Figure 4.8 shows the q-PCR data for 7-stage differentiation protocol. Similar to the 5-stage protocol, *PDX1* was first expressed after stage-3 treatment and the expression was continued in higher amount until stage-7. After stage-3 treatment (which marks the formation of posterior foregut) (Rezania *et al*, 2014), expression of *PDX1* was increased significantly (p-value <0.0001) compared to the previous step until stage-6-day-7 (precursors of $NKX6.1^{+}/INS^{+}$ cells). Significantly lower expression of *PDX1* was observed after stage-6-day-15 ($NKX6.1^{+}/INS^{+}$ cells) compared to the earlier stage and the expression was increased again after stage-7 ($NKX6.1^{+}/INS^{+}$ beta-like cells). Significant expression of *NEUROD1* and *NKX6.1* was first observed after stage-4 (pancreatic endoderm) and expression was continued till the end (stage-7). The change of expression of both markers was not significant after stage-5 (endocrine precursors) compared to the level of stage-4 and after stage-6-day-15 compared to the expression of stage-6-day-7. However, the expressions after stage-6-day-7 and stage-7 were significantly higher compared to the respective previous stage. Expression of *NGN3* was first observed after stage-5 treatment and the expression gradually decreased until stage-7. Expression of *INS* was first observed after stage-6-day-7 treatment at low amount (more than 80-fold compared to untreated condition) and the same level of expression was continued after stage-6-day-15. The expression was significantly increased after the final stage-7. *SST* was expressed only after stage-7 which indicated the presence of delta-like cells along with beta-like cells. In this 7-stage protocol, after stage-4 the cells were cultured at an air-liquid interface on a special filter (see materials and methods for details), so technically it was very difficult to conduct immunofluorescence analysis on cells at final stages and hence such studies were not performed.

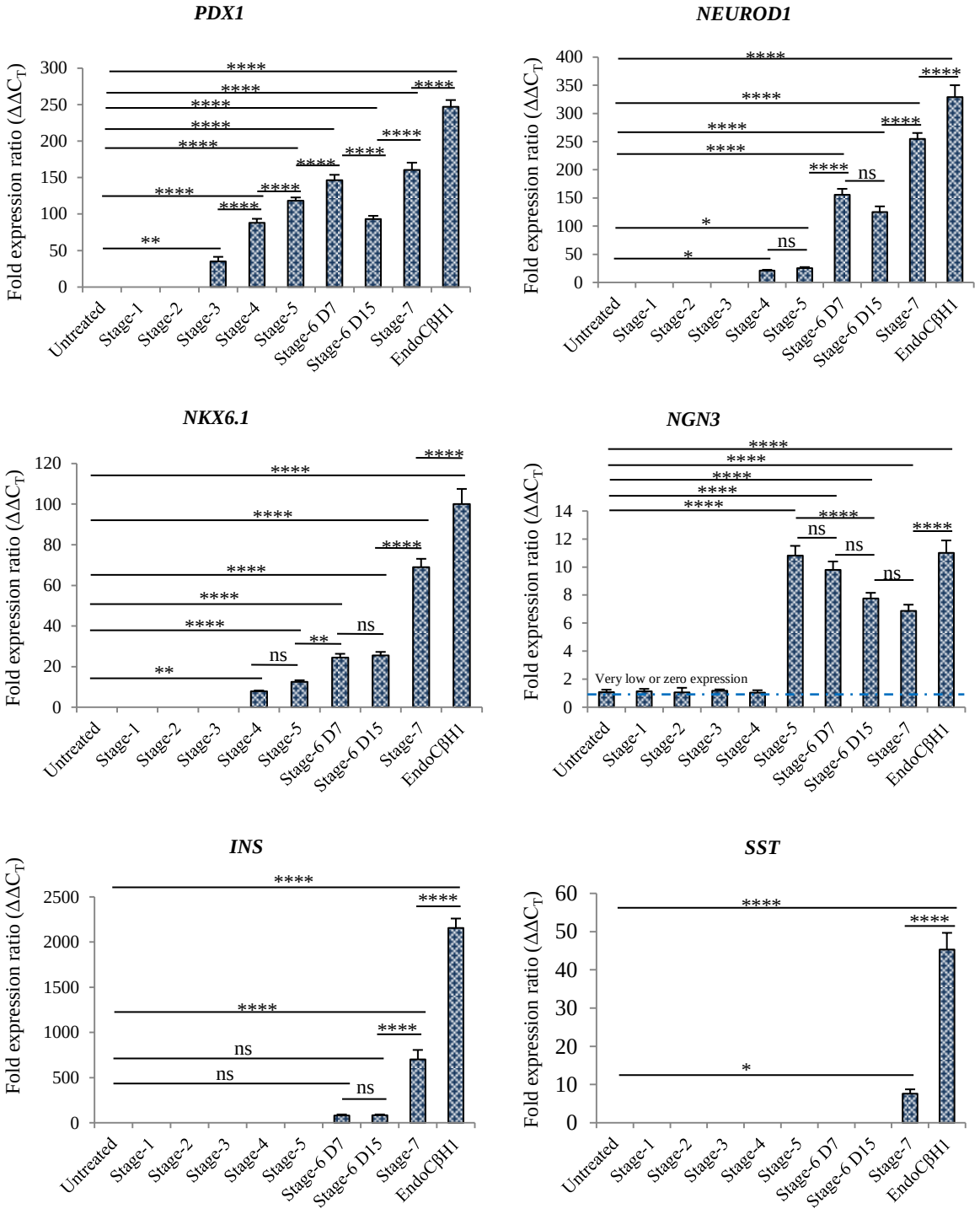

Figure 4.8: **Gene expression changes of beta cell-specific marker genes in CHI-iPS cells at different stages of the 7-stage differentiation protocol**. Expression patterns of *PDX1*, *NEUROD1*, *NKX6.1*, *NGN3*, *INS* and *SST* are illustrated here. Values were normalised with the expression of *GAPDH* in each condition. Blue dotted line in the graph for *NGN3* expression indicates the level for very low or zero expression. n = 3; 3 independent experiments; **** - $p < 0.0001$; ** - $p < 0.01$; * - $p < 0.05$; ns = not significant; one-way ANOVA. Data are presented as mean ± SEM.

4.2.4 Introduction of a homozygous mutation in CHI-iPS cells using CRISPR-Cas9 system

4.2.4.1 Design of guide RNAs and single-stranded oligo donor targeted to introduce a homozygous mutation in CHI-iPS cells

After showing that CHI-iPS cells were able to differentiate into insulin-expressing beta cells, this cell line was used to generate a CHI-like *in vitro* model. It is mentioned earlier that the CHI-iPS cell line carries a heterozygous recessive mutation in *ABCC8* gene exon 6 which introduces a purine transition (from G to A), and there is a change in amino acid sequence because of this mutation (Figure 4.3). Although this mutated cell line was generated from a CHI patient, however the cells that were used to make the CHI-iPS cell line were from the healthy tissue at the edge of the focal lesion (Kellaway, 2016). So, the cells were healthy and carried the inactive recessive mutation. Since the heterozygous recessive mutation could not show any deleterious effect on *ABCC8* expression, it was hypothesized that introduction of a second mutation in the *ABCC8* gene to make the mutated locus homozygous would make the gene inactive or non-functional. Further, insulin-producing cells differentiated from this edited CHI-iPS cells might behave as CHI-like cells

CRISPR-Cas9, a well-known genome engineering tool, was used to introduce a second mutation to transform the heterozygous locus into homozygous. Guide RNAs (gRNAs), single-stranded oligo donor (ssODN) required for homology-directed repair (HDR) and potential primers spanning the mutation locus were designed using the web tool developed by Sanger Institute (Figure 4.9). Two potential gRNAs were cloned into expression vector pSpCas9(BB)-2A-GFP (PX458) and verified by the Genome Editing Services at the Transgenic Unit, the University of Manchester, UK. This vector was amplified using *E. coli* DH5α and used for downstream transfection experiments. Guides were designed to flank the mutation locus of the *ABCC8* exon 6. After transfection of cells with CRISPR reagents and guide RNAs, *ABCC8* at the specific locus was expected to be excised by concurrent actions of guide RNAs and Cas9 nuclease. A second mutation was hoped to be introduced by the HDR pathway using ssODN as a repair template.

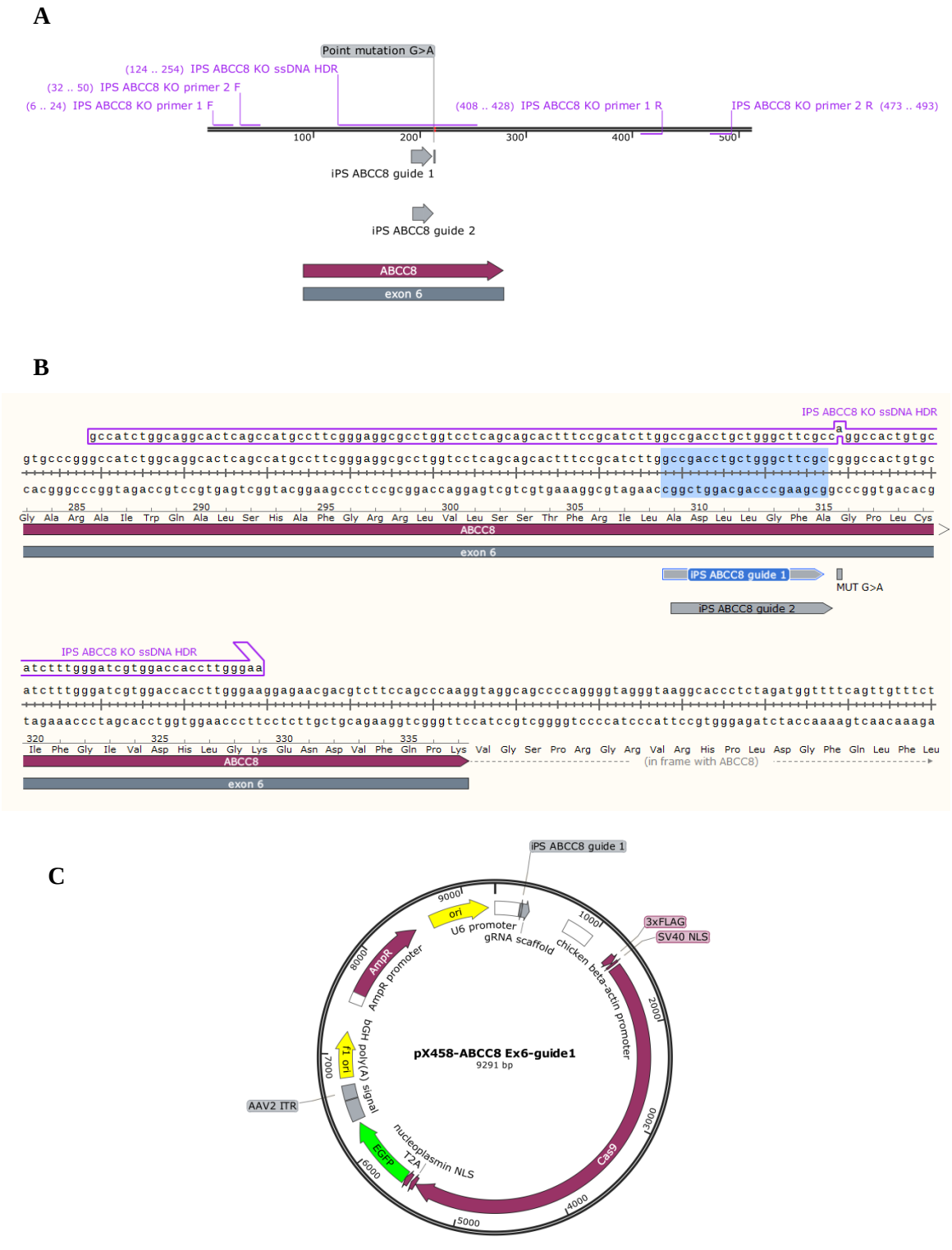

Figure 4.9: **Schematic representation of guide RNAs, ssODN and primers designed for *ABCC8* gene modification in CHI-iPS cells**. A. Illustrative map of *ABCC8* exon 6 zoomed to represent loci of guide RNAs and ssODN. B. Sequence view (partial) of ssODN with target mutation. The sequence of guide RNA 1 is highlighted in the image. C. Graphical representation of the expression vector pX458 cloned with guide RNA 1. Images were drawn using SnapGene 3.3.3 software.

4.2.4.2 Optimisation of cellular transfection method for transfection of CHI-iPS cells with plasmid DNA encoding gRNA

A number of previous studies reported transfection of ES and iPS cells using chemical or electroporation methods (Byrne *et al*, 2014; Tabar *et al*, 2014; Yang *et al*, 2014a; Yang *et al*, 2014b; Li *et al*, 2016; Luo *et al*, 2016). Byrne *et al*. (2014), Yang *et al*. (2014a) and Yang *et al*. (2014b) reported the detailed protocol to transfect iPS cells through electroporation method using the Amaxa Primary Cell 4D-Nucleofector X Unit.

In this study, Amaxa nucleofector, Lipofectamine 2000 (Thermo Fisher Scientific) and ViaFect (Promega, UK) were examined to find the most suitable and efficient method to transfect the CHI-iPS cells. From the observed fluorescent images, Amaxa nucleofector was found to transfect a relatively higher amount of CHI-iPS cells (Figure 4.10).

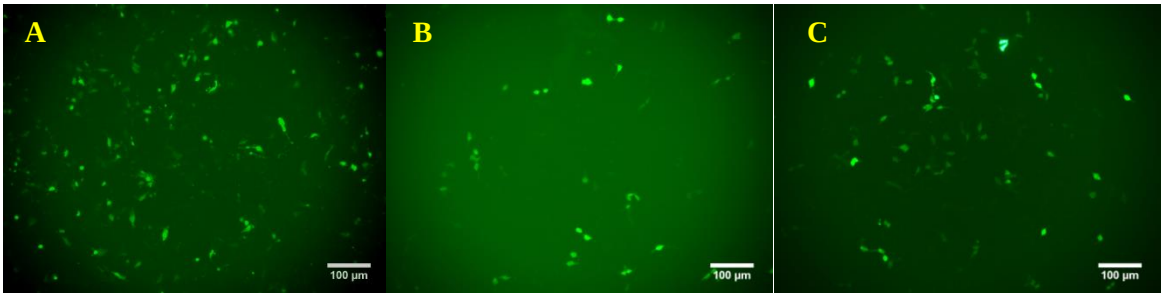

Figure 4.10: **Relative green fluorescence emitted by CHI-iPS cells after transfection with plasmid encoding GFP using different transfection methods**. The images are a representative image for different transfection methods with the best combination of transfection reagents (materials and methods chapter for details) that generated the highest proportion of transfected cells. A) Cells transfected with Amaxa nucleofector; B) cells transfected with ViaFect and C) cells transfected with Lipofectamine 2000. Images were taken using an Olympus IX83 inverted microscope.

4.2.4.3 Transfection of CHI-iPS cells with gRNA-encoding plasmid DNA and ssODN and validation of transfection

To introduce homozygous mutation, CHI-iPS cells were transfected with plasmid DNA encoding guide RNA 1 and guide RNA 2 separately using Amaxa Nucleofector. ssODN was co-transfected along with plasmid DNA to ensure homology-directed mutation in the specific locus. Green fluorescent protein (GFP) gene was integrated into the plasmids and hence, expression of the GFP confirmed the transfection of cells with both gRNAs (Figure 4.11 A and B). PCR products covering the mutation locus in the *ABCC8* gene

were digested with the restriction enzyme, BstNI. The amplified region naturally includes three restriction cutting sites of BstNI. Introduction of a G→A mutation results in another cutting site. So, PCR products from wild-type homozygous cells should generate three DNA fragments of 329, 107 and 25 base pairs (bp) after digestion with BstNI (Figure 4.11 C). PCR products from mutated homozygous cells should break 329 bp fragment and generate four DNA fragments of 183, 146, 107 and 25 bp. PCR products from heterozygous cells should generate five DNA fragments with 329, 183, 146, 107 and 25 bp. Figure 4.11 D illustrates that all three cell types - untreated CHI-iPS cells, cells transfected with guide RNA 1 and guide RNA 2 – generated restriction profiles similar to that of a theoretical heterozygous cell. However, the band intensity of 329 bp fragment is significantly lower (~50%) in transfected cells. The smaller fragment of 25 bp was out of the gel for all three samples as the gel was run for long to separate the larger fragments from one another.

4.2.4.4 Single cell sorting and clonal propagation of CRISPR induced mutated CHI-iPS cells

Usually, eukaryotic cells excrete any transfected plasmid vector in two-three days. Similarly, CHI-iPS cells should have excreted the transfected vector within a couple of days. Hence, GFP was expressed transiently by CHI-iPS cells transfected with both guide RNA 1 and 2. GFP was used as a selection marker to sort CHI-iPS cells which were introduced with homozygous mutation by CRISPR-mediated gene editing system. Only cells which showed expression of the GFP were sorted as single cells using the fluorescence-activated cell sorting (FACS) method. Representative FACS data shows that GFP expression was observed only in 2.4% and 1.8% cells (experiments with gRNA 1 and 2 respectively) of all seeded cells (Figure 4.12). After 10-12 days, some of the clonally propagated single cells were visible as a cluster-like cell colony. However, rates of cell growth and propagation were different for different clonal cells (cell colonies generated from single cells). After two weeks of incubation time, some clonal cells were propagated to large, visible cell-clusters whereas some were observed to grow as very small colony (Figure 4.13). From four individual transfection experiments with both gRNA 1 and 2, a total of 1920 GFP-positive cells were seeded as single cells (240 cells in 4 x 96-well plates, for each guide RNA in each experiment). Among the seeded cells, a total of 82 single cells were propagated to cell colony and from them, only 27 clones survived after first sub-culture.

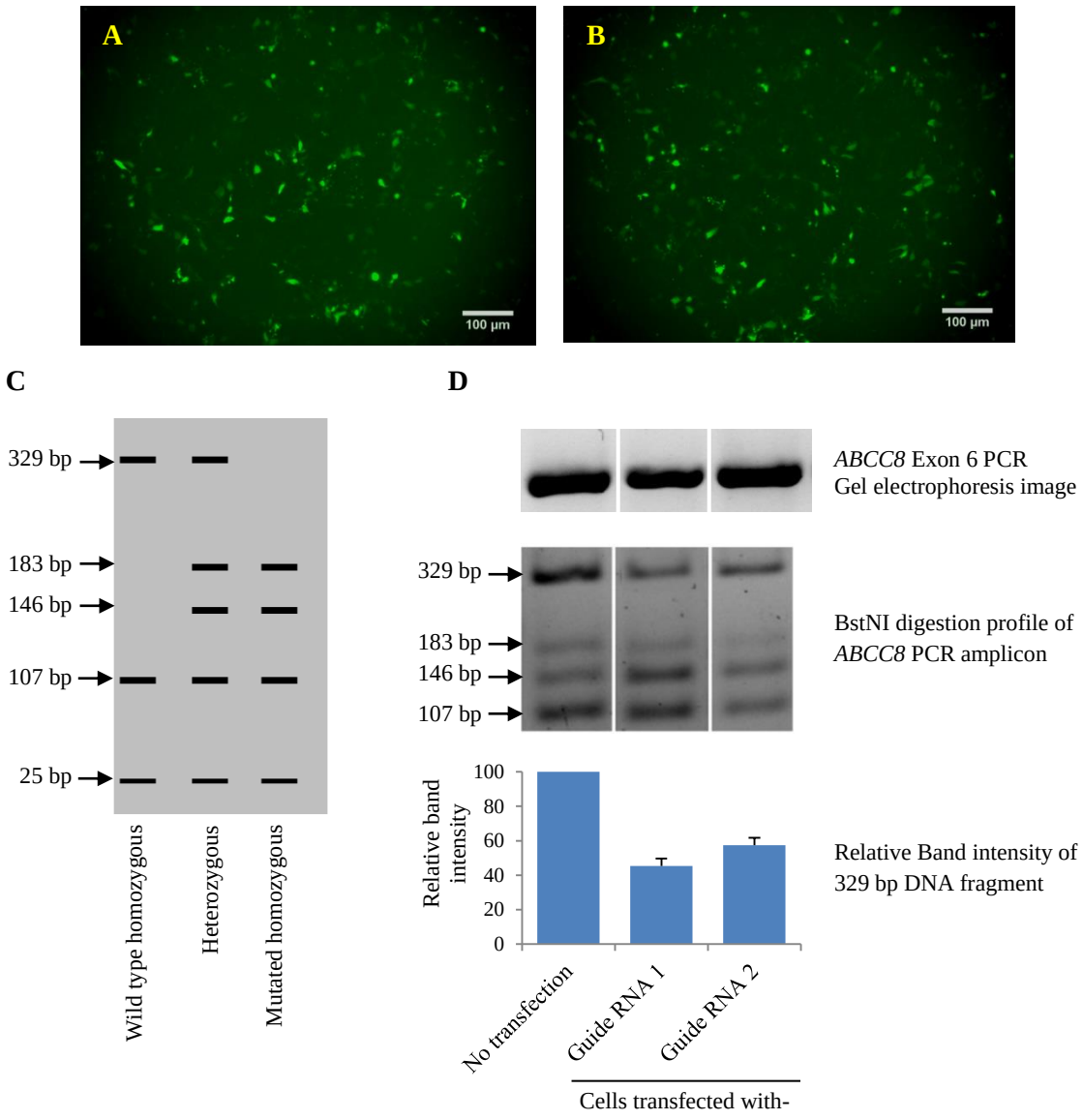

Figure 4.11: **Transfection of CHI-iPS cells with CRISPR guide RNA and ssODN, and validation of transfection.** Panel A and B represent CHI-iPS cells emitting green fluorescence after transfection with guide RNA 1 and guide RNA 2 respectively. Images were taken using an Olympus IX83 inverted microscope and analysed using ImageJ software. Panel C is a representational illustration of theoretical restriction enzyme cutting profile of homozygous and heterozygous cells with or without the mutation. Panel D illustrates the data confirming validation of CRISPR mediated transfection and introduction homozygous mutation. Lane 1, 2 and 3 represent cells without transfection, cells transfected with guide RNA 1 and cells transfected with guide RNA 2 respectively. The restricted fragments were separated in a 3% agarose gel. Band intensity of the largest fragment (329 bp) was measured using ImageJ software.

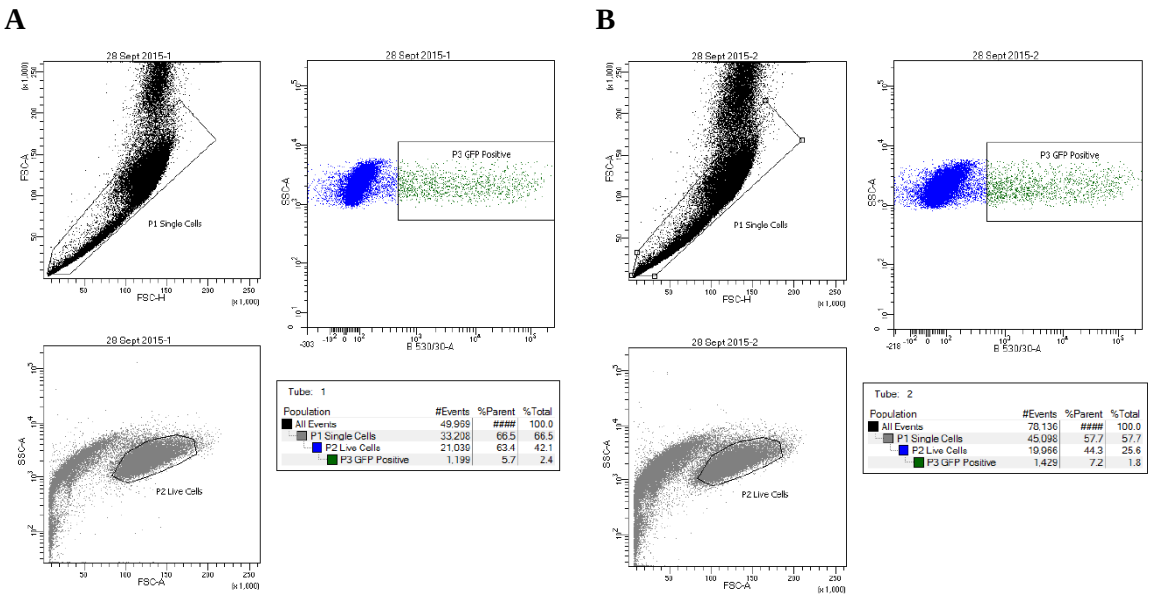

Figure 4.12: **FACS data of GFP-expressing edited CHI-iPS cells**. Only GFP-positive cells were sorted and collected for clonal propagation. Panels A and B illustrate representative FACS data of CHI-iPS cells transfected with guide RNA 1 and 2, respectively.

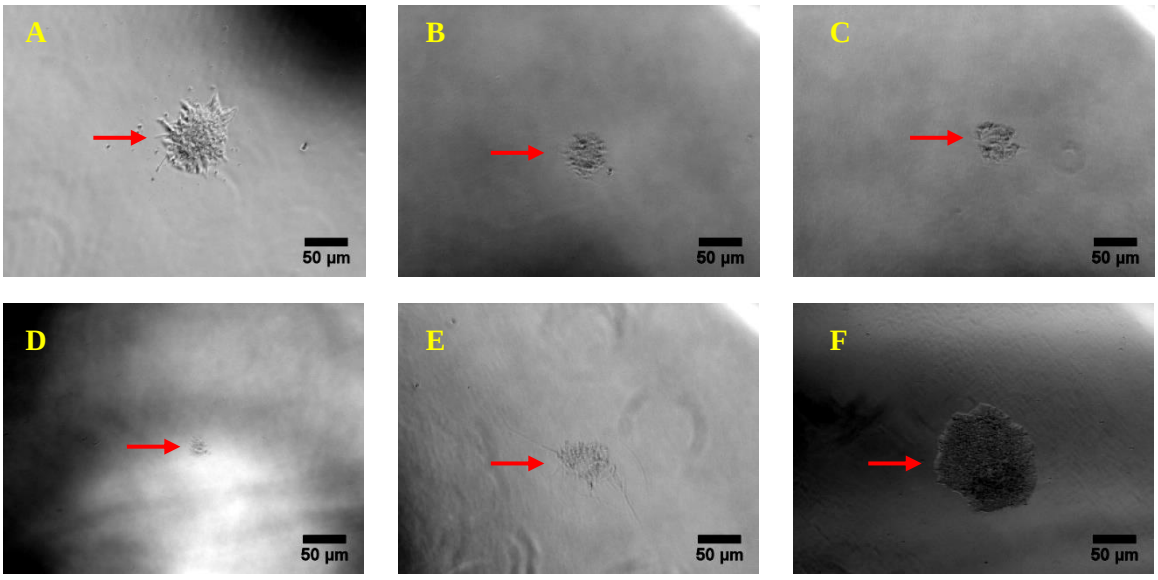

Figure 4.13: **Single-cell clonal propagation of edited CHI-iPS cells**. All the cell images were captured after 10 days of the single cell sorting experiment. Individual representative images correspond to untreated CHI-iPS (A), Guide1 clone 2 (B), Guide 1 clone 7 (C), Guide 1 clone 9 (D), Guide 2 clone 6 (E) and Guide 2 clone 7 (F) cells. The term "Guide X clone Y" indicates Y^{th} survived clone from transfection experiment with guide RNA X. Red arrow indicates the location of the cell colony. The bright field images were taken using an Olympus CKX41 inverted microscope.

4.2.4.5 Characterization of clonally propagated edited CHI-iPS cells

All the clonal cells generated from edited CHI-iPS single cells showed robust growth in supplemented E8 culture media. However, diverse morphologic features were shown by the cells and the cells appeared to be differentiated to different cell types (Figure 4.14 B-H). Only 6 clones out of 27 clones showed cell morphology similar to CHI-iPS cells. However, the growth rate of all the clones was observed to differ greatly from that of control untransfected CHI-iPS cells. More than twice the amount of time (7-10 days) was required for clonal cells to achieve 70-80% confluency compared to untransfected CHI-iPS cells (3 days). The cells were investigated to confirm the insertion of the homozygous mutation in the target loci of *ABCC8* exon 6. Amplified PCR products from the cell genomic DNA were digested with the restriction enzyme, BstNI. Successful incorporation of homozygous mutation should have a restriction profile similar to that illustrated in panel C of Figure 4.11. However, homozygous restriction profile was not observed in any of the edited clones (Figure 4.15). A band accounting for a DNA fragment of 329 bp was observed in all clonal cells. In addition, variations in restriction enzyme digestion profile were observed in most of the clones which could be explained as potential incorporation of random mutations in non-specific loci of the gene in CHI-iPS cells because of transfection treatments.

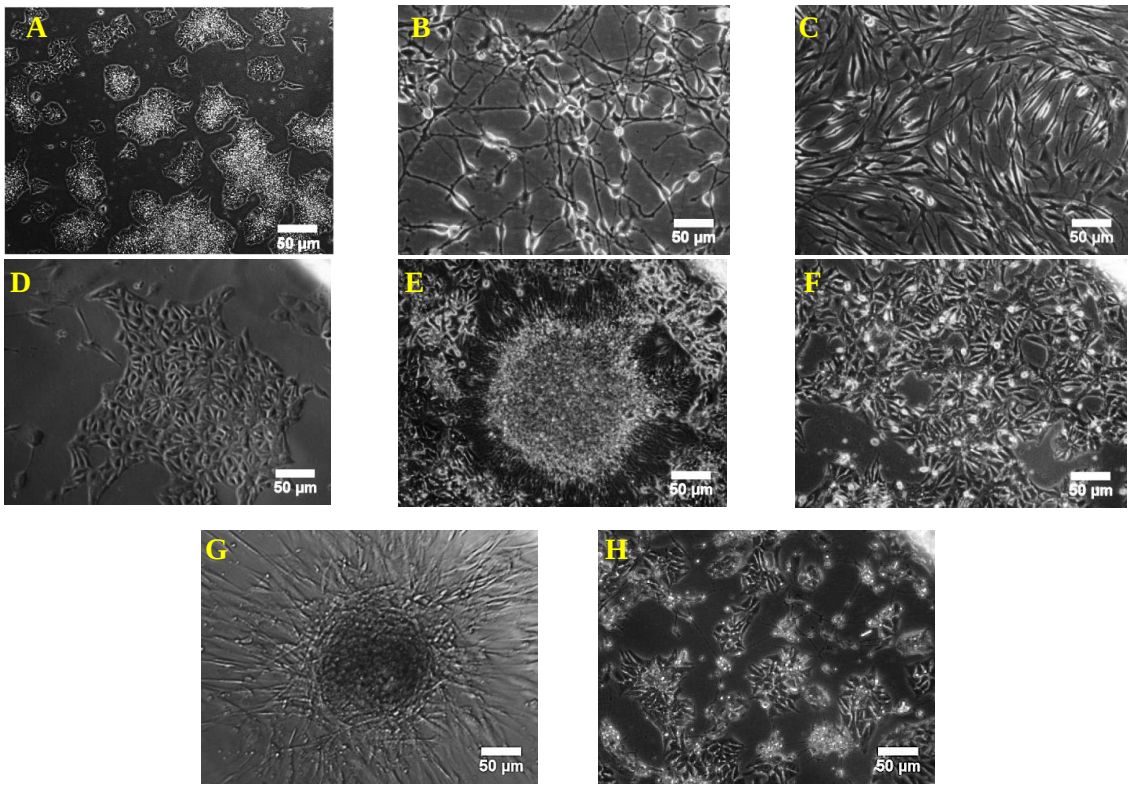

Figure 4.14: **Morphological features of clonal cells generated from CRISPR-edited CHI-iPS cells**. Individual images correspond to untreated CHI-iPS cell (A), Guide 1 clone 1 cell (B), Guide 1 clone 7 cell (C), Guide 1 clone 12 cell (D), Guide 2 clone 3 cell (E), Guide 2 clone 6 cell (F), Guide 2 clone 8 cell (G) and Guide 2 clone 15 cell (H). The term "Guide X clone Y" indicates Y^{th} survived clone from transfection experiment with guide RNA X. The bright field images were taken using an Olympus CKX41 inverted microscope.

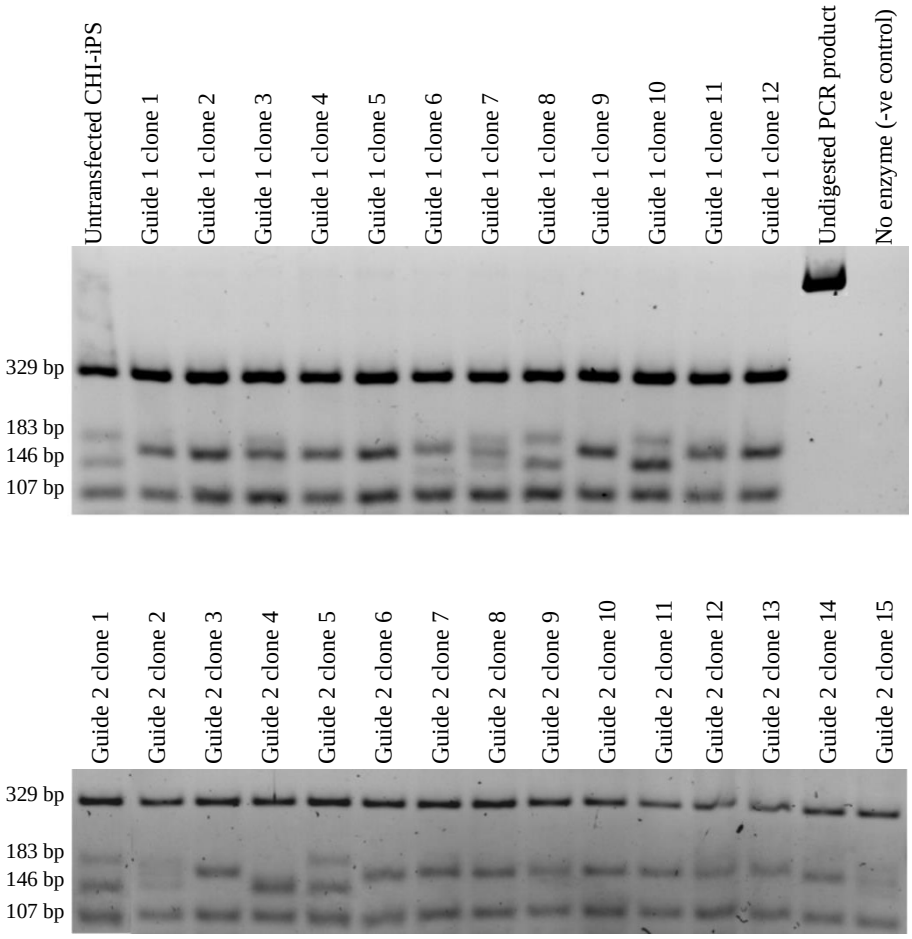

Figure 4.15: **Genetic screening and restriction enzyme profiles of clonal cells generated from edited CHI-iPS cells**. Transfections of CHI-iPS cells were conducted with CRISPR guide RNAs and ssODN. The top panel shows the restriction profiles of clones generated from treatment with guide RNA 1, along with controls. The bottom panel shows the restriction profiles of clones generated from treatment with guide RNA 2. The smaller fragments were out of the gel for all samples and were not visible in the gel. None of the cells shows homozygous mutated cell-like restriction enzyme profile.

To investigate the incorporation of random mutations in the *ABCC8* gene in the clonal cells, PCR amplicons were sequenced. A number of random mutations were identified in each clonal cell compared to CHI-iPS cells while analysed by multiple sequence alignment (Figure 4.16 A). Phylogenetic trees were constructed to observe the genomic distance of each clonal cells comparing to CHI-iPS cells (Figure 4.16 B and C). The phylogenetic trees show that 12 out of 27 clones acquired heavily random mutations and thus show very high differences in the gene sequence. To investigate whether random mutations induced any differentiation of clonal cell to insulin-producing cells, RT-PCR was carried out with 12 clonal cells (based on differences in restriction profiles) to observe insulin mRNA expression (Figure 4.17 A). A PCR amplicon of the desired size (along with some undesired non-specific DNA fragments) was observed in two of the clones (guide 1 clone 11 and guide 2 clone 13). However, no insulin protein production was observed in any of the cells while analysed with immunofluorescence studies (Figure 4.17 B).

From these above-mentioned observations, it can be concluded that CHI-iPS cells can be transfected with guide vectors and the target gene can be edited. However, clonal propagation of the edited cells resulted in differentiation into random cell types and the cells lost their stem cell characteristics. Also, random mutations were introduced in the cell genome without any control and none of them possessed the target homozygous mutations. So, these clonal cell lines generated from these experiments could not be used for any downstream experiment.

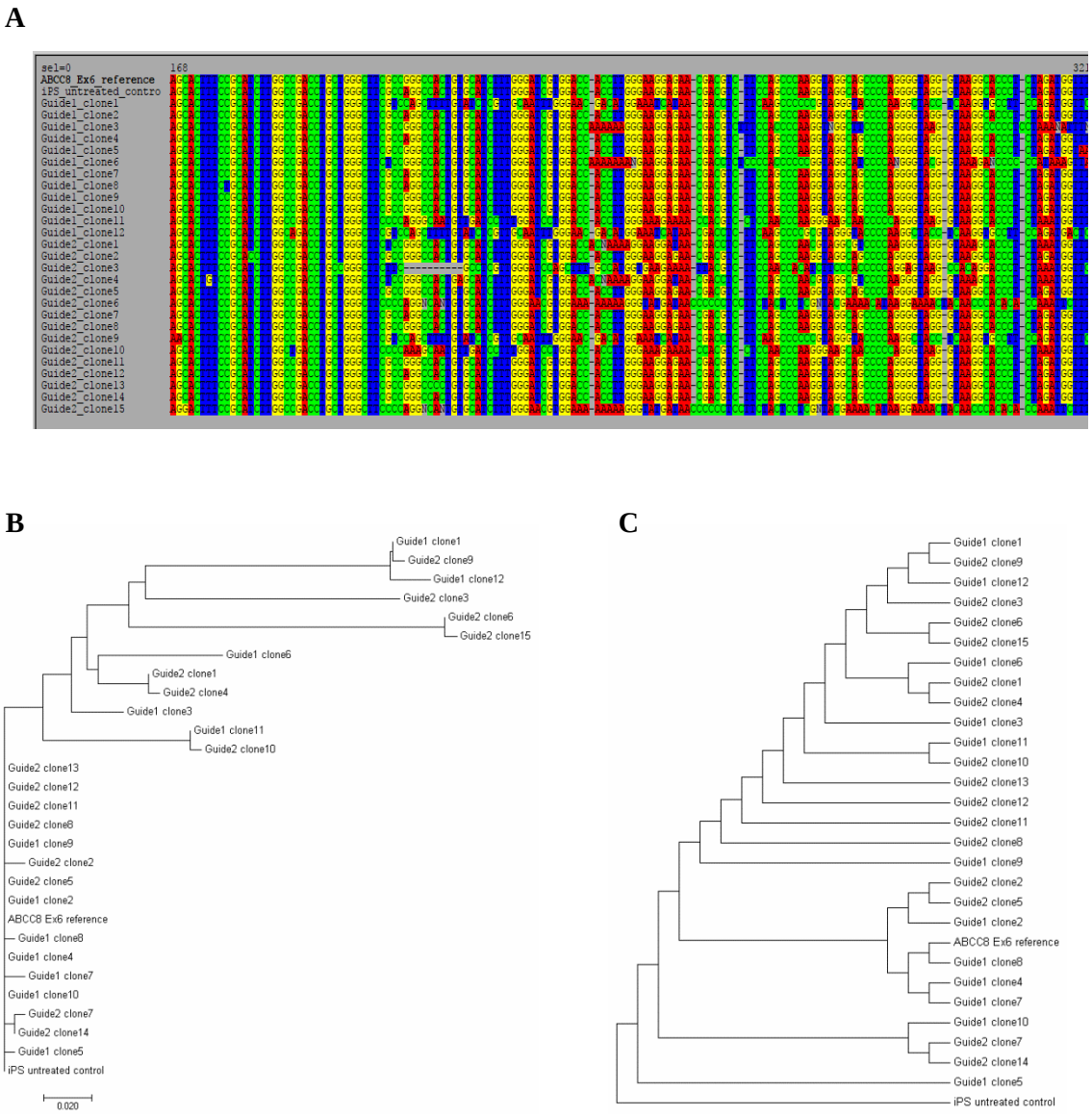

Figure 4.16: **Schematic representation of the genomic relation of clonal cells generated from edited CHI-iPS cells**. Panel A shows the multiple sequences alignment constructed using the software, SeaView 4.6.2 (Gouy *et al*, 2010). Panel B and C show the genomic relation of clonal cells represented as phylogenetic trees constructed in two different visualizations – tree style and topology style, respectively. CHI-iPS cell was used as the root of the tree. *ABCC8* Exon 6 sequence was also added as the reference sequence. The sequences were analysed following the Neighbor-Joining method (Saitou and Nei, 1987; Tamura *et al*, 2004). The trees were constructed using the software, MEGA7 (Kumar *et al*, 2016).

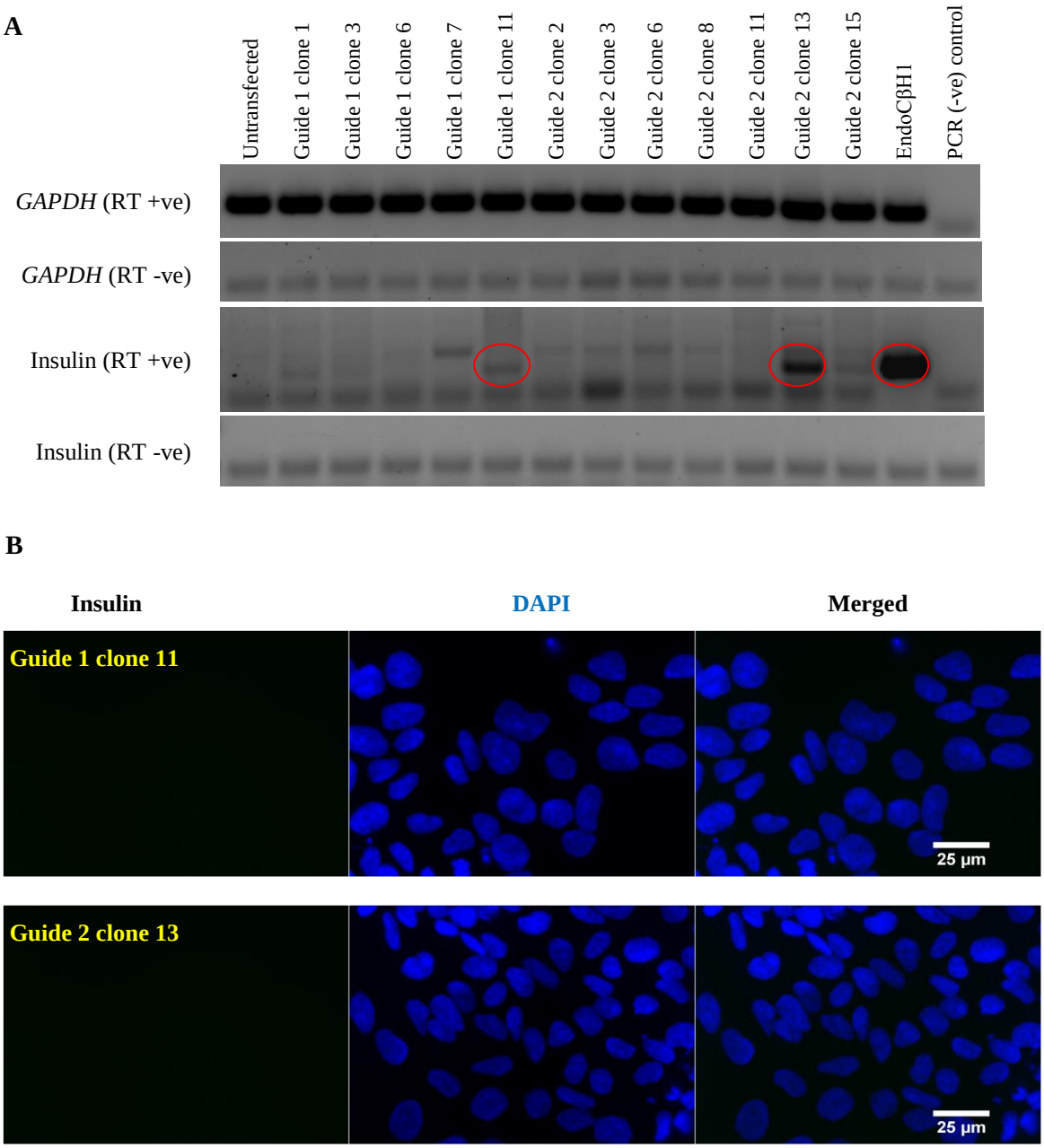

Figure 4.17: **Analysing insulin expression in clonal cells generated from edited CHI-iPS cells.** A. RT-PCR products separated on 2% agarose gel (stained with GelRed staining solution). *GAPDH* was used as RNA amount control. RT+ve and RT-ve correspond to the presence and absence of reverse transcriptase for cDNA synthesis, respectively. EndoCβH1 cell was used as insulin-positive control. RT-ve PCR products show only primer dimers. PCR amplicons indicating the possible presence of insulin in Guide 1 clone 11 and Guide 2 clone 13 cells are marked with red circles. B. Immunofluorescence imaging study showed no expression of insulin in Guide 1 clone 11 and Guide 2 clone 13 cells. Nuclei were stained with DAPI (blue). Images were taken using an Olympus BX51 upright microscope.

4.2.4.6 Applying alternative methods to transfect CHI-iPS cells and propagation of sorted single cells

A number of edited CHI-iPS clonal cells were generated following the above-discussed methods of transfection, single cell sorting using FACS and subsequent culturing of single cells. However, random mutations were introduced into the cells through the process and the cells were observed to be differentiated to undesired cell types and lose their viability as pluripotent cells. It was concluded that the process followed for generating viable clonal population from a single edited CHI-iPS cell was not the proper method of choice. So, alternative following methods were tried to generate viable edited CHI-iPS cells from the transfected single cells (Table 4.1). The cells were transfected with guide RNA 1 and 2 using Lipofectamine 2000 or ViaFect following the recommended protocols. The number of successfully transfected cells was very poor compared to Amaxa nucleofector method (Figure 4.10). Also, the cells were co-transfected with a puromycin-encoding plasmid to select puromycin-resistant cells. Single cells were sorted and cultured as previously described (section 2.8.7). However, not a single cell was observed to propagate after 3 weeks time.

In another attempt, cells were transfected using all three transfection methods, all the GFP expressing cells were sorted and collected altogether using the FACS method, and allowed to grow as a mixed population. After 2 weeks of growth, when the cells were growing properly, then the cells were detached from the culture plates, seeded as single cells and cultured individually in a single well of culture plates. However, no single survived cell colony was observed from these experiments.

Alternatively, the culture conditions were modified once single cells were sorted and plated (Table 4.1). The growth surface coating reagents, Matrigel or Vitronectin were used in each experimental approach. A small molecule cocktail of 4 inhibitors (SMC4) (a cocktail of Chir99021, PD0325901, SB431542, and Thiazovivin) was used in place of ROCK inhibitor (ROCKi). SMC4 was reported earlier to enhance stem cell survival in single cell condition (Valamehr *et al*, 2012; Byrne *et al*, 2014). As previously seen, these attempts were also failed to generate a single viable cell colony. A summary of the aforementioned alternative experiments is shown in Table 4.1.

Finally, a different cell culture media, Cellartis iPSC Single-Cell Cloning DEF-CS Culture Media Kit (Clontech, Takara Bio inc., Japan) was used for electroporation and subsequent culture of sorted single cells. The growth medium was claimed to enhance robust clonal propagation of iPS single cells (accessed at http://www.clontech.com/US/Products/Stem_Cell_Research/Resources/Technical_Notes/DEF-CS_Single-Cell_Cloning). But again, no clonal propagation was observed from the sorted single CHI-iPS cells. Since viable clonal propagation was not possible with edited CHI-iPS cells, hence, no further single nucleotide editing experiments were performed with this CHI-iPS cells.

Table 4.1: **Utilised alternative methods of single cell clonal propagation.**

Culturing sorted single cells in growth media with supplements (time duration)	***Continuation of Culturing cells in growth media without supplements (time duration, up to)***	***Coating reagent***	***Clonal propagation observed***
First 2 days post-seeding with ROCKi, then next 6 days with fresh ROCKi	3 weeks	Vitronectin	No
First 1 or 2 day(s) post-seeding with ROCKi	3 weeks	Matrigel / Vitronectin	No
First 1 or 2 week(s) with ROCKi	1 or 2 week(s)	Matrigel / Vitronectin	No
First 2 days with SMC4, then next 6 days with fresh SMC4	3 weeks	Matrigel / Vitronectin	No
First 1 or 2 day(s) with SMC4	3 weeks	Matrigel / Vitronectin	No
First 1 or 2 week(s) with SMC4	1 or 2 week(s)	Matrigel / Vitronectin	No

4.2.5 Introduction of a deletion mutation in EndoCβH1 cells using CRISPR-Cas9 system to knock out *ABCC8* or *KCNJ11* genes

4.2.5.1 Design of guide RNAs targeted to knock out genes in EndoCβH1 cells

Since a number of approaches failed to generate a stable homozygous mutated cell line from the CHI-iPS cell line, as an alternative approach, EndoCβH1 cells were used for further gene-editing experiments. It was hypothesised that any deletion of K_{ATP} channel subunit genes (*ABCC8* and *KCNJ11*) might make the channel non-functional and thus

induce the cells to have CHI behaviour. In order to create a CHI-like *in vitro* model system, attempts were made to knock out either the *ABCC8* or the *KCNJ11* gene. In Chapter 3, it was presented that chemical modification of growth media did not introduce any CHI-like characteristics in this cell line. So, the following experiments were focused on introducing a knock out mutation of *ABCC8* or *KCNJ11* gene in a controlled way with an expectation that the cell would behave as a CHI-like model system.

To knock out the *ABCC8* or *KCNJ11* genes in EndoCβH1, the CRISPR-Cas9 method was again used. *ABCC8* is a multi-exonic gene (39 exons) whereas *KCNJ11* contains one single coding exon (Figure 4.18) (Adi *et al*, 2015). gRNAs and potential primers spanning the mutation locus of *ABCC8* or *KCNJ11* gene were designed using the web tool developed by Sanger Institute (Figure 4.19). Exon 2 of *ABCC8* was predicted as the critical exon by the algorithm of the software to successfully knock down the gene product. Four potential gRNAs were designed for each gene and cloned into expression vector pSpCas9(BB)-2A-GFP (PX458) and verified by the Genome Editing Services at the Transgenic Unit, the University of Manchester, UK. This vector was amplified using *E. coli* DH5α and used for downstream transfection experiments.

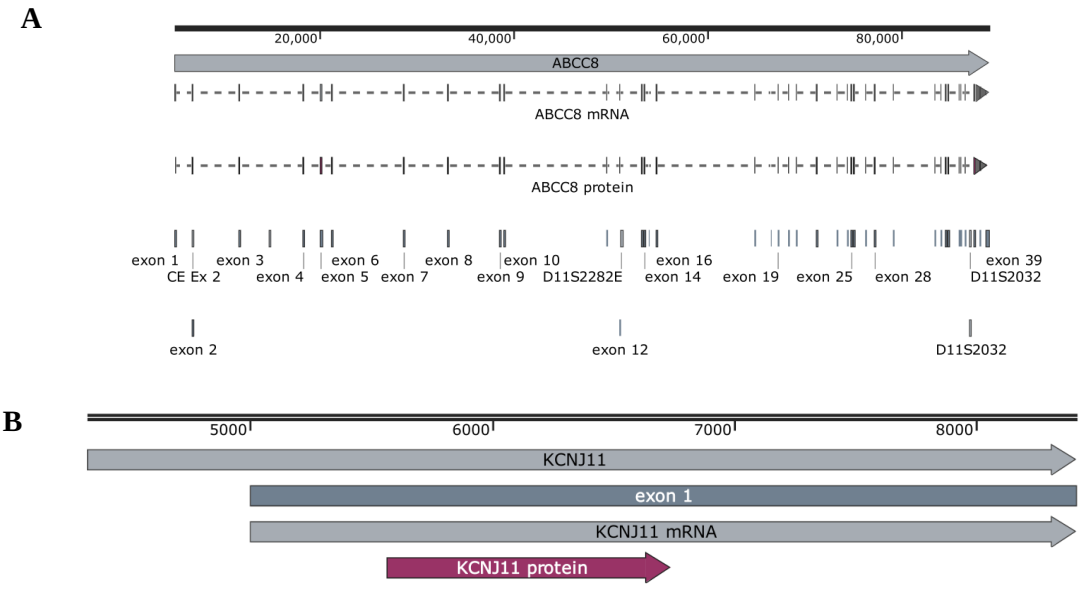

Figure 4.18: **Schematic representation of the gene map of human *ABCC8* and *KCNJ11* genes**. Image A and B show the maps of *ABCC8* and *KCNJ11*, respectively. Locations of exons in the gene are illustrated in the images. *ABCC8* is very big gene having 83960 bp of DNA. *KCNJ11* is a comparatively small gene spanning 3411 bp of DNA. Images were drawn using SnapGene 3.3.3 software.

A

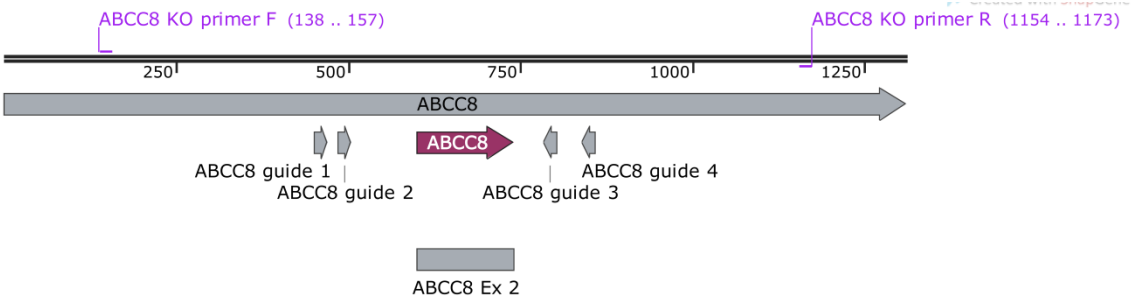

B

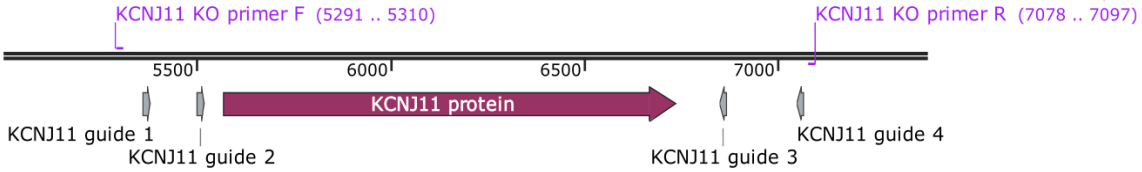

C

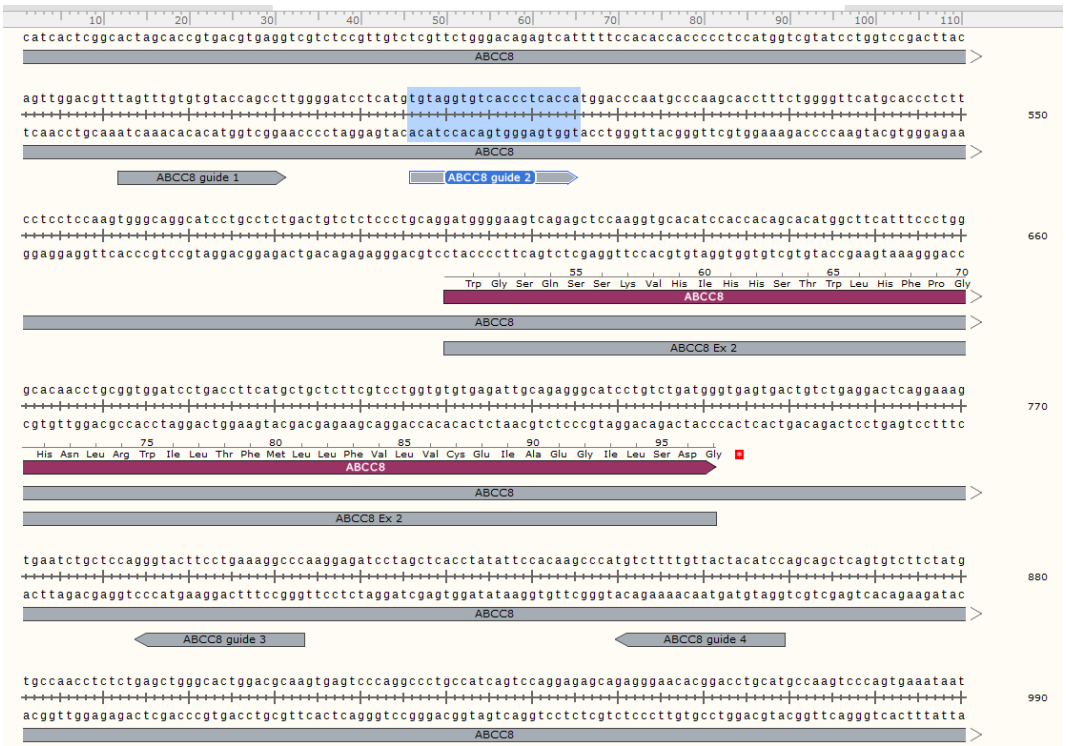

(Continued on next page..)

D

E

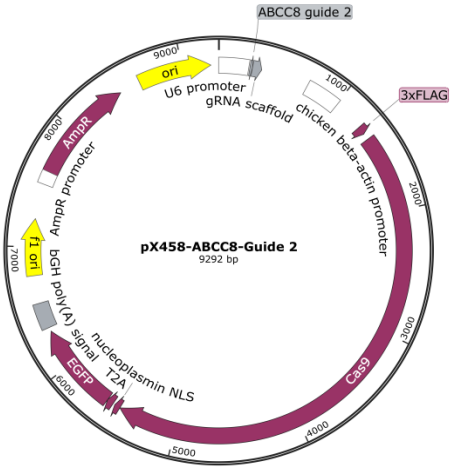

Figure 4.19: **Schematic representation of the location of guide RNAs and primers designed for *ABCC8* and *KCNJ11* gene knock out experiments in EnodCβH1 cells**. Image A and B illustrates the map of *ABCC8* exon 2 and *KCNJ11* exon, respectively, zoomed to represent loci of guide RNAs. Image C and D shows a sequence view (partial) of the location of guide RNAs. The sequence of guide RNA 2 for each gene is highlighted in the images. Image E is a graphical representation of the expression vector pX458 cloned with guide RNA 1 targeted to *ABCC8*. Images were drawn using SnapGene 3.3.3 software.

4.2.5.2 Optimising cell culture conditions for EndoCβH1 single cell clonal propagation

It is mentioned that for proper growth and survival EndoCβH1 cells require high cell seeding density (Section 2.1.1). Since the generation of edited clonal cell line requires single cell clonal propagation, a number of methods were explored to grow EndoCβH1 as a single cell, maintain the cells and then expand the cells. In all methods, cells were sorted as a single cell by using either FACS method or limiting dilution. In some approaches, the time for replacing spent media with fresh media was varied. In other approaches, used culture media, which might contain growth factors favourable for single cell growth, was filter purified and used as growth media for single cell culture. As indicated for the experiments using CHI-iPS cells, ROCKi and SMC4 were added to culture media in some experiments for possible enhancement of single cell propagation. However, all of these attempts failed to generate any single cell colony for up to 12 weeks of total incubation time.

Using a different approach, cells were transfected with a puromycin-encoding plasmid along with plasmid encoding guide RNA. The cells were cultured for two days in growth medium containing puromycin. After 2 days, the spent medium was replaced with fresh growth medium without puromycin supplementation and incubated for 5 more days to promote proper cell growth of surviving cells. However, after 7 days of post-cell-seeding, the surviving cells did not show proper cell growth as a colony. In one approach, the cells were allowed to grow in the growth media for up to 12 weeks. However, no propagation of surviving cells was observed. In another approach, surviving cells (after 7-days or 12-weeks post-cell-seeding) were picked manually using Scienceware cloning cylinders (Sigma-Aldrich) or Scienceware cloning discs (Sigma-Aldrich) and transferred to 96-well or 24-well plates, respectively. The cells were incubated in normal growth media for up to 12 weeks with media replacement in every 5 days. But, again, no clonal propagation was observed from the single EndoCβH1 cells. A summary of the above-mentioned experiments is mentioned in Table 4.2.

Since single cell clonal propagation was not successful in EndoCβH1 under any conditions, so subsequent experiments were focused on the capacity to generate a mixed population containing a minority of wild-type cells, with a higher percentage of knocked out cells.

Table 4.2.: **Attempted methods of EndoCβH1 single cell clonal propagation.**

Cell type	Culture condition	Continuation of culturing cells (time duration)	Clonal propagation observed
serial-diluted/FACS-sorted transfected single cells	Culturing in normal growth media and replacement of spent media in every 5 days	Total 12 weeks	No
	Culturing in normal growth media for 2 weeks without media replacement and then replacement of spent media in every 5 days	Total 12 weeks	No
	Culturing in previously used normal growth media and replacement with fresh media in every 5 days	Total 12 weeks	No
	Culturing in previously used normal growth media for 2 weeks without media replacement and then replacement of spent media in every 5 days	Total 12 weeks	No
	Culturing in normal growth media with ROCKi for 2 days and then replacement with normal media in every 5 days	Total 12 weeks	No
	Culturing in normal growth media with SMC4 for 2 days and then replacement with normal media in every 5 days	Total 12 weeks	No
Cells transfected with puromycin-encoding plasmid	Culturing in growth media with puromycin as mixed cell population for 2 days and then in normal growth media without puromycin for 5 more days. Colonies were picked using cloning cylinder/disc and seeded in a well of culture plate. Spent media was replaced in every 5 days.	Total 12 weeks	No

4.2.5.3 Selection of transfection method for transfecting EndoCβH1 cells with plasmid DNA

No previous studies were reported where EndoCβH1 cells were transfected successfully with plasmid at the time of these experiments. A number of commercially available cell transfection kits were examined to find a suitable method to transfect the EndoCβH1 cells. Since single cell clonal propagation of EndoCβH1 cell, reported in the earlier section, was not made possible, the aim of these transfection experiments was to find out the method which would yield the highest number of transfected *i.e.* knocked out cells. Four chemical based transfection kits - Lipofectamine 3000 (Thermo Fisher Scientific),

Lipofectamine LTX (Thermo Fisher Scientific), ViaFect (Promega, UK) and FuGENE HD (Promega, UK) were explored. In addition, Amaxa nucleofector was also tried as a mean to transfect the cells. A combination of cell seeding density, the amount of plasmid DNA and the amount of kit specific transfection reagents were explored to find out the most successful method.

Among all the conditions, the ViaFect transfection kit gave the highest number of transfected cells under the following combination of conditions; 3x cell density, 1µg plasmid DNA and 3 µl transfection reagent (for a well of 24-well plate) (Figure 4.20). The reaction combinations which generated the visible amount of GFP-expressing transfected cells are summarized in Table 4.3.

Table 4.3: **Reaction combinations for successful EndoCβH1 cell transfection (24-well plate)**

Lipofectamine 3000 (Thermo Fisher Scientific)		
Cell seeding density	*Plasmid DNA (µg)*	*P3000 reagent (µl)*
2x	2	6
Lipofectamine LTX (Thermo Fisher Scientific)		
Cell seeding density	*Plasmid DNA (µg)*	*LTX reagent (µl)*
2x	2	4
ViaFect (Promega, UK)		
Cell seeding density	*Plasmid DNA (µg)*	*transfection reagent (µl)*
3x	1	3
3x	1	5
3x	2	6
3x	3	9
2x	1	3
FuGENE HD (Promega, UK)		
Cell seeding density	*Plasmid DNA (µg)*	*transfection reagent (µl)*
3x	2	4
3x	3	6

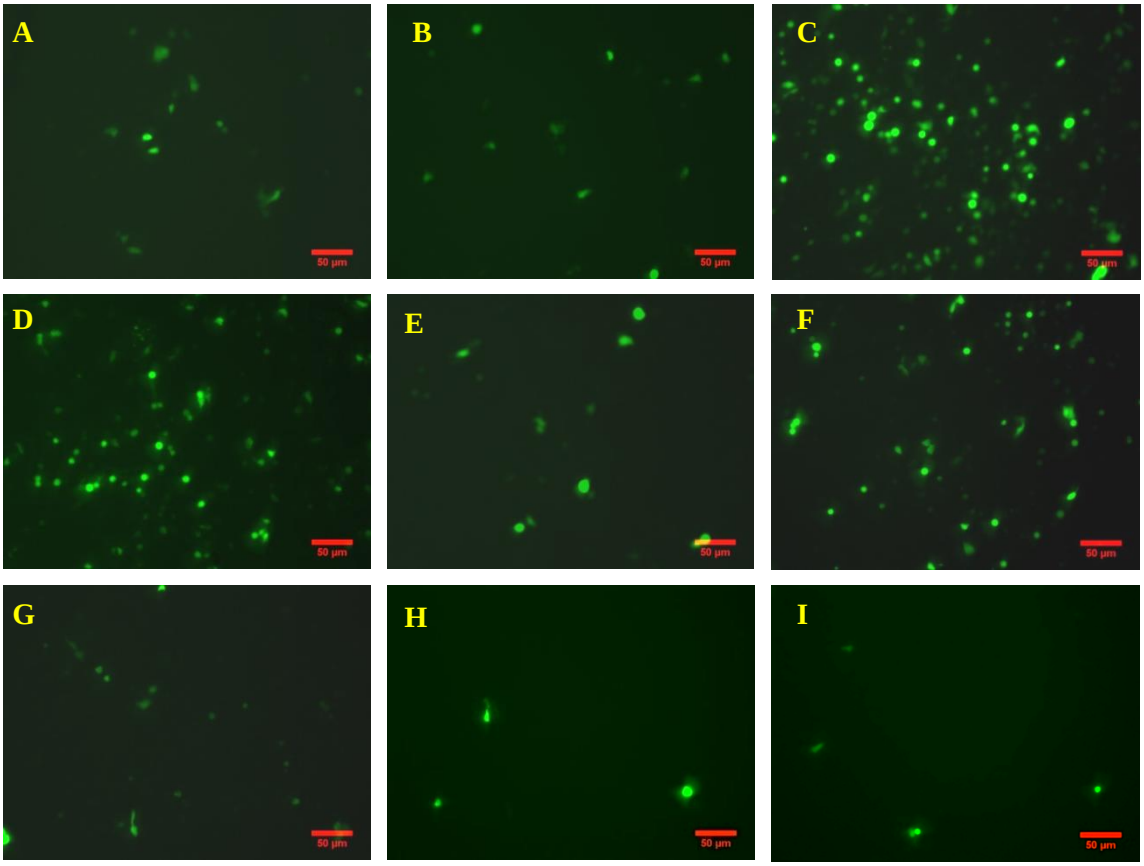

Figure 4.20: **Relative transfection efficiencies of explored transfection kits used for EndoCβH1 cells**. Green fluorescences are emitted by cells after transfection with plasmid encoding GFP. The images represent the best transfection reaction combinations to generate transfected EndoCβH1 cells. The individual images correspond to cells transfected with A) Lipofectamine 3000 (2x cell seeding density + 2 µl plasmid + 6 µl transfection reagent), B) Lipofectamine LTX (2x cell seeding density + 2 µl plasmid + 4 µl transfection reagent), C) ViaFect (3x cell seeding density + 1 µl plasmid + 3 µl transfection reagent), D) ViaFect (3x cell seeding density + 1 µl plasmid + 5 µl transfection reagent), E) ViaFect (3x cell seeding density + 2 µl plasmid + 6 µl transfection reagent), F) ViaFect (3x cell seeding density + 3 µl plasmid + 9 µl transfection reagent), G) ViaFect (2x cell seeding density + 1 µl plasmid + 3 µl transfection reagent), H) FuGENE HD (3x cell seeding density + 2 µl plasmid + 4 µl transfection reagent), and I) FuGENE HD (3x cell seeding density + 3 µl + 6 µl transfection reagent). This transfection data represent three individual experiments with three replicates. Images were taken using an Olympus IX83 inverted microscope. The scale bar in the images represents 50 µm.

4.2.5.4 Selection of best CRISPR guide RNAs to knock out *ABCC8* and *KCNJ11* genes in EndoCβH1 cells

In section 4.2.5.1, it is mentioned that four gRNAs were designed, constructed and cloned into plasmid vector pX458 for both of the *ABCC8* and *KCNJ11* genes. Among the four gRNAs, two were targeted for the forward strand and two were designed for the reverse strand. The strategy of the knock out experiments was to introduce a double-strand break (DSB) in two distantly located site of DNA mediated by one forward strand gRNA and one reverse strand gRNA. As a result, a big segment of the genes could be perturbed by these two DSB.

All four gRNAs for each of the genes were examined for their mutation introduction efficiencies. EndoCβH1 cells were transfected with all gRNAs individually using the ViaFect transfection method. After three days of post-transfection, genomic DNA was extracted from each of the samples. PCR products covering the target mutation regions in the *ABCC8* and *KCNJ11* genes were digested with T7 endonuclease I (T7EI). T7EI recognises and cleaves mismatched heteroduplex DNA which arises from hybridization of wild-type and mutant DNA strands (Mashal *et al,* 1995; Babon *et al,* 2003). From the gel-electrophoresis image of digested samples, the *ABCC8* PCR amplicon was found to naturally possess a single nucleotide polymorphism (SNP) as all transfected and un-transfected samples of EndoCβH1 showed a smaller DNA fragment (Figure 4.21 B). gRNA 2 (forward strand) and gRNA 4 (reverse strand) designed for the *ABCC8* gene were considered better efficient introducing mutations in target loci after observing the gel image of digested products (Figure 4.21 B). So, for final mutation experiments on the *ABCC8* gene, gRNA 2 and 4 were decided to co-transfect the cells.

Figure 4.21 C and D show PCR and T7EI digested image of the *KCNJ11* gene of EndoCβH1 cells. Unfortunately, none of the guide RNAs designed for this gene showed sufficient efficiencies to introduce mutations in the gene. Due to time constraints, new attempts to design guide RNAs and subsequent knock out experiments for the *KCNJ11* were not conducted further.

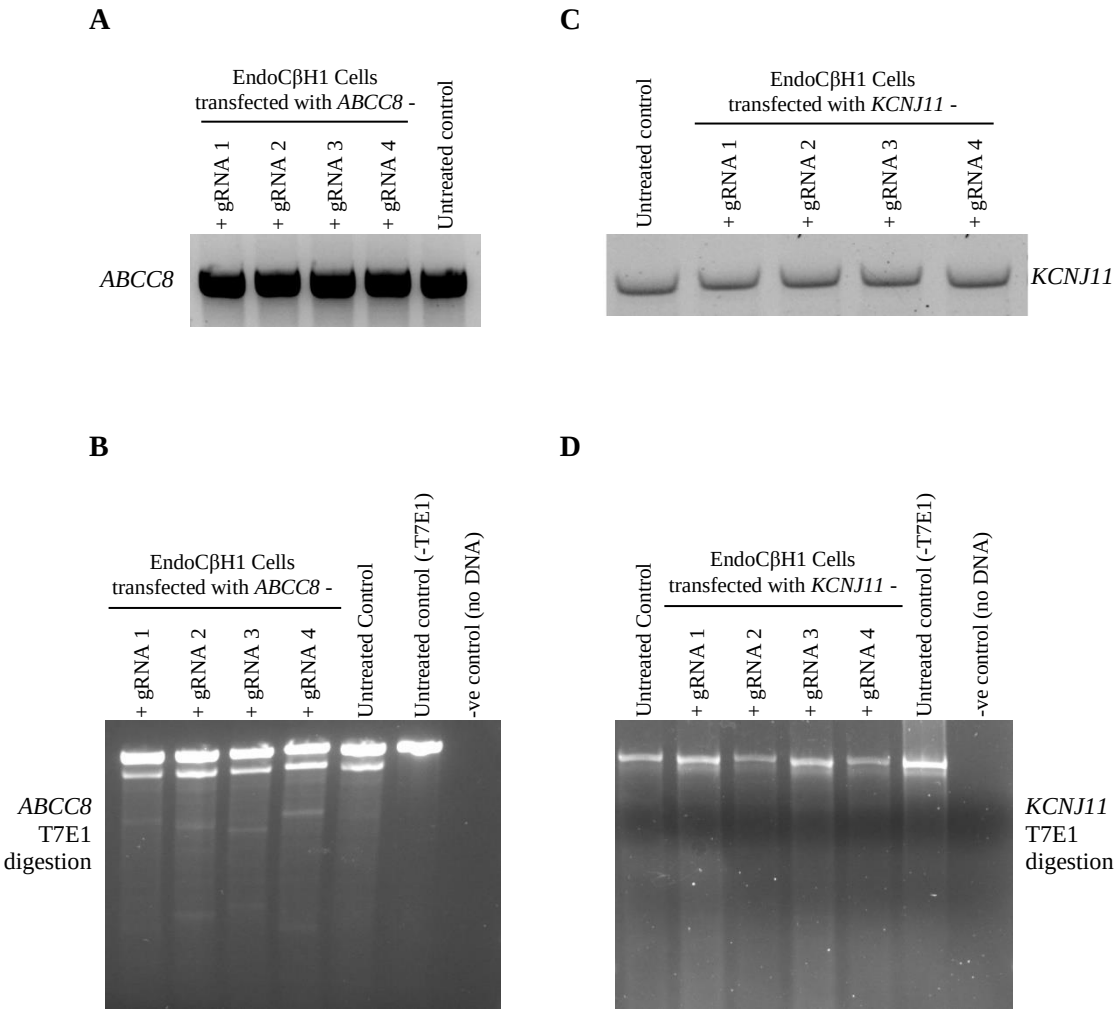

Figure 4.21: **Transfection efficiencies of guide RNAs used to knock out *ABCC8* and *KCNJ11* genes in EndoCβH1 cells**. Images A and C represent PCR amplicons of *ABCC8* and *KCNJ11* genes, respectively, from transfected and non-transfected cells of EndoCβH1. Images B and D show T7EI digestion pattern on PCR products of *ABCC8* and *KCNJ11* genes, respectively, from transfected and non-transfected cells of EndoCβH1.

4.2.5.5 Generation of *ABCC8* knock-out EndoCβH1 cell population and their characterization

As mentioned earlier single cell clonal isolation and expansion were not successful in EndoCβH1 under any conditions, despite many attempts to optimise the culture conditions. Therefore subsequent experiments were focused to generate a mixed population containing a minority of wild-type cells, with a higher percentage of knocked out cells (as described in section 4.2.5.3). gRNA 2 and gRNA 4 were selected to co-transfect EndoCβH1 cells to knock out the *ABCC8* gene. So, the cells were transfected with plasmids encoding gRNA 2 and gRNA 4. Then the cells were cultured for two days in normal growth media. After two days, cells were sorted based on the GFP expression using FACS. All the sorted cells were then allowed to grow together as a mixed population. The cells were sub-cultured until a sufficient number of cells was achieved for further analysis. To increase the percentage of successfully knocked out cells in the mixed population of transfected cells, another approach was applied. The EndoCβH1 cells were transfected with plasmids, encoding guide RNA 2 and gRNA 4 along with plasmid encoding puromycin resistance gene. Then the cells were cultured for two days in growth media containing puromycin antibiotic to select puromycin-resistant cells only. This selection approach was explored to kill the non-transfected cells and also to increase the percentage of successfully knocked out cells in the cell population. After two days of post-transfection spent media was replaced with fresh growth media without puromycin supplementation and incubated for two more days to promote proper cell growth of surviving cells. Then the cells were sub-cultured altogether as a mixed population until sufficient cell number was achieved to do further analysis.

Both the transfection experiments show a good number of successfully transfected cells (Figure 4.22). Amplification of the targeted mutated region of the *ABCC8* gene was carried out using PCR. A deletion mutation resulted because of the dual effect of two guide RNAs. As a result, an additional smaller DNA fragment was observed in the transfected cell population compared to untreated EndoCβH1 cells (Figure 4.23 A). Successful gene editing experiments were confirmed through the presence of smaller DNA fragments in the PCR amplicons. However, the percentage of cells having this deletion mutation was very poor in the population. Less than 30% of cells of the populations, generated from two approaches, were edited and knocked out through the

experiments (Figure 4.23 B). As expected, multiple smaller DNA fragments were observed when PCR amplicons were digested with T7EI (Figure 4.23 C).

Hence, whilst the designed guide RNAs were efficient to knock out the *ABCC8* gene and also transfection experiments were successful to generate knocked out cells, the low percentage of cells with the desired genotype made the transfected cell population inappropriate for use in further analyses.

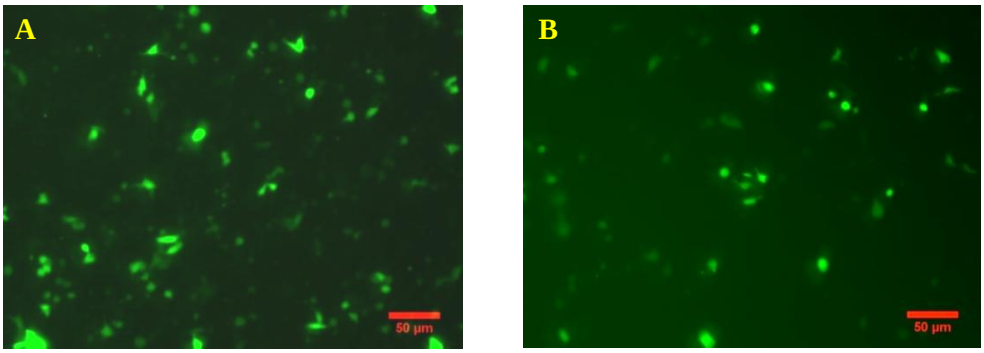

Figure 4.22: **Successfully transfected EndoCβH1 cells expressing GFP**. Image A represents cells transfected with plasmids encoding guide RNAs only. Image B represents cells transfected with plasmids, encoding guide RNAs along with plasmid, encoding puromycin resistance gene. The images were captured two days after transfection. Images were taken using an Olympus IX83 inverted microscope and analysed using ImageJ software.

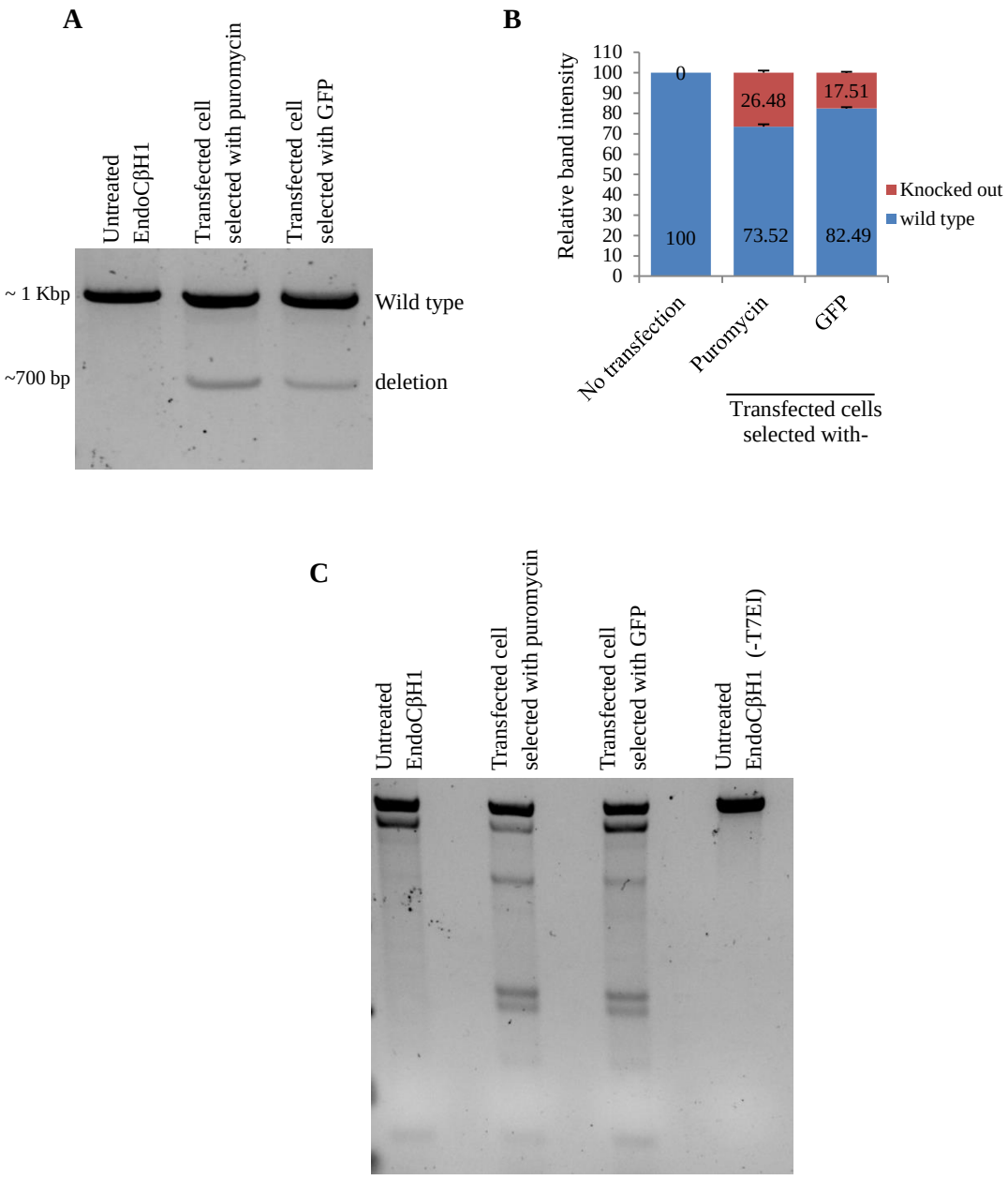

Figure 4.23: **Genetic screening of transfected EndoCβH1 cell population for *ABCC8* mutation**. Cells were transfected with guide RNAs encoding plasmids with or without co-transfection with the puromycin-encoding plasmid. Transfected cells were selected by either GFP or puromycin selection methods. Image A represents PCR amplicons of the *ABCC8* gene covering the targeted mutation region. Image B corresponds to a graphical representation of relative Band intensity observed in image A. 26.5% and 17.5% cells were *ABCC8* knocked out among the cell population while selected by puromycin and GFP based methods, respectively. Data are presented as mean ± SEM. Image C illustrates T7EI digestion pattern of PCR products of the *ABCC8* gene from experimental cells of EndoCβH1.

4.2.6 Introduction of a deletion mutation in the *ABCC8* gene in CHI-iPS cells

Since single cell clonal propagation was unsuccessful for EndoCβH1 cells and generated *ABCC8* knocked out cell population was not suitable for further studies, as a final attempt, CHI-iPS cells were targeted for introducing *ABCC8* deletion mutation using the guide RNAs designed for EndoCβH1 cells. CHI-iPS cells were transfected with plasmids encoding gRNA 2 and gRNA 4 targeted for *ABCC8* gene using Amaxa nucleofector. As described earlier, the transfected cells were sorted by either limiting dilution or using FACS. However, not a single cell was found to propagate clonally after seeding 540 single cells in three separate experiments. The transfected cells were then allowed to grow as a mixed population. A smaller DNA fragment (because of deletion mutation) was generated after PCR amplification of the *ABCC8* gene from the mixed cell population (Figure 4.24). However, less than 10% of cells were observed to have deletion mutation in three separate experiments. And again the low percentage of knocked out cells in the cell population made the CHI-iPS transfected cell population inappropriate for use in further analyses.

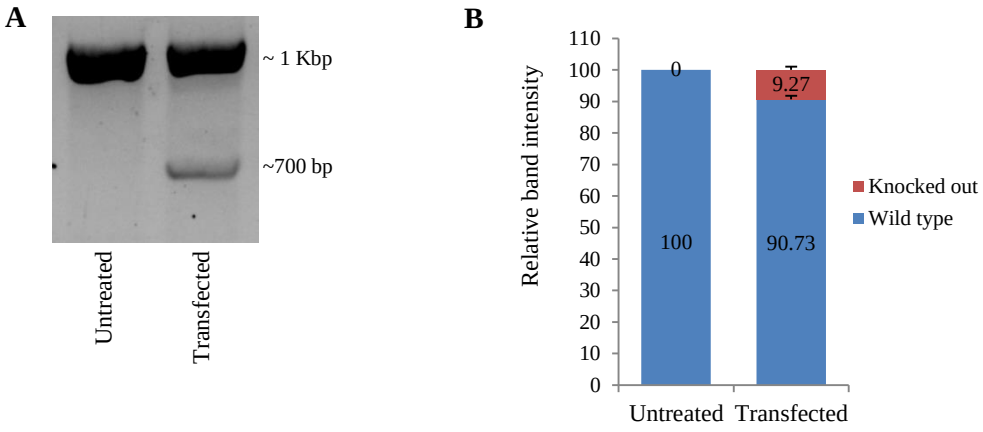

Figure 4.24: **Genetic screening of the *ABCC8* gene knocked out CHI-iPS cell population**. Image A represents PCR amplicons of the *ABCC8* gene from control and transfected cell population. Image B shows relative band intensities observed in PCR experiments. Data are presented as mean ± SEM. Band intensity was measured using ImageJ software.

4.3 Discussion

4.3.1 General

The principal aim of this thesis was to generate a population of insulin-producing model pancreatic beta cells that act like CHI affected cells and could be used for further analysis in order to gain an insight into key molecular processes involved in CHI development in patients.

In chapter 3, attempts were made to transform beta cells into CHI-like cells by modifying *in vitro* culture conditions. However, those attempts were unable to generate CHI-like cells. The aim of the experiments presented in this chapter was to generate a population of CHI-like model cells by editing the *ABCC8* gene directly using gene editing methods. CRISPR-Cas9 mediated gene editing method was explored to introduce either homozygous mutation in the *ABCC8* gene in CHI-iPS cells or deletion mutations in the *ABCC8* gene in either CHI-iPS cells or EndoCβH1 cells. Failure of clonal propagation of edited cells made it unsuccessful to generate viable CHI model cells.

4.3.2 CHI-iPS cell and its potential to generate insulin-producing cells

The expression of several key TFs including Oct4, Sox2, c-Myc and Klf4 are inherent to pluripotent stem cells (Takahashi and Yamanaka, 2006; Schmidt and Plath, 2012). It was reported earlier that CHI-iPS cells express all of these TFs (Kellaway, 2016). To investigate whether a stem or iPS cell line maintains its stem cell properties, expression of some pluripotency marker proteins including Oct4, Sox2, Nanog and SSEA4 are routinely examined ((Henderson *et al*, 2002; Chambers *et al*, 2003; Okumura-Nakanishi *et al*, 2005; Gang *et al*, 2007; Zhou *et al*, 2011; Amini *et al*, 2014). Before conducting any downstream experiment, the CHI-iPS cells were examined whether they maintained their stem cell characteristics. Immunofluorescence assays were designed to investigate the expression of abovementioned marker proteins in CHI-iPS cells. The cells were found to maintain stable expression of these pluripotency markers and this finding suggested that the cells were suitable for further experiments.

It was reported earlier that iPS cells might preserve an epigenetic memory of the original somatic tissue from which they have been established. iPS cell differentiation towards

cells of origin might be enhanced because of the possible influence of the retained epigenetic memories (Kim *et al,* 2010; Bar-Nur *et al,* 2011; Vaskova *et al,* 2013; Liang and Zhang, 2013). As mentioned earlier, the CHI-iPS cell line was established from pancreatic tissue. So, the CHI-iPS cells were examined for their ability to differentiate into insulin-producing beta cells.

A number of differentiation protocols were reported earlier to transform stem cells (ES and iPS cells) into mature and functional insulin-producing pancreatic beta cells (Zhang *et al,* 2009; Rezania *et al,* 2012; Pagliuca *et al,* 2014; Rezania *et al,* 2014; Millman *et al,* 2016). Differential expression of a set of key TFs involved in pancreatic beta cell development is the key to the differentiation of iPS cells into insulin-producing cells (Rezania *et al,* 2014; Millman *et al,* 2016). The key TFs are *PDX1* (a key critical factor of pancreatic endoderm) (Roberts, 1999; Sambathkumar *et al,* 2016), *NEUROD1* (required for transition to endocrine cell type) (Flasse *et al,* 2013; Mastracci *et al,* 2013), *NK6.1* (required for islet cell identity) (Schaffer *et al*. 2013; Taylor *et al,* 2013) and *NGN3* (an endocrine progenitor marker) (Gu *et al,* 2002b; *Li et al,* 2010b; Afrikanova *et al,* 2012). Two differentiation methods, recently published by Rezania *et al*. (2012) and Rezania *et al*. (2014), were used in this study. Since it was not certain which differentiation protocol would lead to a desired insulin-producing cells from edited CHI-iPS cells, so both the protocols were optimised for CHI-iPS cell line.

In the 5-stage protocol (Rezania *et al,* 2012) that ended with insulin-producing cell-clusters, *PDX1* was expressed from stage-3 (marks formation of posterior foregut) and the expression was continued in increasing amount until stage-5 (insulin-producing cell-clusters) (Figure 4.6) as it was observed in the findings of Rezania *et al*. (2012). *NEUROD1* and *NKX6.1* were expressed from stage-4 (pancreatic endoderm) significantly and the expressions were continued in increasing amount until stage-5. However, these findings were in contrast to the findings obtained by Rezania *et al*. (2012) where expression of these TFs was first detected at stage-3. Expression of *NGN3* was observed only after stage-5 treatment in contrast to the study of Rezania *et al*. (2012) where expression of this marker was first detected at stage-3. Unlike the observations reported by Rezania *et al*. (2012) where expressions of the *INS* and *SST* genes were detected first at a low level at stage-3, here in this study, expression of these genes was evident only at stage-5 treatment.

In the 7-stage protocol (Rezania *et al,* 2014) that ended with insulin-producing beta-like cells, *PDX1* expression was first detected at stage-3 (posterior foregut) similar to the 5-stage protocol and the expression was continued over the following steps. A similar observation was reported by Rezania *et al*. (2014). *NEUROD1* was expressed from stage-4 (pancreatic endoderm) and the expression was increased gradually until stage-7 (*NKX6.1*$^{+}$/*INS*$^{+}$ beta-like cells). However, there was a reduction in the expression of *NEUROD1* at stage-6-day-15 (*NKX6.1*$^{+}$/*INS*$^{+}$ cells) compared to the expression level observed at stage-6-day-7 (precursors of *NKX6.1*$^{+}$/*INS*$^{+}$ cells). Similar expression pattern of *NEUROD1* was reported by Rezania *et al*. (2014). *NKX6.1* was expressed from stage-4 and the expression was increased gradually until stage-7. A similar finding was reported by Rezania *et al*. (2014), except that there was a reduction in expression of the gene at stage-6-day-15 compared to the expression level observed at stage-6-day-7. *NGN3* expression was started in a comparatively higher amount in stage-5 (pancreatic endocrine precursors) and then the expression was gradually decreased in the following stages. A similar finding was also reported by Rezania *et al*. (2014). No expression was observed for *SST* in any stages of the differentiation, similar to the report of Rezania *et al*. (2014). Insulin was found to be expressed from stage-6-day-7 and the expression was increased at stage 7 similar to the expression pattern reported by Rezania *et al*. (2014).

For both the 5-stage and 7-stage protocols, the observed differences in the pattern of gene expressions could be associated with the difference in the cell line used. H1 human ES cell line was used by Rezania *et al*. (2012) and Rezania *et al*. (2014) whereas in this study the CHI-iPS cell line was used. The cell lines might respond to the reagents used for the differentiation differently and that might promote the observed variations in expression.

Both the optimized differentiation protocols were able to generate insulin-producing viable cells. However, because of the nature of the differentiation method, the generated insulin-producing cells were unable to propagate further in culture media. So, further extensive experimentations including gene editing were not possible using the CHI-iPS derived final differentiated cells. So experiments were designed to edit the CHI-iPS cells first, then differentiate them into insulin-producing cells and then to carry out downstream experiments.

As mentioned previously (section 4.2.1), CHI-iPS cell line was established from a Fo-CHI pancreatic tissue with a heterozygous recessive mutation in the *ABCC8* gene. The cells that were used to make the CHI-iPS cell line were from the healthy tissue at the edge of the focal lesion. This means the cells were healthy and carried the recessive allele but would not act as if it has CHI. It was hypothesised that the heterozygous recessive mutation might not have any deleterious effect on *ABCC8* expression *in vitro* which, otherwise, induced CHI in some cells *in vivo*. It was assumed that homozygous mutation might be helpful to induce CHI in *in vitro* condition since homozygous mutations in the *ABCC8* gene were reported earlier in CHI patients (Yan *et al*, 2007; Flanagan *et al*, 2009; Rahman *et al*, 2015a; Nessa *et al*, 2016). Hence, experimental approaches were considered to introduce a second mutation in at the mutated locus so that both copies of the gene became mutated and the gene became inactive. The establishment of insulin-producing pancreatic beta-like cells from edited CHI-iPS cell might provide added benefit to generate CHI *in vitro* model cell line.

4.3.3 Introducing homozygous mutation in the *ABCC8* gene in CHI-iPS cell line

Successful generations of *ABCC8* deficient human ES cell lines mediated by CRISPR-Cas9 method were reported (Guo *et al,* 2016; Guo *et al,* 2016a) after starting of these gene editing experiments on CHI-iPS cells. Insulin-producing CHI-like model cell line was also reported recently to be generated from these *ABCC8* deficient ES cell lines (Guo *et al,* 2017). The idea of a generation of a CHI-like model cell line from *ABCC8* knocked out CHI-iPS cell lines is well supported by these three recently published reports.

A number of studies reported earlier for successful transfection of iPS cells, generated from different cell types, using electroporation-based methods (Chatterjee *et al,* 2011; Byrne *et al,* 2014; Yang *et al,* 2014a; Yang *et al,* 2014b; Byrne and Church, 2015; Li *et al,* 2016). In addition, some studies have reported using chemical-based approaches to transfect embryonic stem (ES) cells (Tabar *et al,* 2014; Luo *et al,* 2016). Experiments were designed to investigate the efficiencies of a couple of available chemical-based and one electroporation-based transfection systems on CHI-iPS cells. Amaxa nucleofector, an electroporation-based transfection method was found most efficient to transfect the cells with plasmid vectors and hence was selected for transfecting CHI-iPS cells.

To introduce a specific mutation at the target locus of a target gene, use of a repair template in the form of ssODN along with transfection vectors encoding gRNAs is recommended (Sander and Joung, 2014; Xue *et al,* 2014; Yoshimi *et al,* 2016; Song and Stieger, 2017). If the cells are introduced with a mutation in a target locus, the restriction enzyme profile will be different for a homozygous or a heterozygous mutant compared to a wild-type cell. So, experiments were designed to transfect the CHI-iPS cells with designed gRNAs along with a designed ssODN and then sort potentially edited cells as single cells for clonal propagation. Efficient transfection followed by gene excision and repair was observed in transfected CHI-iPS cells. Close to 50% of cells were predicted to be edited in the transfected cell population which indicates good efficiencies of designed gRNAs. The transfected cells carrying a potential target mutation in the target loci of the *ABCC8* gene were sorted as single cells following the previously reported protocols (Byrne *et al,* 2014; Yang *et al,* 2014a). However, only ~1.5% of sorted single cells were survived and were established as clonal cell lines.

Unlike the CHI-iPS cells, differences in the growth rate of cell colony formation and diverse morphologic features were observed from different established clonal cell lines. Moreover, the undifferentiated state of most of the survived single cell clones was appeared to be compromised after a couple of passages as this phenomenon was reported by Valamehr *et al*. (2011). None of the edited clones was observed to have the desired homozygous mutation at the target locus of *ABCC8*. Rather, incorporation of random mutations was identified through DNA sequencing of the target locus. A similar observation was reported earlier where single cell expansion of ES and iPS cells resulted with random genomic mutation as well as increased cell death (Amit *et al,* 2000; Eiges *et al,* 2001).

Since the clones generated from above-mentioned transfection method were observed to be diversified, differentiated and not carrying the properties of the cell of origin, a number of alternative methods were explored to generate viable edited CHI-iPS cells. Single cell culture media composition was modified; single cell culture practice was changed, different growth surface coating reagents were used, even the transfection experiments were switched to the chemical-based method. However, none of the changes was able to propagate any viable single cell.

Since the experiments to introduce a homozygous mutation in the *ABCC8* gene in CHI-iPS cells were not successful, in another approach, the *ABCC8* gene knock out was tried by deleting a critical exon (exon 2). Similar approaches were reported by Guo *et al*. (2016) and Guo *et al*. (2016a). However, after transfection, sorted knocked out single cells of CHI-iPS failed to propagate. When sorted transfected cells were grown as a mixed population only ~10% of cells were observed to have deletion mutation in the *ABCC8* gene. The very low percentage of knocked out cells in the cell population made the CHI-iPS transfected cell population inappropriate for considering for differentiation into pancreatic beta-like cells.

In summary, CHI-iPS cells generated from a Fo-CHI patient were able to maintain stem cell properties and also to be differentiated into insulin-producing cells. To generate a CHI-like model cell line from CHI-iPS, the cells were treated to introduce a homozygous mutation in the *ABCC8* gene in one approach and to knock out the gene by deleting a crucial exon in another approach. Both approaches were observed to be efficient to transfect the cells. However, the very poor rate of survival in single cell clonal expansion as well as the uncontrolled differentiation of survived cells into different mature cell types made the edited CHI-iPS cells unusable for further studies. The reasons behind the poor rate of single cell survival and also the incorporation of random non-specific mutations could be attributed to multiple factors. CHI-iPS cells might be very sensitive to the culture conditions when they are in a single cell format, rather than being in cell cluster-like format. So, transfection reagents as well as high pressure, applied by FACS during single cell sorting, might promote adverse effects on single cells which induce random mutation for survival. Most of the mutations might have some lethal effects which could explain the low survival of transfected single CHI-iPS cells.

4.3.4 Knocking out the *ABCC8* and *KCNJ11* genes in EndoCβH1 cell line

Since the generation of a stable homozygous mutated cell line from CHI-iPS cell line was not successful, as an alternative option, the EndoCβH1 cell line was considered again. *ABCC8* is a multi-exonic gene (39 exons) whereas *KCNJ11* contains one single coding exon (Babenko *et al,* 2006; Adi *et al,* 2015). Exon 2 of the *ABCC8* was predicted as one of the critical exons required for the *ABCC8* protein to be functional (Guo *et al,* 2016;

Guo *et al,* 2016a). Experiments were designed to delete exon 2 of the *ABCC8* gene and the only exon in the *KCNJ11* gene.

As already explained, the successful generation of a knocked out cell line requires clonal propagation from single cells. But a requirement of high cell seeding density for proper growth and survival of EndoCβH1 cells is a major limiting factor of the cells used in gene editing experiments. No previous studies have reported the successful clonal propagation of single EndoCβH1 cells. Various attempts were explored in this study to enhance single cell growth of these cells. However, none of the methods was observed to be favourable for single cell growth. So, the experimental strategies were switched to find a suitable transfection method which would generate a higher percentage of transfected cells. This population would be useful for studying further to understand the pathophysiology of CHI. Since no study was reported earlier (at the time of these experiments) where EndoCβH1 cells had been transfected successfully with plasmid, a number of commercially available transfection kits were explored for EndoCβH1 cells. Although Lipofectamine 2000 reagent was reported by Velayos *et al*. (2017) recently to be used to transfect EndoCβH1 cells, however, in this current study, ViaFect lipid reagent was found to be most efficient for EndoCβH1 cells transfection with plasmids.

Unpredictable random mutations like insertion, deletion, or frameshifting could result in the genome if the cells are transfected with single gRNA (Ran *et al,* 2013; Wang *et al,* 2013; Wu *et al,* 2013; Maruyama *et al,* 2015). Transfection with two or more gRNAs could facilitate to mediate larger deletions in the genome (Chen *et al,* 2011; Cong *et al,* 2013). It was hypothesised that transfecting EndoCβH1 cells with two gRNAs (against forward and reverse strand of the target gene) could introduce a large deletion in the gene and thus make the gene inactive. So, potential gRNAs were designed for both the *ABCC8* and *KCNJ11* genes. All four gRNAs for *ABCC8* were found to be more or less similarly effective. Among them, guide RNA 2 (forward strand) and guide RNA 4 (reverse strand) were considered for final knock out experiments. On the other hand, none of the gRNAs designed for the *KCNJ11* gene showed sufficient efficiencies to introduce mutations in the gene. Attempts to design a new set of gRNAs and subsequent knock out experiments were not conducted due to time constraints.

In one approach, EndoCβH1 cells, transfected with both guide RNA 2 and 4 simultaneously to delete exon 2 of the *ABCC8* gene, were sorted and cultured as a mixed population. In another approach, in an attempt to increase the percentage of successfully knocked out cells in the population of transfected cells, cells were transfected with plasmids, encoding puromycin resistance gene along with the plasmids, encoding guide RNA 2 and 4 (Howden *et al,* 2011; Ovchinnikov *et al,* 2014; Cerbini *et al,* 2015). Puromycin-resistant cells were then selected and allowed to grow as a mixed population. However, only 26.5% and 17.5% cells of the mixed population were observed to be *ABCC8* knocked out in puromycin and GFP selected cell population, respectively.

Briefly, to generate a CHI-like model cell line from EndoCβH1 cells, experiments were designed to knock out the K_{ATP} channel genes by deleting a crucial exon of the genes. Guide RNAs were designed manually for both *ABCC8* and *KCNJ11* genes since no reference guide RNA for the genes was available in the literature. Since EndoCβH1 cells were unable to grow as a single cell, so, the transfected cells were cultured as a mixed population of cells Although the experiments were designed as best as possible, the percentage of target knocked out cells in mixed cell population was very poor (below 30%). Because of this very low percentage, the cell populations of the knocked out EndoCβH1 cells was considered unfit for further studies.

In summary, multiple experiments were performed to edit either the *ABCC8* gene in CHI-iPS cells or the *ABCC8* and *KCNJ11* genes in EndoCβH1 cells to inactivate the genes in an attempt to introduce CHI-like behaviour in the cells. However, none of the attempts was successful to generate viable CHI model cells. So it was concluded that the methods explored in this study were not the proper methods to transform either the CHI-iPS or EndoCβH1 cells into CHI-like cells. However, due to time constraints, no further approaches were performed to edit genes in these cell lines.

Chapter 5

Genome-wide gene expression microarray analysis of CHI-affected pancreatic tissues

5.1 Introduction

5.1.1 General

It is well noted that a single biological function is a combined effort of multiple biological factors. A variety of activation or inhibition factors are required to carry out a single function (Leung and Cavalieri, 2003). A disease could be a very complex biological phenomenon where multiple genetic and non-genetic factors could be involved and multiple metabolic and regulatory pathways could be altered (Gu *et al,* 2002a; Smith, 2007; Panoutsopoulou and Zeggini, 2009; Jin *et al,* 2014; Kao *et al,* 2017). Yet until recently, very little has been known about the genetic basis of most known complex diseases (Wang *et al,* 2007; Jin *et al,* 2014). Previously, experiments were performed in a reductionist approach to understand the aetiology of a complex biological phenomenon by trying to identify associated central genes or proteins (Panoutsopoulou and Zeggini, 2009). But it was not sufficient to understand the complex nature of the biological abnormality (Wang *et al,* 2007; Jin *et al,* 2014).

Until recently, several genes have been identified to be associated with CHI. Yet, a major portion of patients with CHI does not have any recognisable aetiology (Stevens *et al,* 2013). Like other complex diseases, CHI could be due to a combined effect of multiple factors and multiple pathways. In addition, as was reported for other complex diseases, the microenvironment surrounding the insulin-secreting pancreatic beta cells might also contribute to the development of this disease (Hussain *et al,* 2005a; Bagyánszki and Bodi, 2012; Nyitray *et al,* 2014; Hui and Chen, 2015; Rothschild and Banerjee, 2015; Aamodt and Powers, 2017; Jeffery *et al,* 2017). Therefore, genome-wide gene expression studies could be a suitable approach to gain new information which might help for better understanding of the disease (Wang *et al,* 2007; Panoutsopoulou and Zeggini, 2009; Kao *et al,* 2017).

The principal focus of this research project was to generate an *in vitro* CHI model cell line and then analyse the genome-wide gene expression pattern of the model cells in comparison with the gene expression data from CHI affected tissue in efforts to provide some new information regarding CHI development. Although the attempts to generate suitable CHI model cell lines failed (as mentioned in Chapter 3 and Chapter 4), genome-wide gene expression analysis on CHI tissues was thought to be helpful to identify novel candidate genes and the pathways that could be associated with the disease. No previous studies have been reported earlier where healthy tissues (as control) and lesion tissues, both from CHI affected pancreas, were used for differential gene expression assay in order to identify potential candidate genes as well as the disease associated relevant pathways. Hence, microarray-based differential gene expression assays were conducted in the present study to compare differential gene expressions from control and lesion tissues both from CHI patients in an attempt to identify potential candidate genes and related pathways associated with CHI.

5.1.2 An overview of gene expression microarray

Genome-wide gene expression experiment using microarray technique is a very state-of-art analytic tool to measure the expression of thousands of genes in parallel in a biological sample under certain condition (Schena *et al*. 1995; Alon *et al,* 1999; Callow *et al,* 2000; Trevino *et al,* 2007; Sealfon and Chu, 2011). This technology offers a suitable way to identify relevant disease-associated gene regulatory network and pathways by analysing differentially expressed genes (Gu *et al,* 2002a; Kaul and Eichinger, 2006; Trevino *et al,* 2007; Sealfon and Chu, 2011). Most prominently, microarray experiments are used to measure the level of RNA transcription from thousands of genes from a sample (Trevino *et al,* 2007). Microarray technology has also been used to identify single nucleotide polymorphisms (Gunderson *et al,* 2005; Homer *et al,* 2008; Di Candia *et al,* 2009; Harel *et al,* 2015), alteration of gene copy numbers (Pinkel *et al,*1998; Snijders *et al,* 2001; Tannour-Louet *et al,* 2014), RNA splicing (French *et al,* 2007; Arnold *et al,* 2013; Highley *et al,* 2014), pattern of methylation (Bell *et al,* 2010; Wippermann *et al,* 2014; Jaffe *et al,* 2016), and chromosomal insertion or deletion (Sahoo *et al,* 2006; Probst *et al,* 2007; Day *et al,* 2007).

The basic principle behind microarray technology is the property of single-stranded nucleotide sequences to hybridize with complementary sequences (Lou *et al,* 2001; Trevino *et al,* 2007; Selvaraj and Natarajan, 2011). An expression array is basically an organized arrangement of DNA probes attached to a solid surface and these probes correspond to individual genes of an organism (Schulze and Downward, 2001; Kaul and Eichinger, 2006). Mostly, two types of microarray expression arrays are being used in research- one is complementary DNA (cDNA)-based and the other one is oligonucleotide-based.

The cDNA-based array was the first widely used array platform (Schena *et al*. 1995; Sasik *et al,* 2004; Kaul and Eichinger, 2006). This platform uses PCR-amplified cDNA fragments as probes which represent individual target genes of an organism. RNA from target samples (control and test) are extracted and converted to cDNA in the presence of different fluorescently labelled dNTPs. Then the labelled cDNA are mixed and hybridized to the probes on the expression arrays. The hybridized probes are then scanned and the levels of expression of different genes are analysed based on the colour intensity ratio (Sasik *et al,* 2004; Kaul and Eichinger, 2006; Ness, 2007; Trevino *et al,* 2007). The probes used in this technology can be prepared in laboratories as a customised array. However, the limitations of using cDNA probes are the uneven melting temperatures of the probes because of the differences in probe size and GC content (the percentage of the combined number of guanine and cytosine residues in an oligonucleotide), as well as possible cross-hybridization of similar sequences and overlapped genes (Sasik *et al,* 2004; Chang *et al,* 2006; Ness, 2007; Trevino *et al,* 2007). However, these limitations can be normalised by using multiple different probes for a single gene (Sasik *et al,* 2004; Trevino *et al,* 2007).

The oligonucleotide-based array is designed in a way that can overcome the limitations of the cDNA-based array. In this array, *in situ* synthesized small single-stranded oligonucleotides attached to the surface of glass slides are used as probes. Every single gene is represented by ~20 distinct oligonucleotides on this array. RNAs from different test samples are fluorescently labelled, hybridized with the probes and scanned separately in this array technology. Colour intensities are then analysed and compared to measure differential gene expression (Sasik *et al,* 2004; Ness, 2007; Trevino *et al,* 2007). These arrays are manufactured by commercial providers like Affymetrix (Thermo Fisher

Scientific) and are usually very expensive. In the present study, an oligonucleotide-based array was used to study comparative gene expression in CHI tissues. Figure 5.1 shows a schematic diagram of the overall process of the two above mentioned methods.

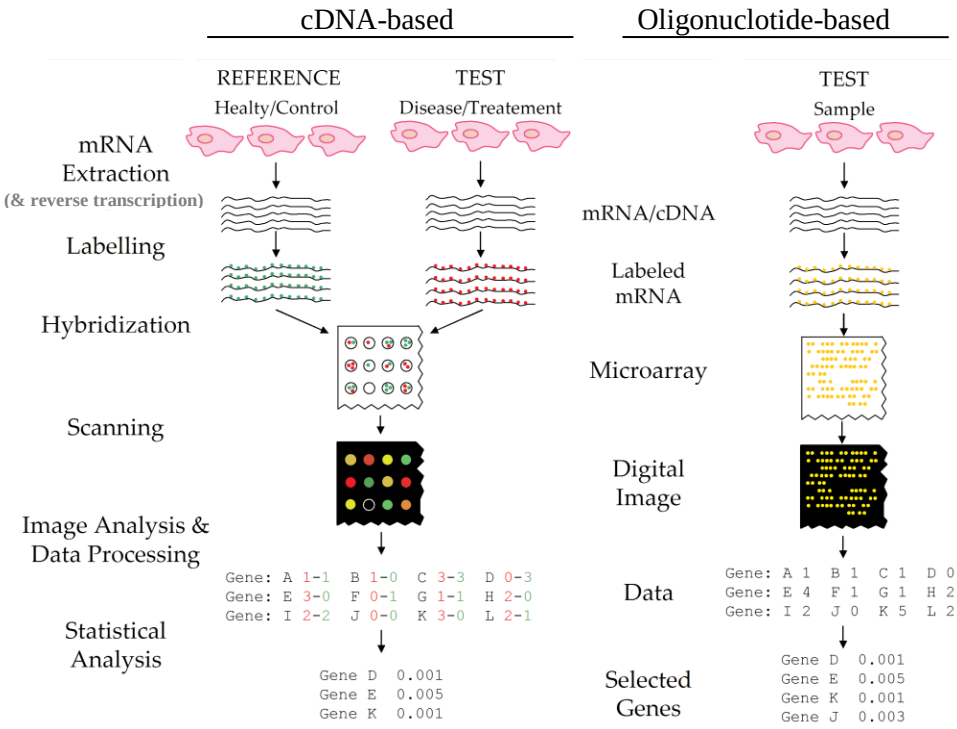

Figure 5.1: **Schematic representation of two major types of arrays used in gene expression microarray**. In complementary DNA (cDNA)-based microarray, RNAs are extracted from both control and test samples and then reverse transcribed to cDNA in the presence of different fluorescently labelled deoxyribonucleoside triphosphates (dNTPs). cDNA from both the samples are then together allowed to hybridize with the PCR-amplified cDNA probes prepared in laboratories as a customised array. The hybridized probes are then scanned and the levels of expression of different genes are analysed based on the colour intensity ratio. In an oligonucleotide-based microarray, RNAs from different samples (test and control) are extracted, reverse transcribed to cDNA and fluorescently labelled similarly to the cDNA array. However, the hybridization of the labelled cDNAs to the probes (manufactured by commercial providers) and the scanning are performed separately for different samples. Colour intensities are then analysed and compared to measure differential gene expression. The image is adapted from Trevino *et al*. (2007).

5.1.3 General approaches for analysing data obtained from gene expression microarray

Expression changes of tens of thousands of genes are measured in a single microarray experiment and so a huge amount of data is normally generated. With the generation of large datasets from these kinds of experiments, it is a challenging task to address and analyse data properly. Elucidating new and accurate information from a gene expression microarray experiment mostly depends on how the data are analysed and how they are interpreted (Chang *et al*, 2006; Ness, 2007; Selvaraj and Natarajan, 2011). Typically, gene expression microarray experiments generate a large dataset containing a list of genes which are changed in their expression level and so are known as differentially expressed genes (Wei *et al*, 2004; Selvaraj and Natarajan, 2011). Since it is a quite strenuous effort to describe every single gene (and its effect) in a large dataset, a popular practice of scientific community is to utilize clustering approach to discuss the change in large datasets and describe the processes that could be altered significantly because of the gene expression changes (Swift *et al*, 2004; Juan and Huang, 2007; Ness, 2007; Hume *et al*, 2010; Selvaraj and Natarajan, 2011). There are a few popular methods based on clustering approach to analyse and interpret microarray data. One of the methods is class comparison which is also known as gene discovery. This analytical approach primarily focuses on identifying groups of differentially expressed genes in samples corresponding to certain biological conditions (like after drug treatments or in disease conditions). These differentially expressed genes are theoretically associated with the biological conditions under study. This analysis does not require any prior knowledge of the behaviour of the samples. The list of differentially expressed genes then can be used to explore the pathways or biological processes which could be associated with those biological conditions (Ness, 2007; Selvaraj and Natarajan, 2011).

Class prediction is another method that requires previous knowledge of a given set of samples of different biological conditions. The pattern of gene expression of the target samples can be analysed and compared with the pre-classified samples and hence, the samples are assigned to one of the known classes. This technique is mainly used for clinical purposes and can be used to design proper treatment systems for a certain patient. This is a comparatively complex process of analysis since it requires a large number of pre-classified samples (Schulze and Downward, 2001; Leung and Cavalieri, 2003; Chang

et al, 2006; Chen *et al,* 2007; Selvaraj and Natarajan, 2011). An emerging approach to analyse gene expression microarray data is pathway or network analysis based on interaction information already available in the literature. This method can help to identify new potential candidate genes associated with the biological conditions under study, and also can help decipher new information for higher level understanding of the condition (Chang *et al,* 2006; Selvaraj and Natarajan, 2011; Roy *et al,* 2014; Zhang and Yin, 2016; Chu *et al,* 2017)

5.1.4 Web-based resources explored in this study to analyse gene expression microarray data

As mentioned before, gene expression microarray data analysis is the most challenging and crucial part to elucidate new and proper information regarding a particular biological condition. Nowadays, a large number of software programs, both free and commercial, are available to assist researchers to manage and analyse microarray data (Koschmieder *et al,* 2011; Mehta and Rani, 2011). Raw expression data are processed and normalised using many of the available programs by dedicated technical experts in research institutes and are then, handed over to the researchers who actually analyse the normalised data and generate novel meaningful information. Typically, researchers filter the list of differentially expressed genes based on an arbitrary fold change in which all the changes are statistically significant (p-value ≤ 0.05). Addition of this filter to narrow down the size of the list of genes enhances the power of analysis (Ness, 2007; Dalman *et al,* 2012). This relatively short list of differentially expressed genes then can be analysed in groups or clusters to determine biological functions associated with those genes (Swift *et al,* 2004; Juan and Huang, 2007; Ness, 2007; Selvaraj and Natarajan, 2011).

To analyse normalised and filtered experimental gene expression data, three web-based software programs were explored in this study and all of these programs utilise clustering method for analysing data. The programs are- DAVID, PANTHER and IPA.

The software program DAVID (the Database for annotation, visualisation and integrated discovery) is a web-based analytical tool that can analyse large set of differentially expressed genes obtained from genomic data and can provide functional annotations to

understand biological meaning comprehensively (Dennis *et al,* 2003; Huang *et al,* 2009a; Huang *et al,* 2009b). A number of previous studies have used this tool to analyse their data and to predict relevant functional biological processes (Chamberlain *et al,* 2011; Depiereux *et al,* 2015; Kotani *et al,* 2015). This software is publicly free to use and can be accessed online at https:// david.ncifcrf.gov.

The PANTHER (protein analysis through evolutionary relationships) classification system is a web-based software program that can help to analyse large biological dataset to predict functional classes by unifying all the available information regarding a particular gene (Thomas *et al,* 2003; Mi *et al,* 2013a; Mi *et al,* 2013b). This classification system performs Gene Ontology (GO) term enrichment analyses at three levels of functional annotations- molecular function, biological process and cellular location to define the biological activities (Ashburner *et al,* 2000; Gene ontology consortium, 2001; Mi *et al,* 2016). A number of previous studies have utilised this classification system to cluster the biological attributes of differentially expressed genes within datasets (Schaefer *et al,* 2008; Tagaya *et al,* 2009; Melville *et al,* 2011). This software is publicly free to use and can be accessed online at http://www.pantherdb.org.

One of the high-throughput analytical tools that can analyse large datasets like whole genome gene expression array to decipher new biological information based on published literature is Ingenuity Pathway Analysis (IPA) (QIAGEN Inc., Redwood City, CA, USA). IPA maintains a high-quality up-to-date knowledge base of biological interactions and functional annotations that are manually curated (Shapira *et al,* 2009; Wittkop *et al,* 2013; Ben-Ari Fuchs *et al,* 2016; IPA website, 2017). The software provides a number of analytical tools by which one can predict upstream or downstream effects caused by differential gene expression and can generate predictive pathway or network models for better understanding of a biological condition (Adriaens *et al,* 2008). A number of studies have used IPA to analyse gene expression microarray datasets (Jiménez-Marín *et al,* 2009; Shapira *et al,* 2009; Haddad *et al,* 2016; Yu *et al,* 2016). This is commercial software and can be accessed at https://www.qiagenbioinformatics.com/products/ ingenuity-pathway-analysis/.

5.1.5 Analysing gene expression microarray data using network biology

The way a biological component, like a cell, carries out its overall activities is complex (Kitano, 2002). At the cellular level, interactions among genes, proteins, regulators, metabolites etc. are conducted to carry out a single function. To understand the functional interactions at the cellular level, systems biology is one of the popular approaches (Stevens *et al,* 2014). Network biology is one of the tools to study systems biology. The function of network biology is to analyse the patterns of interactions between cellular components to understand their roles in complex biological functions linked with various metabolic and regulatory pathways (Barabási and Oltvai, 2004; Pujol *et al,* 2010; Stevens *et al,* 2014). Many studies have utilised a network biology approach to decipher new information regarding biological processes (Ergün *et al,* 2007; Schmid and McMahon, 2007; Chen *et al,* 2008; Jesmin *et al,* 2010; Cahan *et al,* 2014).

The network biology analyses are carried out based on already published protein-protein interactions (PPI) information of the differentially expressed genes of the datasets being examined. Protein-protein interaction partners (PIPs) (either experimentally proven or predicted) of the genes are available in various widely used PPI databases like human protein reference database (HPRD) (Peri *et al,* 2004), biological general repository for interaction datasets (BioGRID) (Stark *et al,* 2006), REACTOME (Croft *et al,* 2011), database of interacting proteins (DIP) (Xenarios *et al,* 2000), biomolecular interaction network database (BIND) (Bader *et al,* 2001), IntAct (Hermjakob *et al,* 2004), HomoMINT (Persico *et al,* 2005), OrthoDB (O'Brien *et al,* 2004), online predicted human interaction database (OPHID) (Brown *et al,* 2005), search tool for recurring instances of neighbouring genes (STRING) (Snel *et al,* 2000) etc. PPI information can be extracted from these databases individually. More recently, a PIPs search tool, unified human interactome (UniHi) was developed which facilitates extracting PPI information automatically from the above-mentioned databases (Chaurasia *et al,* 2007; Kalathur *et al,* 2014). Based on the PPI information, biological networks can be generated and analysed using a number of available software programs. Cytoscape is an open source software program that can be used for visualising molecular interaction networks and analysing them (Shannon *et al,* 2003; Cline *et al,* 2007; Smoot *et al,* 2011). This is one of the most widely used software programs that can integrate networks with gene expression data and functional annotations (Killcoyne *et al,* 2009; Jesmin *et al,* 2010; Kohl *et al,* 2010; Su *et*

al, 2014). A number of publicly free plugins are available for analysing networks with this program (Lotia *et al*, 2013).

5.1.6 Aim and objectives of this study

The **aims of this series of studies** were –

1. To generate an informatics resource of mRNA expression profiles derived from CHI tissues.
2. To use network modelling to analyse mRNA expression profiles to understand the mechanisms of disease.

In order to support this aim, the objectives of this chapter were -

a) To perform genome-wide gene expression microarray analysis on healthy and CHI pancreatic tissues to generate an mRNA expression profile.
b) To use informatics resources to analyse the mRNA expression profiles for the identification of novel gene/protein associations with CHI.
c) To use informatics resources to analyse the mRNA expression profiles for predicting biological processes and pathways potentially associated with CHI.
d) To explore protein-protein interaction and network modelling to analyse the mRNA expression profiles for predicting novel genes/proteins and pathways of CHI.

5.2 Results

5.2.1 Tissues used for genome-wide analysis of gene expression

A number of fresh pancreatic tissues from different CHI patients were received from surgeons from the Royal Manchester Children's Hospital, Manchester, UK. Tissues which were used for analysing the CHI conditions were extracted from lesion regions of the CHI-affected pancreas (section 2.11 for details). Tissues used for control conditions were taken from the healthy regions of the pancreas of the CHI patients. For a few cases, both lesion and healthy region tissues from the same pancreas samples were collected for analysis. In other cases, only lesion or healthy tissues were obtainable for gene expression analysis. So the number of tissue samples for both CHI and control conditions were not the same (Table 5.1). Since the sizes of the received tissues were very small and hence, the amount of total RNA was limited, only one microarray experiment from each sample was performed. All the patients were diagnosed with Focal-CHI with either *ABCC8* or *KCNJ11* mutations. Because of the limited number of patient samples and the impossibility in repeat experiments with a single sample, all the available tissue samples were considered for microarray experiments and further downstream analysis.

Table 5.1: **Tissues used for genome-wide gene expression analysis**

	Patient ID	Type of mutation
Control condition	Nes163	*ABCC8*
	Nes167	*ABCC8*
	Nes168	*KCNJ11*
	Nes169	*ABCC8*
	Nes176	*ABCC8*
CHI condition	Nes162	*ABCC8*
	Nes163	*ABCC8*
	Nes167	*ABCC8*
	Nes168	*KCNJ11*
	Nes170	*ABCC8*
	Nes175	*ABCC8*

5.2.2 Validation of normalised expression data obtained from microarray analysis

Total RNAs extracted from these tissues were used for analysing genome-wide gene expression changes, by Genomic Technologies Core Facility (GTCF) of the University of Manchester, Manchester, UK. The quality, quantity and sizes of the extracted RNAs were assessed using Agilent RNA ScreenTape assays in the facility (Figure 5.2). RNA integrity number (RIN), a tool developed by Agilent technologies, is used to assess and indicate RNA quality and integrity. RIN is represented by a number ranging from 1 to 10 where 1 represents very low-quality RNA (highly degraded) and 10 represents very high quality (intact) RNA. Samples with a high RIN (>7.0) were considered as good quality RNA for gene expression studies (Fleige and Pfaffl, 2006; Raman *et al*, 2009). Microarray experiments on those tissue samples were then performed by the GTCF. After the experiments, normalised data were received for downstream analysis.

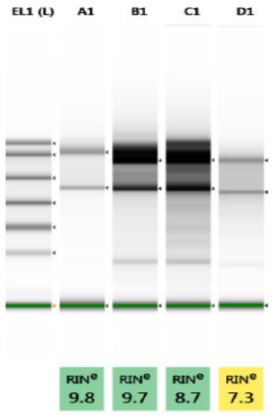

Figure 5.2: **Quality control analysis of total RNA isolated from CHI tissues**. The gel image is a representative data of RNA quality control analyses**.** Lanes A1, B1, C1 and D1 represent RNAs from Nes163, Nes167, Nes168 and Nes169, respectively, from control samples. Lane EL1(L) corresponds to the RNA ladder. These quality control analyses were conducted by the GTCF at The University of Manchester, UK.

Since the sample number in control and CHI condition were not equal, before conducting further analysis, the array data were checked for their normalisation state. It is always recommended to check the normalisation state before downstream analysis with data; otherwise false positive or negative findings might be ended if there is any error in data normalisation (Quackenbush, 2002; Pichler *et al*, 2004). M-A plot is one of the tools to analyse the state of normalisation of the data by visualising the distribution of the data. An M-A plot is a graphical method for visualising intensity-dependent ratio of raw microarray data where "M" represents the binary log of intensity ratio and "A" stands for the average log intensity of the gene expression (Dudoit *et al*, 2002; Yang *et al*, 2002; Quackenbush, 2002) (details in section 2.11). Properly normalised data should generate

an MA plot with most of the intensity data showing values close to zero (0) as most of the genes are unchanged in their expression (Tseng *et al,* 2001). An M-A plot was drawn using the normalised data generated from these CHI microarray experiments (Figure 5.3). Since most of the intensity data were found to be close to zero values (since $Log_2(1)$ is 0), it was considered that the data were normalised properly and needed no further normalisation (Quackenbush, 2002; Bolstad *et al,* 2004; Pichler *et al,* 2004).

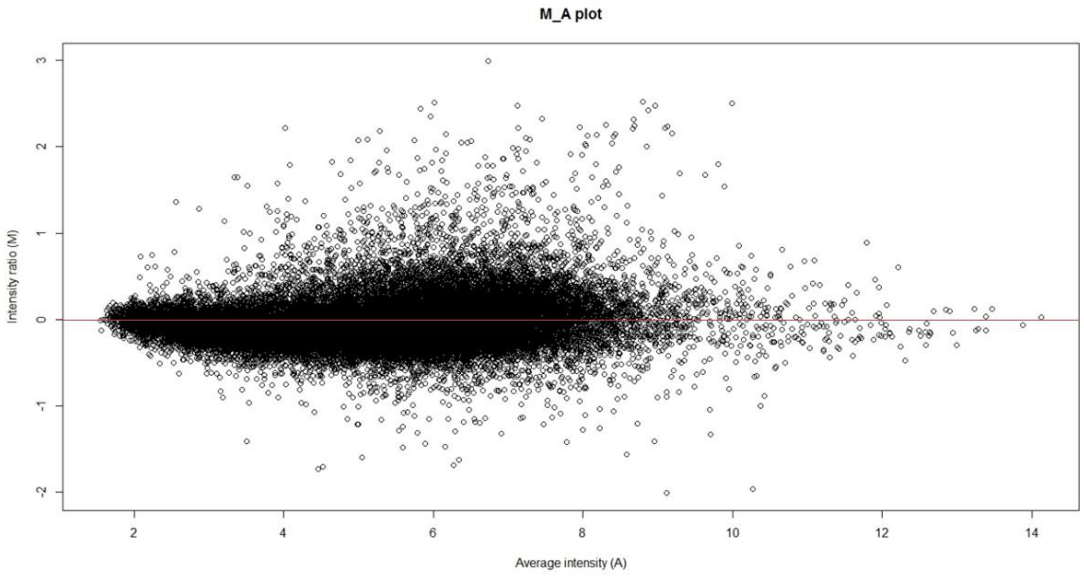

Figure 5.3: **M-A plot representing the normalisation state of microarray data**. Log value of intensity ratio (M) (lesion/control) of each gene is plotted on the Y-axis. The X-axis represents the average log intensity (A) of the gene. The red straight line running on the zero value of M indicates data purity and need no further data normalisation. This analysis was conducted using R version 3.4.0 and Bioconductor packages.

5.2.3 Basic analysis of gene expression data obtained from microarray experiments

Normalised raw data obtained from the microarray experiments were used for some basic analysis- like distribution of data, the range of fold change in differentially expressed genes *etc*. Data were analysed to understand the distribution of expression intensities of the genes and to find out any abnormally high or low expression of any gene. To visualise the distribution of gene expression intensities, an intensity scatter plot was drawn using the normalised mean (average expression intensity value) data (Figure 5.4) (Quackenbush, 2001; Yue *et al,* 2001). This plot is one of the simple most analytical tools

for microarray data visualisation. In this plot, expression values of genes in two conditions (control and CHI) are represented by each data point. Most of the genes were observed to express close to equal in both conditions and hence, were located close to the identity line (diagonal). Genes with higher expression values in either condition were found to be spotted further away from the line. No abnormal higher expression of any gene was found in the distribution plot of mean values.

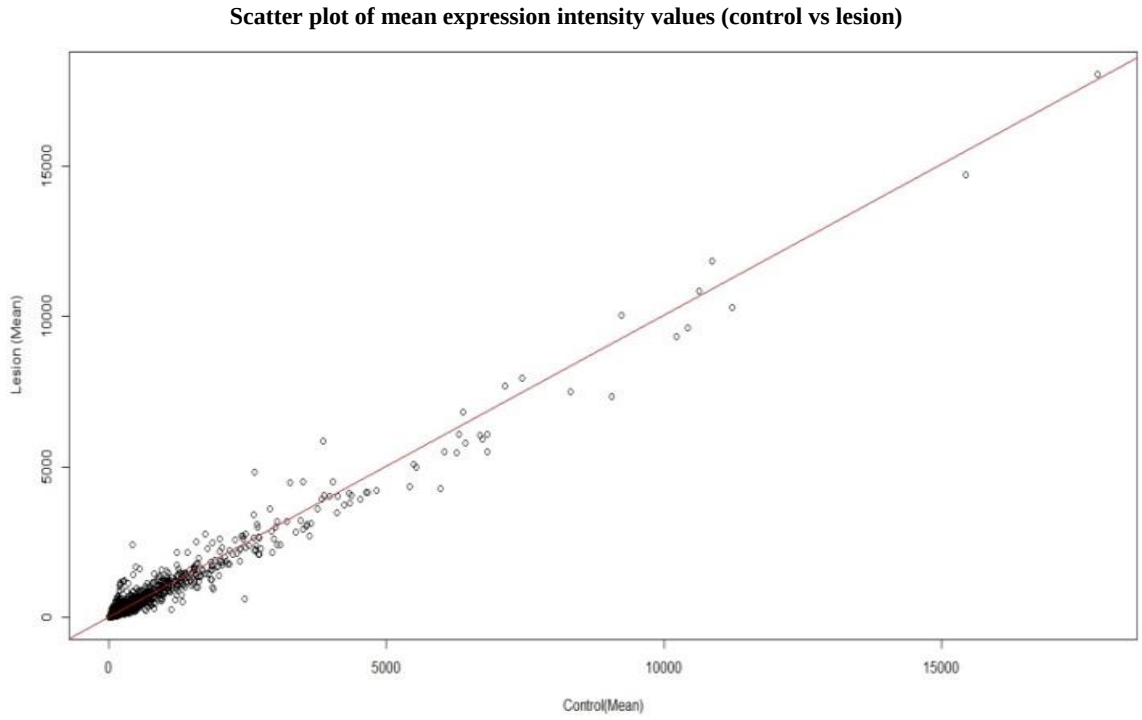

Figure 5.4: **Intensity scatter plot showing the relative distribution of gene expression intensities of individual genes in control and disease conditions**. The plot was drawn using the average gene expression intensity values of control tissues on X-axis and that of lesion tissues on Y-axis. The unit of intensities is arbitrary. The red diagonal line corresponds to identity or reference line where the values of both axes are equal. This plot was constructed using R version 3.4.0 and Bioconductor packages.

It is mentioned in section 2.11 that the microarray experiments were conducted using GeneChip Human Transcriptome Array 2.0. A total of 33720 genes that includes coding as well as non-coding genes such as small nucleolar RNAs (snoRNA), long non-coding RNAs (lncRNA) and microRNAs (miRNA) were analysed successfully for their expression. Among these 33720 genes, only 391 genes (1.16 %) were observed to be

expressed differentially at a significant level in tissues with lesions when the data were analysed with statistical program, R. For this analysis, only genes with at least 2 fold expression changes and false discovery rate (FDR) adjusted p-value (or q-value) with at most 0.05 were considered significant. 247 genes were observed to be over-expressed in the range of 2-3 folds followed by 54 and 45 genes in the range of 3-4 folds (over-expression) and 2-3 folds (down-expression), respectively (Figure 5.5). Very few genes were found to be expressed in the range of 4-8 folds (over-expression) and 3-5 folds (down-expression).

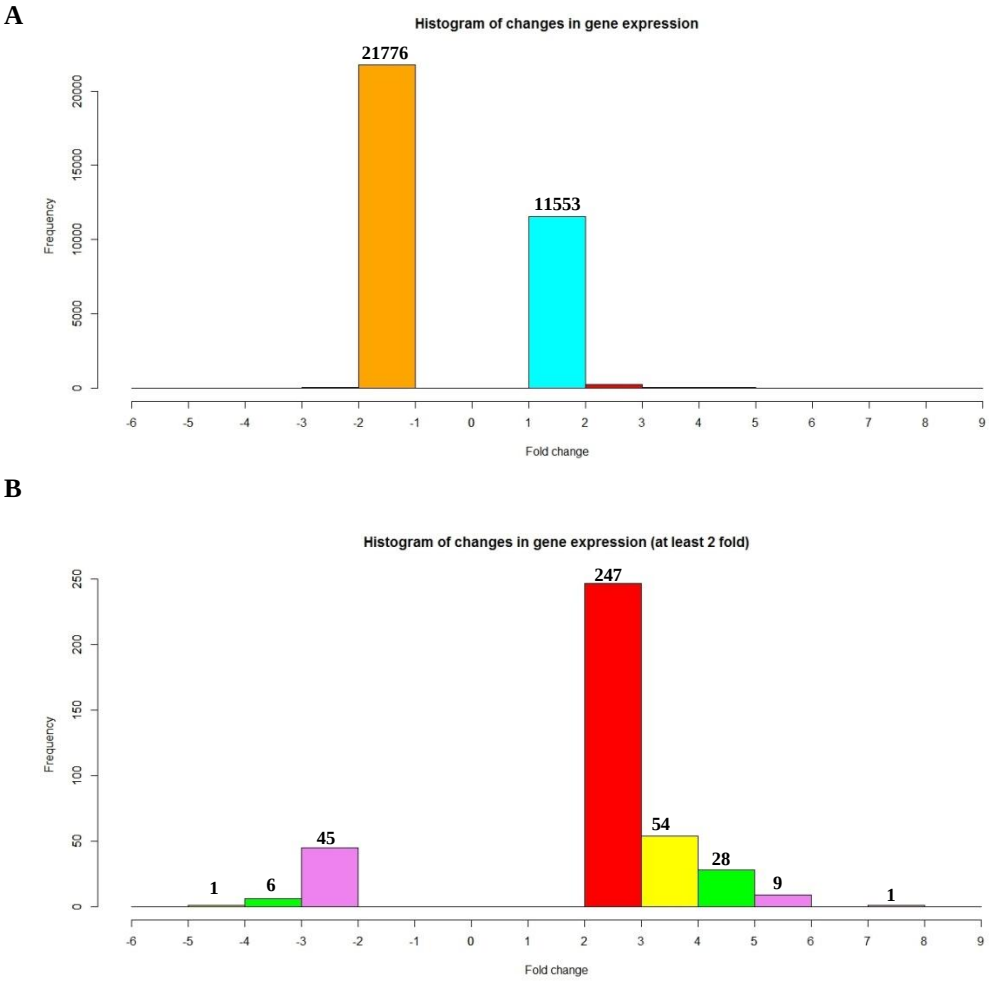

Figure 5.5: **Histogram plots showing the frequency of genes showing differential gene expression in microarray analysis**. A) A general histogram showing frequency distribution of genes covering all range of fold changes including non-significant ones. B) Histogram showing frequency distribution of genes with at least 2-fold changes of gene expression. The number on the top of each bar of the histogram denotes the number of genes showing expression changes in that particular fold range.

As it was mentioned previously in section 5.2.1, for control and disease condition, five and six tissue samples, respectively, were used in this microarray analysis. However, both healthy and lesion region tissues were possible to collect from only three patient samples- Nes163, Nes167 and Nes168, and hence, were used in the analysis for both conditions. All the downstream analyses were designed primarily based on the mean values of all five controls and six disease conditions data. However, some separate analyses were also performed for the data generated from the above mentioned three samples (from here on termed as 'complete samples') along with the mean data (of all experimental samples). It was expected that the data analyses from the complete samples could illustrate the variability of gene expression pattern in the individual patient since tissues of both conditions were provided by these patient samples. With this aim in mind, the pattern of gene expression was analysed for these three complete samples and compared with the mean data of all experimental samples (Figure 5.6).

It was observed that the pattern of gene expressions across these three patient data and mean data were quite similar while considering all the data values (both significant and non-significant expression changes) (Figure 5.6). Inter-quartile range (IQR) (mid 50% quartile) and median values were similar for all the samples, although variable numbers of outliers were observed in each sample (Figure 5.6 A). However, with the expression data with significant changes (at least 2-fold, q-value ≤ 0.05), variability in IQR and median values was observed among the samples (Figure 5.6 B). From both the IQR and median values in all of these three complete samples data and mean data, it could be inferred that the number of over-expressed genes was quite greater than the number of down-expressed genes in CHI tissues. This finding was also confirmed by the manual counting of over-expressed and down-expressed genes from the raw normalised dataset (Figure 5.6 C). High variability of the number of over-expressed and down-expressed genes in individual patient data and mean data were also observed. Variability of a number of genes was also observed when analysing a number of common genes that were differentially expressed in each different samples (Figure 5.6 D).

So, the basic analysis of these data indicates that the disease in the patients under study was not because of any significant changes in any particular genes; rather it could be the result of the combined effect of the differential changes in multiple genes. The variability

of the differential genes in the complete samples also pointed to the involvement of multiple genes in the progression of the disease.

A

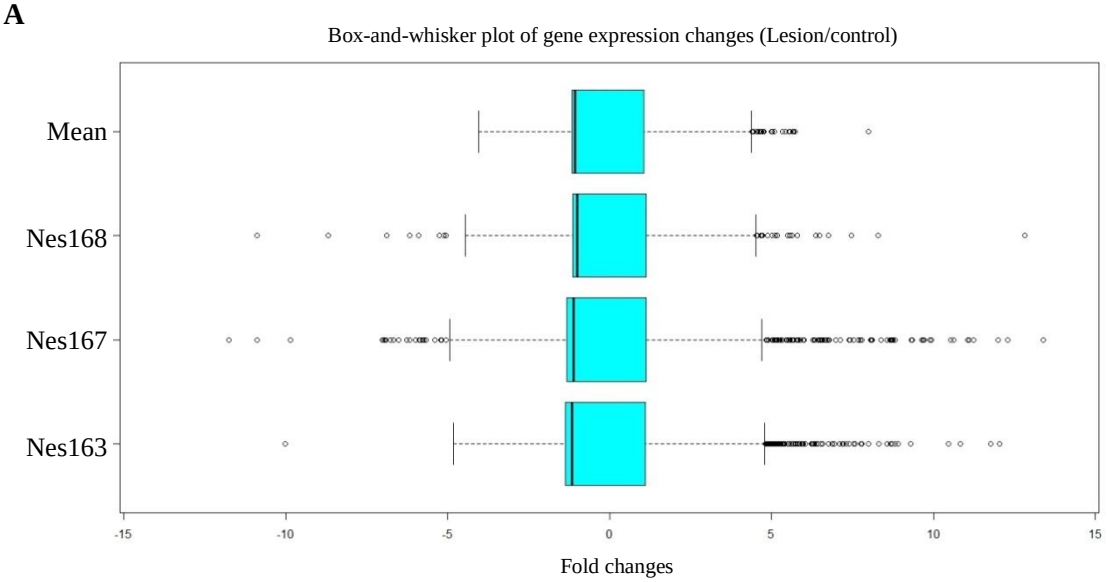

B

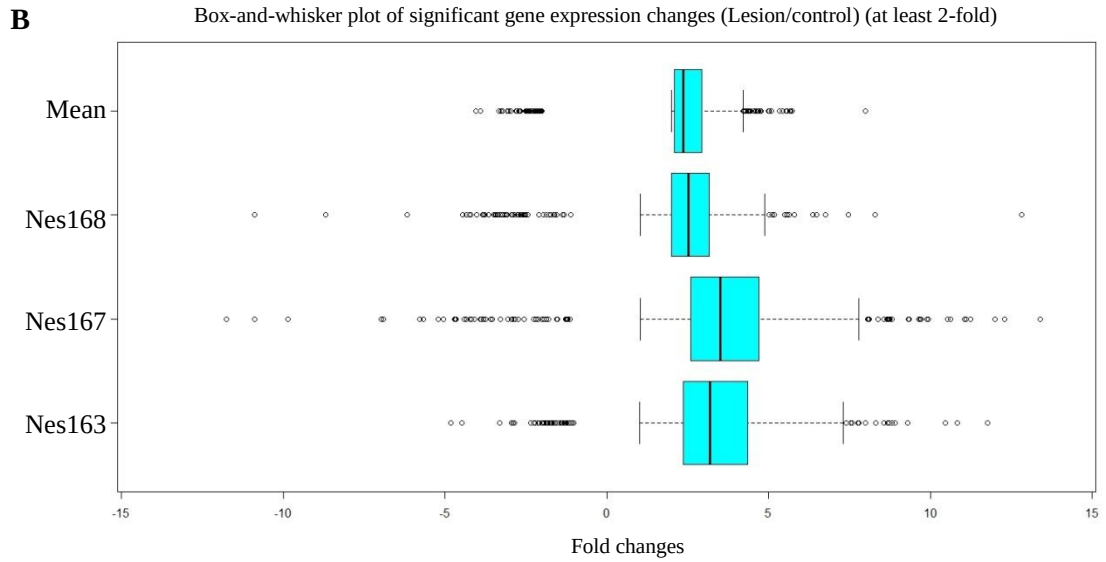

(continued on next page)

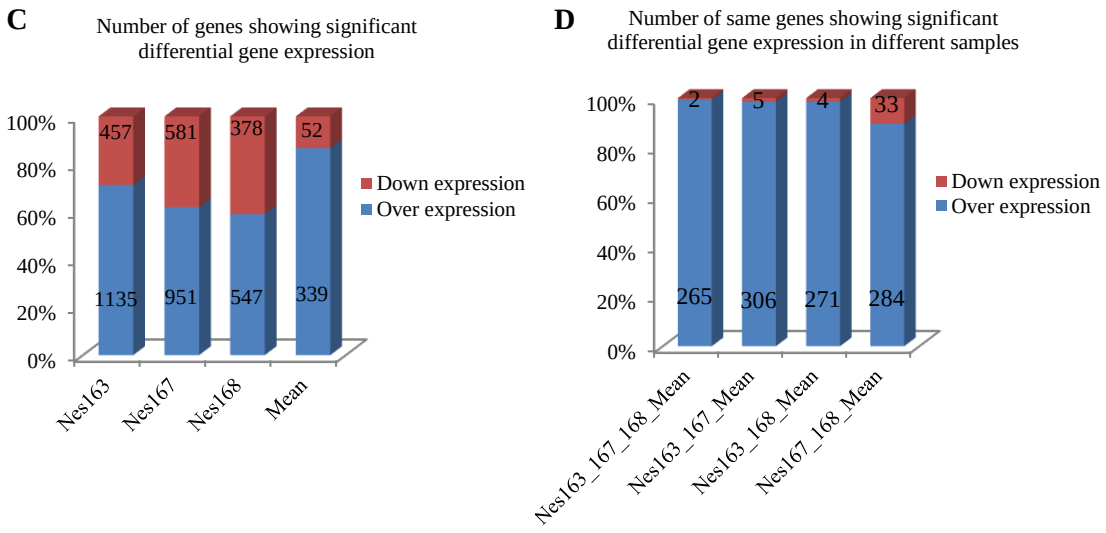

Figure 5.6: **Pattern of gene expressions in three individual complete CHI samples data in comparison with mean CHI data**. Panel A shows the distribution of gene expression changes (fold changes) (both significant and non-significant) in all the experimental genes while panel B represents the distribution of significant changes only. At least 2-fold change in gene expression with q-value ≤ 0.05 was considered significant. The box-and-whisker plots show the overall range of fold changes with upper (75^{th}) and lower quartiles (25^{th}). The central box represents the IQR and the line inside the box represents the median value. Individual plotted points denote the outliers. Panel C illustrates the percentage of significantly over-expressed and down-expressed genes analysed from each complete sample and the mean data. Panel D shows the number of same common genes that were differentially expressed in different set of samples. The numbers on the bars denote the number of genes in each particular data either over-expressed or down-expressed.

5.2.4 Analysing expression of genes potentially associated with CHI pathobiology

As it was mentioned previously in section 1.3, a number of genes linked with insulin secretion regulation have already been identified as being associated with CHI such as - *ABCC8*, *KCNJ11*, *GCK*, *HADH*, *GLUD1*, *SLC16A1*, *HNF1A*, *HNF4A* and *UCP2*. Data from this microarray experiment was analysed to investigate the changes in the expression of these genes in order to find out the possible association of these genes with the disease in the patients under study. The expression of genes in three "complete samples" (Nes163, Nes167 and Nes168) were found similar as was observed in mean data of all samples (Figure 5.7 A). Significant gene over-expression in disease tissues were observed only for *ABCC8* and *HADH* (hydroxyacyl-CoA dehydrogenase) while the

expression of other genes was found to be unchanged. In addition to the above mentioned CHI genes, expression of some genes for hormones and receptors associated with blood glucose regulation were also analysed (Figure 5.7 B). The overall expression of pancreatic hormones like insulin (*INS*), somatostatin (*SST*) and glucagon (*GCG*) was found unchanged in disease conditions. In addition, higher expression was observed for genes of two hormone receptors- *SSTR2* (somatostatin receptor 2) and *GLP1R* (glucagon-like-protein 1 receptor) while expression of other somatostatin receptors (*SSTR1*, *SSTR3* to *5*) was unchanged.

A number of transcription factors (TFs) were reported in previous studies (Pan and Wright, 2011; Shih *et al*, 2013) to play role in different stages of pancreas organogenesis and mature beta-cell generation. With a hypothesis that some of these TFs might be potentially associated with CHI pathobiology, gene expression of TFs was analysed from the experimental microarray data. The expression patterns of TFs in the three "complete samples" were similar to the mean data (Figure 5.8). Significantly (at least 2-fold, q-value ≤ 0.05) higher expression was observed in all disease conditions for the TFs – *NKX6.1* (NK6 homeobox 1), *NEUROD1* (neuronal differentiation 1), *RFX6* (regulatory factor X6), *PAX6* (paired box 6), *ISL1* (ISL LIM homeobox 1) and *INSM1* (insulinoma-associated 1). All of these TFs are expressed in Endocrine precursors in developmental stages and play a role in the generation of mature pancreatic beta cells (Pan and Wright, 2011).

A number of genes were identified recently using whole-genome SNP genotyping and exome sequencing and were believed to play roles in CHI development (Proverbio *et al*, 2013). Expression of these reported genes was investigated here from the experimental data (Figure 5.9 A). Although variability in expression of genes was observed in individual samples, expression of only *CACNA1A* (calcium voltage-gated channel subunit alpha1 A) gene was found significantly higher in all disease conditions. *CACNA1A* gene has already been reported for its potential roles in the regulation of insulin secretion (Chandra *et al*, 2014).

Irregular and uncontrolled insulin secretion is the major feature of CHI, so expression changes of genes associated with insulin secretion regulation were examined from the experimental microarray data. Genes that play roles in insulin secretion were listed from KEGG (Kyoto Encyclopedia of Genes and Genomes), (Kanehisa and Goto, 2000;

Kanehisa *et al*, 2016). KEGG is a widely used collection of databases that present information of genomes, biological pathways, diseases, drugs, and chemical substances. This database is a kind of reference knowledge base for understanding genomic information towards their higher order functional information (Kanehisa and Goto, 2000). The list of genes associated with insulin secretion is accessible at http://www.genome.jp /dbget-bin/www_bget?pathway:map04911. Amongst the 67 reported genes, the expressions of 10 were significantly higher in the diseased tissue. Figure 5.9 B shows the expression of only those 10 over-expressing genes.

In summary, apart from known CHI genes, a number of genes were identified in the present study from the basic analysis of experimental microarray data which were differentially expressed in CHI tissues and hence, could be potentially associated with CHI pathobiology. The genes were found to be associated with various biological processes involving glucose homeostasis, pancreatic cell differentiation, regulation of exocytosis etc. The genes are listed in Table 5.2, their differential expression is illustrated in Figure 5.10 and their roles in various biological functions are illustrated in Table 5.3.

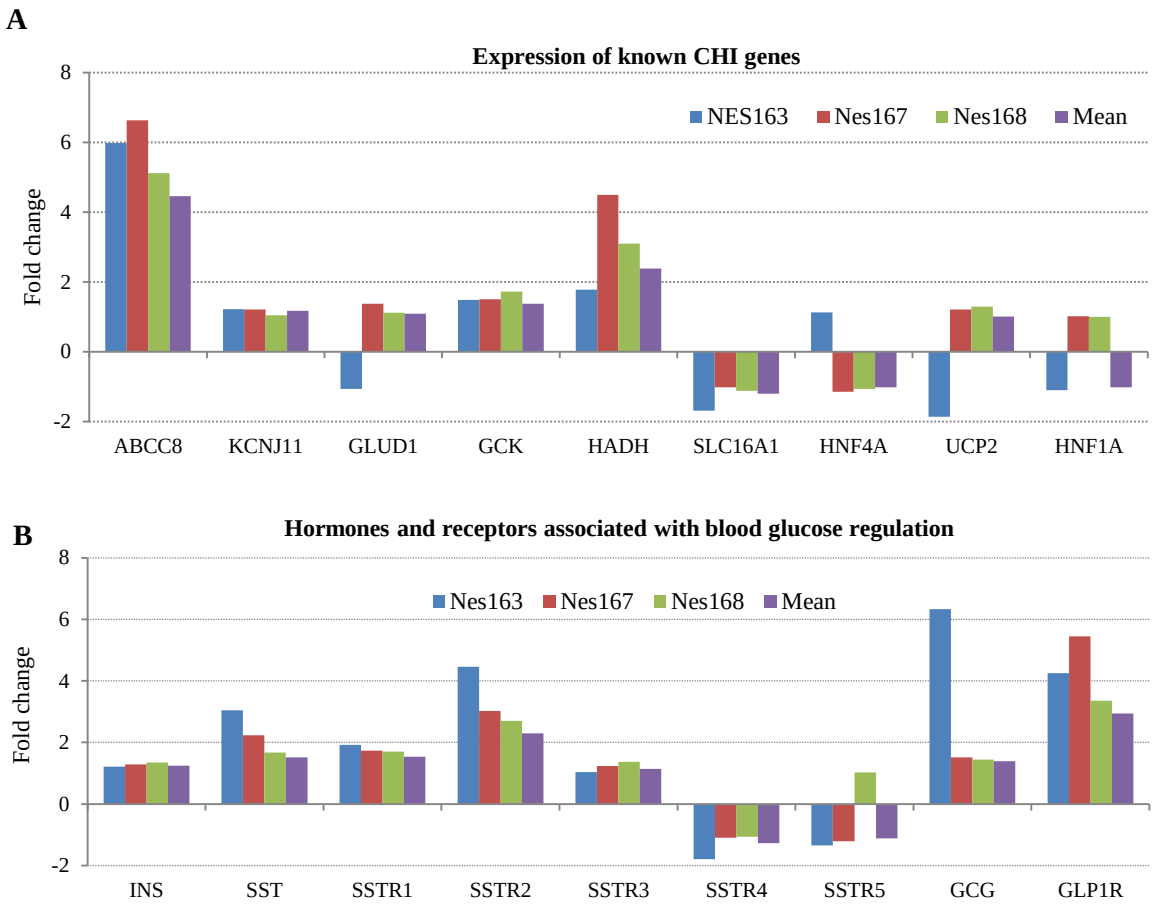

Figure 5.7: **Differential expression in CHI tissues of known CHI genes and genes for hormones and receptors associated with blood glucose regulation.** Panel A shows the expression pattern of previously reported known CHI genes. Panel B denotes the expression of genes encoding hormones and the receptors participating in blood glucose regulation. Nes163, Nes167 and Nes168 represent three complete patient samples from which healthy and lesion tissues were obtained, analysed and compared for differential gene expression. Mean represent average values of all five controls and six disease conditions differential gene expression data.

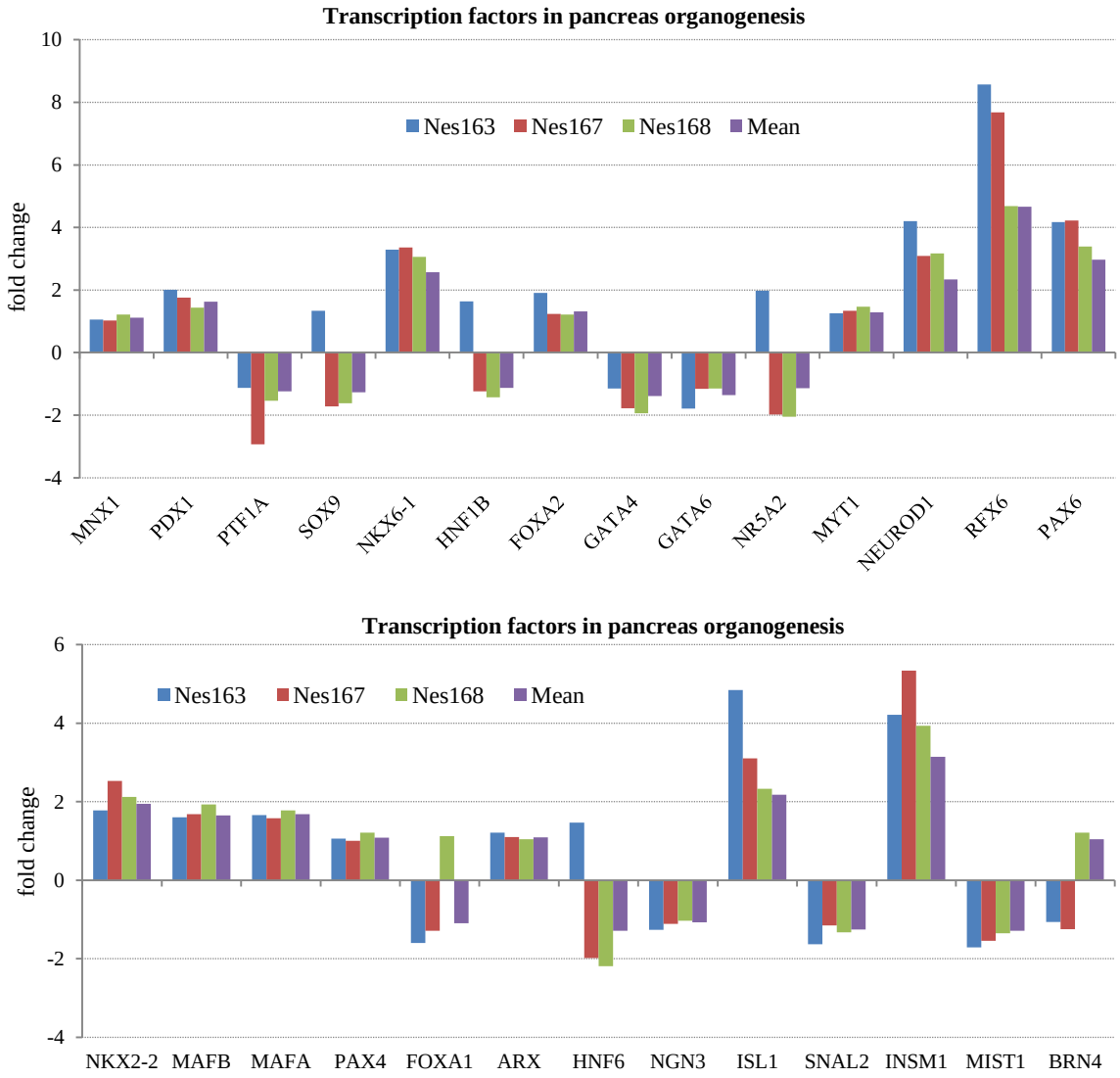

Figure 5.8: **Differential expression in CHI tissues of genes associated with pancreas organogenesis and mature beta-cell generation.** Nes163, Nes167 and Nes168 represent three complete patient samples from which healthy and lesion tissues were obtained, analysed and compared for differential gene expression. Mean represent average values of all five controls and six disease conditions differential gene expression data.

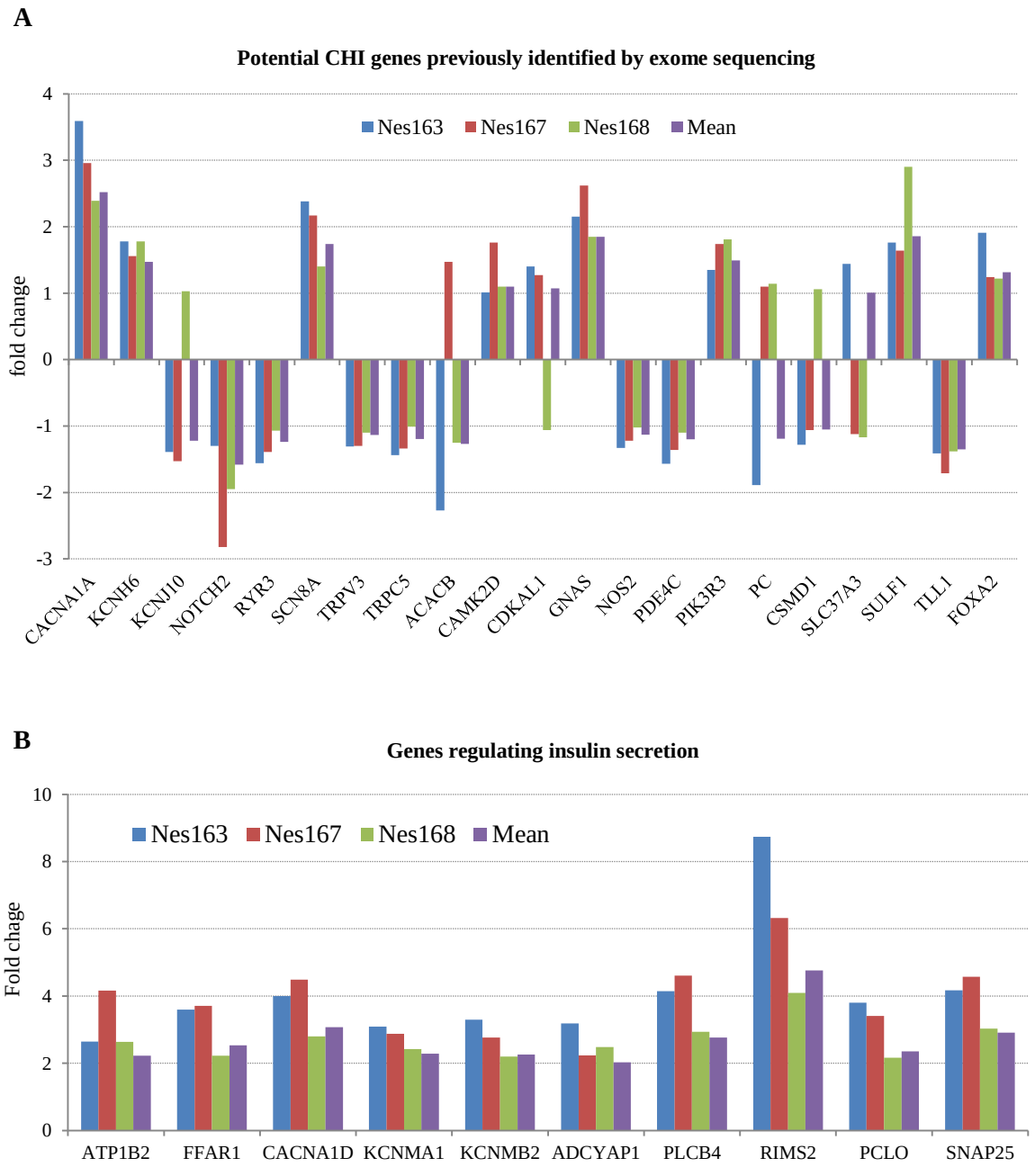

Figure 5.9: **Differential expression in CHI tissues of genes previously predicted potentially associated with CHI and genes regulating insulin secretion**. Panel A shows the differential expression of potential CHI associated genes identified by exome sequencing (Proverbio *et al*, 2013). Panel B shows the expression of genes regulating insulin secretion in beta cells (KEGG database). Nes163, Nes167 and Nes168 represent three complete patient samples from which healthy and lesion tissues were obtained, analysed and compared for differential gene expression. Mean represent average values of all five controls and six disease conditions differential gene expression data.

Table 5.2: **List of potential CHI associated genes identified from the basic analysis of experimental microarray data**

Gene ID	Gene name
SSTR2	Somatostatin receptor 2
GLP1R	Glucagon-like-protein 1 receptor
NKX6.1	NK6 homeobox 1
NEUROD1	Neuronal differentiation 1
RFX6	Regulatory factor X6
PAX6	Paired box 6
ISL1	ISL LIM homeobox 1
INSM1	Insulinoma-associated 1
CACNA1A	Calcium voltage-gated channel subunit alpha1 A
ATP1B2	ATPase Na^+/K^+ transporting subunit beta 2
FFAR1	Free fatty acid receptor 1
CACNA1D	Calcium voltage-gated channel subunit alpha1 D
KCNMA1	Potassium calcium-activated channel subfamily M alpha 1
KCNMB2	Potassium calcium-activated channel subfamily M regulatory beta subunit 2
ADCYAP1	Adenylate cyclase activating polypeptide 1
PLCB4	Phospholipase C beta 4
RIMS2	Regulating synaptic membrane exocytosis 2
PCLO	Piccolo presynaptic cytomatrix protein
SNAP25	Synaptosome associated protein 25

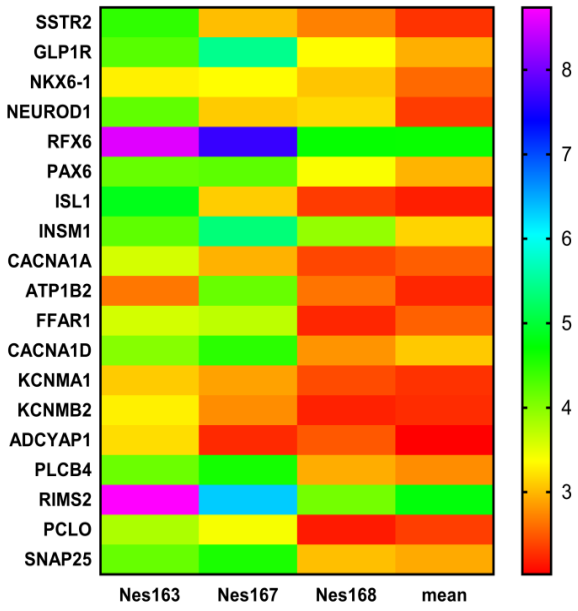

Figure 5.10: **Differential gene expression pattern of identified potential CHI associated genes**. Here differential gene expression values are represented as a colour-coded heat map. Lanes labelled as "Nes163", "Nes167" and "Nes168" represent three complete patient samples. Lane labelled as "Mean" represent average values of all controls and disease conditions gene expression data. Range of colours (from red to violet) in the scale bar indicates range of fold change in gene expression in the disease condition.

Table 5.3: **List of biological processes in which identified potential CHI associated genes participate**

Biological process	Gene count	% of total genes	p-Value
Insulin secretion	11	61.11	3.45E-16
Regulation of insulin secretion	6	33.33	5.18E-09
cAMP-mediated signaling	4	22.22	7.11E-06
Type B pancreatic cell differentiation	3	16.67	3.46E-05
Glucose homeostasis	4	22.22	1.35E-04
Cellular response to glucocorticoid stimulus	3	16.67	1.81E-04
Endocrine pancreas development	3	16.67	3.09E-04
Pituitary gland development	3	16.67	3.59E-04
Potassium ion transport	3	16.67	0.003055
Pancreatic A cell differentiation	2	11.11	0.004044
Positive regulation of cytosolic calcium ion concentration	3	16.67	0.007948
Cellular potassium ion homeostasis	2	11.11	0.012085
Transcription from RNA polymerase II promoter	4	22.22	0.014008
Positive regulation of transcription from RNA polymerase II promoter	5	27.78	0.014948
Spinal cord motor neuron differentiation	2	11.11	0.01708
Signal transduction involved in regulation of gene expression	2	11.11	0.019071
Synaptic vesicle exocytosis	2	11.11	0.022051
Chemical synaptic transmission	3	16.67	0.024023
Positive regulation of calcium ion transport	2	11.11	0.026011
Regulation of exocytosis	2	11.11	0.026011
Response to starvation	2	11.11	0.034865
Positive regulation of cell differentiation	2	11.11	0.036822
Cerebellum development	2	11.11	0.036822
Calcium ion-regulated exocytosis of neurotransmitter	2	11.11	0.038776
Activation of adenylate cyclase activity	2	11.11	0.039751
Positive regulation of insulin secretion	2	11.11	0.040726

~This list of the biological process was generated using DAVID v6.8 (Dennis *et al*, 2003; Huang *et al*, 2009a; Huang *et al*, 2009b). This is a knowledge base that provides functional annotation of lists of genes derived from genomic studies to understand biological meaning comprehensively. Here in this Table the term "Gene count" represents the number of genes from the query genes that were predicted to be associated with the individual biological process. The titles of the biological processes listed here were provided by the software program.

5.2.5 Exploring biological processes related to differentially expressed genes

It was mentioned in section 5.1.3 that class comparison is one of the tools to analyse gene expression data to identify prospective candidate genes and biological processes or pathways potentially associated with a biological condition. To identify CHI associated potential candidate genes and pathways, this class comparison approach was used to analyse the data from the present study (details in section 5.1.3). This section and all the next sections in this chapter present the analyses based on this class comparison approach to identify potential CHI genes and related pathways. As there is no software program available which can analyse a set of data accurately to identify potential disease-related genes and related pathways, multiple software programs like DAVID, PANTHER and IPA (described in section 5.1.4) were used for analysis using this class comparison approach.

Raw mean data obtained from the microarray experiments were used to analyse genome-wide gene expression in terms of significant fold changes (at least two-fold, q-value $\leq$ 0.05) on comparing the results between the control and disease conditions studied. Among 33720 genes that were studied, only a small proportion of genes (391 genes) were observed to meet the cutoff criteria and be expressed significantly in disease conditions. Figure 5.11 shows a volcano plot which combines the statistical significance (q-value) with the magnitude of the gene expression change (fold change). This combination of measurement provides a visual illustration of genes that met the cutoff criteria and displayed genes with large degree changes (Cui and Churchill, 2003; Li, 2012). This illustration shows that very few genes were differentially expressed in CHI tissues and no abnormally high or low expression was observed for any genes.

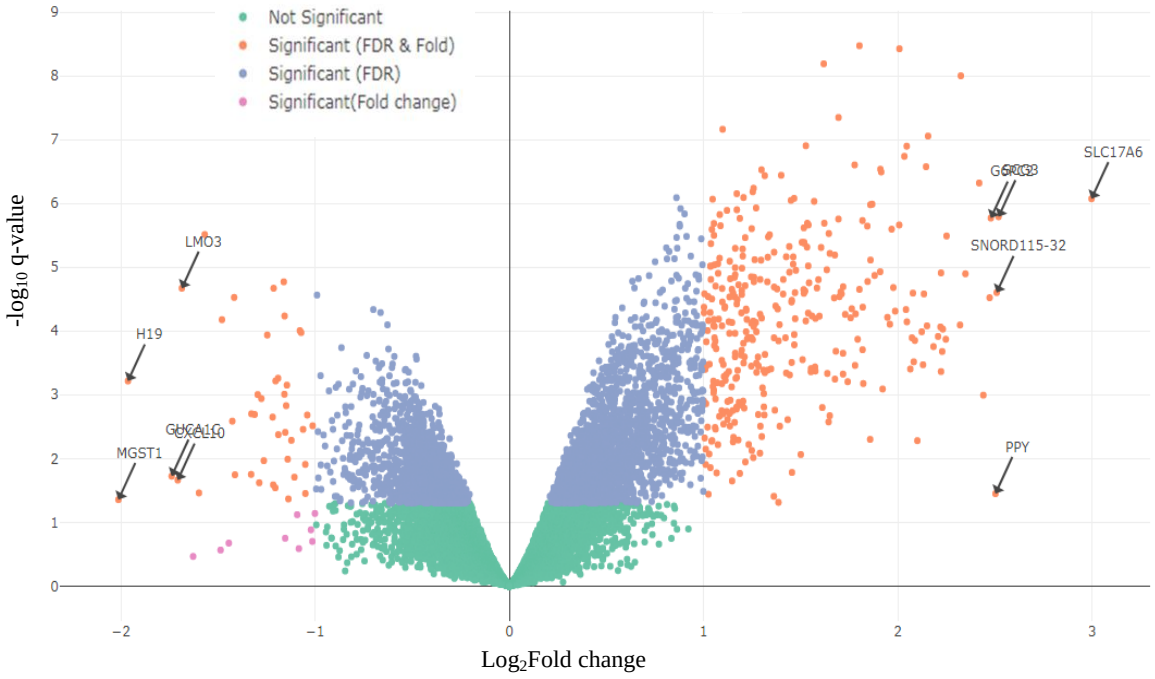

Figure 5.11: **Volcano plot to visualise statistically significant changes in gene expression**. The plot illustrates significance versus fold-change on y- and x- axes, respectively. The parameters of visualisation are- not significant (fold change < |2|, q-value > 0.05), significant FDR (fold change < |2|, q-value ≤ 0.05), significant Fold change (fold change ≥ |2|, q-value > 0.05), significant FDR and Fold (fold change ≥ |2|, q-value ≤ 0.05). Top five (in terms of fold change) over-expressed and down-expressed genes are indicated by the pointed arrows. This plot was constructed using statistical program R, version 3.4.0 and Bioconductor packages.

Total 132 biological functions were identified by the DAVID knowledgebase where the genes, which show significant expression changes in CHI condition, participate in the human body. Among them, the top 40 statistically significant biological processes are mentioned in Table 5.4. The Table shows diverse categories of biological processes including insulin secretion regulation, glucose homeostasis, beta cell differentiation regulation, ion transport, exocytosis, *etc*. and all of these processes are linked to the phenotypes typically displayed by CHI patients (Dunne *et al*, 2004; James *et al*, 2009; Arya *et al*, 2014; Yorifuji, 2014). The DAVID knowledgebase also predicts some other biological pathways like inflammation, nervous system development and signal transduction which can be associated with CHI.

Table 5.4: **List of statistically significant biological processes identified by DAVID knowledgebase altered in CHI conditions**

Biological process	Gene count	% of total genes	p-Value
Regulation of insulin secretion	12	3.23	1.54E-08
Calcium ion-regulated exocytosis of neurotransmitter	8	2.16	3.64E-06
Regulation of calcium ion-dependent exocytosis	7	1.89	2.43E-05
Inflammatory response	20	5.39	2.70E-05
Insulin secretion	6	1.62	1.61E-04
Glucose homeostasis	9	2.42	3.22E-04
Type B pancreatic cell differentiation	4	1.08	3.77E-04
Potassium ion transport	8	2.16	4.84E-04
Regulation of exocytosis	5	1.35	9.05E-04
Chemical synaptic transmission	12	3.23	0.002731
Calcium ion import	4	1.08	0.002758
Ion transmembrane transport	11	2.96	0.003205
Vesicle fusion	6	1.62	0.003222
Positive regulation of insulin secretion	5	1.35	0.005022
Cellular calcium ion homeostasis	7	1.89	0.005038
Pancreas development	4	1.07	0.005131
Positive regulation of endothelial cell proliferation	6	1.62	0.006309
Chemokine-mediated signaling pathway	6	1.62	0.007113
Nervous system development	12	3.23	0.010137
Neurotransmitter secretion	5	1.35	0.010864
Cell-cell signaling	11	2.96	0.011719
Exocytosis	6	1.62	0.013473
Anion transmembrane transport	4	1.08	0.014002
Central nervous system development	7	1.89	0.016579
Positive regulation of cAMP-mediated signaling	3	0.81	0.016934
Adenylate cyclase-modulating G-protein coupled receptor signalling pathway	4	1.08	0.024577
cAMP-mediated signaling	4	1.08	0.026357
Response to insulin	5	1.35	0.027037
Regulation of G-protein coupled receptor protein signalling pathway	4	1.08	0.028204
Response to glucose	5	1.35	0.028356
Positive regulation of calcium ion-dependent exocytosis	3	0.81	0.02945

Biological process	Gene count	% of total genes	p-Value
Positive regulation of GTPase activity	17	4.58	0.032371
Positive regulation of inflammatory response	5	1.35	0.03552
Signal transduction	29	7.82	0.038891
Signal transduction involved in regulation of gene expression	3	0.81	0.040596
Regulation of ion transmembrane transport	6	1.62	0.040794
Positive regulation of tumour necrosis factor production	4	1.08	0.045371
Sodium ion transport	5	1.35	0.048967
Positive regulation of high voltage-gated calcium channel activity	2	0.54	0.050061
Insulin processing	2	0.54	0.050061

~This list of the biological processes was generated using DAVID v6.8. Here in this Table the term "Gene count" represents the number of genes from the query genes that were predicted to be associated with the individual biological process. The titles of the biological processes listed here were provided by the software program.

5.2.6 Gene functional classification by Gene Ontology (GO)

Table 5.4 lists broadly-classified biological processes identified in this study to be associated with CHI potentially. To narrow down the broad processes and to investigate the biological activities potentially affected due to the gene mutations in CHI patients, gene functional analyses were conducted using The PANTHER Classification System version 10.0. This classification system performs Gene Ontology (GO) term enrichment analyses at three levels of functional annotations- molecular functions, cellular components and biological process to define the biological activities. These three hierarchical levels of annotations provide some information to understand where in the cells and what types of biological functions are altered in a given condition.

5.2.6.1 Molecular functions altered in CHI conditions

The PANTHER classification system was utilised to cluster the differentially expressed genes obtained from the experimental microarray datasets according to the molecular

functions (in broad range) they perform. The broad molecular functions that resulted from the analyses and were predicted to be associated with the differentially expressed genes were- binding, catalytic activity, channel regulator activity, receptor activity, signal transducer activity, structural molecule activity, translation regulatory activity, and transporter activity (Figure 5.12). In CHI conditions, the top four molecular functions where larger number of differentially expressed genes were predicted to be associated were - catalytic activity, with 84 over-expressed and 15 down-expressed genes, binding, with 79 over-expressed and 18 down-expressed genes, transporter activity, with 33 over-expressed and only 1 down-expressed gene, and receptor activity, with 16 over-expressed and only 2 down-expressed genes. Signal transducer activity was predicted to show 100% up-regulation with 9 over-expressed genes and no down-expressed gene in the category.

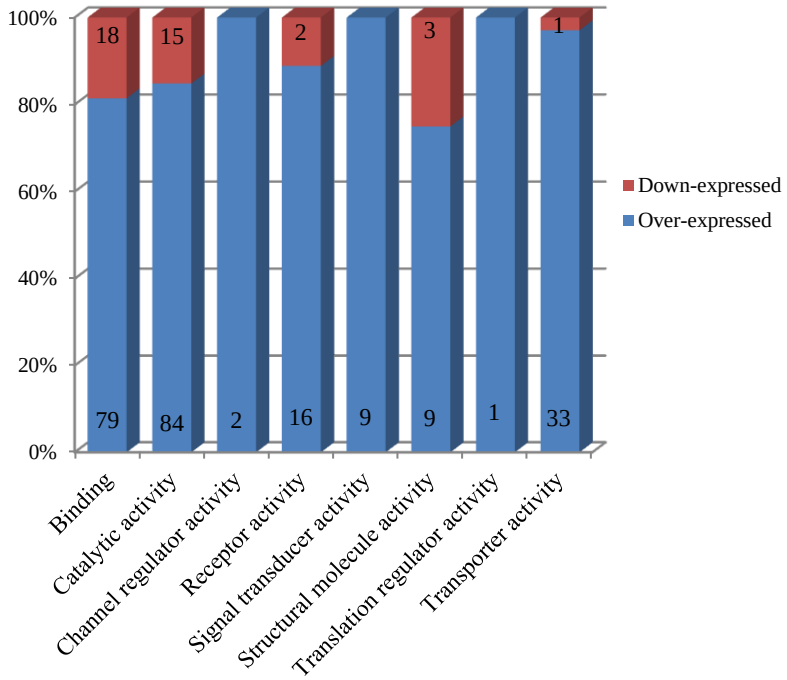

Figure 5.12: **Classification of the differentially expressed genes based on the molecular functions**. Eight broad molecular functions were predicted by the PANTHER system to be associated with the differentially expressed genes in CHI conditions. In each category of function, the percentage of over-expressed genes is represented by the blue area whereas the percentage of down-expressed genes is represented by the red area. The numbers mentioned in the blue and red area in each bar represent the number of over-expressed and down-expressed genes, respectively, in each category.

5.2.6.2 Biological processes altered in CHI conditions

As part of the gene ontology term enrichment analyses, the PANTHER classification system was used to identify biological processes potentially altered in CHI condition. The differentially expressed genes were clustered according to the biological processes they are associated with. Both the over-expressed and down-expressed genes were found to participate in the same twelve broad categories of biological processes (Figure 5.13). The number of over-expressed genes in each process was observed to be much higher than down-expressed genes, except two processes- immune system process and locomotion, where the number of down-expressed genes was found higher. In CHI conditions, the top four biological processes identified by PANTHER where a larger number of differentially expressed genes were observed to be associated were – cellular process, with 141 over-expressed and 25 down-expressed genes, metabolic process, with 91 over-expressed and 12 down-expressed genes, biological regulation, with 57 over-expressed and 12 down-expressed genes, and "response to stimulus", with 44 over-expressed and 16 down-expressed genes.

Among the twelve categories of biological processes, the highest numbers of both over-expressed (141) and down-expressed (25) genes were observed to be associated with one category, cellular process. The PANTHER system was used to further explore this biological process to identify the sub-biological processes within this category. It was found that the category, cellular process was sub-divided into six sub-processes (Figure 5.14). Among them, three sub-processes were found to have a higher number of over-expressed genes and they are - cell communication, with 53 over-expressed and 13 down-expressed genes, cell cycle, with 14 over-expressed and 2 down-expressed genes, and cellular component movement, with 6 over-expressed and 5 down-expressed genes. One sub-process, cell proliferation was found to be associated with 1 over-expressed and 3 down-expressed genes. Two sub-processes were found to be associated with only over-expressed genes and they are- cell recognition, with 1 over-expressed gene and cytokinesis with 4 over-expressed genes.

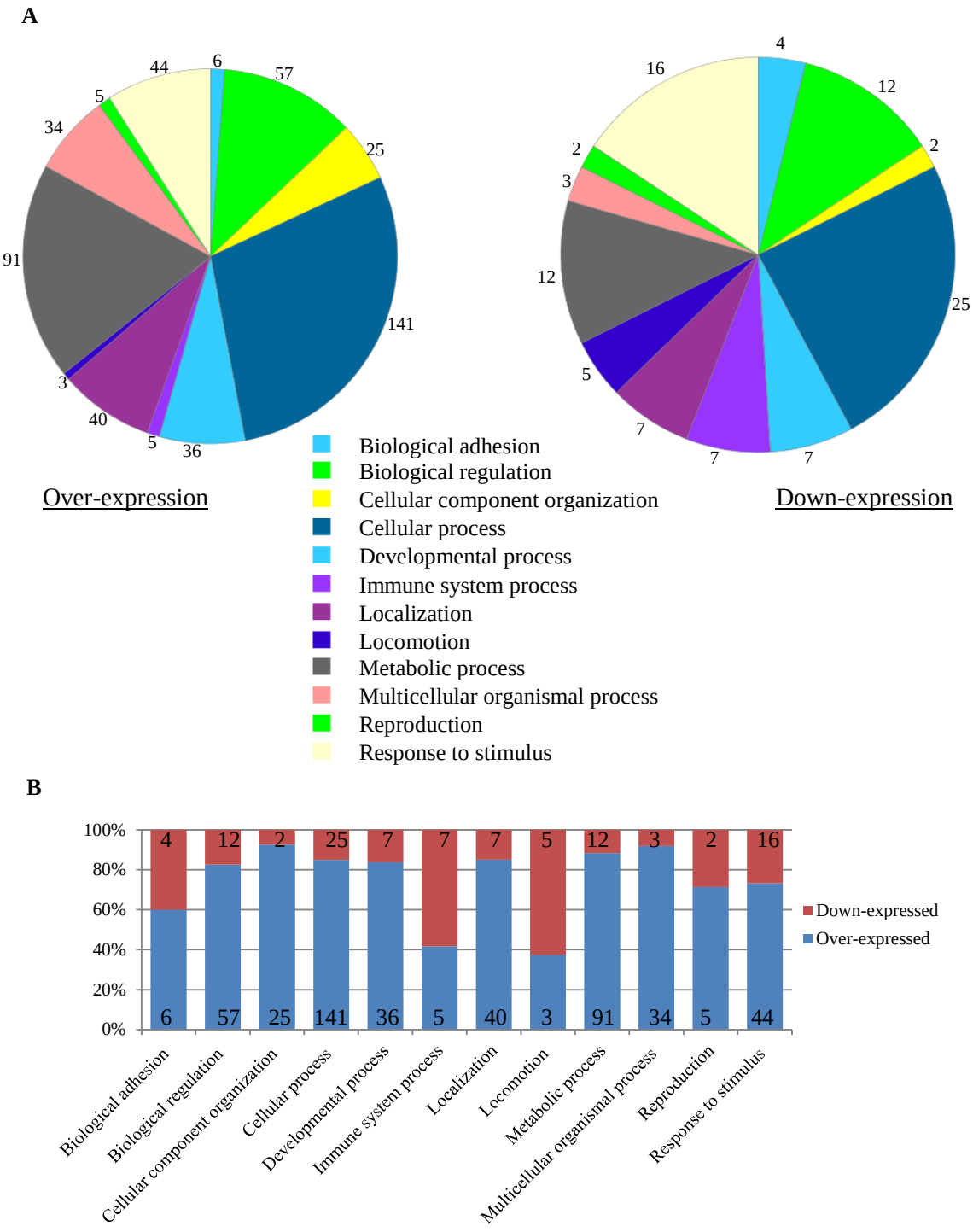

Figure 5.13: **Classification of the differentially expressed genes based on the biological process**. Twelve broad biological processes predicted by the PANTHER system to be associated with the differentially expressed genes in CHI conditions. Panel A shows the pie charts illustrating the predicted biological processes where over-expressed and down-expressed genes participate. The number adjacent to each pie section denotes the number of genes (over-expressed or down-expressed) associated with each biological process. Panel B represents a simplistic visualisation of the percentage of over-expressed or down-expressed

genes in each category of biological process. Percentage of over-expressed genes is represented by the blue area whereas the percentage of down-expressed genes is represented by the red area in each bar. The numbers mentioned in the blue and red area in each bar represent the number of over-expressed and down-expressed genes, respectively, in each category.

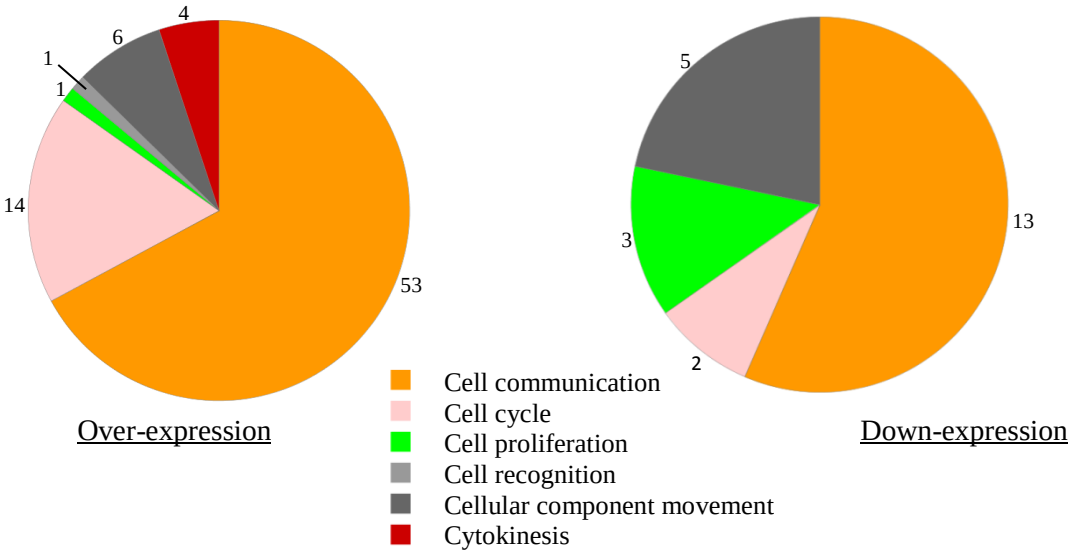

Figure 5.14: **Breakdown of the major biological process category, cellular process, into sub-biological processes**. Six broad sub-biological processes were predicted by the PANTHER system to be clustered under the category, cellular process. The number adjacent to each pie section denotes the number of genes (over-expressed or down-expressed) associated with each sub-biological process.

5.2.6.3 Cellular components altered in CHI conditions

Cellular component is the third domain of gene ontology annotation system which describes the location of the cells or its extracellular environment where a gene product functions. Cellular components of differentially expressed genes in CHI conditions were identified using the PANTHER classification system and were illustrated as clusters according to the sub-cellular locations where they perform their roles. A total of eight sub-cellular locations were identified to be associated with the differentially expressed genes (Figure 5.15). Among them, four sub-cellular locations were found to be associated with a higher number of over-expressed genes and they are - cell part, with 89 over-expressed and 7 down-expressed genes, extracellular region, with 10 over-expressed and

7 down-expressed genes, membrane, with 30 over-expressed genes and 1 down-expressed gene, and organelle, with 41 over-expressed genes and 1 down-expressed gene. One sub-cellular location, extracellular matrix, was found to be associated with an equal number (1) of the over-expressed and down-expressed gene. Three sub-cellular locations were found to be associated with only over-expressed genes and they are- cell junction, with 2 over-expressed genes, macromolecular complex, with 15 over-expressed genes, and synapse with 4 over-expressed genes.

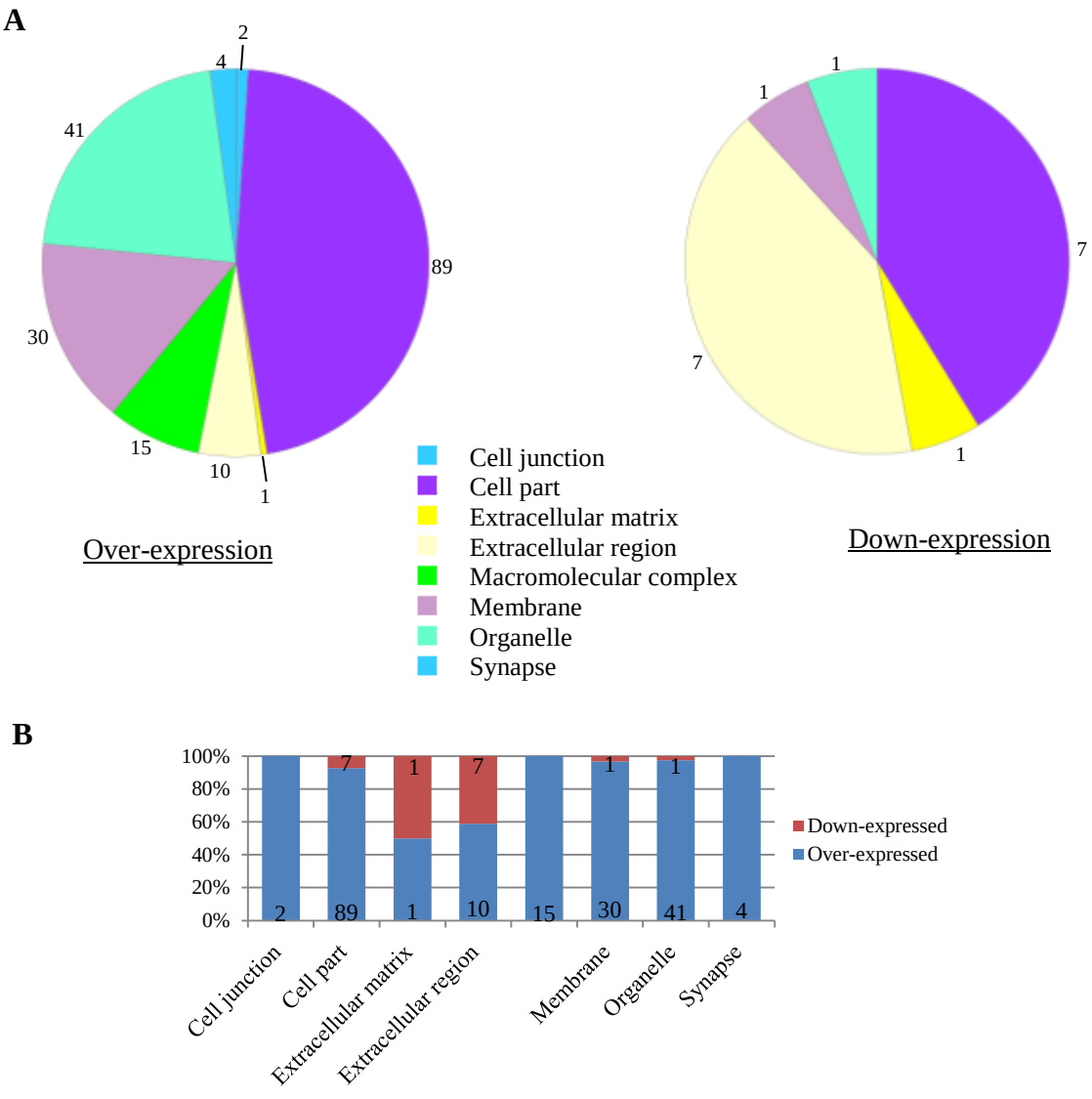

Figure 5.15: **Classification of the differentially expressed genes based on the cellular components associated with them**. Eight broad sub-cellular locations were predicted by the PANTHER system to be associated with the differentially expressed genes in CHI conditions. Panel A shows the pie charts illustrating the predicted sub-cellular locations where over-expressed and down-expressed genes carry out their functions. The number

adjacent to each pie section denotes the number of genes (over-expressed or down-expressed) associated with each location. Panel B represents a simplistic visualisation of the percentage of over-expressed or down-expressed genes associated with each category of cellular location. Percentage of over-expressed genes is represented by the blue area whereas the percentage of down-expressed genes is represented by the red area in each bar. The numbers mentioned in the blue and red area in each bar represent the number of over-expressed and down-expressed genes, respectively, in each category.

So, based on the gene expression data, the PANTHER classification system through its own computational algorithm predicted some biological processes (in broad category) like cellular process (including cell communication, cell cycle regulation), metabolic processes and biological regulation to be altered in CHI which could affect some molecular functions like catalytic activities of proteins, protein-protein interactions and activities of some receptors. However, the software program is not efficiently designed yet to predict biological outcomes accurately based on the analysis of data (Mi *et al,* 2013a; Mi *et al,* 2013b). Hence, the software program could not identify which specific biological processes and associated genes or proteins could be altered in CHI. Nonetheless, some broad biological processes were predicted by the software program which could be associated with CHI. Alteration of one or more of these processes might induce the cells to acquire CHI condition. Future studies might consider investigating these processes to have a better understanding of CHI mechanism.

5.2.7 High-throughput expression analysis of experimental microarray data

Since there is no software program available which can predict biological outcomes precisely based on the analysis of data, it is recommended to use more than one software program to analyse the data to have better ideas of possible biological outcomes (Selvaraj and Natarajan, 2011; Cahan *et al,* 2014; Stevens *et al,* 2014). Since the PANTHER classification system was only able to predict the broad category of biological processes and the software was not perfectly efficient to predict the outcomes, another software program was explored to cross-validate the findings of this PANTHER program. Hence, genome-wide gene expression raw data obtained from microarray experiments were also analysed using IPA as part of the class comparison approach. IPA is one of the most

powerful analytical software programs available to explore datasets acquired from high-throughput expression analysis like microarray and it provides annotations based on a manually curated knowledge base of biological functions (Eisenstein, 2006; Shapira *et al*, 2009; Thomas and Bonchev, 2010; Jin *et al*, 2014; Ben-Ari Fuchs *et al*, 2016). In addition to predicting biological processes, the software can also predict potential upstream regulators and downstream genes/proteins which can be altered because of the genes that are found differentially expressed in the experimental datasets (Ben-Ari Fuchs *et al*, 2016; Haddad *et al*, 2016; Yu *et al*, 2016). To analyse the datasets, the cutoff criteria were selected as fold change ≥ 2 for both, up-regulated and down-regulated genes with q-value ≤ 0.05. A list of 391 differentially expressed genes was generated by IPA analysis that met the cutoff criteria. *SLC17A6* (solute carrier family 17 member 6) which shows transmembrane transporter activity was found to be the most up-regulated gene (7.99 fold). Whereas *MGST1* (microsomal glutathione S-transferase 1) was observed to be the most down-regulated gene (-4.03 fold). Details for all the up- and down-regulated genes for the CHI conditions analysed are provided in Appendices II and III. A brief summary of the IPA analysis of the microarray data is provided in Table 5.5.

Table 5.5: **Summary of the IPA analysis of experimental microarray data**

Molecular and Cellular Functions		
Name	**p-value**	**Number of molecules**
Molecular transport	6.64E-04 - 2.93E-16	127
Cellular development	6.14E-04 - 2.62E-11	55
Cellular function and maintenance	7.62E-04 - 9.28E-11	106
Cell-to-cell signalling and interaction	6.64E-04 - 9.51E-11	97
Small molecule biochemistry	7.62E-04 - 5.86E-10	96

Physiological System Development and Function		
Name	**p-value**	**Number of molecules**
Behaviour	6.98E-04 - 1.53E-16	79
Nervous system development and function	7.62E-04 - 1.71E-13	118
Endocrine system development and function	7.27E-04 - 6.05E-12	49
Organ development	6.97E-04 - 6.05E-12	44
Tissue morphology	6.64E-04 - 1.56E-11	85

Experimental Fold Change up-regulated (top five)		
Gene ID	**Gene name**	**fold change**
SLC17A6	Solute carrier family 17 member 6	↑ 7.987
SCG3	Secretogranin III	↑ 5.732
SNORD115-32	Small nucleolar RNA, C/D box 115-32	↑ 5.694
PPY	Pancreatic polypeptide	↑ 5.669
G6PC2	Glucose-6-phosphatase, catalytic subunit 2	↑ 5.576

Experimental Fold Change down-regulated (top five)		
Gene ID	**Gene name**	**fold change**
MGST1	Microsomal glutathione S-transferase 1	↓-4.03489
H19	H19, imprinted maternally expressed transcript (non-protein coding)	↓-3.89967
GUCA1C	Guanylate cyclase activator 1C	↓-3.33672
CXCL10	C-X-C motif chemokine ligand 10	↓-3.26505
LMO3	LIM domain only 3	↓-3.21735

~This summary of the analyses was generated by the IPA software program. Here in this Table the term "Number of Molecules" represent the number of genes from the query differentially expressed genes that were predicted by the program to be associated with the individual biological process. The titles of the biological processes listed here were provided by the software program. Fold change ≥ 2 for both, up-regulated and down-regulated genes with q-value ≤ 0.05 was considered significant in the analysis with this software.

5.2.7.1 Analysing canonical pathways and processes associated with differentially expressed genes in CHI conditions

In addition to DAVID and PANTHER programs, IPA software was explored to predict potential pathways and processes which are associated with the differentially expressed genes in CHI conditions. As previously, for this analysis, the cutoff criteria were set as fold change ≥ 2 for both, up-regulated and down-regulated genes with q-value ≤ 0.05.

Fifty-three canonical pathways were predicted by the IPA software to be associated with the genes differentially expressed in CHI. Figure 5.16 shows the canonical pathways predicted to be associated with the differentially expressed genes in CHI observed in the experimental datasets. The top ten statistically significant canonical pathways (in order of significance, from higher to lower) were- LXR/RXR (Liver X receptor/ Retinoid X receptor) activation, pathogenesis of multiple sclerosis, maturity-onset diabetes of young (MODY) signalling, axonal guidance signalling, dopamine-DARPP32 feedback in cAMP signalling, cardiac β-adrenergic signalling, IL-17 signalling, amyotrophic lateral sclerosis signalling, CREB signalling in neurons, GPCR-mediated nutrient sensing in enteroendocrine cells (pathway titles as provided by the software program).

Among the statistically significant 53 canonical pathways predicted from this gene expression datasets, 7 pathways were calculated to be activated significantly in CHI conditions and they were (in order of z-score, from higher to lower) - cardiac hypertrophy signalling, CREB signalling in neurons, neuropathic pain signalling in dorsal horn neurons, P2Y purigenic receptor signalling pathway, thrombin signalling, calcium signalling, and melatonin signalling (pathway titles as provided by the software program). No pathways were found to be inhibited according to the expression datasets. The z-score is a statistical measurement of the state of activation or inhibition of the pathways and was calculated by the IPA software by comparing the information in the datasets being examined and the information available in the IPA knowledge base. Positive z-score indicates activation while a negative score indicates inhibition. An absolute z-score of ≥ 2 was considered statistically significant.

Figure 5.16**: Significant canonical Pathways identified to be associated with differentially expressed genes in CHI conditions**. The pathways were predicted by using IPA software. A graph was generated having the pathways on the x-axis and the significance (–log of p-value) on the y-axis. The pathways are presented in descending order of significance. Pathways with predicted activation (with a positive z-score) are shown in orange. The intensity of the orange colour in the pathway bars corresponds to the level of activation. Pathways that were unchanged (with z-score = 0) are shown in white colour. Pathway for which no activity pattern was observed is marked in grey colour. No pathways were predicted to be inhibited (with a negative z-score). A threshold line was drawn to indicate the data point where the p-value is 0.05. The orange points on each bar indicate the ratio value of the number of genes associated with each pathway that met the cutoff criteria and the total number of reference genes associated with that particular pathway.

Significantly activated canonical pathways were further explored using IPA tools to understand the possible role of the molecules in the data sets being analysed in each pathway. Top two significant canonical pathways are illustrated below (Figure 5.17 and Figure 5.18) which were generated by the IPA program. The molecules from the experimental datasets which were predicted to be part of the pathway being explored were highlighted in pink colour in the pathway diagram. Over-expressed (or up-regulated) and down-expressed (down-regulated) molecules in the diagram were highlighted with red and green colour, respectively. Furthermore, a prediction tool in IPA, "Molecule Activity Predictor" (MAP), was used to predict the activation or inhibition status of the molecules in the pathway being analysed.

Cardiac hypertrophy signalling (p-value = 2.11E-03, and z-score = 2.646) was predicted to be the most activated canonical pathway associated with the differentially expressed genes in the present datasets. Cardiac hypertrophy is a heart's response (like abnormal enlargement, thickening of the muscle *etc*.) to different forms of cardiac anomalies (e.g. hypertension, valvular disease, congenital heart disease) (Molkentin *et al,* 1998; Heineke and Molkentin, 2006; Sala *et al,* 2012). Figure 5.17 shows the cardiac hypertrophy signalling pathway. One of the IPA tools, MAP, was used to predict the relationship (activation or inhibition) of the molecules in the pathway. 10 genes from the datasets being examined were found to be part of this canonical pathway and all of them were observed to be over-expressed in CHI conditions (Table 5.6).

The second most significant canonical pathway predicted to be activated by the differentially expressed genes being analysed was CREB signalling in neurons. This pathway was predicted to have a p-value of 1.40E-03 and a z-score of 2.449. This signalling pathway plays an important role to integrate new memory and also information processing within neuronal networks (Impey *et al,* 1998; Benito and Barco, 2010; Pugazhenthi *et al,* 2011). Figure 5.18 shows the illustrated diagram of the CREB signalling pathway in neurons. IPA tool, MAP, was again used to predict the relationship (activation or inhibition) of the molecules in the pathway. 9 genes from the datasets being examined were found to be part of this canonical pathway and all of them were observed to be over-expressed in CHI conditions (Table 5.7). Six of these nine genes are also part of the above-mentioned cardiac hypertrophy signalling pathway (Table 5.6).

Although the predicted canonical pathways seem, at first sight, not to be relevant with CHI pathobiology directly, however, the software program predicted activation to these pathways based on the differential gene expression in CHI tissues. Cardiac hypertrophy can develop because of endocrine disorders (Molkentin *et al*, 1998; Kim *et al*, 2008) and CREB signalling is known to be associated with glucose homeostasis (Herzig *et al*, 2001; Altarejos and Montminy, 2011; Oh *et al*, 2013). So, either these pathways play roles directly or indirectly to the progression of CHI, or activation of these pathways could be the outcome of CHI. In total, 13 genes from the present datasets were predicted to be associated with these two canonical pathways, 3 of these genes were identified in the basic analysis of the datasets (described in section 5.2.4). So future analysis can explore these 10 more genes for studying their possible role in CHI development.

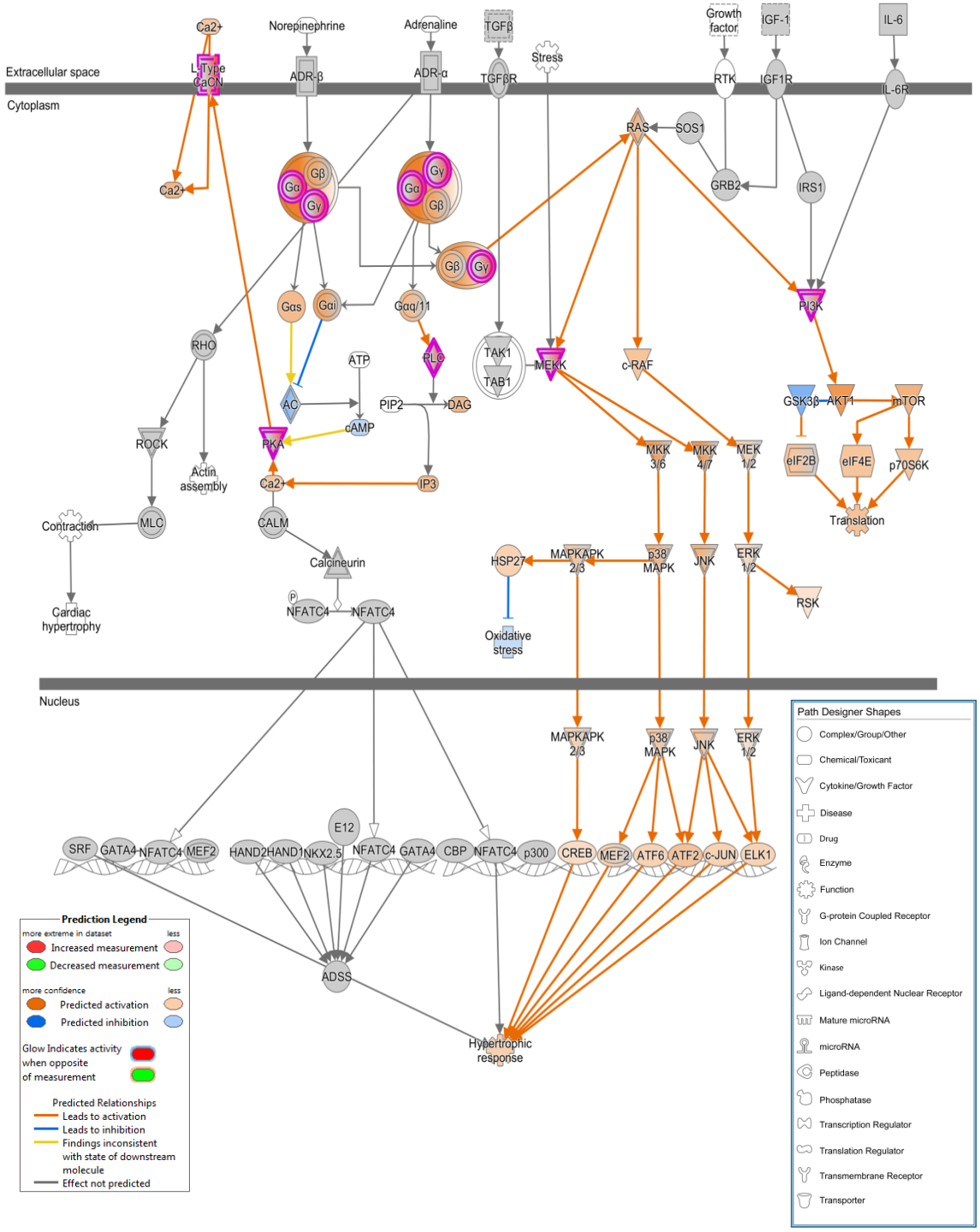

Figure 5.17: **Cardiac hypertrophy signalling pathway**. The pathway was generated using the IPA software. Molecules from the datasets which were found to be part of the pathway are highlighted in pink. Predicted activations or inhibitions of molecules by other molecules in the pathway are also illustrated here. Molecules in the pathway which were found in the datasets being examined but did not meet the cutoff criteria are highlighted in grey. Molecules which are in the pathway reference knowledge base but not in the datasets are indicated by white.

Table 5.6: **Differentially expressed genes in the experimental microarray datasets found to be associated with the cardiac hypertrophy signalling pathway**

Gene ID	*Gene name*	*Experimental fold change*	*Experimental p-value*	*Cellular location*
CACNA1A	Calcium voltage-gated channel subunit alpha1 A	2.519	3.35E-06	Plasma Membrane
CACNA1D	Calcium voltage-gated channel subunit alpha1 D	3.078	2.05E-06	Plasma Membrane
GNA12	G protein subunit alpha 12	2.073	9.37 E-04	Plasma Membrane
GNAO1	G protein subunit alpha O1	2.754	8.97 E-06	Plasma Membrane
GNG4	G protein subunit gamma 4	4.425	2.66 E-07	Plasma Membrane
KL	Klotho	2.078	1.69 E-04	Extracellular Space
MAP3K15	Mitogen-activated protein kinase kinase kinase 15	2.781	1.12 E-05	Other
PLCB4	Phospholipase C beta 4	2.765	1.14 E-04	Cytoplasm
PLCH2	Phospholipase C eta 2	2.061	3.15 E-05	Cytoplasm
PRKACB	Protein kinase cAMP-activated catalytic subunit beta	3.489	2.23 E-05	Cytoplasm

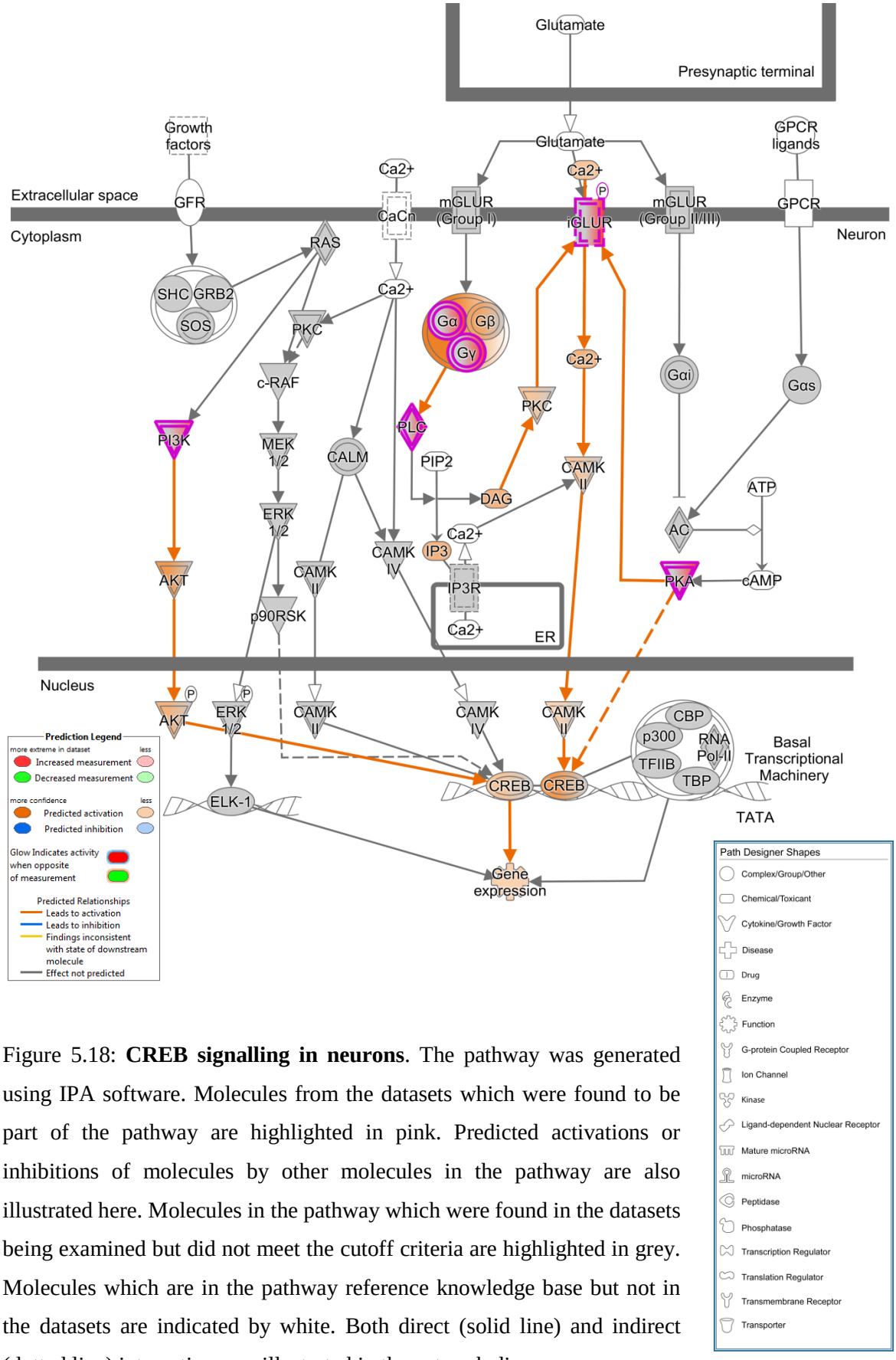

Figure 5.18: **CREB signalling in neurons**. The pathway was generated using IPA software. Molecules from the datasets which were found to be part of the pathway are highlighted in pink. Predicted activations or inhibitions of molecules by other molecules in the pathway are also illustrated here. Molecules in the pathway which were found in the datasets being examined but did not meet the cutoff criteria are highlighted in grey. Molecules which are in the pathway reference knowledge base but not in the datasets are indicated by white. Both direct (solid line) and indirect (dotted line) interactions are illustrated in the network diagrams.

Table 5.7: **Differentially expressed genes in the experimental microarray datasets found to be associated with the CREB signalling pathway in neurons**

Gene ID	*Gene name*	*Experimental fold change*	*Experimental p-value*	*Cellular location*
GNA12	G protein subunit alpha 12	2.073	9.37E-04	Plasma membrane
GNAO1	G protein subunit alpha O1	2.754	8.97E-06	Plasma membrane
GNG4	G protein subunit gamma 4	4.425	2.66E-07	Plasma membrane
GRIA2	Glutamate ionotropic receptor AMPA type subunit 2	2.329	4.76E-05	Plasma membrane
GRIA3	Glutamate ionotropic receptor AMPA type subunit 3	2.512	1.70E-05	Plasma membrane
KL	Klotho	2.078	1.69E-04	Extracellular space
PLCB4	Phospholipase C beta 4	2.765	1.14E-04	Cytoplasm
PLCH2	Phospholipase C eta 2	2.061	3.15E-05	Cytoplasm
PRKACB	Protein kinase cAMP-activated catalytic subunit beta	3.489	2.23E-05	Cytoplasm

5.2.7.2 Predicting upstream regulators that can regulate genes to express differentially in CHI condition

In order to conduct a biological function, a gene/protein might need to be regulated by the upstream regulators, the molecules which can induce or inhibit the expression of other molecules. These upstream regulators might need to be activated or inhibited before regulating downstream target genes/proteins. The IPA software was used to predict upstream regulators that could be activated or inhibited and thus could be accountable for the differential expression of genes in the datasets being studied. Knowledge of these predicted upstream regulators was then used to generate hypotheses to understand how a downstream biological function could be regulated by the activation or inhibition of the regulators. Table 5.8 shows the list of predicted of upstream regulators activated or

inhibited and Table 5.9 presents the list of target molecules and functions predicted to be regulated by the upstream regulators. This list of target molecules was sorted based on the consistency score. This consistency score is a measurement of causal consistency and level of connectivity of a network (Barabási and Oltvai, 2004; Ben-Ari Fuchs *et al*, 2016). The IPA software can generate regulator effect network based on the interaction patterns of the upstream regulators and their target molecules. The regulator effect network with the highest consistency score (Table 5.9) is presented as a network diagram in Figure 5.19. Here in this network, the regulators mainly influence immune responses of cells. Another network that shows the modulation of the expression of *ABCC8* (a CHI gene) and regulates glucose sensitivity, as well as neuron development, is also presented here as an example in Figure 5.20. So, this analysis provides a list of potential upstream regulators (mentioned in Table 5.8) which can be activated or inhibited in CHI condition to alter some biological functions (listed in Table 5.9) by means of inducing differential expression of genes. Future studies to understand the mechanisms of how these regulators are being activated or inhibited in CHI conditions might be helpful to explain the CHI mechanism properly.

Table 5.8: **List of predicted of upstream regulators activated or inhibited**

Upstream Regulator	*Molecule Type*	*Predicted Activation State*	*Activation z-score*
HNF1A	Transcription regulator	Activated	3.322
NEUROG3	Transcription regulator	Activated	3.261
BDNF	Growth factor	Activated	3.090
NEUROD1	Transcription regulator	Activated	2.789
TGF beta	Group	Activated	2.75
PAX6	Transcription regulator	Activated	2.649
P2RY14	G-protein coupled receptor	Activated	2.646
TGFB1	Growth factor	Activated	2.636
DICER1	Enzyme	Activated	2.433
MKNK1	Kinase	Activated	2.236
BCL2	Transporter	Activated	2.204
ADIPOQ	Hormone	Activated	2.177

Upstream Regulator	*Molecule Type*	*Predicted Activation State*	*Activation z-score*
ADCYAP1	Receptor-ligand	Activated	2.08
EGFR	Kinase	Activated	2.006
ASCL1	Transcription regulator	Activated	2.000
NEUROG2	Transcription regulator	Activated	2.000
IFNA1/IFNA13	Cytokine	Inhibited	-2.172
IFNL1	Cytokine	Inhibited	-2.205
Hedgehog	Group	Inhibited	-2.219
IL27	Cytokine	Inhibited	-2.320
IFNA2	Cytokine	Inhibited	-2.377
IFNB1	Cytokine	Inhibited	-2.411
IFN gamma	Complex	Inhibited	-2.418
IFNG	Cytokine	Inhibited	-2.640
PRL	Cytokine	Inhibited	-2.762
IL1B	Cytokine	Inhibited	-2.884
REST	Transcription regulator	Inhibited	-3.126

Table 5.9: **List of target molecules and functions predicted to be regulated by the upstream regulators**

Consistency Score	*Regulators*	*Target Molecules in Dataset*	*Functions*
25.981	EGFR, IFNG, Ifn gamma, IFNA2, IFNB1, IL1B, IL27, PRL	*C3*, *C4A/C4B*, *CCL11*, *CCL2*, *CXCL10*, *CXCL11*, *CXCL12*, *CXCL9*, *CYBB*, *TLR3*, *TNFSF14*, *VEGFA*	Binding of mononuclear leukocytes, cell movement of microglia, chemoattraction, migration of dendritic cells, recruitment of inflammatory leukocytes
23.035	BCL2, BDNF, MKNK1, NEUROG2, P2RY14, REST	*ADCYAP1*, *CASR*, *CBFA2T2*, *CCND2*, *CHGA*, *CHGB*, *CRMP1*, *DDX25*, *ENO2*, *GAD2*, *GJD2*, *GLP1R*, *GLRA1*, *GNAO1*, *GRIA2*, *INA*, *KCNJ6*, *KIF5A*, *MAP1B*, *NEUROD1*, *NKX6-1*, *PAX6*, *PCLO*, *PCSK1*,	Cellular degradation, coordination, degeneration of cells, degeneration of nervous system, exocytosis, glucose metabolism disorder, movement Disorders, neurodegeneration, organisation of cytoskeleton, perinatal death, quantity of neurons, quantity of vesicles,

Consistency Score	*Regulators*	*Target Molecules in Dataset*	*Functions*
		PTPRN, *RGS7*, *SCG2*, *SLC17A6*, *SLC2A2*, *SNAP25*, *SORL1*, *SSTR2*, *STXBP5L*, *SYN1*, *SYT4*, *SYT7*, *UCHL1*, *VEGFA*	reflex, release of neurotransmitter, seizures, size of body, transport of molecule
11.225	EGFR, Ifn gamma, IFNB1, PRL	*CCL2*, *CDH2*, *CXCL10*, *CXCL11*, *CXCL12*, *CXCL9*, *CYBB*, *MX1*, *PTGS2*, *SERPINA3*, *SLC4A7*, *TLR3*, *UCHL1*, *VEGFA*	Binding of mononuclear leukocytes, cell movement of microglia, migration of dendritic cells, neuromuscular disease, organ degeneration, perinatal death
7.839	NEUROD1, NEUROG2, NEUROG3	*ABCC8*, *CBFA2T2*, *CDH2*, *CHGA*, *IAPP*, *INSM1*, *ISL1*, *NKX6-1*, *PAX6*, *PCSK1*, *PCSK2*	Development of neurons, glucose tolerance, morbidity or mortality, quantity of neurons
7.333	ADIPOQ, IFNA1/ IFNA13, IFNL1	*CCL2*, *CXCL10*, *CXCL11*, *CXCL9*, *CYBB*, *IFI44L*, *MX1*, *PTGS2*, *TLR3*	Binding of mononuclear leukocytes, cell death, neoplasia of cells
5.814	ASCL1, EUROD1, NEUROG2, NEUROG3	*CDH2*, *INSM1*, *NFASC*, *NKX6-1*, *PAX6*	Development of neurons, quantity of neurons
3.411	BDNF, DICER1, REST	*ADCYAP1*, *CCND2*, *CHGB*, *CRMP1*, *GAD2*, *GLRA1*, *GNAO1*, *GRIA2*, *KCNJ6*, *KIF5A*, *MAP1B*, *NEUROD1*, *PCSK1*, *PTPRN*, *PTPRN2*, *SCG2*, *SERPINF1*, *SNAP25*, *SORL1*, *SYN1*, *SYT4*, *UCHL1*	Cognition, seizures
3.051	Hedgehog, HNF1A, NEUROD1, PAX6	*ABCC8*, *CCND2*, *FFAR1*, *G0S2*, *GLP1R*, *IAPP*, *NPTX2*, *PCSK1*, *PCSK2*, *SLC2A2*, *TMOD2*, *TRPM3*, *VEGFA*	Behaviour, glucose tolerance
1.333	Tgf beta, TGFB1	*CCL2*, *CXCL10*, *CYBB*, *GCNT1*, *MMP7*, *OLR1*, *P2RY1*, *PTGS2*, *VEGFA*	Hypertension

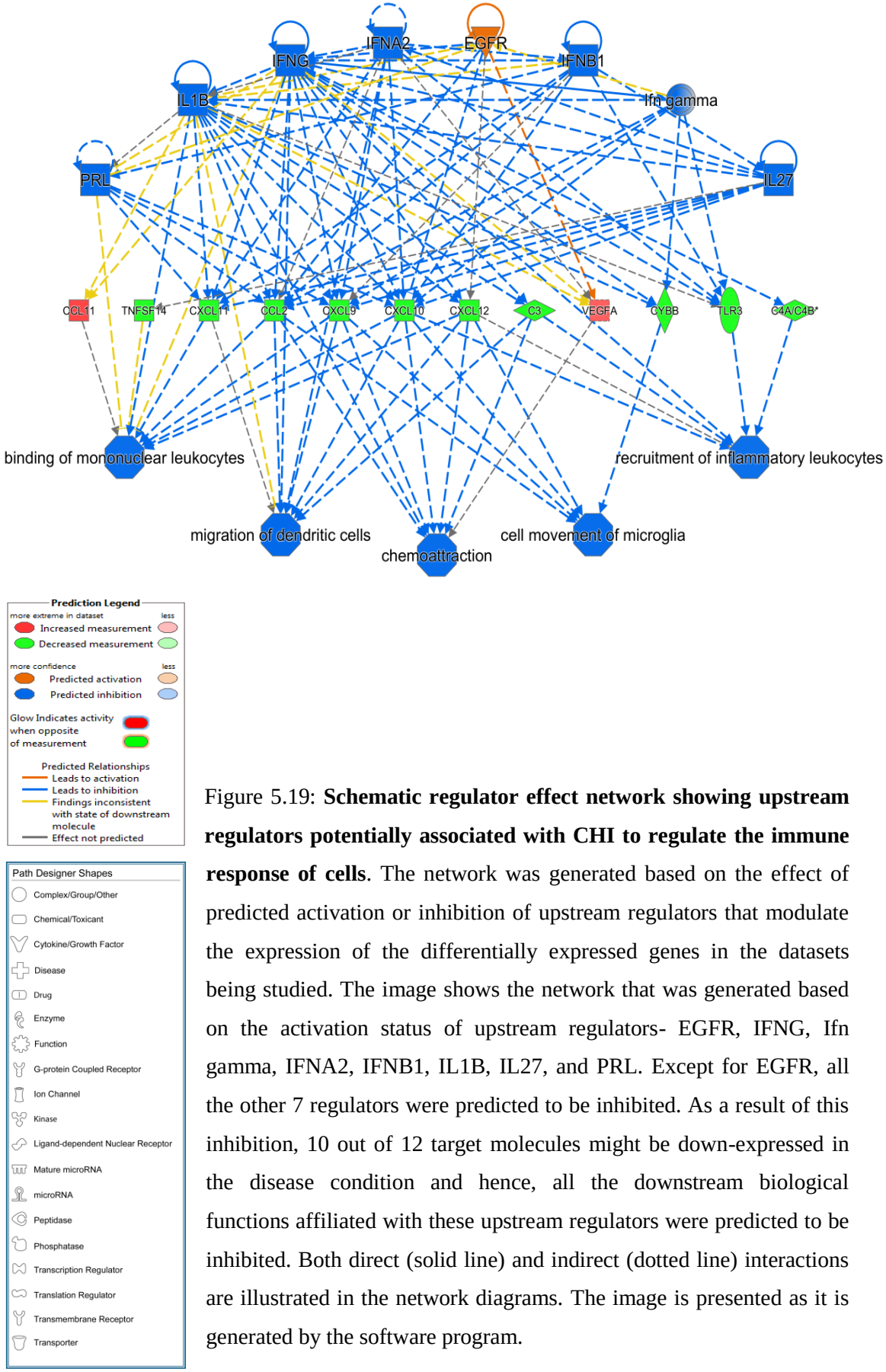

Figure 5.19: **Schematic regulator effect network showing upstream regulators potentially associated with CHI to regulate the immune response of cells**. The network was generated based on the effect of predicted activation or inhibition of upstream regulators that modulate the expression of the differentially expressed genes in the datasets being studied. The image shows the network that was generated based on the activation status of upstream regulators- EGFR, IFNG, Ifn gamma, IFNA2, IFNB1, IL1B, IL27, and PRL. Except for EGFR, all the other 7 regulators were predicted to be inhibited. As a result of this inhibition, 10 out of 12 target molecules might be down-expressed in the disease condition and hence, all the downstream biological functions affiliated with these upstream regulators were predicted to be inhibited. Both direct (solid line) and indirect (dotted line) interactions are illustrated in the network diagrams. The image is presented as it is generated by the software program.

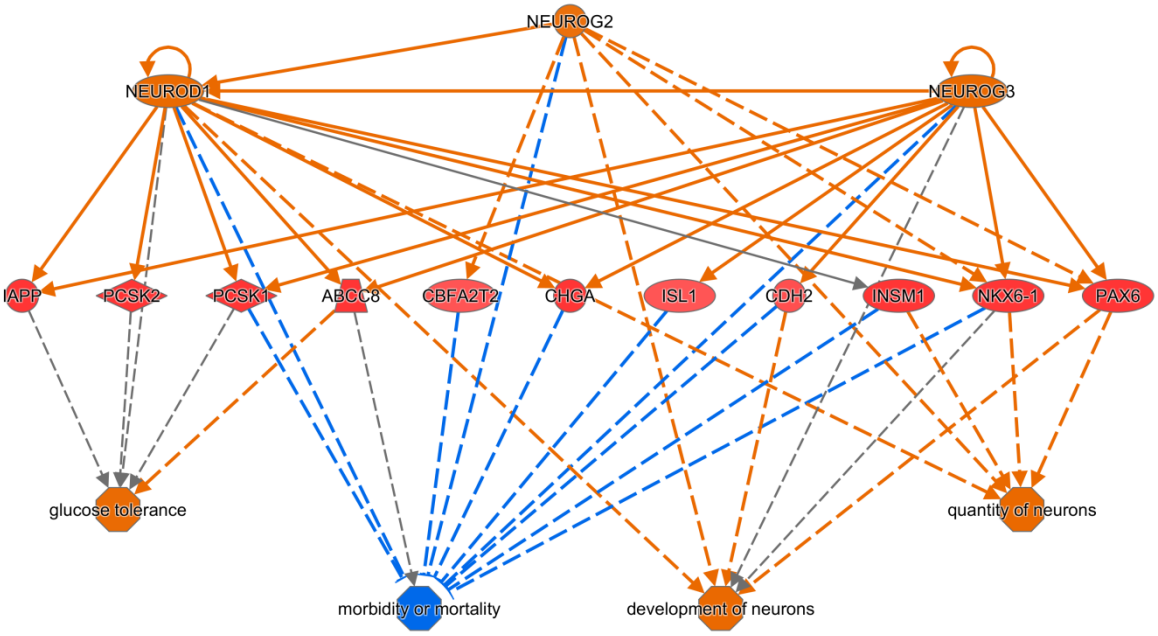

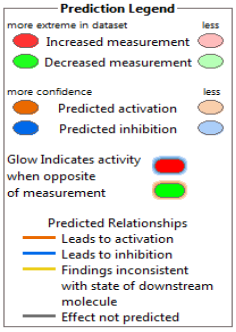

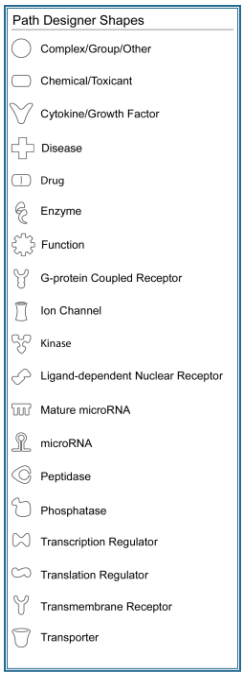

Figure 5.20: **Schematic regulator effect network showing upstream regulators potentially associated with CHI to regulate glucose sensitivity as well as neuron development**. The network was generated based on the effect of predicted activation or inhibition of upstream regulators that modulate the expression of the differentially expressed genes in the datasets being studied. The image illustrates the network that was generated based on the activation status of upstream regulators- NEUROD1, NEUROG2, and NEUROG3. All the 7 regulators were predicted to be activated. All of the 11 target molecules might result in over-expression in the disease condition. And the over-expression of these target molecules was then predicted to activate 3 downstream functions and inhibit one function. Both direct (solid line) and indirect (dotted line) interactions are illustrated in the network diagrams. The image is presented as it is generated by the software program.

5.2.7.3 IPA analysis of biological functions predicted to be altered because of differentially expressed genes

As part of class comparison approach (as mentioned in section 5.2.5), biological functions potentially altered in CHI conditions were also predicted by IPA. One of the advantages of using IPA software was not only it provided the list of biological functions potentially altered in CHI but also it provided the list of genes related to those functions. 23 biological functional networks (in broad categories) were predicted to be altered from the experimental datasets by the IPA software. This prediction was based on the interaction information of molecules available in the IPA knowledge base. Among the 23 networks, top 10 networks are listed in Table 5.10. The lists of genes from the datasets which were calculated to participate in each predicted functional network are also mentioned in the Table. Top two networks are illustrated here as graphical representations for a better understanding of the role of the genes in the respective networks (Figure 5.21 and Figure 5.22). So this analysis provides a list of potentially important genes for CHI which can modulate a number of important functional networks like nervous system development, endocrine system development, cell signalling, cell cycle, transport of small molecules etc. Alteration of any these genes and functional networks might be the result of CHI or could be the reason behind the CHI development.

Table 5.10: **List of top functions networks predicted by IPA from experimental gene expression datasets**

Molecules in network (over-expressed in blue and down-expressed in green)	*Focus Molecules*	*Top Functions*
AP3B2, ATP1B2, BMP5, CADPS, CNIH2, G6PC2, GRIA2, GRIA3, INPP5F, KCNA5, KCNB2, KIF5A, KIF5C, MTMR7, NFASC, PARM1, PFKFB2, PLAC8, PPP1R1A, PTPRN, RAB11A, RCAN2, REG3A, SCD5, SGPP2, SLC22A17 ,SLC4A7, SV2A	28	Nervous system development and function, molecular transport, neurological disease
ABCC8, ASB9, C4A/C4B, CHGA, CHGB, CPE, IAPP, INSM1, KLKB1, NEUROD1, NKX6-1, PAM, PAX6, PCSK1, PCSK2, PTPRN2, RASD1, SCG2, SCG3, SCGN, SEMA5A, SERPING1, SLC2A2, ST18, TRPM3	25	Cellular development, endocrine system development and function, digestive system development and function
ANXA13, BEX1, CCL11, CFB, CXCL9, CXCL10, CXCL11, DEUP1, EDARADD, G0S2, GAD2, GCH1, HACD3, IFI44L, IL13RA2, PCLO, RAB3C, REG3G, RIMS2, SERPINA3, TFPI2, TLR3, TMOD2, TNFSF14, UNC13A	25	Cell-to-cell signalling and interaction, cellular movement, haematological system development and function

Molecules in network (over-expressed in blue and down-expressed in green)	*Focus Molecules*	*Top Functions*
CMIP, ELAVL4, INA, KIAA2022, LRRC39, MSANTD4, MYO3A, PAM, PITPNC1, PRPS1, RASGEF1B, RGS7, SEPT3, SEZ6L2, SGTB, SLC17A6, SLC8A1, SYT13, TMOD2, UNC79	20	Behaviour, cellular function and maintenance, small molecule biochemistry
ARG2, CD200, CHN1, GNAO1, HDAC9, KCNJ5, KCNJ6, PLCB4, PLCH2, PPM1E, RGS7, RGS9, RGS17, SCIN, SERPINE2, SH3GL2, STMN1, TCN1, TNFRSF11A,	19	Cell cycle, nervous system development and function, visual system development and function
CACNA1A, CACNA1D, CACNA2D1, CACNB2, GNG4, H19, HHATL, JAKMIP2, PCP4, PPP1R14C, PPY, RAB3B, RIMBP2, SLC4A10, SLC8A1, SNAP25, SYN1, SYT4, SYT7	19	Cardiovascular disease, cellular function and maintenance, molecular transport
ATP2A3, CASR, CXCL12, ERO1B, HEPACAM2, INA, LMO3, MAP1B, mir-368, PNMA1, RFX6, RIMS2, SCGN, SLC30A8, ST8SIA3, STXBP5L, TMEM27, TSPYL4	18	Cell signalling, molecular transport, vitamin and mineral metabolism
ACE2, CAMK2N1, CYBB, EDIL3, EDN3, EEF1A2, ENO2, EPM2AIP1, FRZB, MMP7, OLR1, QPCT, RUNDC3A, SERPINF1, SORL1, SYT17, WNT4	17	Cellular movement, haematological system development and function, immune cell trafficking
ANKH, ATP6AP1, ATP6V0A1, CCND2, EML5, ETV1, FGF10, HOPX, ISL1, MEIS2, PDZK1, PLXNC1, ROBO2, SLC36A4, SLC7A2, SLC7A8, TMOD1	17	Cell morphology, nervous system development and function, respiratory system development and function
ABI3BP, CBFA2T2, CERKL, CHGA, H19, KCNMB2, KIAA0319, KIF5A, LONRF2, LRRTM3, MOB1B, PAPSS2, PDK3, PLEKHS1, STMN1, TNFSF14, ZNF483	17	Cellular assembly and organization, cell morphology, nervous system development

In summary, the analyses performed by the IPA software program predicted a list of potential CHI-associated genes which can play roles in some important biological pathways including transport of molecules, nervous system development, endocrine system development, cellular development, digestive system development, cell signalling *etc*. All of these functional pathways are related to the phenotypes linked with CHI (James *et al*, 2009; Stevens *et al*, 2013; Arya et al, 2014). In addition, a number of upstream regulators were predicted through these analyses. These regulators can play roles in alteration of expression of genes and thus can mediate the development of CHI. All of these predicted genes could be the subject of future studies for a better understanding of CHI development.

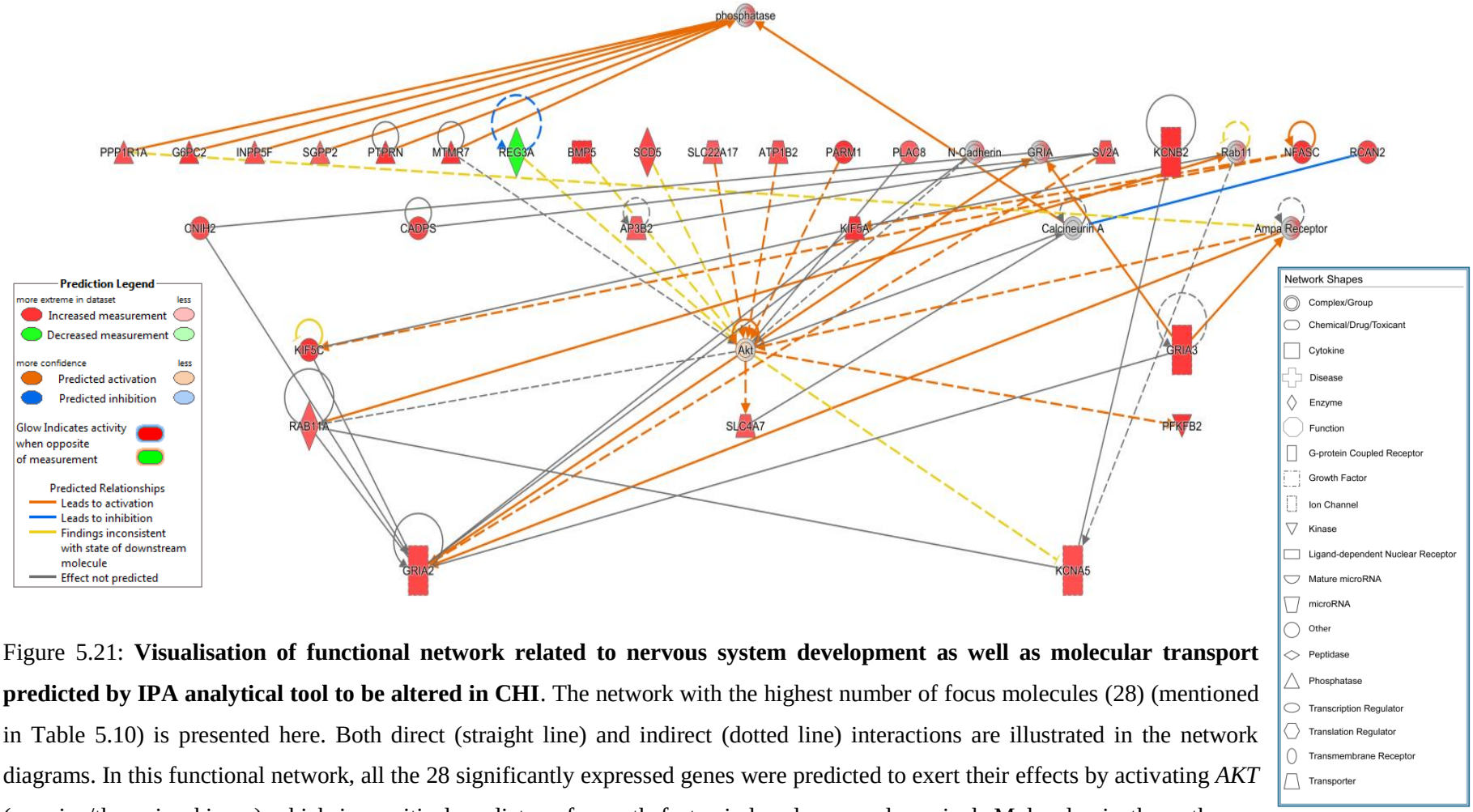

Figure 5.21: **Visualisation of functional network related to nervous system development as well as molecular transport predicted by IPA analytical tool to be altered in CHI**. The network with the highest number of focus molecules (28) (mentioned in Table 5.10) is presented here. Both direct (straight line) and indirect (dotted line) interactions are illustrated in the network diagrams. In this functional network, all the 28 significantly expressed genes were predicted to exert their effects by activating *AKT* (a serine/threonine kinase) which is a critical mediator of growth factor-induced neuronal survival. Molecules in the pathways which were found in the datasets being examined but did not meet the cutoff criteria are highlighted in grey. The image is presented as it is generated by the software program.

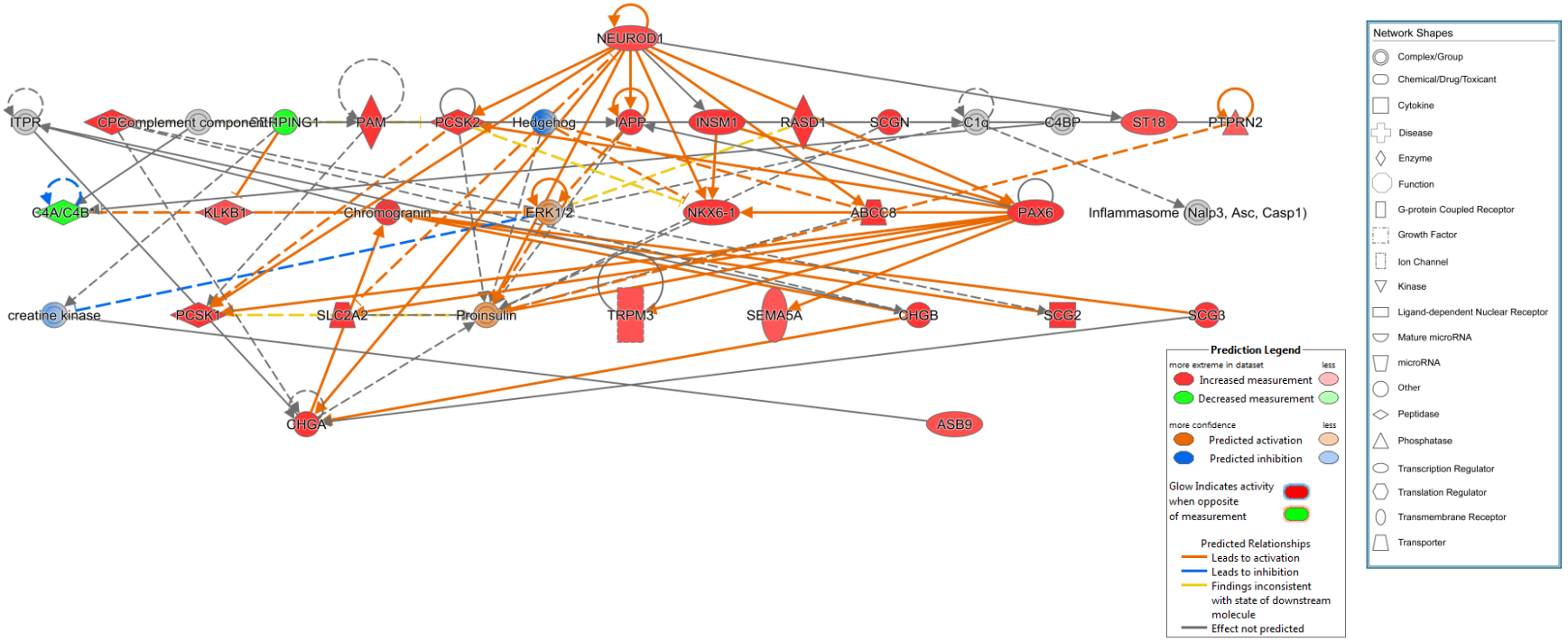

Figure 5.22: **Visualisation of functional network related to endocrine system development as well as cellular development predicted by IPA analytical tool to be altered in CHI**. The network with the second highest number of focus molecules (25) (mentioned in Table 5.10) is presented here. Both direct (straight line) and indirect (dotted line) interactions are illustrated in the network diagrams. In this functional network, all the focus genes were predicted to act by inter-acting multiple genes. Among them, transcription factors, *NEUROD1* and *PAX6* were found the most crucial components of the network. Molecules in the pathways which were found in the datasets being examined but did not meet the cutoff criteria are highlighted in grey. The image is presented as it is generated by the software program.

5.2.8 Expression analysis of experimental microarray data using protein-protein interaction and network biology

In addition to the class comparison approaches (described in section 5.2.5 to section 5.2.7), network biology approach was explored here to predict key potential CHI candidate genes. It is mentioned in the section 5.1.5 that network biology utilises the patterns of interactions between cellular components (gene, RNA or protein) to identify key regulatory component for a given condition (Barabási and Oltvai, 2004; Pujol *et al*, 2010; Stevens *et al,* 2014). Hence, network biology approach was utilized to analyse differentially expressed genes in the datasets to filter out the genes potentially important in CHI pathobiology. This network analysis was carried out based on protein-protein interaction (PPI) information already cited in previous studies and available in different PPI databases. From the experimental dataset, top 50 in total over-expression and down-expression genes (based on fold change) were selected and their protein-protein interaction partners (PIPs) (experimentally proven or predicted) were listed using a web-tool, UniHi (Chaurasia *et al*, 2007; Kalathur *et al,* 2014). Table 5.11 lists the top 50 differentially expressed genes whose PIPs information was available in the PPI databases. Table 5.12 shows the list of differentially expressed genes (mainly encoding different types of non-coding RNAs) which were not included in this network biology analysis because of lack of information regarding their PIPs.

Table 5.11: **List of top differentially expressed genes included for network biology analysis**

Gene ID	*Experimental fold change*	*No of PIPs*	*Gene ID*	*Experimental fold change*	*No of PIPs*
Over-expression					
SLC17A6	7.98662	3	*CXorf57*	3.96371	10
SCG3	5.73173	3	*INA*	3.93723	33
PPY	5.66877	207	*SLC38A4*	3.91409	1
G6PC2	5.57633	1	*NOL4*	3.85513	11
BMP5	5.42886	19	*FAM105A*	3.77095	2
PCSK1	5.34898	18	*GAD2*	3.75709	23
SYT13	5.00993	1	*HEPACAM2*	3.68313	34
RIMS2	4.76136	20	*EDARADD*	3.6518	19
RFX6	4.66785	27	*VAT1L*	3.62934	3
ABCC8	4.45723	26	*RASD1*	3.62796	13
GNG4	4.42531	58	*SYT14*	3.59173	3

Gene ID	*Experimental fold change*	*No of PIPs*	*Gene ID*	*Experimental fold change*	*No of PIPs*
SCGB2A1	4.37755	15	*IL13RA2*	3.58845	15
NEFM	4.12996	44	*SORL1*	3.53053	33
RAB3B	4.09549	28	*SLC2A2*	3.5281	61
IAPP	4.02412	109	*CHGA*	3.4891	14
SCGN	4.02137	23	*PRKACB*	3.48855	241
Down-expression					
MGST1	-4.03489	16	*COLEC12*	-2.78824	17
H19	-3.89967	1	*FABP4*	-2.72098	80
GUCA1C	-3.33672	17	*C4B*	-2.68705	17
CXCL10	-3.26505	224	*SERPING1*	-2.66952	148
LMO3	-3.21735	37	*REG1B*	-2.51265	4
THRSP	-3.09056	26	*MMP7*	-2.51005	91
CXCL9	-3.02664	220	*CXCL11*	-2.48133	216
C3	-2.96514	272	*CYBB*	-2.45412	33
UCP1	-2.8019	76	*C4A*	-2.42248	54

Table 5.12: **List of top differentially expressed genes not included for network biology analysis**

Gene ID	*Gene name*	*Experimental fold change*
SNORD115-32	Small nucleolar RNA, C/D box 115-32	5.69395
PARM1	Prostate androgen-regulated mucin-like protein 1	5.55203
LOC101927457	Uncharacterized LOC101927457	5.09246
SNORD115-22	Small nucleolar RNA, C/D box 115-22	4.99572
SNORD115-5	Small nucleolar RNA, C/D box 115-5	4.74847
SNORD115-6	Small nucleolar RNA, C/D box 115-6	4.69781
SNORD115-44	Small nucleolar RNA, C/D box 115-44	4.68766
SNORD115-27	Small nucleolar RNA, C/D box 115-27	4.66783
SNORD115-10	Small nucleolar RNA, C/D box 115-10	4.65885
SNORD115-11	Small nucleolar RNA, C/D box 115-11	4.61906
SNORD115-25	Small nucleolar RNA, C/D box 115-25	4.54399
SNORD115-1	Small nucleolar RNA, C/D box 115-1	4.44017
MIR7-3HG	MIR7-3 host gene (non-protein coding)	4.39157
SNORD115-16	Small nucleolar RNA, C/D box 115-16	4.35774

Gene ID	*Gene name*	*Experimental fold change*
FAM159B	Family with sequence similarity 159, member B	4.2898
SNORD115-40	Small nucleolar RNA, C/D box 115-40	4.25136
SNORD115-31	Small nucleolar RNA, C/D box 115-31	4.23499
LOC101929550	Uncharacterized LOC101929550	4.22272
SNORD115-38	Small nucleolar RNA, C/D box 115-38	4.20774
SNORD115-33	Small nucleolar RNA, C/D box 115-33	4.18358
SNORD115-24	Small nucleolar RNA, C/D box 115-24	4.13269
SNORD115-21	Small nucleolar RNA, C/D box 115-21	4.11915
RP11-531A24.3	Novel transcript	3.889
RP11-38P22.2	Novel transcript	3.78973
CFC1B	Cripto, FRL-1, cryptic family 1B	3.75938
LINC01112	Long intergenic non-protein coding RNA 1112	3.62479
SNORD115-28	Small nucleolar RNA, C/D box 115-28	3.53716
RP11-77M5.1	Putative novel transcript	-2.66178

Combining all the PIPs of top 50 differentially expressed genes in the dataset being studied, an integrated PPI network was generated using Cytoscape (Shannon *et al,* 2003; Cline *et al,* 2007; Smoot *et al,* 2011; Sun, 2016; Wang *et al,* 2016a; Zhang *et al,* 2016b). This network helps to visualise the important molecules that might act as central molecules (interaction hubs) and modulate activation state of pathways by influencing the pathway molecules. Figure 5.23 shows the complex integrated PPI network that was generated using Cytoscape based on the PIPs of top 50 genes being analysed. A number of central molecules (genes) with a high number of interaction partners were observed in the network. The network was then filtered to identify important genes having at least 10 PIPs and again a new diagram was generated (Figure 5.24). Network analyser plugin of Cytoscape software was then explored to identify key components of the network by analysing network properties including average shortest path length, betweenness centrality, closeness centrality, clustering coefficient, and degree as a measure of confidence of prediction (section 2.12.3 for details). A degree value of ≥ 10 was set as a cutoff value to predict the most important component of the network. Table 5.13 presents the analysed properties of the generated network and nodes with a degree value of ≥ 10.

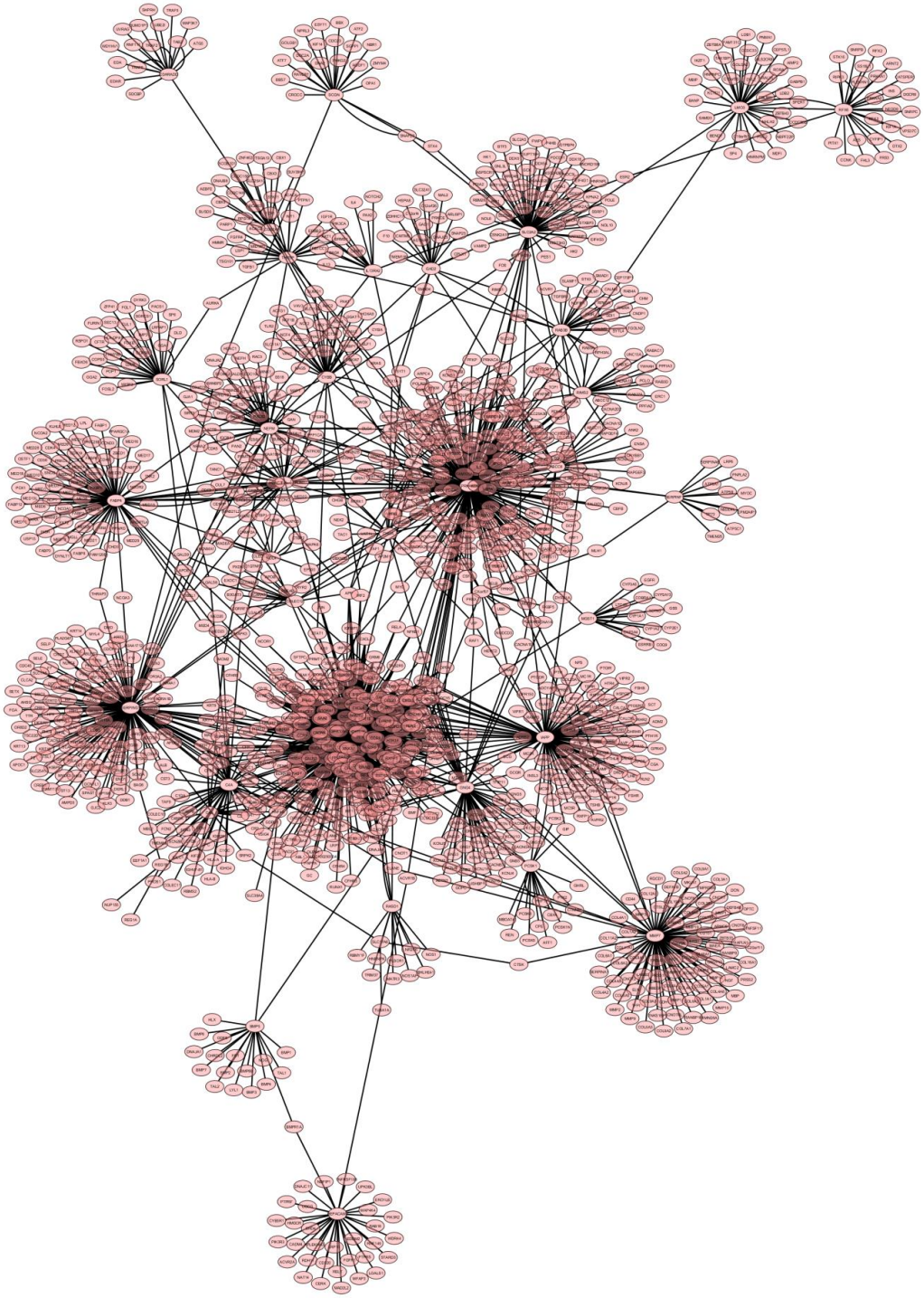

Figure 5.23: **Integrated protein-protein interaction network generated based on interaction partners of the top 50 differentially expressed genes being studied**. All the PIPs of the genes were fetched from PPI databases using web tool UniHi and the network was generated using Cytoscape software. In the diagram, all the nodes represent biological entities like genes or proteins and the connecting edges represent pairwise protein-protein interaction (experimentally verified or computationally predicted). Nodes in the centre of a cluster with a larger number of connections are considered important for the overall function of the network. The image is presented as it is generated by the software program.

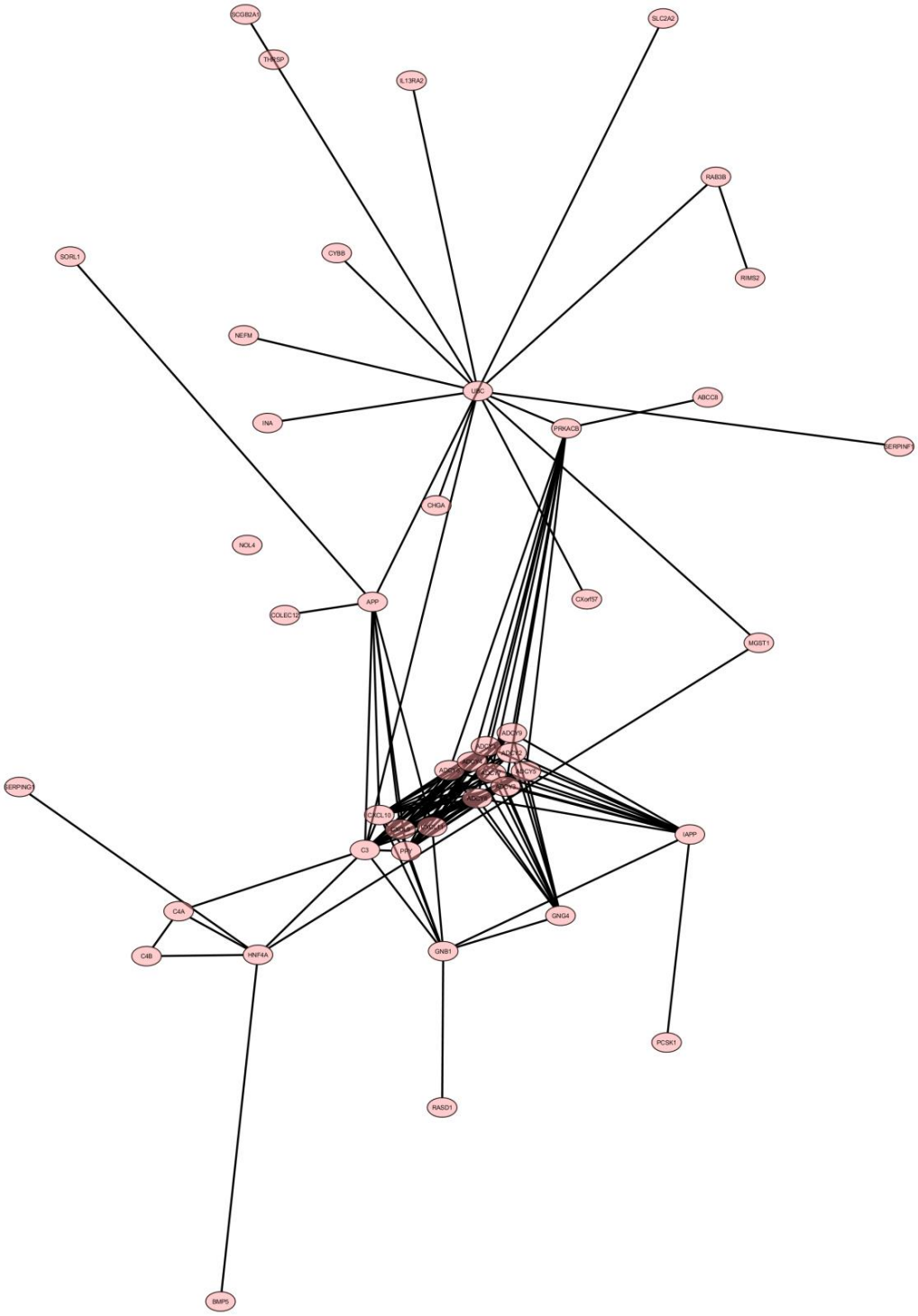

Figure 5.24: **Visualisation of filtered integrated protein-protein interaction network with central nodes having at least 10 interaction partners in the original network**. The network was generated using Cytoscape software. Only the central nodes in a cluster with at least 10 interaction partners illustrated in Figure 5.23 are presented here. In the diagram, all the nodes represent biological entities like genes or proteins and the connecting edges represent pairwise protein-protein interaction. The image is presented as it is generated by the software program.

Table 5.13: **Analysed properties of the integrated PPI network generated from the top 50 differentially expressed genes in the dataset being used**

Average Shortest Path Length (A)	Betweenness Centrality (B)	Closeness Centrality (C)	Clustering Coefficient (D)	Degree (E)	Pearson correlation between E and A	Pearson correlation between E and B	Pearson correlation between E and C	Pearson correlation between E and D	Gene ID
2.811948	0.251419	0.355625	0.0229	272	-0.22234	0.749278	0.283647	0.03754	*C3*
2.775967	0.444109	0.360235	0.000444	233					*PRKACB*
3.039375	0.063965	0.329015	0.016376	224					*CXCL10*
3.044128	0.05522	0.328501	0.016936	220					*CXCL9*
3.129667	0.042322	0.319523	0.017452	217					*CXCL11*
3.137135	0.029121	0.318762	0.038225	207					*PPY*
3.315003	0.19264	0.301659	0	147					*SERPING1*
3.811948	0.118898	0.262333	0.00051	109					*IAPP*
3.812627	0.113724	0.262286	0	92					*MMP7*
3.851324	0.089337	0.259651	0	79					*FABP4*
3.844535	0.083011	0.260109	0	61					*SLC2A2*
3.802444	0.052531	0.262989	0	58					*GNG4*
3.404616	0.041742	0.293719	0.024458	54					*C4A*
3.633401	0.05365	0.275224	0	43					*NEFM*
4.5241	0.063833	0.221038	0	37					*LMO3*
4.607604	0.043818	0.217033	0	34					*HEPACAM2*
3.704005	0.032617	0.269978	0	33					*INA*
3.81738	0.037415	0.26196	0	32					*SORL1*
3.837746	0.037299	0.26057	0	32					*CYBB*

Average Shortest Path Length (A)	Betweenness Centrality (B)	Closeness Centrality (C)	Clustering Coefficient (D)	Degree (E)	Pearson correlation between E and A	Pearson correlation between E and B	Pearson correlation between E and C	Pearson correlation between E and D	Gene ID
3.916497	0.033514	0.25533	0.007937	28					*RAB3B*
4.321792	0.023961	0.231385	0	26					*THRSP*
5.066531	0.032818	0.197374	0	26					*RFX6*
3.613035	0.017355	0.276776	0.036923	26					*ABCC8*
4.466395	0.023436	0.223894	0	23					*GAD2*
4.942295	0.026332	0.202335	0	22					*SCGN*
4.181942	0.017305	0.239123	0.015789	20					*RIMS2*
4.373388	0.025965	0.228656	0	19					*BMP5*
4.226748	0.016425	0.236589	0.022059	17					*PCSK1*
4.150713	0.006098	0.240922	0.080882	17					*C4B*
3.786151	0.016385	0.26412	0	17					*COLEC12*
4.693143	0.02027	0.213077	0	16					*EDARADD*
4.001358	0.018231	0.249915	0	15					*SCGB2A1*
3.72573	0.031235	0.268404	0	15					*IL13RA2*
3.753564	0.019391	0.266413	0	15					*MGST1*
3.021045	0.135421	0.331011	0	14					*UBC*
3.520027	0.015629	0.284089	0	14					*CHGA*
4.002716	0.015681	0.24983	0	14					*SERPINF1*
4.564155	0.012188	0.219099	0	12					*RASD1*
3.983707	0.01144	0.251022	0	10					*CXorf57*
4.851324	0.009897	0.206129	0	10					*NOL4*

To be considered as a viable molecule in an integrated PPI network, confidence parameters such as betweenness centrality, closeness centrality and clustering coefficient of each node (gene) should be in between a value of 0 and 1 (Barabási and Oltvai, 2004). A node with a value 0 in either parameter indicates that the node is an isolated molecule in the integrated network and might be comparatively less important for regulating downstream functions. Considering the facts in mind, from the above-mentioned network analysis (presented in the Table 5.13), 13 out of 40 molecules (genes) were found to meet the selection criteria and could be considered important molecules in CHI pathobiology. The list of these important 13 genes predicted from the network biology analysis is presented in Table 5.14 and their associated biological functions predicted by DAVID are listed in Table 5.15. Among these 13 genes, *ABCC8* is already a known CHI gene, *RIMS2* was also predicted by basic analyses of the present datasets (described in section 5.2.4), and *PRKACB* was also identified by the IPA software program after analysing the present datasets (described in section 5.2.7.1).

Table 5.14: **List of predicted genes by network biology potentially associated with CHI**

Gene ID	*Gene name*	*Experimental fold change*
C3	Complement component 3	-2.96514
PRKACB	Protein kinase, cAMP-dependent, catalytic, beta	3.48855
CXCL10	Chemokine (C-X-C motif) ligand 10	-3.26505
CXCL9	Chemokine (C-X-C motif) ligand 9	-3.02664
CXCL11	Chemokine (C-X-C motif) ligand 11	-2.48133
PPY	Pancreatic polypeptide	5.66877
IAPP	Islet amyloid polypeptide	4.02412
C4A	Complement component 4A	-2.42248
RAB3B	RAB3B, member RAS oncogene family	4.09549
ABCC8	ATP-binding cassette, sub-family C member 8	4.45723
RIMS2	Regulating synaptic membrane exocytosis 2	4.76136
PCSK1	Proprotein convertase subtilisin/kexin type 1	5.34898
C4B	Complement component 4B	-2.68705

Table 5.15: **List of biological functions linked with genes predicted by network biology (generated by DAVID pathway database)**

Biological process	Gene count	% of total genes	p-Value
Cell-cell signalling	6	46.15	5.53E-07
Inflammatory response	6	46.15	3.97E-06
Positive regulation of cAMP metabolic process	3	23.08	7.01E-06
Positive regulation of apoptotic cell clearance	3	23.08	9.81E-06
Positive regulation of cAMP-mediated signaling	3	23.08	3.08E-05
Signal transduction	7	53.85	6.93E-05
Positive regulation of leukocyte chemotaxis	3	23.08	7.12E-05
Positive regulation of release of sequestered calcium ion into cytosol	3	23.08	1.63E-04
Response to lipopolysaccharide	4	30.77	1.89E-04
Regulation of complement activation	3	23.08	2.01E-04
Chemokine-mediated signalling pathway	3	23.08	0.001132
Complement activation	3	23.08	0.001693
Complement activation, classical pathway	3	23.08	0.002185
Immune response	4	30.77	0.002908
Negative regulation of endopeptidase activity	3	23.08	0.003242
Chemotaxis	3	23.08	0.003295
Proteolysis	4	30.77	0.004723
T cell chemotaxis	2	15.38	0.005704
Regulation of cell proliferation	3	23.08	0.00741
Regulation of exocytosis	2	15.38	0.018429
G-protein coupled receptor signalling pathway	4	30.77	0.023398
Cell chemotaxis	2	15.38	0.045489

In summary, in addition to the class comparison approach performed by software programs like DAVID, PANTHER and IPA, the network biology approach conducted by software programs like UniHi and Cytoscape also provided a list of genes which can be potentially associated with CHI. These genes play roles in functions related to cell signalling, the immune response of the cell *etc*. Similar functions were predicted by the class comparison approach to be linked with CHI. So, along with the genes identified by class comparison approach, genes identified by this network biology approach could also be considered as the potential candidate genes of CHI. However, both the class

comparison and network biology approaches were unable to identify or predict key CHI associated genes among the potential candidate genes because of the limitations of the algorithms of the software programs. The software programs can only identify a list of genes/proteins potentially associated with a biological function. It will require experimental validations to identify key genes among the potential candidate genes.

5.3 Discussion

5.3.1 General

The principal objective of the experiments described in this chapter was to identify or predict novel candidate genes and pathways that could be associated with CHI. Hence, genome-wide gene expression microarray analyses were performed to compare the transcriptional expression profiles of diseased and control pancreas tissues. Here both the healthy tissues (as control) and lesion tissues were collected from CHI affected pancreas for the differential gene expression assays.

A total of 391 genes were observed to be expressed differentially in tissues with lesions among the 33720 genes that were analysed for their transcriptional expression. A total of 29 differentially expressed genes were predicted through the basic and class comparison analyses of the experimental array datasets and a total of 10 more genes were predicted through network biology analyses to be associated with CHI. These genes were predicted to be involved in various biological functions including insulin secretion, regulation of insulin secretion, cAMP-mediated signalling, type B pancreatic cell differentiation, glucose homeostasis, cell cycle regulation, and cell proliferation. All of the processes are highly linked to insulin secretion pathway. In addition, 27 upstream regulators were predicted through class comparison approach to be activated or inhibited which could affect downstream regulatory or metabolic pathways directly or indirectly and could take part in the development of CHI. However, the analyses of the gene expression datasets

using the software programs only predicted a list of candidate CHI-associated genes/proteins. Further experimental validations are required to identify key genes among these potential candidate genes.

5.3.2 Experimental design and microarray experiments

Genome-wide gene expression experiment using microarray technique is a very prominent and widely used analytic tool where expressions of tens of thousands of genes in a biological sample in certain condition can be monitored simultaneously (Alon *et al,* 1999; Callow *et al,* 2000; Trevino *et al,* 2007; Sealfon and Chu, 2011). A number of previous studies were reported to use microarray technologies to monitor the differential expression of subsets of genes in various altered conditions like colon cancer (Alon *et al,* 1999; Bertucci *et al,* 2004; Resnick *et al,* 2005), lung cancer (Wang *et al,* 2000b; Gordon *et al,* 2002; Kim *et al,* 2006b), breast cancer (Van't Veer *et al,* 2002; Sotiriou *et al,* 2003; Chang *et al,* 2005), tumorigenesis (Bonner *et al,* 2003; Chakraborty *et al,* 2007; Zhao *et al,* 2009), drug response (Staunton *et al,* 2001; Brachat *et al,* 2002; Dan *et al,* 2002), psychiatric disorders (Bezchlibnyk *et al,* 2001; Novak *et al,* 2002a; Mimmack *et al,* 2002), diabetes (Mootha *et al,* 2003; Wolter *et al,* 2009; Reynier *et al,* 2010; Bugliani *et al,* 2013) etc. for better understanding the reasons behind the particular physiological abnormalities. Novel candidate genes for certain disease/abnormal conditions were reported to be predicted using microarray-based genome-wide gene expression analysis (Zhao *et al,* 2009; Györffy *et al,* 2010; Gelernter *et al,* 2014; Ramos *et al,* 2014; Sanayama *et al,* 2014; Michailidou *et al,* 2015).

Similarly, very few microarray experiments were conducted earlier on CHI tissues to understand the disease pathobiology. Change of expression of two genes – *DPP-4* (dipeptidyl peptidase-4) and *PYY* (peptide YY), associated with glucose homeostasis, were observed using cDNA microarray in CHI patient tissues (Rahman *et al,* 2015b). IGF-1/mTOR/Akt pathway was reported to be observed to be associated with CHI through gene expression analysis (Senniappan *et al,* 2016). Another study was reported to conduct whole genome gene expression microarray experiments on archived formalin-fixed, paraffin-embedded (FFPE) pancreatic tissue affected with CHI in comparison with age-matched control pancreatic tissues (Michelsen *et al,* 2011). It was shown by this study that archived FFPE sample could be a good biological source of valuable CHI-

specific information and could be feasible for genome-wide gene expression studies. Further, in addition to differential gene expressions of some glycolysis and calcium-homeostasis related genes, change of expressions of few cancer-related genes were also observed in this study and these cancer-related genes might be accountable for the hypertrophy observed in some CHI cases (Kloppel *et al,* 1999; Reinecke-Lüthge *et al,* 2000; Fournet *et al,* 2001; Kloppel *et al,* 2008). In addition to gene expression microarray, a couple of studies were reported to use whole genome single nucleotide polymorphisms (SNP) microarray to identify novel mutations in CHI genes (Di Candia *et al,* 2009; Harel *et al,* 2015).

To our knowledge, so far, no previous studies were reported where healthy tissues (as control) and lesion tissues, both from CHI affected pancreas, were used for differential gene expression assay in order to identify potential candidate genes as well as the disease associated relevant pathways. In this study, five CHI-affected tissues and six healthy region tissues were used which were collected from the pancreas of six different CHI-affected individuals. For three instances, both healthy and lesion tissues were received from the same individual and hence, a few downstream analyses were carried out separately using the data generated from these tissues to understand the variability in gene expression in different individuals.

As was mentioned previously, microarray experiments are a very efficient high-throughput system to analyse and compare the pattern of expression of thousands of genes simultaneously in different biological conditions. However, this multi-step experiment is vulnerable to variability because of the process to carry out each step (Schuchhardt *et al,* 2000; Novak *et al,* 2002b; Thomas *et al,* 2010; Bryant *et al,* 2011; Jaksik *et al,* 2015). Unless these variabilities are normalised properly, there may be an increase of falsely discovered data (Draghici *et al,* 2006; Chen *et al,* 2007).

The microarray quality control (MAQC) consortium has been established to provide reference guidelines for conducting microarray experiments to minimize the outcome variability and false discovery as well as to enhance reproducibility of the findings (Ji and Davis, 2006; Patterson *et al,* 2006; Chen *et al,* 2007; Shi *et al.* 2008). One of the key steps for successful and reproducible microarray experiments is the sample preparation *i.e.* extraction of total RNA. The outcome of the gene expression studies and further

downstream analysis primarily depends on the quality of RNA with high integrity (Copois *et al,* 2007; Raman *et al,* 2009; Diaz and Barisone, 2011; Viljoen and Blackburn, 2013). Quality of RNA with high integrity is usually measured before setting up the array experiment. This quality assessment of RNA can be performed using traditional optical density (OD) measurement or modern high-throughput chip-based capillary electrophoresis system provided by technologies like Bioanalyzer 2100 (Agilent Technologies, USA) and Experion (Bio-Rad Laboratories, USA) (Fleige and Pfaffl, 2006; Copois *et al,* 2007; Raman *et al,* 2009; Podolska *et al,* 2011). Furthermore, RNA integrity number (RIN), a tool developed by Agilent technologies, is used to assess and indicate RNA quality and integrity (Fleige and Pfaffl, 2006; Schroeder *et al,* 2006). RIN is presented by a number ranging from 1 to 10 where 1 represents very low-quality RNA (highly degraded) and 10 represents very high quality (intact) RNA. For gene expression analysis, it is recommended to use RNA with RIN value not less than 5 (Fleige and Pfaffl, 2006; Raman *et al,* 2009). For this study, it was made sure that all the gene expression experiments were carried out with the RNA samples that met the quality criteria.

5.3.3 Basic comparative analysis of genome-wide gene expression data generated from microarray experiments

As it is mentioned earlier, microarray data is prone to variability and bias, and thus resulting in false findings unless the gene expression raw data generated from microarray experiments are normalised properly. There are a number of sources of variability and bias in raw microarray data which need to be addressed prior to data analysis. These sources are- amounts of RNA samples, differences in labelling, efficiencies in fluorescent dye detection, systematic variations in the level of gene expression measured in the experiments etc. (Quackenbush, 2002; Johnson *et al,* 2006b). These systematic variations that resulted from nonbiological sources can be minimized and corrected by adjusting raw gene expression data using various normalisation methods (Yang *et al,* 2002; Smyth and Speed, 2003; Fujita *et al,* 2006; Johnson *et al,* 2006b). Normalised data then can be used for downstream analysis and for comparison to understand actual and meaningful biological changes (Yang *et al,* 2002; Fujita *et al,* 2006). For this study, raw data normalisations were performed properly by Bioinformatics Core Facilities, University of Manchester, Manchester, UK and the generated data were suitable for downstream analysis.

To analyse gene expression data generated in this study, at least 2 fold gene expression changes (over-expression or down-expression) with an FDR-adjusted p-value (or q-value) ≤ 0.05 were considered significant. FDR in a microarray experiment is a measurement that corresponds the proportion of false positives among the stated differentially expressed genes (Reiner *et al,* 2002; Aubert *et al,* 2004; Pawitan *et al,* 2005). In accordance with this cutoff value, only 339 genes were observed to be significantly over-expressed with the fold change ranging 2 to 7.98 and 52 genes to be significantly down-expressed with fold change ranging -2 to -4.03. Variability in the number of the differentially expressed gene was observed in datasets generated from the samples of three CHI-affected individuals (Nes163, Nes167 and Nes168) in comparison with the mean value of all datasets. It was mentioned earlier that all the tissue samples carry different mutations in the *ABCC8* gene (except one individual that carries a mutation in the *KCNJ11* gene). From this observed gene expression variability, it can be inferred that apart from the effect of the mutation in the *ABCC8* (or *KCNJ11*), there might be some other important genes (regulatory or functional) whose expression could be altered differently. Hence, effect of these alterations, separately or in combination, might be involved in development of the disease condition in individual patients using different regulatory or metabolic pathways (Grimberg *et al,* 2001; James *et al,* 2009; Banerjee *et al,* 2013; Stevens *et al,* 2013; Yorifuji, 2014; Szymanowski *et al,* 2016; Senniappan *et al,* 2016). These genes could be either other known CHI associated genes or could be novel genes that were not reported earlier to be linked with CHI.

There are no previous studies that report CHI as a combination of the effect of the known CHI genes (*ABCC8*, *KCNJ11*, *GCK*, *HADH*, *GLUD1*, *SLC16A1*, *HNF1A*, *HNF4A* and *UCP2*). Experimental datasets were analysed to investigate whether co-regulation of these known CHI genes was one of the factors behind the development of CHI in the patients under study. Only *ABCC8* and *HADH* were observed to be expressed differentially in CHI affected tissue samples (including the three individual samples separately). So, the disease in the studied patients was not because of the simultaneous regulation of known CHI genes. Since most of the affected tissues (except one sample) were mutated in the *ABCC8* gene, so it was believed that the mutation might cause an altered SUR1 protein (K_{ATP} channel accessory subunit). Because of this altered SUR1 protein, the K_{ATP} channels on beta cell membrane might be malfunctional and remain

closed constitutively which promoted membrane depolarisation and insulin secretion. However, these affected tissues were observed to over-express the transcription of the *ABCC8* gene and this could be explained as a surviving attempt of the cells to compensate for the loss of expression of functional channel subunit. On the other hand, Nes168 patient sample was mutated in the *KCNJ11* gene, not in the *ABCC8* gene. But the expression of *ABCC8* was observed much higher in lesion tissue and interestingly, the expression of *KCNJ11* was not compensated for the loss of function. The mutation in the *KCNJ11* gene in this sample might be not detrimental and there might be some other factors involved which regulated the expression of the *ABCC8* gene.

Since CHI is a glucose metabolism disorder, it was thought that glucose metabolism-related hormones and their receptors might be involved with the development of this disease. So, data were analysed for the expression of genes encoding the hormones and their receptors. Only *SSTR2* (somatostatin type 2 receptor) and *GLP1R* (glucagon-like-protein 1 receptor) were found to have differential expression in all datasets (mean and three individual datasets). Among the five different receptor subtypes of somatostatin, type 2 receptor is the most expressed and functionally dominant receptor in human pancreatic alpha and beta cells (Portela-Gomes *et al,* 2000; Kailey *et al,* 2012). It was reported earlier that the activation of SSTR2 results with inhibition of insulin secretion (Atiya *et al,* 1997; Brunicardi *et al,* 2003). One study was reported to observe lower expression of SSTR2 in a few CHI-affected tissues (Shi, 2014). However, in contrast, the experimental CHI tissues in this study were found to show higher expression of this receptor in comparison to control tissues. Because of this over-expression of SSTR2, the patients might be responsive to octreotide treatment as octreotide binds to somatostatin receptors and inhibit insulin secretion (Hussain, 2008; Arnoux *et al*, 2011). However, there could be a possibility that although SSTR2 were transcriptionally over-expressed, the receptor protein could be down-expressed in its translational level which needs further validation. On the other hand, the activation of SSTR2 could be involved in some other pathways yet to be reported to be linked with CHI development. GLP-1 (glucagon-like-protein 1), an incretin hormone that enhances insulin secretion from pancreatic beta cells in a glucose-dependent manner, exerts its effects through GLP1 receptors (Light *et al,* 2002; MacDonald *et al,* 2002; Doyle and Egan, 2007; Meloni *et al,* 2013). Activation of this receptor in cells could result with increased insulin production, insulin secretion, beta cell proliferation and neogenesis (Kwon *et al,* 2004; Doyle and Egan, 2007; Portha *et al,*

2011; Meloni *et al,* 2013). So, over-expression of the GLP1 receptor in CHI tissues might be involved in enhanced insulin secretion and beta cell proliferation (Kassem *et al,* 2000; Lovisolo *et al,* 2010; Shi *et al,* 2015) observed in CHI patients.

Previous studies reported a number of transcription factors (TFs) which are involved in various stages of pancreas development (Pan and Wright, 2011; Shih *et al,* 2013). It was hypothesised that any of these TFs might be regulated differently and this altered TF can activate or inhibit number to downstream proteins to promote CHI development. From this point of view, these experimental microarray data were analysed to assess the expression of the TFs related to pancreas development. TFs- *NKX6.1*, *NEUROD1*, *RFX6*, *PAX6*, *ISL1* and *INSM1* were found to be over-expressed in all CHI datasets (mean and three individual datasets). NKX6.1 was reported to be important in the regulation of insulin secretion as well as beta cell proliferation (Sander *et al,* 2000; Schisler *et al,* 2005; Tessem *et al,* 2014; Ray *et al,* 2016). All the other 5 TFs were reported to be involved in the regulation of insulin secretion directly or indirectly in beta cells (Chu and Tsai, 2005; Gosmain *et al,* 2012; Chen *et al,* 2013; Chandra *et al,* 2014; Jia *et al,* 2015). As all of these six differentially expressed TFs are related to insulin secretion regulation, these genes could be considered as candidate genes for CHI.

As CHI is characterised by irregular and uncontrolled insulin secretion from pancreatic beta cells (Dunne *et al,* 2004; James *et al,* 2009; Arya *et al,* 2014) and since TFs related to insulin secretion regulation were observed to be differentially expressed, so, all the known genes associated with insulin secretion were examined for their expression pattern in the array datasets. Kyoto Encyclopedia of Genes and Genomes (KEGG) (Kanehisa and Goto, 2000; Kanehisa *et al,* 2016) is a well-known and widely used curated and annotated database of information on genes and associated functional pathways (Kitano, 2002; Proverbio *et al,* 2013; Stevens *et al,* 2014). This database was explored to list the genes reported earlier to be associated with insulin secretion pathways. Among the listed 67 reference genes in the KEGG database linked with insulin secretion pathway, 10 genes were found to be differentially expressed in mean and all three individual datasets. These genes were also concluded as potential CHI genes based on this experimental gene expression data.

As mentioned earlier, CHI affected tissues were reported to show altered cell proliferation (Kassem *et al*, 2000; Lovisolo *et al*, 2010). To find out which genes associated with cell proliferation could be altered in CHI condition, the genes listed in KEGG pathway database as reference genes to be associated with cell cycle pathway (accessed at http://www. genome.jp/dbget-bin/www_bget?pathway:map04110) were checked for gene expression. 20 genes were identified to have altered expression and they were - *RASGEF1B*, *RXRG*, *MYO3A*, *MIA2*, *MYO1D*, *VEGFA*, *CCDC67*, *SEPT3*, *TSPYL4*, *MOB1B*, *HDAC9*, *PRKACB*, *TSPYL5*, *DNAH5*, *CCND2*, *FGF10*, *TNFRSF11A*, *CXCL9*, *CXCL10*, *CXCL11*. These 20 genes might be involved in CHI development and so their particular roles are required to be verified.

From these basic analyses of the experimental array datasets, total 19 differentially expressed genes were predicted as novel candidate genes which could affect downstream regulatory or metabolic pathways directly or indirectly and could take part in the development of CHI. Some biological processes known to be associated with these proteins encoded by these genes are- insulin secretion, regulation of insulin secretion, cAMP-mediated signalling, type B pancreatic cell differentiation, glucose homeostasis, cell cycle regulation, cell proliferation *etc*. All of the processes are highly linked to insulin secretion pathway.

CACNA1A which encodes alpha 1A subunit of voltage-dependent calcium channel has been predicted earlier as a potential candidate gene of CHI by whole genome exome sequencing, however, no study has confirmed it yet (Proverbio *et al*, 2013). To our knowledge, all the other 18 genes (predicted so far through above-mentioned basic analyses) were not reported earlier to be considered as potential candidate genes for CHI. However, this finding is required to be validated further.

5.3.4 Functional analysis of the differentially expressed genes in the experimental microarray datasets

In general, a disease could be a combination of the effects of multiple genetic and non-genetic factors which could alter a number of metabolic and regulatory processes and pathways (Gu *et al*, 2002a; Smith, 2007; Panoutsopoulou and Zeggini, 2009; Jin *et al*, 2014; Kao *et al*, 2017). As it is mentioned earlier that it is quite a difficult task to describe

every single gene (and its effect) in a large dataset. So, a popular practice is to utilize clustering methods to discuss the change in large datasets and describe the processes that could be altered significantly because of the gene expression changes (Swift *et al*, 2004; Juan and Huang, 2007; Ness, 2007; Hume *et al*, 2010; Selvaraj and Natarajan, 2011). Hence in this study data were analysed following the clustering method and potential CHI related genes, biological processes or pathways were predicted following class comparison approach, one of the approaches to analyse microarray data (Ness, 2007; Selvaraj and Natarajan, 2011). Three software programs- DAVID, PANTHER and IPA were used for this purpose. These programs use clustering methods to describe biological functions related to large datasets. Since every software programs used different algorithms for analysing data and as none of these programs was 100% efficient for prediction, hence it was decided to use multiple programs.

As CHI is a metabolic disorder with uncontrolled insulin secretion, it is obvious that this disorder is associated with insulin secretion and regulation related pathway as well as glucose metabolism and homeostasis related pathway (James *et al*, 2009; Steven *et al*, 2013; Yorifuji, 2014; Rahman *et al*, 2015b; Nessa *et al*, 2016). In addition, IGF-1/mTOR/Akt pathway was also reported to be associated with CHI (Senniappan *et al*, 2016). It was believed that CHI might be related to some other processes as a major portion of the patients with CHI didn't have any recognisable aetiology and mechanisms of the disease (Stevens *et al*, 2013). So, approach was considered to analyse the gene expression data to find out pathways and biological processes potentially altered in CHI.

Based on the differentially expressed 391 genes in the datasets, all of the three software programs predicted a number of pathways and biological processes which are somehow involved with glucose metabolism, insulin secretion, calcium or potassium ion transport, exocytosis, beta cell differentiation regulation *etc*. – all of them are crucial for CHI development. In addition, some other pathways like- inflammation, nervous system development, cell signalling and signal transduction were also predicted by all of these programs to be related to CHI potentially. Further, cell cycle, cell proliferation, cellular assembly & organisation, endocrine system development related pathways were also predicted to be altered in CHI by more than one programs. Functions like catalytic activity, protein-protein interaction, receptor activity, ion transport activity, protein

translation regulation *etc*. might be altered in CHI as predicted by the program PANTHER and thus above-mentioned pathways might be altered in CHI.

In addition, seven canonical pathways were predicted to be activated in CHI condition by the program IPA. Top two pathways were studies here and they are- cardiac hypertrophy signalling and CREB signalling in neurons. As it was mentioned earlier, Cardiac hypertrophy is a heart's response (like abnormal enlargement, thickening of the muscle *etc*.) to different forms of cardiac anomalies (Molkentin *et al,* 1998; Heineke and Molkentin, 2006; Kim *et al,* 2008; Sala *et al,* 2012). These malfunctions could be developed because of cardiac problems like myocardial infarction, hypertension, cardiac arrhythmias, and also genetic mutations in cardiac protein genes (Molkentin *et al,* 1998). In addition, hypertrophy can be developed because of endocrine disorders (Molkentin *et al,* 1998; Kim *et al,* 2008). Prolonged and sustained hypertrophy can cause heart failure, arrhythmia and unexpected death (Molkentin *et al,* 1998; Heineke and Molkentin, 2006; Sala *et al,* 2012). Ten genes in the datasets were reported to be associated with this pathway. Among the genes, *CACNA1A* and *CACNA1D* encode high voltage-activated Ca^{2+} channel proteins found in pancreatic beta cells and involved in the regulation of insulin secretion (Braun *et al,* 2008; Rorsman *et al,* 2012; Fridlyand *et al,* 2013). The function of GNA12 in the beta cell is not well documented but this G protein subunit might be involved in exocytosis process in beta cells (Kowluru *et al,* 1997; Wang and Thurmond, 2009; Doussau *et al,* 2000; Kimple *et al,* 2014). KL (Klotho) was reported to be involved in insulin secretion regulation, beta cell proliferation, and also beta cell apoptosis in certain cases (Lin and Sun, 2012; Lin and Sun, 2015a; Lin and Sun, 2015b). To our knowledge so far, the other genes were not reported earlier to be linked with any pancreas function. The other activated canonical pathway studied here was CREB signalling in neurons. This signalling pathway is involved in integrating new memory and information processing within neuronal networks (Impey *et al,* 1998; Benito and Barco, 2010; Pugazhenthi *et al,* 2011). Crucial factors in this pathway are cAMP responsive element binding protein (CREB), activating transcription factor (ATF) and cAMP response element modulator (CREM). CREB signalling pathway was reported earlier to be associated with cell proliferation and survival of different types of cells including pancreatic beta cells (Della Fazia *et al,* 1997; Arnould *et al,* 2002; Hussain *et al,* 2006; Kovach *et al,* 2006;). This pathway was observed to be involved in glucose homeostasis (Herzig *et al,* 2001; Altarejos and Montminy, 2011; Oh *et al,* 2013). As reported earlier

CHI is associated with altered glucose homeostasis (Hussain *et al,* 2007). Thus, CREB signalling could be of importance in CHI development. Also, PI3K-Akt was predicted by the IPA program as a part of this pathway and since PI3K-Akt is part of the insulin signal pathway, this pathway could be affected by the increased secreted insulin observed in CHI (Boucher et al, 2014; Mackenzie and Elliott, 2014) Nine differentially expressed genes from the experimental datasets were found to be part of this canonical pathway. Seven of these genes were identified to be associated with cardiac hypertrophy signalling canonical pathway mentioned above. It was reported that GRIA2 and GRIA3 (both, glutamate ionotropic receptor AMPA type) might be involved in the regulation of insulin secretion (Bertrand *et al,* 1992; Molnar *et al,* 1995; Wu *et al,* 2012). So, based on these findings, it was inferred that these pathways could play roles in CHI development since some of the genes in these pathways are related to insulin secretion regulation. Also, these pathways might not be the reason to develop CHI, rather they could be activated because of the malfunction of other CHI related pathways and thus enhance the complexities related to CHI.

In some cases, a group of proteins known as the upstream regulators might need to be activated or inhibited before regulating downstream target genes/proteins. The observed differential expression of genes in CHI samples might be the result of activation or inhibition of these upstream regulators. It was hypothesised that identification of the cascade of upstream regulators which could play roles in the observed gene expression in the present datasets might help us to understand the disease mechanism. IPA software was used to predict upstream regulators. 27 transcriptional regulators were predicted to have altered activation status. As a consequence a number of biological functions like glucose homeostasis, exocytosis, neurological functions, regulation of cell signalling, inflammatory responses, transport of molecules etc. were predicted to be changed and all of these functions were predicted earlier from the other data analyses approaches mentioned above.

In summary, the basic analyses and class comparison based analyses of present datasets performed by three software programs generated a list of potential CHI candidate genes. These genes were never reported to be associated with CHI earlier. These genes play role in different biological functional pathways like glucose homeostasis, insulin secretion, calcium or potassium ion transport, exocytosis, nervous system development, endocrine

system development, cell communication *etc*. All of these functional pathways are somewhat related to the phenotypes linked with CHI (James *et al*, 2009; Stevens *et al*, 2013; Arya et al, 2014). The possible role of these candidate genes and identified functional pathways need to be checked to provide a new understanding of the disease mechanism.

5.3.5 Using network biology approach to identify key genes associated with CHI

Network biology-based approach is another way to analyse gene expression dataset. It utilises the already published protein-protein interaction (PPI) information. The algorithm of this approach is such that it analyses the patterns of interactions between cellular components (gene, RNA or protein) to identify key regulatory component for a given condition (Barabási and Oltvai, 2004; Pujol *et al*, 2010; Stevens *et al*, 2014). This sort of analytical approach has never been used in CHI research. However, it was believed that this sort of analysis might facilitate the discovery of new insights for CHI management in near future (Banerjee *et al*, 2013, Stevens *et al*, 2013, Stevens *et al*, 2014). So, it was assumed that network biology analysis of the present gene expression datasets might generate a different list of candidate CHI genes as it used a different algorithm. Some of the genes might be in the list generated by class comparison approach earlier in the current study and these common genes could be considered as the most important key genes possibly associated with CHI. Hence, the network biology analysis was carried out based on already published PPI information of the differentially expressed genes of the present datasets. Protein-protein interaction partners (PIPs) (experimentally proven or predicted) of the genes were listed using the PPI search tool, UniHi. This search tool was reported in recent studies to extract authentic PPI information of genes or proteins (Jesmin *et al*, 2010; Wallach *et al*, 2013; Liu *et al*, 2015; Bhargava *et al*, 2015).

Total 50 differentially expressed genes (in order of fold change) whose PPI information was available in PPI databases, were selected for this analysis. The reason to limit the number of differentially expressed genes was to identify crucial and more important genes which could be essential for CHI development. In the process of selecting these analysable genes, 28 genes were not considered since no PPI information was available for them. These genes mainly encode different types of non-coding RNAs (ncRNAs) like small nucleolar RNA. ncRNAs are very important to regulate gene expression through

post-transcriptional modification of ribosomal RNAs (Stepanov *et al,* 2015). Activation or inhibition of these ncRNAs could result in various complex biological diseases like cancer, neurodegenerative disorders *etc*. (Sahoo *et al,* 2008; Chu *et al,* 2012; Mei *et al,* 2012; Stepanov *et al,* 2015). So the identified ncRNAs could be involved in CHI development which needs to be validated further.

The Cytoscape software program was used to analyse biological networks which were generated based on the PPI information listed using UniHi. A good number of genes and proteins were observed in the network to act as central molecules in interaction clusters. Central or highly connected molecules in a biological network are considered essential in a biological process and also believed to be evolved slowly (Yu *et al,* 2004; Kim *et al,* 2006a). In addition, genes or proteins which are essential or very important in biological pathways usually appear to be a central molecule or hub in biological networks (He and Zhang, 2006). However, not all the central molecules are necessary to be important for a particular condition as the central molecules might be essential for a particular function or pathway but they might not be involved in communicating with other functions or pathways and so can be considered comparatively not important in integrated systems of biology (Barabási and Oltvai, 2004; Ye *et al,* 2010; Mao and Zhang, 2013). The network was filtered and analysed to identify truly important genes/proteins. The network was analysed in terms of 5 confidence parameters - average shortest path length (ASP), betweenness centrality (BC), closeness centrality (CC), clustering coefficient (CCo), and degree. ASP is a measurement that indicates an average number of steps that is required by a node in a network to communicate with another node. It is a measure of efficiency to transfer information between nodes in a network (Ye *et al,* 2010; Mao and Zhang, 2013). A node with smaller ASP is considered as important in the network. BC of a node in a network is a measurement that indicates the level of control or influence of the node over transferring information to the other nodes in the network (Newman, 2005; Yoon *et al,* 2006). CC is a measure describing how fast information can transfer from a given node to other nodes in a network, *i.e*. how close a node in a network to all of the other nodes (Newman, 2005). CCo is a measure that describes how well a node in a cluster is connected with neighbour clusters (Barabási and Oltvai, 2004). Degree is the most basic measurement of a node that indicates the number of other nodes it is connected to a network (Barabási and Oltvai, 2004). A node with a high degree number is considered as an important molecule in the network (Barabási and Oltvai, 2004). A node with a high

degree should have a smaller ASP value *i.e.* degree and ASP have a negative correlation (Barabási and Oltvai, 2004; Mao and Zhang, 2013). Pearson correlation between degree and ASP in the network in the present study was calculated to be less than zero that confirmed the negative correlation between them. A node with a high degree should have a higher value of BC, CC and CCo *i.e.* a positive correlation exists between degree and BC, CC and CCo individually (Barabási and Oltvai, 2004; Newman, 2005). However, CCo is independent of the degree of a node (Barabási and Oltvai, 2004). Positive Pearson correlation value was observed between degree and the other three parameters in this analysis. From this network biology approach, 13 genes were predicted as potential candidate genes for CHI. These genes were found to be associated with functions related to cell signalling, immune response, response to chemical stimuli, cell proliferation, exocytosis *etc*. To our knowledge, except *ABCC8*, none of them was previously predicted to be associated with CHI. Interestingly, except *ABCC8*, none of the genes predicted by this network biology approach was predicted by class comparison approach. So based on this network biology analysis, these genes could be important regulatory molecules for CHI development. So, these genes (except *ABCC8*) also could be considered as potential CHI candidate genes.

5.3.6 Validation of the outcomes of the gene expression microarray experiments

In this study, a few potential candidate genes and a number of biological processes were predicted to be linked with CHI through analysing gene expression microarray data. However, these results should be validated before drawing any conclusion. The validation experiments can be carried out at the mRNA level through performing RT-PCR or quantitative qRT-PCR or at the protein level through conducting immunofluorescent studies and western blot experiments.

One of the most recommended and widely used methods to validate the outcomes of microarray data is performing real-time qRT-PCR to compare the expression of target genes in target biological conditions (Rajeevan *et al,* 2001; Sinicropi *et al,* 2006; Qin *et al,* 2006; Thallinger *et al,* 2012). The reason to choose qRT-PCR could be because of the advancement of the method like technical sensitivity, high precision, dynamicity of quantification, reproducibility, low requirement of sample, no post-PCR operations etc. (Klein, 2002; Valasek and Repa, 2005; Sinicropi *et al,* 2006; Francino *et al,* 2006).

However, several studies were reported earlier to observe different levels of agreement between the findings of microarray and qRT-PCR experiments (Beckman *et al,* 2004; Etienne *et al,* 2004; Dallas *et al,* 2005; Wang *et al,* 2006; Thallinger *et al,* 2012). This observed discrepancy of correlation between the findings of microarray and qRT-PCR could be the result of various influencing factors. Both of the methods consist of multiple steps and they differ in various aspects like the method of reverse transcription, reaction chemistries etc. (Thallinger *et al,* 2012). A small change in sample preparation could have a higher impact on the outcomes of the analyses (Freeman *et al.* 1999). The normalisation of the raw data also differs considerably between these methods. In qRT-PCR, data normalisation is carried out by comparing with reference genes which are used to show a constant level of expression irrespective of samples and experimental conditions (Vandesompele *et al,* 2002; Schmittgen and Livak, 2008; Thallinger *et al,* 2012). However, in microarray experiments, data is normalised considering all or a large set of expressed genes to correct the systematic errors (Quackenbush, 2002; Fujita *et al,* 2006; Morey *et al,* 2006). In addition, oligonucleotides in microarray probes and PCR primers might not be the same which could influence the correlation (Thallinger *et al,* 2012). So, the variation of correlation between the outcomes of microarray and qRT-PCR experiments could be resulted because of their own limitation which could influence the data generated from them (Freeman *et al.* 1999; Klein, 2002; Couzin, 2006). Also, different available platforms to conduct microarray and qRT-PCR experiments could be another reason to add variability in the final results (Bustin, 2000; Brazeau, 2004; Mah *et al,* 2004). But it is possible to achieve considerably good correlated results between microarray and qRT-PCR experiments if the cutoff filters (like p-value, fold change etc.) and appropriate normalisation procedures are engaged properly while analysing the raw microarray data (Morey *et al,* 2006). And also, use of more than one platform for both experimentation methods as a cross-validation approach might be helpful to obtain true positive and correlated results (Warnat *et al,* 2005; Bosotti *et al,* 2007; Zhang *et al,* 2016a).

One of the limitations of the gene expression microarray experiments is not to consider the genes that do not pass all the cutoff criteria. Some of the genes might have shown a considerable level of change of expression but the changes might not be statistically significant. Some of the genes might have shown differential gene expression very close but below to the cutoff criteria. These genes might be observed as significant in cross-

platform experiments. It might be helpful to include them in the analysis since these genes could have some important roles in the progression of the disease or the functional anomaly under study. So, the cutoff filters should be selected carefully to obtain proper information from the gene expression study (Morey *et al*, 2006). With these conditions in mind, the cutoff filters for analysing the data of this present gene expression experiments was set to produce reliable and viable information regarding CHI with a high degree of confidence.

5.3.7 Conclusion

The experiments described in this chapter attempted to predict a set of novel candidate genes and pathways that could play roles in the development of CHI. From genome-wide gene expression analyses, a total of 39 genes were predicted by software programs to be important in CHI development. In addition, 27 upstream regulators were predicted to play roles in CHI. All of these predicted genes and regulators are reported to be involved in various biological functions related to insulin secretion regulation. To validate the findings of these microarray data being examined, qRT-PCR could be conducted using RNA extracted from the same tissue samples used for array experiments. However, it was mentioned earlier that the amount of received tissues was very limited; hence no RNA samples were retained to conduct the confirmatory qRT-PCR. Also as it was discussed in Chapter 3 and Chapter 4 that multiple attempts to generate a stable CHI model cell line also failed, so suitable stable CHI model cells were not available to confirm the findings of microarray experiments. Hence, limitation in the availability of CHI tissue samples as well as limited amount of extracted RNA from the tissue samples used in the present study made it impossible to validate the involvement of these genes in CHI. So, further experiments will be required to validate the findings described in this chapter as well as to identify key genes among these predicted potential candidate genes.

Chapter 6

K_{ATP} channel knock-down and generation of transient *in vitro* CHI model

6.1 Introduction

6.1.1 General

It is described in the previous chapter (Chapter 5) that through the genome-wide gene expression experiments of CHI tissues a number of genes and associated biological functions/pathways were predicted to be associated with CHI. However, limitation in the availability of CHI tissue samples as well as a limited amount of extracted RNA from the tissue samples used in the present study made it difficult to validate the involvement of these genes in CHI. Multiple attempts to generate a stable CHI model cell line also failed (discussed in Chapter 3 and Chapter 4). Therefore, suitable stable CHI model cells were not available to confirm the findings of microarray experiments. With a view to validate the findings from the genome-wide gene expression experiments (described in Chapter 5), as an alternative approach, the generation of a transient CHI model cell line was hypothesised to be helpful.

An siRNA-mediated gene silencing approach was explored in the present study to knock-down the expression of K_{ATP} channels in EndoCβH1 cells to generate a population of cells with non-functional channels. It was hypothesised that the cells would acquire CHI characteristics because of these non-functional channel proteins. These defective cells, therefore, would have the potential to validate the findings of gene expression microarray analyses from CHI-affected tissues (described in Chapter 5). Although most of the tissues used in the microarray experiments were affected by *ABCC8* mutations, because of the lack of a suitable antibody against SUR1 (subunit of K_{ATP} channel, product of *ABCC8*) to confirm the gene silencing, the other subunit of the channel, Kir6.2 was targeted to be knocked down by *KCNJ11* gene-specific siRNA to make the channel non-functional. A

suitable antibody against Kir6.2 (product of *KCNJ11*) was available to confirm the gene silencing.

6.1.2 Overview of siRNA-based gene silencing

Knocking out or knocking down a gene is one of the most powerful tools for understanding the function of the target gene product in a cellular system (Santiago *et al,* 2008; Boettcher and McManus, 2015; Shalem *et al,* 2015). One of the pioneering approaches that brought revolution in the ways to knock-out genes utilizes tools that explore RNA interference (RNAi) pathway for repressing the expression of genes (Shalem *et al,* 2015). The RNAi-based knock-out approach was first reported by Fire *et al*. (1998). This pathway is conserved across all eukaryotic organisms (Agrawal *et al,* 2003; Shabalina and Koonin, 2008; Chang *et al,* 2012; Shalem *et al,* 2015). Here in this pathway, target mRNA molecules are degraded, facilitated by a short RNA oligonucleotide with a sequence complementary to the target mRNA (Fire *et al,* 1998; Rana, 2007; Shabalina and Koonin, 2008; Naito and Ui-Tei, 2012). This gene silencing tool was shown earlier to be one of the potent approaches to generate disease model cells (Hommel *et al,* 2003; Rodríguez-Pascau *et al,* 2012; Szlachcic *et al,* 2017). RNAi-based gene knock-out approach has been reported to generate information regarding the overall function of target genes (Root *et al,* 2006; Rana, 2007; Boutros and Ahringer, 2008; Naito and Ui-Tei, 2012).

Several small non-coding RNA molecules are central to the RNAi pathway based gene knock-down strategy. Prominent small RNA molecules are long double-stranded RNA (dsRNA) (Fire *et al,* 1998; Yu *et al,* 2013; Zhou *et al,* 2014), short hairpin RNA (shRNA) (Hommel *et al,* 2003; Root *et al,* 2006; Rodríguez-Pascau *et al,* 2012; Szlachcic *et al,* 2017), microRNA (miRNA) (He and Hannon, 2004; Chendrimada *et al,* 2005; McBride *et al,* 2008) and small interfering RNA (siRNA) (Harborth *et al,* 2001; Elbashir *et al,* 2001; Martinez *et al,* 2002; Morris *et al,* 2004; Han *et al,* 2012). Although all of the above-mentioned RNA molecules can silence target genes, they differ in their mechanism of action, specificity, delivery and hence clinical applications (Rao *et al,* 2009; Lam *et al,* 2015; Xin *et al,* 2017).

6.1.3 siRNA: mechanism of action

Gene-specific synthetic siRNAs are usually manufactured commercially. siRNAs are typically 21-22 nucleotide-long double-stranded RNA molecules with 2 nucleotide overhangs at the 3′ ends (Rana, 2007; Wittrup *et al,* 2015). The two strands of the siRNA have the sequences that are sense and anti-sense to the target region of target mRNA. siRNA molecules are administered into the cells exogenously with the help of different delivery systems depending on cell types. To be functionally active, siRNA needs to be phosphorylated at 5′ ends. Upon entering the cells, siRNA molecules become phosphorylated by an endogenous kinase, Clp1 (Weitzer and Martinez, 2007; Zlatev *et al,* 2016). siRNA processing mediated by Dicer, an RNase III-type enzyme, is conducted in a multiprotein complex known as RNA-induced silencing complex (RISC). This multiprotein complex includes Dicer, Argonaute protein (Ago2, in human RISC), TRBP (HIV-1 transactivation responsive element RNA-binding protein) and other cellular factors (Chendrimada *et al,* 2005; Rana, 2007). TRBP interacts with Dicer complex and then brings Ago2 into the complex (Haase *et al,* 2005; Chendrimada *et al,* 2005; Gregory *et al,* 2005). Once in the RISC complex, the sense strand of the siRNA duplex is discarded, and the antisense strand remains to guide the complex to the target area of the target mRNA. Ago2, an endonuclease, then cleaves the mRNA between nucleotides 10 and 11 upstream of the 5′ end (Elbashir *et al,* 2001; Rana, 2007). Activated RISC can be recycled and can perform silencing of additional mRNAs and thus can amplify the gene silencing effect (Hutvágner and Zamore, 2002; Rana, 2007; Whitehead *et al,* 2009). A schematic representation of the siRNA-mediated gene silencing pathways is illustrated in Figure 6.1.

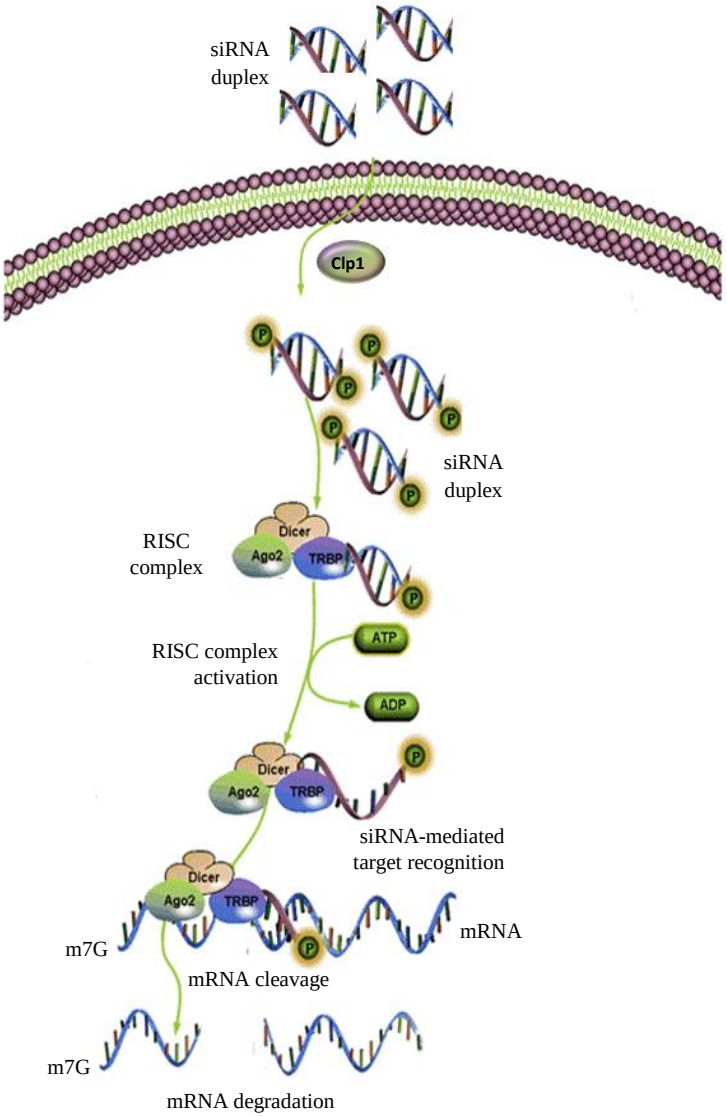

Figure 6.1: **A schematic illustration of the mode of action of siRNA-based gene silencing**. Exogenous synthetic siRNA duplexes get phosphorylated after entering the cell (by Clp1, an endogenous kinase). Then these small RNAs get assembled into the protein complex, known as RNA-induced silencing complex (RISC), along with Dicer, Ago2, TRBP and other factors. Based on the sequence complementarity of guide strands of siRNA duplexes, activated RISC then cleaves target mRNA and thus carries out gene silencing. The image is adapted from http://www.sabiosciences.com/pathway.php?sn=RNAi_Pathway.

6.1.4 Aim and objectives of this study

The **aim of this series of studies** was to generate genetically manipulated transient models of CHI β-cells to support additional studies of the mechanisms of disease.

In order to support this aim, the objectives of this Chapter were:-

a) To use molecular techniques to generate transient models of CHI β-cells following the silencing of K_{ATP} channel genes expression in EndoCβH1 cells by siRNA.

b) To characterise the basic insulin secretion properties of transient models of CHI β-cells.
c) To examine the actions of insulin-secretagogues on insulin secretion in the transient models of CHI β-cells to correlate the gene silencing with insulin secretion.

6.2 Results

6.2.1 siRNA-mediated knocking down of the expression of *KCNJ11* in EndoCβH1 cells

Experiments were designed to knock-down the expression of the *KCNJ11* gene (encoding Kir6.2, the pore-forming subunits of K_{ATP} channel in beta cells) in EndoCβH1 cells with a view to generating transient CHI-like model cells. Here, *KCNJ11* gene-specific siRNA (Pre-designed Silencer Select) was transfected using RNAiMAX reagent (Thermo Fisher Scientific). The efficiency of knock-down of the gene and expression of the protein product, Kir6.2, was measured through Western blot experiments (Figure 6.2). It was found that cells treated with siRNA for 6 days (with the replacement of fresh reagent at day 3) showed better gene knock-down effect compared to the shorter treatments. Treatment with more than 6 days resulted in cell death (data not shown). With the 6-day treatment, ~55% of the expression the Kir6.2 protein was knocked down in the siRNA-transfected cell population in comparison to that of control cell population (Figure 6.3).

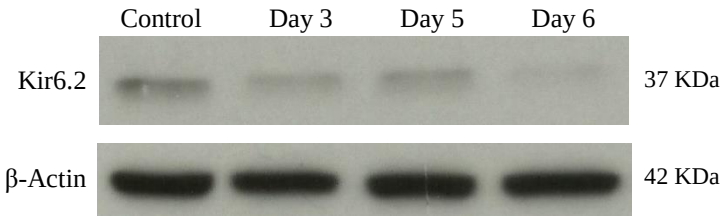

Figure 6.2: **Western blot experiment showing the time course of siRNA-mediated knock-down of *KCNJ11* gene in EndoCβH1 cells**. The image represents the blot showing the relative level of Kir6.2 protein expression in siRNA-treated cell population in different time points (day 3, day 5 and day 6). β-Actin is a housekeeping gene and was used as loading control in the experiment.

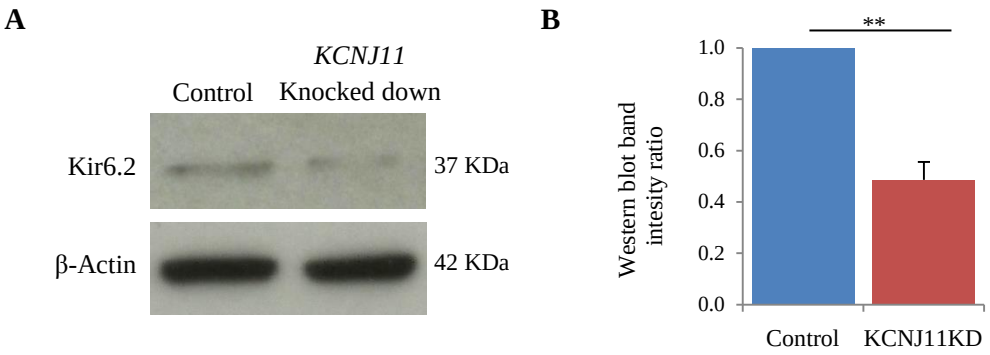

Figure 6.3: **Western blot experiment showing the level of siRNA-mediated knock-down of *KCNJ11* gene in EndoCβH1 cells**. Image A represents the blot images showing the relative level of Kir6.2 protein expression in siRNA-treated cell population. β-Actin is a housekeeping gene and was used as loading control in the experiment. Image B is showing the relative numerical comparison of protein band intensity of Kir6.2 observed in western blot experiments. Data are presented as mean ± SEM (n = 3; 3 independent experiments; ** - p <0.01; unpaired t-test). KCNJ11KD = cells with *KCNJ11* knock-down via siRNA.

To assess changes in the *KCNJ11* gene expression at the transcriptional level, qRT-PCR was performed. Expressions of the *ABCC8* and *INS* genes were investigated as controls. Close to 70% gene knock-down was observed for the *KCNJ11* siRNA-treated cell population (Figure 6.4 A). No effect on gene transcription was observed for *ABCC8*, encoding the other subunit of K_{ATP} channel, in treated cells as expected (Figure 6.4 B). Change of mRNA level of *INS* in siRNA-treated cells was also examined and no significant changes were observed in the expression of that gene (Figure 6.4 C).

The experimental approaches used in the present study could not knock-down all the cells in the siRNA-treated cell population for the expression of the Kir6.2 protein. However, ~55% of cells in the siRNA-treated cell population were knocked down which was viewed as satisfactory. Hence, this cell population was considered for downstream analyses.

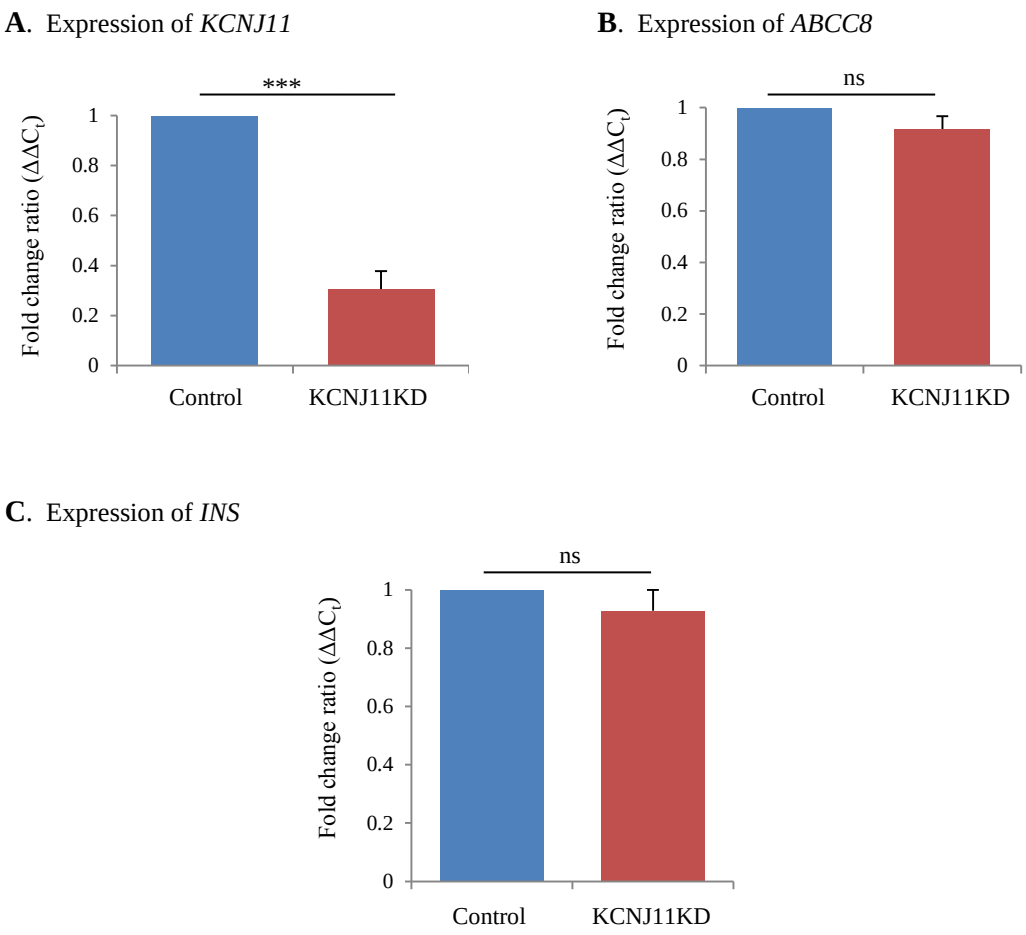

Figure 6.4: **Relative gene expression changes of *KCNJ11, ABCC8* and *INS* in siRNA-mediated knocked down EndoCβH1 cell population**. Values were normalised with the expression of *GAPDH* in each condition. n = 3; 3 independent experiments; *** - p <0.001; ns = not significant; unpaired t-test. Data are presented as mean ± SEM. KCNJ11KD = cells with *KCNJ11* knock-down via siRNA.

6.2.2 Glucose-stimulated insulin secretion assay of *KCNJ11* knocked down EndoCβH1 cells

It was mentioned earlier in chapter 3 that one of the predominant phenotypes of CHI is uncontrolled increased insulin secretion from pancreatic beta cells. To investigate how the *KCNJ11* knocked down (KCNJ11KD) cells behaved in terms of insulin secretion, ELISA-based insulin secretion assays were carried out in the presence of low and high glucose concentrations.

6.2.2.1 KCNJ11KD cells have increased basal insulin secretion

The experiments described here focused on investigating the basal insulin secretion level in KCNJ11KD cells. Significantly increased levels of insulin were observed to be secreted by KCNJ11KD cells in comparison with control EndoCβH1cells (Figure 6.5). In both low (0.5 mM) and high (15 mM) glucose conditions, secretion was significantly higher than the control cells. The secretion was more than five times that in low glucose, and more than 3 times that in high glucose conditions in control cells. Significantly higher insulin secretion was also observed in the presence of high glucose in KCNJ11KD cells compared to the low glucose conditions in KCNJ11KD cells. So, these data indicated that the KCNJ11KD cells acquired increased basal insulin secretion capacity and non-functional K_{ATP} channels in the cells could be the reason for this altered secretion capacity.

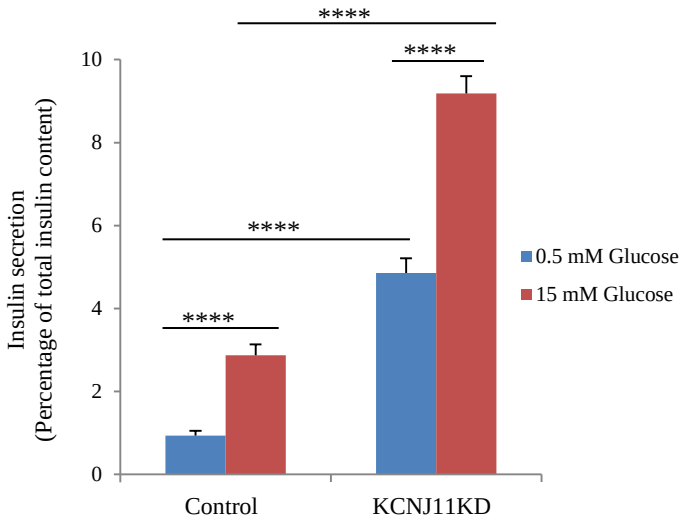

Figure 6.5: **Quantitative assays for glucose-stimulated insulin secretion in KCNJ11KD cells**. Values were normalised and expressed as the percentage of the amount of insulin secreted by the cells from the total insulin content of the cells in individual conditions. n = 3; 3 independent experiments; **** - p <0.0001; unpaired t-test). Data are presented as mean ± SEM

6.2.2.2 Insulin secretion assay of KCNJ11KD cells in presence of insulin secretagogues, tolbutamide

Following on from the previous experiments, the next step was to determine whether the phenomenon of increased insulin secretion in the KCNJ11KD cells was caused by non-

functional K_{ATP} channels (knock-down of *KCNJ11*). Both the control and KCNJ11KD cells were treated with tolbutamide, a known insulin secretagogue which induces secretion by blocking K_{ATP} channels (Mariot *et al*, 1998; Proks *et al*, 2002; Ishiyama *et al*, 2006). Insulin secretions from the treated cells were then investigated.

Insulin secretion was induced significantly in both low and high glucose condition from tolbutamide-treated EndoCβH1 cells compared to untreated control cells. In contrast, no significant changes in insulin secretion were observed in tolbutamide-treated KCNJ11KD cells compared to untreated KCNJ11KD cells in both low and high glucose conditions (Figure 6.6). However, a significantly higher amount of insulin was secreted from tolbutamide-treated KCNJ11KD cells in high glucose conditions than to low glucose condition. Further, in both low and high glucose conditions, insulin secretion from tolbutamide-treated KCNJ11KD cells was observed to be slightly higher (p-value < 0.01 in low glucose; p-value < 0.05 in high glucose) compared to the secretions observed in tolbutamide-treated EndoCβH1 cells. All of these facts indicate the knock-down effect of a proportion of channel proteins in cells.

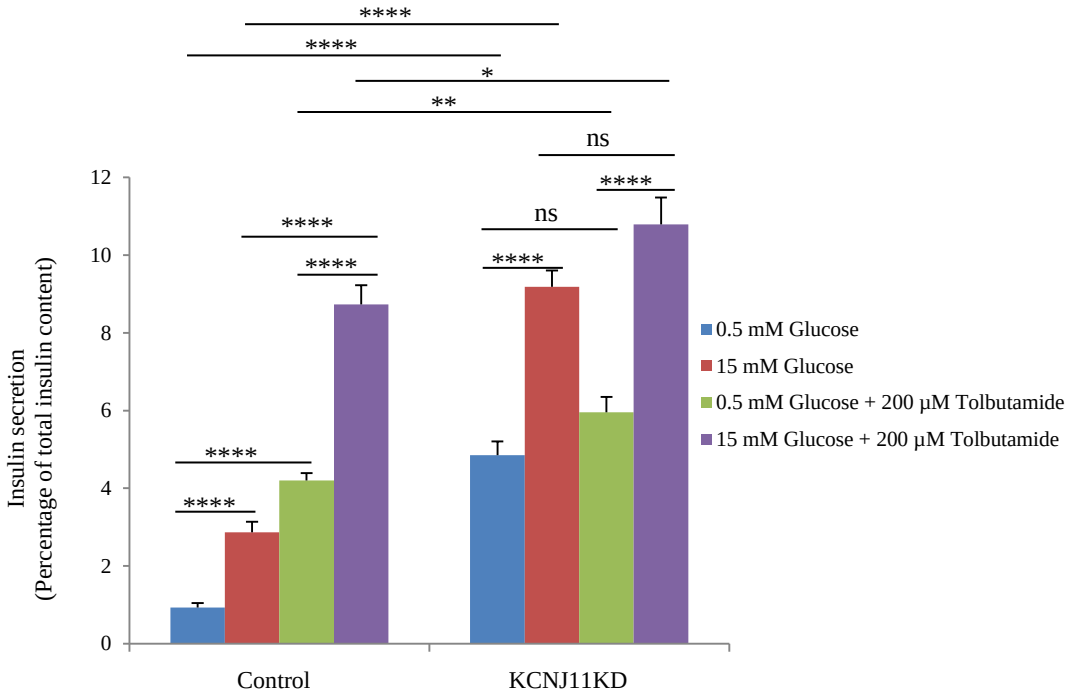

Figure 6.6: **Quantitative assay for glucose-stimulated insulin secretion in KCNJ11KD cells treated with tolbutamide**. Values were normalised and expressed as the percentage of the amount of insulin secreted by the cells from the total insulin content of the cells in individual conditions. n = 3; 3 independent experiments; **** - p <0.0001; ** - p <0.01; * - p <0.05; ns = not significant; unpaired t-test. Data are presented as mean ± SEM.

6.2.2.3 Insulin secretion assay of KCNJ11KD cells in the presence of insulin secretion inhibitor, diazoxide

As described above, tolbutamide could not increase insulin secretion in the KCNJ11KD cells thus suggesting a CHI-like phenotype. Further the effects of channel activation on insulin secretion in KCNJ11KD cells were measured. Diazoxide, a commonly used medication for CHI, is a known K_{ATP} channel activator and thus indirectly insulin secretion inhibitor (mentioned in Chapter 3). Insulin secretion from control EndoCβH1 cells was inhibited significantly after treatment with diazoxide and the secretion could not increase from the basal level even in high glucose concentration (Figure 6.7). In KCNJ11KD cells, the insulin secretion was also inhibited in diazoxide-treated cells in comparison with untreated cells. However, unlike the control cells, insulin secretion was not inhibited to basal level in the diazoxide-treated KCNJ11KD cells. Rather a significant level of insulin secretion was observed in diazoxide-treated KCNJ11KD cells compared to diazoxide-treated control cells. Overall, these data suggest that loss of functional K_{ATP} channel was the reason behind the lower inhibitory effect of diazoxide observed in KCNJ11KD cells. A significant proportion of K_{ATP} channels might be malfunctional because of *KCNJ11*-specific siRNA treatment and these channels turned out to be insensitive to diazoxide treatment. Thus because of the loss of functional K_{ATP} channels increased insulin secretion was observed in KCNJ11KD cells.

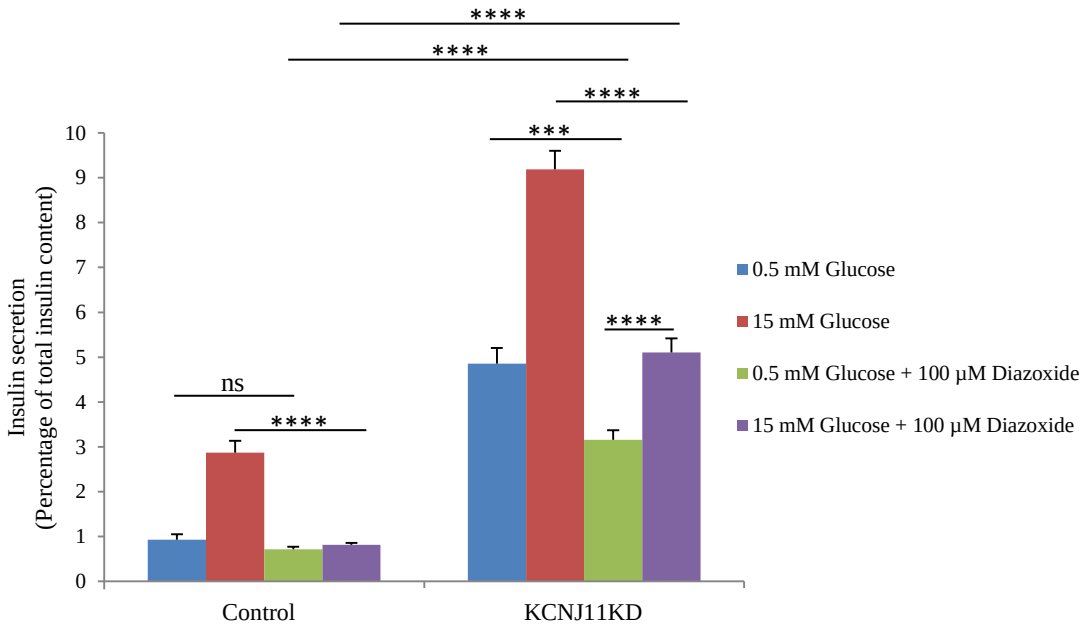

Figure 6.7: **Quantitative assay for glucose-stimulated insulin secretion in KCNJ11KD cells treated with diazoxide**. Values were normalised and expressed as the percentage of the amount of insulin secreted by the cells from the total insulin content of the cells in individual conditions. n = 3; 3 independent experiments; **** - p <0.0001; *** - p <0.001; ns = not significant; unpaired t-test. Data are presented as mean ± SEM.

6.2.2.4 Insulin secretion assay of KCNJ11KD cells in the presence of calcium channel inhibitor, nifedipine

The increased insulin secretion from KCNJ11KD cells could be the result of the altered activity of voltage-activated L-type calcium channels in the cell membrane. These calcium channels in cells could get altered or constitutively activated due to the treatment with siRNA and associated transfection reagents and increased insulin secretion could result. To examine this hypothesis, experiments were designed to investigate the effect of calcium channel inhibition on KCNJ11KD cells insulin secretion property. The cells were treated with nifedipine, a known L-type calcium channel blocker. Insulin secretion from control EndoCβH1 cells was inhibited to the basal secretion level after treatment with nifedipine in both low and high glucose conditions (Figure 6.8). Similar to the nifedipine-treated control cells, insulin secretion from KCNJ11KD cells was also inhibited significantly after treatment with nifedipine. These data suggest that L-type calcium

channels in the cell membrane were not responsible for the increased insulin secretion observed in KCNJ11KD cells. It was observed that insulin secretion was inhibited to basal level in low glucose condition in both nifedipine-treated control and KCNJ11KD cells. However, in high glucose condition, although nifedipine-treated control cells showed the inhibition of insulin secretion, a significantly higher level of insulin secretion was observed in nifedipine-treated KCNJ11KD cells. It was not possible to investigate the reasons behind this increased insulin secretion phenomenon due to time constraints. However, it was hypothesised that a calcium-independent pathway might be activated by a high concentration of glucose that could increase the rate of exocytosis and thus insulin secretion in a ca^{2+}-independent manner (Ämmälä *et al,* 1993; Komatsu *et al,* 1995; Sato *et al,* 1998; Heart *et al,* 2006). So, although nifedipine did not completely abolish insulin secretion in KCNJ11KD cells, the overall inhibition was substantial. From these observations, it can be inferred that L-type calcium channels in the cell membrane were not altered in KCNJ11KD cells. Hence, the observed increased insulin secretion in KCNJ11KD cells was because of the malfunctional K_{ATP} channels.

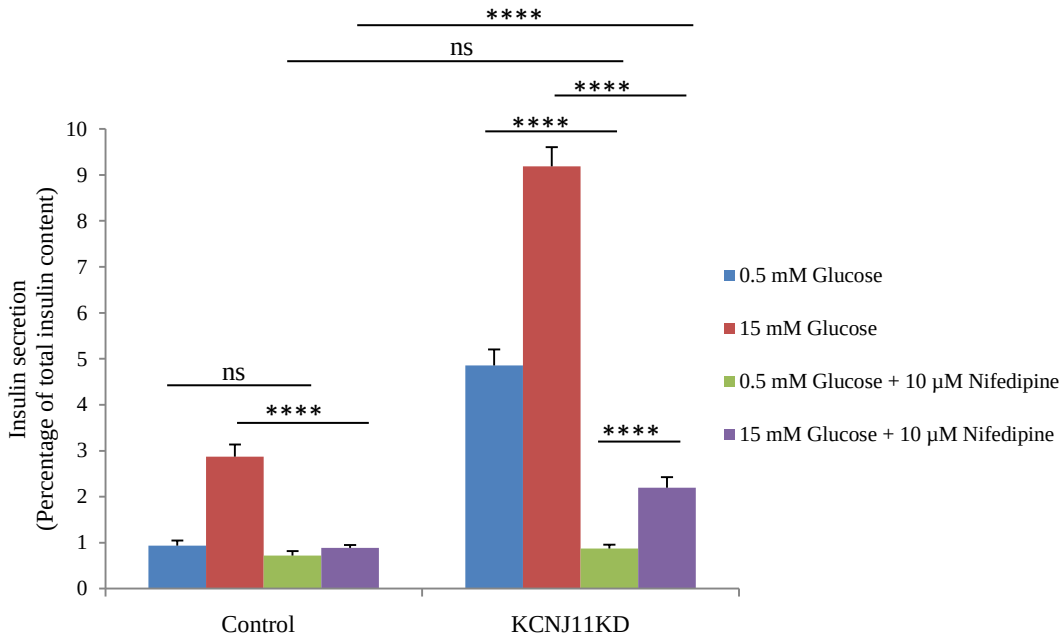

Figure 6.8: **Quantitative assay for glucose-stimulated insulin secretion in KCNJ11KD cells treated with nifedipine.** Values were normalised and expressed as the percentage of the amount of insulin secreted by the cells from the total insulin content of the cells in individual conditions. n = 3; 3 independent experiments; **** - p <0.0001; ns = not significant; unpaired t-test. Data are presented as mean ± SEM.

6.3 Discussion

The principal objective of the experiments described in this chapter was to generate a transient CHI model cell line which would provide a way to validate the findings from the genome-wide gene expression experiments in CHI tissues (described in Chapter 5). Here, siRNA-mediated gene silencing approach was utilised to knock-down the expression of K_{ATP} channels in EndoCβH1 cells with a view to generating a population of cells with non-functional K_{ATP} channels. It was hypothesised that these non-functional K_{ATP} channels could induce the cells to acquire CHI characteristic.

Kir6.2 (pore-forming subunit, the product of *KCNJ11*) expression in EndoCβH1 cells was targeted to be knocked down as a suitable antibody against this protein was available to confirm the gene silencing. ~55% of cells in the *KCNJ11* specific siRNA-treated cell population were knocked down which was viewed as satisfactory for downstream analyses. The KCNJ11KD cells showed increased basal insulin secretion as like CHI. Experimental data from the treatment of KCNJ11KD cells with K_{ATP} channel inhibitor and activator as well as L-type calcium channel inhibitor confirmed that this increased insulin secretion was because of the malfunctional K_{ATP} channels as it is observed in CHI (Inagaki *et al,* 1995; Dunne *et al,* 1997; Shyng *et al,* 1998; Eichmann *et al,* 1999). However, due to time constraints, this transient CHI model cell line could not be used in the validation of the findings from the genome-wide gene expression experiments in CHI tissues (described in Chapter 5).

siRNA is one of the widely used powerful tools to be used to repress genes of interest selectively (Wilson and Doudna, 2013; Jin *et al,* 2016). This tool was used previously to successfully suppress the expression of target genes in different mammalian cells *in vitro* (Elbashir *et al,* 2001; Kosciolek *et al,* 2003; Jin *et al,* 2016; Pileczki *et al,* 2016) as well as *in vivo* (Sørensen *et al,* 2003; Soutschek *et al,* 2004; Zimmermann *et al,* 2006; Alvarez-Erviti *et al,* 2011).

This gene silencing tool was also shown to be effective in suppressing gene expression in different mammalian model pancreatic beta cells *in vitro* and *in vivo* (Goldsworthy *et al,* 2008; Okamoto *et al,* 2012; Wong *et al,* 2013; Scoville *et al,* 2015). The human model pancreatic beta cell line, EndoCβH1, was also shown to be amenable to gene silencing via

siRNA to validate the function of target genes (Scoville *et al,* 2015; Pal *et al,* 2016; Thomsen *et al,* 2016; Grieco *et al,* 2017).

Kir6.2 was targeted in this approach to be knocked down by gene-specific siRNA to make the channel non-functional since suitable antibody against SUR1 (accessory subunit of K_{ATP} channel, the product of *ABCC8*) was not available to confirm the gene silencing. No previous studies have reported using siRNA for suppressing the gene expression of *KCNJ11* in pancreatic cell lines. It was hypothesised that knock-down of the expression of this gene product would make the K_{ATP} channels non-functional and hence, the cells would acquire the CHI characteristics in terms of insulin secretion. So, experiments were designed to knock-down the Kir6.2 protein (pore-forming subunit of K_{ATP} channels). ~55% of the level of expression of Kir6.2 was observed to be suppressed in this gene silencing experiments that resulted in significant up-regulation of insulin secretion in KCNJ11KD cells. This phenomenon resembles the phenotypes associated with CHI (Aynsley-Green *et al,* 1981; González-Barroso *et al,* 2008; Henquin *et al,* 2011; Rahman *et al,* 2015; Guo *et al,* 2017). So the experiment of KCNJ11 gene silencing was considered satisfactory.

Experiments were conducted to investigate whether this excess insulin secretion could be the result of other factors like hyper-activation of voltage-gated L-type calcium channels or different modification of the K_{ATP} channel itself, not because of suppression of the expression of the K_{ATP} channel. To confirm the association of Kir6.2 knock-down with the observed increased insulin secretion in KCNJ11KD cells, experiments were designed to treat the cells with a K_{ATP} channel inhibitor (tolbutamide), a K_{ATP} channel activator (diazoxide) and/or a calcium channel inhibitor (nifedipine) in separate experiments.

Tolbutamide binds to K_{ATP} channel subunit, SUR1 and induces the channel closure (de Wet and proks, 2015). As a consequence, the membrane becomes depolarized that activates voltage-dependent L-type Ca^{2+} channels. The influx of Ca^{2+} then promotes insulin secretion (Mariot *et al,* 1998; Ashcroft and Rorsman, 1989; Proks *et al,* 2002; Dunne *et al,* 2004; Johnson *et al,* 2007a; Henquin and Nenquin, 2016). It was reported in earlier studies that tolbutamide was unable to enhance insulin secretion further in CHI tissues (Grimberg *et al,* 2001; Straub *et al,* 2001; Huopio *et al,* 2002; Henquin *et al,* 2011). It was hypothesised that tolbutamide might not be able to inhibit all those K_{ATP}

channels which were already malfunctional due to siRNA-mediated *KCNJ11* gene silencing. Hence, if the increased basal insulin secretion, observed in the KCNJ11KD cells, were because of these malfunctional K_{ATP} channels, then there should not be much difference in insulin secretion in tolbutamide-treated and untreated KCNJ11KD cells. Experiments were designed to treat the KCNJ11KD cells with tolbutamide to investigate this abovementioned hypothesis. Experimental data suggested that tolbutamide could not enhance insulin secretion any more in KCNJ11KD cells. This finding was similar to what was reported in earlier studies where tolbutamide was unable to enhance insulin secretion further in K_{ATP} channel knock-out mouse models (Miki *et al,* 1998; Seghers *et al,* 2000). This observation indicated that the KCNJ11KD cells truly exhibited CHI-like behaviour. Most of the secreted insulin might be contributed by the uncontrolled secretion of cells because of the knock-down effect of the K_{ATP} channels on the membrane. Henceforth, tolbutamide might not be able to show its overall secretion augmentation activity on the cell population and the contribution of tolbutamide was not reflected in the amount of total secreted insulin.

Diazoxide is a K_{ATP} channel agonist that binds to the channel subunit, SUR1 and induces the channel to be open. Thus it prevents membrane depolarization and consequently inhibits glucose-stimulated insulin secretion from the cells (Mariot *et al,* 1998; Schöfl *et al,* 2000; Dunne *et al,* 2004; Henquin *et al,* 2011). It was hypothesised that diazoxide might not be able to activate all those K_{ATP} channels which were already malfunctional due to siRNA-mediated *KCNJ11* gene silencing. Hence, insulin secretion might not be inhibited completely in the diazoxide-treated KCNJ11KD cells as it would be in the diazoxide-treated control cells. Experiments were designed to treat the KCNJ11KD cells with diazoxide to investigate this abovementioned hypothesis. Experimental data suggested that KCNJ11KD cells showed some inhibitions in insulin secretion activity in both low and high glucose conditions when challenged with diazoxide. Despite diazoxide having an inhibitory effect on KCNJ11KD cells, the level of insulin secretion was still higher than that seen in diazoxide-treated control cells. This inhibition could be the result of the sensitivity to diazoxide of the remaining functional channel proteins which were not knocked down. These channels might be kept open after binding with diazoxide and hence prevented a proportion of insulin secretion. For this inhibitory property, diazoxide is used in the treatment of CHI patients to reduce the secretion of insulin. However, depending on the causative mutations (particularly mutations in K_{ATP} channel genes)

some patients are resistant to diazoxide (Dunne *et al,* 2004; Bakker and Oostdijk, 2006; MacMullen *et al,* 2011; Arnoux *et al,* 2011; Hu *et al,* 2012; Petraitienė *et al,* 2014; Welters *et al,* 2015; Saint-Martin *et al,* 2015; Rahman *et al,* 2015). The experimental KCNJ11KD cell population was showing a similar behaviour towards diazoxide as those CHI patients. KCNJ11KD cells were observed to show some resistance to diazoxide in high glucose. Altogether, these data suggested that increased basal level insulin secretion in KCNJ11KD cells could be due to the malfunctional K_{ATP} channels.

Further, to investigate whether the excess insulin secretion in KCNJ11KD cells could be the result of hyper-activation of voltage-gated L-type calcium channels, experiments were designed to treat the cells with nifedipine, an inhibitor of voltage-gated L-type calcium channel. Nifedipine prevents the exocytosis of insulin-containing granules and consequently insulin secretion (Giugliano *et al,* 1980; Dunne *et al,* 2004; Qureshi *et al,* 2015). It was hypothesised that if the increased insulin secretion observed in KCNJ11KD cells was because of the alteration or hyper-activation of voltage-gated L-type calcium channels, then treatment with nifedipine would not change the insulin secretion much. Nifedipine would not be able to inhibit these calcium channels in KCNJ11KD cells and thus would not be able to inhibit insulin secretion. Experiments were designed to treat the KCNJ11KD cells with nifedipine to investigate this abovementioned hypothesis. In this study, insulin secretion was inhibited in nifedipine-treated control EndoCβH1 cells in both low and high glucose conditions as observed in earlier studies on rodent pancreatic model beta cells (Yaluri *et al,* 2015; Kursan *et al,* 2017). KCNJ11KD cells were found to show strong inhibitions in insulin secretion activity in both low and high glucose conditions when challenged with nifedipine similar to previously reported K_{ATP} channel knock-out mouse models (Munoz *et al,* 2005; Seghers *et al,* 2000). However, the KCNJ11KD cells still exhibited some glucose sensitivity and increased insulin secretion after stimulation with high glucose. A calcium independent pathway might be activated by glucose that could increase the rate of exocytosis and insulin secretion in a ca^{+2}-independent manner (Ämmälä *et al,* 1993; Komatsu *et al,* 1995; Sato *et al,* 1998; Heart *et al,* 2006). So, although nifedipine did not completely put an end to insulin secretion in KCNJ11KD cells, the overall inhibition was significant. From these observations, it can be concluded that the observed increased insulin secretion in KCNJ11KD cells was because of the *KCNJ11* knock-down and thus malfunction of K_{ATP} channels, not because of any alteration in voltage-activated calcium channels or other proteins.

From all of the above-mentioned experiments with KCNJ11KD cells challenged with different K_{ATP} channel activator, inhibitor and calcium channel inhibitor, and the observed pattern of insulin secretion, KCNJ11KD cells can be considered a potential model cell line that can mimic the CHI condition to some extent in terms of increased insulin secretion. Moreover, ongoing research has shown that KCNJ11KD cells exhibit similar gene expression (for some genes that were investigated) to CHI tissue as it was identified in gene expression experiments described in Chapter 5 (A. Ryan and M. Dunne, personal communications). For example, *RAB3B* (member, RAS oncogene family) and *RIMS2* (Regulating synaptic membrane exocytosis 2) were reported earlier to be associated with insulin secretion regulation (Andersson *et al*, 2012; Steneberg *et al*, 2013). Both of these genes, as well as GLP1R (glucagon-like-protein 1 receptor), were observed to be over-expressed in CHI condition (mentioned in Chapter 5). Unpublished work from Dunne research group showed the over-expression of *RAB3B*, *RIMS2* and *GLP1R* genes in the KCNJ11KD cells (A. Ryan and M. Dunne, personal communications). In addition, RNA-sequence arrays were generated from these KCNJ11KD cells. Data from these arrays would be helpful in future to identify novel genes associated with CHI. Thus, this KCNJ11KD cell line could be considered as a potential model CHI-like cell line. Because of time constraints, this cell line could not be used to validate the findings of microarray experiments described in Chapter 5. Future studies may focus on using this cell line to validate the association of potential candidate CHI genes identified in Chapter 5.

Chapter 7

Discussion

7.1 Summary

A number of studies have previously attempted to understand the mechanism of CHI and have identified a number of genes involved in the insulin secretion pathway that are associated with this disease (Nessa *et al*, 2015; Rahman *et al*, 2015). However, in many instances, the aetiology of the disease is yet to be identified (Banerjee *et al*, 2011; Stevens *et al*, 2013; Seniappan *et al*, 2015). A major problem in studying the mechanisms that underlie CHI is that the number of patients is very limited, and thus access to live tissue samples from these patients is also limited. An *in vitro* CHI disease model would, therefore, be helpful to decipher the mechanisms underlying this disease. Thus, the primary focus of the present study was to try to generate a suitable model cell line with CHI-like properties. The other main aim was to generate an informatics resource of mRNA expression profiles from pancreatic tissues obtained from CHI patients in order to identify novel CHI candidate genes.

Briefly, three different approaches were explored to establish a CHI-like model cell line. The first approach was to use insulin secretagogues (ISGs) as chemical inducers of insulin hypersecretion and hyperproliferation of pancreatic beta cells- markers of CHI. ISGs (KCl, tolbutamide, arginine, leucine and glibenclamide) were unable to induce either insulin hypersecretion or hyperproliferation in beta cells. Hence this induction approach was concluded not to be a suitable method to transform beta cells into a CHI-like model system. As an alternative approach, K_{ATP} channel gene, *ABCC8* (encodes the accessory subunit, SUR1 of the K_{ATP} channels), was edited with the CRISPR-Cas9 method in the CHI-iPS and the EndoCβH1 cells with a view to expressing nonfunctional K_{ATP} channels. The CHI-iPS cell line was derived in our laboratory from *ex vivo* expanded pancreas tissue of a CHI patient with a heterozygous recessive mutation in the *ABCC8* gene. The cells were healthy but did not show insulin over-secretion as with CHI. It was postulated that homozygous mutation might be able to induce CHI in these cells in

in vitro condition. In addition, EndoCβH1 cells (a pancreatic beta cell model of human origin) were also tested. Successful target gene editing was observed in a proportion of both CHI-iPS and EndoCβH1 cell populations. However, none of the clonal cell lines generated from single edited CHI-iPS cells retained their stem cell properties beyond a couple of passages. Moreover, edited EndoCβH1 cells were unable to survive as single cells. So editing the *ABCC8* gene to induce CHI characteristics was shown to be an unsuitable approach for generating model CHI-like beta cells from either the CHI-iPS or EndoCβH1 cells. The third approach was to attempt K_{ATP} channel gene knock-down by targeting the *KCNJ11* gene which encodes for the pore-forming subunit, Kir6.2 of the channel proteins using siRNA. In this way, it was hypothesised that it should be possible to produce transient knock-down of K_{ATP} channel function and thereby produce a transient CHI-like model cell line (KCNJ11KD, derived from the EndoCβH1 cell line). As anticipated, KCNJ11KD cells showed CHI-like behaviour in terms of insulin hypersecretion. However, since the effect of siRNA was transient, it was not possible to carry out experiments to determine if these cells were hyperproliferative. The successful generation of this transient cell line thus partially achieved the primary aim of the thesis. Future studies with this model CHI-like cell line will aid better understanding of CHI.

According to the second main aim of the thesis, genome-wide differential gene expression was studied in pancreas tissue samples to identify novel CHI candidate genes and associated pathways. Unlike the previously reported studies where control tissues were derived from non-CHI patients, here in the present study both the control and diseased tissues were collected from CHI patients. Three of these control and diseased tissues were from the same patients (tissue-matched controls). So, the differential gene expression data of CHI tissues in comparison with tissue-matched control tissues were expected to be more reliable and more accurate to be able to predict key CHI-associated genes and pathways. A number of pathways including regulation of insulin secretion, regulation of calcium ion-dependent exocytosis, type B pancreatic cell differentiation, glucose homeostasis, cell cycle regulation, and cell proliferation were identified as potential key CHI-associated pathways based on the differential gene expression. In addition, a total of 39 potential candidate genes were predicted from the differential gene expression datasets to be linked with CHI. Among them, *SSTR2* (somatostatin type 2 receptor) and *GLP1R* (glucagon-like protein 1 receptor) genes were predicted to be among the key genes potentially involved in CHI development. Both of these genes are

involved in insulin secretion and beta cell proliferation (Kailey *et al*, 2012; Meloni *et al*, 2013). In addition, *PPY* (pancreatic polypeptide) was predicted to be another potential key CHI-associated gene. This gene was reported to be involved in the regulation of insulin secretion and glucose homeostasis (Shi *et al*, 2015). Future studies for experimental validation of these predicted candidate genes may provide valuable information for better understanding of CHI mechanism.

To conclude, this thesis work has successfully generated a transient CHI-like model cell line (KCNJ11KD) and has been able to identify a number of potential CHI candidate genes and key pathways. These findings need to be validated further to confirm their association with CHI and their roles in the mechanism(s) underlying CHI. The KCNJ11KD cell line could provide a model with which to study the association of these predicted candidate genes with CHI and for the other future studies on CHI.

7.2 Contribution to the understanding of CHI

7.2.1 Establishment of CHI-like model cell line

This thesis work primarily attempted on establishing a suitable *in vitro* CHI model cell line following three approaches- ISG-based induction, K_{ATP} channel gene editing, and siRNA-based K_{ATP} channel gene silencing approach.

7.2.1.1 ISG-based induction method

Insulin, supplied as nutrient supplement, was reported to stimulate cell proliferation, and increased beta cell proliferation has been reported to be associated with increased insulin secretion (Heni *et al*, 2011; Dadon *et al*, 2012; Li *et al*, 2017). This present study attempted to stimulate cells using insulin secretagogues (ISGs) for insulin hypersecretion to bring changes in cell proliferation as well as insulin secretion capacities. However, no acquired changes were observed in cells. No studies were reported earlier to use ISGs for inducing CHI characteristics in pancreatic beta cells. As this approach was not successful, hence, it was concluded that ISG-based cell induction approach may not be suitable to transform beta cells into the CHI-like model systems and hence, this approach should not be used in future studies.

7.2.1.2 K_{ATP} channel gene-editing approach

The most common cause of CHI is the loss of functional K_{ATP} channels in beta cells (Yorifuji, 2014; Nessa *et al*, 2016). Before the commencement of the present study, there were no reports of attempts to edit K_{ATP} channel genes in order to induce CHI-like characteristics in cells. However, in the latter stages of the project, one group did report a CHI-like model cell line by introducing mutations in the *ABCC8* gene (encoding SUR1 subunit of K_{ATP} channel) into a stem cell line (H1) using the CRISPR-Cas9 gene-editing method (Guo *et al*, 2017).

As indicated earlier, in the present study target gene editing of *ABCC8* using CRISPR-Cas9 was successful in CHI-iPS cells. However, control of these gene-edited cells to create stable and undifferentiated cells lines was not achieved. Unfortunately, Guo *et al.* (2017) did not report their method for growing the edited stem cells. So it was not possible to compare the two studies to identify any discrepancies that may account for the different outcomes. Nevertheless, since Guo and colleagues have shown that it is possible to establish CHI-like model cell line from stem cells through the modification of K_{ATP} channel genes, it should be possible to generate CHI-like model cell line from CHI-iPS cells in future. However, a viable protocol to grow the edited stem cells as an undifferentiated stem cell line will be necessary. It was suggested that irradiated mouse embryonic fibroblast (MEF) cells can be used as feeder cells to enhance the survival of the edited single cells (Yang *et al*, 2013; Byrne *et al*, 2014). These MEF cells can grow in culture but can not propagate because of the irradiation treatment (Byrne *et al*, 2014). However, MEF cells are able to secrete several important growth factors which could be helpful for the survival and single-cell clonal propagation of the edited stem cells and maintain their pluripotency (Hongisto *et al*, 2012; Yang *et al*, 2013; Singhal *et al*, 2016). A very recent study demonstrated the Stem-Flex media (a commercially available stem cell growth media) is efficient for single-cell cloning of stem cells to support genome-editing experiments (Chen and Pruett-Miller, 2018). Future studies may explore these approaches to enhance the stability of edited CHI-iPS cells.

The present study has also shown that it is possible to use the CRISPR-Cas9 method for successful gene editing in EndoCβH1 cells. However, the failure of the single-cell clonal propagation of EndoCβH1 cells makes the cells inappropriate for generating CHI-like

model cells. No study was reported earlier to conduct gene-editing experiments on EndoCβH1 cells followed by single-cell clonal propagation of the cells. A viable protocol for single-cell clonal propagation will be necessary to use these cells for the generation of CHI-like model cells. Inter-α-inhibitor (IαI), a human serum-derived protein has been reported to enhance single-cell survival and supports clonal expansion (Pijuan-Galito *et al*, 2016). Also, earlier studies suggest that epidermal growth factor and fibroblast growth factor support the clonal expansion of mammalian cells which are difficult to culture as single cells (Lee *et al*, 1997; Xu *et al*, 2005; Levenstein *et al*, 2006). Future studies could attempt to optimize the single-cell culture protocol for this cell line by adding the growth factors mentioned above. Alternatively, single-cell clonal expansion of EndoCβH1 cells could be conducted by growing the cells on irradiated fibroblasts cells as feeder cells (Byrne *et al*, 2014; Yang *et al*, 2014a).

7.2.1.3 siRNA-based K_{ATP} channel gene silencing approach

Since the above-mentioned two approaches failed to establish a stable CHI-like model cell line, hence, this study attempted to generate transient CHI-like cells by siRNA-based gene silencing approach. No previous studies had been reported where K_{ATP} channel genes were knocked down transiently by gene-specific siRNAs to induce CHI characteristics in beta cells. These transient CHI-like cells (KCNJ11KD) showed increased basal insulin secretion; consistent with reports highlighting the importance of non-functional K_{ATP} channels in CHI (Kapoor *et al*, 2013; Nessa *et al*, 2016). Since generating the KCNJ11KD cell line was part of this thesis work, further characterisation of these cells has been undertaken in the Dunne laboratory. This further work has shown that KCNJ11KD cells exhibit gene expression similar to CHI tissue (A. Ryan and M. Dunne, personal communications). For example, *GLP1R* and *PPY* genes showed differential expression in these KCNJ11KD cells similar to the CHI tissues. In addition, *RAB3B* (Ras-associated small molecular mass GTP-binding protein), and *RIMS2* (regulating synaptic membrane exocytosis 2) were found to be upregulated in CHI tissues. These genes have previously been reported to be associated with regulation of insulin secretion (Lezzi *et al*, 1999; Kashima *et al*, 2001; Norlin *et al*, 2005). Notably, upregulation in these genes was also observed in the KCNJ11KD cells. These observations support our earlier findings and provide further evidence that KCNJ11KD cells have CHI-like properties. Thus - a good starting model for further investigations.

The limitation of this cell model is that the effect of K_{ATP} channel knockdown is transient and therefore, the cell line is not stable. Thus, for each experiment, pancreatic beta cells would need to be treated again with siRNA to produce knockdown of K_{ATP} channel expression. Importantly however, this KCNJ11KD cell line did exhibit characteristics similar to CHI and so is a potential model cell system that can be used in further research (some examples are mentioned in section 7.3) to better understand the mechanisms underlying CHI.

7.2.2 Differential gene expression study using microarray

As described elsewhere, CHI is genotypically multifactorial, genes/proteins from multiple pathways are likely to be involved in the development of the disease (Stevens *et al*, 2013). A transcriptomic dataset would, therefore, be a highly valuable resource to help gain further understanding of how CHI is associated with altered expression of different genes and proteins (Wang *et al,* 2007; Kao *et al,* 2017). Two previous studies have attempted to study differential gene expression in CHI tissues to identify candidate genes and pathways associated with CHI (Rahman *et al,* 2015b; Senniappan *et al,* 2016). These studies used CHI tissues and age-matched control pancreatic tissues (tissues from non-CHI patients) to look at differential gene expression. In the present study, however, both the healthy tissues (as control) and lesion tissues were collected from CHI affected pancreas. Moreover, three of these control and diseased tissues were from the same individual patient (tissue-matched controls). No previous study has been reported earlier where both the healthy tissues and lesion tissues were collected from CHI affected pancreas and used for differential gene expression-based CHI study. Similar approaches of using control and lesion tissues from diseased patients for differential gene expression assays were reported previously for colon cancer, lung cancer and tumorigenesis-related studies (Resnick *et al,* 2005; Kim *et al,* 2006; Zhao *et al,* 2009). It was hypothesised that comparing the transcriptional expression profiles between healthy and lesion tissues, both from CHI affected pancreas, would lead to more reliable identification of CHI related genes and pathways (Stevens *et al,* 2013; Senniappan *et al,* 2016). However, it is not evident whether there is any difference in the outcome of the studies if not the control and lesion tissues are from same individual patients.

A number of pathways including regulation of insulin secretion, regulation of calcium ion-dependent exocytosis, glucose homeostasis, type B pancreatic cell differentiation, cell cycle regulation, and cell proliferation were predicted as potential key CHI-associated pathways based on the differential gene expression patterns observed in the present study. Previous studies have reported the association of CHI with some of these pathways including insulin secretion, glucose homeostasis and cell cycle regulation (Kassem *et al*, 2010; Senniappan *et al*, 2012; Rahman *et al*, 2015a). Senniappan *et al.* (2016) reported the IGF-1/mTOR/Akt pathway as a potential CHI pathway, however, the present study did not find the association of this pathway with CHI. A total of 39 potential CHI candidate genes were predicted from the present study. Among them, *SSTR2, GLP1R* and *PPY* genes were predicted to be among the key genes potentially involved in CHI development. These genes are involved in the regulation of insulin secretion, glucose homeostasis, and beta cell proliferation (Kailey *et al*, 2012; Meloni *et al*, 2013; Shi *et al*, 2015). Ongoing research in the Dunne laboratory has shown similar CHI-like differential expression of *GLP1R* and *PPY* genes in KCNJ11KD cells. Rahman *et al.* (2015b) reported *DPP-4* and *PYY* genes as potential CHI genes based on differential gene expression-based studies. However, these genes were not identified as CHI genes in the present study. The differences in the sources of control tissues could be the reasons behind these observed variances, though there is no previous report in support of this hypothesis. Among the previously identified CHI genes (mentioned in Chapter 1), *ABCC8* and *HADH* are the two genes whose differential expression was observed in all CHI tissue samples in the present study.

The predicted 39 candidate genes from the present differential gene expression study have not previously been reported to be linked with CHI. These candidate genes are either directly or indirectly related to glucose homeostasis and insulin secretion, so they could play vital roles in disease progression. Experimental validation of these candidate genes may provide valuable information for better understanding of CHI mechanism in future.

7.3 Future perspectives

The transient CHI-like cell line, KCNJ11KD showed uncontrolled increased insulin secretion. On-going research has shown gene expression in these cells (for some genes that were investigated) similar to the differential gene expression datasets generated from

CHI tissues in the present study (mentioned in section 7.2.1.3) (A. Ryan and M. Dunne, personal communications). Further, RNA-sequence arrays (RNA-Seq) were generated from these KCNJ11KD cells by the Dunne Laboratory as the facility for this experiment was available at the University of Manchester. In compared to gene expression microarray, RNA-Seq is more sensitive and accurate in detecting the expression of genes (Zhao *et al*, 2014; Rai *et al*, 2018; Rao *et al*, 2019). This technology is also better in detecting gene isoforms as well as novel transcripts which could be potentially associated with a biological phenomenon (Rai *et al*, 2018). Data from these assays would be helpful in future to identify novel genes and pathways potentially associated with CHI.

In addition to the previously reported CHI-associated genes (mentioned in section 1.3), the present study also identified 39 more potential candidate genes. Among them, *SSTR2*, *GLP1R* and *PPY* genes were predicted to be the key genes. However, these genes need to be experimentally validated. As discussed above, KCNJ11KD cell line could provide a useful model to validate these potential gene candidates in CHI. Quantitative PCR (qRT-PCR) based comparative gene expression studies in KCNJ11KD cells could be an option for validating these genes. Further, comparative studies between the data from differential gene expression of CHI tissues and RNA-sequence arrays from the KCNJ11KD cells would be more supportive to identify key candidate genes. siRNA-mediated gene knock-down experiments in the EndoCβH1 cells could also be used to validate the involvement of these key genes in CHI.

7.4 Concluding remarks

To conclude, a siRNA-mediated K_{ATP} channel gene knock-down approach was successfully used to generate a transient CHI-like model cell line (KCNJ11KD) that showed CHI-like behaviour in terms of uncontrolled insulin secretion, and thus partially achieved the primary aim of the thesis. Subsequent experiments conducted in the Dunne lab have obtained gene expression data that are also consistent with CHI-like properties of these cells. Future studies with this model CHI-like cell line could thus provide valuable information for a better understanding of CHI. Differential gene expression microarray analyses on pancreas tissue from CHI patients identified a total of 39 potential candidate genes that are predicted to be linked with CHI. Future studies for experimental

validation and identifying key genes among the predicted candidate genes will provide valuable information for better understanding of CHI mechanism.

References

Aamodt, K. I. & Powers, A. C. (2017). Signals in the pancreatic islet microenvironment influence β-cell proliferation. *Diabetes, obesity and metabolism,* 19(S1)**,** 124-136.

Adi, A., Abbas, B. B., Hamed, M. A., Tassan, N. A. & Bakheet, D. (2015). Screening for Mutations in *ABCC8* and *KCNJ11* Genes in Saudi Persistent Hyperinsulinemic Hypoglycemia of Infancy (PHHI) Patients. *Genes,* 6(2)**,** 206-215.

Adriaens, M. E., Jaillard, M., Waagmeester, A., Coort, S. L., Pico, A. R. & Evelo, C. T. (2008). The public road to high-quality curated biological pathways. *Drug discovery today,* 13(19-20)**,** 856-862.

Affourtit, C. & Brand, M. D. (2008). Uncoupling protein-2 contributes significantly to high mitochondrial proton leak in INS-1E insulinoma cells and attenuates glucose-stimulated insulin secretion. *Biochemical journal,* 409(1)**,** 199-204.

Afrikanova, I., Kayali, A., Lopez, A. & Hayek, A. (2012). Is stage-specific embryonic antigen 4 a marker for human ductal stem/progenitor cells? *BioResearch open access,* 1(4)**,** 184-191.

Agrawal, N., Dasaradhi, P., Mohmmed, A., Malhotra, P., Bhatnagar, R. K. & Mukherjee, S. K. (2003). RNA interference: biology, mechanism, and applications. *Microbiology and molecular biology reviews,* 67(4)**,** 657-685.

Aguilar-Bryan, L. & Bryan, J. (1999). Molecular biology of adenosine triphosphate-sensitive potassium channels. *Endocrine reviews,* 20(2)**,** 101-135.

Aguilar-Bryan, L., Nichols, C. G., Wechsler, S. W., Clement, J. P., Boyd, A., Gonzalez, G., Herrera-Sosa, H., Nguy, K., Bryan, J. & Nelson, D. A. (1995). Cloning of the β-cell high-affinity sulfonylurea receptor: a regulator of insulin secretion. *Science,* 268(5209)**,** 423-426.

Ahlgren, U., Jonsson, J., Jonsson, L., Simu, K. & Edlund, H. (1998). β-Cell-specific inactivation of the mouseIpf1/Pdx1 gene results in loss of the β-cell phenotype and maturity onset diabetes. *Genes & development,* 12(12)**,** 1763-1768.

Alon, U., Barkai, N., Notterman, D. A., Gish, K., Ybarra, S., Mack, D. & Levine, A. J. (1999). Broad patterns of gene expression revealed by clustering analysis of tumor and normal colon tissues probed by oligonucleotide arrays. *Proceedings of the national academy of sciences,* 96(12)**,** 6745-6750.

Altarejos, J. Y. & Montminy, M. (2011). CREB and the CRTC co-activators: sensors for hormonal and metabolic signals. *Nature reviews molecular cell biology,* 12(3)**,** 141-151.

Alvarez-Erviti, L., Seow, Y., Yin, H., Betts, C., Lakhal, S. & Wood, M. J. (2011). Delivery of siRNA to the mouse brain by systemic injection of targeted exosomes. *Nature biotechnology,* 29(4)**,** 341-345.

Amin, R., Chen, H.-Q., Tannous, M., Gibbs, R. & Kowluru, A. (2002). Inhibition of glucose-and calcium-induced insulin secretion from βTC3 cells by novel inhibitors of protein isoprenylation. *Journal of pharmacology and experimental therapeutics,* 303(1)**,** 82-88.

Amini, S., Fathi, F., Mobalegi, J., Sofimajidpour, H. & Ghadimi, T. (2014). The expressions of stem cell markers: Oct4, Nanog, Sox2, nucleostemin, Bmi, Zfx, Tcl1, Tbx3, Dppa4, and Esrrb in bladder, colon, and prostate cancer, and certain cancer cell lines. *Anatomy & cell biology,* 47(1)**,** 1-11.

Amit, M., Carpenter, M. K., Inokuma, M. S., Chiu, C.-P., Harris, C. P., Waknitz, M. A., Itskovitz-Eldor, J. & Thomson, J. A. (2000). Clonally derived human embryonic stem cell lines maintain pluripotency and proliferative potential for prolonged periods of culture. *Developmental biology,* 227(2)**,** 271-278.

Ammala, C., Ashcroft, F. M. & Rorsman, P. (1993). Calcium-independent potentiation of insulin release by cyclic AMP in single β-cells. *Nature,* 363(6427)**,** 356-358.

Ammala, C., Moorhouse, A. & Ashcroft, F. (1996a). The sulphonylurea receptor confers diazoxide sensitivity on the inwardly rectifying K^+ channel Kir6. 1 expressed in human embryonic kidney cells. *The journal of physiology,* 494(3)**,** 709-714.

Ammala, C., Moorhouse, A., Gribble, F., Ashfleld, R., Proks, P., Smith, P. A., Sakura, H., Coles, B., Ashcroft, S. J. & Ashcroft, F. M. (1996b). Promiscuous coupling between the sulphonylurea receptor and inwardly rectifying potassium channels. *Nature,* 379(6565)**,** 545-548.

Andersson, L. E., Valtat, B., Bagge, A., Sharoyko, V. V., Nicholls, D. G., Ravassard, P., Scharfmann, R., Spégel, P. & Mulder, H. (2015). Characterization of stimulus-secretion coupling in the human pancreatic EndoC-βH1 beta cell line. *PLoS one,* 10(3)**,** e0120879.

Andersson, S. A., Olsson, A. H., Esguerra, J. L., Heimann, E., Ladenvall, C., Edlund, A., Salehi, A., Taneera, J., Degerman, E. & Groop, L. (2012). Reduced insulin secretion correlates with decreased expression of exocytotic genes in pancreatic islets from patients with type 2 diabetes. *Molecular and cellular endocrinology,* 364(1-2), 36-45.

Anello, M., Ucciardello, V., Piro, S., Patané, G., Frittitta, L., Calabrese, V., Giuffrida Stella, A., Vigneri, R., Purrello, F. & Rabuazzo, A. (2001). Chronic exposure to high leucine impairs glucose-induced insulin release by lowering the ATP-to-ADP ratio. *American journal of physiology-endocrinology and metabolism,* 281(5)**,** E1082-E1087.

Antonucci, S., Tagliavini, A. & Pedersen, M. G. (2015). Reactive oxygen and nitrogen species disturb Ca^{2+} oscillations in insulin-secreting MIN6 β-cells. *Islets,* 7(4)**,** e1107255.

Arnold, E. S., Ling, S.-C., Huelga, S. C., Lagier-Tourenne, C., Polymenidou, M., Ditsworth, D., Kordasiewicz, H. B., McAlonis-Downes, M., Platoshyn, O. & Parone, P. A. (2013). ALS-linked TDP-43 mutations produce aberrant RNA splicing and adult-onset motor neuron disease without aggregation or loss of nuclear TDP-43. *Proceedings of the national academy of sciences,* 110(8)**,** E736-E745.

Arnould, T., Vankoningsloo, S., Renard, P., Houbion, A., Ninane, N., Demazy, C., Remacle, J. & Raes, M. (2002). CREB activation induced by mitochondrial dysfunction is a new signaling pathway that impairs cell proliferation. *The EMBO journal,* 21(1-2)**,** 53-63.

Arnoux, J.-B., Verkarre, V., Saint-Martin, C., Montravers, F., Brassier, A., Valayannopoulos, V., Brunelle, F., Fournet, J.-C., Robert, J.-J. & Aigrain, Y. (2011). Congenital hyperinsulinism: current trends in diagnosis and therapy. *Orphanet journal of rare diseases,* 6**,** 63.

Arya, V., Mohammed, Z., Blankenstein, O., De Lonlay, P. & Hussain, K. (2014). Hyperinsulinaemic hypoglycaemia. *Hormone and metabolic research,* 46(03)**,** 157-170.

Asfari, M., Janjic, D., Meda, P., Li, G., Halban, P. A. & Wollheim, C. B. (1992). Establishment of 2-mercaptoethanol-dependent differentiated insulin-secreting cell lines. *Endocrinology,* 130(1)**,** 167-178.

Ashburner, M., Ball, C. A., Blake, J. A., Botstein, D., Butler, H., Cherry, J. M., Davis, A. P., Dolinski, K., Dwight, S. S. & Eppig, J. T. (2000). Gene Ontology: tool for the unification of biology. *Nature genetics,* 25(1)**,** 25-29.

Ashcroft, F. M. (1988). Adenosine 5'-triphosphate-sensitive potassium channels. *Annual review of neuroscience,* 11(1), 97-118.

Ashcroft, F. M., Harrison, D. E. & Ashcroft, S. J. (1984). Glucose induces closure of single potassium channels in isolated rat pancreatic β-cells. *Nature,* 312(5993)**,** 446-448.

Ashcroft, F. M. & Rorsman, P. (1989). Electrophysiology of the pancreatic β-cell. *Progress in biophysics and molecular biology,* 54(2)**,** 87-143.

Ashcroft, S. J., Weerasinghe, L. C. C. & Randle, P. J. (1973). Interrelationship of islet metabolism, adenosine triphosphate content and insulin release. *The biochemical.j ournal,* 132**,** 223-231.

Atiya, A. W., Moldovan, S., Adrian, T. E., Coy, D., Walsh, J. & Brunicardi, F. C. (1997). Intraislet somatostatin inhibits insulin (via a subtype-2 somatostatin receptor) but not islet amyloid polypeptide secretion in the isolated perfused human pancreas. *Journal of gastrointestinal surgery,* 1(3)**,** 251-256.

Aubert, J., Bar-Hen, A., Daudin, J.-J. & Robin, S. (2004). Determination of the differentially expressed genes in microarray experiments using local FDR. *BMC bioinformatics,* 5(1)**,** 125.

Avatapalle, B. H., Banerjee, I. I., Shah, S., Pryce, M., Nicholson, J., Rigby, L., Caine, L., Didi, M., Skae, M. & Ehtisham, S. (2013). Abnormal neurodevelopmental outcomes are common in children with transient congenital hyperinsulinism. *Frontiers in endocrinology,* 4**,** 60.

Avrahami, D., Li, C., Yu, M., Jiao, Y., Zhang, J., Naji, A., Ziaie, S., Glaser, B. & Kaestner, K. H. (2014). Targeting the cell cycle inhibitor p57 Kip2 promotes adult human β cell replication. *The Journal of clinical investigation,* 124(2), 670-674.

Axelsson, A., Mahdi, T., Nenonen, H., Singh, T., Hänzelmann, S., Wendt, A., Bagge, A., Reinbothe, T., Millstein, J. & Yang, X. (2017). Sox5 regulates beta-cell phenotype and is reduced in type 2 diabetes. *Nature communications,* 8**,** 15652.

Aynsley-Green, A., Hussain, K., Hall, J., Saudubray, J., Nihoul-Fekete, C., De Lonlay-Debeney, P., Brunelle, F., Otonkoski, T., Thornton, P. & Lindley, K. (2000). Practical management of hyperinsulinism in infancy. *Archives of disease in childhood-fetal and neonatal edition,* 82(2)**,** F98-F107.

Aynsley-Green, A., Polak, J., Bloom, S., Gough, M., Keeling, J., Ashcroft, S., Turner, R. & Baum, J. (1981). Nesidioblastosis of the pancreas: definition of the syndrome and the management of the severe neonatal hyperinsulinaemic hypoglycaemia. *Archives of disease in childhood,* 56(7)**,** 496-508.

Azmi, A. S., Beck, F. W., Bao, B., Mohammad, R. M. & Sarkar, F. H. (2011). Aberrant epigenetic grooming of miRNAs in pancreatic cancer: a systems biology perspective. *Epigenomics,* 3(6), 747-759.

Babenko, A. P., Polak, M., Cavé, H., Busiah, K., Czernichow, P., Scharfmann, R., Bryan, J., Aguilar-Bryan, L., Vaxillaire, M. & Froguel, P. (2006). Activating mutations in the *ABCC8* gene in neonatal diabetes mellitus. *New England journal of medicine,* 355(5)**,** 456-466.

Babon, J., McKenzie, M. & Cotton, R. (2003). The use of resolvases T4 endonuclease VII and T7 endonuclease I in mutation detection. *Molecular biotechnology,* 23(1)**,** 73-81.

Bach, S. P., Renehan, A. G. & Potten, C. S. (2000). Stem cells: the intestinal stem cell as a paradigm. *Carcinogenesis,* 21(3)**,** 469-476.

Bader, G. D., Donaldson, I., Wolting, C., Ouellette, B. F., Pawson, T. & Hogue, C. W. (2001). BIND-the biomolecular interaction network database. *Nucleic acids research,* 29(1)**,** 242-245.

Bagyánszki, M. & Bódi, N. (2012). Diabetes-related alterations in the enteric nervous system and its microenvironment. *World journal of diabetes,* 3(5)**,** 80-93.

Bakker, B. & Oostdijk, W. (2006). Diagnosis and management of congenital hyperinsulinism: a case report. *European journal of endocrinology,* 155(suppl 1)**,** S153-S155.

Ball, A. J., Flatt, P. R. & McClenaghan, N. H. (2000). Desensitization of sulphonylurea-and nutrient-induced insulin secretion following prolonged treatment with glibenclamide. *European journal of pharmacology,* 408(3)**,** 327-333.

Banerjee, I., Avatapalle, B., Padidela, R., Stevens, A., Cosgrove, K., Clayton, P. & Dunne, M. (2013). Integrating genetic and imaging investigations into the clinical management of congenital hyperinsulinism. *Clinical endocrinology,* 78(6)**,** 803-813.

Banerjee, I., Skae, M., Flanagan, S. E., Rigby, L., Patel, L., Didi, M., Blair, J., Ehtisham, S., Ellard, S. & Cosgrove, K. E. (2011). The contribution of rapid K_{ATP} channel gene mutation analysis to the clinical management of children with congenital hyperinsulinism. *European journal of endocrinology,* 164(5)**,** 733-740.

Bar-Nur, O., Russ, H. A., Efrat, S. & Benvenisty, N. (2011). Epigenetic memory and preferential lineage-specific differentiation in induced pluripotent stem cells derived from human pancreatic islet beta cells. *Cell stem cell,* 9(1)**,** 17-23.

Barabasi, A.-L. & Oltvai, Z. N. (2004). Network biology: understanding the cell's functional organization. *Nature reviews genetics,* 5(2)**,** 101-113.

Bas, F., Darendeliler, F., Demirkol, D., Bundak, R., Saka, N. & Günöz, H. (1999). Successful therapy with calcium channel blocker (nifedipine) in persistent neonatal hyperinsulinemic hypoglycemia of infancy. *Journal of pediatric endocrinology and metabolism,* 12(6)**,** 873-878.

Beckman, K. B., Lee, K. Y., Golden, T. & Melov, S. (2004). Gene expression profiling in mitochondrial disease: assessment of microarray accuracy by high-throughput Q-PCR. *Mitochondrion,* 4(5)**,** 453-470.

Beith, J. L., Alejandro, E. U. & Johnson, J. D. (2008). Insulin stimulates primary β-cell proliferation via Raf-1 kinase. *Endocrinology,* 149(5)**,** 2251-2260.

Bell, C. G., Teschendorff, A. E., Rakyan, V. K., Maxwell, A. P., Beck, S. & Savage, D. A. (2010). Genome-wide DNA methylation analysis for diabetic nephropathy in type 1 diabetes mellitus. *BMC medical genomics,* 3(1)**,** 33.

Beltrami, A. P., Barlucchi, L., Torella, D., Baker, M., Limana, F., Chimenti, S., Kasahara, H., Rota, M., Musso, E. & Urbanek, K. (2003). Adult cardiac stem cells are multipotent and support myocardial regeneration. *Cell,* 114(6)**,** 763-776.

Ben-Ari Fuchs, S., Lieder, I., Stelzer, G., Mazor, Y., Buzhor, E., Kaplan, S., Bogoch, Y., Plaschkes, I., Shitrit, A. & Rappaport, N. (2016). GeneAnalytics: an integrative gene set analysis tool for next generation sequencing, RNAseq and microarray data. *Omics: a journal of integrative biology,* 20(3)**,** 139-151.

Benito, E. & Barco, A. (2010). CREB's control of intrinsic and synaptic plasticity: implications for CREB-dependent memory models. *Trends in neurosciences,* 33(5)**,** 230-240.

Bertrand, G., Gross, R., Puech, R., Loubatières-Mariani, M. & Bockaert, J. (1992). Evidence for a glutamate receptor of the AMPA subtype which mediates insulin release from rat perfused pancreas. *British journal of pharmacology,* 106(2)**,** 354-359.

Bertucci, F., Salas, S., Eysteries, S., Nasser, V., Finetti, P., Ginestier, C., Charafe-Jauffret, E., Loriod, B., Bachelart, L. & Montfort, J. m. (2004). Gene expression profiling of colon cancer by DNA microarrays and correlation with histoclinical parameters. *Oncogene,* 23(7)**,** 1377.

Bezchlibnyk, Y. B., Wang, J. F., McQueen, G. M. & Young, L. T. (2001). Gene expression differences in bipolar disorder revealed by cDNA array analysis of post-mortem frontal cortex. *Journal of neurochemistry,* 79(4)**,** 826-834.

Bhargava, A., Herzel, H. & Ananthasubramaniam, B. (2015). Mining for novel candidate clock genes in the circadian regulatory network. *BMC systems biology,* 9(1)**,** 78.

Boettcher, M. & McManus, M. T. (2015). Choosing the right tool for the job: RNAi, TALEN, or CRISPR. *Molecular cell,* 58(4)**,** 575-585.

Boisset, J.-C. & Robin, C. (2012). On the origin of hematopoietic stem cells: progress and controversy. *Stem cell research,* 8(1)**,** 1-13.

Bolstad, B., Collin, F., Simpson, K., Irizarry, R. & Speed, T. (2004). Experimental design and low-level analysis of microarray data. *International review of neurobiology,* 60, 25-58.

Bonner, A., Lemon, W. & You, M. (2003). Gene expression signatures identify novel regulatory pathways during murine lung development: implications for lung tumorigenesis. *Journal of medical genetics,* 40(6)**,** 408-417.

Bonser, A. M., Garcia-Webb, P. & Harrison, L. C. (1984). C-peptide measurement: methods and clinical utility. *CRC critical reviews in clinical laboratory sciences,* 19(4), 297-352.

Bosotti, R., Locatelli, G., Healy, S., Scacheri, E., Sartori, L., Mercurio, C., Calogero, R. & Isacchi, A. (2007). Cross platform microarray analysis for robust identification of differentially expressed genes. *BMC bioinformatics,* 8(1)**,** S5.

Boucher, J., Kleinridders, A. & Kahn, C. R. (2014). Insulin receptor signaling in normal and insulin-resistant states. *Cold spring harbor perspectives in biology,* 6(1), a009191.

Boutros, M. & Ahringer, J. (2008). The art and design of genetic screens: RNA interference. *Nature reviews genetics,* 9(7)**,** 554-566.

Brachat, A., Pierrat, B., Xynos, A., Brecht, K., Simonen, M., Brüngger, A. & Heim, J. (2002). A microarray-based, integrated approach to identify novel regulators of cancer drug response and apoptosis. *Oncogene,* 21(54)**,** 8361-8371.

Bränström, R., Efendic, S., Berggren, P.-O. & Larsson, O. (1998). Direct inhibition of the pancreatic β-cell ATP-regulated potassium channel by α-ketoisocaproate. *Journal of biological chemistry,* 273(23)**,** 14113-14118.

Braun, M., Ramracheya, R., Bengtsson, M., Zhang, Q., Karanauskaite, J., Partridge, C., Johnson, P. R. & Rorsman, P. (2008). Voltage-gated ion channels in human pancreatic β-cells: electrophysiological characterization and role in insulin secretion. *Diabetes,* 57(6)**,** 1618-1628.

Brazeau, D. A. (2004). Combining genome-wide and targeted gene expression profiling in drug discovery: microarrays and real-time PCR. *Drug discovery today,* 9(19)**,** 838-845.

Brennan, L., Hewage, C., Malthouse, J., McClenaghan, N. H., Flatt, P. R. & Newsholme, P. (2006). Investigation of the effects of sulfonylurea exposure on pancreatic beta cell metabolism. *The FEBS journal,* 273(22)**,** 5160-5168.

Brereton, M. F., Vergari, E., Zhang, Q. & Clark, A. (2015). Alpha-, delta-and PP-cells: are they the architectural cornerstones of islet structure and co-ordination? *Journal of histochemistry & cytochemistry,* 63(8)**,** 575-591.

Broche, B., Fradj, S. B., Aguilar, E., Sancerni, T., Bénard, M., Makaci, F., Berthault, C., Scharfmann, R., Alves-Guerra, M.-C. & Duvillié, B. (2018). Mitochondrial protein UCP2 controls pancreas development. *Diabetes,* 67(1), 78-84.

Brown, K. R. & Jurisica, I. (2005). Online predicted human interaction database. *Bioinformatics,* 21(9)**,** 2076-2082.

Brunicardi, F. C., Atiya, A., Moldovan, S., Lee, T. C., Fagan, S. P., Kleinman, R. M., Adrian, T. E., Coy, D. H., Walsh, J. H. & Fisher, W. E. (2003). Activation of somatostatin receptor subtype 2 inhibits insulin secretion in the isolated perfused human pancreas. *Pancreas,* 27(4)**,** e84-e89.

Bryant, P. A., Smyth, G. K., Robins-Browne, R. & Curtis, N. (2011). Technical variability is greater than biological variability in a microarray experiment but both are outweighed by changes induced by stimulation. *PLoS one,* 6(5)**,** e19556.

Bugliani, M., Liechti, R., Cheon, H., Suleiman, M., Marselli, L., Kirkpatrick, C., Filipponi, F., Boggi, U., Xenarios, I. & Syed, F. (2013). Microarray analysis of isolated human islet transcriptome in type 2 diabetes and the role of the ubiquitin–proteasome system in pancreatic beta cell dysfunction. *Molecular and cellular endocrinology,* 367(1-2)**,** 1-10.

Burkhardt, A. M. & Zlotnik, A. (2013). Translating translational research: mouse models of human disease. *Cellular & molecular immunology,* 10(5), 373-374.

Bustin, S. A. (2000). Absolute quantification of mRNA using real-time reverse transcription polymerase chain reaction assays. *Journal of molecular endocrinology,* 25(2)**,** 169-193.

Byrne, S. M. & Church, G. M. (2015). CRISPR-Mediated Gene Targeting of Human Induced Pluripotent Stem Cells. *Current protocols in stem cell biology***,** 2015(sup35), 5A. 8.1-5A. 8.22.

Byrne, S. M., Mali, P. & Church, G. M. (2014). Genome editing in human stem cells, in Doudna, J. A. and Sontheimer E. J. (eds.) *Methods in enzymology, volume 546: the use of CRISPR/cas9, ZFNs, TALENs in generating site-specific genome alterations*. Elsevier, pp. 120-138.

Cahan, P., Li, H., Morris, S. A., Da Rocha, E. L., Daley, G. Q. & Collins, J. J. (2014). CellNet: network biology applied to stem cell engineering. *Cell,* 158(4)**,** 903-915.

Callow, M. J., Dudoit, S., Gong, E. L., Speed, T. P. & Rubin, E. M. (2000). Microarray expression profiling identifies genes with altered expression in HDL-deficient mice. *Genome research,* 10(12)**,** 2022-2029.

Calvano, S. E., Xiao, W., Richards, D. R., Felciano, R. M., Baker, H. V., Cho, R. J., Chen, R. O., Brownstein, B. H., Cobb, J. P. & Tschoeke, S. K. (2005). A network-based analysis of systemic inflammation in humans. *Nature,* 437(7061)**,** 1032-1037.

Cao, H. & Shockey, J. M. (2012). Comparison of TaqMan and SYBR Green qPCR methods for quantitative gene expression in tung tree tissues. *Journal of agricultural and food chemistry,* 60(50)**,** 12296-12303.

Capito, C., de Lonlay, P., Verkarre, V., Jaubert, F., Rahier, J., Nihoul-Fékété, C. & Aigrain, Y. (2011). The surgical management of atypical forms of congenital hyperinsulinism. *Seminars in pediatric surgery,* 20(1), 54-55.

Cartier, E. A., Conti, L. R., Vandenberg, C. A. & Shyng, S.-L. (2001). Defective trafficking and function of K_{ATP} channels caused by a sulfonylurea receptor 1 mutation associated with persistent hyperinsulinemic hypoglycemia of infancy. *Proceedings of the national academy of sciences,* 98(5)**,** 2882-2887.

Cerbini, T., Luo, Y., Rao, M. S. & Zou, J. (2015). Transfection, selection, and colony-picking of human induced pluripotent stem cells TALEN-targeted with a GFP gene into the AAVS1 safe harbor. *Journal of visualized experiments: JoVE,* 96, e52504.

Chakraborty, S., Khare, S., Dorairaj, S. K., Prabhakaran, V. C., Prakash, D. R. & Kumar, A. (2007). Identification of genes associated with tumorigenesis of retinoblastoma by microarray analysis. *Genomics,* 90(3)**,** 344-353.

Chamberlain, C. S., Brounts, S. H., Sterken, D. G., Rolnick, K. I., Baer, G. S. & Vanderby, R. (2011). Gene profiling of the rat medial collateral ligament during early healing using microarray analysis. *Journal of applied physiology,* 111(2)**,** 552-565.

Chambers, I., Colby, D., Robertson, M., Nichols, J., Lee, S., Tweedie, S. & Smith, A. (2003). Functional expression cloning of Nanog, a pluripotency sustaining factor in embryonic stem cells. *Cell,* 113(5)**,** 643-655.

Chan, C. B., De Leo, D., Joseph, J. W., McQuaid, T. S., Ha, X. F., Xu, F., Tsushima, R. G., Pennefather, P. S., Salapatek, A. M. F. & Wheeler, M. B. (2001). Increased uncoupling protein-2 levels in β-cells are associated with impaired glucose-stimulated insulin secretion: mechanism of action. *Diabetes,* 50(6)**,** 1302-1310.

Chan, C. B. & Harper, M.-E. (2006). Uncoupling proteins: role in insulin resistance and insulin insufficiency. *Current diabetes reviews,* 2(3)**,** 271-283.

Chan, C. B., MacDonald, P. E., Saleh, M. C., Johns, D. C., Marbàn, E. & Wheeler, M. B. (1999). Overexpression of uncoupling protein 2 inhibits glucose-stimulated insulin secretion from rat islets. *Diabetes,* 48(7)**,** 1482-1486.

Chandra, V., Albagli-Curiel, O., Hastoy, B., Piccand, J., Randriamampita, C., Vaillant, E., Cave, H., Busiah, K., Froguel, P., Vaxillaire, M., Rorsman, P., Polak, M. & Scharfmann, R. RFX6 Regulates Insulin Secretion by Modulating Ca $^{2+}$ Homeostasis in Human β Cells. *Cell reports*, 9, 2206-2218.

Chandran, S., Peng, F. Y. K., Rajadurai, V. S., Te Lu, Y., Chang, K. T., Flanagan, S., Ellard, S. & Hussain, K. (2013). Paternally inherited A*BCC8* mutation causing diffuse congenital hyperinsulinism. *Endocrinology, diabetes & metabolism case reports,* 2013, 130041.

Chang, H. Y., Nuyten, D. S., Sneddon, J. B., Hastie, T., Tibshirani, R., Sørlie, T., Dai, H., He, Y. D., van't Veer, L. J. & Bartelink, H. (2005). Robustness, scalability, and integration of a wound-response gene expression signature in predicting breast cancer survival. *Proceedings of the national academy of sciences,* 102(10)**,** 3738-3743.

Chang, H. Y., Thomson, J. A. & Chen, X. (2006). Microarray analysis of stem cells and differentiation. *Methods in enzymology,* 420**,** 225-254.

Chang, S.-S., Zhang, Z. & Liu, Y. (2012). RNA interference pathways in fungi: mechanisms and functions. *Annual review of microbiology,* 66**,** 305-323.

Charles, S., Tamagawa, T. & Henquin, J.-C. (1982). A single mechanism for the stimulation of insulin release and $^{86}Rb^{+}$ efflux from rat islets by cationic amino acids. *Biochemical journal,* 208(2)**,** 301-308.

Chatterjee, P., Cheung, Y. & Liew, C. (2011). Transfecting and nucleofecting human induced pluripotent stem cells. *Journal of visualized experiments: JoVE,* 56, e3110.

Chaurasia, G., Iqbal, Y., Hänig, C., Herzel, H., Wanker, E. E. & Futschik, M. E. (2007). UniHI: an entry gate to the human protein interactome. *Nucleic acids research,* 35(suppl_1)**,** D590-D594.

Chen, B.-S., Yang, S.-K., Lan, C.-Y. & Chuang, Y.-J. (2008). A systems biology approach to construct the gene regulatory network of systemic inflammation via microarray and databases mining. *BMC medical genomics,* 1(1)**,** 46.

Chen, F., Pruett-Miller, S. M., Huang, Y., Gjoka, M., Duda, K., Taunton, J., Collingwood, T. N., Frodin, M. & Davis, G. D. (2011). High-frequency genome editing using ssDNA oligonucleotides with zinc-finger nucleases. *Nature methods,* 8(9)**,** 753-755.

Chen, J., Fu, R., Cui, Y., Li, Y.-s., Pan, J.-r., Liu, J.-l., Luo, H.-s., Yin, J.-d., Li, D.-f. & Cui, S. (2013). LIM-homeodomain transcription factor Isl-1 mediates the effect of leptin on insulin secretion in mice. *Journal of biological chemistry,* 288(17)**,** 12395-12405.

Chen, J. J., Hsueh, H.-M., Delongchamp, R. R., Lin, C.-J. & Tsai, C.-A. (2007). Reproducibility of microarray data: a further analysis of microarray quality control (MAQC) data. *BMC bioinformatics,* 8(1)**,** 412.

Chendrimada, T. P., Gregory, R. I., Kumaraswamy, E., Norman, J., Cooch, N., Nishikura, K. & Shiekhattar, R. (2005). TRBP recruits the Dicer complex to Ago2 for microRNA processing and gene silencing. *Nature,* 436(7051)**,** 740-744.

Cheng, K., Delghingaro-Augusto, V., Nolan, C. J., Turner, N., Hallahan, N., Andrikopoulos, S. & Gunton, J. E. (2012). High passage MIN6 cells have impaired insulin secretion with impaired glucose and lipid oxidation. *PLoS one,* 7(7)**,** e40868.

Christesen, H. B., Jacobsen, B. B., Odili, S., Buettger, C., Cuesta-Munoz, A., Hansen, T., Brusgaard, K., Massa, O., Magnuson, M. A. & Shiota, C. (2002). The second activating glucokinase mutation (A456V): implications for glucose homeostasis and diabetes therapy. *Diabetes,* 51(4)**,** 1240-1246.

Chu, K. & Tsai, M.-J. (2005). Neuronatin, a downstream target of BETA2/NeuroD1 in the pancreas, is involved in glucose-mediated insulin secretion. *Diabetes,* 54(4)**,** 1064-1073.

Chu, L., Su, M. Y., Maggi, L. B., Lu, L., Mullins, C., Crosby, S., Huang, G., Chng, W. J., Vij, R. & Tomasson, M. H. (2012). Multiple myeloma–associated chromosomal translocation activates orphan snoRNA ACA11 to suppress oxidative stress. *The Journal of clinical investigation,* 122(8)**,** 2793-2806.

Chu, S., Wang, H. & Yu, M. (2017). A putative molecular network associated with colon cancer metastasis constructed from microarray data. *World journal of surgical oncology,* 15(1)**,** 115.

Chu, V. T., Weber, T., Wefers, B., Wurst, W., Sander, S., Rajewsky, K. & Kühn, R. (2015). Increasing the efficiency of homology-directed repair for CRISPR-Cas9-induced precise gene editing in mammalian cells. *Nature biotechnology,* 33(5)**,** 543-548.

Clayton, P. T., Eaton, S., Aynsley-Green, A., Edginton, M., Hussain, K., Krywawych, S., Datta, V., Malingré, H. E., Berger, R. & van den Berg, I. E. (2001). Hyperinsulinism in short-chain L-3-hydroxyacyl-CoA dehydrogenase deficiency reveals the importance of β-oxidation in insulin secretion. *Journal of clinical investigation,* 108(3)**,** 457-465.

Clement IV, J. P., Kunjilwar, K., Gonzalez, G., Schwanstecher, M., Panten, U., Aguilar-Bryan, L. & Bryan, J. (1997). Association and stoichiometry of K_{ATP} channel subunits. *Neuron,* 18(5)**,** 827-838.

Cline, M. S., Smoot, M., Cerami, E., Kuchinsky, A., Landys, N., Workman, C., Christmas, R., Avila-Campilo, I., Creech, M. & Gross, B. (2007). Integration of biological networks and gene expression data using Cytoscape. *Nature protocols,* 2(10)**,** 2366-2382.

Cong, L., Ran, F. A., Cox, D., Lin, S., Barretto, R., Habib, N., Hsu, P. D., Wu, X., Jiang, W. & Marraffini, L. (2013). Multiplex genome engineering using CRISPR/Cas systems. *Science***,** 339(6121), 819-823.

Gene Ontology Consortium, (2001). Creating the gene ontology resource: design and implementation. *Genome research,* 11(8)**,** 1425-1433.

Cook, D. L. & Hales, N. (1984). Intracellular ATP directly blocks K^+ channels in pancreatic B-cells. *Nature*, 311(5983), 271-273.

Copois, V., Bibeau, F., Bascoul-Mollevi, C., Salvetat, N., Chalbos, P., Bareil, C., Candeil, L., Fraslon, C., Conseiller, E. & Granci, V. (2007). Impact of RNA degradation on gene expression profiles: assessment of different methods to reliably determine RNA quality. *Journal of biotechnology,* 127(4)**,** 549-559.

Couzin, J. (2006). Microarray data reproduced, but some concerns remain. *Science,* 313(5793), 1559.

Craig, T. J., Ashcroft, F. M. & Proks, P. (2008). How ATP inhibits the open K_{ATP} channel. *The Journal of general physiology,* 132(1)**,** 131-144.

Croft, D., O'Kelly, G., Wu, G., Haw, R., Gillespie, M., Matthews, L., Caudy, M., Garapati, P., Gopinath, G. & Jassal, B. (2011). Reactome: a database of reactions, pathways and biological processes. *Nucleic acids research,* 39(suppl_1)**,** D691-D697.

Cryer, P. E. (2007). Hypoglycemia, functional brain failure, and brain death. *The Journal of clinical investigation,* 117(4)**,** 868-870.

Cuesta-Muñoz, A. L., Huopio, H., Otonkoski, T., Gomez-Zumaquero, J. M., Näntö-Salonen, K., Rahier, J., López-Enriquez, S., García-Gimeno, M. A., Sanz, P. & Soriguer, F. C. (2004). Severe persistent hyperinsulinemic hypoglycemia due to a de novo glucokinase mutation. *Diabetes,* 53(8)**,** 2164-2168.

Cui, X. & Churchill, G. A. (2003). Statistical tests for differential expression in cDNA microarray experiments. *Genome biology,* 4(4)**,** 210.

da Silva, T. A., Lemes, R. M., Oliveira, C. J. F., da Silva Almeida, A. & Chica, J. E. L. (2016). Data on morphometric analysis of the pancreatic islets from C57BL/6 and BALB/c mice. *Data in brief,* 8**,** 1094-1098.

Dadon, D., Tornovsky-Babaey, S., Furth-Lavi, J., Ben-Zvi, D., Ziv, O., Schyr-Ben-Haroush, R., Stolovich-Rain, M., Hija, A., Porat, S. & Granot, Z. (2012). Glucose metabolism: key endogenous regulator of β-cell replication and survival. *Diabetes, obesity and metabolism,* 14(s3)**,** 101-108.

Dallas, P. B., Gottardo, N. G., Firth, M. J., Beesley, A. H., Hoffmann, K., Terry, P. A., Freitas, J. R., Boag, J. M., Cummings, A. J. & Kees, U. R. (2005). Gene expression levels assessed by oligonucleotide microarray analysis and quantitative real-time RT-PCR–how well do they correlate? *BMC genomics,* 6(1)**,** 59.

Dalman, M. R., Deeter, A., Nimishakavi, G. & Duan, Z.-H. (2012). Fold change and p-value cutoffs significantly alter microarray interpretations. *BMC bioinformatics*, 13(Suppl 2), S11.

Damaj, L., Le Lorch, M., Verkarre, V., Werl, C., Hubert, L., Nihoul-Fékété, C., Aigrain, Y., De Keyzer, Y., Romana, S. & Bellanne-Chantelot, C. (2008). Chromosome 11p15 paternal isodisomy in focal forms of neonatal hyperinsulinism. *The Journal of clinical endocrinology & metabolism,* 93(12)**,** 4941-4947.

Dan, S., Tsunoda, T., Kitahara, O., Yanagawa, R., Zembutsu, H., Katagiri, T., Yamazaki, K., Nakamura, Y. & Yamori, T. (2002). An integrated database of chemosensitivity to 55 anticancer drugs and gene expression profiles of 39 human cancer cell lines. *Cancer research,* 62(4)**,** 1139-1147.

Day, W. A., Rasmussen, S. L., Carpenter, B. M., Peterson, S. N. & Friedlander, A. M. (2007). Microarray analysis of transposon insertion mutations in Bacillus anthracis: global identification of genes required for sporulation and germination. *Journal of bacteriology,* 189(8)**,** 3296-3301.

de Lonlay-Debeney, P., Poggi-Travert, F., Fournet, J.-C., Sempoux, C., Vici, C. D., Brunelle, F., Touati, G., Rahier, J., Junien, C. & Nihoul-Fékété, C. (1999). Clinical features of 52 neonates with hyperinsulinism. *New England journal of medicine,* 340(15)**,** 1169-1175.

de Lonlay, P., Fournet, J.-C., Rahier, J., Gross-Morand, M.-S., Poggi-Travert, F., Foussier, V., Bonnefont, J.-P., Brusset, M.-C., Brunelle, F. & Robert, J.-J. (1997). Somatic deletion of the imprinted 11p15 region in sporadic persistent hyperinsulinemic hypoglycemia of infancy is specific of focal adenomatous hyperplasia and endorses partial pancreatectomy. *Journal of clinical investigation,* 100(4)**,** 802-807.

De Souza, C. T., Araújo, E. P., Stoppiglia, L. F., Pauli, J. R., Ropelle, E., Rocco, S. A., Marin, R. M., Franchini, K. G., Carvalheira, J. B. & Saad, M. J. (2007). Inhibition of UCP2 expression reverses diet-induced diabetes mellitus by effects on both insulin secretion and action. *The FASEB journal,* 21(4)**,** 1153-1163.

de Wet, H. and Proks, P. (2015). Molecular action of sulphonylureas on K_{ATP} channels: a real partnership between drugs and nucleotides. *Biochemical society transactions,* 43(5), 901-907.

Della Fazia, M. A., Servillo, G. & Sassone-Corsi, P. (1997). Cyclic AMP signalling and cellular proliferation: regulation of CREB and CREM. *FEBS letters,* 410(1)**,** 22-24.

Delonlay, P., Simon, A., Galmiche-Rolland, L., Giurgea, I., Verkarre, V., Aigrain, Y., Santiago-Ribeiro, M.-J., Polak, M., Robert, J.-J. & Bellanne-Chantelot, C. (2007). Neonatal hyperinsulinism: clinicopathologic correlation. *Human pathology,* 38(3)**,** 387-399.

Dennis, G., Sherman, B. T., Hosack, D. A., Yang, J., Gao, W., Lane, H. C. & Lempicki, R. A. (2003). DAVID: database for annotation, visualization, and integrated discovery. *Genome biology,* 4(9)**,** R60.

Depiereux, S., De Meulder, B., Bareke, E., Berger, F., Le Gac, F., Depiereux, E. & Kestemont, P. (2015). Adaptation of a bioinformatics microarray analysis workflow for a toxicogenomic study in rainbow trout. *PLoS one,* 10(7)**,** e0128598.

Desbois-Mouthon, C., Cadoret, A., Blivet-Van Eggelpoël, M.-J., Bertrand, F., Caron, M., Atfi, A., Cherqui, G. & Capeau, J. (2000). Insulin-mediated cell proliferation and survival involve inhibition of c-Jun N-terminal kinases through a phosphatidylinositol 3-kinase-and mitogen-activated protein kinase phosphatase-1-dependent pathway. *Endocrinology,* 141(3)**,** 922-931.

Di Candia, S., Gessi, A., Pepe, G., Valin, P. S., Mangano, E., Chiumello, G., Gianolli, L., Proverbio, M. & Mora, S. (2009). Identification of a diffuse form of hyperinsulinemic hypoglycemia by ^{18}F-DOPA PET/CT in a patient carrying a novel mutation of the HADH gene. *European journal of endocrinology,* 160(6), 1019-1023.

Diaz, E. & Barisone, G. A. (2011). DNA microarrays: sample quality control, array hybridization and scanning. *Journal of visualized experiments: JoVE,* 49, 2546.

Doussau, F., Gasman, S., Humeau, Y., Vitiello, F., Popoff, M., Boquet, P., Bader, M.-F. & Poulain, B. (2000). A Rho-related GTPase is involved in Ca^{2+}-dependent neurotransmitter exocytosis. *Journal of biological chemistry,* 275(11)**,** 7764-7770.

Doyle, M. E. & Egan, J. M. (2007). Mechanisms of action of glucagon-like peptide 1 in the pancreas. *Pharmacology & therapeutics,* 113(3)**,** 546-593.

Draghici, S., Khatri, P., Eklund, A. C. & Szallasi, Z. (2006). Reliability and reproducibility issues in DNA microarray measurements. *TRENDS in genetics,* 22(2)**,** 101-109.

Drain, P., Li, L. & Wang, J. (1998). K_{ATP} channel inhibition by ATP requires distinct functional domains of the cytoplasmic C terminus of the pore-forming subunit. *Proceedings of the national academy of sciences,* 95(23)**,** 13953-13958.

Dudoit, S., Yang, Y. H., Callow, M. J. & Speed, T. P. (2002). Statistical methods for identifying differentially expressed genes in replicated cDNA microarray experiments. *Statistica sinica***,** 12, 111-139.

Dullaart, R., Hoogenberg, K., Rouwé, C. W. & Stulp, B. (2004). Family with autosomal dominant hyperinsulinism associated with A456V mutation in the glucokinase gene. *Journal of internal medicine,* 255(1)**,** 143-145.

Duncan, S. A., Navas, M. A., Dufort, D., Rossant, J. & Stoffel, M. (1998). Regulation of a transcription factor network required for differentiation and metabolism. *Science,* 281(5377)**,** 692-695.

Dunn-Meynell, A. A., Sanders, N. M., Compton, D., Becker, T. C., Eiki, J.-i., Zhang, B. B. & Levin, B. E. (2009). Relationship among brain and blood glucose levels and spontaneous and glucoprivic feeding. *Journal of neuroscience,* 29(21)**,** 7015-7022.

Dunne, M., Harding, E., Jaggar, J. & Squires, P. E. (1994). Ion channels and the molecular control of insulin secretion. *Biochemical society transaction,* 22(1), 6-12.

Dunne, M. J., Cosgrove, K. E., Shepherd, R. M., Aynsley-Green, A. & Lindley, K. J. (2004). Hyperinsulinism in infancy: from basic science to clinical disease. *Physiological reviews,* 84(1)**,** 239-275.

Dunne, M. J., Kane, C., Shepherd, R. M., Sanchez, J. A., James, R. F., Johnson, P. R., Aynsley-Green, A., Lu, S., Clement, J. P. & Lindley, K. J. (1997). Familial persistent hyperinsulinemic hypoglycemia of infancy and mutations in the sulfonylurea receptor. *New England journal of medicine,* 336(10)**,** 703-706.

Dunne, M. J. & Petersen, O. H. (1986). Intracellular ADP activates K^+ channels that are inhibited by ATP in an insulin-secreting cell line. *FEBS letters,* 208(1)**,** 59-62.

Efanova, I. B., Zaitsev, S. V., Zhivotovsky, B., Köhler, M., Efendić, S., Orrenius, S. & Berggren, P.-O. (1998). Glucose and tolbutamide induce apoptosis in pancreatic β-Cells a process dependent on intracellular Ca^{2+} concentration. *Journal of biological chemistry,* 273(50)**,** 33501-33507.

Eichmann, D., Hufnagel, M., Quick, P. & Santer, R. (1999). Treatment of hyperinsulinaemic hypoglycaemia with nifedipine. *European journal of pediatrics,* 158(3)**,** 204-206.

Eiges, R., Schuldiner, M., Drukker, M., Yanuka, O., Itskovitz-Eldor, J. & Benvenisty, N. (2001). Establishment of human embryonic stem cell-transfected clones carrying a marker for undifferentiated cells. *Current biology,* 11(7)**,** 514-518.

Eisenstein, M. (2006). Microarrays: quality control. *Nature,* 442(7106)**,** 1067-1070.

Elbashir, S. M., Harborth, J., Lendeckel, W., Yalcin, A., Weber, K. & Tuschl, T. (2001). Duplexes of 21-nucleotide RNAs mediate RNA interference in cultured mammalian cells. *Nature,* 411(6836)**,** 494-498.

Enkvetchakul, D., Loussouarn, G., Makhina, E. & Nichols, C. (2001). ATP interaction with the open state of the K_{ATP} channel. *Biophysical journal,* 80(2)**,** 719-728.

Ergün, A., Lawrence, C. A., Kohanski, M. A., Brennan, T. A. & Collins, J. J. (2007). A network biology approach to prostate cancer. *Molecular systems biology,* 3(1)**,** 82.

Etienne, W., Meyer, M. H., Peppers, J. & Meyer, R. A. (2004). Comparison of mRNA gene expression by RT-PCR and DNA microarray. *Biotechniques,* 36(4)**,** 618-627.

Fan, Z., Ni, J., Yang, L., Hu, L., Ma, S., Mei, M., Sun, B., Wang, H., & Zhou, W. (2015). Uncovering the molecular pathogenesis of congenital hyperinsulinism by panel gene sequencing in 32 Chinese patients. *Molecular Genetics & Genomic Medicine,* 3(6), 526-536.

Fearon, I. M., Gaca, M. D. & Nordskog, B. K. (2013). *In vitro* models for assessing the potential cardiovascular disease risk associated with cigarette smoking. *Toxicology in vitro,* 27(1)**,** 513-522.

Fekete, C. N., De Lonlay, P., Jaubert, F., Rahier, J., Brunelle, F. & Saudubray, J. (2004). The surgical management of congenital hyperinsulinemic hypoglycemia in infancy. *Journal of pediatric surgery,* 39(3)**,** 267-269.

Fergusson, G., Éthier, M., Guévremont, M., Chrétien, C., Attané, C., Joly, E., Fioramonti, X., Prentki, M., Poitout, V. & Alquier, T. (2014). Defective insulin secretory response to intravenous glucose in C57Bl/6J compared to C57Bl/6N mice. *Molecular metabolism,* 3(9)**,** 848-854.

Ferrara, C. T., Boodhansingh, K. E., Paradies, E., Giuseppe, F., Steinkrauss, L. J., Topor, L. S., Quintos, J. B., Ganguly, A., De Leon, D. D. & Palmieri, F. (2017). Novel Hypoglycemia Phenotype in Congenital Hyperinsulinism Due to Dominant Mutations of Uncoupling Protein 2. *The Journal of clinical endocrinology & metabolism,* 102(3)**,** 942-949.

Fire, A., Xu, S., Montgomery, M. K., Kostas, S. A., Driver, S. E. & Mello, C. C. (1998). Potent and specific genetic interference by double-stranded RNA in Caenorhabditis elegans. *Nature,* 391(6669)**,** 806-811.

Flanagan, S., Kapoor, R., Banerjee, I., Hall, C., Smith, V., Hussain, K. & Ellard, S. (2011). Dominantly acting *ABCC8* mutations in patients with medically unresponsive hyperinsulinaemic hypoglycaemia. *Clinical genetics,* 79(6)**,** 582-587.

Flanagan, S., Kapoor, R., Mali, G., Cody, D., Murphy, N., Schwahn, B., Siahanidou, T., Banerjee, I., Akcay, T. & Rubio-Cabezas, O. (2010). Diazoxide-responsive hyperinsulinemic hypoglycemia caused by *HNF4A* gene mutations. *European journal of endocrinology,* 162(5)**,** 987-992.

Flanagan, S. E., Clauin, S., Bellanné-Chantelot, C., de Lonlay, P., Harries, L. W., Gloyn, A. L. & Ellard, S. (2009). Update of mutations in the genes encoding the pancreatic beta-cell K_{ATP} channel subunits Kir6. 2 (*KCNJ11*) and sulfonylurea receptor 1 (*ABCC8*) in diabetes mellitus and hyperinsulinism. *Human mutation,* 30(2)**,** 170-180.

Flanagan, S., Damhuis, A., Banerjee, I., Rokicki, D., Jefferies, C., Kapoor, R., Hussain, K. & Ellard, S. (2012). Partial *ABCC8* gene deletion mutations causing diazoxide-unresponsive hyperinsulinaemic hypoglycaemia, *Pediatric diabetes,* 13(3), 285-289.

Flasse, L. C., Pirson, J. L., Stern, D. G., Von Berg, V., Manfroid, I., Peers, B. & Voz, M. L. (2013). Ascl1b and Neurod1, instead of Neurog3, control pancreatic endocrine cell fate in zebrafish. *BMC biology,* 11(1)**,** 78.

Fleige, S. & Pfaffl, M. W. (2006). RNA integrity and the effect on the real-time qRT-PCR performance. *Molecular aspects of medicine,* 27(2-3)**,** 126-139.

Fournet, J.-C., Mayaud, C., de Lonlay, P., Gross-Morand, M.-S., Verkarre, V., Castanet, M., Devillers, M., Rahier, J., Brunelle, F. & Robert, J.-J. (2001). Unbalanced expression of 11p15 imprinted genes in focal forms of congenital hyperinsulinism: association with a reduction to homozygosity of a mutation in *ABCC8* or *KCNJ11*. *The American journal of pathology,* 158(6)**,** 2177-2184.

Fournet, J.-C., Mayaud, C., de Lonlay, P., Verkarre, V., Rahier, J., Brunelle, F., Robert, J.-J., Nihoul-Fékété, C., Saudubray, J.-M. & Junien, C. (2000). Loss of imprinted genes and paternal SUR1 mutations lead to focal form of congenital hyperinsulinism. *Hormone research in paediatrics,* 53(Suppl. 1)**,** 2-6.

Francino, O., Altet, L., Sanchez-Robert, E., Rodriguez, A., Solano-Gallego, L., Alberola, J., Ferrer, L., Sánchez, A. & Roura, X. (2006). Advantages of real-time PCR assay for diagnosis and monitoring of canine leishmaniosis. *Veterinary parasitology,* 137(3-4)**,** 214-221.

Fred, R. G., Kappe, C., Ameur, A., Cen, J., Bergsten, P., Ravassard, P., Scharfmann, R. & Welsh, N. (2015). Role of the AMP kinase in cytokine-induced human EndoC-βH1 cell death. *Molecular and cellular endocrinology,* 414**,** 53-63.

Freeman, W. M., Walker, S. J. & Vrana, K. E. (1999). Quantitative RT-PCR: pitfalls and potential. *Biotechniques,* 26(1)**,** 112-125.

French, P. J., Peeters, J., Horsman, S., Duijm, E., Siccama, I., Van Den Bent, M. J., Luider, T. M., Kros, J. M., van der Spek, P. & Smitt, P. A. S. (2007). Identification of differentially regulated splice variants and novel exons in glial brain tumors using exon expression arrays. *Cancer research,* 67(12)**,** 5635-5642.

Fridlyand, L. E., Jacobson, D. A. & Philipson, L. (2013). Ion channels and regulation of insulin secretion in human β-cells: a computational systems analysis. *Islets,* 5(1)**,** 1-15.

Fujita, A., Sato, J. R., de Oliveira Rodrigues, L., Ferreira, C. E. & Sogayar, M. C. (2006). Evaluating different methods of microarray data normalization. *BMC bioinformatics,* 7(1)**,** 469.

Fujiwara, T., Kanazawa, S., Ichibori, R., Tanigawa, T., Magome, T., Shingaki, K., Miyata, S., Tohyama, M. & Hosokawa, K. (2014). L-arginine stimulates fibroblast proliferation through the GPRC6A-ERK1/2 and PI3K/Akt pathway. *PLoS one,* 9(3)**,** e92168.

Gang, E. J., Bosnakovski, D., Figueiredo, C. A., Visser, J. W. & Perlingeiro, R. C. (2007). SSEA-4 identifies mesenchymal stem cells from bone marrow. *Blood,* 109(4)**,** 1743-1751.

Gelernter, J., Sherva, R., Koesterer, R., Almasy, L., Zhao, H., Kranzler, H. R. & Farrer, L. (2014). Genome-wide association study of cocaine dependence and related traits: FAM53B identified as a risk gene. *Molecular psychiatry,* 19(6)**,** 717-723.

Gembal, M., Gilon, P. & Henquin, J.-C. (1992). Evidence that glucose can control insulin release independently from its action on ATP-sensitive K^+ channels in mouse B cells. *The Journal of clinical investigation,* 89(4)**,** 1288-1295.

Giersbergen, P. L., Treiber, A., Clozel, M., Bodin, F. & Dingemanse, J. (2002). *In vivo* and *in vitro* studies exploring the pharmacokinetic interaction between bosentan, a dual endothelin receptor antagonist, and glyburide. *Clinical pharmacology & therapeutics,* 71(4)**,** 253-262.

Giugliano, D., Torella, R., Cacciapuoti, F., Gentile, S., Verza, M. & Varricchio, M. (1980). Impairment of insulin secretion in man by nifedipine. *European journal of clinical pharmacology,* 18(5)**,** 395-398.

Giurgea, I., Bellanné-Chantelot, C., Ribeiro, M., Hubert, L., Sempoux, C., Robert, J.-J., Blankenstein, O., Hussain, K., Brunelle, F. & Nihoul-Fékété, C. (2006). Molecular mechanisms of neonatal hyperinsulinism. *Hormone research in paediatrics,* 66(6)**,** 289-296.

Glaser, B., Kesavan, P., Heyman, M., Davis, E., Cuesta, A., Buchs, A., Stanley, C. A., Thornton, P. S., Permutt, M. A. & Matschinsky, F. M. (1998). Familial hyperinsulinism caused by an activating glucokinase mutation. *New England journal of medicine,* 338(4)**,** 226-230.

Glaser, B., Thornton, P., Otonkoski, T. & Junien, C. (2000). Genetics of neonatal hyperinsulinism. *Archives of disease in childhood-fetal and neonatal edition,* 82(2)**,** F79-F86.

Glick, E., Leshkowitz, D. & Walker, M. D. (2000). Transcription factor BETA2 acts cooperatively with E2A and PDX1 to activate the insulin gene promoter. *Journal of biological chemistry,* 275(3)**,** 2199-2204.

Goldsworthy, M., Hugill, A., Freeman, H., Horner, E., Shimomura, K., Bogani, D., Pieles, G., Mijat, V., Arkell, R. & Bhattacharya, S. (2008). Role of the transcription factor sox4 in insulin secretion and impaired glucose tolerance. *Diabetes,* 57(8)**,** 2234-2244.

Gong, Y., Ma, Y., Sinyuk, M., Loganathan, S., Thompson, R. C., Sarkaria, J. N., Chen, W., Lathia, J. D., Mobley, B. C. & Clark, S. W. (2015). Insulin-mediated signaling promotes proliferation and survival of glioblastoma through Akt activation. *Neuro-oncology,* 18(1)**,** 48-57.

Goni, R., García, P. & Foissac, S. (2009). The qPCR data statistical analysis. *Integromics white paper***,** 1-9.

González-Barroso, M. M., Giurgea, I., Bouillaud, F., Anedda, A., Bellanné-Chantelot, C., Hubert, L., De Keyzer, Y., De Lonlay, P. & Ricquier, D. (2008). Mutations in *UCP2* in congenital hyperinsulinism reveal a role for regulation of insulin secretion. *PLoS one,* 3(12)**,** e3850.

González, F. (2016). CRISPR/Cas9 genome editing in human pluripotent stem cells: harnessing human genetics in a dish. *Developmental dynamics,* 245(7)**,** 788-806.

Goossens, A., Gepts, W., Saudubray, J., Bonnefont, J., Heitz, P. & Klöppel, G. (1989). Diffuse and focal nesidioblastosis. A clinicopathological study of 24 patients with persistent neonatal hyperinsulinemic hypoglycemia. *The American journal of surgical pathology,* 13(9)**,** 766-775.

Gordon, G. J., Jensen, R. V., Hsiao, L.-L., Gullans, S. R., Blumenstock, J. E., Ramaswamy, S., Richards, W. G., Sugarbaker, D. J. & Bueno, R. (2002). Translation of microarray data into clinically relevant cancer diagnostic tests using gene expression ratios in lung cancer and mesothelioma. *Cancer research,* 62(17)**,** 4963-4967.

Gosmain, Y., Katz, L. S., Masson, M. H., Cheyssac, C., Poisson, C. & Philippe, J. (2012). Pax6 is crucial for β-cell function, insulin biosynthesis, and glucose-induced insulin secretion. *Molecular endocrinology,* 26(4)**,** 696-709.

Gouy, M., Guindon, S. & Gascuel, O. (2009). SeaView version 4: a multiplatform graphical user interface for sequence alignment and phylogenetic tree building. *Molecular biology and evolution,* 27(2)**,** 221-224.

Greene, J. M., Feugang, J. M., Pfeiffer, K. E., Stokes, J. V., Bowers, S. D. & Ryan, P. L. (2013). L-arginine enhances cell proliferation and reduces apoptosis in human endometrial RL95-2 cells. *Reproductive biology and endocrinology,* 11(1)**,** 15.

Gregory, R. I., Chendrimada, T. P., Cooch, N. & Shiekhattar, R. (2005). Human RISC couples microRNA biogenesis and posttranscriptional gene silencing. *Cell,* 123(4)**,** 631-640.

Gribble, F. M., Ashfield, R., Ammälä, C. & Ashcroft, F. M. (1997a). Properties of cloned ATP-sensitive K^+ currents expressed in Xenopus oocytes. *The Journal of physiology,* 498(1)**,** 87-98.

Gribble, F. M., Tucker, S. J. & Ashcroft, F. M. (1997b). The essential role of the Walker A motifs of SUR1 in K-ATP channel activation by Mg-ADP and diazoxide. *The EMBO journal,* 16(6)**,** 1145-1152.

Grieco, F. A., Sebastiani, G., Juan-Mateu, J., Villate, O., Marroqui, L., Ladrière, L., Tugay, K., Regazzi, R., Bugliani, M. & Marchetti, P. (2017). MicroRNAs miR-23a-3p, miR-23b-3p, and miR-149-5p regulate the expression of proapoptotic BH3-only proteins DP5 and PUMA in human pancreatic β-cells. *Diabetes,* 66(1)**,** 100-112.

Grimberg, A., Ferry, R., Kelly, A., Koo-McCoy, S., Polonsky, K., Glaser, B., Permutt, M., Aguilar-Bryan, L., Stafford, D. & Thornton, P. (2001). Dysregulation of insulin secretion in children with congenital hyperinsulinism due to sulfonylurea receptor mutations. *Diabetes,* 50(2)**,** 322-328.

Gu, C. C., Rao, D., Stormo, G., Hicks, C. & Province, M. A. (2002a). Role of gene expression microarray analysis in finding complex disease genes. *Genetic epidemiology,* 23(1)**,** 37-56.

Gu, G., Dubauskaite, J. & Melton, D. A. (2002b). Direct evidence for the pancreatic lineage: $NGN3^+$ cells are islet progenitors and are distinct from duct progenitors. *Development,* 129(10)**,** 2447-2457.

Gunderson, K. L., Steemers, F. J., Lee, G., Mendoza, L. G. & Chee, M. S. (2005). A genome-wide scalable SNP genotyping assay using microarray technology. *Nature genetics,* 37(5)**,** 549-554.

Guo, D., Liu, H., Gao, G., Ruzi, A., Wang, K., Wu, H., Lai, K., Liu, Y., Yang, F. & Lai, L. (2016a). Generation of an *ABCC8* heterozygous mutation human embryonic stem cell line using CRISPR/Cas9. *Stem cell research,* 17(3)**,** 670-672.

Guo, D., Liu, H., Gao, G., Ruzi, A., Wang, K., Wu, H., Lai, K., Liu, Y., Yang, F. & Lai, L. (2016b). Generation of an *ABCC8* homozygous mutation human embryonic stem cell line using CRISPR/Cas9. *Stem cell research,* 17(3)**,** 640-642.

Guo, D., Liu, H., Ruzi, A., Gao, G., Nasir, A., Liu, Y., Yang, F., Wu, F., Xu, G. & Li, Y.-x. (2017). Modeling Congenital Hyperinsulinism with *ABCC8*-Deficient Human Embryonic Stem Cells Generated by CRISPR/Cas9. *Scientific reports,* 7(1)**,** 3156.

Gupta, R. K., Vatamaniuk, M. Z., Lee, C. S., Flaschen, R. C., Fulmer, J. T., Matschinsky, F. M., Duncan, S. A. & Kaestner, K. H. (2005). The MODY1 gene *HNF-4*α regulates selected genes involved in insulin secretion. *The Journal of clinical investigation,* 115(4)**,** 1006-1015.

Gurgul-Convey, E., Kaminski, M. T. & Lenzen, S. (2015). Physiological characterization of the human EndoC-βH1 β-cell line. *Biochemical and biophysical research communications,* 464(1)**,** 13-19.

Györffy, B., Lanczky, A., Eklund, A. C., Denkert, C., Budczies, J., Li, Q. & Szallasi, Z. (2010). An online survival analysis tool to rapidly assess the effect of 22,277 genes on breast cancer prognosis using microarray data of 1,809 patients. *Breast cancer research and treatment,* 123(3)**,** 725-731.

Haase, A. D., Jaskiewicz, L., Zhang, H., Lainé, S., Sack, R., Gatignol, A. & Filipowicz, W. (2005). TRBP, a regulator of cellular PKR and HIV-1 virus expression, interacts with Dicer and functions in RNA silencing. *EMBO reports,* 6(10)**,** 961-967.

Haddad, D., Socci, N., Chen, C.-H., Chen, N. G., Zhang, Q., Carpenter, S. G., Mittra, A., Szalay, A. A. & Fong, Y. (2016). Molecular network, pathway, and functional analysis of time-dependent gene changes associated with pancreatic cancer susceptibility to oncolytic vaccinia virotherapy. *Molecular therapy-oncolytics,* 3, 16008.

Han, X., Cheng, W., Jing, H., Zhang, J.-W. & Tang, L.-L. (2012). Neuroepithelial Transforming Protein 1 Short Interfering RNA–Mediated Gene Silencing With Microbubble and Ultrasound Exposure Inhibits the Proliferation of Hepatic Carcinoma Cells *In Vitro*. *Journal of ultrasound in medicine,* 31(6)**,** 853-861.

Hanley, K. P., Hearn, T., Berry, A., Carvell, M. J., Patch, A.-M., Williams, L. J., Sugden, S. A., Wilson, D. I., Ellard, S. & Hanley, N. A. (2010). *In vitro* expression of NGN3 identifies RAB3B as the predominant Ras-associated GTP-binding protein 3 family member in human islets. *Journal of Endocrinology,* 207, 151-161.

Harborth, J., Elbashir, S. M., Bechert, K., Tuschl, T. & Weber, K. (2001). Identification of essential genes in cultured mammalian cells using small interfering RNAs. *Journal of cell science,* 114(24)**,** 4557-4565.

Hardy, O. T., Hernandez-Pampaloni, M., Saffer, J. R., Scheuermann, J. S., Ernst, L. M., Freifelder, R., Zhuang, H., MacMullen, C., Becker, S. & Adzick, N. S. (2007a). Accuracy of [18F] fluorodopa positron emission tomography for diagnosing and localizing focal congenital hyperinsulinism. *The Journal of clinical endocrinology & metabolism,* 92(12)**,** 4706-4711.

Hardy, O. T., Hernandez-Pampaloni, M., Saffer, J. R., Suchi, M., Ruchelli, E., Zhuang, H., Ganguly, A., Freifelder, R., Adzick, N. S. & Alavi, A. (2007b). Diagnosis and localization of focal congenital hyperinsulinism by ^{18}F-fluorodopa PET scan. *The Journal of pediatrics,* 150(2)**,** 140-145.

Hardy, O. T., Hohmeier, H. E., Becker, T. C., Manduchi, E., Doliba, N. M., Gupta, R. K., White, P., Stoeckert Jr, C. J., Matschinsky, F. M. & Newgard, C. B. (2007c). Functional genomics of the β-cell: short-chain 3-hydroxyacyl-coenzyme A dehydrogenase regulates insulin secretion independent of K^+ currents. *Molecular endocrinology,* 21(3)**,** 765-773.

Harel, S., Cohen, A. S., Hussain, K., Flanagan, S. E., Schlade-Bartusiak, K., Patel, M., Courtade, J., Li, J. B., Van Karnebeek, C. & Kurata, H. (2015). Alternating hypoglycemia and hyperglycemia in a toddler with a homozygous p. R1419H *ABCC8* mutation: an unusual clinical picture. *Journal of pediatric endocrinology and metabolism,* 28(3-4)**,** 345-351.

Harris, A. (1994). Somatostatin and somatostatin analogues: pharmacokinetics and pharmacodynamic effects. *Gut,* 35(3 Suppl), S1-S4.

Hatlapatka, K., Matz, M., Schumacher, K., Baumann, K. & Rustenbeck, I. (2011). Bidirectional Insulin Granule Turnover in the Submembrane Space During K^+ Depolarization-Induced Secretion. *Traffic,* 12(9)**,** 1166-1178.

Hatlapatka, K., Willenborg, M. & Rustenbeck, I. (2009). Plasma membrane depolarization as a determinant of the first phase of insulin secretion. *American journal of physiology-endocrinology and metabolism,* 297(2)**,** E315-E322.

Hatzis, P. & Talianidis, I. (2001). Regulatory mechanisms controlling human hepatocyte nuclear factor 4α gene expression. *Molecular and Cellular Biology,* 21(21)**,** 7320-7330.

He, L. & Hannon, G. J. (2004). MicroRNAs: small RNAs with a big role in gene regulation. *Nature reviews genetics,* 5(7)**,** 522-531.

He, X. & Zhang, J. (2006). Why do hubs tend to be essential in protein networks? *PLoS genetics,* 2(6)**,** e88.

Heart, E., Corkey, R. F., Wikstrom, J. D., Shirihai, O. S. & Corkey, B. E. (2006). Glucose-dependent increase in mitochondrial membrane potential, but not cytoplasmic calcium, correlates with insulin secretion in single islet cells. *American journal of physiology-endocrinology and metabolism,* 290(1)**,** E143-E148.

Heineke, J. & Molkentin, J. D. (2006). Regulation of cardiac hypertrophy by intracellular signalling pathways. *Nature reviews molecular cell biology,* 7(8)**,** 589-600.

Henderson, J., Draper, J., Baillie, H., Fishel, S., Thomson, J., Moore, H. & Andrews, P. (2002). Preimplantation human embryos and embryonic stem cells show comparable expression of stage-specific embryonic antigens. *Stem cells,* 20(4)**,** 329-337.

Heni, M., Hennige, A. M., Peter, A., Siegel-Axel, D., Ordelheide, A.-M., Krebs, N., Machicao, F., Fritsche, A., Häring, H.-U. & Staiger, H. (2011). Insulin promotes glycogen storage and cell proliferation in primary human astrocytes. *PLoS one,* 6(6)**,** e21594.

Henquin, J.-C. & Nenquin, M. (2016). Dynamics and regulation of insulin secretion in pancreatic islets from normal young children. *PLoS one,* 11(11)**,** e0165961.

Henquin, J.-C., Nenquin, M., Sempoux, C., Guiot, Y., Bellanné-Chantelot, C., Otonkoski, T., de Lonlay, P., Nihoul-Fékété, C. & Rahier, J. (2011). *In vitro* insulin secretion by pancreatic tissue from infants with diazoxide-resistant congenital hyperinsulinism deviates from model predictions. *The Journal of clinical investigation,* 121(10), 3932-3942.

Henquin, J.-C., Nenquin, M., Stiernet, P. & Ahren, B. (2006). *In vivo* and *in vitro* glucose-induced biphasic insulin secretion in the mouse: pattern and role of cytoplasmic Ca^{2+} and amplification signals in β-cells. *Diabetes,* 55(2)**,** 441-451.

Henquin, J. C. & Meissner, H. P. (1981). Effects of amino acids on membrane potential and $86Rb^+$ fluxes in pancreatic beta-cells. *American journal of physiology-endocrinology and metabolism,* 240(3)**,** E245-E252.

Hermjakob, H., Montecchi-Palazzi, L., Lewington, C., Mudali, S., Kerrien, S., Orchard, S., Vingron, M., Roechert, B., Roepstorff, P. & Valencia, A. (2004). IntAct: an open source molecular interaction database. *Nucleic acids research,* 32(suppl_1)**,** D452-D455.

Herzig, S., Long, F., Jhala, U. S., Hedrick, S., Quinn, R., Bauer, A., Rudolph, D., Schutz, G., Yoon, C. & Puigserver, P. (2001). CREB regulates hepatic gluconeogenesis through the coactivator PGC-1. *Nature,* 413(6852)**,** 179-183.

Heslegrave, A. J. & Hussain, K. (2013). Novel insights into fatty acid oxidation, amino acid metabolism, and insulin secretion from studying patients with loss of function mutations in 3-hydroxyacyl-CoA dehydrogenase. *The Journal of clinical endocrinology & metabolism,* 98(2)**,** 496-501.

Highley, J. R., Kirby, J., Jansweijer, J. A., Webb, P. S., Hewamadduma, C. A., Heath, P. R., Higginbottom, A., Raman, R., Ferraiuolo, L. & Cooper-Knock, J. (2014). Loss of nuclear TDP-43 in amyotrophic lateral sclerosis (ALS) causes altered expression of splicing machinery and widespread dysregulation of RNA splicing in motor neurones. *Neuropathology and applied neurobiology,* 40(6)**,** 670-685.

Hilderink, J., Spijker, S., Carlotti, F., Lange, L., Engelse, M., Blitterswijk, C., Koning, E., Karperien, M. & Apeldoorn, A. (2015). Controlled aggregation of primary human pancreatic islet cells leads to glucose-responsive pseudoislets comparable to native islets. *Journal of cellular and molecular medicine,* 19(8)**,** 1836-1846.

Hill, D. & Milner, R. (1985). Insulin as a growth factor. *Pediatric research,* 19(9)**,** 879-886.

Hoenig, M. & Sharp, G. W. (1986). Glucose induces insulin release and a rise in cytosolic calcium concentration in a transplantable rat insulinoma. *Endocrinology,* 119(6)**,** 2502-2507.

Holland, P. M., Abramson, R. D., Watson, R. & Gelfand, D. H. (1991). Detection of specific polymerase chain reaction product by utilizing the 5'-3'exonuclease activity of Thermus aquaticus DNA polymerase. *Proceedings of the national academy of sciences,* 88(16)**,** 7276-7280.

Homer, N., Szelinger, S., Redman, M., Duggan, D., Tembe, W., Muehling, J., Pearson, J. V., Stephan, D. A., Nelson, S. F. & Craig, D. W. (2008). Resolving individuals contributing trace amounts of DNA to highly complex mixtures using high-density SNP genotyping microarrays. *PLoS genetics,* 4(8)**,** e1000167.

Hommel, J. D., Sears, R. M., Georgescu, D., Simmons, D. L. & DiLeone, R. J. (2003). Local gene knockdown in the brain using viral-mediated RNA interference. *Nature medicine,* 9(12)**,** 1539-1544.

Hongisto, H., Vuoristo, S., Mikhailova, A., Suuronen, R., Virtanen, I., Otonkoski, T. & Skottman, H. (2012). Laminin-511 expression is associated with the functionality of feeder cells in human embryonic stem cell culture. *Stem cell research,* 8(1), 97-108.

Hovorka, R. & Jones, R. H. (1994). How to measure insulin secretion. *Diabetes/metabolism reviews,* 10(2), 91-117.

Howden, S. E., Gore, A., Li, Z., Fung, H.-L., Nisler, B. S., Nie, J., Chen, G., McIntosh, B. E., Gulbranson, D. R. & Diol, N. R. (2011). Genetic correction and analysis of induced pluripotent stem cells from a patient with gyrate atrophy. *Proceedings of the national academy of sciences,* 108(16)**,** 6537-6542.

Hsu, P. D., Lander, E. S. & Zhang, F. (2014). Development and applications of CRISPR-Cas9 for genome engineering. *Cell,* 157(6)**,** 1262-1278.

Hu, S., Xu, Z., Yan, J., Liu, M., Sun, B., Li, W. & Sang, Y. (2012). The treatment effect of diazoxide on 44 patients with congenital hyperinsulinism. *Journal of pediatric endocrinology and metabolism,* 25(11-12)**,** 1119-1122.

Huan, T., Zhang, B., Wang, Z., Joehanes, R., Zhu, J., Johnson, A. D., Ying, S., Munson, P. J., Raghavachari, N. & Wang, R. (2013). A Systems Biology Framework Identifies Molecular Underpinnings of Coronary Heart DiseaseSignificance. *Arteriosclerosis, thrombosis, and vascular biology,* 33(6)**,** 1427-1434.

Huang, D. W., Sherman, B. T. & Lempicki, R. A. (2009a). Bioinformatics enrichment tools: paths toward the comprehensive functional analysis of large gene lists. *Nucleic acids research,* 37(1)**,** 1-13.

Huang, D. W., Sherman, B. T. & Lempicki, R. A. (2009b). Systematic and integrative analysis of large gene lists using DAVID bioinformatics resources. *Nature protocols,* 4(1)**,** 44-57.

Huang, L., Shen, H., Atkinson, M. A. & Kennedy, R. T. (1995). Detection of exocytosis at individual pancreatic beta cells by amperometry at a chemically modified microelectrode. *Proceedings of the national academy of sciences,* 92(21)**,** 9608-9612.

Hui, L. & Chen, Y. (2015). Tumor microenvironment: Sanctuary of the devil. *Cancer letters,* 368(1)**,** 7-13.

Hume, D. A., Summers, K. M., Raza, S., Baillie, J. K. & Freeman, T. C. (2010). Functional clustering and lineage markers: insights into cellular differentiation and gene function from large-scale microarray studies of purified primary cell populations. *Genomics,* 95(6)**,** 328-338.

Huopio, H., Jaaskelainen, J., Komulainen, J., Miettinen, R., Karkkainen, P., Laakso, M., Tapanainen, P., Voutilainen, R. & Otonkoski, T. (2002). Acute insulin response tests for the differential diagnosis of congenital hyperinsulinism. *The Journal of clinical endocrinology & metabolism,* 87(10)**,** 4502-4507.

Huopio, H., Reimann, F., Ashfield, R., Komulainen, J., Lenko, H.-L., Rahier, J., Vauhkonen, I., Kere, J., Laakso, M. & Ashcroft, F. (2000). Dominantly inherited hyperinsulinism caused by a mutation in the sulfonylurea receptor type 1. *Journal of clinical investigation,* 106(7)**,** 897-906.

Hussain, K. (2005). Congenital hyperinsulinism. *Seminars in fetal and neonatal medicine,* 10(4), 369-376.

Hussain, K. (2008). Diagnosis and management of hyperinsulinaemic hypoglycaemia of infancy. *Hormone research in paediatrics,* 69(1)**,** 2-13.

Hussain, K., Blankenstein, O., De Lonlay, P. & Christesen, H. T. (2007). Hyperinsulinaemic hypoglycaemia: biochemical basis and the importance of maintaining normoglycaemia during management. *Archives of disease in childhood,* 92(7)**,** 568-570.

Hussain, K., Bryan, J., Christesen, H. T., Brusgaard, K. & Aguilar-Bryan, L. (2005a). Serum glucagon counterregulatory hormonal response to hypoglycemia is blunted in congenital hyperinsulinism. *Diabetes,* 54(10)**,** 2946-2951.

Hussain, K., Clayton, P. T., Krywawych, S., Chatziandreou, I., Mills, P., Ginbey, D., Geboers, A. J., Berger, R., van den Berg, I. E. & Eaton, S. (2005b). Hyperinsulinism of infancy associated with a novel splice site mutation in the *SCHAD* gene. *The Journal of pediatrics,* 146(5)**,** 706-708.

Hussain, K., Flanagan, S. E., Smith, V. V., Ashworth, M., Day, M., Pierro, A. & Ellard, S. (2008). An *ABCC8* gene mutation and mosaic uniparental isodisomy resulting in atypical diffuse congenital hyperinsulinism. *Diabetes,* 57(1)**,** 259-263.

Hussain, K., Hindmarsh, P. & Aynsley-Green, A. (2003). Neonates with symptomatic hyperinsulinemic hypoglycemia generate inappropriately low serum cortisol counterregulatory hormonal responses. *The Journal of clinical endocrinology & metabolism,* 88(9)**,** 4342-4347.

Hussain, M. A., Porras, D. L., Rowe, M. H., West, J. R., Song, W.-J., Schreiber, W. E. & Wondisford, F. E. (2006). Increased pancreatic β-cell proliferation mediated by CREB binding protein gene activation. *Molecular and cellular biology,* 26(20)**,** 7747-7759.

Hutvágner, G. & Zamore, P. D. (2002). A microRNA in a multiple-turnover RNAi enzyme complex. *Science,* 297(5589)**,** 2056-2060.

Hwang, W. S., Ryu, Y. J., Park, J. H., Park, E. S., Lee, E. G., Koo, J. M., Jeon, H. Y., Lee, B. C., Kang, S. K. & Kim, S. J. (2004). Evidence of a pluripotent human embryonic stem cell line derived from a cloned blastocyst. *Science,* 303(5664)**,** 1669-1674.

Imai, Y., Patel, H. R., Hawkins, E. J., Doliba, N. M., Matschinsky, F. M. & Ahima, R. S. (2007). Insulin secretion is increased in pancreatic islets of neuropeptide Y-deficient mice. *Endocrinology,* 148(12)**,** 5716-5723.

Impey, S., Smith, D. M., Obrietan, K., Donahue, R., Wade, C. & Storm, D. R. (1998). Stimulation of cAMP response element (CRE)-mediated transcription during contextual learning. *Nature neuroscience,* 1(7)**,** 595-601.

Inagaki, N., Gonoi, T., Clement, J. P., Namba, N., Inazawa, J., Gonzalez, G., Aguilar-Bryan, L., Seino, S. & Bryan, J. (1995). Reconstitution of I_{KATP}: an inward rectifier subunit plus the sulfonylurea receptor. *Science,* 270(5239)**,** 1166-1170.

Ish-Shalom, D., Christoffersen, C., Vorwerk, P., Sacerdoti-Sierra, N., Shymko, R., Naor, D. & De Meyts, P. (1997). Mitogenic properties of insulin and insulin analogues mediated by the insulin receptor. *Diabetologia,* 40(2)**,** S25-S31.

Ishihara, H., Asano, T., Tsukuda, K., Katagiri, H., Inukai, K., Anai, M., Kikuchi, M., Yazaki, Y., Miyazaki, J.-I. & Oka, Y. (1993). Pancreatic beta cell line MIN6 exhibits characteristics of glucose metabolism and glucose-stimulated insulin secretion similar to those of normal islets. *Diabetologia,* 36(11)**,** 1139-1145.

Ishihara, H., Wang, H., Drewes, L. R. & Wollheim, C. B. (1999). Overexpression of monocarboxylate transporter and lactate dehydrogenase alters insulin secretory responses to pyruvate and lactate in β cells. *Journal of clinical investigation,* 104(11)**,** 1621-1629.

Ishiyama, N., Ravier, M. A. & Henquin, J.-C. (2006). Dual mechanism of the potentiation by glucose of insulin secretion induced by arginine and tolbutamide in mouse islets. *American journal of physiology-endocrinology and metabolism,* 290(3)**,** E540-E549.

Iype, T., Francis, J., Garmey, J. C., Schisler, J. C., Nesher, R., Weir, G. C., Becker, T. C., Newgard, C. B., Griffen, S. C. & Mirmira, R. G. (2005). Mechanism of insulin gene regulation by the pancreatic transcription factor Pdx-1 application of pre-mRNA analysis and chromatin immunoprecipitation to assess formation of functional transcriptional complexes. *Journal of biological chemistry,* 280(17)**,** 16798-16807.

Jaffe, A. E., Gao, Y., Deep-Soboslay, A., Tao, R., Hyde, T. M., Weinberger, D. R. & Kleinman, J. E. (2016). Mapping DNA methylation across development, genotype and schizophrenia in the human frontal cortex. *Nature neuroscience,* 19(1)**,** 40-47.

Jaksik, R., Iwanaszko, M., Rzeszowska-Wolny, J. & Kimmel, M. (2015). Microarray experiments and factors which affect their reliability. *Biology direct,* 10(1)**,** 46.

James, C., Kapoor, R. R., Ismail, D. & Hussain, K. (2009). The genetic basis of congenital hyperinsulinism. *Journal of medical genetics,* 46(5)**,** 289-299.

Jeffery, N., Richardson, S., Beall, C. & Harries, L. (2017). The species origin of the cellular microenvironment influences markers of beta cell fate and function in EndoC-βH1 cells. *Experimental cell research,* 361(2)**,** 284-291.

Jesmin, J., Rashid, M., Jamil, H., Hontecillas, R. & Bassaganya-Riera, J. (2010). Gene regulatory network reveals oxidative stress as the underlying molecular mechanism of type 2 diabetes and hypertension. *BMC medical genomics,* 3**,** 45.

Ji, H. & Davis, R. W. (2006). Data quality in genomics and microarrays. *Nature biotechnology,* 24(9)**,** 1112-1113.

Jia, J., Liu, X., Chen, Y., Zheng, X., Tu, L., Huang, X. & Wang, X. (2014). Establishment of a pancreatic β cell proliferation model *in vitro* and a platform for diabetes drug screening. *Cytotechnology,* 66(4)**,** 687-697.

Jia, S., Ivanov, A., Blasevic, D., Müller, T., Purfürst, B., Sun, W., Chen, W., Poy, M. N., Rajewsky, N. & Birchmeier, C. (2015). Insm1 cooperates with Neurod1 and Foxa2 to maintain mature pancreatic β-cell function. *The EMBO journal,* 34(10)**,** 1417-1433.

Jiménez-Marín, Á., Collado-Romero, M., Ramirez-Boo, M., Arce, C. & Garrido, J. J. (2009). Biological pathway analysis by ArrayUnlock and ingenuity pathway analysis. *BMC proceedings,* 3(suppl 4), S6.

Jin, L., Zuo, X.-Y., Su, W.-Y., Zhao, X.-L., Yuan, M.-Q., Han, L.-Z., Zhao, X., Chen, Y.-D. & Rao, S.-Q. (2014). Pathway-based analysis tools for complex diseases: a review. *Genomics, proteomics & bioinformatics,* 12(5)**,** 210-220.

Jin, Z., Li, R., Zhou, C., Shi, L., Zhang, X., Yang, Z. & Zhang, D. (2016). Efficient gene knockdown in mouse oocytes through peptide nanoparticle-mediated sirna transfection. *PLoS One,* 11(3)**,** e0150462.

Johnson, B., Shindo, N., Rathjen, P., Rathjen, J. & Keough, R. (2008). Understanding pluripotency—how embryonic stem cells keep their options open. *Molecular human reproduction,* 14(9)**,** 513-520.

Johnson, D., Shepherd, R. M., Gill, D., Gorman, T., Smith, D. M. & Dunne, M. J. (2007a). Glucose-dependent modulation of insulin secretion and intracellular calcium ions by GKA50, a glucokinase activator. *Diabetes,* 56(6)**,** 1694-1702.

Johnson, W. E., Li, C. & Rabinovic, A. (2007b). Adjusting batch effects in microarray expression data using empirical Bayes methods. *Biostatistics,* 8(1)**,** 118-127.

Jonsson, J., Carlsson, L., Edlund, T. & Edlund, H. (1994). Insulin-promoter-factor 1 is required for pancreas development in mice. *Nature,* 371(6498)**,** 606-609.

Juan, H.-F. & Huang, H.-C. (2007). Bioinformatics: microarray data clustering and functional classification, in Rampal, J. B. (ed.) *Microarrays: volume 2, applicaton and data analysis* 2nd edn. Springer, pp. 405-416.

Justice, M. J. & Dhillon, P. (2016). Using the mouse to model human disease: increasing validity and reproducibility. *Disease models & mechanisms,* 9(2), 101-103.

Kaestner, K. H., Lee, C. S., Scearce, L. M., Brestelli, J. E., Arsenlis, A., Le, P. P., Lantz, K. A., Crabtree, J., Pizarro, A. & Mazzarelli, J. (2003). Transcriptional program of the endocrine pancreas in mice and humans. *Diabetes,* 52(7)**,** 1604-1610.

Kailey, B., van de Bunt, M., Cheley, S., Johnson, P. R., MacDonald, P. E., Gloyn, A. L., Rorsman, P. & Braun, M. (2012). SSTR2 is the functionally dominant somatostatin receptor in human pancreatic β-and α-cells. *American journal of physiology-endocrinology and metabolism,* 303(9)**,** E1107-E1116.

Kalathur, R. K. R., Pinto, J. P., Hernandez-Prieto, M. A., Machado, R. S., Almeida, D., Chaurasia, G. & Futschik, M. E. (2013). UniHI 7: an enhanced database for retrieval and interactive analysis of human molecular interaction networks. *Nucleic acids research,* 42(D1)**,** D408-D414.

Kanazawa, T., Konno, A., Hashimoto, Y. & Kon, Y. (2010). Hepatocyte nuclear factor 4 alpha is related to survival of the condensed mesenchyme in the developing mouse kidney. *Developmental dynamics,* 239(4)**,** 1145-1154.

Kane, C., Shepherd, R., Squires, P., Johnson, P., James, R., Milla, P., Aynsley-Green, A., Lindley, K. & Dunne, M. (1996). Loss of functional K_{ATP} channels in pancreatic β-cells causes persistent hyperinsulinemic hypoglycemia of infancy. *Nature medicine,* 2(12), 1344-1347.

Kanehisa, M., Furumichi, M., Tanabe, M., Sato, Y. & Morishima, K. (2016). KEGG: new perspectives on genomes, pathways, diseases and drugs. *Nucleic acids research,* 45(D1)**,** D353-D361.

Kanehisa, M. & Goto, S. (2000). KEGG: kyoto encyclopedia of genes and genomes. *Nucleic acids research,* 28(1)**,** 27-30.

Kao, P. Y., Leung, K. H., Chan, L. W., Yip, S. P. & Yap, M. K. (2017). Pathway analysis of complex diseases for GWAS, extending to consider rare variants, multi-omics and interactions. *Biochimica et Biophysica Acta (BBA)-General Subjects,* 1861(2)**,** 335-353.

Kao, R. L., Ha, T., Li, C., Gao, X., Zhang, F., Yiang, Z., Chen, Y. & Ma, W. (2011). Stem cell therapy for myocardial regeneration: the Chinese experience, in Prakash, S. and Shum-Tim, D (eds.) *Stem cell bioengineering and tissue engineering microenvironment.* World Scientific, pp. 457-480.

Kapoor, R. R., Flanagan, S. E., Arya, V. B., Shield, J. P., Ellard, S. & Hussain, K. (2013). Clinical and molecular characterisation of 300 patients with congenital hyperinsulinism. *European journal of endocrinology,* 168(4)**,** 557-564.

Kapoor, R. R., Flanagan, S. E., Fulton, P., Chakrapani, A., Chadefaux, B., Ben-Omran, T., Banerjee, I., Shield, J. P., Ellard, S. & Hussain, K. (2009a). Hyperinsulinism–hyperammonaemia syndrome: novel mutations in the *GLUD1* gene and genotype–phenotype correlations. *European journal of endocrinology,* 161(5)**,** 731-735.

Kapoor, R. R., Heslegrave, A. & Hussain, K. (2010). Congenital hyperinsulinism due to mutations in *HNF4A* and *HADH. Reviews in endocrine and metabolic disorders,* 11(3)**,** 185-191.

Kapoor, R. R., James, C., Flanagan, S. E., Ellard, S., Eaton, S. & Hussain, K. (2009b). 3-Hydroxyacyl-coenzyme A dehydrogenase deficiency and hyperinsulinemic hypoglycemia: characterization of a novel mutation and severe dietary protein sensitivity. *The Journal of clinical endocrinology & metabolism,* 94(7)**,** 2221-2225.

Kapoor, R. R., Locke, J., Colclough, K., Wales, J., Conn, J. J., Hattersley, A. T., Ellard, S. & Hussain, K. (2008). Persistent hyperinsulinemic hypoglycemia and maturity-onset diabetes of the young due to heterozygous *HNF4A* mutations. *Diabetes,* 57(6)**,** 1659-1663.

Kassem, S., Ariel, I., Thornton, P., Hussain, K., Smith, V., Lindley, K., Aynsley-Green, A. & Glaser, B. (2001). p57KIP2 expression in normal islet cells and in hyperinsulinism of infancy. *Diabetes,* 50(12)**,** 2763-2769.

Kassem, S., Ariel, I., Thornton, P., Scheimberg, I. & Glaser, B. (2000). Beta-cell proliferation and apoptosis in the developing normal human pancreas and in hyperinsulinism of infancy. *Diabetes,* 49(8)**,** 1325-1333.

Kassem, S., Bhandari, S., Rodríguez-Bada, P., Motaghedi, R., Heyman, M., García-Gimeno, M. A., Cobo-Vuilleumier, N., Sanz, P., Maclaren, N. K. & Rahier, J. (2010). Large islets, beta-cell proliferation, and a glucokinase mutation. *New England journal of medicine,* 362(14)**,** 1348-1350.

Kaul, M. & Eichinger, L. (2006). Analysis of gene expression using cDNA microarrays, in Eichinger, L. and Rivero, F. (eds.) *Dictyostelium discoideum protocols.* Springer, pp. 75-93.

Kellaway, S. (2016). *Stem cells from patients with congenital hyperinsulinism.* Ph.D. University of Manchester.

Kelly, A., Ng, D., Ferry, R. J., Grimberg, A., Koo-McCoy, S., Thornton, P. S. & Stanley, C. A. (2001). Acute insulin responses to leucine in children with the hyperinsulinism/ hyperammonemia syndrome. *Journal of clinical endocrinology & metabolism,* 86(8)**,** 3724-3728.

Killcoyne, S., Carter, G. W., Smith, J. & Boyle, J. (2009). Cytoscape: a community-based framework for network modeling, in Nilolsky, Y. and Bryant, J. (eds.) *Protein networks and pathway analysis.* Springer, pp. 219-239.

Kim, J.-W., Seghers, V., Cho, J.-H., Kang, Y., Kim, S., Ryu, Y., Baek, K., Aguilar-Bryan, L., Lee, Y.-D. & Bryan, J. (2002). Transactivation of the mouse sulfonylurea receptor I gene by BETA2/NeuroD. *Molecular endocrinology,* 16(5)**,** 1097-1107.

Kim, J., Song, G., Wu, G., Gao, H., Johnson, G. A. & Bazer, F. W. (2013). Arginine, leucine, and glutamine stimulate proliferation of porcine trophectoderm cells through the MTOR-RPS6K-RPS6-EIF4EBP1 signal transduction pathway. *Biology of reproduction,* 88(5)**,** 113, 1-9.

Kim, J., Wende, A. R., Sena, S., Theobald, H. A., Soto, J., Sloan, C., Wayment, B. E., Litwin, S. E., Holzenberger, M. & LeRoith, D. (2008). Insulin-like growth factor I receptor signaling is required for exercise-induced cardiac hypertrophy. *Molecular endocrinology,* 22(11)**,** 2531-2543.

Kim, K., Doi, A., Wen, B., Ng, K., Zhao, R., Cahan, P., Kim, J., Aryee, M., Ji, H. & Ehrlich, L. (2010). Epigenetic memory in induced pluripotent stem cells. *Nature,* 467(7313)**,** 285-290.

Kim, P. M., Lu, L. J., Xia, Y. & Gerstein, M. B. (2006a). Relating three-dimensional structures to protein networks provides evolutionary insights. *Science,* 314(5807)**,** 1938-1941.

Kim, S., Kim, D., Cho, S. W., Kim, J. & Kim, J.-S. (2014). Highly efficient RNA-guided genome editing in human cells via delivery of purified Cas9 ribonucleoproteins. *Genome research,* 24(6)**,** 1012-1019.

Kim, Y., Girard, L., Giacomini, C., Wang, P., Hernandez-Boussard, T., Tibshirani, R., Minna, J. & Pollack, J. (2006b). Combined microarray analysis of small cell lung cancer reveals altered apoptotic balance and distinct expression signatures of MYC family gene amplification. *Oncogene,* 25(1)**,** 130.

Kimple, M. E., Neuman, J. C., Linnemann, A. K. & Casey, P. J. (2014). Inhibitory G proteins and their receptors: emerging therapeutic targets for obesity and diabetes. *Experimental & molecular medicine,* 46(6)**,** e102.

Kitano, H. (2002). Computational systems biology. *Nature,* 420(6912)**,** 206.

Klein, D. (2002). Quantification using real-time PCR technology: applications and limitations. *Trends in molecular medicine,* 8(6)**,** 257-260.

Kloppel, G., Anlauf, M., Raffel, A., Perren, A. & Knoefel, W. T. (2008). Adult diffuse nesidioblastosis: genetically or environmentally induced? *Human pathology,* 39(1)**,** 3-8.

Kloppel, G., Reinecke-Lüthge, A. & Koschoreck, F. (1999). Focal and diffuse beta cell changes in persistent hyperinsulinemic hypoglycemia of infancy. *Endocrine pathology,* 10(4)**,** 299-304.

Koh, S. & Piedrahita, J. A. (2014). From "ES-like" cells to induced pluripotent stem cells: a historical perspective in domestic animals. *Theriogenology,* 81(1)**,** 103-111.

Koh, T., Aynsley-Green, A., Tarbit, M. & Eyre, J. (1988). Neural dysfunction during hypoglycaemia. *Archives of disease in childhood,* 63(11)**,** 1353-1358.

Kohl, M., Wiese, S. & Warscheid, B. (2011). Cytoscape: software for visualization and analysis of biological networks, in Hamacher, M, Eisenacher, M. and Stephan, C. (eds.) *Data Mining in Proteomics: from standards to application.* Springer, pp. .291-303.

Komatsu, M., Schermerhorn, T., Aizawa, T. & Sharp, G. (1995). Glucose stimulation of insulin release in the absence of extracellular Ca^{2+} and in the absence of any increase in intracellular Ca^{2+} in rat pancreatic islets. *Proceedings of the national academy of sciences,* 92(23)**,** 10728-10732.

Koren, D. & Palladino, A. (2016). Hypoglycemia, in Weiss, R. E. and Refetoff, S. (eds.) *Genetic diagnosis of endocrine disorders.* 2nd edn. Elsevier, pp. 31-75.

Koschmieder, A., Zimmermann, K., Trißl, S., Stoltmann, T. & Leser, U. (2011). Tools for managing and analyzing microarray data. *Briefings in bioinformatics,* 13(1)**,** 46-60.

Kosciolek, B. A., Kalantidis, K., Tabler, M. & Rowley, P. T. (2003). Inhibition of Telomerase Activity in Human Cancer Cells by RNA Interference1. *Molecular cancer therapeutics,* 2(3)**,** 209-216.

Kotani, K., Kawabe, J., Morikawa, H., Akahoshi, T., Hashizume, M. & Shiomi, S. (2015). Comprehensive screening of gene function and networks by DNA microarray analysis in Japanese patients with idiopathic portal hypertension. *Mediators of inflammation,* 2015, 349215.

Kovach, S. J., Price, J. A., Shaw, C. M., Theodorakis, N. G. & McKillop, I. H. (2006). Role of cyclic-AMP responsive element binding (CREB) proteins in cell proliferation in a rat model of hepatocellular carcinoma. *Journal of cellular physiology,* 206(2)**,** 411-419.

Kowluru, A., Li, G., Rabaglia, M. E., Segu, V. B., Hofmann, F., Aktories, K. & Metz, S. A. (1997). Evidence for differential roles of the Rho subfamily of GTP-binding proteins in glucose-and calcium-induced insulin secretion from pancreatic β cells. *Biochemical pharmacology,* 54(10)**,** 1097-1108.

Krishnan, K., Ma, Z., Björklund, A. & Islam, M. S. (2015). Calcium signaling in a genetically engineered human pancreatic β-cell line. *Pancreas,* 44(5)**,** 773-777.

Kumar, B., Kumar, P., Rajput, R., Daga, M., Singh, V. & Khanna, M. (2012). Comparative reproducibility of SYBR Green I and TaqMan real-time PCR chemistries for the analysis of matrix and hemagglutinin genes of Influenza A viruses. *International journal of collaborative research on internal medicine & public health,* 4(7)**,** 1346-1352.

Kumar, G., Breen, E. J. & Ranganathan, S. (2013). Identification of ovarian cancer associated genes using an integrated approach in a Boolean framework. *BMC systems biology,* 7(1)**,** 12.

Kumar, S., Stecher, G. & Tamura, K. (2016). MEGA7: molecular evolutionary genetics analysis version 7.0 for bigger datasets. *Molecular biology and evolution,* 33(7)**,** 1870-1874.

Kursan, S., McMillen, T. S., Beesetty, P., Dias-Junior, E., Almutairi, M. M., Sajib, A. A., Kozak, J. A., Aguilar-Bryan, L. & Di Fulvio, M. (2017). The neuronal K^+ Cl^- co-transporter 2 (Slc12a5) modulates insulin secretion. *Scientific reports,* 7(1)**,** 1732.

Kwon, G., Marshall, C. A., Pappan, K. L., Remedi, M. S. & McDaniel, M. L. (2004). Signaling elements involved in the metabolic regulation of mTOR by nutrients, incretins, and growth factors in islets. *Diabetes,* 53(suppl 3)**,** S225-S232.

Lam, J. K., Chow, M. Y., Zhang, Y. & Leung, S. W. (2015). siRNA versus miRNA as therapeutics for gene silencing. *Molecular therapy-nucleic acids,* 4(9), e252.

Landgraf, R., Landgraf-Leurs, M. & Hoerl, R. (1974). L-Leucine and L-phenylalanine induced insulin release and the influence of D-glucose. *Diabetologia,* 10(5)**,** 415-420.

Lantz, K. A., Vatamaniuk, M. Z., Brestelli, J. E., Friedman, J. R., Matschinsky, F. M. & Kaestner, K. H. (2004). *Foxa2* regulates multiple pathways of insulin secretion. *The Journal of clinical investigation,* 114(4)**,** 512-520.

Lau, J., Grapengiesser, E. & Hellman, B. (2016). Small Mouse Islets Are Deficient in Glucagon-Producing Alpha Cells but Rich in Somatostatin-Secreting Delta Cells. *Journal of diabetes research,* 4930741.

Le Brigand, L., Virsolvy, A., Peyrollier, K., Manechez, D., Godfroid, J.-J., Guardiola-Lemaître, B. & Bataille, D. (1997). Stimulation of insulin release from the MIN6 cell line by a new imidazoline compound, S-21663: evidence for the existence of a novel imidazoline site in β cells. *British journal of pharmacology,* 122(4)**,** 786-791.

Le Lay, J. & Stein, R. (2006). Involvement of PDX-1 in activation of human insulin gene transcription. *Journal of endocrinology,* 188(2)**,** 287-294.

Leeper, N. J., Hunter, A. L. & Cooke, J. P. (2010). Stem cell therapy for vascular regeneration: adult, embryonic, and induced pluripotent stem cells. *Circulation,* 122(5)**,** 517-526.

Leung, Y. F. & Cavalieri, D. (2003). Fundamentals of cDNA microarray data analysis. *TRENDS in genetics,* 19(11)**,** 649-659.

Li, C., Chen, P., Palladino, A., Narayan, S., Russell, L. K., Sayed, S., Xiong, G., Chen, J., Stokes, D. & Butt, Y. M. (2010a). Mechanism of hyperinsulinism in short-chain 3-hydroxyacyl-CoA dehydrogenase deficiency involves activation of glutamate dehydrogenase. *Journal of biological chemistry,* 285(41)**,** 31806-31818.

Li, H. L., Gee, P., Ishida, K. & Hotta, A. (2016). Efficient genomic correction methods in human iPS cells using CRISPR–Cas9 system. *Methods,* 101**,** 27-35.

Li, P., Wei, J., Gao, X., Wei, B., Lin, H., Huang, R., Niu, Y., Lim, K., Jing, K. & Chu, J. (2017). Insulin Promotes the Proliferation of Human Umbilical Cord Matrix-Derived Mesenchymal Stem Cells by Activating the Akt-Cyclin D1 Axis. *Stem cells international,* 2017, 7371615.

Li, W.-C., Rukstalis, J. M., Nishimura, W., Tchipashvili, V., Habener, J. F., Sharma, A. & Bonner-Weir, S. (2010b). Activation of pancreatic-duct-derived progenitor cells during pancreas regeneration in adult rats. *Journal of cell science,* 123(16)**,** 2792-2802.

Li, W. (2012). Volcano plots in analyzing differential expressions with mRNA microarrays. *Journal of bioinformatics and computational biology,* 10(6)**,** 1231003.

Liang, G. & Zhang, Y. (2013). Embryonic stem cell and induced pluripotent stem cell: an epigenetic perspective. *Cell research,* 23(1)**,** 49-69.

Light, P. E., Manning Fox, J. E., Riedel, M. J. & Wheeler, M. B. (2002). Glucagon-like peptide-1 inhibits pancreatic ATP-sensitive potassium channels via a protein kinase A-and ADP-dependent mechanism. *Molecular endocrinology,* 16(9)**,** 2135-2144.

Lin, Y. & Sun, Z. (2012). Antiaging gene Klotho enhances glucose-induced insulin secretion by up-regulating plasma membrane levels of TRPV2 in MIN6 β-cells. *Endocrinology,* 153(7)**,** 3029-3039.

Lin, Y. & Sun, Z. (2015a). Anti-aging Gene Klotho Attenuates Pancreatic β Cell Apoptosis in Type I Diabetes. *Diabetes***,** 64(12), 4298-4311.

Lin, Y. & Sun, Z. (2015b). In vivo pancreatic β cell-specific expression of anti-aging gene Klotho, a novel approach for preserving β cells in type II diabetes. *Diabetes***,** 64(4), 1444-1458.

Liu, S., Qu, Y., Stewart, T. J., Howard, M. J., Chakrabortty, S., Holekamp, T. F. & McDonald, J. W. (2000). Embryonic stem cells differentiate into oligodendrocytes and myelinate in culture and after spinal cord transplantation. *Proceedings of the national academy of sciences,* 97(11)**,** 6126-6131.

Liu, Y.-Z., Zhou, Y., Zhang, L., Li, J., Tian, Q., Zhang, J.-G. & Deng, H.-W. (2015). Attenuated monocyte apoptosis, a new mechanism for osteoporosis suggested by a transcriptome-wide expression study of monocytes. *PLoS one,* 10(2)**,** e0116792.

Liu, Z., Jeppesen, P. B., Gregersen, S., Larsen, L. B. & Hermansen, K. (2012). Chronic exposure to leucine *in vitro* induces β-cell dysfunction in INS-1E cells and mouse islets. *Journal of endocrinology,* 215(1)**,** 79-88.

Lones, M. A., Smith, S. L., Tyrrell, A. M., Alty, J. E. & Jamieson, D. S. (2013). Characterising neurological time series data using biologically motivated networks of coupled discrete maps. *BioSystems,* 112(2)**,** 94-101.

Lord, K. & De León, D. D. (2013). Monogenic hyperinsulinemic hypoglycemia: current insights into the pathogenesis and management. *International journal of pediatric endocrinology,* 2013(1)**,** 3.

Loscalzo, J., Kohane, I. & Barabasi, A. L. (2007). Human disease classification in the postgenomic era: a complex systems approach to human pathobiology. *Molecular systems biology,* 3(1)**,** 124.

Lotia, S., Montojo, J., Dong, Y., Bader, G. D. & Pico, A. R. (2013). Cytoscape app store. *Bioinformatics,* 29(10)**,** 1350-1351.

Lou, X. J., Schena, M., Horrigan, F. T., Lawn, R. M. & Davis, R. W. (2001). Expression monitoring using cDNA microarrays: a general protocol, in Starkey, M. P. and Elaswarapu, R. (eds.) *Genomics protocols.* Springer, pp. 323-340.

Lovisolo, S. M., Mendonça, B. B., Pinto, E. M., Manna, T. D., Saldiva, P. H. N. & Zerbini, M. C. N. (2010). Congenital hyperinsulinism in brazilian neonates: a study of histology, K_{ATP} channel genes, and proliferation of β cells. *Pediatric and developmental pathology,* 13(5)**,** 375-384.

Lund, S. S., Tarnow, L., Frandsen, M., Nielsen, B. B., Hansen, B. V., Pedersen, O., Parving, H.-H. & Vaag, A. A. (2009). Combining insulin with metformin or an insulin secretagogue in non-obese patients with type 2 diabetes: 12 month, randomised, double blind trial. *BMJ,* 339**,** b4324.

Luo, C., Lü, D., Pan, J. & Long, M. (2016). Improving the gene transfection in human embryonic stem cells: balancing with cytotoxicity and pluripotent maintenance. *ACS applied materials & interfaces,* 8(13)**,** 8367-8375.

Ma, F., Chen, F., Chi, Y., Yang, S., Lu, S. & Han, Z. (2012). Isolation of pancreatic progenitor cells with the surface marker of hematopoietic stem cells. *International journal of endocrinology,* 948683.

MacDonald, P. & Wheeler, M. (2003). Voltage-dependent K^+ channels in pancreatic beta cells: role, regulation and potential as therapeutic targets. *Diabetologia,* 46(8)**,** 1046-1062.

MacDonald, P. E., El-kholy, W., Riedel, M. J., Salapatek, A. M. F., Light, P. E. & Wheeler, M. B. (2002). The multiple actions of GLP-1 on the process of glucose-stimulated insulin secretion. *Diabetes,* 51(suppl 3)**,** S434-S442.

Macfarlane, W. M., Frayling, T. M., Ellard, S., Evans, J. C., Allen, L. I., Bulman, M. P., Ayres, S., Shepherd, M., Clark, P. & Millward, A. (1999). Missense mutations in the insulin promoter factor-1 gene predispose to type 2 diabetes. *The journal of clinical investigation,* 104(9)**,** R33-R39.

Mackenzie, R. W. & Elliott, B. T. (2014). Akt/PKB activation and insulin signaling: a novel insulin signaling pathway in the treatment of type 2 diabetes. *Diabetes, metabolic syndrome and obesity: targets and therapy,* 7, 55-64.

MacMullen, C. M., Zhou, Q., Snider, K. E., Tewson, P. H., Becker, S. A., Aziz, A. R., Ganguly, A., Shyng, S.-L. & Stanley, C. A. (2011). Diazoxide-unresponsive congenital hyperinsulinism in children with dominant mutations of the β-cell sulfonylurea receptor SUR1. *Diabetes,* 60(6)**,** 1797-1804.

Mah, N., Thelin, A., Lu, T., Nikolaus, S., Kühbacher, T., Gurbuz, Y., Eickhoff, H., Klöppel, G. n., Lehrach, H. & Mellgard, B. (2004). A comparison of oligonucleotide and cDNA-based microarray systems. *Physiological genomics,* 16(3)**,** 361-370.

Mao, G. & Zhang, N. (2013). Analysis of average shortest-path length of scale-free network. *Journal of applied mathematics,* 2013, 865643.

Mar, J. C., Kimura, Y., Schroder, K., Irvine, K. M., Hayashizaki, Y., Suzuki, H., Hume, D. & Quackenbush, J. (2009). Data-driven normalization strategies for high-throughput quantitative RT-PCR. *BMC bioinformatics,* 10(1)**,** 110.

Mariot, P., Gilon, P., Nenquin, M. & Henquin, J.-C. (1998). Tolbutamide and diazoxide influence insulin secretion by changing the concentration but not the action of cytoplasmic Ca^{2+} in beta-cells. *Diabetes,* 47(3)**,** 365-373.

Martens, G. A., Vervoort, A., Van de Casteele, M., Stangé, G., Hellemans, K., Van Thi, H. V., Schuit, F. & Pipeleers, D. (2007). Specificity in beta cell expression of L-3-hydroxyacyl-CoA dehydrogenase, short chain, and potential role in down-regulating insulin release. *Journal of biological chemistry,* 282(29)**,** 21134-21144.

Marthinet, E., Bloc, A., Oka, Y., Tanizawa, Y., Wehrle-Haller, B., Bancila, V., Dubuis, J.-M., Philippe, J. & Schwitzgebel, V. M. (2005). Severe congenital hyperinsulinism caused by a mutation in the Kir6. 2 subunit of the adenosine triphosphate-sensitive potassium channel impairing trafficking and function. *Journal of clinical endocrinology & metabolism,* 90(9)**,** 5401-5406.

Martinez, J., Patkaniowska, A., Urlaub, H., Lührmann, R. & Tuschl, T. (2002). Single-stranded antisense siRNAs guide target RNA cleavage in RNAi. *Cell,* 110(5)**,** 563-574.

Maruyama, T., Dougan, S. K., Truttmann, M. C., Bilate, A. M., Ingram, J. R. & Ploegh, H. L. (2015). Increasing the efficiency of precise genome editing with CRISPR-Cas9 by inhibition of nonhomologous end joining. *Nature biotechnology,* 33(5)**,** 538-542.

Mashal, R. D., Koontz, J. & Sklar, J. (1995). Detection of mutations by cleavage of DNA heteroduplexes with bacteriophage resolvases. *Nature genetics,* 9(2)**,** 177-183.

Mastracci, T. L., Anderson, K. R., Papizan, J. B. & Sussel, L. (2013). Regulation of Neurod1 contributes to the lineage potential of Neurogenin3^{+} endocrine precursor cells in the pancreas. *PLoS genetics,* 9(2)**,** e1003278.

Matschinsky, F., Liang, Y., Kesavan, P., Wang, L., Froguel, P., Velho, G., Cohen, D., Permutt, M., Tanizawa, Y. & Jetton, T. (1993). Glucokinase as pancreatic beta cell glucose sensor and diabetes gene. *The Journal of clinical investigation,* 92(5)**,** 2092-2098.

Mayorga, A. J. & Lucki, I. (2001). Limitations on the use of the C57BL/6 mouse in the tail suspension test. *Psychopharmacology,* 155(1)**,** 110-112.

McBride, J. L., Boudreau, R. L., Harper, S. Q., Staber, P. D., Monteys, A. M., Martins, I., Gilmore, B. L., Burstein, H., Peluso, R. W. & Polisky, B. (2008). Artificial miRNAs mitigate shRNA-mediated toxicity in the brain: implications for the therapeutic development of RNAi. *Proceedings of the national academy of sciences,* 105(15)**,** 5868-5873.

McCall, M. N., McMurray, H. R., Land, H. & Almudevar, A. (2014). On non-detects in qPCR data. *Bioinformatics,* 30(16)**,** 2310-2316.

McQuarrie, I. (1954). Idiopathic spontaneously occurring hypoglycemia in infantsClinical significance of problem and treatment. *AMA American journal of diseases of children,* 87(4)**,** 399-428.

Mehta, J. P. & Rani, S. (2011). Software and tools for microarray data analysis, in O'Driscoll, L. (ed.) *Gene expression profiling: methods and protocols.* Springer, pp. 41-53.

Mei, Y., Liao, J., Shen, J., Yu, L., Liu, B., Liu, L., Li, R., Ji, L., Dorsey, S. & Jiang, Z. (2012). Small nucleolar RNA 42 acts as an oncogene in lung tumorigenesis. *Oncogene,* 31(22)**,** 2794-2804.

Meissner, T., Wendel, U., Burgard, P., Schaetzle, S. & Mayatepek, E. (2003). Long-term follow-up of 114 patients with congenital hyperinsulinism. *European journal of endocrinology,* 149(1)**,** 43-51.

Meloni, A., DeYoung, M., Lowe, C. & Parkes, D. (2013). GLP-1 receptor activated insulin secretion from pancreatic β-cells: mechanism and glucose dependence. *Diabetes, obesity and metabolism,* 15(1)**,** 15-27.

Melville, M., Doolan, P., Mounts, W., Barron, N., Hann, L., Leonard, M., Clynes, M. & Charlebois, T. (2011). Development and characterization of a Chinese hamster ovary cell-specific oligonucleotide microarray. *Biotechnology letters,* 33(9)**,** 1773-1779.

Menni, F., de Lonlay, P., Sevin, C., Touati, G., Peigné, C., Barbier, V., Nihoul-Fékété, C., Saudubray, J.-M. & Robert, J.-J. (2001). Neurologic outcomes of 90 neonates and infants with persistent hyperinsulinemic hypoglycemia. *Pediatrics,* 107(3)**,** 476-479.

Mi, H., Huang, X., Muruganujan, A., Tang, H., Mills, C., Kang, D. & Thomas, P. D. (2016). PANTHER version 11: expanded annotation data from Gene Ontology and Reactome pathways, and data analysis tool enhancements. *Nucleic acids research,* 45(D1)**,** D183-D189.

Mi, H., Muruganujan, A., Casagrande, J. T. & Thomas, P. D. (2013a). Large-scale gene function analysis with the PANTHER classification system. *Nature protocols,* 8(8)**,** 1551-1566.

Mi, H., Muruganujan, A. & Thomas, P. D. (2013b). PANTHER in 2013: modeling the evolution of gene function, and other gene attributes, in the context of phylogenetic trees. *Nucleic acids research,* 41(D1)**,** D377-D386.

Michailidou, K., Beesley, J., Lindstrom, S., Canisius, S., Dennis, J., Lush, M. J., Maranian, M. J., Bolla, M. K., Wang, Q. & Shah, M. (2015). Genome-wide association analysis of more than 120,000 individuals identifies 15 new susceptibility loci for breast cancer. *Nature genetics,* 47(4)**,** 373-380.

Michelsen, N. V., Brusgaard, K., Tan, Q., Thomassen, M., Hussain, K. & Christesen, H. T. (2011). Investigation of archived formalin-fixed paraffin-embedded pancreatic tissue with whole-genome gene expression microarray. *ISRN Pathology,* 2011, 275102.

Mikhailov, M. V., Campbell, J. D., de Wet, H., Shimomura, K., Zadek, B., Collins, R. F., Sansom, M. S., Ford, R. C. & Ashcroft, F. M. (2005). 3-D structural and functional characterization of the purified K_{ATP} channel complex Kir6. 2–SUR1. *The EMBO journal,* 24(23)**,** 4166-4175.

Miki, T., Nagashima, K., Tashiro, F., Kotake, K., Yoshitomi, H., Tamamoto, A., Gonoi, T., Iwanaga, T., Miyazaki, J.-i. & Seino, S. (1998). Defective insulin secretion and enhanced insulin action in KATP channel-deficient mice. *Proceedings of the national academy of sciences,* 95(18)**,** 10402-10406.

Millman, J. R., Xie, C., Van Dervort, A., Gürtler, M., Pagliuca, F. W. & Melton, D. A. (2016). Generation of stem cell-derived β-cells from patients with type 1 diabetes. *Nature communications,* 7**,** 11463.

Mimmack, M. L., Ryan, M., Baba, H., Navarro-Ruiz, J., Iritani, S., Faull, R. L., McKenna, P. J., Jones, P. B., Arai, H. & Starkey, M. (2002). Gene expression analysis in schizophrenia: reproducible up-regulation of several members of the apolipoprotein L family located in a high-susceptibility locus for schizophrenia on chromosome 22. *Proceedings of the national academy of sciences,* 99(7)**,** 4680-4685.

Miura, A., Yamagata, K., Kakei, M., Hatakeyama, H., Takahashi, N., Fukui, K., Nammo, T., Yoneda, K., Inoue, Y. & Sladek, F. M. (2006). Hepatocyte nuclear factor-4α is essential for glucose-stimulated insulin secretion by pancreatic β-cells. *Journal of biological chemistry,* 281(8)**,** 5246-5257.

Miyazaki, J.-I., Araki, K., Yamato, E., Ikegami, H., Asano, T., Shibasaki, Y., Oka, Y. & Yamamura, K.-I. (1990). Establishment of a pancreatic β cell line that retains glucose-inducible insulin secretion: special reference to expression of glucose transporter isoforms. *Endocrinology,* 127(1)**,** 126-132.

Mohamed, Z., Arya, V. B. & Hussain, K. (2012). Hyperinsulinaemic hypoglycaemia: genetic mechanisms, diagnosis and management. *Journal of clinical research in pediatric endocrinology,* 4(4)**,** 169-181.

Mohnike, K., Blankenstein, O., Minn, H., Mohnike, W., Fuchtner, F. & Otonkoski, T. (2008). [18F]-DOPA positron emission tomography for preoperative localization in congenital hyperinsulinism. *Hormone research in paediatrics,* 70(2)**,** 65-72.

Molkentin, J. D., Lu, J.-R., Antos, C. L., Markham, B., Richardson, J., Robbins, J., Grant, S. R. & Olson, E. N. (1998). A calcineurin-dependent transcriptional pathway for cardiac hypertrophy. *Cell,* 93(2)**,** 215-228.

Molnar, E., McIlhinney, R. J. & Ashcroft, S. J. (1995). Identification of functional ionotropic glutamate receptor proteins in pancreatic β-cells and in islets of Langerhans. *FEBS letters,* 371(3)**,** 253-257.

Molven, A., Matre, G. E., Duran, M., Wanders, R. J., Rishaug, U., Njølstad, P. R., Jellum, E. & Søvik, O. (2004). Familial hyperinsulinemic hypoglycemia caused by a defect in the SCHAD enzyme of mitochondrial fatty acid oxidation. *Diabetes,* 53(1)**,** 221-227.

Mootha, V. K., Lindgren, C. M., Eriksson, K.-F., Subramanian, A., Sihag, S., Lehar, J., Puigserver, P., Carlsson, E., Ridderstråle, M. & Laurila, E. (2003). PGC-1α-responsive genes involved in oxidative phosphorylation are coordinately downregulated in human diabetes. *Nature genetics,* 34(3)**,** 267-273.

Morey, J. S., Ryan, J. C. & Dolah, F. M. (2006). Microarray validation: factors influencing correlation between oligonucleotide microarrays and real-time PCR. *Biological procedures online,* 8(1)**,** 175-193.

Morris, K. V., Chan, S. W.-L., Jacobsen, S. E. & Looney, D. J. (2004). Small interfering RNA-induced transcriptional gene silencing in human cells. *Science,* 305(5688)**,** 1289-1292.

Mullooly, N., Vernon, W., Smith, D. M. & Newsholme, P. (2014). Elevated levels of branched-chain amino acids have little effect on pancreatic islet cells, but l-arginine impairs function through activation of the endoplasmic reticulum stress response. *Experimental physiology,* 99(3)**,** 538-551.

Munoz, A., Hu, M., Hussain, K., Bryan, J., Aguilar-Bryan, L. & Rajan, A. S. (2005). Regulation of glucagon secretion at low glucose concentrations: evidence for adenosine triphosphate-sensitive potassium channel involvement. *Endocrinology,* 146(12)**,** 5514-5521.

Murry, C. E. & Keller, G. (2008). Differentiation of embryonic stem cells to clinically relevant populations: lessons from embryonic development. *Cell,* 132(4)**,** 661-680.

Musunuru, K. (2013). Genome editing of human pluripotent stem cells to generate human cellular disease models. *Disease models & mechanisms,* 6(4)**,** 896-904.

Naito, Y. & Ui-Tei, K. (2012). siRNA design software for a target gene-specific RNA interference. *Frontiers in genetics,* 3**,** 102.

Narsinh, K. H., Plews, J. & Wu, J. C. (2011). Comparison of human induced pluripotent and embryonic stem cells: fraternal or identical twins? *Molecular therapy,* 19(4)**,** 635-638.

Naya, F. J., Stellrecht, C. & Tsai, M.-J. (1995). Tissue-specific regulation of the insulin gene by a novel basic helix-loop-helix transcription factor. *Genes & Development,* 9(8)**,** 1009-1019.

Nelson, D. L. & Cox, M. M. (2008). *Lehninger principles of biochemistry*. 8th edn. New York: W H Freeman and company.

Ness, S. A. (2007). Microarray analysis: basic strategies for successful experiments. *Molecular biotechnology,* 36(3)**,** 205-219.

Nessa, A., Aziz, Q. H., Thomas, A. M., Harmer, S. C., Tinker, A. & Hussain, K. (2015). Molecular mechanisms of congenital hyperinsulinism due to autosomal dominant mutations in *ABCC8*. *Human molecular genetics,* 24(18)**,** 5142-5153.

Nessa, A., Rahman, S. A. & Hussain, K. (2016). Hyperinsulinemic hypoglycemia–the molecular mechanisms. *Frontiers in endocrinology,* 7**,** 29.

Nestorowicz, A., Inagaki, N., Gonoi, T., Schoor, K. P., Wilson, B. A., Glaser, B., Landau, H., Stanley, C. A., Thornton, P. S. & Seino, S. (1997). A nonsense mutation in the inward rectifier potassium channel gene, Kir6. 2, is associated with familial hyperinsulinism. *Diabetes,* 46(11), 1743-1748.

Nestorowicz, A., Wilson, B. A., Schoor, K. P., Inoue, H., Glaser, B., Landau, H., Stanley, C. A., Thornton, P. S., Clement IV, J. P. & Bryan, J. (1996). Mutations in the sulfonylurea receptor gene are associated with familial hyperinsulinism in Ashkenazi Jews. *Human molecular genetics,* 5(11), 1813-1822.

Newman, M. E. (2005). A measure of betweenness centrality based on random walks. *Social networks,* 27(1)**,** 39-54.

Nichols, C., Shyng, S.-L., Nestorowicz, A., Glaser, B., Clement, J. t., Gonzalez, G., Aguilar-Bryan, L., Permutt, M. & Bryan, J. (1996). Adenosine diphosphate as an intracellular regulator of insulin secretion. *Science,* 272(5269)**,** 1785-1787.

Novak, G., Kim, D., Seeman, P. and Tallerico, T. (2002). Schizophrenia and Nogo: elevated mRNA in cortex, and high prevalence of a homozygous CAA insert. *Molecular brain research*, 107(2), 183-189.

Novak, J. P., Sladek, R. & Hudson, T. J. (2002b). Characterization of variability in large-scale gene expression data: implications for study design. *Genomics,* 79(1)**,** 104-113.

Nyitray, C. E., Chavez, M. G. & Desai, T. A. (2014). Compliant 3D microenvironment improves β-cell cluster insulin expression through mechanosensing and β-catenin signaling. *Tissue engineering part A,* 20(13-14)**,** 1888-1895.

O'Brien, K. P., Westerlund, I. & Sonnhammer, E. L. (2004). OrthoDisease: a database of human disease orthologs. *Human mutation,* 24(2)**,** 112-119.

Ocal, G., Flanagan, S. E., Hacihamdioğlu, B., Berberoğlu, M., Şiklar, Z., Ellard, S., Erdeve, Ş. S., Okulu, E., Akin, I. M. & Atasay, B. (2011). Clinical characteristics of recessive and dominant congenital hyperinsulinism due to mutation (s) in the *ABCC8/KCNJ11* genes encoding the ATP-sensitive potasium channel in the pancreatic beta cell. *Journal of pediatric endocrinology and metabolism,* 24(11-12)**,** 1019-1023.

Odom, D. T., Zizlsperger, N., Gordon, D. B., Bell, G. W., Rinaldi, N. J., Murray, H. L., Volkert, T. L., Schreiber, J., Rolfe, P. A. & Gifford, D. K. (2004). Control of pancreas and liver gene expression by HNF transcription factors. *Science,* 303(5662)**,** 1378-1381.

Odorico, J. S., Kaufman, D. S. & Thomson, J. A. (2001). Multilineage differentiation from human embryonic stem cell lines. *Stem cells,* 19(3)**,** 193-204.

Offield, M. F., Jetton, T. L., Labosky, P. A., Ray, M., Stein, R. W., Magnuson, M. A., Hogan, B. & Wright, C. (1996). PDX-1 is required for pancreatic outgrowth and differentiation of the rostral duodenum. *Development,* 122(3)**,** 983-995.

Oh, K.-J., Han, H.-S., Kim, M.-J. & Koo, S.-H. (2013). CREB and FoxO1: two transcription factors for the regulation of hepatic gluconeogenesis. *BMB reports,* 46(12)**,** 567-574.

Ohlsson, H., Karlsson, K. & Edlund, T. (1993). IPF1, a homeodomain-containing transactivator of the insulin gene. *The EMBO journal,* 12(11)**,** 4251-4259.

Okamoto, K., Iwasaki, N., Doi, K., Noiri, E., Iwamoto, Y., Uchigata, Y., Fujita, T. & Tokunaga, K. (2012). Inhibition of glucose-stimulated insulin secretion by KCNJ15, a newly identified susceptibility gene for type 2 diabetes. *Diabetes,* 61(7)**,** 1734-1741.

Okita, K. & Yamanaka, S. (2011). Induced pluripotent stem cells: opportunities and challenges. *Philosophical transactions of the royal society B,* 366(1575)**,** 2198-2207.

Okumura-Nakanishi, S., Saito, M., Niwa, H. & Ishikawa, F. (2005). Oct-3/4 and Sox2 regulate Oct-3/4 gene in embryonic stem cells. *Journal of biological chemistry,* 280(7)**,** 5307-5317.

Omenn, G. S., Yocum, A. K. & Menon, R. (2010). Alternative splice variants, a new class of protein cancer biomarker candidates: findings in pancreatic cancer and breast cancer with systems biology implications. *Disease markers,* 28(4)**,** 241-251.

Oshima, H., Rochat, A., Kedzia, C., Kobayashi, K. & Barrandon, Y. (2001). Morphogenesis and renewal of hair follicles from adult multipotent stem cells. *Cell,* 104(2)**,** 233-245.

Otonkoski, T., Jiao, H., Kaminen-Ahola, N., Tapia-Paez, I., Ullah, M. S., Parton, L. E., Schuit, F., Quintens, R., Sipilä, I. & Mayatepek, E. (2007). Physical Exercise–Induced Hypoglycemia Caused by Failed Silencing of Monocarboxylate Transporter 1 in Pancreatic β Cells. *The American journal of human genetics,* 81(3)**,** 467-474.

Otonkoski, T., Kaminen, N., Ustinov, J., Lapatto, R., Meissner, T., Mayatepek, E., Kere, J. & Sipilä, I. (2003). Physical exercise-induced hyperinsulinemic hypoglycemia is an autosomal-dominant trait characterized by abnormal pyruvate-induced insulin release. *Diabetes,* 52(1)**,** 199-204.

Ovchinnikov, D. A., Titmarsh, D. M., Fortuna, P. R., Hidalgo, A., Alharbi, S., Whitworth, D. J., Cooper-White, J. J. & Wolvetang, E. J. (2014). Transgenic human ES and iPS reporter cell lines for identification and selection of pluripotent stem cells in vitro. *Stem cell research,* 13(2)**,** 251-261.

Oyama, K., Minami, K., Ishizaki, K., Fuse, M., Miki, T. & Seino, S. (2006). Spontaneous recovery from hyperglycemia by regeneration of pancreatic β-cells in Kir6. 2G132S transgenic mice. *Diabetes,* 55(7)**,** 1930-1938.

Pagliuca, F. W., Millman, J. R., Gürtler, M., Segel, M., Van Dervort, A., Ryu, J. H., Peterson, Q. P., Greiner, D. & Melton, D. A. (2014). Generation of functional human pancreatic β cells *in vitro*. *Cell,* 159(2)**,** 428-439.

Pal, A., Potjer, T. P., Thomsen, S. K., Ng, H. J., Barrett, A., Scharfmann, R., James, T. J., Bishop, D. T., Karpe, F. & Godsland, I. F. (2016). Loss-of-function mutations in the cell-cycle control gene CDKN2A impact on glucose homeostasis in humans. *Diabetes***,** 65(2), 527-533.

Palladino, A. A. & Stanley, C. A. (2010). The hyperinsulinism/hyperammonemia syndrome. *Reviews in endocrine and metabolic disorders,* 11(3)**,** 171-178.

Pan, F. C. & Wright, C. (2011). Pancreas organogenesis: from bud to plexus to gland. *Developmental dynamics,* 240(3)**,** 530-565.

Panoutsopoulou, K. & Zeggini, E. (2009). Finding common susceptibility variants for complex disease: past, present and future. *Briefings in functional genomics and proteomics,* 8(5)**,** 345-352.

Paterson, Y., Kafarnik, C. & Guest, D. (2017). Characterization of companion animal pluripotent stem cells. *Cytometry part A,* 93(1), 137-148.

Patterson, T. A., Lobenhofer, E. K., Fulmer-Smentek, S. B., Collins, P. J., Chu, T.-M., Bao, W., Fang, H., Kawasaki, E. S., Hager, J. & Tikhonova, I. R. (2006). Performance comparison of one-color and two-color platforms within the MicroArray Quality Control (MAQC) project. *Nature biotechnology,* 24(9)**,** 1140-1150.

Pawitan, Y., Michiels, S., Koscielny, S., Gusnanto, A. & Ploner, A. (2005). False discovery rate, sensitivity and sample size for microarray studies. *Bioinformatics,* 21(13)**,** 3017-3024.

Pearson, E. R., Boj, S. F., Steele, A. M., Barrett, T., Stals, K., Shield, J. P., Ellard, S., Ferrer, J. & Hattersley, A. T. (2007). Macrosomia and hyperinsulinaemic hypoglycaemia in patients with heterozygous mutations in the *HNF4A* gene. *PLoS medicine,* 4(4)**,** e118.

Peri, S., Navarro, J. D., Kristiansen, T. Z., Amanchy, R., Surendranath, V., Muthusamy, B., Gandhi, T., Chandrika, K., Deshpande, N. & Suresh, S. (2004). Human protein reference database as a discovery resource for proteomics. *Nucleic acids research,* 32(suppl_1)**,** D497-D501.

Persico, M., Ceol, A., Gavrila, C., Hoffmann, R., Florio, A. & Cesareni, G. (2005). HomoMINT: an inferred human network based on orthology mapping of protein interactions discovered in model organisms. *BMC bioinformatics,* 6(4)**,** S21.

Petraitienė, I., Barauskas, G., Gulbinas, A., Malcius, D., Hussain, K., Verkauskas, G. & Verkauskienė, R. (2014). Congenital hyperinsulinism. *Medicina,* 50(3)**,** 190-195.

Pichler, F., Black, M., Williams, L. & Love, D. (2004). Design, normalization, and analysis of spotted microarray data. *Methods in cell biology,* 77, 521-543.

Pierro, A. & Nah, S. A. (2011). Surgical management of congenital hyperinsulinism of infancy. *Seminars in pediatric surgery,* 20(1), 50-53.

Pileczki, V., Pop, L., Braicu, C., Budisan, L., Morar, G. B., del C Monroig-Bosque, P., Sandulescu, R. V. & Berindan-Neagoe, I. (2016). Double gene siRNA knockdown of mutant p53 and TNF induces apoptosis in triple-negative breast cancer cells. *Onco targets and therapy,* 9**,** 6921-6933.

Pinkel, D., Segraves, R., Sudar, D., Clark, S., Poole, I., Kowbel, D., Collins, C., Kuo, W.-L., Chen, C. & Zhai, Y. (1998). High resolution analysis of DNA copy number variation using comparative genomic hybridization to microarrays. *Nature genetics,* 20(2)**,** 207-211.

Pinney, S. E., MacMullen, C., Becker, S., Lin, Y.-W., Hanna, C., Thornton, P., Ganguly, A., Shyng, S.-L. & Stanley, C. A. (2008). Clinical characteristics and biochemical mechanisms of congenital hyperinsulinism associated with dominant K_{ATP} channel mutations. *The journal of clinical investigation,* 118(8)**,** 2877-2886.

Pittenger, M. F., Mackay, A. M., Beck, S. C., Jaiswal, R. K., Douglas, R., Mosca, J. D., Moorman, M. A., Simonetti, D. W., Craig, S. & Marshak, D. R. (1999). Multilineage potential of adult human mesenchymal stem cells. *Science,* 284(5411)**,** 143-147.

Podolska, A., Kaczkowski, B., Litman, T., Fredholm, M. & Cirera, S. (2011). How the RNA isolation method can affect microRNA microarray results. *Acta bochimica polonica,* 58(4), 535-540.

Popiela, H. & Moore, W. (1991). Tolbutamide stimulates proliferation of pancreatic beta cells in culture. *Pancreas,* 6(4)**,** 464-469.

Porat, S., Weinberg-Corem, N., Tornovsky-Babaey, S., Schyr-Ben-Haroush, R., Hija, A., Stolovich-Rain, M., Dadon, D., Granot, Z., Ben-Hur, V. & White, P. (2011). Control of pancreatic β cell regeneration by glucose metabolism. *Cell metabolism,* 13(4)**,** 440-449.

Portela-Gomes, G. M., Stridsberg, M., Grimelius, L., Öberg, K. & Janson, E. T. (2000). Expression of the five different somatostatin receptor subtypes in endocrine cells of the pancreas. *Applied immunohistochemistry & molecular morphology,* 8(2)**,** 126-132.

Portha, B., Tourrel-Cuzin, C. & Movassat, J. (2011). Activation of the GLP-1 receptor signalling pathway: a relevant strategy to repair a deficient beta-cell mass. *Experimental diabetes research*, 2011, 376509.

Probst, F. J., Roeder, E. R., Enciso, V. B., Ou, Z., Cooper, M. L., Eng, P., Li, J., Gu, Y., Stratton, R. F. & Chinault, A. C. (2007). Chromosomal microarray analysis (CMA) detects a large X chromosome deletion including FMR1, FMR2, and IDS in a female patient with mental retardation. *American journal of medical genetics part A*, 143(12)**,** 1358-1365.

Proks, P., Reimann, F., Green, N., Gribble, F. & Ashcroft, F. (2002). Sulfonylurea stimulation of insulin secretion. *Diabetes*, 51(suppl 3)**,** S368-S376.

Proverbio, M. C., Mangano, E., Gessi, A., Bordoni, R., Spinelli, R., Asselta, R., Valin, P. S., Di Candia, S., Zamproni, I. & Diceglie, C. (2013). Whole genome SNP genotyping and exome sequencing reveal novel genetic variants and putative causative genes in congenital hyperinsulinism. *PLoS one*, 8(7)**,** e68740.

Pugazhenthi, S., Wang, M., Pham, S., Sze, C.-I. & Eckman, C. B. (2011). Downregulation of CREB expression in Alzheimer's brain and in Aβ-treated rat hippocampal neurons. *Molecular neurodegeneration*, 6(1)**,** 60.

Pujol, A., Mosca, R., Farrés, J. & Aloy, P. (2010). Unveiling the role of network and systems biology in drug discovery. *Trends in pharmacological sciences*, 31(3)**,** 115-123.

Qin, L.-X., Beyer, R. P., Hudson, F. N., Linford, N. J., Morris, D. E. & Kerr, K. F. (2006). Evaluation of methods for oligonucleotide array data via quantitative real-time PCR. *BMC bioinformatics*, 7(1)**,** 23.

Qiu, Y., Guo, M., Huang, S. & Stein, R. (2002). Insulin gene transcription is mediated by interactions between the p300 coactivator and PDX-1, BETA2, and E47. *Molecular and cellular biology*, 22(2)**,** 412-420.

Quackenbush, J. (2001). Computational genetics: computational analysis of microarray data. *Nature reviews genetics*, 2(6)**,** 418-427.

Quackenbush, J. (2002). Microarray data normalization and transformation. *Nature genetics*, 32**,** 496-501.

Qureshi, F. M., Dejene, E. A., Corbin, K. L. & Nunemaker, C. S. (2015). Stress-induced dissociations between intracellular calcium signaling and insulin secretion in pancreatic islets. *Cell calcium*, 57(5-6)**,** 366-375.

Radvanyi, F., Christgau, S., Baekkeskov, S., Jolicoeur, C. & Hanahan, D. (1993). Pancreatic beta cells cultured from individual preneoplastic foci in a multistage tumorigenesis pathway: a potentially general technique for isolating physiologically representative cell lines. *Molecular and cellular biology*, 13(7)**,** 4223-4232.

Rahier, J., Fält, K., Müntefering, H., Becker, K., Gepts, W. & Falkmer, S. (1984). The basic structural lesion of persistent neonatal hypoglycaemia with hyperinsulinism: deficiency of pancreatic D cells or hyperactivity of B cells? *Diabetologia*, 26(4)**,** 282-289.

Rahier, J., Guiot, Y. & Sempoux, C. (2011). Morphologic analysis of focal and diffuse forms of congenital hyperinsulinism. *Seminars in pediatric surgery*, 20, 3-12.

Rahman, S. A., Nessa, A. & Hussain, K. (2015a). Molecular mechanisms of congenital hyperinsulinism. *Journal of molecular endocrinology*, 54(2)**,** R119-R129.

Rahman, S. A., Senniappan, S., Sherif, M., Tahir, S. & Hussain, K. (2015b). Dipeptidyl peptidase-4 expression in pancreatic tissue from patients with congenital hyperinsulinism. *International journal of clinical and experimental pathology*, 8(7)**,** 8199-8208.

Rai, M. F., Tycksen, E. D., Sandell, L. J. & Brophy, R. H. (2018). Advantages of RNA-seq compared to RNA microarrays for transcriptome profiling of anterior cruciate ligament tears. *Journal of Orthopaedic Research*, 36(1), 484-497.

Rajeevan, M. S., Ranamukhaarachchi, D. G., Vernon, S. D. & Unger, E. R. (2001). Use of real-time quantitative PCR to validate the results of cDNA array and differential display PCR technologies. *Methods,* 25(4)**,** 443-451.

Raman, T., O'Connor, T. P., Hackett, N. R., Wang, W., Harvey, B.-G., Attiyeh, M. A., Dang, D. T., Teater, M. & Crystal, R. G. (2009). Quality control in microarray assessment of gene expression in human airway epithelium. *BMC genomics,* 10(1)**,** 493.

Ramos, Y. F., den Hollander, W., Bovée, J. V., Bomer, N., van der Breggen, R., Lakenberg, N., Keurentjes, J. C., Goeman, J. J., Slagboom, P. E. & Nelissen, R. G. (2014). Genes involved in the osteoarthritis process identified through genome wide expression analysis in articular cartilage; the RAAK study. *PLoS one,* 9(7)**,** e103056.

Ran, F. A., Hsu, P. D., Wright, J., Agarwala, V., Scott, D. A. & Zhang, F. (2013). Genome engineering using the CRISPR-Cas9 system. *Nature protocols,* 8(11)**,** 2281-2308.

Rana, T. M. (2007). Illuminating the silence: understanding the structure and function of small RNAs. *Nature reviews molecular cell biology,* 8(1)**,** 23-36.

Rao, D. D., Vorhies, J. S., Senzer, N. & Nemunaitis, J. (2009). siRNA vs. shRNA: similarities and differences. *Advanced drug delivery reviews,* 61(9)**,** 746-759.

Rao, M. S., Van Vleet, T. R., Ciurlionis, R., Buck, W. R., Mittelstadt, S. W., Blomme, E. A. & Liguori, M. J. (2018). Comparison of RNA-seq and microarray gene expression platforms for the toxicogenomic evaluation of liver from short-term rat toxicity studies. *Frontiers in genetics,* 9, 636.

Ravassard, P., Hazhouz, Y., Pechberty, S., Bricout-Neveu, E., Armanet, M., Czernichow, P. & Scharfmann, R. (2011). A genetically engineered human pancreatic β cell line exhibiting glucose-inducible insulin secretion. *The Journal of clinical investigation,* 121(9)**,** 3589-3597.

Ray, J. D., Kener, K. B., Bitner, B. F., Wright, B. J., Ballard, M. S., Barrett, E. J., Hill, J. T., Moss, L. G. & Tessem, J. S. (2016). Nkx6. 1-mediated insulin secretion and β-cell proliferation is dependent on upregulation of c-Fos. *FEBS letters,* 590(12)**,** 1791-1803.

Reinecke-Lüthge, A., Koschoreck, F. & Klöppel, G. (2000). The molecular basis of persistent hyperinsulinemic hypoglycemia of infancy and its pathologic substrates. *Virchows Archiv,* 436(1)**,** 1-5.

Reiner, A., Yekutieli, D. & Benjamini, Y. (2003). Identifying differentially expressed genes using false discovery rate controlling procedures. *Bioinformatics,* 19(3)**,** 368-375.

Resnick, M. B., Konkin, T., Routhier, J., Sabo, E. & Pricolo, V. E. (2005). Claudin-1 is a strong prognostic indicator in stage II colonic cancer: a tissue microarray study. *Modern pathology,* 18(4)**,** 511-518.

Reynier, F., Pachot, A., Paye, M., Xu, Q., Turrel-Davin, F., Petit, F., Hot, A., Auffray, C., Bendelac, N. & Nicolino, M. (2010). Specific gene expression signature associated with development of autoimmune type-I diabetes using whole-blood microarray analysis. *Genes and immunity,* 11(3)**,** 269-278.

Rezania, A., Bruin, J. E., Arora, P., Rubin, A., Batushansky, I., Asadi, A., O'dwyer, S., Quiskamp, N., Mojibian, M. & Albrecht, T. (2014). Reversal of diabetes with insulin-producing cells derived in vitro from human pluripotent stem cells. *Nature biotechnology,* 32(11)**,** 1121-1133.

Rezania, A., Bruin, J. E., Riedel, M. J., Mojibian, M., Asadi, A., Xu, J., Gauvin, R., Narayan, K., Karanu, F. & O'Neil, J. J. (2012). Maturation of human embryonic stem cell–derived pancreatic progenitors into functional islets capable of treating pre-existing diabetes in mice. *Diabetes,* 61(8)**,** 2016-2029.

Ribeiro, M.-J., De Lonlay, P., Delzescaux, T., Boddaert, N., Jaubert, F., Bourgeois, S., Dollé, F., Nihoul-Fékété, C., Syrota, A. & Brunelle, F. (2005). Characterization of hyperinsulinism in infancy assessed with PET and ^{18}F-fluoro-L-DOPA. *Journal of nuclear medicine,* 46(4)**,** 560-566.

Roat, R., Rao, V., Doliba, N. M., Matschinsky, F. M., Tobias, J. W., Garcia, E., Ahima, R. S. & Imai, Y. (2014). Alterations of pancreatic islet structure, metabolism and gene expression in diet-induced obese C57BL/6J mice. *PLoS one,* 9(2)**,** e86815.

Roberts, D. (1999). Embryology of gastrointestinal tract, in Sanderson, I. R. and Walker, W. A. (eds.) *Development of the gastrointestinal tract.* USA: PMPH, pp. 1-12.

Rodríguez-Pascau, L., Coll, M. J., Casas, J., Vilageliu, L. & Grinberg, D. (2012). Generation of a human neuronal stable cell model for Niemann-pick C disease by RNA interference. *JIMD reports-case and research reports,* 4, 29-37.

Root, D. E., Hacohen, N., Hahn, W. C., Lander, E. S. & Sabatini, D. M. (2006). Genome-scale loss-of-function screening with a lentiviral RNAi library. *Nature methods,* 3(9)**,** 715-719.

Rorsman, P., Braun, M. & Zhang, Q. (2012). Regulation of calcium in pancreatic α-and β-cells in health and disease. *Cell calcium,* 51(3-4)**,** 300-308.

Rothschild, E. & Banerjee, D. (2015). Subverting subversion: a review on the breast cancer microenvironment and therapeutic opportunities. *Breast cancer: basic and clinical research,* 9**(**suppl 2), 7-15.

Roy, S., Bhattacharyya, D. K. & Kalita, J. K. (2014). Reconstruction of gene co-expression network from microarray data using local expression patterns. *BMC bioinformatics,* 15(7)**,** S10.

Rozenkova, K., Malikova, J., Nessa, A., Dusatkova, L., Bjørkhaug, L., Obermannova, B., Dusatkova, P., Kytnarova, J., Aukrust, I., Najmi, L. A., Rypackova, B., Sumnik, Z., Lebl, J., Njolstad, P. R., Hussain, K. & Pruhova, S. (2015). High incidence of heterozygous *ABCC8* and *HNF1A* mutations in Czech patients with congenital Hyperinsulinism. *The Journal of clinical endocrinology & metabolism,* 100(12)**,** E1540-E1549.

Sahoo, T., del Gaudio, D., German, J. R., Shinawi, M., Peters, S. U., Person, R. E., Garnica, A., Cheung, S. W. & Beaudet, A. L. (2008). Prader-Willi phenotype caused by paternal deficiency for the HBII-85 C/D box small nucleolar RNA cluster. *Nature genetics,* 40(6)**,** 719-721.

Sahoo, T., Peters, S. U., Madduri, N. S., Glaze, D. G., German, J. R., Bird, L. M., Barbieri-Welge, R., Bichell, T. J., Beaudet, A. L. & Bacino, C. A. (2006). Microarray based comparative genomic hybridization testing in deletion bearing patients with Angelman syndrome: genotype-phenotype correlations. *Journal of medical genetics,* 43(6)**,** 512-516.

Saint-Martin, C., Zhou, Q., Martin, G. M., Vaury, C., Leroy, G., Arnoux, J. B., de Lonlay, P., Shyng, S. L. & Bellanné-Chantelot, C. (2015). Monoallelic ABCC8 mutations are a common cause of diazoxide-unresponsive diffuse form of congenital hyperinsulinism. *Clinical genetics,* 87(5)**,** 448-454.

Saitou, N. & Nei, M. (1987). The neighbor-joining method: a new method for reconstructing phylogenetic trees. *Molecular biology and evolution,* 4(4)**,** 406-425.

Sala, V., Gallo, S., Leo, C., Gatti, S., Gelb, B. D. & Crepaldi, T. (2012). Signaling to cardiac hypertrophy: insights from human and mouse RASopathies. *Molecular medicine,* 18(1)**,** 938-947.

Salisbury, R. J., Han, B., Jennings, R. E., Berry, A. A., Stevens, A., Mohamed, Z., Sugden, S. A., De Krijger, R., Cross, S. E. & Johnson, P. P. (2015). Altered phenotype of β-cells and other pancreatic cell lineages in patients with diffuse Congenital Hyperinsulinism in Infancy due to mutations in the ATP-sensitive K-channel. *Diabetes***,** 64(9), 3182-3188.

Sambathkumar, R., Kalo, E., Van Rossom, R., Faas, M. M., de Vos, P. & Verfaillie, C. M. (2016). Epigenetic induction of definitive and pancreatic endoderm cell fate in human fibroblasts. *Stem cells international*, 7654321.

Sanayama, Y., Ikeda, K., Saito, Y., Kagami, S. i., Yamagata, M., Furuta, S., Kashiwakuma, D., Iwamoto, I., Umibe, T. & Nawata, Y. (2014). Prediction of Therapeutic Responses to Tocilizumab in Patients With Rheumatoid Arthritis: Biomarkers Identified by Analysis of Gene Expression in Peripheral Blood Mononuclear Cells Using Genome-Wide DNA Microarray. *Arthritis & rheumatology*, 66(6)**,** 1421-1431.

Sánchez-Alvarez, R., Paíno, T., Herrero-González, S., Medina, J. M. & Tabernero, A. (2006). Tolbutamide reduces glioma cell proliferation by increasing connexin43, which promotes the up-regulation of p21 and p27 and subsequent changes in retinoblastoma phosphorylation. *Glia*, 54(2)**,** 125-134.

Sander, J. D. & Joung, J. K. (2014). CRISPR-Cas systems for editing, regulating and targeting genomes. *Nature biotechnology*, 32(4)**,** 347-355.

Sander, M., Sussel, L., Conners, J., Scheel, D., Kalamaras, J., Cruz, F. D., Schwitzgebel, V., Hayes-Jordan, A. & German, M. (2000). Homeobox gene Nkx6. 1 lies downstream of Nkx2. 2 in the major pathway of beta-cell formation in the pancreas. *Development*, 127(24)**,** 5533-5540.

Sang, Y., Xu, Z., Liu, M., Yan, J., Wu, Y., Zhu, C. & Ni, G. (2014). Mutational analysis of ABCC8, KCNJ11, GLUD1, HNF4A and GCK genes in 30 Chinese patients with congenital hyperinsulinism. *Endocrine journal*, 61(9)**,** 901-910.

Santiago, Y., Chan, E., Liu, P.-Q., Orlando, S., Zhang, L., Urnov, F. D., Holmes, M. C., Guschin, D., Waite, A. & Miller, J. C. (2008). Targeted gene knockout in mammalian cells by using engineered zinc-finger nucleases. *Proceedings of the national academy of sciences*, 105(15)**,** 5809-5814.

Sasik, R., Woelk, C. & Corbeil, J. (2004). Microarray truths and consequences. *Journal of molecular endocrinology*, 33(1)**,** 1-9.

Sato, Y., Nenquin, M. & Henquin, J.-C. (1998). Relative contribution of Ca^{2+}-dependent and Ca^{2+}-independent mechanisms to the regulation of insulin secretion by glucose. *FEBS letters*, 421(2)**,** 115-119.

Schaefer, K.-L., Eisenacher, M., Braun, Y., Brachwitz, K., Wai, D. H., Dirksen, U., Lanvers-Kaminsky, C., Juergens, H., Herrero, D. & Stegmaier, S. (2008). Microarray analysis of Ewing's sarcoma family of tumours reveals characteristic gene expression signatures associated with metastasis and resistance to chemotherapy. *European journal of cancer*, 44(5)**,** 699-709.

Schaffer, A. E., Taylor, B. L., Benthuysen, J. R., Liu, J., Thorel, F., Yuan, W., Jiao, Y., Kaestner, K. H., Herrera, P. L. & Magnuson, M. A. (2013). Nkx6. 1 controls a gene regulatory network required for establishing and maintaining pancreatic Beta cell identity. *PLoS genetics*, 9(1)**,** e1003274.

Scheen, A. J. (2016). Investigational insulin secretagogues for type 2 diabetes. *Expert opinion on investigational drugs*, 25(4)**,** 405-422.

Schena, M., Shalon, D., Davis, R. W. & Brown, P. O. (1995). Quantitative monitoring of gene expression patterns with a complementary DNA microarray. *Science*, 270(5235)**,** 467-470.

Schisler, J. C., Jensen, P. B., Taylor, D. G., Becker, T. C., Knop, F. K., Takekawa, S., German, M., Weir, G. C., Lu, D. & Mirmira, R. G. (2005). The Nkx6. 1 homeodomain transcription factor suppresses glucagon expression and regulates glucose-stimulated insulin secretion in islet beta cells. *Proceedings of the national academy of sciences,* 102(20)**,** 7297-7302.

Schmid, E. M. & McMahon, H. T. (2007). Integrating molecular and network biology to decode endocytosis. *Nature,* 448(7156)**,** 883-888.

Schmidt, R. & Plath, K. (2012). The roles of the reprogramming factors Oct4, Sox2 and Klf4 in resetting the somatic cell epigenome during induced pluripotent stem cell generation. *Genome biology,* 13(10)**,** 251.

Schmittgen, T. D. & Livak, K. J. (2008). Analyzing real-time PCR data by the comparative C_T method. *Nature protocols,* 3(6)**,** 1101-1108.

Schmitz, O., Lund, S., Andersen, P. H., Jønler, M. & Pørksen, N. (2002). Optimizing insulin secretagogue therapy in patients with type 2 diabetes: a randomized double-blind study with repaglinide. *Diabetes Care,* 25(2)**,** 342-346.

Schneeberger, C., Speiser, P., Kury, F. & Zeillinger, R. (1995). Quantitative detection of reverse transcriptase-PCR products by means of a novel and sensitive DNA stain. *Genome research,* 4(4)**,** 234-238.

Schöfl, C., Börger, J., Mader, T., Waring, M., von zur Mühlen, A. & Brabant, G. (2000). Tolbutamide and diazoxide modulate phospholipase C-linked Ca^{2+} signaling and insulin secretion in β-cells. *American journal of physiology-endocrinology and metabolism,* 278(4)**,** E639-E647.

Schramm, T. K., Gislason, G. H., Vaag, A., Rasmussen, J. N., Folke, F., Hansen, M. L., Fosbøl, E. L., Køber, L., Norgaard, M. L. & Madsen, M. (2011). Mortality and cardiovascular risk associated with different insulin secretagogues compared with metformin in type 2 diabetes, with or without a previous myocardial infarction: a nationwide study. *European heart journal,* 32(15)**,** 1900-1908.

Schroeder, A., Mueller, O., Stocker, S., Salowsky, R., Leiber, M., Gassmann, M., Lightfoot, S., Menzel, W., Granzow, M. & Ragg, T. (2006). The RIN: an RNA integrity number for assigning integrity values to RNA measurements. *BMC molecular biology,* 7(1)**,** 3.

Schuchhardt, J., Beule, D., Malik, A., Wolski, E., Eickhoff, H., Lehrach, H. & Herzel, H. (2000). Normalization strategies for cDNA microarrays. *Nucleic acids research,* 28(10)**,** e47-e47.

Schulze, A. & Downward, J. (2001). Navigating gene expression using microarrays—a technology review. *Nature cell biology,* 3(8)**,** E190-E195.

Scoville, D. W., Cyphert, H. A., Liao, L., Xu, J., Reynolds, A., Guo, S. & Stein, R. (2015). MLL3 and MLL4 methyltransferases bind to the MAFA and MAFB transcription factors to regulate islet β-cell function. *Diabetes,* 64(11)**,** 3772-3783.

Sealfon, S. C. & Chu, T. T. (2011). RNA and DNA microarrays, in Khademhosseini, A., Suh, K. -Y. and Zourob, M. (eds.) *Biological microarrays: mehods and protocols.* Springer, pp. 3-34.

Seghers, V., Nakazaki, M., DeMayo, F., Aguilar-Bryan, L. & Bryan, J. (2000). SUR1 knockout mice A model for K_{ATP} channel-independent regulation of insulin secretion. *Journal of biological chemistry,* 275(13)**,** 9270-9277.

Sellers, R. S. (2017). Translating mouse models: immune variation and efficacy testing. *Toxicologic pathology,* 45(1), 134-145.

Selvaraj, S. & Natarajan, J. (2011). Microarray data analysis and mining tools. *Bioinformation,* 6(3)**,** 95-99.

Sempoux, C., Capito, C., Bellanne-Chantelot, C., Verkarre, V., De Lonlay, P., Aigrain, Y., Fekete, C., Guiot, Y. & Rahier, J. (2011). Morphological mosaicism of the pancreatic islets: a novel anatomopathological form of persistent hyperinsulinemic hypoglycemia of infancy. *The Journal of clinical endocrinology & metabolism,* 96(12)**,** 3785-3793.

Sempoux, C., Guiot, Y., Dubois, D., Nollevaux, M.-C., Saudubray, J., Nihoul-Fekete, C. & Rahier, J. (1998a). Pancreatic B-cell proliferation in persistent hyperinsulinemic hypoglycemia of infancy: an immunohistochemical study of 18 cases. *Modern pathology: an official journal of the United States and Canadian academy of pathology, Inc,* 11(5)**,** 444-449.

Sempoux, C., Guiot, Y., Lefevre, A., Nihoul-Fékété, C., Jaubert, F., Saudubray, J. & Rahier, J. (1998b). Neonatal hyperinsulinemic hypoglycemia: heterogeneity of the syndrome and keys for differential diagnosis. *Journal of clinical endocrinology & metabolism,* 83(5)**,** 1455-1461.

Senniappan, S., Alexandrescu, S., Tatevian, N., Shah, P., Arya, V., Flanagan, S., Ellard, S., Rampling, D., Ashworth, M. & Brown, R. E. (2014). Sirolimus therapy in infants with severe hyperinsulinemic hypoglycemia. *New England journal of medicine,* 370(12)**,** 1131-1137.

Senniappan, S., Brown, R. E. & Hussain, K. (2016). Genomic and morphoproteomic correlates implicate the IGF-1/mTOR/Akt pathway in the pathogenesis of diffuse congenital hyperinsulinism. *Internation journal of clinical and experimental pathology,* 9(2)**,** 548-562.

Senniappan, S., Sadeghizadeh, A., Flanagan, S. E., Ellard, S., Hashemipour, M., Hosseinzadeh, M., Salehi, M. & Hussain, K. (2015). Genotype and phenotype correlations in Iranian patients with hyperinsulinaemic hypoglycaemia. *BMC research notes,* 8(1)**,** 350.

Senniappan, S., Shanti, B., James, C. & Hussain, K. (2012). Hyperinsulinaemic hypoglycaemia: genetic mechanisms, diagnosis and management. *Journal of inherited metabolic disease,* 35(4)**,** 589-601.

Seok, J., Warren, H. S., Cuenca, A. G., Mindrinos, M. N., Baker, H. V., Xu, W., Richards, D. R., McDonald-Smith, G. P., Gao, H. & Hennessy, L. (2013). Genomic responses in mouse models poorly mimic human inflammatory diseases. *Proceedings of the national academy of sciences,* 110(9), 3507-3512.

Serup, P., Petersen, H., Pedersen, E., Edlund, H., Leonard, J., Petersen, J., Larsson, L. & Madsen, O. (1995). The homeodomain protein IPF-1/STF-1 is expressed in a subset of islet cells and promotes rat insulin 1 gene expression dependent on an intact E1 helix-loop-helix factor binding site. *Biochemical journal,* 310(Pt 3)**,** 997-1003.

Shabalina, S. A. & Koonin, E. V. (2008). Origins and evolution of eukaryotic RNA interference. *Trends in ecology & evolution,* 23(10)**,** 578-587.

Shalem, O., Sanjana, N. E. & Zhang, F. (2015). High-throughput functional genomics using CRISPR–Cas9. *Nature reviews genetics,* 16(5)**,** 299-311.

Shanbag, P., Pathak, A., Vaidya, M. & Shahid, S. K. (2002). Persistent hyperinsulinemic hypoglycemia of infancysuccessful therapy with nifedipine. *The Indian journal of pediatrics,* 69(3)**,** 271-272.

Shanks, N., Greek, R. & Greek, J. (2009). Are animal models predictive for humans? *Philosophy, ethics, and humanities in medicine,* 4(1)**,** 2.

Shannon, P., Markiel, A., Ozier, O., Baliga, N. S., Wang, J. T., Ramage, D., Amin, N., Schwikowski, B. & Ideker, T. (2003). Cytoscape: a software environment for integrated models of biomolecular interaction networks. *Genome research,* 13(11)**,** 2498-2504.

Shapira, S. D., Gat-Viks, I., Shum, B. O., Dricot, A., de Grace, M. M., Wu, L., Gupta, P. B., Hao, T., Silver, S. J. & Root, D. E. (2009). A physical and regulatory map of host-influenza interactions reveals pathways in H1N1 infection. *Cell,* 139(7)**,** 1255-1267.

Sherer, T. B., Betarbet, R., Stout, A. K., Lund, S., Baptista, M., Panov, A. V., Cookson, M. R. & Greenamyre, J. T. (2002). An *in vitro* model of Parkinson's disease: linking mitochondrial impairment to altered α-synuclein metabolism and oxidative damage. *The journal of neuroscience,* 22(16)**,** 7006-7015.

Shi, L., Perkins, R. G., Fang, H. & Tong, W. (2008). Reproducible and reliable microarray results through quality control: good laboratory proficiency and appropriate data analysis practices are essential. *Current opinion in biotechnology,* 19(1)**,** 10-18.

Shi, Y. (2014). *Congenital Hyperinsulinism: a unique model to study pancreatic islet cell development and maintenance*. Ph.D. University of Manchester.

Shi, Y., Avatapalle, H. B., Skae, M. S., Padidela, R., Newbould, M., Rigby, L., Flanagan, S. E., Ellard, S., Rahier, J. & Clayton, P. E. (2015). Increased plasma incretin concentrations identifies a subset of patients with persistent congenital hyperinsulinism without K_{ATP} channel gene defects. *The journal of pediatrics,* 166(1)**,** 191-194.

Shi, Y. C., Loh K., Bensellam, M., Lee, K., Zhai, L., Lau, J., Cantley, J., Luzuriaga, J., Laybutt, D. R. & Herzog, H. (2015). *Endocrinology*, 156(9), 3122-3136.

Shih, H. P., Wang, A. and Sander, M. (2013). Pancreas Organogenesis: from lineage determination to morphogenesis. *Annual review of cell and developmental biology*, 29, 81-105.

Shyng, S.-L., Ferrigni, T. & Nichols, C. (1997a). Control of rectification and gating of cloned K_{ATP} channels by the Kir6. 2 subunit. *The journal of general physiology,* 110(2)**,** 141-153.

Shyng, S.-L., Ferrigni, T. & Nichols, C. (1997b). Regulation of K_{ATP} channel activity by diazoxide and MgADP: distinct functions of the two nucleotide binding folds of the sulfonylurea receptor. *The journal of general physiology,* 110(6)**,** 643-654.

Shyng, S.-L., Ferrigni, T., Shepard, J. B., Nestorowicz, A., Glaser, B., Permutt, M. A. & Nichols, C. G. (1998). Functional analyses of novel mutations in the sulfonylurea receptor 1 associated with persistent hyperinsulinemic hypoglycemia of infancy. *Diabetes,* 47(7)**,** 1145-1151.

Sidhu, K. S., Chayosumrit, M. & Lie, K. H. (2012). Stem Cells, Definition, Classification and Sources in Sidhu, K. S. (ed) *Frontiers in Pluripotent Stem Cells Research and Therapeutic Potentials: Bench-to-bedside*. Australia: Bentham ebooks.

Singhal, P. K., Sassi, S., Lan, L., Au, P., Halvorsen, S. C., Fukumura, D., Jain, R. K. and Seed, B. (2016). Mouse embryonic fibroblasts exhibit extensive developmental and phenotypic diversity. *Proceedings of the National Academy of Sciences,* 113(1),122-127.

Sinicropi, D., Cronin, M. & Liu, M.-L. (2006). Gene expression profiling utilizing microarray technology and RT-PCR, in Ferrari, M., Ozkan, M. and Heller, M. (eds.) *BioMEMS and biomedical nanotechnology: micro/nano technologies for genomics and proteomics*. Springer, pp. 23-46.

Smith, P. A., Sakura, H., Coles, B., Gummerson, N., Proks, P. & Ashcroft, F. (1997). Electrogenic arginine transport mediates stimulus-secretion coupling in mouse pancreatic beta-cells. *The Journal of physiology,* 499(3)**,** 625-635.

Smith, S. C. (2007). Multiple risk factors for cardiovascular disease and diabetes mellitus. *The American journal of medicine,* 120(3)**,** S3-S11.

Smoot, M. E., Ono, K., Ruscheinski, J., Wang, P.-L. & Ideker, T. (2011). Cytoscape 2.8: new features for data integration and network visualization. *Bioinformatics,* 27(3)**,** 431-432.

Smyth, G. K. & Speed, T. (2003). Normalization of cDNA microarray data. *Methods,* 31(4)**,** 265-273.

Snel, B., Lehmann, G., Bork, P. & Huynen, M. A. (2000). STRING: a web-server to retrieve and display the repeatedly occurring neighbourhood of a gene. *Nucleic acids research,* 28(18)**,** 3442-3444.

Snider, K., Becker, S., Boyajian, L., Shyng, S.-L., MacMullen, C., Hughes, N., Ganapathy, K., Bhatti, T., Stanley, C. & Ganguly, A. (2013). Genotype and phenotype correlations in 417 children with congenital hyperinsulinism. *The journal of clinical endocrinology & metabolism,* 98(2)**,** E355-E363.

Snijders, A. M., Nowak, N., Segraves, R., Blackwood, S., Brown, N., Conroy, J., Hamilton, G., Hindle, A. K., Huey, B. & Kimura, K. (2001). Assembly of microarrays for genome-wide measurement of DNA copy number. *Nature genetics,* 29(3)**,** 263-264.

Song, F. & Stieger, K. (2017). Optimizing the DNA donor template for homology-directed repair of double-strand breaks. *Molecular therapy-nucleic acids,* 7**,** 53-60.

Sookoian, S. & Pirola, C. J. (2013). Systems biology elucidates common pathogenic mechanisms between nonalcoholic and alcoholic-fatty liver disease. *PLoS one,* 8(3)**,** e58895.

Sørensen, D. R., Leirdal, M. & Sioud, M. (2003). Gene silencing by systemic delivery of synthetic siRNAs in adult mice. *Journal of molecular biology,* 327(4)**,** 761-766.

Sotiriou, C., Neo, S.-Y., McShane, L. M., Korn, E. L., Long, P. M., Jazaeri, A., Martiat, P., Fox, S. B., Harris, A. L. & Liu, E. T. (2003). Breast cancer classification and prognosis based on gene expression profiles from a population-based study. *Proceedings of the national academy of sciences,* 100(18)**,** 10393-10398.

Soutschek, J., Akinc, A., Bramlage, B., Charisse, K., Constien, R., Donoghue, M., Elbashir, S., Geick, A., Hadwiger, P. & Harborth, J. (2004). Therapeutic silencing of an endogenous gene by systemic administration of modified siRNAs. *Nature,* 432(7014)**,** 173-178.

Sprague, J. E. & Arbeláez, A. M. (2011). Glucose counterregulatory responses to hypoglycemia. *Pediatric endocrinology reviews,* 9(1)**,** 463-475.

Stanescu, D. E., Hughes, N., Kaplan, B., Stanley, C. A. & De León, D. D. (2012). Novel Presentations of Congenital Hyperinsulinism due to Mutations in the MODY genes: *HNF1A* and *HNF4A*. *Journal of clinical endocrinology & metabolism,* 97(10)**,** E2026-E2030.

Stanley, C. & Baker, L. (1976). Hyperinsulinism in infancy: diagnosis by demonstration of abnormal response to fasting hypoglycemia. *Pediatrics,* 57(5)**,** 702-711.

Stanley, C. A. (1997). Hyperinsulinism in infants and children. *Pediatric clinics of north America,* 44(2)**,** 363-374.

Stanley, C. A. (2004). Hyperinsulinism/hyperammonemia syndrome: insights into the regulatory role of glutamate dehydrogenase in ammonia metabolism. *Molecular genetics and metabolism,* 81**,** 45-51.

Stanley, C. A. (2009). Regulation of glutamate metabolism and insulin secretion by glutamate dehydrogenase in hypoglycemic children–. *The American journal of clinical nutrition,* 90(3)**,** 862S-866S.

Stanley, C. A. (2016). Perspective on the genetics and diagnosis of congenital hyperinsulinism disorders. *The journal of clinical endocrinology & metabolism,* 101(3)**,** 815-826.

Stanley, C. A., Lieu, Y. K., Hsu, B. Y., Burlina, A. B., Greenberg, C. R., Hopwood, N. J., Perlman, K., Rich, B. H., Zammarchi, E. & Poncz, M. (1998). Hyperinsulinism and hyperammonemia in infants with regulatory mutations of the glutamate dehydrogenase gene. *New England journal of medicine,* 338(19)**,** 1352-1357.

Stark, C., Breitkreutz, B.-J., Reguly, T., Boucher, L., Breitkreutz, A. & Tyers, M. (2006). BioGRID: a general repository for interaction datasets. *Nucleic acids research,* 34(suppl_1)**,** D535-D539.

Staunton, J. E., Slonim, D. K., Coller, H. A., Tamayo, P., Angelo, M. J., Park, J., Scherf, U., Lee, J. K., Reinhold, W. O. & Weinstein, J. N. (2001). Chemosensitivity prediction by transcriptional profiling. *Proceedings of the national academy of sciences,* 98(19)**,** 10787-10792.

Steinkrauss, L., Lipman, T. H., Hendell, C. D., Gerdes, M., Thornton, P. S. & Stanley, C. A. (2005). Effects of hypoglycemia on developmental outcome in children with congenital hyperinsulinism. *Journal of pediatric nursing: nursing care of children and families,* 20(2)**,** 109-118.

Steneberg, P., Bernardo, L., Edfalk, S., Backlund, F., Lundberg, L., Östenson, C.-G. & Edlund, H. (2013). The type 2 diabetes associated gene Ide is required for insulin secretion and suppression of α-synuclein levels in β-cells. *Diabetes,* 62(6), 2004-2014.

Stepanov, G. A., Filippova, J. A., Komissarov, A. B., Kuligina, E. V., Richter, V. A. & Semenov, D. V. (2015). Regulatory role of small nucleolar RNAs in human diseases. *BioMed research international,* 2015, 206849.

Sterneckert, J. L., Reinhardt, P. & Schöler, H. R. (2014). Investigating human disease using stem cell models. *Nature reviews genetics,* 15(9)**,** 625-639.

Stevens, A., Cosgrove, K. E., Padidela, R., Skae, M. S., Clayton, P. E., Banerjee, I. & Dunne, M. J. (2013). Can network biology unravel the aetiology of congenital hyperinsulinism? *Orphanet journal of rare diseases,* 8(1)**,** 21.

Stevens, A., De Leonibus, C., Hanson, D., Dowsey, A., Whatmore, A., Meyer, S., Donn, R., Chatelain, P., Banerjee, I. & Cosgrove, K. (2014). Network analysis: a new approach to study endocrine disorders. *Journal of molecular endocrinology,* 52(1)**,** R79-R93.

Stoffers, D. A., Zinkin, N. T., Stanojevic, V., Clarke, W. L. & Habener, J. F. (1997). Pancreatic agenesis attributable to a single nucleotide deletion in the human IPF1 gene coding sequence. *Nature genetics,* 15(1)**,** 106-110.

Straub, S. G., Cosgrove, K. E., Ämmälä, C., Shepherd, R. M., O'brien, R. E., Barnes, P. D., Kuchinski, N. a., Chapman, J. C., Schaeppi, M. & Glaser, B. (2001). Hyperinsulinism of Infancy: The Regulated Release of Insulin by KATP Channel—Independent Pathways. *Diabetes,* 50(2)**,** 329-339.

Su, G., Morris, J. H., Demchak, B. & Bader, G. D. (2014). Biological network exploration with cytoscape 3. *Current protocols in bioinformatics***,** 47, 8.13. 1-8.13. 24.

Sun, H. (2016). Identification of key genes associated with gastric cancer based on DNA microarray data. *Oncology letters,* 11(1)**,** 525-530.

Swift, S., Tucker, A., Vinciotti, V., Martin, N., Orengo, C., Liu, X. & Kellam, P. (2004). Consensus clustering and functional interpretation of gene-expression data. *Genome biology,* 5(11)**,** R94.

Swinnen, S., Dain, M. P., Mauricio, D., DeVries, J., Hoekstra, J. & Holleman, F. (2010). Continuation versus discontinuation of insulin secretagogues when initiating insulin in type 2 diabetes. *Diabetes, obesity and metabolism,* 12(10)**,** 923-925.

Szlachcic, W. J., Wiatr, K., Trzeciak, M., Figlerowicz, M. & Figiel, M. (2017). The Generation of Mouse and Human Huntington Disease iPS Cells Suitable for In vitro Studies on Huntingtin Function. *Frontiers in molecular neuroscience,* 10**,** 253.

Szymanowski, M., Estebanez, M. S., Padidela, R., Han, B., Mosinska, K., Stevens, A., Damaj, L., Pihan-Le Bars, F., Lascouts, E. & Reynaud, R. (2016). mTOR inhibitors for the treatment of severe congenital hyperinsulinism: perspectives on limited therapeutic success. *The Journal of clinical endocrinology & metabolism*, 101(12)**,** 4719-4729.

Tabar, M. S., Hesaraki, M., Esfandiari, F., Samani, F. S., Vakilian, H. & Baharvand, H. (2015). Evaluating electroporation and lipofectamine approaches for transient and stable transgene expressions in human fibroblasts and embryonic stem cells. *Cell journal*, 17(3)**,** 438-450.

Tagaya, M., Oka, M., Ueda, M., Takagaki, K., Tanaka, M., Ohgi, T. & Yano, J. (2009). Eviprostat suppresses proinflammatory gene expression in the prostate of rats with partial bladder-outlet obstruction: A genome-wide DNA microarray analysis. *Cytokine*, 47(3)**,** 185-193.

Takahashi, K. & Yamanaka, S. (2006). Induction of pluripotent stem cells from mouse embryonic and adult fibroblast cultures by defined factors. *Cell*, 126(4)**,** 663-676.

Tamura, K., Nei, M. & Kumar, S. (2004). Prospects for inferring very large phylogenies by using the neighbor-joining method. *Proceedings of the national academy of sciences*, 101(30)**,** 11030-11035.

Tanizawa, Y., Matsuda, K., Matsuo, M., Ohta, Y., Ochi, N., Adachi, M., Koga, M., Mizuno, S., Kajita, M. & Tanaka, Y. (2000). Genetic analysis of Japanese patients with persistent hyperinsulinemic hypoglycemia of infancy: nucleotide-binding fold-2 mutation impairs cooperative binding of adenine nucleotides to sulfonylurea receptor 1. *Diabetes*, 49(1)**,** 114-120.

Tanizawa, Y., Nakai, K., Sasaki, T., Anno, T., Ohta, Y., Inoue, H., Matsuo, K., Koga, M., Furukawa, S. & Oka, Y. (2002). Unregulated elevation of glutamate dehydrogenase activity induces glutamine-stimulated insulin secretion: identification and characterization of a GLUD1 gene mutation and insulin secretion studies with MIN6 cells overexpressing the mutant glutamate dehydrogenase. *Diabetes*, 51(3)**,** 712-717.

Tannour-Louet, M., Han, S., Louet, J.-F., Zhang, B., Romero, K., Addai, J., Sahin, A., Cheung, S. W. & Lamb, D. J. (2014). Increased gene copy number of VAMP7 disrupts human male urogenital development through altered estrogen action. *Nature medicine*, 20(7)**,** 715-724.

Taschenberger, G., Mougey, A., Shen, S., Lester, L. B., LaFranchi, S. & Shyng, S.-L. (2002). Identification of a familial hyperinsulinism-causing mutation in the sulfonylurea receptor 1 that prevents normal trafficking and function of KATP channels. *Journal of biological chemistry*, 277(19), 17139-17146.

Taylor, B. L., Liu, F.-F. & Sander, M. (2013). Nkx6. 1 is essential for maintaining the functional state of pancreatic beta cells. *Cell reports*, 4(6)**,** 1262-1275.

Tessem, J. S., Moss, L. G., Chao, L. C., Arlotto, M., Lu, D., Jensen, M. V., Stephens, S. B., Tontonoz, P., Hohmeier, H. E. & Newgard, C. B. (2014). Nkx6. 1 regulates islet β-cell proliferation via Nr4a1 and Nr4a3 nuclear receptors. *Proceedings of the national academy of sciences*, 111(14)**,** 5242-5247.

Thallinger, G. G., Obermayr, E., Charoentong, P., Tong, D., Trajanoski, Z. and Zellinger, R. (2012). A sequence based validation of gene expression microarray data. *American journal of bioinformatics*, 1(1), 1-9.

Thomas Jr, C. G., Underwood, L. E., Carney, C. N., Dolcourt, J. L. & Whitt, J. J. (1977). Neonatal and infantile hypoglycemia due to insulin excess: new aspects of diagnosis and surgical management. *Annals of surgery*, 185(5)**,** 505-516.

Thomas, P., Ye, Y. & Lightner, E. (1996). Mutation of the pancreatic islet inward rectifier Kir6. 2 also leads to familial persistent hyperinsulinemic hypoglycemia of infancy. *Human molecular genetics*, 5(11)**,** 1809-1812.

Thomas, P. D., Kejariwal, A., Campbell, M. J., Mi, H., Diemer, K., Guo, N., Ladunga, I., Ulitsky-Lazareva, B., Muruganujan, A. & Rabkin, S. (2003). PANTHER: a browsable database of gene products organized by biological function, using curated protein family and subfamily classification. *Nucleic acids research,* 31(1)**,** 334-341.

Thomas, P. M., Cote, G. J., Wohllk, N., Haddad, B., Mathew, P., Rabl, W., Aguilar-Bryan, L., Gagel, R. F. & Bryan, J. (1995). Mutations in the sulfonylurea receptor gene in familial persistent hyperinsulinemic hypoglycemia of infancy. *Science,* 268(5209)**,** 426-429.

Thomas, R., de la Torre, L., Chang, X. & Mehrotra, S. (2010). Validation and characterization of DNA microarray gene expression data distribution and associated moments. *BMC bioinformatics,* 11(1)**,** 576.

Thomas, S. & Bonchev, D. (2010). A survey of current software for network analysis in molecular biology. *Human genomics,* 4(5)**,** 353-360.

Thomsen, S. K., Ceroni, A., van de Bunt, M., Burrows, C., Barrett, A., Scharfmann, R., Ebner, D., McCarthy, M. I. & Gloyn, A. L. (2016). Systematic functional characterization of candidate causal genes for type 2 diabetes risk variants. *Diabetes***,** 65(12),3805-3811 .

Thornton, P. S., MacMullen, C., Ganguly, A., Ruchelli, E., Steinkrauss, L., Crane, A., Aguilar-Bryan, L. & Stanley, C. A. (2003). Clinical and molecular characterization of a dominant form of congenital hyperinsulinism caused by a mutation in the high-affinity sulfonylurea receptor. *Diabetes,* 52(9)**,** 2403-2410.

Tian, J.-M. & Schibler, U. (1991). Tissue-specific expression of the gene encoding hepatocyte nuclear factor 1 may involve hepatocyte nuclear factor 4. *Genes & development,* 5(12a)**,** 2225-2234.

Toma, J. G., Akhavan, M., Fernandes, K. J., Barnabé-Heider, F., Sadikot, A., Kaplan, D. R. & Miller, F. D. (2001). Isolation of multipotent adult stem cells from the dermis of mammalian skin. *Nature cell biology,* 3(9)**,** 778-784.

Tornovsky-Babeay, S., Dadon, D., Ziv, O., Tzipilevich, E., Kadosh, T., Haroush, R. S.-B., Hija, A., Stolovich-Rain, M., Furth-Lavi, J. & Granot, Z. (2014). Type 2 diabetes and congenital hyperinsulinism cause DNA double-strand breaks and p53 activity in β cells. *Cell metabolism,* 19(1)**,** 109-121.

Tosur, M. & Jeha, G. S. (2017). A Novel Intragenic *SLC16A1* Mutation Associated With Congenital Hyperinsulinism. *Global pediatric health,* 4**,** 1-3.

Trevino, V., Falciani, F. & Barrera-Saldaña, H. A. (2007). DNA microarrays: a powerful genomic tool for biomedical and clinical research. *Molecular medicine,* 13(9-10)**,** 527-541.

Tseng, G. C., Oh, M.-K., Rohlin, L., Liao, J. C. & Wong, W. H. (2001). Issues in cDNA microarray analysis: quality filtering, channel normalization, models of variations and assessment of gene effects. *Nucleic acids research,* 29(12)**,** 2549-2557.

Tyson, J. J., Chen, K. & Novak, B. (2001). Network dynamics and cell physiology. *Nature reviews molecular cell biology,* 2(12)**,** 908-916.

Valamehr, B., Abujarour, R., Robinson, M., Le, T., Robbins, D., Shoemaker, D. & Flynn, P. (2012). A novel platform to enable the high-throughput derivation and characterization of feeder-free human iPSCs. *Scientific reports,* 2**,** 213.

Valamehr, B., Tsutsui, H., Ho, C.-M. & Wu, H. (2011). Developing defined culture systems for human pluripotent stem cells. *Regenerative medicine,* 6(5)**,** 623-634.

Valasek, M. A. & Repa, J. J. (2005). The power of real-time PCR. *Advances in physiology education,* 29(3)**,** 151-159.

Van't Veer, L. J., Dai, H., Van De Vijver, M. J., He, Y. D., Hart, A. A., Mao, M., Peterse, H. L., Van Der Kooy, K., Marton, M. J. & Witteveen, A. T. (2002). Gene expression profiling predicts clinical outcome of breast cancer. *Nature,* 415(6871)**,** 530-536.

van Vuren, P. J., Grobbelaar, A., Storm, N., Conteh, O., Konneh, K., Kamara, A., Sanne, I. & Paweska, J. T. (2016). Comparative evaluation of the diagnostic performance of the prototype Cepheid GeneXpert Ebola assay. *Journal of clinical microbiology,* 54(2)**,** 359-367.

Vanderford, N. L., Cantrell, J. E., Popa, G. J. & Özcan, S. (2008). Multiple kinases regulate mafA expression in the pancreatic beta cell line MIN6. *Archives of biochemistry and biophysics,* 480(2)**,** 138-142.

Vandesompele, J., De Preter, K., Pattyn, F., Poppe, B., Van Roy, N., De Paepe, A. & Speleman, F. (2002). Accurate normalization of real-time quantitative RT-PCR data by geometric averaging of multiple internal control genes. *Genome biology,* 3(7)**,** research0034. 1-0034.11.

VanGuilder, H. D., Vrana, K. E. & Freeman, W. M. (2008). Twenty-five years of quantitative PCR for gene expression analysis. *Biotechniques,* 44(5)**,** 619-625.

Vaskova, E., Stekleneva, A., Medvedev, S. & Zakian, S. (2013). "Epigenetic memory" phenomenon in induced pluripotent stem cells. *Acta naturae,* 5(4), 15-21.

Velayos, T., Martínez, R., Alonso, M., Garcia-Etxebarria, K., Aguayo, A., Camarero, C., Urrutia, I., de LaPiscina, I. M., Barrio, R. & Santin, I. (2017). An activating mutation in STAT3 results in neonatal diabetes through reduced insulin synthesis. *Diabetes,* 66(4)**,** 1022-1029.

Verkarre, V., Fournet, J.-C., de Lonlay, P., Gross-Morand, M.-S., Devillers, M., Rahier, J., Brunelle, F., Robert, J.-J., Nihoul-Fékété, C. & Saudubray, J.-M. (1998). Paternal mutation of the sulfonylurea receptor (SUR1) gene and maternal loss of 11p15 imprinted genes lead to persistent hyperinsulinism in focal adenomatous hyperplasia. *Journal of clinical investigation,* 102(7)**,** 1286-1291.

Vignali, S., Leiss, V., Karl, R., Hofmann, F. & Welling, A. (2006). Characterization of voltage-dependent sodium and calcium channels in mouse pancreatic A-and B-cells. *The Journal of physiology,* 572(3)**,** 691-706.

Viljoen, K. S. & Blackburn, J. M. (2013). Quality assessment and data handling methods for Affymetrix Gene 1.0 ST arrays with variable RNA integrity. *BMC genomics,* 14(1)**,** 14.

Vogel, C. & Marcotte, E. M. (2012). Insights into the regulation of protein abundance from proteomic and transcriptomic analyses. *Nature reviews genetics,* 13(4), 227-232.

Vozza, A., Parisi, G., De Leonardis, F., Lasorsa, F. M., Castegna, A., Amorese, D., Marmo, R., Calcagnile, V. M., Palmieri, L. & Ricquier, D. (2014). UCP2 transports C4 metabolites out of mitochondria, regulating glucose and glutamine oxidation. *Proceedings of the national academy of sciences,* 111(3)**,** 960-965.

Wabitsch, M., Lahr, G., Van de Bunt, M., Marchant, C., Lindner, M., Von Puttkamer, J., Fenneberg, A., Debatin, K., Klein, R. & Ellard, S. (2007). Heterogeneity in disease severity in a family with a novel G68V *GCK* activating mutation causing persistent hyperinsulinaemic hypoglycaemia of infancy. *Diabetic medicine,* 24(12)**,** 1393-1399.

Wallach, T., Schellenberg, K., Maier, B., Kalathur, R. K. R., Porras, P., Wanker, E. E., Futschik, M. E. & Kramer, A. (2013). Dynamic circadian protein–protein interaction networks predict temporal organization of cellular functions. *PLoS genetics,* 9(3)**,** e1003398.

Wang, H.-M., Dong, J.-H., Li, Q., Hu, Q., Ning, S.-L., Zheng, W., Cui, M., Chen, T.-S., Xie, X. & Sun, J.-P. (2014). A stress response pathway in mice upregulates somatostatin level and transcription in pancreatic delta cells through Gs and β-arrestin 1. *Diabetologia,* 57(9)**,** 1899-1910.

Wang, H., Maechler, P., Antinozzi, P. A., Hagenfeldt, K. A. & Wollheim, C. B. (2000a). Hepatocyte nuclear factor 4α regulates the expression of pancreatic β-cell genes implicated in glucose metabolism and nutrient-induced insulin secretion. *Journal of biological chemistry,* 275(46)**,** 35953-35959.

Wang, H., Yang, H., Shivalila, C. S., Dawlaty, M. M., Cheng, A. W., Zhang, F. & Jaenisch, R. (2013). One-step generation of mice carrying mutations in multiple genes by CRISPR/Cas-mediated genome engineering. *Cell,* 153(4)**,** 910-918.

Wang, K., Li, M. & Bucan, M. (2007). Pathway-based approaches for analysis of genomewide association studies. *The American journal of human genetics,* 81(6)**,** 1278-1283.

Wang, T., Hopkins, D., Schmidt, C., Silva, S., Houghton, R., Takita, H., Repasky, E. & Reed, S. G. (2000b). Identification of genes differentially over-expressed in lung squamous cell carcinoma using combination of cDNA subtraction and microarray analysis. *Oncogene,* 19(12)**,** 1519.

Wang, W., Shi, Q., Guo, T., Yang, Z., Jia, Z., Chen, P. & Zhou, C. (2016b). PDX1 and ISL1 differentially coordinate with epigenetic modifications to regulate insulin gene expression in varied glucose concentrations. *Molecular and cellular endocrinology,* 428**,** 38-48.

Wang, Y., Barbacioru, C., Hyland, F., Xiao, W., Hunkapiller, K. L., Blake, J., Chan, F., Gonzalez, C., Zhang, L. & Samaha, R. R. (2006). Large scale real-time PCR validation on gene expression measurements from two commercial long-oligonucleotide microarrays. *BMC genomics,* 7(1)**,** 59.

Wang, Z. & Thurmond, D. C. (2009). Mechanisms of biphasic insulin-granule exocytosis–roles of the cytoskeleton, small GTPases and SNARE proteins. *Journal of cell science,* 122(7)**,** 893-903.

Warnat, P., Eils, R. & Brors, B. (2005). Cross-platform analysis of cancer microarray data improves gene expression based classification of phenotypes. *BMC bioinformatics,* 6(1)**,** 265.

Watkins-Chow, D. E. & Pavan, W. J. (2008). Genomic copy number and expression variation within the C57BL/6J inbred mouse strain. *Genome research,* 18(1)**,** 60-66.

Wei, C., Li, J. & Bumgarner, R. E. (2004). Sample size for detecting differentially expressed genes in microarray experiments. *BMC genomics,* 5(1)**,** 87.

Weir, G. C. & Bonner-Weir, S. (2011). Finally! A human pancreatic β cell line. *The journal of clinical investigation,* 121(9), 3395-3397.

Weitzer, S. & Martinez, J. (2007). hClp1, A Novel Kinase Revitalizes RNA Metabolism. *Cell cycle,* 6(17)**,** 2133-2137.

Welters, A., Lerch, C., Kummer, S., Marquard, J., Salgin, B., Mayatepek, E. & Meissner, T. (2015). Long-term medical treatment in congenital hyperinsulinism: a descriptive analysis in a large cohort of patients from different clinical centers. *Orphanet journal of rare diseases,* 10(1)**,** 150.

Whitehead, K. A., Langer, R. and Anderson, D. G. (2009). Knocking down barriers: advances in siRNA delivery. *Nature reviews*, 8(2), 129-138.

Wilson, R. C. & Doudna, J. A. (2013). Molecular mechanisms of RNA interference. *Annual review of biophysics,* 42**,** 217-239.

Wippermann, A., Klausing, S., Rupp, O., Albaum, S. P., Büntemeyer, H., Noll, T. & Hoffrogge, R. (2014). Establishment of a CpG island microarray for analyses of genome-wide DNA methylation in Chinese hamster ovary cells. *Applied microbiology and biotechnology,* 98(2)**,** 579-589.

Wittkop, T., TerAvest, E., Evani, U. S., Fleisch, K. M., Berman, A. E., Powell, C., Shah, N. H. & Mooney, S. D. (2013). STOP using just GO: a multi-ontology hypothesis generation tool for high throughput experimentation. *BMC bioinformatics,* 14(1)**,** 53.

Wittrup, A., Ai, A., Liu, X., Hamar, P., Trifonova, R., Charisse, K., Manoharan, M., Kirchhausen, T. & Lieberman, J. (2015). Visualizing lipid-formulated siRNA release from endosomes and target gene knockdown. *Nature biotechnology,* 33(8)**,** 870-876.

Wolter, T. R., Wong, R., Sarkar, S. A. & Zipris, D. (2009). DNA microarray analysis for the identification of innate immune pathways implicated in virus-induced autoimmune diabetes. *Clinical immunology,* 132(1)**,** 103-115.

Wong, N., Morahan, G., Stathopoulos, M., Proietto, J. & Andrikopoulos, S. (2013). A novel mechanism regulating insulin secretion involving Herpud1 in mice. *Diabetologia,* 56(7)**,** 1569-1576.

Wu, J. & Belmonte, J. C. I. (2016). Stem cells: a renaissance in human biology research. *Cell,* 165(7)**,** 1572-1585.

Wu, Y., Liang, D., Wang, Y., Bai, M., Tang, W., Bao, S., Yan, Z., Li, D. & Li, J. (2013). Correction of a genetic disease in mouse via use of CRISPR-Cas9. *Cell stem cell,* 13(6)**,** 659-662.

Wu, Z. Y., Zhu, L. J., Zou, N., Bombek, L. K., Shao, C. Y., Wang, N., Wang, X. X., Liang, L., Xia, J. & Rupnik, M. (2012). AMPA receptors regulate exocytosis and insulin release in pancreatic β cells. *Traffic,* 13(8)**,** 1124-1139.

Xenarios, I., Rice, D. W., Salwinski, L., Baron, M. K., Marcotte, E. M. & Eisenberg, D. (2000). DIP: the database of interacting proteins. *Nucleic acids research,* 28(1)**,** 289-291.

Xin, Y., Huang, M., Guo, W. W., Huang, Q., zhen Zhang, L. & Jiang, G. (2017). Nano-based delivery of RNAi in cancer therapy. *Molecular cancer,* 16(1)**,** 134.

Xue, W., Chen, S., Yin, H., Tammela, T., Papagiannakopoulos, T., Joshi, N. S., Cai, W., Yang, G., Bronson, R. & Crowley, D. G. (2014). CRISPR-mediated direct mutation of cancer genes in the mouse liver. *Nature,* 514(7522)**,** 380-384.

Yaluri, N., Modi, S., Rodríguez, M. L., Stančáková, A., Kuusisto, J., Kokkola, T. & Laakso, M. (2015). Simvastatin impairs insulin secretion by multiple mechanisms in MIN6 cells. *PLoS one,* 10(11)**,** e0142902.

Yan, F.-F., Lin, Y.-W., MacMullen, C., Ganguly, A., Stanley, C. A. & Shyng, S.-L. (2007). Congenital Hyperinsulinism–Associated *ABCC8* Mutations That Cause Defective Trafficking of ATP-Sensitive K^+ Channels: Identification and Rescue. *Diabetes,* 56(9), 2339-2348.

Yan, L., Figueroa, D. J., Austin, C. P., Liu, Y., Bugianesi, R. M., Slaughter, R. S., Kaczorowski, G. J. & Kohler, M. G. (2004). Expression of voltage-gated potassium channels in human and rhesus pancreatic islets. *Diabetes,* 53(3)**,** 597-607.

Yang, H., Wang, H., Shivalila, C. S., Cheng, A. W., Shi, L. & Jaenisch, R. (2013). One-step generation of mice carrying reporter and conditional alleles by CRISPR/Cas-mediated genome engineering. *Cell,* 154(6)**,** 1370-1379.

Yang, J., Chi, Y., Burkhardt, B. R., Guan, Y. & Wolf, B. A. (2010). Leucine metabolism in regulation of insulin secretion from pancreatic beta cells. *Nutrition reviews,* 68(5)**,** 270-279.

Yang, J., Wong, R. K., Park, M., Wu, J., Cook, J. R., York, D. A., Deng, S., Markmann, J., Naji, A. & Wolf, B. A. (2006). Leucine regulation of glucokinase and ATP synthase sensitizes glucose-induced insulin secretion in pancreatic β-cells. *Diabetes,* 55(1)**,** 193-201.

Yang, J., Wong, R. K., Wang, X., Moibi, J., Hessner, M. J., Greene, S., Wu, J., Sukumvanich, S., Wolf, B. A. & Gao, Z. (2004). Leucine culture reveals that ATP synthase functions as a fuel sensor in pancreatic β-cells. *Journal of biological chemistry,* 279(52)**,** 53915-53923.

Yang, L., Mali, P., Kim-Kiselak, C. & Church, G. (2014a). CRISPR-Cas-mediated targeted genome editing in human cells, in Storici, F. (ed.) *Gene correction: methods and protocols.* Springer, 245-267.

Yang, L., Yang, J. L., Byrne, S., Pan, J. & Church, G. M. (2014b). CRISPR/Cas9-Directed Genome Editing of Cultured Cells. *Current protocols in molecular biology***,** 107, 31.1. 1-31.1. 17.

Yang, Y. H., Dudoit, S., Luu, P., Lin, D. M., Peng, V., Ngai, J. & Speed, T. P. (2002). Normalization for cDNA microarray data: a robust composite method addressing single and multiple slide systematic variation. *Nucleic acids research,* 30(4)**,** e15-e15.

Yao, T. & Asayama, Y. (2017). Animal-cell culture media: history, characteristics, and current issues. *Reproductive medicine and biology,* 16(2), 99-117.

Ye, Q., Wu, B. & Wang, B. (2010). Distance distribution and average shortest path length estimation in real-world networks, in Cao, L., Zhong, J. and Feng, Y. (eds.) *International conference on advanced data mining and applications*. Springer, pp. 322-333.

Yoon, J., Blumer, A. & Lee, K. (2006). An algorithm for modularity analysis of directed and weighted biological networks based on edge-betweenness centrality. *Bioinformatics,* 22(24)**,** 3106-3108.

Yorifuji, T. (2014). Congenital hyperinsulinism: current status and future perspectives. *Annals of pediatric endocrinology & metabolism,* 19(2)**,** 57-68.

Yorifuji, T., Muroi, J., Uematsu, A., Hiramatsu, H. & Momoi, T. (1999). Hyperinsulinism-hyperammonemia syndrome caused by mutant glutamate dehydrogenase accompanied by novel enzyme kinetics. *Human genetics,* 104(6)**,** 476-479.

Yoshimi, K., Kunihiro, Y., Kaneko, T., Nagahora, H., Voigt, B. & Mashimo, T. (2016). ssODN-mediated knock-in with CRISPR-Cas for large genomic regions in zygotes. *Nature communications,* 7**,** 10431.

Yu, H. & Cowan, C. A. (2016). Minireview: genome editing of human pluripotent stem cells for modeling metabolic disease. *Molecular endocrinology,* 30(6)**,** 575-586.

Yu, H., Greenbaum, D., Lu, H. X., Zhu, X. & Gerstein, M. (2004). Genomic analysis of essentiality within protein networks. *TRENDS in genetics,* 20(6)**,** 227-231.

Yu, J., Gu, X. & Yi, S. (2016). Ingenuity pathway analysis of gene expression profiles in distal nerve stump following nerve injury: insights into Wallerian degeneration. *Frontiers in cellular neuroscience,* 10(274), 1-12.

Yu, N., Christiaens, O., Liu, J., Niu, J., Cappelle, K., Caccia, S., Huvenne, H. & Smagghe, G. (2013). Delivery of dsRNA for RNAi in insects: an overview and future directions. *Insect science,* 20(1)**,** 4-14.

Yue, H., Eastman, P. S., Wang, B. B., Minor, J., Doctolero, M. H., Nuttall, R. L., Stack, R., Becker, J. W., Montgomery, J. R. & Vainer, M. (2001). An evaluation of the performance of cDNA microarrays for detecting changes in global mRNA expression. *Nucleic acids research,* 29(8)**,** e41-e41.

Zhang, D., Jiang, W., Liu, M., Sui, X., Yin, X., Chen, S., Shi, Y. & Deng, H. (2009). Highly efficient differentiation of human ES cells and iPS cells into mature pancreatic insulin-producing cells. *Cell research,* 19(4)**,** 429-438.

Zhang, H. & Yin, T. (2016). Identifying candidate genes for wood formation in poplar based on microarray network analysis and graph theory. *Tree genetics & genomes,* 12(3)**,** 61.

Zhang, J., Ni, S., Xiang, Y., Parvin, J. D., Yang, Y., Zhou, Y. & Huang, K. (2013). Gene Co-expression analysis predicts genetic aberration loci associated with colon cancer metastasis. *International journal of computational biology and drug design,* 6(1-2)**,** 60-71.

Zhang, W., Yi, X., Sun, X. & Zhang, Y. (2008). Surface modification of non-woven poly (ethylene terephthalate) fibrous scaffold for inproving cell attachment in animal cell culture. *Journal of Chemical Technology & Biotechnology,* 83, 904-911.

Zhang, X.-F., Ou-Yang, L., Zhao, X.-M. & Yan, H. (2016a). Differential network analysis from cross-platform gene expression data. *Scientific reports,* 6**,** 34112.

Zhang, Y., Wang, N., Ma, J., Chen, X., Li, Z. & Zhao, W. (2016b). Expression profile analysis of new candidate genes for the therapy of primary osteoporosis. *European reveiw for medical and pharmacological sciences,* 20(3)**,** 433-40.

Zhao, J.-J., Yang, J., Lin, J., Yao, N., Zhu, Y., Zheng, J., Xu, J., Cheng, J. Q., Lin, J.-Y. & Ma, X. (2009). Identification of miRNAs associated with tumorigenesis of retinoblastoma by miRNA microarray analysis. *Child's nervous system,* 25(1)**,** 13-20.

Zhao, S., Fung-Leung, W.-P., Bittner, A., Ngo, K. & Liu, X. (2014). Comparison of RNA-Seq and microarray in transcription profiling of activated T cells. *PLOS One,* 9(1), e78644.

Zhou, R., Mohr, S., Hannon, G. J. & Perrimon, N. (2014). Inducing RNAi in Drosophila cells by soaking with dsRNA. *Cold spring harbor protocols,* 2014(5)**,** pdb. prot080747.

Zhou, X., Zhou, Y.-P., Huang, G.-R., Gong, B.-L., Yang, B., Zhang, D.-X., Hu, P. & Xu, S.-R. (2011). Expression of the stem cell marker Nanog in human endometrial adenocarcinoma. *International journal of gynecological pathology,* 30(3)**,** 262-270.

Zimmermann, T. S., Lee, A. C., Akinc, A., Bramlage, B., Bumcrot, D., Fedoruk, M. N., Harborth, J., Heyes, J. A., Jeffs, L. B. & John, M. (2006). RNAi-mediated gene silencing in non-human primates. *Nature,* 441(7089)**,** 111-114.

Zingman, L. V., Alekseev, A. E., Bienengraeber, M., Hodgson, D., Karger, A. B., Dzeja, P. P. & Terzic, A. (2001). Signaling in channel/enzyme multimers: ATPase transitions in SUR module gate ATP-sensitive K^+ conductance. *Neuron,* 31(2)**,** 233-245.

Zlatev, I., Foster, D. J., Liu, J., Charisse, K., Brigham, B., Parmar, R. G., Jadhav, V., Maier, M. A., Rajeev, K. G. & Egli, M. (2016). 5′-C-Malonyl RNA: Small Interfering RNAs Modified with 5′-Monophosphate Bioisostere Demonstrate Gene Silencing Activity. *ACS chemical biology,* 11(4)**,** 953-960.

Appendix I

List of primers used in RT-PCR

Gene name/ NCBI ref. no	Primer	Primer sequence 5′ → 3′	T_m (°C)	Product size (bp)
ABCC8 (human) NM_000352.4	Forward	GCCTTCCTGACAGCGAGATA	62	84
	Reverse	CGGGGCCTCTCTTCCTGAT		
ABCC8 (mouse) NM_001357538.1	Forward	GAGATGCAGAGGGTCTCCG	62	99
	Reverse	CTCTGGGTTGCTTGTCCTGA		
CACNA1A (mouse) NM_001252059.1	Forward	TCGGGAACTACACCCTGCT	60	100
	Reverse	GCCTCTTCCTCTTCTTGCTCA		
CACNA1B (mouse) NM_001042528.2	Forward	TACTTCCGGGACCTGTGGAA	62	90
	Reverse	GGATCCTCCCATGAAGCTCG		
CACNA1C (mouse) NM_001159533.2	Forward	TTCCTCATCGTCATTGGGAGC	60	97
	Reverse	TCTCCTCTGCACTCATAGAGG		
CACNA1D (human) NM_000720.3	Forward	GTCTCTGGTGCTGGTGGAGA	59	100
	Reverse	CGTCGGCTGAGTTTGGATTT		
CACNA1H (human) NM_001005407.1	Forward	ACCAGCCACTATCTCGACCT	62	94
	Reverse	CCAGCGACTTGGGTTGGTTA		
GAPDH (human) NM_001256799.2	Forward	ATTGCCCTCAACGACCAC	60	79
	Reverse	GGTCCACCACCCTGTTGC		
GAPDH (mouse) NM_001289726.1	Forward	TAAGAGGGATGCTGCCCTTAC	60	115
	Reverse	CCAAATCCGTTCACACCGAC		
INS (human) NM_001185097.1	Forward	GCATCTGTCCCTCTACCA	59	107
	Reverse	CAAGGGTTTATTCCATCTCTCT		
INS (mouse) NM_008386.4	Forward	TGGCTTCTTCTACACACCCAAG	62	132
	Reverse	ACAATGCCACGCTTCTGCC		
KCNB1 (human) NM_004975.3	Forward	TGCCAAGATCCTTGCCATAATTT	62	97
	Reverse	CTCATCGAGGCTCTGTAGCTC		
KCNB1 (mouse) NM_008420.4	Forward	GGTGGCCGCCAAGATCCTGG	60	107
	Reverse	CGAATTCGTCCAGGCTCTGT		
KCNB2 (human) NM_004770.2	Forward	GTCATTGGCGAAGGGGATCG	60	124
	Reverse	GACAAAGCTAGCTCCCACAGAC		

Gene name/ NCBI ref. no	**Primer**	**Primer sequence 5′ → 3′**	**T_m (°C)**	**Product size (bp)**
KCNB2 (mouse) NM_001098528.2	Forward	GAGTTTGATAACACCTGCTGCC	60	97
	Reverse	CGATGGCCAGGATCTTTGCAG		
KCNC2 (human) NM_001260497.1	Forward	AGGAAAGGAATTAGAAATGGGCA	60	115
	Reverse	CCAGCATATTTAATCTTCCAGCTT		
KCNJ11 (human) NM_000525.3	Forward	GTCTGGTGGGGAGTTATCTCAG	62	99
	Reverse	TAGGGCCTCACTGCAGAGTC		
KCNJ11 (mouse) NM_001204411.1	Forward	CAGACACACGCCAGGGAAG	60	97
	Reverse	GCAGCCAGCTGCTCGTGC		
KCNMA1 (mouse) NM_001253358.1	Forward	CATCCCGTCCACAGCAAATC	62	100
	Reverse	CTTTTCTGCTTGGCCCATTCT		
NEUROD1 (human) NM_002500.4	Forward	CTCGGACTTTTCTGCCTGAG	58	275
	Reverse	GAAGTTGCCATTGATGCTGA		
NKX6.1 (human) NM_006168.2	Forward	AAAGACGGGAAGAGAAAACA	58	298
	Reverse	CCAGAGGCTTATTGTAGTCG		
PDX1 (human) NM_000209.3	Forward	AACAACTATTCACGAGCCAGTA	58	203
	Reverse	GCATTTCCCACAAACATAAC		
SCN8A (human) NM_001177984.2	Forward	GTTGCTCAAGTGGACAGCCT	60	90
	Reverse	TTCACCACCACAGCCACAATG		
SCN9A (human) NM_002977.3	Forward	ACCCTAGAGAGTGAAGAAGACT	58	99
	Reverse	ACACTGACCTGAATCTGTGCT		
SCN9A (mouse) NM_001290674.1	Forward	TGCTGAGAGTGAAGAAGAATTGA	62	99
	Reverse	GGACACTGCCCTGAATCTGT		

Appendix II

List of differentially expressed genes (over-expressed) in CHI tissues

Gene Symbol	Gene name	Fold-Change
SLC17A6	Solute carrier family 17 member 6	7.98662
SCG3	Secretogranin III	5.73173
SNORD115-32	Small nucleolar RNA, C/D box 115-32	5.69395
PPY	Pancreatic polypeptide	5.66877
G6PC2	Glucose-6-phosphatase, catalytic, 2	5.57633
PARM1	Prostate androgen-regulated mucin-like protein 1	5.55203
BMP5	Bone morphogenetic protein 5	5.42886
PCSK1	Proprotein convertase subtilisin/kexin type 1	5.34898
LOC101927457	Uncharacterized LOC101927457	5.09246
SYT13	Synaptotagmin XIII	5.00993
SNORD115-22	Small nucleolar RNA, C/D box 115-22	4.99572
RIMS2	Regulating synaptic membrane exocytosis 2	4.76136
SNORD115-5	Small nucleolar RNA, C/D box 115-5	4.74847
SNORD115-6	Small nucleolar RNA, C/D box 115-6	4.69781
SNORD115-44	Small nucleolar RNA, C/D box 115-44	4.68766
RFX6	Regulatory factor X, 6	4.66785
SNORD115-27	Small nucleolar RNA, C/D box 115-27	4.66783
SNORD115-10	Small nucleolar RNA, C/D box 115-10	4.65885
SNORD115-11	Small nucleolar RNA, C/D box 115-11	4.61906
SNORD115-25	Small nucleolar RNA, C/D box 115-25	4.54399
ABCC8	ATP-binding cassette, sub-family C member 8	4.45723
SNORD115-1	Small nucleolar RNA, C/D box 115-1	4.44017
GNG4	Guanine nucleotide binding protein gamma 4	4.42531
MIR7-3HG	MIR7-3 host gene (non-protein coding)	4.39157
SCGB2A1	Secretoglobin, family 2A, member 1	4.37755
SNORD115-16	Small nucleolar RNA, C/D box 115-16	4.35774
FAM159B	Family with sequence similarity 159, member B	4.2898
SNORD115-40	Small nucleolar RNA, C/D box 115-40	4.25136
SNORD115-31	Small nucleolar RNA, C/D box 115-31	4.23499
LOC101929550	Uncharacterized LOC101929550	4.22272
SNORD115-38	Small nucleolar RNA, C/D box 115-38	4.20774
SNORD115-33	Small nucleolar RNA, C/D box 115-33	4.18358
SNORD115-24	Small nucleolar RNA, C/D box 115-24	4.13269
NEFM	Neurofilament, medium polypeptide	4.12996
SNORD115-21	Small nucleolar RNA, C/D box 115-21	4.11915
RAB3B	RAB3B, member RAS oncogene family	4.09549
IAPP	Islet amyloid polypeptide	4.02412
SCGN	Secretagogin, EF-hand calcium binding protein	4.02137

Gene Symbol	Gene name	Fold-Change
CXorf57	Chromosome X open reading frame 57	3.96371
INA	Internexin neuronal intermediate filament protein, alpha	3.93723
SLC38A4	Solute carrier family 38, member 4	3.91409
RP11-531A24.3	Novel transcript	3.889
NOL4	Nucleolar protein 4	3.85513
RP11-38P22.2	Novel transcript	3.78973
FAM105A	Family with sequence similarity 105, member A	3.77095
CFC1B	Cripto, FRL-1, cryptic family 1B	3.75938
GAD2	Glutamate decarboxylase 2	3.75709
HEPACAM2	HEPACAM family member 2	3.68313
EDARADD	EDAR-associated death domain	3.6518
VAT1L	Vesicle amine transport 1-like	3.62934
RASD1	RAS, dexamethasone-induced 1	3.62796
LINC01112	Long intergenic non-protein coding RNA 1112	3.62479
SYT14	Synaptotagmin XIV	3.59173
IL13RA2	Interleukin 13 receptor, alpha 2	3.58845
SNORD115-28	Small nucleolar RNA, C/D box 115-28	3.53716
SORL1	Sortilin-related receptor 1	3.53053
SLC2A2	Solute carrier family 2 member 2	3.5281
UNC79	Unc-79 homolog, NALCN channel complex subunit	3.52703
CHGA	Chromogranin A	3.4891
PRKACB	Protein kinase, cAMP-dependent, catalytic, beta	3.48855
SNORD115-41	Small nucleolar RNA, C/D box 115-41	3.46676
GCH1	GTP cyclohydrolase 1	3.44092
LINC00643	Long intergenic non-protein coding RNA 643	3.43492
UNC13A	Unc-13 homolog A	3.42988
PCSK2	Proprotein convertase subtilisin/kexin type 2	3.39423
ELAVL4	ELAV like neuron-specific RNA binding protein 4	3.38101
CLGN	Calmegin	3.34569
EGFEM1P	EGF-like and EMI domain containing 1, pseudogene	3.31601
LOC653513	Phosphodiesterase 4D interacting protein pseudogene	3.29166
RAB3C	RAB3C, member RAS oncogene family	3.29073
LOC100288310	Uncharacterized LOC100288310	3.29023
CASR	Calcium-sensing receptor	3.27355
STXBP5L	Syntaxin binding protein 5-like	3.26314
SLC4A10	Solute carrier family 4 member 10	3.24838
CPE	Carboxypeptidase E	3.23779
LOC100129046	Uncharacterized LOC100129046	3.23716
SNORD115-39	Small nucleolar RNA, C/D box 115-39	3.20723
SAMD5	Sterile alpha motif domain containing 5	3.19696
PAM	Peptidylglycine alpha-amidating monooxygenase	3.19536
KIAA1377	Kiaa1377	3.18808
INSM1	Insulinoma-associated 1	3.13923

Gene Symbol	Gene name	Fold-Change
SNORD115-30	Small nucleolar RNA, C/D box 115-30	3.13827
KIF5C	Kinesin family member 5C	3.12774
SNORD115-17	Small nucleolar RNA, C/D box 115-17	3.12521
CHST9	Carbohydrate (N-acetylgalactosamine 4-0) sulfotransferase 9	3.11132
TOX	Thymocyte selection-associated high mobility group box	3.10553
CACNA1D	Calcium channel, voltage-dependent, L type, alpha 1D subunit	3.0776
PTPRN	Protein tyrosine phosphatase, receptor type, N	3.07146
SYT16	Synaptotagmin XVI	3.0558
GJD2	Gap junction protein, delta 2, 36kda	3.04259
JAKMIP2	Janus kinase and microtubule interacting protein 2	3.02476
ST8SIA3	ST8 alpha-N-acetyl-neuraminide alpha-2,8-sialyltransferase 3	3.01376
SCG2	Secretogranin II	2.99804
ZNF483	Zinc finger protein 483	2.9823
SLC8A1	Solute carrier family 8 member A1	2.98091
SNORD115-14	Small nucleolar RNA, C/D box 115-14	2.97705
PAX6	Paired box 6	2.9682
GLP1R	Glucagon-like peptide 1 receptor	2.94456
TMOD2	Tropomodulin 2	2.93484
SNORD115-8	Small nucleolar RNA, C/D box 115-8	2.93386
SNAP25	Synaptosome associated protein 25	2.91474
CHGB	Chromogranin B	2.9082
PFKFB2	6-phosphofructo-2-kinase/fructose-2,6-biphosphatase 2	2.90615
ERO1LB	ERO1-like beta (S. Cerevisiae)	2.90557
NFASC	Neurofascin	2.8968
CHN1	Chimerin 1	2.89388
UCHL1	Ubiquitin carboxyl-terminal esterase L1	2.88167
MYO3A	Myosin IIIA	2.88099
VWDE	Von Willebrand factor D and EGF domains	2.87407
SLC6A17	Solute carrier family 6 member 17	2.86543
SYT4	Synaptotagmin IV	2.86295
KCNB2	Potassium voltage-gated channel, Shab-related subfamily, member 2	2.86128
KCNK16	Potassium channel, subfamily K, member 16	2.86107
UNC80	Unc-80 homolog (C. Elegans)	2.8586
DZIP3	DAZ interacting zinc finger protein 3	2.848
SEPT3	Septin 3	2.84134
MBOAT4	Membrane bound O-acyltransferase domain containing 4	2.83005
MAP3K15	Mitogen-activated protein kinase kinase kinase 15	2.78051
FMN2	Formin 2	2.77357
NBEA	Neurobeachin	2.77226
PDK3	Pyruvate dehydrogenase kinase, isozyme 3	2.76507
PLCB4	Phospholipase C, beta 4	2.76465
SRD5A1	Steroid-5-alpha-reductase	2.76348

Gene Symbol	Gene name	Fold-Change
QPCT	Glutaminyl-peptide cyclotransferase	2.75469
GNAO1	G protein subunit alpha o1	2.75411
EMB	Embigin	2.74236
DPP6	Dipeptidyl-peptidase 6	2.74074
CSRNP3	Cysteine-serine-rich nuclear protein 3	2.73935
EDN3	Endothelin 3	2.73817
SYT7	Synaptotagmin VII	2.73258
CAMK2N1	Calcium/calmodulin-dependent protein kinase II inhibitor 1	2.72015
TMEM63C	Transmembrane protein 63C	2.71787
KIAA2022	Kiaa2022	2.71626
ELMO1	Engulfment and cell motility 1	2.70073
TMEM27	Transmembrane protein 27	2.68684
CA8	Carbonic anhydrase VIII	2.68637
MEG3	Maternally expressed 3 (non-protein coding)	2.67962
SLC7A8	Solute carrier family 7 member 8	2.65811
ZNF674-AS1	ZNF674 antisense RNA 1	2.65672
MIR670HG	MIR670 host gene (non-protein coding)	2.639
CACNA2D1	Calcium channel, voltage-dependent, alpha 2/delta subunit 1	2.62588
LINC01014	Long intergenic non-protein coding RNA 1014	2.6236
FAR2P2	Fatty acyl coa reductase 2 pseudogene 2	2.61387
CCDC67	Coiled-coil domain containing 67	2.61347
MTMR7	Myotubularin related protein 7	2.60595
ARG2	Arginase 2	2.60028
KIF5A	Kinesin family member 5A	2.58659
LRRC39	Leucine rich repeat containing 39	2.57985
SNORD115-4	Small nucleolar RNA, C/D box 115-4	2.57318
NKX6-1	NK6 homeobox 1	2.57299
LPPR4	Lipid phosphate phosphatase-related protein type 4	2.57206
TCN1	Transcobalamin I (	2.57063
LGI2	Leucine-rich repeat LGI family, member 2	2.54477
FFAR1	Free fatty acid receptor 1	2.53223
CACNA1A	Calcium voltage-gated channel subunit alpha 1A	2.51922
SLC4A8	Solute carrier family 4, member 8	2.51588
GPR98	G protein-coupled receptor 98	2.51512
GRIA3	Glutamate receptor, ionotropic, AMPA 3	2.51173
DAPL1	Death associated protein-like 1	2.49027
C1QL1	Complement component 1, q subcomponent-like 1	2.48925
PLCXD3	Phosphatidylinositol-specific phospholipase C, X domain containing 3	2.48847
SLC36A4	Solute carrier family 36 member 4	2.48482
MIR376B	Microrna 376b	2.48059
CAPN13	Calpain 13	2.47982
MAP1B	Microtubule-associated protein 1B	2.4768

Gene Symbol	Gene name	Fold-Change
HDAC9	Histone deacetylase 9	2.46846
EMBP1	Embigin pseudogene 1	2.46258
SLC30A8	Solute carrier family 30 member 8	2.46119
GLRA1	Glycine receptor, alpha 1	2.45983
SCIN	Scinderin	2.45558
RPS6KA6	Ribosomal protein S6 kinase A6	2.44992
RGS9	Regulator of G-protein signaling 9	2.44809
GCNT1	Glucosaminyl (N-acetyl) transferase 1, core 2	2.44705
KATNAL1	Katanin catalytic subunit A1 like 1	2.44645
ATP6V0A1	Atpase, H+ transporting, lysosomal V0 subunit a1	2.43349
SNORD115-3	Small nucleolar RNA, C/D box 115-3	2.43135
GPR148	G protein-coupled receptor 148	2.42921
TSPAN2	Tetraspanin 2	2.41652
MYO1D	Myosin ID	2.41544
CADPS	Calcium dependent secretion activator	2.41529
RIMBP2	RIMS binding protein 2	2.41297
LINC01146	Long intergenic non-protein coding RNA 1146	2.41027
NPTX2	Neuronal pentraxin II	2.40063
APLP1	Amyloid beta precursor-like protein 1	2.39463
CERKL	Ceramide kinase-like	2.39385
ATP8A1	Atpase phospholipid transporter 8A1	2.39224
SLCO5A1	Solute carrier organic anion transporter family, member 5A1	2.3913
WDR17	WD repeat domain 17	2.38874
RNU6-267P	RNA, U6 small nuclear 267, pseudogene	2.38862
RCAN2	Regulator of calcineurin 2	2.38405
HADH	Hydroxyacyl-coa dehydrogenase	2.38355
RNU6-162P	RNA, U6 small nuclear 162, pseudogene	2.3759
PPM1E	Protein phosphatase, Mg2+/Mn2+ dependent, 1E	2.37514
CD200	CD200 molecule	2.3724
CCL11	Chemokine (C-C motif) ligand 11	2.37214
PIGA	Phosphatidylinositol glycan anchor biosynthesis, class A	2.37181
IDS	Iduronate 2-sulfatase	2.37114
PCLO	Piccolo presynaptic cytomatrix protein	2.35033
SNORD113-1	Small nucleolar RNA, C/D box 113-1	2.35006
NEUROD1	Neuronal differentiation 1	2.33771
B3GALT2	Beta 1,3-galactosyltransferase 2	2.33443
GRIA2	Glutamate receptor, ionotropic, AMPA 2	2.32927
SCD5	Stearoyl-coa desaturase 5	2.32815
GPR158	G protein-coupled receptor 158	2.328
PTGS2	Prostaglandin-endoperoxide synthase 2	2.32189
TMEM196	Transmembrane protein 196	2.32069
KCNJ6	Potassium inwardly-rectifying channel, subfamily J, member 6	2.32068
TFCP2L1	Transcription factor CP2-like 1	2.31487

Gene Symbol	Gene name	Fold-Change
PITPNC1	Phosphatidylinositol transfer protein, cytoplasmic 1	2.31255
LONRF2	LON peptidase N-terminal domain and ring finger 2	2.30777
CNIH2	Cornichon family AMPA receptor auxiliary protein 2	2.30689
RGS17	Regulator of G-protein signaling 17	2.30593
NMNAT2	Nicotinamide nucleotide adenylyltransferase 2	2.30359
BEX1	Brain expressed, X-linked 1	2.30084
RGS7	Regulator of G-protein signaling 7	2.29946
ITGBL1	Integrin subunit beta-like 1	2.29492
ST18	Suppression of tumorigenicity 18	2.2944
SYT17	Synaptotagmin XVII	2.29277
SH3GL2	SH3-domain GRB2-like 2	2.29243
ROBO2	Roundabout guidance receptor 2	2.29227
SSTR2	Somatostatin receptor 2	2.2921
LINC00948	Long intergenic non-protein coding RNA 948	2.28975
KLKB1	Kallikrein B1	2.28728
RUNDC3A	RUN domain containing 3A	2.27687
A1CF	APOBEC1 complementation factor	2.27684
MEIS2	Meis homeobox 2	2.26971
PAPSS2	3-phosphoadenosine 5-phosphosulfate synthase 2	2.26643
SLC7A2	Solute carrier family 7 member 2	2.26395
INPP5F	Inositol polyphosphate-5-phosphatase F	2.25906
KCNMB2	Potassium calcium-activated channel subfamily M regulatory beta subunit 2	2.25556
SV2A	Synaptic vesicle glycoprotein 2A	2.25268
CDH2	Cadherin 2	2.25199
KCNA5	Potassium voltage-gated channel subfamily A member 5	2.25198
TSPYL5	TSPY-like 5	2.2516
ATRNL1	Attractin-like 1	2.25024
ANXA13	Annexin A13	2.24962
P2RY1	Purinergic receptor P2Y, G-protein coupled, 1	2.24359
ASB9	Ankyrin repeat and SOCS box containing 9	2.23963
LOC154761	Family with sequence similarity 115, member C pseudogene	2.23957
PPP1R1A	Protein phosphatase 1 regulatory inhibitor subunit 1A	2.23922
WNT4	Wingless-type MMTV integration site family, member 4	2.23896
LPPR5	Lipid phosphate phosphatase-related protein type 5	2.23832
SGTB	Small glutamine-rich tetratricopeptide repeat containing beta	2.23823
WSCD2	WSC domain containing 2	2.23707
XXbac-BPG55C20.7	Novel transcript	2.23491
SEZ6L2	Seizure related 6 homolog like 2	2.23461
MIR889	Microrna 889	2.22549
ATP1B2	Atpase Na+/K+ transporting subunit beta 2	2.22251
TSPYL4	TSPY-like 4	2.22232
PLXNC1	Plexin C1	2.21932

Gene Symbol	Gene name	Fold-Change
ETV1	Ets variant 1	2.21493
TRPM3	Transient receptor potential cation channel subfamily M member 3	2.21423
ANKH	ANKH inorganic pyrophosphate transport regulator	2.21308
FRZB	Frizzled-related protein	2.21105
CACNB2	Calcium voltage-gated channel auxiliary subunit beta 2	2.20081
ATP6AP1	Atpase H+ transporting accessory protein 1	2.20016
TMEM150C	Transmembrane protein 150C	2.19768
SYN1	Synapsin I	2.19629
AC011891.5	Putative novel transcript	2.1952
NUPR1L	Nuclear protein, transcriptional regulator, 1-like	2.19511
CBFA2T2	CBF2/RUNX1 translocation partner 2	2.19415
TMEM178B	Transmembrane protein 178B	2.18908
PPP1R14C	Protein phosphatase 1, regulatory (inhibitor) subunit 14C	2.18841
ISL1	ISL LIM homeobox 1	2.17963
SNORD113-2	Small nucleolar RNA, C/D box 113-2	2.17889
SEPT5-GP1BB	SEPT5-GP1BB readthrough	2.17437
MIR1179	Microrna 1179	2.17232
STMN1	Stathmin 1	2.1695
ARHGEF9	Cdc42 guanine nucleotide exchange factor 9	2.16287
ELOVL4	ELOVL fatty acid elongase 4	2.15932
SLC4A7	Solute carrier family , member 7	2.15673
SEMA5A	Semaphoring 5A	2.15203
PDZK1P2	PDZ domain containing 1 pseudogene 2	2.14798
KIAA0319	Kiaa0319	2.1467
MOB1B	MOB kinase activator 1B	2.144
TNFRSF11A	TNF receptor superfamily, member 11a	2.14131
PNMA1	Paraneoplastic Ma antigen 1	2.13925
SEZ6L	Seizure related 6 homolog like	2.13751
LOC642366	Uncharacterized LOC642366	2.1368
LRRTM3	Leucine rich repeat transmembrane neuronal 3	2.13613
RXRG	Retinoid X receptor, gamma	2.13498
EDIL3	EGF-like repeats and discoidin I-like domains 3	2.13397
CRMP1	Collapsin response mediator protein 1	2.12478
NBEAP1	Neurobeachin pseudogene 1	2.11915
ACE2	Angiotensin I converting enzyme 2	2.1178
PCP4	Purkinje cell protein 4	2.11602
FAR2P3	Fatty acyl coa reductase 2 pseudogene 3	2.11121
AMACR	Alpha-methylacyl-coa racemase	2.10708
MANSC4	MANSC domain containing 4	2.10546
DGKG	Diacylglycerol kinase, gamma 90kda	2.10534
LOC100507661	Uncharacterized LOC100507661	2.10023
SUCNR1	Succinate receptor 1	2.09587

Gene Symbol	Gene name	Fold-Change
KRT222	Keratin 222	2.09233
DNAJC6	Dnaj (Hsp40) homolog, subfamily C, member 6	2.08771
PDZK1	PDZ domain containing 1	2.08769
RASGEF1B	Rasgef domain family, member 1B	2.08735
PTPRN2	Protein tyrosine phosphatase, receptor type, N polypeptide 2	2.08581
EPM2AIP1	EPM2A (laforin) interacting protein 1	2.08395
FAM169A	Family with sequence similarity 169, member A	2.07981
LOC646903	Uncharacterized LOC646903	2.07977
SLC22A17	Solute carrier family 22, member 17	2.0786
KL	Klotho	2.07836
EML5	Echinoderm microtubule associated protein like 5	2.07611
MCF2L2	MCF.2 cell line derived transforming sequence-like 2	2.07582
AP3B2	Adaptor-related protein complex 3, beta 2 subunit	2.07546
KIAA1244	Kiaa1244	2.07471
GNA12	Guanine nucleotide binding protein (G protein) alpha 12	2.07318
PAXBP1-AS1	PAXBP1 antisense RNA 1	2.07258
RAB11A	RAB11A, member RAS oncogene family	2.07193
RAB39B	RAB39B, member RAS oncogene family	2.06784
ENO2	Enolase 2 (gamma, neuronal)	2.06613
SNORD109B	Small nucleolar RNA, C/D box 109B	2.06227
PLCH2	Phospholipase C, eta 2	2.06063
TMOD1	Tropomodulin 1	2.06059
SNORD114-22	Small nucleolar RNA, C/D box 114-22	2.05779
DNAH5	Dynein, axonemal, heavy chain 5	2.05342
HOPX	HOP homeobox	2.05323
VEGFA	Vascular endothelial growth factor A	2.0515
EEF1A2	Eukaryotic translation elongation factor 1 alpha 2	2.04992
LINC01370	Long intergenic non-protein coding RNA 1370	2.04983
SGPP2	Sphingosine-1-phosphate phosphatase 2	2.04856
SERPINE2	Serpin peptidase inhibitor, clade E (nexin, plasminogen act	2.04298
MSANTD4	Myb/SANT-like DNA-binding domain containing 4 with coiled-coils	2.04083
DDX25	DEAD (Asp-Glu-Ala-Asp) box helicase 25	2.03602
PTPLAD1	Protein tyrosine phosphatase-like A domain containing 1	2.03502
CMIP	C-Maf inducing protein	2.03314
HMGCLL1	3-hydroxymethyl-3-methylglutaryl-coa lyase-like 1	2.02899
ADAM22	ADAM metallopeptidase domain 22	2.02897
ADCYAP1	Adenylate cyclase activating polypeptide 1 (pituitary)	2.02463
ATP2A3	Atpase sarcoplasmic/endoplasmic reticulum Ca2+ transporting 3	2.01994
PLAC8	Placenta-specific 8	2.0181
RP11-343D24.2	Novel transcript	2.01579
CRISP3	Cysteine-rich secretory protein 3	2.01543
CERS6	Ceramide synthase 6	2.01243

Gene Symbol	Gene name	Fold-Change
MIA2	Melanoma inhibitory activity 2	2.00811
HHATL	Hedgehog acyltransferase-like	2.00664
PRPS1	Phosphoribosyl pyrophosphate synthetase 1	2.00345
TMEM200A	Transmembrane protein 200A	2.00315
CNTNAP5	Contactin associated protein-like 5	2.0023

Appendix III

List of differentially expressed genes (down-expressed) in CHI tissues

Gene Symbol	Gene name	Fold-Change
MGST1	Microsomal glutathione S-transferase 1	4.03489
H19	H19, imprinted maternally expressed transcript (non-protein coding)	3.89967
GUCA1C	Guanylate cyclase activator 1C	3.33672
CXCL10	Chemokine (C-X-C motif) ligand 10	3.26505
LMO3	LIM domain only 3 (rhombotin-like 2)	3.21735
THRSP	Thyroid hormone responsive	3.09056
CXCL9	Chemokine (C-X-C motif) ligand 9	3.02664
C3	Complement component 3	2.96514
UCP1	Uncoupling protein 1	2.8019
COLEC12	Collectin sub-family member 12	2.78824
FABP4	Fatty acid binding protein 4	2.72098
C4B	Complement component 4B	2.68705
SERPING1	Serpin peptidase inhibitor, clade G (C1 inhibitor), member 1	2.66952
RP11-77M5.1	Putative novel transcript	2.66178
REG1B	Regenerating islet-derived 1 beta	2.51265
MMP7	Matrix metallopeptidase 7	2.51005
CXCL11	Chemokine (C-X-C motif) ligand 11	2.48133
CYBB	Cytochrome b-245, beta chain	2.45412
IFI44L	Interferon-induced protein 44-like	2.44106
C4A	Complement component 4A	2.42248
SERPINF1	Serpin famaily F member 1	2.40125
ACADL	Acyl-coa dehydrogenase, long chain	2.37189
REG3A	Regenerating islet-derived 3 alpha	2.32703
CLDN10-AS1	CLDN10 antisense RNA 1	2.32187
PLA2G7	Phospholipase A2 group VII	2.31881
REG3G	Regenerating islet-derived 3 gamma	2.30506
CCDC80	Coiled-coil domain containing 80	2.30271
CFB	Complement factor B	2.28211
CXCL12	Chemokine (C-X-C motif) ligand 12	2.28015
TNFSF14	Tumor necrosis factor (ligand) superfamily, member 14	2.23638
TFPI2	Tissue factor pathway inhibitor 2	2.23111
KCNJ5	Potassium inwardly-rectifying channel, subfamily J, member 5	2.22986
PYGL	Phosphorylase, glycogen, liver	2.22527
SRPX	Sushi-repeat containing protein, X-linked	2.22444
SERPINA3	Serpin peptidase inhibitor family A member 3	2.21725
TLR3	Toll-like receptor 3	2.21137
AOX1	Aldehyde oxidase 1	2.20513

Gene Symbol	Gene name	Fold-Change
MX1	MX dynamin like GTPase 1	2.19983
FGF10	Fibroblast growth factor 10	2.17648
CCL2	Chemokine (C-C motif) ligand 2	2.1532
REG1P	Regenerating islet-derived 1 pseudogene	2.13169
ADIPOQ	Adiponectin, C1Q and collagen domain containing	2.11897
MIR4451	Microrna 4451	2.11151
OLR1	Oxidized low density lipoprotein receptor 1	2.10191
LYZ	Lysozyme	2.08729
ABI3BP	ABI family, member 3 binding protein	2.07111
G0S2	G0/G1 switch 2	2.0701
CCND2	Cyclin D2	2.05656
HBB	Hemoglobin, beta	2.02958
CD36	CD36 molecule	2.01923
PLEKHS1	Pleckstrin homology domain containing, family S member 1	2.01725
SNORA71B	Small nucleolar RNA, H/ACA box 71B	2.00093